

29th Benelux Meeting
on
Systems and Control

March 30 – April 1, 2010

Heeze, The Netherlands

Book of Abstracts

The 29th Benelux Meeting on Systems and Control is sponsored by



Netherlands Organisation for Scientific Research

and supported by



Hans Stigter and Gjerrit Meinsma (eds.)
Book of Abstracts 29th Benelux Meeting on Systems and Control

Wageningen University – Biometris
P.O. Box 9101
6700 HB Wageningen
The Netherlands

A catalog record is available from Wageningen University Library.

Alle rechten voorbehouden. Niets uit deze uitgave mag worden vermenigvuldigd en/of openbaar gemaakt worden door middel van druk, fotokopie, microfilm, elektronisch of op welke andere wijze ook zonder voorafgaande schriftelijke toestemming van de uitgever.

All rights reserved. No part of the publication may be reproduced in any form by print, photo print, microfilm or by any other means without prior permission in writing from the publisher.

ISBN: 978-90-8585-672-6

Part 1

Programmatic Table of Contents

Tuesday, March 30, 2010

P0	Welcome and opening	Samenspel
Chair: Gjerrit Meinsma		11.25–11.30

Plenary: P1	System Identification of ... (Part 1)	Samenspel
	Håkan Hjalmarsson	
Chair: Hans Stigter		11.30–12.30

System Identification of Complex and Structured Systems (Part 1) **183**
Håkan Hjalmarsson

TuM01	Systems Theory A	Samenspel
Chair: Arjan van der Schaft		13.45–15:50

TuM01-1 **13.45–14.10**
Putting reaction-diffusion systems into port-Hamiltonian framework **19**
M. Seslija University of Groningen
A.J. van der Schaft University of Groningen
J.M.A. Scherpen University of Groningen

TuM01-2 **14.10–14.35**
The achievable dynamics via control by interconnection **20**
Harsh Vinjamoor University of Groningen
Arjan van der Schaft University of Groningen

TuM01-3 **14.35–15.00**
Hamiltonian dynamics on graphs **21**
Arjan van der Schaft University of Groningen

TuM01-4 **15.00–15.25**
Finding a good window size for evolving graph analysis **22**
Gautier M. Krings Université Catholique de Louvain
Marton Karsai Helsinki University of Technology
Jari Saramäki Helsinki University of Technology
Vincent D. Blondel

TuM01-5 **15.25–15.50**
A Deficiency in a Classical Sampling Formula and its Remedy in the Framework of Colombeau's Algebra . . **23**
M. Seslija University of Groningen

TuM02	Optimal Control A	Samenkomst
Chair: Jan Swevers		13.45–15:50

TuM02-1 **13.45–14.10**
A two-level optimization-based learning controller for wet clutches **24**
Bruno Depraetere Katholieke Universiteit Leuven
Gregory Pinte Flanders Mechatronics Technology Centre
Jan Swevers Katholieke Universiteit Leuven

TuM02-2 **14.10–14.35**
A general optimization based approach to iterative learning control **25**

M. Volckaert Katholieke Universiteit Leuven
M. Diehl Katholieke Universiteit Leuven
J. Swevers Katholieke Universiteit Leuven

TuM02-3 **14.35–15.00**
Model-free norm optimal ILC for LTI systems **26**

Pieter Janssens Katholieke Universiteit Leuven
Goele Pipeleers Katholieke Universiteit Leuven
Jan Swevers Katholieke Universiteit Leuven

TuM02-4 **15.00–15.25**
A Performance Study of a Novel Dynamic Real-Time Optimisation Engine **27**

Pablo A Folandi Process Systems Enterprise Ltd
Jose A Romagnoli Luisiana State University

TuM02-5 **15.25–15.50**
Control of fresh air and exhaust in a diesel engine . . . **28**

C.H.A. Criens Eindhoven University of Technology

TuM03	System Identification A	Samenwerking
Chair: Okko Bosgra		13.45–15:50

TuM03-1 **13.45–14.10**
Improved Waterflooding Performance Using Model Predictive Control **29**

A. Rezapour Delft University of Technology
G.M. van Essen Delft University of Technology
P.M.J. Van den Hof Delft University of Technology
J.D. Jansen

TuM03-2 **14.10–14.35**
Towards model order selection in view of robust control for motion systems with dominant flexible dynamics . . **30**

Robbert van Herpen Eindhoven University of Technology
Tom Oomen Eindhoven University of Technology
Okko Bosgra Eindhoven University of Technology
Marc van de Wal

TuM03-3 **14.35–15.00**
Behavioral modeling of the thermal dynamics of bore-fields for geothermal applications **31**

Griet Monteyne Vrije Universiteit Brussel
Gerd Vandersteen Vrije Universiteit Brussel

TuM03-4 **15.00–15.25**
Systems & Control in Electron Microscopy **32**

Arturo Tejada Ruiz Delft University of Technology

TuM03-5 **15.25–15.50**
Identification and control of a binary distillation column in view of PLC based control **33**

B. Huyck KaHo Sint-Lieven
F. Logist Katholieke Universiteit Leuven
J. De Brabanter KaHo Sint-Lieven
J. Van Impe, B. De Moor

TuM04	Optimization A	Visie
Chair: Pierre-Antoine Absil		13.45–15:50

TuM04-1 **13.45–14.10**
Fast Oriented Bounding Box Computation Using Particle Swarm Optimization 34

Pierre Borckmans Université Catholique de Louvain
 Pierre-Antoine Absil Université Catholique de Louvain

TuM04-2 **14.10–14.35**
Swarm intelligence for traffic control 35

Z. Cong Delft University of Technology
 B. De Schutter Delft University of Technology
 R. Babuska Delft University of Technology

TuM04-3 **14.35–15.00**
Model-Free Feedforward Control of Inkjet Printhead . 36

Mohamed Ezzeldin Mahdy Eindhoven University of Technology
 Andrej Jokic Eindhoven University of Technology
 Paul van den Bosch Eindhoven University of Technology

TuM04-4 **15.00–15.25**
Tensor- versus matrix-based algorithms in exponential data fitting 37

Mariya Ishteva Université Catholique de Louvain
 P.-A. Absil Université Catholique de Louvain
 Sabine Van Huffel Katholieke Universiteit Leuven
 Lieven De Lathauwer

TuM04-5 **15.25–15.50**
Optimization of jacketed tubular reactors for the production of low-density polyethylene: conceptual approach 38

Peter M.M. Van Erdeghem Katholieke Universiteit Leuven
 Filip Logist Katholieke Universiteit Leuven
 Jan F. Van Impe Katholieke Universiteit Leuven
 Chritoph Dittrich

TuM05 **Uitdaging**
Mechanical Engineering
Chair: Paul van den Hof **13.45–15:50**

TuM05-1 **13.45–14.10**
Modelling thermo-acoustic combustion instability with the flame as a parameter 39

Maarten Hoeijmakers Eindhoven University of Technology
 Viktor Kornliv Eindhoven University of Technology
 Ines Lopez Arteaga Eindhoven University of Technology
 Philip de Goey, Henk Nijmeijer

TuM05-2 **14.10–14.35**
Design of feedback controllers and topography estimator for dual actuated atomic force microscopy 40

S. Kuiper Delft University of Technology
 Anil Kunnappillil Madhusudhanan Delft University of Technology
 Paul M.J. Van den Hof Delft University of Technology
 Georg Schitter

TuM05-3 **14.35–15.00**
Data-driven control for the next generation of wind turbines 41

G.J. van der Veen Delft University of Technology
 J.W. van Wingerden Delft University of Technology
 M. Verhaegen Delft University of Technology

TuM05-4 **15.00–15.25**
Data-Driven Learning of Periodic Disturbances for Load Reduction 42

I. Houtzager Delft University of Technology
 J. W. van Wingerden Delft University of Technology
 M. Verhaegen Delft University of Technology

TuM05-5 **15.25–15.50**
Cruise control design, an LPV approach 43

G.J.L. Naus Eindhoven University of Technology
 R.G.M. Huisman DAF Trucks N.V.
 M.J.G. van de Molengraft Eindhoven University of Technology

TuM06 **Interactie**
Robotics A
Chair: Dragan Kostic **13.45–15:50**

TuM06-1 **13.45–14.10**
Modeling Legged Locomotion via the Max-Plus Algebra 44

Gabriel A. D. Lopes Delft University of Technology
 R. Babuska Delft University of Technology
 A.J.J. van den Boom Delft University of Technology
 B. De Schutter

TuM06-2 **14.10–14.35**
Performance of High-level and Low-level Coordinated Control of Mobile Robots 45

S. Adinandra Eindhoven University of Technology
 J. Caarls Eindhoven University of Technology
 D. Kostic Eindhoven University of Technology
 H. Nijmeijer

TuM06-3 **14.35–15.00**
RoboEarth: Concepts and objectives 46

J. Elfring Eindhoven University of Technology
 R.J.M. Janssen Eindhoven University of Technology
 M.J.G. van de Molengraft Eindhoven University of Technology

TuM06-4 **15.00–15.25**
Modeling, identification and stability of a humanoid robot 47

P.W.M. van Zutven Eindhoven University of Technology
 D. Kostic Eindhoven University of Technology
 H. Nijmeijer Eindhoven University of Technology

TuM06-5 **15.25–15.50**
Collision-free motion coordination of unicycle multi-agent systems 48

D. Kostic Eindhoven University of Technology
 S. Adinandra Eindhoven University of Technology
 J. Caarls Eindhoven University of Technology
 H. Nijmeijer

TuP01 **Samenspel**
Systems Theory B
Chair: Jan-Willem Polderman **16.15–19.00**

TuP01-1 **16.15–16.40**
Computable Semantics for CTL on Discrete-Time and Continuous-Space Dynamic Systems* 49

Ivan S. Zapreev Centrum Wiskunde & Informatica
 Pieter J. Collins Centrum Wiskunde & Informatica

TuP01-2 **16.40–17.05**
Compositional and computable semantics for hybrid systems 50
 Pieter Collins Centrum Wiskunde en Informatica
 Ramon Schiffelers Eindhoven University of Technology
 Davide Bresolin Universida di Verona
 Bert van Beek, Koos Rooda, Tiziano Villa

TuP01-3 **17.05–17.30**
Abstraction Techniques for Automatic Verification of Stochastic Hybrid Systems 51
 Alessandro Abate Delft University of Technology

TuP01-4 **17.45–18.10**
The Information Inequality on Function Spaces 52
 Tzvetan Ivanov Université Catholique de Louvain
 Michel Gevers Université Catholique de Louvain
 P.-A. Absil Université Catholique de Louvain
 Brian D.O. Anderson

TuP01-5 **18.10–18.35**
Tracking and regulation in the behavioral framework . 53
 S. Fiaz University of Groningen
 K. Takaba Kyoto University
 Harry L. Trentelman University of Groningen

TuP01-6 **18.35–19.00**
Fast and robust iterative learning control for lifted systems with bounded model uncertainties 54
 A. Haber Delft University of Technology

TuP02 **Samenkomst**
Optimal Control B
Chair: Jacob Engwerda **16.15–19.00**

TuP02-1 **16.15–16.40**
Necessary and sufficient conditions for Pareto optimality in differential games 55
 J.C. Engwerda Tilburg University
 P.V. Reddy Tilburg University

TuP02-2 **16.40–17.05**
Model-free Monte-Carlo like policy evaluation 56
 Raphael Fonteneau Université de Liège
 Susan A. Murphy University of Michigan
 Damien Ernst Université de Liège
 Louis Wehenkel

TuP02-3 **17.05–17.30**
ACADO Toolkit – An open-source framework for Automatic Control and Dynamic Optimization 57
 H.J. Ferreau Katholieke Universiteit Leuven
 B. Houska Katholieke Universiteit Leuven
 M. Diehl Katholieke Universiteit Leuven

TuP02-4 **17.45–18.10**
Flood control of the Demer with model predictive control 58
 Maarten Breckpot Katholieke Universiteit Leuven
 Toni Barjas Blanco Katholieke Universiteit Leuven
 Bart De Moor Katholieke Universiteit Leuven

TuP02-5 **18.10–18.35**
Optimal Shifting Strategy for a Parallel Hybrid Electric Vehicle 59
 D.V. Ngo Eindhoven University of Technology
 T. Hofman Eindhoven University of Technology
 M. Steinbuch Eindhoven University of Technology
 A. Serrarens

TuP02-6 **18.35–19.00**
Robust fixed-order controller design for time-delay systems with application to the milling process 60
 N.J.M. van Dijk Eindhoven University of Technology
 N. van de Wouw Eindhoven University of Technology
 H. Nijmeijer Eindhoven University of Technology

TuP03 **Samenwerking**
Systems Biology + Medical App. A
Chair: Hans Stigter **16.15–19.00**

TuP03-1 **16.15–16.40**
Accurate Oscillometric Blood Pressure Measurement: an Experimental Approach 61
 Kurt Barbé Vrije Universiteit Brussel
 Wendy Van Moer Vrije Universiteit Brussel
 Lieve Lauwers Vrije Universiteit Brussel
 Danny Schoors

TuP03-2 **16.40–17.05**
Design of a teleoperated palpation device for minimally invasive thoracic surgery 62
 Angelo Buttafuoco Université Libre de Bruxelles
 Amaury Dambour Université Libre de Bruxelles
 Thomas Delwiche Université Libre de Bruxelles
 Michel Kinnaert

TuP03-3 **17.05–17.30**
Selection of circadian clock models for robust entrainment: an analysis based on the phase response curve . 63
 Pierre Sacré Université de Liège
 Marc Hafner Ecole Polytechnique Fédérale de Lausanne (EPFL)
 Rodolphe Sepulchre Université de Liège
 Heinz Koeppel

TuP03-4 **17.45–18.10**
Modeling orienting eye movements 64
 Sebastien Coppe Université Catholique de Louvain
 Jean-Jacques Orban de Xivry Johns Hopkins University
 Gunnar Blohm Queen's University
 Philippe Lefèvre

TuP03-5 **18.10–18.35**
The visuomotor transformation of velocity signals in visually guided manual tracking when the eye is in motion 65
 Guillaume Leclercq Université Catholique de Louvain
 Gunnar Blohm Queen's University
 Philippe Lefèvre Université Catholique de Louvain

TuP03-6 **18.35–19.00**
New model of gaze tracking in 2D: compensation for perturbations of the head. 66
 Pierre M. Daye Université Catholique de Louvain
 Lance M. Optican NIH
 Philippe Lefèvre Université Catholique de Louvain
 Gunnar Blohm

TuP04 **Visie**
Biochemical Engineering A
Chair: Gerrit van Straten **16.15–19.00**

TuP04-1 **16.15–16.40**
Dynamical modeling of alcoholic fermentation and its link with nitrogen consumption 67
 R. David Université Catholique de Louvain-la-Neuve
 D. Dochain Université Catholique de Louvain-la-Neuve
 A. Vande Wouwer University of Mons
 Mouret, Sablayrolles

TuP04-2 **16.40–17.05**
State estimation of simulated moving bed chromatographic processes (SMB) 68
 C. Retamal University of Mons
 M. Kinnaert Université Libre de Bruxelles
 A. Vande Wouwer University of Mons
 C. Vilas

TuP04-3 **17.05–17.30**
Nonlinear model predictive control of animal cell cultures in perfusion mode 69
 Ines Saraiva University of Mons
 Alain Vande Wouwer University of Mons
 Lino O. Santos University of Mons

TuP04-4 **17.45–18.10**
On a reduced order model for the representation of plant bioprocesses 70
 Antoine Delmotte University of Mons
 Johan Mailier University of Mons
 Alain Vande Wouwer University of Mons
 M Cloutier, M. Jolicoeur

TuP04-5 **18.10–18.35**
Robust linearizing control of yeast and bacteria fed-batch cultures 71
 Laurent Dewasme University of Mons
 Alain Vande Wouwer University of Mons
 Daniel Coutinho Pontifícia Universidade do Rio Grande do Sul

TuP04-6 **18.35–19.00**
Microbial kinetics at the growth/inactivation interface: estimation of the maximum growth temperature 72
 Eva Van Derlinden Katholieke Universiteit Leuven
 Jan Van Impe Katholieke Universiteit Leuven

TuP05 **Uitdaging**
Electro-Mechanical Eng. A
Chair: Ming Cao **16.15–19.00**

TuP05-1 **16.15–16.40**
Adaptive detection and isolation of sensor faults in doubly-fed induction generators for wind turbine applications 73
 Manuel Gálvez Université Libre de Bruxelles
 Michel Kinnaert Université Libre de Bruxelles

TuP05-2 **16.40–17.05**
Active damping in precision equipment using piezo . . . 74
 B. Babakhani University of Twente
 T.J.A. de Vries University of Twente

TuP05-3 **17.05–17.30**
Experimental synchronization of Hindmarsh-Rose neurons 75
 E. Steur Eindhoven University of Technology
 P.J. Neefs Eindhoven University of Technology
 H. Nijmeijer Eindhoven University of Technology

TuP05-4 **17.45–18.10**
Over-actuation to compensate for static deformation . . 76
 J. Achterberg Eindhoven University of Technology
 C.M.M. van Lierop Eindhoven University of Technology
 P.P.J. van den Bosch Eindhoven University of Technology

TuP05-5 **18.10–18.35**
Tracking periodic signals for simple hysteretic mechanical systems using repetitive internal model 77
 R. Huisman University of Groningen
 B. Jayawardhana University of Groningen

TuP05-6 **18.35–19.00**
Adaptive controller design for automatic micro-assembly systems under the influence of surface forces 78
 R. Ouyang University of Groningen
 B. Jayawardhana University of Groningen

TuP06 **Interactie**
Non-Linear Control A
Chair: Nelis van Lierop **16.15–19.00**

TuP06-1 **16.15–16.40**
Estimation of the probability of stable operation over a given time interval for discrete-time nonlinear state-space models 79
 Laurent Vanbeylen Vrije Universiteit Brussel
 Anne Van Mulders Vrije Universiteit Brussel
 Johan Schoukens Vrije Universiteit Brussel

TuP06-2 **16.40–17.05**
Numerical solutions to noisy systems 80
 Sanja Zivanovic Centrum voor Wiskunde en Informatica
 Pieter Collins Centrum voor Wiskunde en Informatica

TuP06-3 **17.05–17.30**
Smooth adaptive compensation of the input hysteresis . . 81
 A. Katalenic Eindhoven University of Technology
 C.M.M. van Lierop Eindhoven University of Technology

TuP06-4 17.45–18.10

Predictor based control of a mobile robot subject to a bilateral delay 82

Alejandro Alvarez-Aguirre Eindhoven University of Technology

Henk Nijmeijer Eindhoven University of Technology

Toshiki Oguchi Tokyo Metropolitan University

TuP06-5 18.10–18.35

Synchronization of diffusively coupled systems with time delayed interaction: a passivity based approach 83

E. Steur Eindhoven University of Technology

H. Nijmeijer Eindhoven University of Technology

TuP06-6 18.35–19.00

Lyapunov theory for delay difference inclusions 84

R.H. Gielen Eindhoven University of Technology

M. Lazar Eindhoven University of Technology

I.V. Kolmanovsky Ford Motor Company

Wednesday, March 31, 2010

Plenary: P2 Samenspel
Control of PDEs (Part 1)
Andreas Kugi
Chair: Hans Stigter 8.30– 9.30

Control of PDEs (Part 1: Trajectory Planning and Feed-forward Control) 206
 Andreas Kugi

Plenary: P3 Samenspel
Control of PDEs (Part 2)
Andreas Kugi
Chair: Hans Stigter 10.00–11.00

Control of PDEs (Part 2: Feedback and Tracking Control)223
 Andreas Kugi

Plenary: P4 Samenspel
System Identification of ... (Part 2)
Håkan Hjalmarsson
Chair: Hans Stigter 11.20–12.20

System Identification of Complex and Structured Systems (Part 2) 183
 Håkan Hjalmarsson

Plenary: P5 Samenspel
DISC Award and Certificates
Paul van den Hof
Chair: Hans Stigter 12.20–12.30

WeM01 Samenspel
Systems Theory C
Chair: Gjerrit Meinsma 13.45–15.50

WeM01-1 13.45–14.10
A comparison of approximation algorithms for the joint spectral radius 85
 Chia-Tche Chang Université Catholique de Louvain
 Vincent D. Blondel Université Catholique de Louvain

WeM01-2 14.10–14.35
Fixed-order Robust Controller and Time Domain Response Improvement 86
 Keivan Zavari Katholieke Universiteit Leuven
 Hamid Khatibi Sharif University of Technology
 Jan Swevers Katholieke Universiteit Leuven

WeM01-3 14.35–15.00
On Algebraic Riccati Equations Whose Coefficient Matrices Depend Periodically on a Single State Variable . . 87
 S. Muhammad Delft University of Technology
 J. van der Woude Delft University of Technology

WeM01-4 **15.00–15.25**
Solving systems of polynomial equations: from algebraic geometry to linear algebra 88

Philippe Dreesen Katholieke Universiteit Leuven
 Kim Batselier Katholieke Universiteit Leuven
 Bart De Moor Katholieke Universiteit Leuven

WeM01-5 **15.25–15.50**
Computation of chopped system norm 89

Hanumant Singh Shekhawat University of Twente
 Gjerrit Meinsma University of Twente

WeM02 **Samenkomst**
Optimal Control C
Chair: Bram de Jager **13.45–15.50**

WeM02-1 **13.45–14.10**
An Approximation Method for Stochastic Max-Plus Linear Systems 90

Samira S. Farahani Delft University of Technology
 T. J. J. van den Boom Delft University of Technology
 B. De Schutter Delft University of Technology

WeM02-2 **14.10–14.35**
ACADO Multi-Objective: a toolkit for multiple objective optimal control 91

Filip Logist Katholieke Universiteit Leuven
 Boris Houska Katholieke Universiteit Leuven
 Jan F. Van Impe Katholieke Universiteit Leuven
 Moritz Diehl

WeM02-3 **14.35–15.00**
A solution with reduced conservatism for \mathcal{H}_2 or \mathcal{H}_∞ multi-objective output-feedback control of LTI systems 92

E. Simon Université Catholique de Louvain
 P. Rodriguez-Ayerbe SUPELEC
 V. Wertz Université Catholique de Louvain
 C. Stoica, D. Dumur

WeM02-4 **15.00–15.25**
Hybrid Automata Model Approach for Coordinating Traffic Signal Control 93

Herman Sutarto University of Ghent
 Rene Boel University of Ghent

WeM02-5 **15.25–15.50**
Velocity trajectory optimization in hybrid electric trucks 94

Thijs van Keulen Eindhoven University of Technology
 Bram de Jager Eindhoven University of Technology
 Maarten Steinbuch Eindhoven University of Technology

WeM03 **Samenwerking**
System Identification B
Chair: Johan Schoukens **13.45–15.50**

WeM03-1 **13.45–14.10**
Estimating nonlinear dynamics in nonlinear state-space models 95

Anna Marconato Vrije Universiteit Brussel
 Jonas Sjöberg Vrije Universiteit Brussel
 Johan Schoukens Vrije Universiteit Brussel
 Johan Suykens

WeM03-2 **14.10–14.35**
Assigning the Nonlinear Distortions of a Two-input Single-output System 96

W.D. Widanage Vrije Universiteit Brussel
 J. Schoukens Vrije Universiteit Brussel

WeM03-3 **14.35–15.00**
Using linear system estimates within LS-SVM models . 97

Tillmann Falck Katholieke Universiteit Leuven
 Johan Suykens Katholieke Universiteit Leuven
 Johan Schoukens Vrije Universiteit Brussel
 Bart De Moor

WeM03-4 **15.00–15.25**
Reduction of polynomial nonlinear state-space models by means of nonlinear similarity transforms 98

Anne Van Mulders Vrije Universiteit Brussel
 Laurent Vanbeylen Vrije Universiteit Brussel
 Johan Schoukens Vrije Universiteit Brussel

WeM03-5 **15.25–15.50**
Good short record confidence regions for system identification 99

Kurt Barbé Vrije Universiteit Brussel
 Johan Schoukens Vrije Universiteit Brussel

WeM04 **Optimization B**
Chair: Paul van Dooren **13.45–15.50** **Visie**

WeM04-1 **13.45–14.10**
Spectral clustering of time series: Identifying Profiles in Power Load Data 100

Carlos Alzate Katholieke Universiteit Leuven
 Marcelo Espinoza Katholieke Universiteit Leuven
 Bart De Moor Katholieke Universiteit Leuven
 Johan A.K. Suykens

WeM04-2 **14.10–14.35**
Image segmentation and real-time video tracking using graph based techniques 101

Arnaud Browet Université Catholique de Louvain
 Paul Van Dooren Université Catholique de Louvain
 P.-A. Absil Université Catholique de Louvain

WeM04-3 **14.35–15.00**
Regression on fixed-rank positive semidefinite matrices: a geometric approach 102

Gilles Meyer Université de Liège
 Silvère Bonnabel Mines ParisTech
 Rodolphe Sepulchre Université de Liège

WeM04-4 **15.00–15.25**
Means and medians in nonlinear spaces 103

Anne Collard Université de Liège
 Rodolphe Sepulchre Université de Liège

WeM04-5 **15.25–15.50**
On Adjoint-Based Sequential Convex Programming for Parametric Nonlinear Programming 104

Mr. Tran Dinh Quoc Katholieke Universiteit Leuven
 Prof. Moritz Diehl Katholieke Universiteit Leuven

WeM05	Uitdaging
Networks and Distributed Control	
Chair: Bart De Schutter	13.45–15.50
WeM05-1	13.45–14.10
<i>Synchronization Criteria for Discrete Dynamical Networks via Impulsive Couplings</i>	105
H. Liu	University of Groningen
M. Cao	University of Groningen
J. A. Lu	Wuhan University
WeM05-2	14.10–14.35
<i>An Approach to Observer-Based Decentralized Control under Periodic Protocols</i>	106
N.W. Bauer	Eindhoven University of Technology
M.C.F. Donkers	Eindhoven University of Technology
W.P.M.H. Heemels	Eindhoven University of Technology
N. van de Wouw	
WeM05-3	14.35–15.00
<i>Multi-level model predictive control of large-scale networks</i>	107
N.B. Groot	Delft University of Technology
B.H.K. de Schutter	Delft University of Technology
J. Hellendoorn	Delft University of Technology
WeM05-4	15.00–15.25
<i>Distributed control using decompositions applied to a network of houses with μCHP's.</i>	108
Gunn K.H. Larsen	University of Groningen
Jacquelin M.A. Scherpen	University of Groningen
Nicky D. van Foreest	University of Groningen
WeM05-5	15.25–15.50
<i>Review of Similarity Matrices and Application to Sub-graph Matching</i>	109
T. P. Cason	Université Catholique de Louvain
P.-A. Absil	Université Catholique de Louvain
P. Van Dooren	Université Catholique de Louvain
WeM06	Interactie
Robotics B	
Chair: Dragan Kostic	13.45–15.50
WeM06-2	14.10–14.35
<i>Coordinate transformation as a help for controller design in walking</i>	110
Gijs van Oort	University of Twente
Stefano Stramigioli	University of Twente
WeM06-3	14.35–15.00
<i>Real-time clustering of position and omnivision object observations in the Robocup domain</i>	111
R.J.M. Janssen	Eindhoven University of Technology
M.J.G. van de Molengraft	Eindhoven University of Technology
WeM06-4	15.00–15.25
<i>Application of the IMPACT structure on bilateral teleoperation</i>	112
A. Denasi	Eindhoven University of Technology
D. Kostic	Eindhoven University of Technology
H. Nijmeijer	Eindhoven University of Technology

WeM06-5	15.25–15.50
<i>Transparency in Force-sensorless Teleoperation Setups</i>	113
S.Lichardopol	Eindhoven University of Technology
H. Nijmeijer	Eindhoven University of Technology
WeP01	Samenspel
Distributed Parameter Systems	
Chair: Ming Cao	16.15–19.00
WeP01-1	16.15–16.40
<i>Stabilisation of unstable transition boiling states</i>	114
R.W. van Gils	Eindhoven University of Technology
M.F.M. Speetjens	Eindhoven University of Technology
H. Nijmeijer	Eindhoven University of Technology
WeP01-2	16.40–17.05
<i>Design of optimal deterministic output estimators for distributed parameter systems</i>	115
J.A.W. Vissers	Eindhoven University of Technology
S. Weiland	Eindhoven University of Technology
WeP01-3	17.05–17.30
<i>Cluster synchronization algorithms</i>	116
Weiguo Xia	University of Groningen
Ming Cao	University of Groningen
WeP01-4	17.45–18.10
<i>Feedback control of the sawtooth behavior in nuclear fusion</i>	117
G. Witvoet	Eindhoven University of Technology
M. Steinbuch	Eindhoven University of Technology
E. Westerhof	FOM - Institute for Plasma Physics
N. Doelman, M. de Baar	
WeP01-5	18.10–18.35
<i>Modeling and Control of Inline Separators: An Introduction</i>	118
M. Leskens	Delft University of Technology
A. Huesman	Delft University of Technology
P.M.J. Van den Hof	Delft University of Technology
S. Belfroid, E. Nennie, P. Verbeek, R. Henkes, E. van Donkelaar	
WeP01-6	18.35–19.00
<i>Positivity criteria for Hilbert state-space systems</i>	119
B. Abouzaid	University of Namur (FUNDP)
J. J. Winkin	University of Namur (FUNDP)
V. Wertz	Université Catholique de Louvain
WeP02	Samenkomst
Optimal Control D	
Chair: Yucai Zhu	16.15–19.00
WeP02-1	16.15–16.40
<i>Almost decentralized Lyapunov-based model predictive control</i>	120
Ralph M. Hermans	Eindhoven University of Technology
Mircea Lazar	Eindhoven University of Technology
Andrej Jokic	Eindhoven University of Technology
WeP02-2	16.40–17.05
<i>Time optimal MPC for mechatronic systems</i>	121
Lieboud Van den Broeck	Katholieke Universiteit Leuven
Moritz Diehl	Katholieke Universiteit Leuven
Jan Swevers	Katholieke Universiteit Leuven

WeP02-3 17.05–17.30*Constrained predictive control of fast-sampling linear systems: An inversion-based algebraic approach 122*Jean-François Stumper Technische Universität München
Ralph Kennel Technische Universität München**WeP02-4** 17.45–18.10*Predictive control for non strictly proper and non causal systems 123*Abhishek Dutta Ghent University
Robin De Keyser Ghent University
Bart Wyns Ghent University
Clara Ionescu, Yu Zhong**WeP02-5** 18.10–18.35*Is there free lunch in control? An adaptive disturbance model for MPC 124*Kai Han Zhejiang University
Yucai Zhu Eindhoven University of Technology
Jun Zhao Zhejiang University
Zuhua Xu, Jixin Qian**WeP02-6** 18.35–19.00*Robust Feedforward Control For a DoD Inkjet Printhead 125*Amol A. Khalate Delft Center for Systems and Control
Xavier Bombois Delft University of Technology
Robert Babuska Delft University of Technology
R. Waarsing, W. de Zeeuw, P. Klerken**WeP03** **Samenwerking**
Systems Biology + Medical App. B
Chair: Rodolphe Sepulchre 16.15–19.00**WeP03-1** 16.15–16.40*Global analysis of pulse-coupled oscillators: discrete and continuous models 126*A. Mauroy Université de Liège
R. Sepulchre Université de Liège**WeP03-2** 16.40–17.05*Identification of biochemical reaction systems using semi-definite programming 127*Dirk Fey Université de Liège
Eric Bullinger Université de Liège**WeP03-3** 17.05–17.30*Performance and robustness of bistable systems 128*Laura Trotta Université de Liège
Eric Bullinger Université de Liège
Rodolphe Sepulchre Université de Liège**WeP03-4** 17.45–18.10*Modeling of the interaction force between the instrument and the trocar in minimally invasive surgery 129*Jonathan Verspecht Université Libre de Bruxelles
Thomas Delwiche Past U.L.B.
Angelo Buttafuoco Université Libre de Bruxelles
Laurent Catoire, Serge Torfs, Michel Kinnaert**WeP03-5** 18.10–18.35*Robust patterning in Arabidopsis flowers 130*

Simon van Mourik Wageningen University and Research Center

WeP03-6 18.35–19.00*SK Channels as Regulators of Synaptically Induced Bursting and Neural Synchrony 131*Guillaume Drion Université de Liège
Vincent Seutin Université de Liège
Rodolphe Sepulchre Université de Liège
Anne Collard**WeP04** **Visie**
Biochemical Engineering B
Chair: Jan van Impe 16.15–19.00**WeP04-1** 16.15–16.40*Metabolic Flux Analysis of an Underdetermined Network of CHO Cells Considering Measurement Errors . 132*Francisca Zamorano University of Mons
Alain Vande Wouwer University of Mons
Georges Bastin Université Catholique de Louvain**WeP04-2** 16.40–17.05*The production of food for manned space missions - simple mass balance models for plant growth 133*Heather Maclean Université Catholique de Louvain
Denis Dochain Université Catholique de Louvain
Geoff Waters, Mike Dixon, Laury Chaerle, Dominique Van Der Straeten**WeP04-3** 17.05–17.30*Data reconciliation from an electrochemical biosensor to measure toxicity in water 134*Nienke E. Stein Wageningen University
Karel J. Keesman Wageningen University
Hubertus V. M. Hamelers Wageningen University
Cees J. N. Buisman**WeP04-4** 17.45–18.10*Combined online quality prediction and critical vs. non-critical process disturbance discrimination in (bio-) chemical batch processes 135*G. Gins Katholieke Universiteit Leuven
J. Vanlaer Katholieke Universiteit Leuven
J.F.M. Van impe Katholieke Universiteit Leuven**WeP04-5** 18.10–18.35*Online fault detection and diagnosis of (bio)chemical batch processes 136*P. Van den Kerkhof Katholieke Universiteit Leuven
G. Gins Katholieke Universiteit Leuven
J.F.M. Van impe Katholieke Universiteit Leuven
J. Vanlaer**WeP04-6** 18.35–19.00*The influence of measurement noise on PLS-based data mining techniques 137*J. Vanlaer Katholieke Universiteit Leuven
G. Gins Katholieke Universiteit Leuven
J.F.M. Van Impe Katholieke Universiteit Leuven**WeP05** **Uitdaging**
Electro-Mechanical Eng. B
Chair: Damien Ernst 16.15–19.00

WeP05-1	16.15–16.40	WeP06-5	18.10–18.35
<i>Stress driven security analysis of power systems</i>	<i>138</i>	<i>A Cyclo-dissipativity Condition for Power Factor Improvement in Nonsinusoidal Systems with Significant Source Impedance</i>	<i>148</i>
F. Fonteneau-Belmudes	Université de Liège	D. del Puerto-Flores	University of Groningen
D. Ernst	Université de Liège	R. Ortega	Supelec
L. Wehenkel	Université de Liège	J.M.A. Scherpen	University of Groningen
WeP05-2	16.40–17.05	WeP06-6	18.35–19.00
<i>Coordinated voltage control in electrical power systems</i>	<i>139</i>	<i>Computing the Evolution of Hybrid Systems with Ariadne</i>	<i>149</i>
Mohammad Moradzadeh	University of Gent	Pieter Collins	Centrum Wiskunde en Informatica
René Boel	University of Gent	Ivan Zapreev	Centrum Wiskunde en Informatica
WeP05-3	17.05–17.30	Daive Bresolin	Universida di Verona
<i>Visual Feature-Based Motion Control</i>	<i>140</i>	Luca Geretti, Tiziano Villa, Luca Benvenuti, Alberto Ferrari,	
Jeroen de Best	Eindhoven University of Technology	Christos Sofronis	
Rene van de Molengraft	Eindhoven University of Technology		
Maarten Steinbuch	Eindhoven University of Technology		
WeP05-4	17.45–18.10		
<i>Real-time control of magnetic islands in a fusion plasma</i>	<i>141</i>		
B.A. Hennen	Eindhoven University of Technology		
E. Westerhof	FOM Institute for Plasma Physics Rijnhuizen		
P.W.J.M. Nuij	Eindhoven University of Technology		
M.R. de Baar, M. Steinbuch, TEXTOR team			
WeP05-5	18.10–18.35		
<i>Overactuated feedback control using a decoupling approach</i>	<i>142</i>		
Michael Ronde	Eindhoven University of Technology		
Maurice Schneiders	Eindhoven University of Technology		
René van de Molenfract	Eindhoven University of Technology		
Maarten Steinbuch			
WeP05-6	18.35–19.00		
<i>Two-phase anti-lock braking system using force measurement</i>	<i>143</i>		
Mathieu Gerard	Delft University of Technology		
Michel Verhaegen	Delft University of Technology		
Edward Holweg	Delft University of Technology		
WeP06	Interactie		
Non-Linear Control B			
Chair: Jacqelien Scherpen	16.15–19.00		
WeP06-1	16.15–16.40		
<i>Nonsmooth bifurcations of equilibria in planar continuous systems</i>	<i>144</i>		
J.J.Benjamin Biemond	Eindhoven University of Technology		
Nathan van de Wouw	Eindhoven University of Technology		
Henk Nijmeijer	Eindhoven University of Technology		
WeP06-2	16.40–17.05		
<i>The logarithmic quantiser is not optimal for LQ control</i>	<i>145</i>		
Jean-Charles Delvenne	University of Namur		
WeP06-3	17.05–17.30		
<i>Quantized Continuous-Time Average Consensus</i>	<i>146</i>		
Francesca Ceragioli	Politecnico di Torino		
Claudio De Persis	University of Twente		
Paolo Frasca	C.N.R.		
WeP06-4	17.45–18.10		
<i>Adaptive control of port-Hamiltonian systems</i>	<i>147</i>		
D.A. Dirksz	University of Groningen		
J.M.A. Scherpen	University of Groningen		

Thursday, April 1, 2010

Mini Course: P6 **Samenspel**
Networked Control Systems (Part 1)
 Maurice Heemels and Nathan van de Wouw
Chair: Gjerrit Meinsma **10.00–11.00**

Networked Control Systems (Part 1: Introduction and Overview) **237**
 Maurice Heemels and Nathan van de Wouw

Mini Course: P7 **Samenspel**
Networked Control Systems (Part 2)
 Maurice Heemels and Nathan van de Wouw
Chair: Gjerrit Meinsma **8.30– 9.30**

Networked Control Systems (Part 2: Without Communication Constraints) **242**
 Maurice Heemels and Nathan van de Wouw

Mini Course: P8 **Samenspel**
Networked Control Systems (Part 3)
 Maurice Heemels and Nathan van de Wouw
Chair: Gjerrit Meinsma **11.30–12.30**

Networked Control Systems (Part 3: Communication Constraints) **258**
 Maurice Heemels and Nathan van de Wouw

ThP01 **Samenspel**
Systems Theory A
Chair: Anton A. Stoorvogel **13.45–15.50**

ThP01-1 **13.45–14.10**
Issues on global stabilization of linear systems subject to actuator saturation **150**
 Tao Yang Washington State University
 Anton A. Stoorvogel University of Twente
 Ali Saberi Washington State University

ThP01-2 **14.10–14.35**
Stability criteria for planar linear systems with state reset **151**
 Svetlana Polenkova University of Twente
 Jan Willem Polderman University of Twente
 Rom Langerak University of Twente

ThP01-3 **14.35–15.00**
On existence and uniqueness of solutions for bimodal piecewise affine systems **152**
 Le Quang Thuan University of Groningen
 M. K. Çamlibel University of Groningen

ThP01-4 **15.00–15.25**
Compositional analysis for linear control systems **153**
 Florian Kerber University of Groningen
 Arjan van der Schaft University of Groningen

ThP01-5 **15.25–15.50**
Biological implications of global bifurcations **154**
 G.A.K. van Voorn Wageningen UR
 B.W. Kooi VU Amsterdam

ThP02 **Samenkomst**
Optimal Control E
Chair: Karel Keesman **13.45–15.50**

ThP02-1 **13.45–14.10**
Switch model ILC **155**
 Gang Xu Tongji University / Katholieke Universiteit Leuven
 Marnix Volckaert Katholieke Universiteit Leuven
 Jan Swevers Katholieke Universiteit Leuven

ThP02-2 **14.10–14.35**
Xtreme Motion: Control of non-rigid body dynamics of a high precision positioning stage **156**
 R. Hoogendijk Eindhoven University of Technology

ThP02-3 **14.35–15.00**
Optimal Regenerative Braking with a Pushbelt CVT: an Experimental Study **157**
 Koos van Berkel Eindhoven University of Technology
 Theo Hofman Eindhoven University of Technology
 Bas Vroemen DriveTrain Innovations
 Maarten Steinbuch

ThP02-4 **15.00–15.25**
Real-time control of industrial batch crystallizers: A model-based control approach **158**
 Ali Mesbah Delft University of Technology
 Adrie E.M. Huesman Delft University of Technology
 Herman J.M. Kramer Delft University of Technology
 Paul M.J. Van den Hof

ThP02-5 **15.25–15.50**
Badminton playing robot - a multidisciplinary test case in mechatronics **159**
 J. Stoev FMTC
 S. Gillijns
 A. Bartic
 W. Symens

ThP03 **Samenwerking**
System Identification C
Chair: Rik Pintelon **13.45–15.50**

ThP03-1 **13.45–14.10**
Detection of Nonlinearities in Industrial Motion Stages **160**
 David J. Rijlaarsdam Eindhoven University of Technology
 Pieter W.J.M. Nuij Eindhoven University of Technology
 Maarten Steinbuch Eindhoven University of Technology

ThP03-2 **14.10–14.35**
Identification of linear, periodically time-varying systems **161**
 E. Louarroudi Vrije Universiteit Brussel
 J. Lataire Vrije Universiteit Brussel
 R. Pintelon Vrije Universiteit Brussel

ThP03-3 **14.35–15.00**
Frequency Domain Total Least Squares Estimator of Time-Varying Systems **162**
 John Lataire Vrije Universiteit Brussel
 Rik Pintelon Vrije Universiteit Brussel

ThP03-4 **15.00–15.25**
Frequency domain identification of output error models in matrix fraction description 163
 Rogier S. Blom Delft University of Technology
 Paul M. J. Van den Hof Delft University of Technology
 Hans H. Langen Delft University of Technology
 Rob H. Munnig Schmidt

ThP03-5 **15.25–15.50**
Higher Order Cumulant Based Blind Channel Identification : Enhanced Line Search Solutions 164
 Ignat Domanov Katholieke Universiteit Leuven Campus Kortrijk
 Lieven De Lathauwer Katholieke Universiteit Leuven Campus Kortrijk

ThP04 **Visie**
Optimization and Model Reduction
Chair: Bayu Jayawardhana **13.45–15.50**

ThP04-1 **13.45–14.10**
Model reduction as an identification problem 165
 S. K. Wattamwar student, Eindhoven University of Technology
 Siep Weiland Eindhoven University of Technology
 Ton Backx Eindhoven University of Technology

ThP04-2 **14.10–14.35**
POD model reduction of multi-variable distributed systems 166
 Femke van Belzen Eindhoven University of Technology
 Siep Weiland Eindhoven University of Technology

ThP04-3 **14.35–15.00**
Closed-loop Model Reduction for Controller- and Observer Design 167
 M.E.C. Mutsaers Eindhoven University of Technology
 S. Weiland Eindhoven University of Technology

ThP04-4 **15.00–15.25**
A small-gain theorem for input-to-state convergent systems 168
 B. Besselink Eindhoven University of Technology
 N. van de Wouw Eindhoven University of Technology
 H. Nijmeijer Eindhoven University of Technology

ThP04-5 **15.25–15.50**
Selecting and grouping with multiple graphs 169
 M. Signoretto Katholieke Universiteit Leuven
 J.A. Suykens Katholieke Universiteit Leuven

ThP05 **Uitdaging**
Modeling
Chair: Maarten Steinbuch **13.45–15.50**

ThP05-1 **13.45–14.10**
Very fast temperature pulsing: first results 170
 J. Stolte Eindhoven University of Technology
 A.C.P.M. Backx Eindhoven University of Technology

ThP05-2 **14.10–14.35**
Stability Analysis of Stochastic Networked Control Systems 171
 M.C.F. Donkers Eindhoven University of Technology
 W.P.M.H. Heemels Eindhoven University of Technology
 D. Bernardini University of Siena
 A. Bemporad

ThP05-3 **14.35–15.00**
Modelling a hysteretic relay in a self-oscillating loop . 172
 Paul van der Hulst Piak electronic design b.v.
 A. Veltman Piak electronic design b.v.
 P.P.J. van den Bosch Eindhoven University of Technology

ThP05-4 **15.00–15.25**
Friction Based Actuation and Control Systems in CVT Applications 173
 Irmak Aladagli Eindhoven University of Technology
 Theo Hofman Eindhoven University of Technology
 Maarten Steinbuch Eindhoven University of Technology
 Roell van Druten

ThP05-5 **15.25–15.50**
The C-Lever Project: Haptics for Automotive Applications 174
 E. Garcia-Canseco Eindhoven University of Technology
 A. Ayemlong-Fokem Eindhoven University of Technology
 M. Steinbuch Eindhoven University of Technology
 A. Serrarens

ThP06 **Interactie**
Observers
Chair: Pierre-Antoine Absil **13.45–15.50**

ThP06-1 **13.45–14.10**
Comparison of Decentralized Kalman Filters for Heated Plates 175
 Z. Hidayat Delft University of Technology
 R. Babuška Delft University of Technology
 B. De Schutter Delft University of Technology

ThP06-2 **14.10–14.35**
Distributed estimation for domestic mobile robots: an experimental setup 176
 Andrea Simonetto Delft University of Technology
 Tamas Keviczky Delft University of Technology

ThP06-3 **14.35–15.00**
Nonlinear non-Gaussian state estimation using a land surface model and the particle filter 177
 Douglas A. Plaza University of Ghent

ThP06-4 **15.00–15.25**
A filtering technique on the Grassmann manifold . . . 178
 Q. Rentmeesters Université Catholique de Louvain
 P.-A. Absil Université Catholique de Louvain
 P. Van Dooren Université Catholique de Louvain

ThP06-5 **15.25–15.50**
A comparison of spacecraft attitude estimation filters . 179
 Jeroen Vandersteen Katholieke Universiteit Leuven
 Jan Swevers Katholieke Universiteit Leuven
 Conny Aerts Katholieke Universiteit Leuven

P9	Samenspel
Best Junior Presentation Award ceremony	
Chair: Paul Van den Hof	15.50–16.15

<i>Part 1: Programmatic Table of Contents</i>	3
Overview of scientific program	
<i>Part 2: Contributed Lectures</i>	17
One-page abstracts	
<i>Part 3: Plenary Lectures</i>	181
Presentation materials	
<i>Part 4: List of Participants</i>	273
Alphabetical list	
<i>Part 5: Organizational Comments</i>	293
Comments, overview program, map	

Part 2

Contributed Lectures

Putting reaction-diffusion systems into port-Hamiltonian framework

Marko Šešljija

Faculty of Mathematics and Natural Sciences
University of Groningen
Nijenborgh 4, 9747 AG Groningen
e-mail: m.seslija@rug.nl

Arjan van der Schaft

Faculty of Mathematics and Natural Sciences
University of Groningen
Nijenborgh 9, 9747 AG Groningen
e-mail: A.J.van.der.Schaft@math.rug.nl

Jacqueline M.A. Scherpen

Faculty of Mathematics and Natural Sciences
University of Groningen
Nijenborgh 4, 9747 AG Groningen
e-mail: J.M.A.Scherpen@rug.nl

Abstract

Reaction-diffusion systems model the evolution of the constituents distributed in space under the influence of chemical reactions and diffusion [6], [10]. These systems arise naturally in chemistry [5], but can also be used to model dynamical processes beyond the realm of chemistry such as biology, ecology, geology, and physics. In this paper, by adopting the viewpoint of port-controlled Hamiltonian systems [7] we cast reaction-diffusion systems into the port-Hamiltonian framework. Aside from offering conceptually a clear geometric interpretation formalized by a Stokes-Dirac structure [8], a port-Hamiltonian perspective allows to treat these dissipative systems as interconnected and thus makes their analysis, both quantitative and qualitative, more accessible from a modern dynamical systems and control theory point of view. This modeling approach permits us to draw immediately some conclusions regarding passivity and stability of reaction-diffusion systems.

It is well-known that adding diffusion to the reaction system can generate behaviors absent in the ode case. This primarily pertains to the problem of diffusion-driven instability which constitutes the basis of Turing's mechanism for pattern formation [11], [5]. Here the treatment of reaction-diffusion systems as dissipative distributed port-Hamiltonian systems could prove to be instrumental in supply of the results on absorbing sets, the existence of the maximal attractor and stability analysis.

Furthermore, by adopting a discrete differential geometry-based approach [9] and discretizing the reaction-diffusion system in port-Hamiltonian form, apart from preserving a geometric structure, a compartmental model analogous to the standard one [1], [2] is obtained.

References

- [1] J.A. Jacquez, *Compartmental Analysis in Biology and Medicine*, Amsterdam, The Netherlands: Elsevier, 1972.
- [2] M.R. Jovanovic, M. Arcak, E.D. Sontag, "A passivity-based approach to stability of spatially distributed systems with a cyclic interconnection structure", *IEEE Transactions on Circuits and Systems, Special Issue on Systems Biology*, 55:75–86, 2008.
- [3] G.F. Oster, A.S. Perelson, "Chemical reaction dynamics. Part I: Geometrical structure", *Arch. Rational Mech. Anal.* 55:230-274.
- [4] G.F. Oster, A.S. Perelson, "Chemical reaction dynamics. Part II: Reaction networks", *Arch. Rational Mech. Anal.* 57:31-98, 1974.
- [5] G. Nicolis, I. Prigogine, *Self-Organization in Non-Equilibrium Systems*, Wiley, New York, 1977.
- [6] J. Smoller, *Shock Waves and Reaction Diffusion Equations*, New York: Springer-Verlag, 1994.
- [7] A.J. van der Schaft, *L2-Gain and Passivity Techniques in Nonlinear Control*, Lect. Notes in Control and Information Sciences, Vol. 218, Springer-Verlag, Berlin, 1996, p. 168, 2nd revised and enlarged edition, Springer-Verlag, London, 2000 (Springer Communications and Control Engineering series), p. xvi+249.
- [8] A.J. van der Schaft, B.M. Maschke, "Hamiltonian formulation of distributed-parameter systems with boundary energy flow", *Journal of Geometry and Physics*, vol. 42, pp. 166–194, 2002.
- [9] A.J. van der Schaft, B.M. Maschke, "Conservation laws and open systems on higherdimensional networks", pp. 799–804 in *Proc. 47th IEEE Conf. on Decision and Control*, Cancun, Mexico, December 9–11, 2008.
- [10] R. Temam, *Infinite Dimensional Dynamical Systems in Mechanics and Physics*, 2nd edition, Springer, 1997.
- [11] A.M. Turing, "The chemical basis of morphogenesis", *Philosophical transactions of Royal Society of London, Series B, Biological Sciences*, Volume 237, Issue 641 (Aug. 14, 1952), pp. 37–72.

The achievable dynamics via control by interconnection.

Harsh Vinjamoor
University of Groningen
h.g.vinjamoor@rug.nl

Arjan van der Schaft
University of Groningen
a.j.van.der.schaft@math.rug.nl

1 Abstract

We consider here the problem of finding a controller such that when interconnected to the plant, we obtain a system which is equivalent to a desired system. Here ‘equivalence’ is formalized as ‘bisimilarity’. We give necessary and sufficient conditions for the existence of such a controller. The systems we consider are linear input-state-output systems. A comparison is made with previously obtained results about achievable/implementable behaviors in the behavioral approach to systems theory. Amongst the advantages of using the notion of bisimilarity is the fact that it directly applies to state space systems, while the computations involved are operations on constant matrices.

Hamiltonian dynamics on graphs

A.J. van der Schaft

Johann Bernoulli Institute for Mathematics and Computer Science

University of Groningen

a.j.van.der.schaft@rug.nl

1 Abstract

In this talk we discuss a number of ways to define port-Hamiltonian dynamics on graphs in an intrinsic way [1]. This will be done by defining two canonical Dirac structures on graphs with boundary vertices, namely the *Kirchhoff-Dirac* structure and the *vertex-edge Dirac* structure.

Prime example for the first Dirac structure is the port-Hamiltonian formulation of RLC electrical circuits (with terminals). Examples for the second canonical Dirac structure include standard consensus algorithms (possibly with leader-follower structure), as well coordination control strategies with a passivity interpretation.

The graph Laplacian matrix turns out to have a natural interpretation of a resistive circuit [2]; this observation can be traced back to the classical work of Kirchhoff.

Furthermore, we discuss how the port-Hamiltonian formulation can be employed for analysis and control purposes, generalizing and unifying previously obtained results by other authors.

References

- [1] A.J. van der Schaft, B.M. Maschke, *Port-Hamiltonian dynamics on graphs*, submitted for publication.
- [2] A.J. van der Schaft, *External characterization and partial synthesis of resistive circuits with terminals*, in preparation.

Finding a good window size for evolving graph analysis

Gautier M. Krings
 Université catholique de Louvain
 Avenue Georges Lemaître, 4
 B-1348 Louvain-la-Neuve, Belgium
 gautier.krings@uclouvain.be

Márton Karsai
 Aalto University

Jari Saramäki
 Aalto University

Vincent D. Blondel
 Université catholique de Louvain

1 Introduction

We consider a set of agents, making interactions over time. With the triplets (i, j, t) (further called *events*) we mean that there has been an interaction between i and j at time t . Many graphs that are built from real-world datasets consist of such interactions (e.g. phone calls). When analyzing a real-world evolving graph, one usually splits the time interval into several time windows, and aggregates for each window its events to a graph, which an edge between the nodes i and j if there is at least one event (i, j, \cdot) happening inside the window. The choice of the window length is not an easy task, because some edges appear in the dataset with a high frequency (let us call them the “stable backbone” of the graph), while others appear only a few times. In many applications, a good window length should be the minimum length required to catch the stable backbone. The aim of this work is to provide a methodology to choose the right window size to use.

2 Characterization of a growing graph

Let \mathcal{C} be the set of events belonging to the time window that generates the graph $G(\mathcal{V}, \mathcal{E})$.

Assuming that the events are equally distributed over time, we can define the length of the window as the number of events that it contains.

The growth of \mathcal{C} induces an increase of the number of edges $|\mathcal{E}|$, since new interactions can be discovered. However, the addition of an event to \mathcal{C} does not automatically lead to the discovery of new edges, since some edges appear several times in the dataset.

We characterize the growth of G with the quantity $\beta(|\mathcal{C}|) = \frac{\ln |\mathcal{E}|}{\ln |\mathcal{C}|}$ and its derivative $\beta' = \frac{\frac{\ln |\mathcal{C}|}{|\mathcal{E}|} \frac{d|\mathcal{E}|}{d|\mathcal{C}|} - \frac{\ln |\mathcal{E}|}{|\mathcal{C}|}}{\ln |\mathcal{C}|^2}$. This notation is equivalent to an extension of Heaps’ law, which is commonly used in linguistics and informetrics.

If the total number of edges is bounded and there is an infinite number of events, then the value of $\beta(\cdot)$ decreases from $\beta(1) = 1$ to $\lim_{k \rightarrow \infty} \beta(k) = 0$.

3 β as a measure of redundancy of information

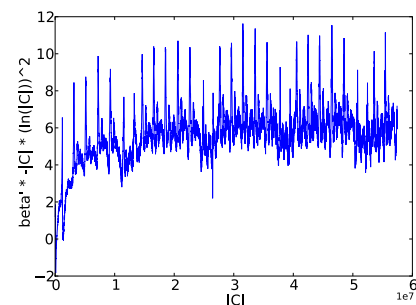
The value of β is a measure of the redundancy of \mathcal{C} . If the events provide diversified information, β is close to 1, and each event contributes significantly to the discovery of new edges. However, when the events provide redundant information, β decreases to 0. This happens when the size of the window is long enough, such that the stable backbone of the network has been completely discovered. In that case, additional events have a high probability to provide information about an edge that is already known.

In such a situation, β' becomes almost proportional to $\frac{-1}{|\mathcal{C}| \ln |\mathcal{C}|^2}$. When this limit is reached, any longer window will generate a graph that contains redundant information, and any shorter window wouldn’t capture all of the stable backbone.

We propose to analyze how β decreases when \mathcal{C} grows, and to fix the window length as the length when β starts to decrease proportionally to $\frac{-1}{|\mathcal{C}| \ln |\mathcal{C}|^2}$.

4 Example on a real network

We applied our methodology to a mobile phone network, and noticed that after around two weeks of data, β decreases on average as fast as the limit given before (on the figure, when the blue curve stabilizes on average). We interpret this as that even if the number of edges still increases, the stable backbone of the network has been totally uncovered, and the optimal window length is reached.



A Deficiency in a Classical Sampling Formula and its Remedy in the Framework of Colombeau's Algebra

Marko Šešlija

Faculty of Mathematics and Natural Sciences
University of Groningen
Nijenborgh 4, 9747 AG Groningen
e-mail: m.seslija@rug.nl

Abstract

In the field of signal and system analysis interpreting signals and discontinuous phenomena as distributions is common. Schwartz's theory of distributions [14] provides a simple and rigorous calculus for distributions, however this theory is based on a vector space rather than on an algebra, so distributions cannot in general be multiplied. But products of distributions naturally arise in many areas of sciences and engineering—the problem of sampling is one of them. Many proposals have been made to define an algebra of generalized functions that will remove the so-called Schwartz's "impossibility result". This is not only a problem of abstract mathematics but also a conceptual problem with many physically reasonable restrictions. J. F. Colombeau in early 1980's defined such an algebra that embeds the Schwartz vector space while retaining its elegance [2]–[5].

The essential aim of this paper is to find a solid theoretical foundation for deriving a Poisson sampling formula [1] that relates the Laplace transform of a sampled and the original signal. Despite this formula appears in standard literature, it is very difficult to find a rigorous proof which clearly indicates the class of functions to which it is applicable. Moreover, many authors [1], [12] avoid introducing the notion of Dirac's delta distribution considering it as ill-defined, nevertheless they implicitly deal with a concepts of weak convergence [6], [9], [10], [13]. Ignoring Schwartz's well established theory of distributions in engineering practice usually leads to a variety of both classical and intuitive methods that suffer from many discrepancies. This paper aims to point out some deficiencies that can be encountered in deriving the key sampling formula.

In this paper I present the application of Colombeau's algebra and a concept of weak equality in deriving the Poisson sampling formula for signals seen as rapidly decreasing generalized functions of bounded rate. The obtained results do not suppress the functional nature of Dirac's delta distribution, hence they differ from those classically acquired. In order to establish a relationship between new and classical results a delayed sampling procedure is introduced.

References

- [1] J. Braslavsky, G. Meinsma, R. Middleton, J. Freudenberg, *On a key sampling formula relating the Laplace and \mathcal{L} transforms*, *Systems Control Letters* 29, 181–190, 1997.
- [2] J.F. Colombeau, *A general multiplication of distributions*, *Comptes Rendus Acad. Sci. Paris* 296, pp. 357–360, 1983.
- [3] ———, *A general multiplication of distributions*, *Bull. AMS* 23,2, pp. 251–268, 1990.
- [4] ———, *Elementary Introduction to new generalized functions*, North Holland, Amsterdam, 1985.
- [5] J. F. Colombeau, A. Meril, *Generalized functions and multiplication of distributions on \mathcal{C}^∞ manifolds*, *J. Math. Anal. Appl.*, 186:357–364, 1994.
- [6] M. Oberguggenberger, *Multiplication of distributions and applications to partial differential equations*, Longman, 1992.
- [7] A.V. Oppenheim, R. W. Schaffer, *Digital signal processing*, Prentice–Hall, Inc., 1975.
- [8] Rosinger, E. Elemér, *Nonlinear partial differential equations. An algebraic view of generalized solutions*, North-Holland Mathematics Studies, 164. North-Holland Publishing Co., Amsterdam, 1990.
- [9] L. Schwartz, *Théorie des distributions*, nouvelle éd., Hermann, 1966.
- [10] S.L. Sobolev, *Méthode nouvelle à résoudre le problème de Cauchy*, *Math. Sbornik* 1, pp. 39–71, 1936.
- [11] R. Steinbauer, *Distributional Methods in General Relativity*, PhD dissertation, Naturwissenschaftlichen Fakultät der Universität Wien, 2000.
- [12] M.R. Stojić, *Digitalni sistemi upravljanja* (in Serbian), IP Nauka, Beograd, 2nd edition, p. 66–72, 1990.
- [13] Tộ Ngọc Trí, *The Colombeau theory of generalized functions*, Master thesis, KdV Institute, Faculty of Science, University of Amsterdam, The Netherlands, 2005.
- [14] A.H. Zemanian, *Distribution theory and transform Analysis*, Dover publications, INC. New York, 1965.

A two-level optimization-based learning controller for wet clutches

Bruno Depraetere¹, Gregory Pinte², Jan Swevers¹

¹ Department of Mechanical Engineering, Division PMA, Katholieke Universiteit Leuven

² Flanders Mechatronics Technology Centre

Celestijnenlaan 300B¹ / 300D², 3001 Heverlee, Belgium

Email: bruno.depraetere@mech.kuleuven.be

1 Introduction

In many mechatronic applications it is not possible to use traditional feedback control or learning techniques like iterative learning control (ILC) since defining suitable reference trajectories is not straightforward. In this work, an alternative learning technique is proposed in the form of a two-level iterative optimization scheme. Instead of indirectly trying to define a reference that leads to a good performance and does not violate certain limitations, the control signal itself is calculated directly by solving a constrained optimization problem on the low level. On the high level, the constraints and models for this optimization problem are updated iteratively to ensure the performance increases as more iterations pass by.

2 Wet clutches

An example of such a mechatronic application is a wet clutch, schematically shown in figure 1. These are typically used in off-highway vehicles and agricultural machines to transmit power from the input shaft to the output shaft by means of friction. To do so, the pressure in the clutch chamber needs to increase such that a hydraulic piston presses two sets of friction plates together. The goal for a good clutch engagement is to engage as fast as possible but without introducing torque spikes. This process can be controlled by sending an appropriate control signal to the solenoid valve in the line to the clutch. Obtaining controllers that perform well under all conditions is difficult since the behavior changes when the piston comes into contact with the plates, and since the dynamics vary as a consequence of wear or changes in the oil temperature [1]. For industrial clutches, these problems are avoided by performing experimental calibrations and repeating this procedure to compensate for system variation. The drawback is that these are time-consuming processes, which require the machine to be taken out of production.

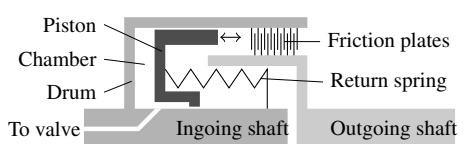


Figure 1: Cross-section of a wet clutch and its components

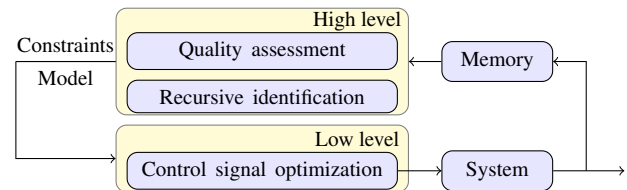


Figure 2: Presented two-level control scheme.

These (re)calibrations can be avoided by using the proposed two-level learning algorithm shown in figure 2. The time required to engage the clutch is minimized by solving a time-optimal control problem on the low level, whereas the high-level learning controller adjusts the constraints based on an assessment of engagement quality, such that torque spikes are avoided and smooth engagements are obtained. The high-level controller also contains a recursive identification algorithm. As a result, the controller adapts to the operating conditions and maintains a good performance.

3 Experimental validation

The developed control scheme has been validated on an experimental test setup. During these experiments the learning controller is initialized with bad parameter values, resulting in poor performance. As more iterations pass and the control signals are iteratively updated, the performance increases. Finally, smooth engagements are obtained with a fast response and without discontinuities or spikes in the transmitted torque, ensuring operator comfort. To demonstrate the robustness, the experiments have been performed at several oil temperatures and at different values of the load. Convergence towards good engagement quality was obtained for all test cases.

Acknowledgement This work has been carried out within the framework of projects IWT-SBO 80032 of the Institute for the Promotion of Innovation through Science and Technology in Flanders (IWT-Vlaanderen) and G.0422.08 of the Research Foundation - Flanders (FWO - Vlaanderen). This work also benefits from K.U.Leuven-BOF EF/05/006 Center-of-Excellence Optimization in Engineering and from the Belgian Programme on Interuniversity Attraction Poles, initiated by the Belgian Federal Science Policy Office.

References

- [1] Z. Sun and K. Hebbale, "Challenges and opportunities in automotive transmission control," in *American Control Conference, 2005. Proceedings of the 2005*, June 2005, pp. 3284–3289 vol. 5.

A general optimization based approach to iterative learning control

Marnix Volckaert¹, Moritz Diehl², Jan Swevers¹

¹ Department of Mechanical Engineering, Katholieke Universiteit Leuven, Belgium

² Department of Electrical Engineering, Katholieke Universiteit Leuven, Belgium

Email: Marnix.Volckaert@mech.kuleuven.be

1 Introduction

This presentation introduces a general formulation of model based iterative learning control (ILC). The formulation is valid for both linear and nonlinear models. It consists of a two step approach, such that after each repetition of the motion two (non)linear least squares problems have to be solved. In the first step an optimal model correction vector is calculated. This is a nonparametric correction to the model to more accurately describe the measured output signal. This model correction is used in the second step, which is a model inversion problem. It is shown that conventional linear ILC is a particular case of this general formulation.

2 General formulation

The aim of ILC is to find, in an iterative way, the control signal u of a system $y = P(u)$, such that the output y exactly follows a reference output y_r .

There exist a number of different ILC schemes: linear and nonlinear ILC, first order and higher order ILC, model free and model based ILC [1]. Model based ILC uses a model $y = \hat{P}(u)$ to calculate u^i . If the model is perfect ($\hat{P} = P$) then the solution of the tracking problem is simply $u = \hat{P}^{-1}(y_r)$. However, in practice the model is never perfect.

In the presented two step approach, the first step is to estimate a correction to the model, while the second step is to invert the corrected model using the reference output. The corrected model $P'(u, \alpha)$ is a function of a time domain signal α , e.g. $P'(u, \alpha) = \hat{P}(u) + \alpha$ or $P'(u, \alpha) = \hat{P}(u + \alpha)$.

Both the model correction estimation and the model inversion are formulated as least squares problems. The solution of the second problem is the input signal that should be applied at the next iteration. The two steps can be written as follows:

$$\alpha^i = \arg \min_{\alpha} \|y^i - P'(u^i, \alpha)\|^2 \quad (1)$$

$$u^{i+1} = \arg \min_u \|y_r - P'(u, \alpha^i)\|^2 \quad (2)$$

In these equations $\|\cdot\|$ means the two-norm.

This formulation is general, and it can be shown that existing ILC approaches are in fact special cases of this formulation, or correspond to solving (1)-(2) using a particular optimization algorithm.

There are many possible extensions to the basic form (1) and (2), for example to extend (1) to penalize a change of α from

one iteration to the next, yields:

$$\alpha^i = \arg \min_{\alpha} \|y^i - P'(u^i, \alpha)\|_2^2 + \|\alpha - \alpha^{i-1}\|^2. \quad (3)$$

It can be shown that this extension corresponds to higher order ILC. A possible extension to (2) is to penalize large input signals, yielding:

$$u^{i+1} = \arg \min_u \|y_r - P'(u, \alpha^i)\|^2 + \|u\|_R^2. \quad (4)$$

In this equation $\|\cdot\|_R$ is the weighted two-norm with R a positive definite weighting matrix.

3 Conventional linear ILC

Model based linear ILC uses an update law of the following form:

$$u^{i+1} = Q[u^i + Le^i]. \quad (5)$$

This update law is written in the lifted-system framework [1], such that $u = [u(0) \ u(1) \ \dots \ u(N-1)]^T$ and $e = [e(1) \ e(2) \ \dots \ e(N)]^T$. The robustness filter Q is often a zero-phase filter, written as

$$Q = \begin{bmatrix} q_0 & q_{-1} & \dots & q_{-(N-1)} \\ q_1 & q_0 & \dots & q_{-(N-2)} \\ \vdots & \vdots & \ddots & \vdots \\ q_{N-1} & q_{N-2} & \dots & q_0 \end{bmatrix}. \quad (6)$$

The learning filter is usually designed as the inverse of the model \hat{P} , such that $L = \hat{P}^{-1}$.

This ILC law is equivalent to the general form if the model correction function $P'(u, \alpha) = \hat{P}(u) + \alpha$ is used, in combination with the objective function of equation (4), using the following weighting matrix:

$$R = \hat{P}^T \hat{P} (Q^{-1} - I) \quad (7)$$

A numerical example illustrates the equivalence of the conventional linear ILC and the general approach under these conditions.

References

- [1] D. A. Bristow, M. Tharayil, A. G. Alleyne, A survey of iterative learning control, IEEE Control Systems Magazine 26 (3) (2006) 96–114.

Model-free norm optimal ILC for LTI systems

Pieter Janssens, Goele Pipeleers and Jan Swevers
 Department of Mechanical Engineering, Katholieke Universiteit Leuven
 Celestijnenlaan 300B, Heverlee B3001, Belgium
 Pieter.Janssens@mech.kuleuven.be

1 Introduction

In iterative learning control (ILC) the tracking performance of a system performing a task iteratively is improved using data from previous trials. In the proposed model-free method an update of the feedforward signal is calculated by convoluting the previous input signal with an optimal convolution vector. This convolution vector is obtained every iteration by solving an optimization problem that minimizes a quadratic next-iteration cost criterion.

2 Method

Consider a reference trajectory $r(t)$ of N samples, a discrete-time linear time-invariant SISO system P and a given sample period T_s . During the first trial a test signal $u_1(t)$ is applied to the system P and a noise-corrupted output $y_1^m(t) = y_1(t) + n(t)$ is measured. $n(t)$ denotes the normally distributed output noise with standard deviation σ_n .

When convoluting a previous input signal $u_k(t)$ with any vector $a(t)$, the corresponding output can be predicted to be $a(t) * y_k^m(t) = a(t) * y_k(t) + a(t) * n(t)$ since the system P is linear and time-invariant. However, the output noise $n(t)$ results in a prediction error $e_{pr} = a(t) * n(t)$ with a standard deviation on the last sample of the trial given by $\sigma_n \sqrt{\sum_{t=1}^N a(t)^2}$. This standard deviation can be reduced by (a) averaging out noise on the output signals (σ_n decreases) and (b) by limiting $\|a(t)\|_2$.

After every trial the next input signal $u_{k+1}(t)$ is calculated as $u_{prev}(t) + a(t) * u_{prev}(t)$ where u_{prev} denotes the average of the M previous input signals. The vector $a(t)$ is obtained by solving the following convex optimization problem which allows input constraints to be accounted for. Robustness is added by penalizing the input signal and/or changes in input signal between 2 trials.

$$\begin{aligned} \min_{a \in \mathbb{R}^N} \quad & \|r(t) - y_{prev}(t) - a(t) * y_{prev}(t)\|_2 \\ & + \gamma_1 \|a(t) * u_{prev}(t)\|_2 + \gamma_2 \|u_{prev} + a(t) * u_{prev}(t)\|_2 \\ \text{s.t.} \quad & u_{k+1}(t) = u_{prev}(t) + a(t) * u_{prev}(t) \\ & |u_{k+1}(t)| \leq u_{max} \\ & |u_{k+1}(t + T_s) - u_{k+1}(t)| \leq \delta u_{max} \\ & \|a\|_2 \leq S \end{aligned}$$

The last constraint limits the standard deviation of the prediction error on the last sample to $\sigma_n \sqrt{(1 + S^2)/M}$.

3 Simulation results

The algorithm is tested in simulation for a flexible system with actuator constraints ($u_{max} = 4V$ and $\delta u_{max} = 1V$) and normally distributed noise on the output. Figure 1 presents the learned input signal and the corresponding output signal and tracking error e after 15 trials together with the optimal tracking error e_{opt} .

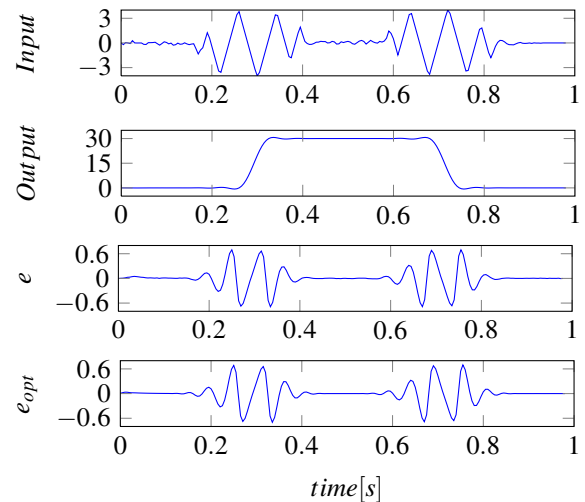


Figure 1: Learned input signal and corresponding output signal and tracking error compared with the optimal tracking error

4 Conclusion

The proposed model-free algorithm for LTI SISO systems learns a noncausal feedforward signal to track a reference signal using information from previous trials. Actuator constraints can easily be taken into account. The effect of noise on the next input signal is reduced using information from multiple trials and by constraining the prediction error.

A Performance Study of a Novel Dynamic Real-Time Optimisation Engine

Pablo A Rolandi

Process Systems Enterprise Ltd,
London, UK

Email: p.rolandi@penterprise.com

José A Romagnoli

Luisiana State University, Luisiana, USA

Email: jose@lsu.edu

For decades, industrial Model Predictive Control (MPC) technology has been based on linear empirical models obtained by identification from input-output process data. Typically, a discrete-time formulation is adopted, and the control problem is posed as an unconstrained optimisation problem with a quadratic-cost objective function. Large-scale first-principles models (of the order of tens of thousands of equations) have seldom been used in advanced model-based control of industrial processes. As a consequence, issues arising from embedding these process models at different levels of the APC control hierarchy have not been addressed satisfactorily; in particular, little emphasis has been placed on using rigorous first-principle models in Dynamic Real-Time Optimisation.

Flexibility (and to some degree interoperability) should be the key technological breakthrough of the next generation of model-based APC systems. For example, such an APC engine would allow embedding linear models as easily as linearised or nonlinear ones. Similarly, this APC engine would support (semi-)empirical models derived from identification- or reduction-based techniques, as well as fundamental mechanistic models derived from first principles. At the same time, the APC system would allow unconstrained, quadratic cost (MPC-like) optimisation-problem formulations or general constrained (RTO-like) ones. Finally, this next-generation APC engine would support discrete- and continuous-time formulations interchangeably (typical of MPC and RTO formalisms, respectively). Since the form of the optimal control problem would not depend on the characteristics of the APC application, a set of mechanisms to formulate (and subsequently interpret) this control problem should be provided to operators and process engineers. In summary, next-generation model-based advanced process control technologies should be centred on an architecture that allows the choice of models, solutions methods, control settings and optimisation strategies seamlessly.

This work describes a model-centric platform for dynamic real-time optimisation (DRTO) based on a generic architecture which supports various models and control problem configurations. This platform

provides an appropriate framework through which key research issues can be investigated and addressed in a thorough and systematic way. The DRTO kernel uses the gPROMS Server as modelling and solution engine (MSE). Other key components of this DRTO are the Event Manager, the Problem Definition Manager and the Solution Feasibility Supervisor, which provide the engine with full flexibility and configurability.

In this work, we present a number of case studies applied to the simulation of an industrial process system. This process is a continuous cooking digester and auxiliary units described by a large-scale model consisting of 14000 algebraic and 1000 differential equations (DAEs). This model, implemented in gPROMS, is used both as virtual plant and as the model server for the DRTO engine.

The performance of the novel DRTO engine is studied in terms of optimality, feasibility and computational speed. We assess the performance of the DRTO engine based on both linear and nonlinear models in disturbance rejection and production transition scenarios. We also investigate optimal formulations of the control problem and their mapping into the receding horizon dynamic optimisation formalism. Finally, we examine the control problem infeasibility aspects and we investigate two infeasibility recuperations mechanisms: ranking and elimination vs identification and relaxation.

Control of Fresh Air and Exhaust in a Diesel Engine

Chris Criens

Department of Mechanical Engineering (Control Systems Technology)

Eindhoven University of Technology

P.O. Box 513, 5600 MB Eindhoven, The Netherlands

Email: c.h.a.criens@tue.nl

1 Problem description

Control over the combustion process in diesel engines is becoming increasingly important due to tightening emission legislation. To accommodate for this, peripherals are added, adding flexibility over the intake conditions. Here, the exhaust gas recirculation (EGR) system and variable turbine geometry (VTG) are the subject of research. An EGR system recirculates exhaust gas through a cooler and a controllable valve into the intake manifold. A VTG has a variable vane angle in the turbine intake. This gives control over the pressure drop over the turbine and the power it transfers to the compressor. The combination of EGR and VTG makes it possible to control the amount of fresh air available for combustion and the amount of EGR-dilution. However, they cannot be controlled independently. Opening the EGR valve will add exhaust gas to the combustion, but this will replace some fresh air. Changing the vane angle of the turbine changes the turbine/compressor speed and hence the fresh air intake, but also the pressure difference between intake and exhaust and consequently the EGR flow.

The goal of the controller is to control the EGR and VTG such that a fixed oxygen percentage ($O_2\%$) and fuel-oxygen ratio λ are obtained in the intake air mixture. The reason for controlling these two parameters is that they are strongly linked with emissions. The $O_2\%$ is strongly correlated to the NOx emissions. Soot and particulate matter emissions are related to λ .

There is a strong preference for model based, optimal control. This allows us to make optimal MIMO controllers in a very systematic way. Robustness and performance trade-offs can be made very clearly. Also, once a framework is completed, it is straightforward to transfer the control design method to a different EGR-VTG engine.

2 Control design

The starting point for control design is a mean value model of a modern heavy duty diesel engine. The model quite accurately predicts e.g. mean air flows, turbine speed and intake and exhaust manifold pressure. It contains data maps to describe e.g. the efficiency of the engine and the turbine for different input conditions. Nonlinear ODEs are used to describe the dynamics. Up to the frequency region where cycle to cycle engine behavior starts playing a role, the model is quite accurate. Problematic for model based control are the nonlinearity of the model and also the data

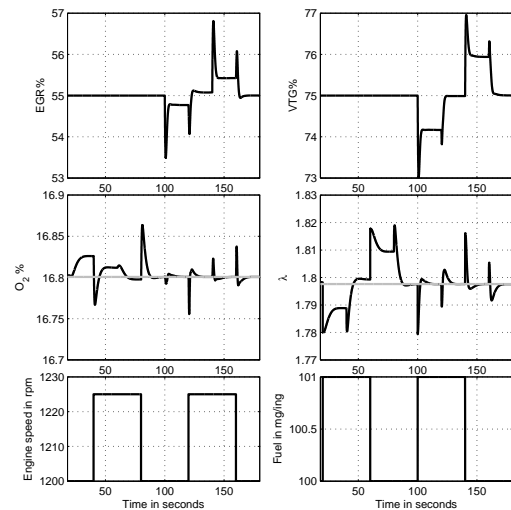


Figure 1: A simulation of the controlled and uncontrolled system. After 100 seconds, the controller is switched on. The top shows two control inputs. The middle graph shows the two outputs and their reference values (grey). The bottom graph shows the engine speed and fuel input.

maps, which make the model difficult to analyze.

The control design will therefore use simulation data as a starting point. This circumvents problems with the model complexity. From simulation data, local LTI models are estimated in a grid of operating points. Using the LTI models, linear controllers are made that locally control the full nonlinear model. By gain scheduling these controllers, a controller for the full operating range can be made.

Model based, H_∞ -optimal control synthesis will be used for the design of the controller. The optimality criterion is a weighted version of tracking performance and the input needed for this. The weight for the system input is higher on high frequencies, because these cause wear of the actuators. The weight on the tracking error is formed from two parts that reflect different types of disturbances. The first part are variations due to the driver input. These are standardized in the European transient cycle (ETC), a cycle that reflects typical road driving. It contains engine speed and torque data for a mix of driving conditions such as city or highway driving. The second source of disturbances are almost static. They are caused by e.g. ambient temperature or pressure. The error-weight combines an integrator for low frequency disturbances with a first order approximation of the frequency response of the ETC. The new controller improves the system response as can be seen in Figure 1.

Improved Waterflooding Performance Using Model Predictive Control

Amin Rezapour
 Delft Center for Systems and Control
 Delft University of Technology
 Mekelweg 2
 2628 CD Delft
 The Netherlands
 Email: aminrezapour@gmail.com

Paul Van den Hof
 Delft Center for Systems and Control
 Delft University of Technology
 Mekelweg 2
 2628 CD Delft
 The Netherlands
 Email: p.m.j.vandenhof@tudelft.nl

Gijs van Essen
 Delft Center for Systems and Control
 Delft University of Technology
 Mekelweg 2
 2628 CD Delft
 The Netherlands
 Email: g.m.vanessen@tudelft.nl

Jan Dirk Jansen
 Department of Geotechnology
 Delft University of Technology
 Stevinweg 1, room 02.05
 2628 CN Delft
 The Netherlands
 Email: j.d.jansen@tudelft.nl

1 Introduction

Hydrocarbon resources around the world are limited, and to satisfy future energy demands more efficient recovery solutions are needed. In oil production, a common method to bring the oil to the surface is to flood a reservoir by injecting water. After properly locating the injection and production wells, injection continues as long as it is profitable, and the wells are shut in afterwards (referred to as reactive control). In order to increase the recovery factor, this task has been cast into an integrated and more structured approach called Closed Loop Reservoir Management (CloReM) [1].

2 Problem Settings

In CloReM methodology, optimal production settings are determined by using adjoint model, and simulating the fluid flow based on reservoir models in a feedback loop. The reservoir dynamics are highly non-linear and models have large number of parameters and states, which are usually expressed with a great deal of uncertainties. Therefore, the performance of the CloReM is highly dependant on quality of the models, which are not updated quite often.

3 Approach

A reference tracking framework using Model Predictive Control (MPC) is investigated in order to provide more rapid corrective responses, to circumvent the unwanted effects of uncertainties. This framework acts like a secondary loop (in addition to the original feedback loop) that has a supervisory task, and reoptimizes the input settings based on low order linear models. Validity (i.e. the prediction horizon) of such

models are relatively short, but they can get updated more often, in several working points through the production life of the reservoir. In this work we have studied the possibility of using system identification methods using Prediction Error Identification (PEI) and Subspace Identification (SubID) to derive Linear Time Invariant (LTI) reservoir models.

4 Results

According to the experiments applied to a 5-spot homogeneous and a 3D multi layered heterogeneous reservoirs, it has been shown that a relatively high simulation fit can be achieved with low order models. However, the accuracy of the models are very much dependent on the availability of a sufficiently informative data. Moreover, it becomes more difficult to acquire higher simulation fits when nonlinearities are more pronounced, e.g. during the water breakthrough. For large number of inputs and outputs, SubID models are able to provide more accurate predictions, while they are computationally more efficient to be implemented in MPC. In general, the proposed methodology can potentially increase the profitability of the above mentioned reservoirs up to 18%, by providing more appropriate input updates [2].

References

- [1] Jansen, J.D., Douma, S.G., Brouwer, D.R., Van den Hof, P.M.J., Bosgra, O.H. and Heemink, A.W. "Closed-Loop Reservoir Management," SPE 119098, 2009 SPE Reservoir Simulation Symposium, USA.
- [2] Rezapour, A., "Improved Waterflooding Performance using Model Predictive Control," MSc Thesis, TU Delft, 2009.

Towards Model Order Selection in View of Robust Control for Motion Systems with Dominant Flexible Dynamics

Robbert van Herpen, Tom Oomen, Okko Bosgra
Eindhoven University of Technology
r.m.a.v.herpen@tue.nl

Marc van de Wal
ASML Research Mechatronics
marc.van.de.wal@asm1.com

Background

Next-generation high-precision positioning systems tend to become lightweight. Generally, lightweight systems exhibit pronounced flexible dynamical behavior in relevant frequency ranges. These flexible dynamics typically are not aligned with the motion degrees-of-freedom, leading to an inherently multivariable dynamical behavior. As a consequence, multivariable controllers are essential to achieve the limits of performance. Model-based control enables a systematic design of such multivariable controllers.

The need for robust-control-relevant model sets

Any physical system is too complex to be represented exactly by a mathematical model. For example, identification of highly complex models of lightly damped flexible dynamical systems is numerically infeasible, as is confirmed in [4]. Hence, any model is approximate. This has two important implications for control design: i) model imperfections should be addressed in a robust control design to guarantee that the designed controller performs adequately when implemented on the physical system and ii) the model should accurately describe those phenomena that need to be compensated explicitly by control, since the quality of approximate models depends on their purpose. Recently, a novel coordinate frame has been presented [1] that transparently connects control-relevant identification of a nominal model, as developed in, e.g., [2], [3], with uncertainty modeling and robust control design.

Re-evaluating model order selection

Although the transparent connection between nominal model identification, uncertainty modeling, and robust control enables a non-conservative multivariable control design to the limits of performance, the desire to construct *control-*

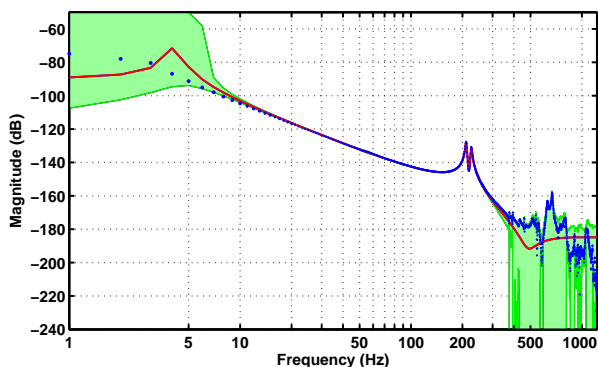


Figure 1: Bode magnitude plot of the true system (dotted), control-relevant 7th order model (solid) and candidate plant set, tight around dominant resonances (shaded).

relevant model sets requires a re-evaluation of model order selection procedures. Indeed, the separate steps of nominal model identification and uncertainty modeling both involve the parametrization and order selection of a dynamical system. A selection procedure should be developed that i) involves both the model order corresponding to the nominal model and to the uncertainty model and ii) evaluates these model orders in light of the control criterion.

First experimental results

Application of the robust-control-relevant identification framework to a next-generation wafer stage for various nominal model orders yields Fig. 1 and Fig. 2. The resulting model sets i) encompass the true system behavior and ii) accurately describe those phenomena that need to be compensated to achieve high performance indeed. (Note that, instead of modeling consecutive control-relevant system artifacts, conventional modeling approaches typically focus on the representation of low-frequency system behavior.) Non-conservative robust control design requires for a dynamical bound on the uncertainty characterization shown. Clearly, an important interplay exists between order selection for the nominal model and the uncertainty bound.

References

- [1] T. Oomen, R. van Herpen, and O. Bosgra. Robust-control-relevant coprime factor identification with application to model validation of a wafer stage. *Proc. 15th IFAC Symp. Sys. Id.*, St. Malo, France, 1044–1049, 2009.
- [2] R. J. P. Schrama. Accurate identification for control: The necessity of an iterative scheme. *IEEE Trans. Automat. Contr.*, 37(7):991–994, 1992.
- [3] R.A. de Callafon and P.M.J. Van den Hof. Suboptimal feedback control by a scheme of iterative identification and control design. *Math. Mod. Syst.*, 3(1):77–101, 1997.
- [4] A. Bultheel, M. Van Barel, Y. Rolain, and R. Pintelon. Numerically Robust Transfer Function Modeling From Noisy Frequency Domain Data. *IEEE Trans. Automat. Contr.*, 50(11):1835–1839, 2005.

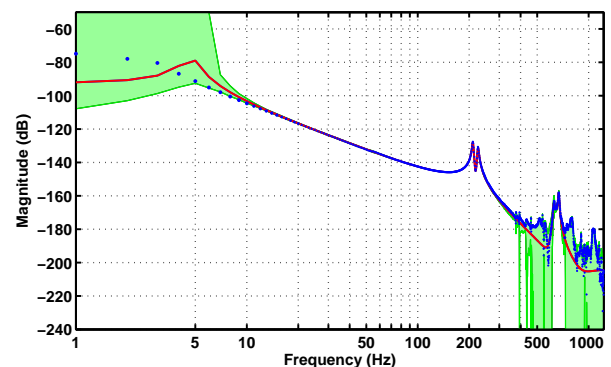


Figure 2: Inclusion of consecutive control-relevant system artifacts in an 11th order model, enabling explicit compensation the high-frequency resonances at 600 Hz.

Behavioral modeling of the thermal dynamics of borefields for geothermal applications

Griet Monteyne and Gerd Vandersteen
 Vrije Universiteit Brussel, Department of Electrical Measurement (ELEC)
 Pleinlaan 2, 1050 Brussels, Belgium
 E-mail: griet.monteyne@vub.ac.be

1 Introduction

This work is related to geothermal heat pumps for central heating and/or cooling using geothermal energy. This is one of the most recommendable methods for heating buildings via so called green energy.

Current controllers don't explicitly take the dynamic behavior of the source-side (the so-called borefields in the ground) into account. The object of this work is to model the thermal dynamic behavior of the surrounding geology. This model can then be used to develop an optimal control strategy that also prevents the exhaustion of the heat from the soil on short and long term.

2 Problem formulation

It is not straightforward to model the thermal dynamic behavior of the surrounding geology. The system dynamics of a ground coupled heat pump is characterized by very diverse time constants. It is important that both the fast and the slow dynamic behavior of the soil are well modeled.

The conductive heat transport between the soil and the fluid is characterized by small time constants (with an order of magnitude of several minutes). On the other hand, the thermal diffusion in the soil is characterized by large time constants (with an order of magnitude of years). An additional problem is that diffusion phenomena can only be approximately described by a rational form in the s -domain (with s the Laplace variable). In order to get more accurate results, rational models in the \sqrt{s} -domain have to be used to model the diffusion properties of the thermal behavior [1].

First a rational model in the \sqrt{s} domain will be fit on simulated data. We will start with the simulation of a very simple heat diffusion problem, namely the heat transfer in a beam. This problem is selected since it can be solved analytically when certain boundary conditions are fulfilled. Thus, the model can be compared with the theoretical solution.

Once the \sqrt{s} model based on the simulated data is satisfactory, temperature measurements will be performed on a heated metal beam. Again a \sqrt{s} model will be verified.

Once this academic problem is fully understood, the analysis of simulated data of the more complicated problem is started, namely the thermal dynamic behavior of the geology that surrounds the heat pump.

The object is to fit a model on the simulated data that can be split into two parts. The first part describes the heat conduction and the second part describes the thermal diffusion.

The conductive part of the problem is characterized by the thermal resistances and capacitances of the materials that assure the heat transfer from the surrounding ground to the water in the borehole. This results in a rational form in the Laplace domain. By limiting the possible solutions for the rational model in the Laplace domain, we want to fit a model that can be interpreted as a combination of resistors and capacitors.

Afterwards, the thermal diffusion will be described by a rational form in the \sqrt{s} -domain.

There are more challenges to be faced. Only a limited amount of measured quantities are easily accessible for the user. The measurement time is limited as well as the possible excitations. Several other identification problems have to be considered, for example, MIMO identification of the thermal diffusion in multiple borefield installations, dealing with missing data, ...

Finally the model will be validated by use of measurements on an operational thermal installation.

3 References

- [1] Rik Pintelon, Johan Schoukens, Laurence Pauwels and Els Van Gheem, "Diffusion Systems: Stability, Modeling and Identification," IEEE Transaction on Instrumentation and Measurement, Vol. 54, No.5, October 2005.
- [2] C. Verhelst, G. Vandersteen, J. Schoukens and L. Helsen, "A linear dynamic borehole model for use in Model based Predictive Control", International Conference on Energy Storage, Effstock 2009, Stockholm, June 2009.

Systems & Control in Electron Microscopy

Arturo Tejada Ruiz
 DCSC - Delft University of Technology
 Mekelweg 2, 2628 CD Delft
 The Netherlands
 a.tejadaruiz@tudelft.nl

1 Abstract

Transmission electron microscopes (TEM) are indispensable tools for research in material science, nanotechnology and biology. Thus, it is expected that in the near future there will be high commercial demand for TEMs that can perform high-throughput, unsupervised measurements in the nano-scale. The development of such tools will certainly benefit from the methods offered by systems and control (S&C) theory. The latter, besides its obvious potential contribution to automation, will also play an important role in developing an analysis framework from which many of the un-explained TEM processes (e.g., sample drift) can be studied. This presentation summarizes several such potential contributions, some of which constitute interesting theoretical problems on their own.

2 Systems & Control in Electron Microscopy

The ideas presented here stem from the current work at the CONDOR project. This project, is a concerted effort between (among others) FEI Company, TU Delft, and the Embedded Systems Institute to automate scanning transmission electron microscopes. One of the projects mayor challenges consists of regulating the parameters of the microscopes optical transfer function. This is currently done through 'auto tuning' algorithms, which generally consist of the following steps: (i) acquire images; (ii) estimate a 'quality factor' from the images; (iii) using a look-up table, find the values of the microscope's 'control knobs' that will shift the quality factor towards a desired value; (iv) repeat as needed.

These algorithms work reasonably well in several situations. However, they do not provide information about the underlying processes in the microscope (since they are model-free), they cannot enforce strict timing requirements, and they cannot be compared systematically.

S&C theory can contribute to alleviate these problems by providing a framework to analyze the microscope behavior. Thus, this talk will emphasize the following topics:

- An integrated control-oriented TEM view [1].
- Methods for measuring optical aberrations (i.e., aberration sensors), with known dynamics and error bounds.

Emphasis will be placed in the latter topic. Measuring optical aberrations from images will be treated as a system identification problem: Images are the two-dimensional output signals of a two-dimensional Wiener system, whose input is the two-dimensional potential function of a specimen. The main research question is: Given input output data, how does one identify a two-dimensional Wiener model? In terms of TEM images, the following questions are of interest:

- The linear portion of the microscope's two-dimensional Wiener model, the so-called optical transfer function, is an infinite-dimensional linear system. Thus, is it possible to derive finite-dimensional approximations for this transfer function, with known approximation errors?
- If an identification experiment is performed and used to fit the approximate finite-dimensional model, how much error is introduced in the identified parameters (which are what one really wants to measure)?
- Is it possible to perform system identification with the limited type of known inputs available to microscopists (e.g. crystals)?

Since this is a new and ongoing research effort, the presentation will emphasize the set up of the system identification approach, and the practical limitations imposed by the microscopes to identification experiments.

Acknowledgements

This research was sponsored by the Condor project at FEI company, under the responsibilities of the Embedded Systems Institute (ESI). This project is partially supported by the Dutch Ministry of Economic Affairs under the BSIK program.

References

- [1] A. Tejada, W. Van den Broek, S.W. van der Hoeven and A.J. den Dekker, "Towards STEM Control: Modeling Framework and Development of a Sensor for Defocus Control," *Proc. Joint 48th IEEE Conference on Decision and Control and 28th Chinese Control Conference* Shanghai, P.R. China, 2009, pp. 8310-8315.

Identification and control of a binary distillation column in view of PLC based control

Bart Huyck, Jos De Brabanter

KaHo Sint Lieven - Department Industrieel Ingenieur

Email: bart.huyck@kahosl.be jos.debrabanter@kahosl.be

Filip Logist, Jan Van Impe

K.U.Leuven - Department of Chemical Engineering (CIT)

Email: filip.logist@cit.kuleuven.be jan.vanimpe@cit.kuleuven.be

Bart De Moor

K.U.Leuven - Department of Electrical Engineering (ESAT - SCD)

Email: bart.demoor@esat.kuleuven.be

1 Introduction

In a world where economic and environmental issues have increasing importance, efficient control systems have become indispensable. When dealing with complex processes, Model Predictive Control (MPC) is one of the possible control strategies [1]. In practice, current linear and non-linear MPC algorithms are most often implemented on powerful computers. However, since Programmable Logic Controllers (PLCs) with less computational power are used a lot in industry, it is interesting to explore the possibilities and limitations of these devices for MPC. For this purpose, a 6 m high pilot scale binary distillation column, is selected as an industrial test example with multiple inputs and outputs.

2 Experimental set-up

In the distillation set-up, four variables can be manipulated (MV): the reboiler duty, the duty of the feed heater and the reflux and feed flow rate. The controlled variables (CV) of the system are the temperatures in the reboiler and at the top of the column. Only these variables are employed for the control of the column as they are strongly related to the quality of the final products. Other measurements are available, but are currently omitted for control.

3 Results

To create a model of the distillation column, system identification is performed [2]. A Pseudo Random Binary excitation signal is applied simultaneously to the four MVs. From former experiments [4], it is known that the dynamics of the system are faster at the top of the column. Therefore, the signal is slightly faster at the top. As distillation columns consist of low order systems, the selected models to be fitted, are first and second order continuous-time transfer functions with time delay. For both the reboiler and bottom temperature, a MISO model is identified and combined into

one MIMO model. Model validation on a different dataset demonstrates that the MISO model describing the reboiler temperature captures the dynamics of the system excellently, while the MISO model for the top temperature has difficulties following the fast temperature variations. Nevertheless the global MIMO model describes all main trends well and, hence, it is implemented in an MPC controller taken from the Matlab Model Predictive Control Toolbox [3]. As a first step towards control on PLCs, this MPC controller is tested while running on a PC. Simulation tests, as well as experiments on the pilot scale set-up have proven that the controller accurately deals with desired setpoint changes without violating constraints.

4 Conclusion

A linear model has been created for a binary distillation column. The model has been validated and employed in an MPC. This controller has proven to be successful in simulation and on the real set-up. Further research will now focus on the translation of the current model predictive control approaches to low level industry standard hardware.

5 Acknowledgements

Work supported in part by Projects OT/09/025/TBA, EF/05/006 (Center-of-Excellence Optimization in Engineering) and IOF-SCORES4CHEM of the Research Council of the Katholieke Universiteit Leuven. J. Van Impe holds the chair Safety Engineering sponsored by the Belgian chemistry and life sciences federation essenscia.

References

- [1] S. J. Qin and T. A. Badgwell. "A survey of industrial model predictive control technology," *Contr Eng Pract*, 11:733764, 2003.
- [2] L. Ljung. *System Identification: Theory for the User*, Second Edition. Prentice Hall, Upper Saddle River, New Jersey, 1999.
- [3] A. Bemporad, M. Morari and N. L. Ricker. *Model Predictive Control Toolbox 3 Users Guide*. The MathWorks, Inc, Natick, 2009.
- [4] F. Logist, B. Huyck, M. Fabre, M. Verwerft, B. Plumeyers, J. De Brabanter, B. De Moor and J. Van Impe. "Identification and control of a pilot scale binary distillation column." *Proc. ECC 09*, p. 4659-4664, 2009.

Fast Oriented Bounding Box Computation Using Particle Swarm Optimization

P. Borckmans

Department of Mathematical Engineering
 Université catholique de Louvain
 pierre.borckmans@uclouvain.be

P.-A. Absil

Department of Mathematical Engineering
 Université catholique de Louvain
 absil@inma.ucl.ac.be

Overview

The problem of finding the optimal oriented bounding box (OBB) for a given set of points in \mathbb{R}^3 , yet simple to state, is computationally challenging. This question arises in many practical applications and notably in vision problems, like collision detection. Existing state-of-the-art methods dealing with this problem are either exact but slow [1], or fast but very approximative and unreliable [2]. We propose a method based on Particle Swarm Optimization (PSO) to approximate solutions both effectively and accurately. The original PSO algorithm is modified so as to search for optimal solutions over the rotation group $SO(3)$. Particles are defined as 3D rotation matrices and operations are expressed over $SO(3)$ using matrix products, exponentials and logarithms. The symmetry of the problem is also exploited. Numerical experiments show that the proposed algorithm outperforms existing methods, often by far. This preliminary experiment indicates that, while being a stochastic method, PSO shows to be both efficient and relatively reliable to solve the OBB problem. Furthermore, this application is encouraging the development of PSO over different search spaces and manifolds.

Description of the method

The idea presented in this article is to exploit a reformulation of the OBB problem as an optimization over the rotation group $SO(3)$ [3]. Finding the minimal volume oriented bounding box can be expressed as follows :

$$\min_{\substack{R \in \mathbb{R}^{3 \times 3} \\ \det(R)=1 \\ R^T R=I}} f(R) = V_{\text{AABB}}(RX) \\ = (x'_{\max} - x'_{\min})(y'_{\max} - y'_{\min})(z'_{\max} - z'_{\min})$$

where $R \in SO(3)$ is the rotation matrix, $X \in \mathbb{R}^{3 \times n}$ denotes the set of points and V_{AABB} is the volume of the so-called axis-aligned bounding box (AABB). For given R and X , the volume of the AABB is simply obtained by rotating the set of points X by R : $X' = RX = (x', y', z')$ and computing the product of the span along each rotated direction. As can be observed with a 2D example, the function $f(R)$ is only C^0 and presents multiple minima. The non-differentiable and multimodal aspects of $f(R)$ make it a good candidate for PSO.

PSO is a stochastic population-based algorithm. The driving force of the optimization process is given by the following update equations (iterated over k), for each particle (indexed by i) :

$$\begin{cases} v_i^{k+1} = \underbrace{w^k v_i^k}_{\text{inertia}} + \underbrace{c \alpha_i^k (x_i^k - y_i^k)}_{\text{nostalgia}} + \underbrace{s \beta_i^k (x_i^k - \hat{y}^k)}_{\text{social}} \\ x_i^{k+1} = x_i^k + v_i^{k+1}, \end{cases}$$

where x denotes position, v denotes velocity, y is the personal best position, \hat{y} is the global best position of the swarm.

In its original form, PSO is described for particles distributed in \mathbb{R}^n so that $x \in \mathbb{R}^n$, $y \in \mathbb{R}^n$ and that the operations involved in the update equations (+, -, .) are the usual vectorial addition, difference and scaling. In this work, we show how to adapt standard PSO to the $SO(3)$ search space, using concepts of differential geometry. Note that the key idea behind PSO is preserved with this adaptation: the new rotation is built using a stochastically weighted combination of the old rotation (with inertia) and attraction towards both personal and global best rotations. Preliminary results can be found in [4].

References

- [1] Joseph O'Rourke. Finding minimal enclosing boxes. *Internat. J. Comput. Inform. Sci.*, 14:183–199, June 1985.
- [2] Darko Dimitrov, Christian Knauer, Klaus Kriegel, and Gunter Rote. Bounds on the Quality of the PCA Bounding Boxes. *Computational Geometry*, 42(8):772 – 789, 2009. Special Issue on the 23rd European Workshop on Computational Geometry.
- [3] Chia-Tche Chang, Bastien Gorissen, and Samuel Melchior. Fast Computation of the Minimal Oriented Bounding Box on the Rotation Group $SO(3)$, 2009. Submitted.
- [4] Pierre Borckmans and Pierre-Antoine Absil. Fast Oriented Bounding Box Computation Using Particle Swarm Optimization. Technical Report UCL-INMA-2009.082, Université catholique de Louvain, Department of Mathematical Engineering, 2009.

Swarm Intelligence for Traffic Control

Zhe Cong, Bart De Schutter, Robert Babuška

Delft Center for Systems and Control

Delft University of Technology

Delft, The Netherlands

Email: {z.cong,b.deschutter,r.babuska}@tudelft.nl

1 Introduction

With the rapid growth of human population and jobs distributed unevenly in different locations, daily commuting between cities is required more than ever, which has created a huge socio-economic issue: traffic congestion. Several measures have been put into practice to solve this problem, such as improving junctions and adding separate lanes for public transportation. However, these methods just relieve the burden of the traffic system temporarily rather than aiming for a long-term solution.

We focus on swarm intelligence for traffic management, which is expected to yield excellent performance in traffic flow optimization. *Swarm Intelligence* is an artificial intelligence method based on the collective behavior of decentralized, self-organized systems and its main goal is to use the simple behavior and local interactions between the agents and their environment, to obtain the desired complex global behavior. We will use it to optimize various traffic control measures (in particular route guidance).

2 Method

For this purpose, the Ant Colony Optimization (ACO) algorithm is introduced and extended. The basic ACO algorithm is inspired by ants and their behavior of finding shortest paths from their nest to sources of food by interacting with their local environment. The ants initially search for food in a random fashion, but when they have found some, they return home while depositing chemicals called pheromones. These pheromones attract other ants to follow the same path, and they in turn also deposit pheromones on their way back. The stronger the pheromones are, the more ants are attracted. Over time, this behavior leads to the emergence of paths that can be shown to be near-optimal.

In ACO the combinatorial optimization problem is represented as a construction graph consisting of a set of vertices and a set of edges connecting the vertices. A solution is a concatenation of components, which are pairs of a vertex and an edge, and form a path from the initial vertices to the final vertices. The algorithm starts with the initialization of M ants at their own origin nodes where they begin their journey to the destination. At each iteration, each ant will have to decide to take which edge to take next edge

based on the pheromone levels. In addition, there is also an option for exploration with a certain probability. After an ant reaches its destination, the ant then retraces its steps depositing pheromone on the edges chosen, and obviously the pheromones deposited should be proportional to the inverse of the cost as we want to minimize the cost.

When applying ACO in a traffic context several changes have to be made. First of all, for traffic we want to steer the system towards the system optimum, whereas the ants in ACO typically look for a user optimum. In fact, in traffic each driver will choose the route that at that moment benefits him most, based on the information he has. However, the drivers do not consider the impact their actions will have in the traffic network. Sometimes the shortest route may become less effective because every driver is inclined to choose it, causing a traffic jam. Hence, we will take into account the number of ants/drivers already traveling on a route and add a penalty on this number. Moreover, we should also take the dynamic nature of the traffic process into account. This will be done by incorporating a dynamic traffic flow model into the ACO algorithm. Finally, several types of costs should be considered, such as travel time, fuel consumption, emissions, and so on. Total cost is then the weighted sum of these individual costs. Through minimizing total cost, we can find the optimal routing which benefits both the network and the drivers.

3 Expected result

We will test the algorithm for a wide variety of set-ups, traffic scenarios, traffic control measures, and cost functions. We expect that this new ACO algorithm for traffic management will result in an efficient and — due to its inherent parallelism - scalable approach that will provide a significant improvement in the performance of the traffic system.

References

- [1] D. Alves. Ant dispersion routing for traffic optimization. Master's thesis, Delft University of Technology, Delft, The Netherlands, 2009.
- [2] J. van Ast, R. Babuška, and B. De Schutter. Ant colony optimization for optimal control. In *Proceedings of the 2008 IEEE Congress on Evolutionary Computation (CEC 2008)*, pages 2040–2046, Hong Kong, June 2008.

Model-Free Feedforward Control of Inkjet Printhead¹

Mohamed Ezzeldin, Andrej Jokic and Paul van den Bosch

Department of Electrical Engineering

Technische Universiteit Eindhoven

P.O. Box 513, 5600 MB Eindhoven

The Netherlands

Email: m.ezz,a.jokic and p.p.j.v.d.bosch@tue.nl

1 Introduction

Inkjet printers are non-impact printers which print text and images by spraying tiny droplets of liquid ink onto paper. Besides the well known small inkjet printers for home and office, there is a market for professional inkjet printers. Inkjet printers are used to form conductive traces for circuits, and color filters in LCD and plasma displays. That makes the printing quality is an important issue. Currently, most inkjet printers use either thermal inkjet or piezoelectric inkjet technology. Most commercial and industrial inkjet printers use a piezoelectric material in an ink-filled chamber behind each nozzle instead of a heating element. When a voltage is applied, the piezoelectric material changes shape or size, which generates a pressure pulse in the fluid forcing a droplet of ink from the nozzle. In my project the piezoelectric inkjet printer is considered.

2 Problem Statement

After a drop is jetted, the fluid-mechanics within an ink channel are not at rest immediately: apparently traveling pressure waves are still present. These are referred to as residual vibrations. These residual vibrations result in changing the speed of the subsequent drops. That is due to the fact that the initial meniscus positions of the subsequent drops are different than the initial meniscus position of the first drop. Usually the fixed actuation pulse is designed under the assumption that all the drops have the same initial meniscus position. To guarantee consistent drop properties, one has to wait for these residual vibrations to be sufficiently damped out to fulfill this assumption. Cross-talk is the phenomenon that one ink channel cannot be actuated without affecting the fluid-mechanics of the neighboring channels. The cross-talk happens due to the fact that the pressure waves within one channel influence other channels. Residual vibrations and cross-talk result in ink drops with different speed and volume which affect the printing quality. The main goal is to improve the printing quality of the printhead that is achieved by keeping both the speed and volume of the ink-drop constant.

¹This work has been carried out as part of the OCTOPUS project with Océ Technologies B.V. under the responsibility of the Embedded Systems Institute. This project is partially supported by the Netherlands Ministry of Economic Affairs under the Bsik program.

3 Model-Free Optimization

Since there are no online measurements for the system variables, a feedforward controller is the only appropriate solution. Optimization of process performance has received attention recently because it represents the natural choice for reducing production costs, improving product quality, and meeting safety requirements and environmental regulations. Process optimization is typically based on a process model that is used by a numerical procedure for computing the optimal solution. In practical situations, however, an accurate process model can rarely be found with affordable effort. Uncertainty results primarily from trying to fit a model of limited complexity to a complex process system [1] and [2]. In this paper, we propose a new input pulse, that consists of two pulses an actuation pulse and quenching pulse. The actuation part is used to formulate and jet the drop while the quenching part is used to dampen the residual vibrations. A lot of efforts have been done to produce a good model for the ink channel [3] and [4], however this model is still incomplete and fails to predict the meniscus position of the drops. In our approach the optimization is carried out on the real set-up instead of using a printhead model. A high speed camera is used to obtain the time history of the drops traveling from the nozzle plate to the paper. An image processing technique is developed to obtain the actual speed of each drop. An optimization technique is used to get the optimal actuation pulse parameters by minimizing the error between the actual drop-speed and a desired reference drop-speed.

References

- [1] D. Bonvin, "Optimal operation of batch reactors-A personal view", *Journal of Process Control*, vol. 8, 1998, pp 355-368.
- [2] J.F. Forbes and T. E. Marlin, "Model accuracy for economic optimizing controllers: The bias update case", *Industrial and Engineering Chemistry Research*, vol. 33, 1994, pp 1919-1929.
- [3] H.M.A. Wijshoff, "Structure- and fluid-dynamics in piezo inkjet printheads," PhD thesis, 2008.
- [4] M. B. Groot Wassink, "Inkjet printhead performance enhancement by feedforward input design based on two-port modeling," PhD thesis, 2007.

Tensor- versus matrix-based algorithms in exponential data fitting

Mariya Ishteva, P.-A. Absil
 Dept. of Mathematical Engineering
 Université catholique de Louvain
 Bâtiment Euler - P13, Av. Georges Lemaître 4
 1348 Louvain-la-Neuve
 Belgium
 Email: mariya.ishteva@uclouvain.be,
<http://www.inma.ucl.ac.be/~absil>

Sabine Van Huffel, Lieven De Lathauwer*
 Dept. of Electrical Engineering ESAT/SCD
 K.U.Leuven
 *and Group Science, Engineering and Technology
 K.U.Leuven Campus Kortrijk
 Belgium
 Email: sabine.vanhuffel@esat.kuleuven.be,
 lieven.delathauwer@kuleuven-kortrijk.be

1 Introduction

The exponentially damped sinusoidal (EDS) model [5] is a simple and widely used model in signal processing applications, including magnetic resonance spectroscopy, magnetic resonance spectroscopic imaging, electroencephalography and audio processing. The exponential data fitting problem consists of estimating the parameters of the EDS model, given a number of samples.

Matrix-based methods for the estimation of the unknown parameters are well-known. Algorithms for the single-channel, multi-channel, and decimative case based on higher-order tensors have also been proposed in the literature. Higher-order tensors are generalizations of vectors (first order tensors) and matrices (second order tensors).

We consider in particular the multi-channel case. A set of signals with identical poles but different complex amplitudes is assumed. The goal is to estimate the poles of the model, i.e., the frequencies and the damping factors, from given samples. We define the problem formally and briefly recall the tensor algorithm proposed in [4].

2 Low multilinear rank approximation of tensors

The best low multilinear rank approximation of tensors is essential for the algorithm [4]. The multilinear rank of a tensor is a direct generalization of column and row rank of a matrix. In this sense, a tensor can be approximated by a tensor having multilinear rank bounded by given numbers. These numbers are related to the model order and to the number of channels.

The computation of the best low multilinear rank approximation of tensors is not as straightforward as in the matrix case. Truncation of a higher-order singular value decomposition leads to a good but suboptimal approximation. A traditional algorithm for further improvement is the higher-order orthogonal iteration [1]. For alternative algorithms see [3] and the references therein.

3 Result

We compare the performance of the tensor-based [4] and its corresponding matrix-based method [6] for the case of closely spaced poles. This problem is more difficult than the case where the poles are well separated. The goal is to find factors indicating in which cases it is better to use the tensor-based instead of the matrix-based method. We present simulations revealing that when the matrix containing the amplitudes of the model is ill-conditioned, reducing the mode-3 rank in the low multilinear rank approximation of the involved tensor improves the performance of the tensor method. As a result it outperforms the matrix-based method, see also [2].

Acknowledgments

Research supported by: (1) the Belgian Federal Science Policy Office: IUAP P6/04 (DYSCO, “Dynamical systems, control and optimization”, 2007–2011), (2) Communauté française de Belgique - Actions de Recherche Concertées, (3) Research Council K.U.Leuven: GOA-AMBioRICS, GOA-MaNet, CoE EF/05/006 Optimization in Engineering (OPTEC), (4) F.W.O. project G.0321.06, “Numerical tensor methods for spectral analysis”. (5) “Impulsfinanciering Campus Kortrijk (2007-2012)(CIF1)” and STRT1/08/023.

References

- [1] L. De Lathauwer, B. De Moor, J. Vandewalle. On the best rank-1 and rank- (R_1, R_2, \dots, R_N) approximation of higher-order tensors. *SIAM J. Matrix Anal. Appl.*, 21(4):1324–1342, 2000.
- [2] M. Ishteva, L. De Lathauwer, S. Van Huffel. Comparison of the performance of matrix and tensor based multi-channel harmonic analysis. In *7th Int. Conf. on Mathematics in Signal Processing, Cirencester, UK*, pp. 77–80, 2006.
- [3] M. Ishteva. *Numerical methods for the best low multilinear rank approximation of higher-order tensors*. PhD thesis, Dept. of Electrical Engineering, K.U.Leuven, December 2009.
- [4] J.-M. Papy, L. De Lathauwer, S. Van Huffel. Exponential data fitting using multilinear algebra: The single-channel and the multi-channel case. *Numer. Linear Algebra Appl.*, 12(8):809–826, 2005.
- [5] P. Stoica, R. Moses. *Spectral Analysis of Signals*. Pearson, Prentice Hall, 2005.
- [6] L. Vanhamme, S. Van Huffel. Multichannel quantification of biomedical magnetic resonance spectroscopy signals. *Proc. of SPIE, Advanced Signal Processing Algorithms, Architectures, and Implementations VIII*, vol. 3461, pp. 237–248, San Diego, 1998.

Optimization of jacketed tubular reactors for the production of low-density polyethylene: conceptual approach

Peter M.M. Van Erdeghem*, Filip Logist*, Christoph Dittrich** and Jan F. Van Impe*

* BioTeC - Department of Chemical Engineering, K.U. Leuven
W. de Croylaan 46, B-3001 Leuven, Belgium

Email: {peter.vanerdeghem, filip.logist, jan.vanimpe}@cit.kuleuven.be

** SABIC Technology Center Geleen,
P.O. Box 319, 6160 AH Geleen, The Netherlands

1 Introduction

Polyethylene is without any doubt the most widespread polymer worldwide. Its annual production is estimated at 80 million tonnes and low-density polyethylene (LDPE) represents about 30 % of the total volume. Nowadays high-pressure tubular reactors stand for 60 % of the total production of LDPE. These reactors consist of a spiral wrapped metallic pipe with a large length to diameter ratio. The polymerization of ethylene is carried out under extreme conditions, e.g., at very high pressures (2000 to 3000 bar) and at a temperature level of 400 to 600 K due to the exothermicity of the free-radical polymerization reaction. The heat of reaction is partially removed through the reactor wall by a cooling system in the jacket around the tube. The ethylene conversion is known to be in the order of 25-35 %.

2 Approach

Setting up a well-defined model based optimization problem of an industrial application is not always as straightforward as it seems. Often researchers seek the shortest way to reach their final goal by going directly to the development of a high-complexity model and optimize this with respect to a certain objective ([1, 2]). Although this approach seems the fastest way to success, it can be a bumpy road with a lot of dead ends (dashed arrow in Figure 1). Due to the high complexity of the model convergence is not ensured, good ini-

tialization is required and calculation time increases rapidly. Hence, for this research project a sustainable strategy of *divide and conquer* is adopted, i.e., first develop a conceptual (low-complexity) model, set up the (multiple objective) optimization problem and later on use the obtained knowledge during the optimization of more complex models.

3 Results

First, this multizone process is modelled as a sequence of conceptual modules which simulate the steady-state characteristics of one reaction and cooling zone. A 1-peak module is composed out of the mass balance of the monomer and initiator and the energy balance along the length of the reactor. Then, this model is fitted to industrial data such that it quantitatively describes the real process. Finally, a multiple objective design optimization problem is formulated, i.e., where along the reactor does initiator have to be injected and in which amount in order to maximize the profit for different economic situations.

4 Acknowledgments

Work supported in part by SABIC (The Netherlands) and Projects OT/09/025/TBA and EF/05/006 (Center-of-Excellence Optimization in Engineering) of the Research Council of the Katholieke Universiteit Leuven, Project 3E090616 (SCORES4CHEM) of the Industrial Research Council of the Katholieke Universiteit Leuven, and the Belgian Program on Interuniversity Poles of Attraction, initiated by the Belgian Federal Science Policy Office. J. Van Impe holds the chair Safety Engineering sponsored by the Belgian chemistry and life sciences federation *essenscia*. The scientific responsibility is assumed by its authors.

References

- [1] M. Astasuain, S.M. Tonelli, A. Brandolin, and J.A. Bandoni. Dynamic simulation and optimisation of tubular polymerisation reactors in gPROMS. *Computers and Chemical Engineering*, 25:509–515, 2001.
- [2] F.Z. Yao, A. Lohi, S.R. Upreti, and R. Dhib. Modeling, simulation and optimal control of ethylene polymerization in non-isothermal, high-pressure tubular reactors. *International Journal of Chemical Reactor Engineering*, 2(2), 2004.

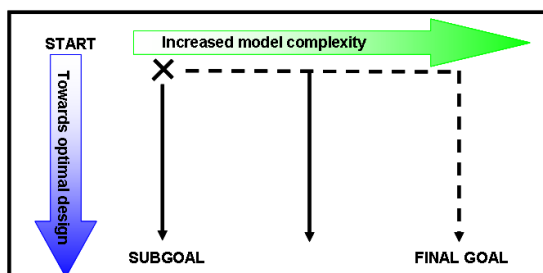


Figure 1: Divide and conquer strategy.

Modelling thermo-acoustic combustion instability with the flame as a parameter

Maarten Hoeijmakers*, Viktor Kornilov, Ines Lopez Arteaga, Philip de Goey, and Henk Nijmeijer

Department of Mechanical Engineering

Eindhoven University of Technology

P.O. Box 513

5600 MB Eindhoven, The Netherlands

Email: *p.g.m.hoeijmakers@tue.nl

1 Introduction

Many combustion devices are highly susceptible to acoustic instability of combustion. This problem is especially pronounced under premixed fuel lean operation, widely used in this kind of systems due to the lower thermal NO_x emissions. Typical examples include domestic boilers and gas turbines.

Thermo-acoustic combustion instabilities usually manifest themselves by the generation of acoustic tone(s) within a combustion system. Such instabilities consist of a feedback loop between acoustic waves and the unsteady flame heat release rate. In most cases the instability is an undesirable effect which is difficult to foresee during the design process and to eliminate in the development stage. Accordingly, the development of methods to predict, prevent or actively control such oscillations is an actual and practically relevant problem [1].

Due to the very nature of the phenomenon both the acoustics of the combustor and the thermo-acoustics of the flame/burner are important. The main focus of the present research is to model, and experimentally verify, the stability of the system as a function of the flame behaviour.

2 Modelling approach

In many practical situations combustor systems consist of assemblies of ducts, vessels, and burners. The transverse dimensions are usually sufficiently small to assume that acoustic waves are longitudinal. Then, one can describe the combustor acoustics using the approach of acoustic network modelling. Within this approach the combustion system can be represented as a network of elements such as tubes, area jumps, flame, open and closed ends, etc. Each of the elements can be represented by a frequency dependent transfer matrix which links the output fluctuating pressure and velocity p'_{out}, u'_{out} to the input pressure and velocity p'_{in}, u'_{in} :

$$\begin{bmatrix} p' \\ u' \end{bmatrix}_{out} = \begin{bmatrix} M_{11}(s) & M_{12}(s) \\ M_{21}(s) & M_{22}(s) \end{bmatrix} \begin{bmatrix} p' \\ u' \end{bmatrix}_{in}$$

For many simple acoustic elements the analytical expressions for the transfer matrices (TM) are known. For the

flame/burner the TM can be expressed in terms of the flame thermo-acoustic transfer function (TF). The flame TF describes the response of the flame heat release to velocity excitations in terms of a frequency dependent gain and phase.

The complete network model of a system can be found by combining the TM's of all elements. Such a set of homogeneous equations has a non-trivial solution if the determinant of the system matrix is equal to zero. This condition allows determining the set of unstable and stable eigen-values (frequencies) of the acoustic system.

To prevent thermo-acoustic instabilities in the design stage two closely related strategies can be considered. One can either try to find an optimal geometry, or one may select a burner which, once installed in a given combustor, provides stable operation. In the current research we are only interested in the second option. Thus, we regard the flame as a parameter and calculate all possible eigen-frequencies in a certain gain and phase range. The result is a complete overview of all possible unstable and stable modes in a combustor for a wide range of practical flames.

3 Results

The analysis is done for a simple combustion system consisting of a gas feed pipe, area change, flame, and an exhaust duct. Experiments on such a set-up are used to verify our results. Comparison of simulation and experiment indicates that the model gives a conservative estimate of stability. The results are valuable in the design stage, i.e. the formulation of criteria which a certain burner should satisfy to prevent instability. On the other hand, the results suggest that the flame can be used as an element to actively suppress instabilities by modifying the flame behaviour (i.e. by an electric field). This also opens possibilities for active control by using the flame as an actuator.

References

- [1] S. Candel, Combustion dynamics and control: Progress and challenges, Proceedings of the Combustion Institute, 2002, 29, 1 - 28

Design of Feedback controllers and Topography Estimator for Dual Actuated Atomic Force Microscopy

Stefan Kuiper^{1,*}, A. Kunnappillil Madhusudhanan¹, Paul M.J. Van den Hof¹, Georg Schitter^{1,2}

¹Delft Center for Systems and Control, ²Precision and Microsystems Engineering
Delft University of Technology

*Corresponding author, email: stefan.kuiper@tudelft.nl

1 Introduction

Atomic Force Microscopy (AFM) is an important tool in nanotechnology, providing sample topography images with molecular resolution by probing the sample with a very sharp tip [1]. One major drawback of AFM, however, is its relatively low imaging speed which makes it impossible to capture dynamic processes on a molecular scale. The goal of this research is to increase the imaging speed of AFM systems by using modern control techniques and improving the overall mechatronic design of these instruments.

2 Dual actuation

One major limitation on the imaging speed of AFM is the bandwidth of the feedback loop controlling the force variations between the tip and the sample. This feedback bandwidth is strongly determined by the dynamics of the piezo actuators which position the sample in vertical direction. Designing these actuators for faster actuation often comes at the price of a reduction in positioning range. In most cases, however, the full positioning range is needed for the slow varying topography changes only. A significant increase in positioning bandwidth can therefore be achieved by combining a relatively slow, long-stroke actuator with a faster, short-stroke actuator to obtain a dual actuated system [2].

3 Problem description

This contribution focusses on controlling the imaging force and estimating the sample topography in dual actuated AFM. Special emphasis is given on providing an optimal trade off between the long-stroke and the short-stroke actuator and to prevent both feedback loops from competing with each other. In order to provide an estimate of the sample topography using the available control signals, a filter has to be designed which captures the system dynamics [3, 4]. As the dynamics of the actuators are slightly different each time the system is setup, the designed feedback controllers and topography estimator should be robust for the variations in the system dynamics.

4 Results

Dual actuation for faster imaging is demonstrated on a modified commercially available AFM setup (Veeco, Santa Barbara, CA, USA). The long-range positioning of the sample is hereby provided by a piezoelectric tube scanner, while the AFM tip is actuated via a short range, high-bandwidth piezoelectric stack actuator mounted on the tip holder. The dynamics of the system have been identified multiple times with different measurement probes and samples, resulting in a model of the nominal system dynamics and a model of the dynamic uncertainty. Using these models, the topography estimator and feedback controllers are designed using μ -synthesis techniques, which guarantee robust performance of the system under the possible variations of the system dynamics. By varying the weights of the optimization, a direct trade-off between the guaranteed bound on the topography estimation error and the resulting control bandwidth is shown. The dual actuated AFM system demonstrates a significant increase in closed-loop bandwidth, and thus imaging speed, as compared to the conventional AFM system. AFM images are obtained at high speed demonstrating a significant reduction of the residual error and reduced variations of the imaging force.

Acknowledgment

This work is supported by TU Delft faculty grant PAL-614, by the Netherlands Organization for Scientific Research (NWO) under Innovational Research Incentives Scheme (VENI DOV.7835), and by the National Institutes of Health under Award R01 GM 065354.

References

- [1] G. Binnig, C.F. Quate, and C. Gerber, *Phys. rev. lett.*, vol. 56, pp. 930-933, 1986.
- [2] G. Schitter, W.F. Rijke, and N. Phan, *Proc. 47th IEEE Conf. Decis. Control*, pp. 5176-5181, 2008.
- [3] G. Schitter, P. Menold, H.F. Knapp, F. Allgower, and A. Stemmer, *Rev. Sci. Instrum.*, vol. 72, pp. 3320-3327, 2001.
- [4] S.M. Salapaka, T. De, and A. Sebastian, *Int. J. Robust Nonlin. Control*, vol. 15, pp. 821-838, 2005.

Data-driven control for the next generation of wind turbines

Gijs van der Veen

G.J.vanderVeen@tudelft.nl

Jan-Willem van Wingerden

J.W.vanWingerden@tudelft.nl

Michel Verhaegen

M.Verhaegen@tudelft.nl

Delft Center for Systems and Control, Delft University of Technology, Delft

Abstract

Two important trends in the wind energy industry are to increase power by increasing rotor diameters to sizes in excess of 140 metres and to move towards off-shore locations. Both these developments bring new challenges with them. Increased rotor sizes call for control systems that are able to handle mechanical loads more adequately and off-shore wind turbines require an even higher reliability than that expected from on-shore generators, with required operational lives of over 20 years.

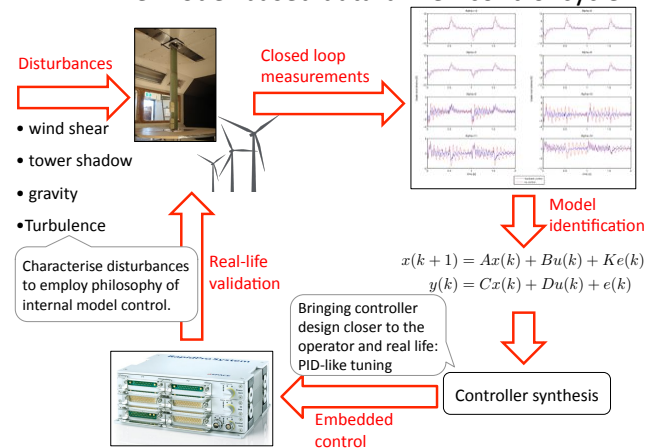
In this PhD research, sponsored by Vestas Wind Systems, several lines of research will be extended to develop control solutions for the next generation of wind turbines. The first main research item is to develop system identification tools suited to wind energy applications. The second part focusses on control methods that use these identified models. Current practice is often to use first-principles models for the design control of systems, while the commissioning of the production turbine often requires a complete re-tuning of controllers and models due to differences between the model and the true system. Obtaining an identified model of the true system may avoid such non-trivial re-tuning.

Regarding the first part, the aim is to develop methods that are especially suited for the identification of wind turbine dynamics. For state-of-the-art turbines this concerns the assembly of rotor-generator together with the blade pitching system. For future turbines, this may include the dynamics of “smart” rotor blades with trailing edge flaps [?]. In these cases of obtaining a model from data, disturbances play an important role since these are to a large extent periodic and non-stochastic in nature. This calls for an extension of existing methods. To deal with disturbances that are periodic in nature, ideas similar to those in [?] are applied to subspace identification. Furthermore, a subspace identification method has been developed can deal with closed-loop systems. Another challenge lies in the fact that the dynamics of a wind turbine change with the operational conditions and therefore a linear time-varying approach may be necessary.

A wind turbine experiences significant dynamic loads, such as turbulence, gravity and wind shear. Due to the size of future rotors and the presence of stochastic and periodic disturbances over the entire lifespan of a turbine, fatigue is a critical issue to wind turbine life and reliability. Therefore,

reduction and alleviation of loads by means of advanced control is an enabling technology for future turbines. To allow industrial implementation of such control systems, it is important that these systems are intuitive, relatively simple and can be tuned in an insightful way. An interesting and intuitive option is the use of predictive control combined with system identification. Research in the past ten years has shown that the prohibitive computational burden traditionally associated with predictive control is not necessary by exploiting structure in the problem [?], allowing sample rates that are sufficiently high for wind energy applications. Additionally, fatigue in mechanical parts can be expressed in terms of signal variances. By taking this into account in the MPC objective, control actions can be optimised to reduce fatigue loads at locations where they are most critical, while taking into account signal constraints.

The model-based data-driven control cycle



References

- [1] J.W. van Wingerden, A.W. Hulskamp, T. Barlas, B. Marrant, G.A.M. van Kuik, D-P. Molenaar and M. Verhaegen, *On the proof of concept of a “Smart” wind turbine rotor blade for load alleviation*, Wind Energy, 2008.
- [2] G.E. van Baars, H. Mosterd and P.M.M. Bongers, *Extension to standard system identification of detailed dynamics of a flexible wind turbine system*, Proceedings of the 32nd IEEE Conference on Decision and Control, 1993.
- [3] Y. Wang and S.P. Boyd, *Fast Model Predictive Control Using Online Optimization*, IFAC World Congress, 2008.

Data-Driven Learning of Periodic Disturbances for Load Reduction

Ivo Houtzager, Jan-Willem van Wingerden, and Michel Verhaegen
 Delft Center for Systems and Control, Delft University of Technology
 Mekelweg 2, 2628 CD Delft, The Netherlands
 Email: I.Houtzager@TUDelft.nl

1 Introduction

The trend in offshore wind turbines is to increase the rotor diameter as much as possible to decrease the cost per kWh. The increasing dimensions have led to a relative increase of the loads on the wind turbine structure, thus it is necessary to react to disturbances in a more detailed way: each blade separately [1]. The load disturbances acting on an individual wind turbine blade are to a large extent deterministic, such as the tower shadow (see Figure 1), wind shear (see Figure 2), yawed error and gravity, and they depend on the rotation angle and speed. A repetitive controller can learn these periodic disturbances for fixed-speed wind turbines and variable-speed wind turbines operating above-rated. For relatively slow changing periodic disturbances it is expected that this control method can significantly reduce the vibrations in the wind turbine structure.

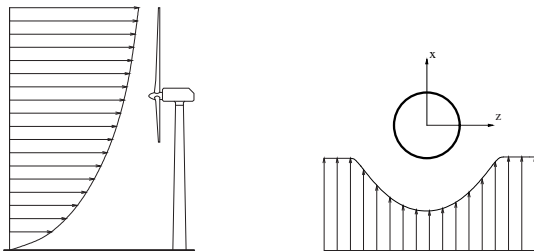


Figure 1: Wind shear effect Figure 2: Tower shadow effect

2 Repetitive Controller Design

The repetitive controller (RC) is designed by formulating a lifted MIMO output-feedback problem such that after a full rotation (trial) the input signals are updated to counteract the described periodic disturbances [2]. For the transition from trial-to-trial, a “lifted” model is derived based on the periodic time-varying state-space model of the system under study. Normally, a feedback controller is already designed to deal with the stability of the system. Therefore, the RC is designed “on top” of the closed-loop wind turbine system.

In simulation, the additional pitch input of the RC gives after a number of trials a considerable reduction in the amplitude. In Figure 3 the power spectral density of the first blade root moment is illustrated. The slicing of the wind by the rotating blades transforms the wind load spectrum seen by the rotating rotor by additional energy at rotor frequency

1P (once-per-revolution) and its multiples. The additional loads at 1P, 2P, and 3P frequencies are clearly visible in the response with only feedback control. Using RC these effects are totally gone.

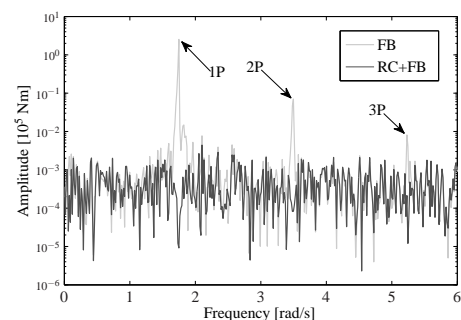


Figure 3: Power spectral density of the first blade root moment over 100 trials. The light grey line uses feedback control only, and the dark grey line with RC added.

3 Data-Driven Implementation

There are some additional challenges relating to the implementation of the RC algorithm, like the memory storage and realtime calculation of the large lifted matrices. Further, it is known that the performance of the RC strongly depends on the precise match between model and system to be controlled, and between the controller’s period and the actual period of the disturbance signal. With even a slight period or model mismatch, the performance of the controller can decrease substantially. As the wind turbine dynamics vary over time, due to the slowly changing environment, the model and period have therefore to be made adaptive. So, the goal is to implement a data-driven RC, which adapts itself to the changing dynamics, using the input and output data and recursive subspace identification techniques [3].

References

- [1] T. G. van Engelen. “Design model and load reduction assessment for multi-rotational mode individual pitch control”, In EWEC conference, 2006.
- [2] J. K. Rice and M. Verhaegen, “Repetitive learning control for stochastic LTV systems”, Submitted, 2009.
- [3] I. Houtzager, J. W. van Wingerden, and M. Verhaegen, “Fast-array recursive closed-loop subspace model identification”, in 15th SYSID conference, 2009.

Cruise control design, an LPV approach

Gerrit Naus, René v.d. Molengraft
Dept. of Mechanical Engineering
Eindhoven University of Technology
P.O. box 513, 5600 MB, Eindhoven,
The Netherlands. Email: g.j.l.naus@tue.nl

Rudolf Huisman
Product Development
DAF Trucks N.V.
Eindhoven, The Netherlands

1 Introduction

Control design and tuning techniques adopted in industry often differ from the state-of-the-art techniques presented in the academic world. Generally, well-known, proven techniques are preferred, rather than theoretically comprehensive techniques, which are often more complex. The automotive industry is a typical example of such an industry.

In this research, different LPV control synthesis approaches are compared, focusing on their practical applicability in industry by means of a relevant problem, namely the design of a cruise control (CC) system for heavy-duty vehicles (HDVs). Within this context, the advantages and disadvantages of using relatively simple ad-hoc gain-scheduling methods and more complex, theoretically comprehensive LPV techniques are discussed [1].

2 Cruise control problem definition

Cruise control is a widespread, commercially available functionality. In this research, a standard CC system is considered, which means that the engine is considered as an actuator enabling automatic propulsion. A tachograph is used to measure the vehicle velocity, see Figure 1.

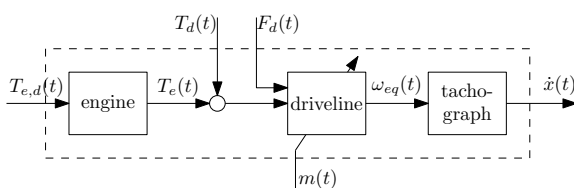


Figure 1: Schematic representation of the system to control, with $T_{e,d}(t)$ and $T_e(t)$ the desired and the brutto engine torque, $T_d(t)$ and $F_d(t)$ disturbance torques and forces, $m(t)$ the vehicle mass, $\omega_{eq}(t)$ the equivalent driveline rotational velocity, and $\dot{x}(t)$ the measured vehicle velocity.

Specifically focusing on HDV's, a large variation in operating conditions has to be dealt with when designing a CC system. The mass of a typical HDV, for example, may vary between 7 and 40 ton. In Figure 2, the corresponding Bode magnitude plots of the open-loop system (see Figure 1) are shown for different mass values. Targeting a bandwidth in the order of 1.0 to 10 rads^{-1} , these plots indicate that

the performance of the cruise control system can be significantly improved when the actual value of the mass is explicitly taken into account in the controller design and tuning.

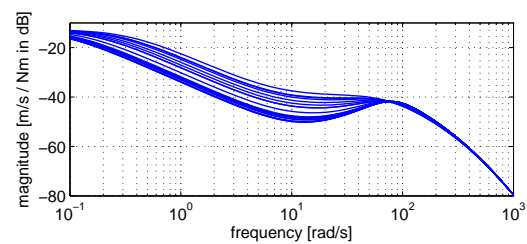


Figure 2: Bode magnitude plot of the open-loop system (see Figure 1) for $m(t) \in [7, 40]$ ton and $T_d(t) = F_d(t) = 0$.

3 LPV controller synthesis

Different LPV control design approaches are compared, focusing on their applicability for the design, tuning and implementation of a cruise control system.

- zero-pole-gain interpolation of operating-point dependent controllers which are designed by manual loopshaping techniques
- state-space interpolation of operating-point dependent \mathcal{H}_∞ -controllers
- LPV controller design using gridding of the total operating range
- LPV controller design making use of the extended Kalman-Yakubovich-Popov (KYP) lemma [3], which is equivalent to the full-block S-procedure [2]

The relative simplicity of the cruise control problem enables to compare the approaches.

References

- [1] W.J. Rugh and J.S. Shamma, Research on gain scheduling, *Automatica*, Vol. 36, pp.1401–1425, 2000.
- [2] C.W. Scherer, LPV control and full block multipliers, *Automatica*, Vol. 37, pp. 361–375, 2001.
- [3] M. Dinh, G. Scorletti, V. Fromion and E. Magarotto, Parameter dependent \mathcal{H}_∞ control by finite dimensional LMI optimization: application to trade-off dependent control, *Int. J. Robust Nonlinear Control*, Vol. 15, pp. 383–406, 2005.

Modeling Legged Locomotion via the Max-Plus Algebra

G.A.D. Lopes, R. Babuška, A.J.J. van den Boom and B. De Schutter
Delft Center for Systems and Control, Delft University of Technology
Mekelweg 2, 2628 CD Delft, The Netherlands

Email: {g.a.delgadolopes, r.babuska, a.j.j.vandenboom} @tudelft.nl, b@deschutter.info

1 Introduction

We present a new class of gait generation and control algorithms based on the Max-Plus modeling framework [1] that allows for the synchronization of multiple legs of walking robots. Transitions between stance and swing phases of each leg are modeled as discrete events on a system described by max-plus-linear state equations.

2 Designing motion gaits

Let $l_i(k)$ be the time instant leg i lifts off the ground and $t_i(k)$ be the time instant it touches the ground, both for the k -th iteration. For a traditional alternating swing/stance gait one can impose that the time instant when the leg touches the ground must equal the time instant it lifted off the ground for the last time plus the time it stays in flight (denoted τ_f):

$$t_i(k) = l_i(k) + \tau_f \quad (1)$$

Analogously, we get a similar relation for the lift off time:

$$l_i(k) = t_i(k-1) + \tau_g, \quad (2)$$

where τ_g is the stance time and t_i uses the previous iteration such that equations (1) and (2) can be used iteratively. Suppose now that one aims to synchronize leg i with leg j in such a way that leg i can only lift off τ_Δ seconds after leg j has touched the ground. One can then write the relation:

$$\begin{aligned} l_i(k) &= \max(t_i(k-1) + \tau_g, t_j(k-1) + \tau_\Delta) \\ &= [\tau_g \quad \tau_\Delta] \otimes \begin{bmatrix} t_i(k-1) \\ t_j(k-1) \end{bmatrix}, \end{aligned} \quad (3)$$

where the symbol \otimes denotes the matrix product operator defined in the Max-Plus algebra [1]. Equation (3) enforces simultaneously that both the leg i stays at least τ_g seconds in stance and will only lift off at least τ_Δ seconds after leg j has touched down. When both conditions are satisfied, lift off takes place. Following this reasoning, one can efficiently represent motion gaits in terms of synchronization of timed events. Figure 1 illustrates a pacing gait for a quadruped. Define the state variables for a quadruped robot $x(k) \in \mathbb{R}_{\max}^8$ by $x(k) = [t_1(k) \ l_1(k) \ \dots \ t_4(k) \ l_4(k)]^T$. Following the relations in Figure 1 one can find the max-plus-linear system matrix for the pacing gait, that we denote A_p . For gait symmetry we assume that $\tau_g > \tau_f$, and $\tau_p = (\tau_g - \tau_f)/2$. The

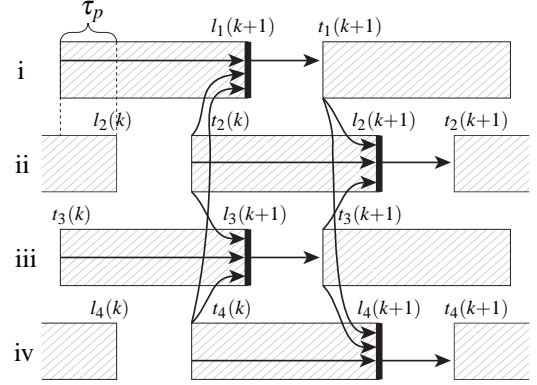


Figure 1: Time evolution of gaits for a quadruped. The hatched boxes represent the leg stance, and the solid thick lines represent the lift off events $l_i(k+1)$. The arrows represent events that must occur for each lift off and touch-down events to happen.

extra parameters $\tau_{fg} = \tau_f + \tau_g$ and $\tau_{pf} = \tau_p + \tau_f$ are introduced for compactness and $\varepsilon = -\infty$ (see [1]).

$$x(k) = A_p \otimes x(k-1)$$

$$A_p = \begin{bmatrix} \tau_{fg} & \varepsilon & \tau_{pf} & \varepsilon & \varepsilon & \varepsilon & \tau_{pf} & \varepsilon \\ \tau_g & \varepsilon & \tau_p & \varepsilon & \varepsilon & \varepsilon & \tau_p & \varepsilon \\ \tau_{pf} + \tau_{fg} & \varepsilon & \tau_{fg} & \varepsilon & \tau_{pf} + \tau_{fg} & \varepsilon & \tau_{fg} & \varepsilon \\ \tau_{pf} + \tau_g & \varepsilon & \tau_g & \varepsilon & \tau_{pf} + \tau_g & \varepsilon & \tau_g & \varepsilon \\ \varepsilon & \varepsilon & \tau_{pf} & \varepsilon & \tau_{fg} & \varepsilon & \tau_{pf} & \varepsilon \\ \varepsilon & \varepsilon & \tau_p & \varepsilon & \tau_g & \varepsilon & \tau_p & \varepsilon \\ \tau_{pf} + \tau_{fg} & \varepsilon & \tau_{fg} & \varepsilon & \tau_{pf} + \tau_{fg} & \varepsilon & \tau_{fg} & \varepsilon \\ \tau_{pf} + \tau_g & \varepsilon & \tau_g & \varepsilon & \tau_{pf} + \tau_g & \varepsilon & \tau_g & \varepsilon \end{bmatrix}$$

3 Conclusions

Experimental results in locomotion have validated the proposed framework. We have concluded that various gaits can be implemented at the discrete events level, and that the Switching Max-Plus framework allows for save transitions between different gaits.

References

- [1] B. Heidergott, G. Olsder, and J. van der Woude. *Max Plus at Work: Modeling and Analysis of Synchronized Systems*. Kluwer, 2006.

Performance of High-level and Low-level Coordinated Control of Mobile Robots

Sisdarmanto Adinandra¹, Jurjen Caarls², Dragan Kostić³, and Henk Nijmeijer⁴

Dynamics and Control, Department of Mechanical Engineering, Technische Universiteit Eindhoven
P.O. Box 513, 5600 MB, Eindhoven, The Netherlands

Email: { ¹s.adinandra, ²j.caarls, ³d.kostic, ⁴h.nijmeijer } @tue.nl

Abstract

We analyse the performance of different strategies for coordinated control of mobile robots. These robots are characterized by the non-holonomic kinematic model of a unicycle. The robots are employed for transportation of goods in an environment of a distribution center.

We propose a control architecture, shown in Figure 1, that contains multiple layers of functionality. The high-level control assigns to each robot the reference trajectory. The low-level control takes care that each robot tracks own reference.

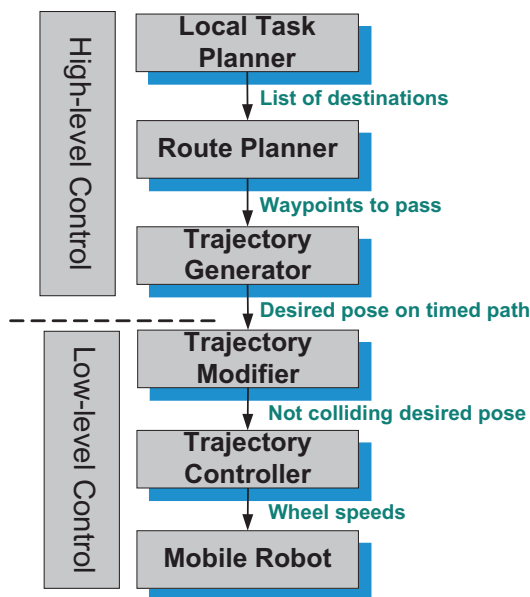


Figure 1: The control architecture

In a distribution center, coordination is needed to guarantee collision-free robot motions and correct robot sequencing. Collisions may occur if there is an obstacle on the robot path or when several robots share the same working space. A correct sequencing of robots is required, since items being transported have to arrive at drop-off points in a specific order based on the customer demands. With our architecture, it is easy to shift responsibilities over coordination of mobile robots to different control layers.

In this work, we investigate performance of two robot coordination strategies. This is done in experiments according to the following scenario: a convoy of seven robots delivers goods along a path where one part of this convoy intersects with another part, so robot coordination is needed to avoid collisions. The coordination strategies are:

1. High-level coordination (HL): at 1 Hz, the robot trajectory generators coordinate their occupation times of intersection, such that only one robot at a time occupies an intersection.
2. Low-level coordination (LL): at 30 Hz, the trajectory modifiers of the robots facing a collision locally override their original reference trajectories using artificial potential fields, such that the robots move away from each other until the imminent collision is averted.

For performance analysis, we consider the following indicators:

- Average travelled time, $\overline{t_{trvl}}[s]$, for all robots to reach their destination.
- Total normalized tracking errors of all robots, $\sum e_{xy}^2[m^2]$, and formation errors $\sum \delta_{ij}^2[m^2]$.

Table 1: Performance Evaluation

Strategies	Indicators		
	$\overline{t_{trvl}}[s]$	$\sum e_{xy}^2[m^2]$	$\sum \delta_{ij}^2[m^2]$
HL	36.06	0.002	0.0014
LL, not coupled	38.458	0.114	0.0021
LL, all robots coupled	38.496	0.123	0.0014

The data given in Table 1 indicate that the high-level coordination leads to shorter travel time and smaller tracking errors. It gives optimal and efficient robot trajectories that are free of collisions. However, this coordination method is less robust to perturbations, since it requires accurate tracking of the reference trajectories. Even though the performance of the low-level coordination is lower, this coordination turns out to be much more robust to uncertainties.

References

- [1] D. Kostić, *et. al.*, "Collision-free Tracking Control of Unicycle Mobile Robot", in *Proc. IEEE Conf. on Decision and Control Shanghai, China*, pp 5677-5672, 2009.

RoboEarth: Concept and Objectives

Jos Elfring, Rob Janssen, and René van de Molengraft

Department of Mechanical Engineering

Eindhoven University of Technology (TU/e)

P.O. Box 513, 5600 MB Eindhoven, The Netherlands

Email: J.Elfring@tue.nl, R.J.M.Janssen@tue.nl, M.J.G.v.d.Molengraft@tue.nl

Abstract

Today's robots are programmed in such a way that they rely, almost completely, on feedback. Based on the consequences of an action performed by the robot, it tries to make the necessary adjustments. Each response to a contingency has to be programmed in advance and every time a robot has to perform a task the same process has to start all over again, *i.e.*, building a world model from sensor data and adjusting its actions in order to successfully accomplish the desired task. A solution to this problem could be to store the robot's knowledge regarding the actions and the environment. Then, any robot that has access to the stored knowledge can benefit from it resulting in an improved action. Such a feed forward strategy prevents reinventing the wheel over and over again.

Recently, a consortium consisting of Eindhoven University of Technology (TU/e), Philips Applied Technology, Universität Stuttgart (USTUTT), Eidgenössische Technische Hochschule Zürich (ETHZ), Universidad de Zaragoza (UNIZAR), and Technische Universität München (TUM) started a project called RoboEarth. The goal is to successfully design and implement a world-wide web-style database called RoboEarth. RoboEarth should receive and store knowledge obtained by a robot and supply it to any robot that can benefit from it, independent of the robot's hardware and configuration. Apart from this database, an interface between the database and the systems referring to the database, and a language that can be used for communication have to be developed. As a proof of principle, a service robot for patient companion in a hospital environment will be built as a demonstrator. This service robot will, *e.g.*, serve a drink or open a screw cap bottle.

A robot will collect environmental data from its sensors. From this data, objects are detected and labeled. These objects, both static and dynamic, are associated with real world objects and are tracked. This constitutes the local world model, mainly deployed by the robot itself. The local world model can benefit from object definitions, *e.g.*, shape, position, size, that are downloaded from RoboEarth. Furthermore, RoboEarth deploys a global world model that manages the consistency between various incoming local world models from different robots. Furthermore it builds up probabilistic models of the initiation, continuation and finalization of objects. Clearly, this knowledge can be beneficial

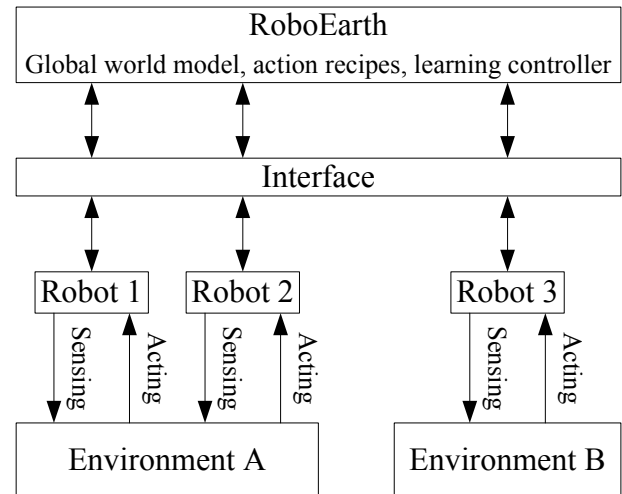


Figure 1: Schematic representation of the interactions between RoboEarth and various robots

for a robot, since it tells the robot, *e.g.*, where to expect objects in the sensor data, or in which direction objects usually move.

If a robot has to perform a task, a plan containing actions and handling for the objects involved can be downloaded from RoboEarth. Such a plan will be called action recipe and it usually consists of a series of actions such as grabbing or moving an object. By downloading action recipes, a robot will be able to perform tasks, even if it never did the task before.

Finally, any robot can upload *e.g.*, control architectures, motion control algorithms and learned parameters, such that all other robots can benefit. This allows learning control on all levels, from control parameters to path planning. A schematic representation of the RoboEarth setup is given in Figure 1.

The focus of the RoboEarth research and technological development will be on 3D sensing, world modeling, action and situation recognition and labeling, learning control, and language for communication. The research leading to these results has received funding from the European Union Seventh Framework Programme FP7/2007-2013 under grant agreement n^o248942 RoboEarth.

Modeling, identification and stability of a humanoid robot

Pieter van Zutven, Dragan Kostić, Henk Nijmeijer
 Eindhoven University of Technology, Department of Mechanical Engineering
 P.O. Box 513, 5600 MB Eindhoven, The Netherlands
 Email: {p.w.m.v.zutven, d.kostic, h.nijmeijer}@tue.nl

Abstract

In this work, we address modeling and identification of bipedal humanoid robots and conduct stability analysis of bipedal locomotion. We propose a theoretical framework for automatic modeling and identification of an arbitrary bipedal robot. Our approach is tested in experiments on the humanoid robot TULip, shown in figure 1. Finally, we argue merits and limitations of the two most common methods for evaluation of stability of bipedal walking.

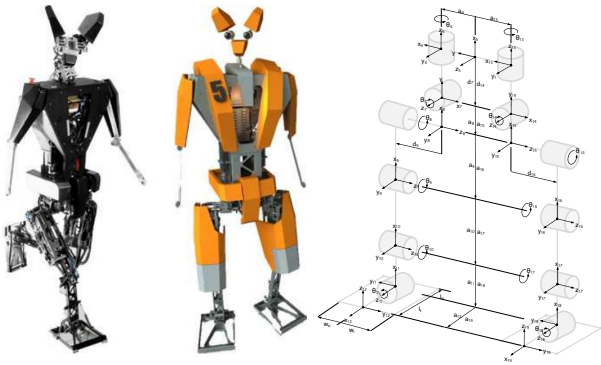


Figure 1: Humanoid TULip: photo, CAD drawing and DH model

Using Denavit Hartenberg's convention for modeling robot kinematics, depicted in figure 1, we contribute an automatic algorithm for derivation of Lagrange-Euler equations of motions for a general bipedal humanoid robot. This algorithm is instantiated on TULip. Furthermore, conditions for ground contact and impact expressions are derived and numerically integrated in a Matlab simulation together with equations of motion using the event detection method [1].

The model parameters of a humanoid robot can be identified in dynamic experiments. In this work, we propose a method for automatic conversion of the robot dynamical equations into a regressor form. Here, the dynamical equations encompass Lagrange-Euler equations of motion, of the actuator dynamics, friction and dynamics of the drive trains [1, 2]. Persistently exciting trajectories are optimized using the regressor of the resulting dynamical model, and these trajectories are used in experiments to estimate parameters of the robot TULip. The estimated parameters are validated in experiments, and results are shown in figure 2.

The Zero Moment Point and Poincaré map methods have been applied for design and stability analysis of bipedal

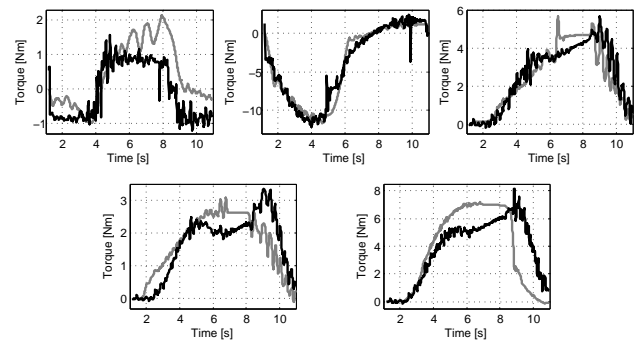


Figure 2: Validation of system identification: measured torque (grey) and model-based torque estimation (black)

walking. Illustrative results are shown in figure 3. Critical evaluation of both methods leads to the conclusion that these methods are neither sufficient nor necessary to guarantee stability of bipedal walking. Consequently, new theoretical formalisms are needed for proper qualification of bipedal locomotion stability and for synthesis of stable gaits [1].

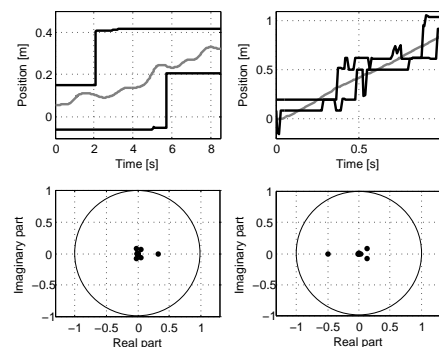


Figure 3: ZMP (top) and Poincaré (bottom) stability for ZMP based gait (left) and limit cycle walking gait (right)

References

- [1] P.W.M. van Zutven. *Modeling, identification and stability of humanoid robots*. Master thesis, DCT 2009.100. Eindhoven University of Technology, 2009.
- [2] P.W.M. van Zutven, D. Kostić, and H. Nijmeijer. Parameter identification of robotic systems with series elastic actuators. 2010. Submitted to *8th IFAC symposium on non-linear control systems*.

Collision-free motion coordination of unicycle multi-agent systems

Dragan Kostić,¹ Sisdamanto Adinandra,² Jurjen Caarls,³ and Henk Nijmeijer⁴

Department of Mechanical Engineering

Technische Universiteit Eindhoven

P.O. Box 513, 5600 MB Eindhoven

The Netherlands

Email: {¹D.Kostic, ²S.Adinandra, ³J.Caarls, ⁴H.Nijmeijer}@tue.nl

Abstract

We propose a collision-free motion coordination of a group of unicycle agents. The agents are characterized by non-holonomic kinematics of a unicycle, such as wheeled mobile robots and unmanned aerial vehicles. While the reference trajectories of interacting agents make a time-varying formation, our control strategy achieves globally asymptotically stable tracking of these trajectories and coordination between the interacting agents, both under constraints on the actuator inputs. The coordination takes care that after perturbation of one or several agents, the formation is recovered even before the tracking errors of all individual agents converge to zero. The proposed strategy is an extension of the control design presented in [1], in terms of mutual coupling of motion controllers of the individual agents. The controller couplings yield robustness of the formation to perturbations.

Robustness is further strengthened by means of an algorithm for collision avoidance. This algorithm runs at each agent locally and is based on the concept of the artificial potential functions. The algorithm achieves collision avoidance by real-time modifications of the reference trajectories of the individual agents.

Quality of the collision-free motion coordination is experimentally verified. A layout of robot paths is shown at the top in Fig.1. To verify formation keeping, we perturb the formation three times, by manual robot repositioning. Each time a robot is repositioned, the other ones start moving away from their reference trajectories aiming to restore the prescribed formation. After recovering the formation, the robots continue tracking their own reference trajectories. At the bottom in Fig.1, we show the tracking errors together with errors in keeping the formation. This figure confirms that the transients of the formation errors are faster than the transients of the tracking errors.

The main contributions are: *i)* Lyapunov based design of saturated feedback tracking controllers that achieve global asymptotic stable motion coordination of multi-agent unicycle systems, *ii)* global asymptotic tracking of time-varying formations, where the forward and steering velocities of the individual agents can all be mutually different, while the steering velocities can even be discontinuous, *iii)* flexible

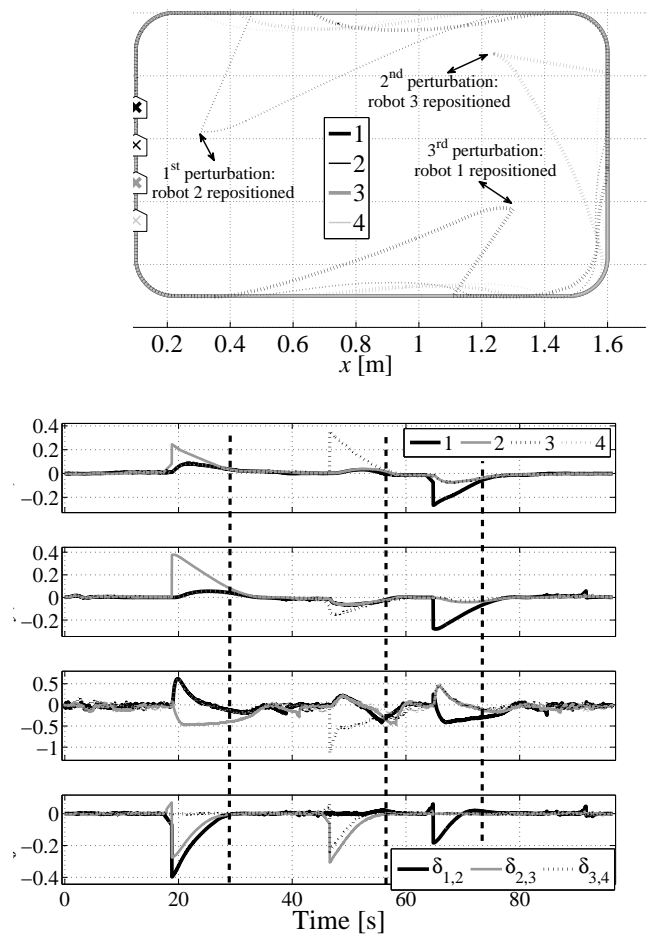


Figure 1: Top: reference (solid) and actual (dotted) paths; bottom: errors in tracking and formation keeping.

controller tuning and intuitive adjustment of robustness of motion coordination with respect to perturbations, *iv)* real-time collision avoidance, and *v)* experimental verification.

References

- [1] D. Kostić, *et al.*, “Collision-free Tracking Control of Unicycle Mobile Robots,” *Proc. IEEE Conf. Dec. and Control*, pp. 5667-5672, Shanghai, China, 2009.

Computable Semantics for CTL* on Discrete-Time and Continuous-Space Dynamic Systems

Pieter Collins and Ivan S. Zapreev

Centrum Wiskunde & Informatica, Science Park 123, 1098 XG Amsterdam

Emails: *Pieter.Collins@cwi.nl*, *I.Zapreev@cwi.nl*

1 Introduction

Many of the high-profile and safety-critical processes in physiology, biology, chemistry and engineering can be naturally modelled as dynamic systems. This resulted in a large amount of work on formal verification thereof but most of the existing methods can only cope with finite-state systems or simple Hybrid systems such as timed automata. The aim of this work is to extend the scope of formal verification to systems with continuous state spaces such as \mathbb{R}^n . Therefore, we consider discrete-time continuous-space dynamic systems (DTCSDSs) for which we study the standard semantics of the branching temporal logic CTL* [1] and give a “computable semantics”, in the sense of Type-2 Theory of Effectivity (TTE) [2], under which most of the *true* system properties can be proven using numerical methods.

2 Overview

CTL* is a strict superset of CTL – Computational Tree Logic and LTL – Linear Temporal Logic. CTL reasons about the infinite computation tree of the system, i. e. allows to specify branching-time properties. LTL reasons about system traces, i. e. allows to specify linear-time properties.

In [3] we first devise a computable semantics for CTL on DTCSDSs. Later in [4], employing path spaces, we extend it to a computable semantics of CTL*. This semantics turns out to be not optimal as it can lead to inconclusive model-checking results even on finite-state models. Further, in [5], we give a new computable semantics for CTL* such that it is exact on finite-state models. The latter is done by showing how the computable model checking of existentially and universally quantified path formulae of LTL can be reduced to solving, respectively, repeated reachability and persistence problems on a model obtained as a parallel composition of the original one and a non-deterministic Büchi automaton (NBA) corresponding to the verified LTL formula.

Our computable semantics are topological, cf. [6], i. e. we work with open sets of states and paths. In the provided semantics, if the verified state formula Φ contains negation, henceforth, or release operators then Φ can be true on a given model M , but not verifiable. Moreover, the formula Φ may be neither verifiable nor falsifiable on M . Yet, if the formula holds in the computable semantics, then it does hold in the original one. Also, our final version of the semantics

for CTL*, cf. [5], is optimal since it is exact on finite-state models, i. e. we can not obtain better verification results by discretizing the system’s state space.

3 Details

The basic computability requirements for our semantics in [3, 4, 5] are: (i) the set of initial system states I is compact; (ii) $\Phi \in \text{CTL}^*$ is in negation normal form (NNF); (iii) the DTCSDS $M = (T, F, L)$ is such that T is a computable Hausdorff space, and F is a continuous map for which the weak and strong pre-images of any open U are computable; (iv) the negation-prefixed atomic propositions of Φ have representations that allow for computing interiors of their complements. The computable semantics for CTL*, introduced in [5], is based on reducing the problem of verifying $\forall\phi$ or $\exists\phi$ on M to a problem of verifying $\forall\Diamond\Box U_F$ or $\exists\Box\Diamond U_F$ on a model obtained using a parallel composition of M and the non-blocking NBA for $\neg\phi$ or ϕ . Here, ϕ is an LTL path formula; $\text{Sat}(U_F)$ is the state space of M times the set of accepting states of the corresponding NBA; $\neg\phi$ and ϕ are in NNF. For verifying $\exists\phi$, we require knowing an separable-type name of I .

4 Acknowledgements

This research was supported by the Nederlandse Organisatie voor Wetenschappelijk Onderzoek (NWO) Vidi grant 639.032.408.

References

- [1] E. A. Emerson and J. Y. Halpern. “sometimes” and “Not Never” Revisited: On Branching versus Linear Time Temporal Logic. *Journal of the Association for Computing Machinery (ACM)*, 33(1):151–178, 1986.
- [2] Klaus Weihrauch. *Computable Analysis: An Introduction*. Springer-Verlag New York, Inc., Secaucus, NJ, USA, 2000.
- [3] Pieter J. Collins and Ivan S. Zapreev. Computable CTL for Discrete-Time and Continuous-Space Dynamic Systems. In *Computability in Europe (CiE)*, pages 110–119, 2009. Pre-conference proceedings volume.
- [4] Pieter J. Collins and Ivan S. Zapreev. Computable CTL* for Discrete-Time and Continuous-Space Dynamic Systems. In *Proceedings of the 3rd International Workshop on Reachability Problems (RP)*, pages 107–119. Springer-Verlag, 2009.
- [5] Pieter J. Collins and Ivan S. Zapreev. Computable CTL* for Discrete-Time and Continuous-Space Dynamic Systems. Submitted to *International Journal of Foundations of Computer Science (IJFCS)*, 2010.
- [6] Philip Kremer and Grigori Mints. Dynamic topological logic. *Annals of Pure and Applied Logic*, 131(1–3):133–158, 2005.

Compositional and Computable Semantics for Hybrid Systems

Pieter Collins
Centrum Wiskunde en Informatica
Amsterdam, Nederland
Pieter.Collins@cwi.nl

Davide Bresolin, Tiziano Villa
Universita di Verona, Italia
bresolin@sci.univr.it
villa@univr.it

Ramon Schiffelers, Bert van Beek, Koos Rooda
Technische Universiteit Eindhoven, Nederland
{r.r.h.schiffelers,d.a.v.beek,j.e.rooda}@tue.nl

1 Motivation

Hybrid systems are commonly used as models of industrial processes. Due to the innate complexity of such systems, considerable attention has been paid to the development of modeling languages for hybrid systems. The Compositional Interchange Format (CIF) [1] is a language for describing hybrid systems which was designed both for modeling and as an intermediate for translation between other frameworks for system specification. The CIF has an *operational semantics* which gives a well-defined mathematical description of the behaviour of a model.

Given a system model, we wish to compute properties of its behaviour. Unfortunately, the CIF allows the construction of models for which the behaviour given by the operational semantics is *uncomputable*, in the sense that there is no algorithm which can be implemented on a digital computer which can compute the set of executions. Worse, it can be shown that there is no semantics of evolution for hybrid systems under which the evolution is computable; we need an *upper-semicomputable semantics* (or simply *upper semantics*) to prove safety properties, and a *lower-semicomputable semantics* to prove liveness properties. The tool Ariadne [2] can compute the evolution of nonlinear hybrid systems without inputs using either the lower or upper semantics.

The main problem we address is to find a subset of the CIF under which upper- or lower-semicomputable semantics of evolution can be given, and show that these semantics behave reasonably under parallel composition.

2 Input/Output Automata

To ensure computability of the evolution, we restrict the discrete and continuous dynamics of a CIF model to be given in explicit form. For example, differential-algebraic equations $f(x, \dot{x}, u)$ are problematic, but differential equations $\dot{x} = f(x, u)$ are allowed. Every state or output variable must be defined exactly once and there may be no algebraic loops, though which variables are inputs and which are outputs may be mode-dependent. Noise variables may not be used in the guards or resets. For upper semantics, we take the

closure of the guard sets, and for lower semantics, the interior. The resulting system model is a variant of *input/output hybrid automata*, and is defined by the equations

$$\begin{aligned} \dot{x} &= f_q(x, u, v) \text{ if } p_q(x) \leq 0; \\ q' &= \gamma(q, e), x' = r_{q,e}(x, u) \text{ if } g_{q,e}(x) \geq 0. \end{aligned}$$

The parallel composition operator can be defined at two levels; at the system definition level, for which the equations governing the system evolution are combined, and at the behavioural level, in which the intersection of the possible individual behaviours is taken. It is also conjectured that the parallel composition of CIF automata yields the same behaviour whether defined on models or on behaviours.

3 Simulation Relations

The main result is that the upper and lower semantics respectively simulate or are simulated by the operational semantics defined in CIF (for CIF models whose computable semantics are defined), and that the semantics behave appropriately under parallel composition. We obtain the following diagram, where \rightarrow denotes the simulation relation, and $S^{C,U,L}$ denote the behaviour of the system S using (respectively) operational, lower and upper semantics.

$$\begin{array}{ccc} S_1^U \parallel S_2^U & \longrightarrow & (S_1 \parallel S_2)^U \\ \downarrow & & \downarrow \\ S_1^C \parallel S_2^C & \longleftrightarrow & (S_1 \parallel S_2)^C \\ \downarrow & & \downarrow \\ S_1^L \parallel S_2^L & \longleftarrow & (S_1 \parallel S_2)^L \end{array}$$

This means that the upper- and lower-semicomputable semantics as used in Ariadne are compatible with the operational semantics defined by CIF, and with the parallel composition operator.

References

- [1] Systems Engineering Group TU/e. CIF language and toolset. <http://se.wtb.tue.nl/sewiki/cif>.
- [2] Control and Systems Theory Group, CWI; Information Processing Systems Group, Verona; PARADES, Roma. Ariadne: An open framework for hybrid systems analysis. <http://trac.univr.rm.cnr.it/ariadne/>.

Abstraction Techniques for Automatic Verification of Stochastic Hybrid Systems

Alessandro Abate

Delft Center for Systems and Control

Faculty of Mechanical, Maritime and Materials Engineering

Technische Universiteit Delft

Mekelweg 2, 2628 CD, Delft

The Netherlands

Email: a.abate@tudelft.nl

Abstract

The goal of this research effort is to formally investigate and develop automatic verification techniques that are directly applicable to general Stochastic Hybrid System (SHS) models while being computationally scalable. Such constructive procedures will simplify SHS models into computationally prone structures, will establish quantitative bounds on the introduced approximations, and will be rigorously formulated as probabilistic bisimulations. This will enable the use of known automatic verification techniques, such as probabilistic model checking, to study properties and devise control schemes for the abstracted structures, and to precisely export the results back to the original SHS.

1 BACKGROUND AND MOTIVATIONS

Stochastic Hybrid Systems (SHS) are dynamical models that are amenable to characterizing the probabilistic evolution of systems with interleaved and interacting continuous and discrete components.

The formal analysis and verification of SHS models represent relevant goals both because of the theoretical generality of SHS and for their applicability to a wealth of studies in the Sciences and in Engineering.

However, the potential complexity of the topological and structural properties of hybrid models, the generality allowed by their hybrid dynamics, and the presence of stochasticity are intrinsically bound to the known complexity of the development of control schemes, as well as the lack of scalability for automatic verification techniques over these models.

2 OBJECTIVES

The overall goal of this research project is to formally develop novel approximate abstraction techniques for general SHS, to formulate them within the framework of probabilistic bisimulation, and to integrate them within automatic verification procedures for probabilistic systems. The objectives of the project will be divided into two parts.

1. The research will investigate the notion of approximate abstraction of SHS, and will establish a formal relationship between this notion and the concept of probabilistic bisimulation for SHS
2. The study will employ this connection to export automatic verification techniques for the abstracted model onto the original SHS, and will develop an integrated software for abstraction and verification of SHS

3 INITIAL RESULTS

With regards to point 1., the work in [1] has studied the problem of characterizing and computing probabilistic bisimulations of certain classes of stochastic processes. A probabilistic bisimulation relation between two processes has been defined through a bisimulation function, and sufficient conditions for the existence of a bisimulation function have been introduced, based on the use of contractivity analysis for probabilistic systems. Furthermore, early research has gained understanding on the notion of approximate abstraction of SHS [2]. The mathematical underpinning of this technique hinges on the use of explicit and tunable bounds on the distance between the probabilistic laws that characterize the concrete SHS and its abstraction. The abstraction is interpreted as a Markov Set-Chain, which is a mathematically well-understood structure.

With regards to point 2., the contribution in [3] has proposed a method for approximate model checking of a class of properties over SHS, with provable approximation guarantees.

References

- [1] A. Abate, "A Contractivity Approach for Probabilistic Bisimulations of Diffusion Processes." Proceedings of the 48th IEEE Conference of Decision and Control, 2009.
- [2] A. Abate, A. D'Innocenzo, and M. Di Benedetto, "Approximate Abstractions of Stochastic Hybrid systems." *Prov. accepted*, IEEE Trans. on Automatic Control, 2010.
- [3] A. Abate, J.P. Katoen, J. Lygeros, and M. Prandini, "Approximate Model Checking of Stochastic Hybrid Systems." To appear, European Journal of Control, 2010.

The Information Inequality on Function Spaces

Tzvetan Ivanov, Michel Gevers, P.-A. Absil

Center for Systems Engineering and

Applied Mechanics (CESAME)

Université Catholique de Louvain

B-1348, Louvain-la-Neuve, Belgium

{tzvetan.ivanov, michel.gevers, pa.absil}
@uclouvain.be

Brian D.O. Anderson

Australian National University

Research School of Inf. Sciences & Eng.

Canberra, ACT 2601,

Australia

brian.anderson@anu.edu.au

1 Introduction

The goal of this work is to extend the scope of classical information inequalities from Euclidean to function spaces. More precisely we derive an ultimate lower bound on the autocovariance function of any unbiased function estimator. Compared to previous work in [1] we are now able to handle the case where the function depends on a statistical structure that has a singular information matrix. This applies, a.o., to reduced order modeling.

2 Autocovariance and Uncertainty

We shall limit ourselves to the case where the function space is an n -dimensional differentiable manifold, call it $\mathcal{P} = \{P : \mathbb{T} \rightarrow \mathbb{C}\}$, whose elements $P \in \mathbb{R}(z)$ are complex-valued real-rational functions on the unit circle \mathbb{T} which correspond to transfer-functions of discrete-time plants. This is merely for the ease of exposition since the theory applies to general function spaces including those associated with MIMO systems.

The autocovariance function of an estimator \hat{P} of P can be used to evaluate natural performance specifications [2], e.g., the following in the context of robust control: With probability not less than α given N samples the maximum mismatch $|\hat{P}(z) - P(z)|$ over all frequencies z in a band $B \subseteq \mathbb{T}$ is bounded from above by ε/N . Using the results in [3] we show that a sufficient condition to satisfy this performance specification is

$$\chi_n^2(\alpha) \cdot (\Phi(z, z) - |\Phi(z, z^{-1})|) \leq 2 \cdot \varepsilon/N, \quad (1)$$

where Φ is the autocovariance function of \hat{P} and $\chi_n^2(\alpha)$ denotes the α -quantile of the Chi-square distribution with n degrees of freedom. The main result in [1], i.e., the information inequality on function spaces, states that the autocovariance function of \hat{P} is bounded from below, in the sense of E.H. Moore [4], by the reproducing kernel K_P of the tangent space $T_P\mathcal{P}$ of \mathcal{P} at P with respect to the Fisher-information metric g_P .

3 Compression Metric and Singularities

In other words for an efficient estimator, i.e., an estimator attaining the lower bound K_P , the Fisher-information metric g_P can be used for autocovariance quantification. However this result can only be applied if the information metric g_P defines a *positive definite* inner-product on the tangent space $T_P\mathcal{P}$. If the information metric on $T_P\mathcal{P}$ is singular the autocovariance function of the estimator \hat{P} becomes unbounded. Notwithstanding this observation, in applications \hat{P} is often used to estimate another function, call it $M : \mathbb{T} \rightarrow \mathbb{C}$, which only partially depends on P . For instance one may think of M as a reduced order model or controller. The mathematical formulation of this is that $M = \mu(P)$ where $\mu : \mathcal{P} \rightarrow \mathcal{M}$ denotes a smooth function between two function spaces. It is a natural question to ask under which conditions on the information metric g_P and the function μ the autocovariance function of $\hat{M} := \mu(\hat{P})$ is bounded. The introduction of a novel concept called a compression metric allows us to answer this question and state the generalized information inequality.

References

- [1] T. Ivanov and M. Gevers, "Parametrization Invariant Covariance Quantification in Identification of Transfer Functions for Linear Systems," in *48th IEEE Conference on Decision and Control*, December 2009, pp. 1544–1550.
- [2] H. Hjalmarsson, "System identification of complex structured systems," *Plenary lecture at ECC 2009, European Journal of Control*, vol. 15, no. 3-4, pp. 276–310, 2009.
- [3] T. Ivanov, B.D.O. Anderson, P.-A. Absil, and M. Gevers, "Using H^2 norm to bound H^∞ norm from above on Real Rational Modules," in *CD-ROM Proc. of European Control Conference*, 2009, pp. 2259–2264.
- [4] E. H. Moore, "On properly positive Hermitian matrices," *Bull. Amer. Math. Soc.*, vol. 23, no. 59, pp. 66–67, 1916.

TRACKING AND REGULATION IN THE BEHAVIORAL FRAMEWORK

S. Fiaz*, K. Takaba** and H.L. Trentelman*

*Johann Bernoulli Institute for Mathematics and Computer Science,

University of Groningen, P.O Box 800, 9700 AV Groningen, The Netherlands, Email: s.fiaz@math.rug.nl and h.l.trentelman@math.rug.nl

**Department of Applied Mathematics and Physics, Kyoto University, Kyoto 606-8501, Japan, Email: takaba@amp.i.kyoto-u.ac.jp.

In this talk we formulate the tracking and regulation problem in the behavioral framework, with control as interconnection. The problem formulation and its resolution are completely representation free, and specified only in terms of the plant and the exosystem dynamics. We start with a plant behavior $\mathcal{P}_{\text{full}} \in \mathcal{L}^{w_1+w_2+c+v}$, with plant variable (w_1, w_2, c, v) . The variables w_2, c, v represent the to be regulated variable (like tracking error), the interconnection variable (like sensor measurements and actuator inputs), and external disturbances, respectively. The interconnection variable c is the plant variable through which we are allowed to interconnect $\mathcal{P}_{\text{full}}$ with a controller $\mathcal{C} \in \mathcal{L}^c$. As the variable v represents reference signal and external disturbances we assume it to be free in $\mathcal{P}_{\text{full}}$ (see [1]). Here we assume that the reference signal and disturbances are generated by an autonomous anti-stable exosystem $\mathcal{E} \in \mathcal{L}^v$ with system variable v .

Define $\mathcal{P}_{\text{full}} \wedge_v \mathcal{E} := \{(w_1, w_2, c, v) \mid (w_1, w_2, c, v) \in \mathcal{P}_{\text{full}} \text{ and } v \in \mathcal{E}\}$, $\mathcal{P}_{\text{full}} \wedge_c \mathcal{C} := \{(w_1, w_2, c, v) \mid (w_1, w_2, c, v) \in \mathcal{P}_{\text{full}} \text{ and } c \in \mathcal{C}\}$, $\mathcal{P}_{\text{full}} \wedge_v \mathcal{E} \wedge_c \mathcal{C} := \{(w_1, w_2, c, v) \mid (w_1, w_2, c, v) \in \mathcal{P}_{\text{full}} \wedge_v \mathcal{E} \text{ and } c \in \mathcal{C}\}$, $\mathcal{N}_{(w_1, w_2, c)}(\mathcal{P}_{\text{full}}) := \{(w_1, w_2, c) \mid (w_1, w_2, c, 0) \in \mathcal{P}_{\text{full}}\}$ and $\mathcal{N}_v((\mathcal{P}_{\text{full}})_{(w_2, c, v)}) := \{v \mid \exists w_1 \text{ s. t. } (w_1, 0, 0, v) \in \mathcal{P}_{\text{full}}\}$.

Problem of tracking and regulation in the behavioral framework can be formulated as follows.

Problem : Given the plant $\mathcal{P}_{\text{full}} \in \mathcal{L}^{w_1+w_2+c+v}$ and the exosystem $\mathcal{E} \in \mathcal{L}^v$, find conditions under which there exists a controller $\mathcal{C} \in \mathcal{L}^c$ such that (1.) the interconnection $\mathcal{P}_{\text{full}} \wedge_c \mathcal{C}$ is regular (see [2]), (2.) v is free in $\mathcal{P}_{\text{full}} \wedge_c \mathcal{C}$, (3.) for all $(w_1, w_2, c, v) \in \mathcal{P}_{\text{full}} \wedge_v \mathcal{E} \wedge_c \mathcal{C}$ we have $\lim_{t \rightarrow \infty} w_2(t) = 0$, and (4.) for all $(w_1, w_2, c, 0) \in \mathcal{P}_{\text{full}} \wedge_v \mathcal{E} \wedge_c \mathcal{C}$ we have $\lim_{t \rightarrow \infty} (w_1(t), w_2(t), c(t)) = (0, 0, 0)$.

Condition (2) above asks the controller not to put any restrictions on the variable v which represents the reference signal and external disturbances acting on the system. Condition (3) asks the controller to achieve regulation of the tracking error, and condition (4) asks the controller to take the system to rest when the disturbance signal is equal to zero. Condition (1) about the regularity of the interconnection $\mathcal{P}_{\text{full}} \wedge_c \mathcal{C}$ will make sure that \mathcal{C} does not re-impose restrictions on the control variable c that are already present in the laws of $\mathcal{P}_{\text{full}}$ (see [2]). A controller which achieves these objectives is

called a *regulator* for $\mathcal{P}_{\text{full}}$ with respect to \mathcal{E} . The following Theorem provides a solution to the above problem.

Theorem 0.1 Let $\mathcal{P}_{\text{full}} \in \mathcal{L}^{w_1+w_2+c+v}$ with system variable (w_1, w_2, c, v) . Assume v is free in $\mathcal{P}_{\text{full}}$. Let $\mathcal{E} \in \mathcal{L}^v$ be an autonomous anti-stable system with system variable v . Assume $\mathcal{E} \cap \mathcal{N}_v((\mathcal{P}_{\text{full}})_{(w_2, c, v)}) = 0$. Then there exists a regulator for $\mathcal{P}_{\text{full}}$ with respect to \mathcal{E} if and only if (1.) (w_1, w_2, v) is detectable from c in $\mathcal{P}_{\text{full}} \wedge_v \mathcal{E}$, $\mathcal{N}_{(w_1, w_2, c)}(\mathcal{P}_{\text{full}})$ is stabilizable (see [1]), and (2.) for all $v \in \mathcal{E}$, there exists maps $L(\frac{d}{dt})$ and $M(\frac{d}{dt})$ such that $(L(\frac{d}{dt})v, 0, M(\frac{d}{dt})v, v) \in \mathcal{P}_{\text{full}}$.

Remark 0.2 Consider a special case of state space systems, where the plant and the exosystem are described by state space equations, $\mathcal{P}_{\text{full}} = \{(w_1, w_2, c = (u, y), v) \mid \dot{w}_1 = A_3 v + A_2 w_1 + B_2 v, y = C_1 v + C_2 w_1, w_2 = D_1 v + D_2 w_1 + E u\}$ and $\mathcal{E} = \{v \mid \dot{v} = A_1 v\}$ with $\sigma(A_1) \subset \mathbb{C}^+$, respectively. Then the conditions of Theorem 0.1 becomes (1.) pair (A_2, B_2) is stabilizable and pair $\left(\begin{pmatrix} C_2 & C_1 \end{pmatrix}, \begin{pmatrix} A_2 & A_3 \\ 0 & A_1 \end{pmatrix} \right)$ is detectable (see [3]), and (2.) there exists $S \in \mathbb{R}^{w_1 \times v}$ and $T \in \mathbb{R}^{v \times v}$ such that $SA_1 - A_2 S - B_2 T = A_3$ and $D_1 + D_2 S + E T = 0$. These conditions coincide with the classical results on state space systems. For example see Theorem 9.2 of [3] and references therein.

Detailed proofs of Theorem 0.1 and Remark 0.2, and an algorithm to construct a regulator will be discussed in the talk.

References

- [1] J.W. Polderman and J.C. Willems, *Introduction to Mathematical Systems Theory: a Behavioral Approach*, Springer-Verlag, Berlin, 1997.
- [2] M.N. Belur and H.L. Trentelman, "Stabilization, pole placement and regular implementability," *IEEE Transactions on Automatic Control*, Vol. 47, nr. 5, pp. 735 - 744, 2002.
- [3] H.L. Trentelman, A.A. Stoorvogel and M.L.J. Hautus, *Control Theory for Linear Systems*, Springer, London, 2001.

Fast and Robust Iterative Learning Control for Lifted Systems with Bounded Model Uncertainties

Aleksandar Haber, MSc.
Delft Center for Systems and Control
Mekelweg 2, 2628 CD Delft, The Netherlands.

In this work we propose a new methodology to synthesize and implement a robust ILC controller for lifted systems. The control law is obtained as a solution of the bounded data uncertainty least squares problem, using bounded model uncertainty in a trial domain. Tight uncertainty bounds in the trial domain are directly obtained from bounded model uncertainty in a sample to sample domain for both LTI and LTV systems, using randomized algorithms approach. Lifted system contains a structure, namely a sequentially semi-separable, which is exploited in both solving bounded data uncertainty least squares problem and in a derivation of the trial domain uncertainty bounds. As a result, the computational complexity of the proposed framework is linear in the number of samples of a trial, in contrast to at least cubic computational complexity of standard robust and optimal control synthesis techniques. Therefore the proposed framework especially suitable for the LTI and LTV uncertain systems with large number of samples in the trial.

Necessary and Sufficient Conditions for Pareto Optimality in Differential Games.

Engwerda J.C.

Tilburg University, Dept. of Econometrics and OR, P.O. Box 90153, 5000 LE Tilburg, The Netherlands
engwerda@uvt.nl

Reddy P.V.

Tilburg University, Dept. of Econometrics and OR, P.O. Box 90153, 5000 LE Tilburg, The Netherlands
p.v.Reddy@uvt.nl

1 Abstract

In this presentation we present as well necessary as sufficient conditions for existence of a Pareto optimum for cooperative differential games. We consider both a finite and infinite planning horizon.

Formally, we consider a dynamic system described by the next differential equation, where the dynamics are influenced by N different players

$$\dot{x}(t) = f(t, x(t), u_1(t), \dots, u_N(t)), x(t_0) = x_0. \quad (1)$$

Here, $x \in \mathbb{R}^n$ is the state of the system and $u_i \in \mathbb{R}^m$ the control used by player i .

Each player i likes to minimize his performance criterion J_i , $i = 1, \dots, N$, given by:

$$\int_{t_0}^T g_i(t, x(t), u_1(t), \dots, u_N(t)) dt + h_i(x(T)). \quad (2)$$

In case $T = \infty$ we assume that $h_i = 0$.

Under the assumption that the players cooperate in trying to minimize their performance, we look for a set of control actions \hat{u} that are such that the resulting individual cost cannot be improved upon by all players simultaneously. The so-called Pareto efficient solutions.

In literature a well-known way to find Pareto solutions is to solve a parameterized optimal control problem (see e.g. [4], [2], [5]). However, in general, it is unclear whether in this way one obtains all Pareto solutions. Here, we present for problem (1,2) necessary conditions for a control to be Pareto efficient and discuss additional conditions from which one can conclude that these necessary conditions are sufficient too. These conditions are in the spirit of the maximum principle.

As far as we know these conditions have not been stated explicitly in the literature before.

It is well-known in optimal control problems that for problems dealing with an infinite planning horizon in general the

corresponding finite-planning horizon transversality conditions do not apply. Only under some additional restrictions on the system and cost functions these transversality conditions continue to hold. We present here restrictions frequently encountered in ordinary optimal control problems, under which the transversality conditions apply in this setting too. We illustrate the main results by some examples.

References

- [1] Engwerda J.C., 2009. Necessary and Sufficient Conditions for Pareto Optimal Solutions of Cooperative Differential Games. Submitted for publication.
- [2] Leitmann G., 1974. *Cooperative and Non-cooperative Many Players Differential Games*. Springer Verlag, Berlin.
- [3] Reddy P.V. and Engwerda J.C., 2010. Necessary and Sufficient Conditions for Pareto Optimality in Infinite Horizon Cooperative Differential Games. To appear in *Contributions to Game Theory and Management*, Vol.3. Editors Leon A. Petrosjan, Nikolay A. Zenkevich, St. Petersburg, Russia.
- [4] Starr A.W. and Ho Y.C., 1969. Nonzero-sum differential games. *Journal of Optimization Theory and Applications*, Vol.3, pp.184-206.
- [5] Yeung D.W.K and Petrosyan L.A., 2005. Subgame consistent solutions of a cooperative stochastic differential game with nontransferable payoffs. *Journal of Optimization Theory and Applications*, Vol.124, pp.701-724.

Model-Free Monte-Carlo like Policy Evaluation

Raphael Fonteneau
Department of EECS
University of Liège
BELGIUM

Susan Murphy
Department of Statistics
University of Michigan
USA

Louis Wehenkel
Department of EECS
University of Liège
BELGIUM

Damien Ernst
Department of EECS
University of Liège
BELGIUM

1 Introduction

We propose an algorithm for estimating the finite-horizon return of a closed loop control policy from an a priori given (off-policy) sample of one-step transitions [1]. It averages cumulated rewards along a set of “broken trajectories” made of one-step transitions selected from the sample on the basis of the control policy. Under some Lipschitz continuity assumptions on the system dynamics, reward function and control policy, we provide bounds on the bias and variance of the estimator that depend only on the Lipschitz constants, on the number of broken trajectories used in the estimator, and on the sparsity of the sample of one-step transitions.

2 Monte-Carlo policy evaluation

Discrete-time stochastic optimal control problems arise in many fields such as finance [2], medicine [3], engineering [4] as well as artificial intelligence [5]. Many techniques for solving such problems use an oracle that evaluates the performance of any given policy in order to navigate rapidly in the space of candidate optimal policies to a (near-)optimal one. When the considered system is accessible to experimentation at low cost, such an oracle can be based on a Monte-Carlo (MC) approach. With such an approach, several “on-policy” trajectories are generated by collecting information from the system when controlled by the given policy, and the cumulated rewards observed along these trajectories are averaged to get an unbiased estimate of the performance of that policy. However if obtaining trajectories under a given policy is very costly, time consuming or otherwise difficult, e.g. in medicine or in safety critical problems, the above approach is not feasible.

3 Model-free Monte-Carlo policy evaluation

In this paper, we propose a policy evaluation oracle in a *model-free* setting. In our setting, the only information available on the optimal control problem is contained in a sample of one-step transitions of the system, that have been gathered by some arbitrary experimental protocol, i.e. independently of the policy that has to be evaluated. Our estimator is inspired by the MC approach. Similarly to the MC estimator, it evaluates the performance of a policy by the average of the cumulated rewards along some trajectories. However, rather than “real” on-policy trajectories of the system generated by fresh experiments, it uses a set of “broken trajectories” that

are rebuilt from the given sample and from the policy that is being evaluated.

4 Preliminary results

Under some Lipschitz continuity assumptions on the system dynamics, reward function and policy, we provide bounds on the bias and variance of our model-free policy evaluator, and show that it behaves like the standard MC estimator when the sample sparsity decreases towards zero. These theoretical properties are illustrated with some promising simulations results.

References

- [1] R. Fonteneau, S. Murphy, L. Wehenkel, and D. Ernst, “Model-free Monte-Carlo like policy evaluation,” *Submitted*, 2010.
- [2] J. Ingersoll, *Theory of Financial Decision Making*. Rowman and Littlefield Publishers, Inc., 1987.
- [3] S. Murphy, “Optimal dynamic treatment regimes,” *Journal of the Royal Statistical Society, Series B*, vol. 65(2), pp. 331–366, 2003.
- [4] D. Bertsekas and J. Tsitsiklis, *Neuro-Dynamic Programming*. Athena Scientific, 1996.
- [5] R. Sutton and A. Barto, *Reinforcement Learning*. MIT Press, 1998.

ACADO Toolkit – An open-source framework for Automatic Control and Dynamic Optimization

Hans Joachim Ferreau, Boris Houska, Moritz Diehl

Electrical Engineering Department (ESAT-SCD) and Optimization in Engineering Center (OPTEC),

K.U. Leuven, Kasteelpark Arenberg 10, 3001 Leuven, Belgium

e-mail: {joachim.ferreau,boris.houska,moritz.diehl}@esat.kuleuven.be

1 Introduction

The last decades have seen a rapidly increasing number of applications where control techniques based on dynamic optimization lead to improved performance. These techniques use a mathematical model in form of differential equations of the process to be controlled to predict its future behavior and calculate optimized control actions. This is performed either offline or online and the numerical solution of optimal control problems is the main algorithmic step within such advanced controllers. Thus, efficient and reliable optimization algorithms for performing this step—possibly on embedded hardware—are of great interest.

Several of those optimization algorithms have been implemented, among them IPOPT, MUSCOD-II, PROPT and dsoa. Moreover, dedicated software packages for model predictive control in the process industry exist. Each of the above packages has its particular strengths for a specific range of applications. However, their software design is tailored to a certain choice of underlying numerical algorithms, which renders it difficult to combine algorithmic ideas from different packages or to extend them with new mathematical concepts. Also do most of these packages require a sound knowledge of programming in C/C++ for using them.

To overcome these issues, the ACADO Toolkit [1] is an efficient implementation that meets the following four key properties:

- The software is *open-source* distributed under the GNU LGPL. This allows researchers to reproduce all results and to try out own modifications.
- The software allows to formulate optimal control problems in a very intuitive and *user-friendly* manner. Also non-experts should be able to formulate their control problems within short time.
- The software design allows for *code extensions* by either linking existing algorithms or by using it as a platform for new developments.
- The ACADO Toolkit is written in a completely *self-contained* manner. This feature is particularly crucial for applications on embedded hardware.

This talk outlines the philosophy and numerical algorithms that are implemented within the ACADO Toolkit.

2 Scope of the Software

ACADO Toolkit 1.0 highlights three important problem classes. The first problem class are offline dynamic optimization problems, where the aim is to find an open-loop control which minimizes a given objective functional. The second class are parameter and state estimation problems, where parameters or unknown control inputs should be identified by measuring an output of a given nonlinear dynamic system. The third class are combined online estimation and model predictive control problems, where parameterized dynamic optimization problems have to be solved repeatedly to obtain a dynamic feedback control law.

Each of these classes leads to a specially structured variant of the following standard optimal control problem:

$$\begin{aligned} & \underset{x(\cdot), z(\cdot), u(\cdot), p, T}{\text{minimize}} && \int_0^T L(\tau, x(\tau), z(\tau), u(\tau), p, T) d\tau \\ & && + M(x(T), z(T), p, T) \\ & \text{subject to} && \\ \forall t \in [0, T]: & \dot{x}(t) &= & f(t, x(t), z(t), u(t), p, T) \\ \forall t \in [0, T]: & 0 &= & g(t, x(t), z(t), u(t), p, T) \\ & & & 0 = r(x(0), z(0), x(T), z(T), p, T) \\ \forall t \in [0, T]: & 0 &\geq & s(t, x(t), z(t), u(t), p, T) \end{aligned}$$

with differential states x , time varying control inputs u , time constant parameters p , and possibly algebraic states z and free end time T .

Extensions to multi-stage formulations, robust optimization and optimal control problems comprising a multi-objective formulation are currently under development.

3 Download

ACADO Toolkit 1.0 is open-source software and freely available at <http://www.acadotoolkit.org>.

References

- [1] B. Houska, H.J. Ferreau, and M. Diehl. ACADO Toolkit – An Open Source Framework for Automatic Control and Dynamic Optimization. *Optimal Control Applications and Methods* (submitted).

Flood control of the Demer with model predictive control

Maarten Breckpot, Toni Barjas Blanco and Bart De Moor

K.U.Leuven, Department of Electrical Engineering (ESAT), SCD-SISTA,

Kasteelpark Arenberg 10, 3001 Leuven, Belgium

{maarten.breckpot,toni.barjas-blanco, bart.demoor}@esat.kuleuven.be

1 Introduction

Floodings are in Europe the most occurring natural disaster. Historical data demonstrate an overall increase in Europe. The Demer, a river in Belgium, has in this context a bad reputation. The Demer often floods during periods of heavy rainfall. In the sixties of last century, counter measures were taken by the local water authority by expanding the storage capacity of the river with flood basins. They installed hydraulic gates to control the flow of water from the river into these basins and vice versa. These hydraulic structures are controlled by an advanced three-position controller. These constructions could not prevent the Demer from flooding again in 1998 and 2002. The main reason for this is that the controller does not take the rain forecasts into account. Therefore the control actions are often suboptimal which forces the operator to overrule. This introduces subjectivity and is dependent of the experience of the operator. This study shows that these drawbacks can be overcome with model predictive control (MPC) and that much better results can be achieved.

2 Model predictive control and flood control

MPC is a control strategy originating from the process industry and is nowadays used in various applications going from chemicals and food processing to automotive and aerospace applications [3]. MPC uses a process model to predict the future process outputs within a specified prediction horizon. MPC solves an optimization problem over this horizon to determine the optimal inputs for the process taking input and output constraints, future disturbances and the process model into account. Only the first input sample of the complete optimal sequence is applied to the process, new samples are taken and the entire procedure is repeated.

Because MPC uses a prediction horizon, it is possible to incorporate the rain predictions in a naturally way. Another advantage is the use of a mathematical model of the river. This makes it possible for the controller to calculate a solution that is optimal for the entire system. This is much better than the solution of the current controller since it only controls the hydraulic structures based on the local water levels close to the structures. The models of the Demer used in this study were provided by the Department of Civil Engineering of the K.U.Leuven. The models are nonlinear state space models which describe the relations between the wa-

ter levels, the volumes, the discharges and the height of the gates. Because of the strong nonlinearities over the range of operation, the model cannot be accurately approximated by one linear model. Therefore it is necessary for flood control to use nonlinear model predictive control. The strategy used in this study is to relinearize the model around the current and the predicted states of the river at each time step and to use these linear models for the optimization problem [2].

3 Results and conclusions

The controller is implemented with the INCA Software of the company IPCOS¹. When there is no uncertainty on the rain predictions the implemented controller outperforms the current control structure. Because MPC takes these predictions into account it uses the available buffer capacity of the basins in a more optimal way. This results in a significant reduction in the number and the height of the floodings [1]. After expanding the MPC controller into a Multiple MPC controller, the controller can successfully deal with uncertainty on the rain predictions and the same conclusions can be made [4].

Until now there is assumed that there is no plant-model mismatch and every state of the river is known at every time sample. Future work will focus on these two topics.

References

- [1] M. Breckpot, "Flood control of the Demer with model predictive control", thesis, Leuven, Belgium, 2009.
- [2] E. Camacho and C. Bordons, "Nonlinear Model Predictive Control: an Introductory Survey" in *Int. Workshop on Assessment and Future Directions of NMPC*, Freudenstadt-Lauterbad, Germany, Aug 2005.
- [3] S. Qin and T. Badgwell, "A survey of industrial model predictive control technology", *Control Engineering Practice*, 7:733-764, 2003.
- [4] P. van Overloop, S. Weijs and S. Dijkstra, "Multiple Model Predictive Control on a drainage canal system", *Control Engineering Practice*, 16:531-540, May 2008.

Acknowledgements

Maarten Breckpot and Toni Barjas Blanco are research assistants at the Katholieke Universiteit Leuven, Belgium. Dr. Bart De Moor is a full professor at the Katholieke Universiteit Leuven, Belgium. Research supported by Research Council KUL: GOA AMBioRICS, GOA MaNet, CoE EF/05/006 Optimization in Engineering(OPTEC), IOF-SCORES4CHEM, several PhD/postdoc & fellow grants; Flemish Government: FWO: PhD/postdoc grants, projects G.0452.04, G.0499.04, G.0211.05, G.0226.06, G.0321.06, G.0302.07, G.0320.08, G.0558.08, G.0557.08, G.0588.09 research communities (ICCoS, ANMMM, MLDM); G.0377.09; IWT: PhD Grants, McKnow-E, Eureka-Flite+, SBO LeCoPro, SBO Climaqs, POM; Belgian Federal Science Policy Office: IUAP P6/04 (DYSCO, Dynamical systems, control and optimization, 2007-2011); EU: ERNSI; FP7-HD-MPC (INFOS-ICT-223854), COST intelliCIS, EMBO-COM; Contract Research: AMINAL; Other: Helmholtz: viCERP, ACCM, Bauknecht, Hoerbiger;

¹www.ipcos.be

Optimal Shifting Strategy for a Parallel Hybrid Electric Vehicle

D.V. Ngo*, T. Hofman*, M. Steinbuch*, A. Serrarens**

* *Department of Mechanical Engineering, Eindhoven University of Technology
PO Box 513, 5600 MB Eindhoven, The Netherlands*

Corresponding author email: d.v.ngo@tue.nl

** *Drivetrain Innovations B.V, Croy 46, 5653 LD Eindhoven, The Netherlands*

1. Introduction

Control strategies for Hybrid Electric Vehicles (HEVs) are generally aimed at optimally choosing power split ratio between the internal combustion engine and the electric motor in order to minimize the fuel consumption. However, for a given drive cycle, the operating points of the hybrid driveline are not only defined by power split ratio but also defined by gear position of the transmission.

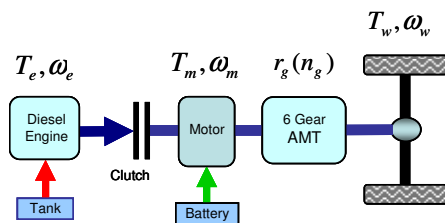


Figure 1: Parallel Hybrid Electric Vehicle topology

In this paper, an optimal shifting strategy based on Dynamic Programming (DP) is proposed for the energy management system of a parallel HEV (see Fig.1) to explore the potential fuel saving by optimizing both the power split ratio and the gear shifting. Then a gradient-based optimal control algorithm is formulated for this optimization problem in comparison of the optimal results and computational performance with that of DP method.

2. Control algorithms

The control problem is to minimize the cost function J of fuel consumption over a drive cycle. It is formulated as follows:

$$u^*(t) = \min_{u(t)} J$$

$$\text{where in: } J = \int_0^{t_f} \dot{m}_f(x(t), u(t)) dt$$

subject to constraints:

$$\dot{x}(t) = f(x(t), u(t)),$$

$$G(x(k)) < 0,$$

wherein: $x(t)$ and $u(t)$ are the state vector and control vector of the powertrain dynamics respectively; $\dot{m}_f(x(t), u(t))$ is the fuel rate; $f(x(t), u(t))$ and $G(x(t))$ are the constraints on the dynamics and operating range of physical components of the system respectively.

The problem is solved by using DP method for global optimal results of battery power command and gear position. In dealing with computational burden occurring

with DP, a gradient-based optimal control algorithm is proposed for this optimization based on the approximated hybrid powertrain model.

3. Simulation results

A mild parallel HEV configuration is chosen in this study. Simulations are performed on New European Drive Cycle (NEDC) along with a prescribed gear shift schedule. The results, in Table 1, show that by optimal controlling the gear shifting, fuel saving can be relatively added up to 10.5% compared to the case of not optimizing the gear position. By using a gradient-based optimal control, fuel economy is nearly equivalent to the case of DP algorithm, but the computational burden is reduced significantly.

Algorithms	Fuel		Computation time(s)
	(gr)	(%)	
Conventional vehicle, using prescribed gear shift	471.29	-	-
HEV, optimizing power ratio by DP, using prescribed gear shift	416.08	11.7	341
HEV, optimizing power ratio and gear shifting by DP	370.92	21.3	2146
HEV, optimizing power ratio and gear shifting by gradient-based optimal control	369.05	21.7	44

Table 1: Simulation results

4. Future research

Analyze engine braking power and its effect on the energy management strategy during regenerative phase.

Optimizing the velocity profile for this hybrid vehicle over a preview route segment to earn more fuel economy is the focus of future research.

References:

- [1] L. Guzzella, A. Sciarretta; "Vehicle Propulsion Systems Introduction to Modeling and Optimization"; Springer, the 2nd ed., 2007, XII.
- [2] M. Koot, J. T. B. A. Kessels, B. de Jager, W. P. M. H. Heemels, P. P. J. van den Bosch and M. Steinbuch; "Energy Management Strategies for Vehicular Electric Power Systems"; *IEEE Trans. Veh. Technol.*, vol. 54, pp. 771, May 2005.
- [3] S. Delprat, J. Lauber, T. M. Guerra, and J. Rimaux; "Control of a parallel hybrid powertrain: optimal control"; *IEEE Trans. Veh. Technol.*, vol. 53, no. 3, pp. 872-881, May 2004.

Robust fixed-order controller design for time-delay systems with application to the milling process

Niels van Dijk*, Nathan van de Wouw and Henk Nijmeijer
 Department of Mechanical Engineering, Eindhoven University of Technology
 P.O. Box 513, 5600 MB Eindhoven, The Netherlands
 Email: *N.J.M.v.Dijk@tue.nl

Introduction

Controller design for systems with one or more time delay can be a difficult task. Due to the infinite dimensional character of a time-delay system, standard (robust) control techniques cannot be applied to time-delay systems. The goal of this study is to develop a robust control strategy for systems with (one or more) time-delays.

Approach

Let us consider the following uncertain linear time-delay model with one delay,

$$\begin{aligned}\dot{\underline{x}}(t) &= \mathbf{A}_0 \underline{x}(t) + \mathbf{A}_1 \underline{x}(t - \tau - \delta\tau) + \mathbf{B} \underline{u}(t), \\ \underline{y}(t) &= \mathbf{C} \underline{x}(t),\end{aligned}\quad (1)$$

where $\mathbf{A}_0 = (A_0 + \delta A_0)$ and $\mathbf{A}_1 = (A_1 + \delta A_1)$. As described in [1] the uncertain system (1) can be represented as a feedback interconnection between

$$\begin{aligned}\dot{\underline{x}}(t) &= A_0 \underline{x}(t) + A_1 \underline{x}(t - \tau) + [D_0, B_1 \tilde{D}_1, B_1 \tilde{A}_1]^T \underline{q}(t) \\ &\quad + \mathbf{B} \underline{u}(t) \\ \underline{y}(t) &= \mathbf{C} \underline{x}(t), \\ \underline{p}(t) &= [E_0 \underline{x}(t), \tilde{E}_1 C_1 \underline{x}(t - \tau) + q_3(t), -C_1 \dot{\underline{x}}(t)]^T\end{aligned}\quad (2)$$

and uncertainties

$$\underline{q}(t) = \left[\delta \bar{A}_0 p_1(t), \delta \bar{A}_1 p_2(t), \frac{1}{w} \int_{t-\tau-\delta\tau}^{t-\tau} p_3(\lambda) d\lambda \right]^T \quad (3)$$

where $\delta A_0 = D_0 \delta \bar{A}_0 E_0$, $(A_1 + D_1 \delta \bar{A}_1 E_1) = B_1 (\tilde{A}_1 + \tilde{D}_1 \delta \bar{A}_1 \tilde{E}_1) C_1$ and $w > 0$ a scaling parameter. Consider a dynamic linear feedback control law,

$$\dot{\underline{\xi}}(t) = A_c \underline{\xi}(t) + B_c \underline{y}(t), \quad \underline{u}(t) = C_c \underline{\xi}(t) + D_c \underline{y}(t). \quad (4)$$

The problem now is to find controller matrices $K = (A_c, B_c, C_c, D_c)$ such that the origin is an asymptotic stable equilibrium of (1) for given uncertainties δA_0 , δA_1 and delay range $\delta\tau$. Or, stated differently, find K such that $\sup_{\omega \geq 0} \mu_{\Delta} P(j\omega, K) < 1$ where $P(j\omega, K)$ denotes the Laplace transform of the lower fractional transformation between (2) and (4) and Δ the Laplace transform of (3), scaled such that $\|\Delta\|_{\infty} \leq 1$. In general μ_{Δ} is difficult to compute. Hereto, the scaled singular value $\min_{D \in \mathcal{D}} \bar{\sigma}(DPD^{-1})$, which

is an upper bound on $\mu_{\Delta}(P)$, is used instead. Then the problem becomes to find D and K such that,

$$\sup_{\omega \geq 0} \bar{\sigma}(DP(j\omega, K)D^{-1}) < 1 \quad (5)$$

which is solved by iterating over D and K . The K -step in this iterative process is a nonsmooth/nonconvex optimisation problem which is solved by using the algorithm as presented in [2].

Application example: the milling process

The occurrence of chatter limits the performance of the milling process and results in heavy vibrations of the cutter and an inferior workpiece quality. One way to increase the performance of the milling process is to use an active control strategy that increases stability of the process for a range of operating points.

Next we apply the control strategy to design a static output-feedback controller that robustly stabilises (i.e. guarantees chatter-free operation) a milling model [3] in a range of spindle speeds and depths of cut.

Figure 1 depicts the stability diagram of a particular milling model [3] with and without control. Note that the control indeed stabilises the range of operating conditions desired.

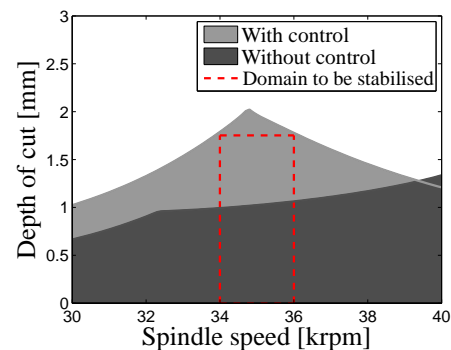


Figure 1: Stability diagram with and without chatter control.

References

- [1] W. Michiels et al., Robustness assessment via stability radii in delay parameters, *Int. J. Rob. Nonlin. Control*, 19 (13), 2009, 1405-1426.
- [2] J.V. Burke et al. A robust gradient sampling algorithm for nonsmooth, nonconvex optimization, *SIAM J. Optim.*, 15(3), 2005, 751-779.
- [3] R.P.H. Faassen, Chatter prediction and control for high speed milling: modelling and experiments, Ph.D. Thesis, Eindhoven University of Technology (2007)

Accurate Oscillometric Blood Pressure Measurement: an Experimental Approach

Kurt Barbé¹, Wendy Van Moer¹, Lieve Lauwers¹ and Danny Schoors²

¹ Dept. ELEC, Vrije Universiteit Brussel, Pleinlaan 2, B-1050 Brussels, Belgium

² Dept. CHVZ, VUB-UZ Brussel, Laarbeeklaan 101, B-1090 Brussels, Belgium

Email: kurt.barbe@vub.ac.be

1. Introduction

One of the most popular medical instruments is the automatic blood pressure meter (BPM). A lot of medicine cupboards contain one and a lot of people use it on a daily basis. Although this measurement instrument is commercially available and widely spread, physicians refuse to use them, due to the poor accuracy of these instruments.

A classical automatic blood pressure meter is based on the oscillometric principle, which records the oscillations in the cuff pressure during the measurement (see figure 1 [1]). Out of this oscillometric waveform a mean arterial pressure as well as a systolic and diastolic pressure is deduced. Each manufacturer of blood pressure meters has developed his proper algorithm which is most of the time patented. However, in general, the systolic and the diastolic pressure are defined as a certain percentage of the mean arterial pressure, [2]. The mean arterial pressure

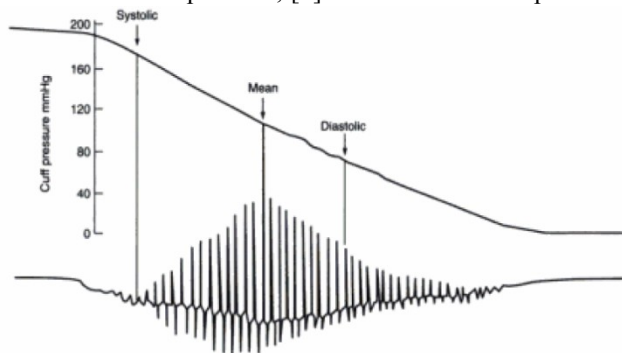


Figure 1: Oscillometric blood pressure waveform

is defined as the maximum of the envelope of the oscillometric waveform.

In order to obtain more accurate measurements, a more robust algorithm must be developed which also takes into account the physical phenomena behind the oscillometric waveform. The final goal is to develop a validation procedure for automatic blood pressure meters.

2. Measurement Campaign

Measuring is knowing. And before one can start to develop a new algorithm, accurate measurements are needed. Therefore the following measurement campaign will be conducted. The blood pressure of 100 patients will be measurement by an automatic blood pressure meter as well as by the classical Korotkoff method [3], where a physician listens through a stethoscope to the Korotkoff sounds. This is referred to as the auscultatory method. In a first measurement, the oscillometric method will be used on the left arm and the auscultatory method on the right.

After 5 minutes the measurement will be repeated but the arms will be switched. This is to omit the difference in blood pressure that exists between both arms. The patients will be selected so that no confounding effects among the patients are possible. The auscultatory measurement will be considered as the golden standard.

3. Mathematical algorithm

Instead of defining the systolic and diastolic pressures as fixed percentages of the mean arterial pressure, we shall use the definition where the systolic and diastolic pressures are defined as the inflexion points of the envelope of the oscillometric waveform, [4].

This brings us to two major theoretical challenges: (i) Can we parametrically estimate the inflexion points in a maximum likelihood framework from the sampled envelope of the oscillometric waveform? (ii) Can we link, by physical laws of pressure, the inflexion points to the Korotkoff sounds which are induced by turbulences in the arteries?

The first problem implies that there is a need for a statistical model for the oscillometric waveform. The second problem is difficult because we are dealing with non-Newtonian fluids in particular blood.

4. Conclusion

In this paper, we discussed a seemingly simple modeling problem to identify the systolic and diastolic blood pressures. To apply oscillometric measurements for more sophisticated medical applications a proper statistical framework should be defined. Furthermore, the relation between oscillometric measurement and the classical Korotkoff methods should be fully explored to being confident that the physician and the automated method are measuring the same quantity.

References

- [1] T. Tien, A. Adiyaman, J. A. Staessen, and J. Deinum, "Bloodpressure measurements in the year 2008: revival of oscillometry?," *The Netherlands Journal of Medicine*, vol. 66, no. 11, pp. 453-456, Dec. 2008.
- [2] A. Ball-llovera, et al., "An Experience in Implementing the Oscillometric Algorithm for the Non-Invasive," in *The 25th Annual International Conference of the IEEE EMBS*, Cancun, Mexico, 2003, pp. 3173-3175.
- [3] M. Turner, C. Speechly, and N. Bignell, "Sphygmomanometer calibration – why, how and how often?," *Australian Family Physician*, vol. 36, no. 10, pp. 834-837, Oct. 2007.
- [4] G. Drzewiecki, "Noninvasive assessment of arterial blood pressure and mechanics," in *The biomedical engineering handbook*. Boca Raton, USA: CRC Press, 1995, ch. 71, pp. 1196-1211.

Design of a teleoperated palpation device for minimally invasive thoracic surgery

Angelo Buttafuoco, Amaury Dambour, Thomas Delwiche and Michel Kinnaert
 Université Libre de Bruxelles (U.L.B.)
 50, Av. F.D. Roosevelt-CP 165/55, B-1050 Brussels, Belgium
 angelo.buttafuoco@ulb.ac.be, michel.kinnaert@ulb.ac.be

1 Introduction

Minimally invasive surgery (MIS) consists in operating through small incisions in which a camera and adapted instruments are inserted. It allows to perform many interventions with reduced trauma for the patient. One of these is the ablation of peripheral pulmonary nodules [1].

Nevertheless, the means for detecting nodules during MIS are limited. In fact, because of the lack of direct contact, the surgeon cannot palpate the lung to find invisible lesions, as he would do in classical open surgery. As a result, only clearly visible nodules can be treated by MIS presently.

2 The palpation device

Our work aims at designing, building and the controlling a teleoperated palpation instrument, in order to extend the possibilities of MIS in the thoracic field. Such an instrument is made of a master device, manipulated by an operator, and a slave device which is in contact with the patient and reproduces the task imposed by the master. Adequate control laws between these two parts allow to restore the operator's haptic sensation [2].

The principle of the palpation instrument (see fig.1) has been established through experiments with thoracic surgeons. The main goals were to identify the most efficient gestures performed by the surgeons during palpation and the kind of information needed when looking for hidden nodules. The results showed that for instruments providing at least 2 degrees of freedom (dof) the kinaesthetic information alone is sufficient. Moreover, the forces applied on the lung do not exceed 12N in compression and 2N in shear. In consequence, the device can be provided with ordinary DC motors.

A pantograph has been designed to be used as the master of the palpation device, since this kind of architecture provides good ergonomics and low inertia. The length of each link has been optimized in order to maximize the manipulability of the device within its workspace. A 2 dof force sensor has also been designed and integrated to the pantograph so that the force applied by the operator can be measured.

The slave device has been designed as a 2 dof clamp, which can be actuated in compression and shear. The form of each

part of the clamp has been chosen so that the forces applied on it can be measured with strain gages. Notice that all the miniaturization issues for MIS have not been taken into account at this point. Both the master and the slave are still under construction.

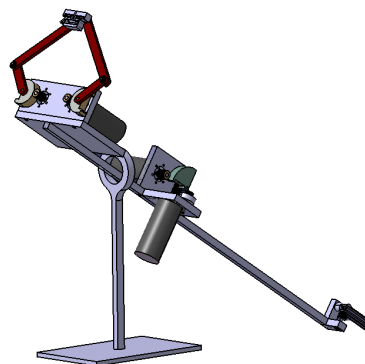


Figure 1: Teleoperated palpation device

3 Future work

The following steps will see further experiments with the surgeons to validate the design of the palpation device and the development of control laws that best suit the needs of palpation [3]. The last part of the project will be dedicated to the miniaturization of the device to meet MIS exigences.

Acknowledgments

The work of Angelo Buttafuoco is supported by a FRIA grant. The experimental setup is financed by the FNRS. This paper presents research results of the Belgian Network DYSCO (Dynamic Systems, Control and Optimization), funded by the Interuniversity Attraction Poles Programme, initiated by the Belgian State, Science Policy Office. The scientific responsibility rests with its authors.

References

- [1] J. Lin, M.D. Iannettoni, The role of thoracoscopy in the management of lung cancer, In *Surgical Oncology*, vol. 12, pp. 195–200, 2003.
- [2] P.F. Hokayem, Bilateral teleoperation : an historical survey, In *Automatica*, vol. 42, pp. 2035–2047, 2006.
- [3] M.C. Cavusoglu, Bilateral Controller Design for Telemanipulation in Soft Environments, In *Proceedings of the 2001 IEEE International Conference on Robotics and Automation*, 2001.

Selection of circadian clock models for robust entrainment: an analysis based on the phase response curve

Pierre Sacré*, Marc Hafner†, Heinz Koepl† and Rodolphe Sepulchre*

*Department of Electrical Engineering and Computer Science, University of Liège, Belgium

†School of Computer and Communication Sciences, EPFL, Switzerland

1 Introduction

Robustness is a ubiquitously observed feature of biological systems. Broadly speaking, this property allows a system to maintain its function despite external and/or internal perturbations. Currently, it is widely believed that the specific structure of a biological control network is responsible for its dynamic behavior and its robust performance. However, the actual mechanisms are still not clear, even in genetic circuits of moderate complexity.

Autonomous oscillations provided by circadian clock architectures have been widely studied in the literature in terms of local and global sensitivity analyses [1, 2]. Nevertheless, the main feature of circadian clocks is their ability to be entrained by the daily light/dark rhythm.

In this research, our goal is to understand how oscillator architectures influence the paradoxical relationship between entrainment (sensitivity to a periodical input) and robustness (insensitivity to perturbations). This general idea is illustrated on particular models of circadian rhythms [3, 4].

2 Combined global and local analyses

We develop a method that combines global and local analyses to quantify the robustness of biochemical oscillator models [5]. A global approach identifies the ‘viable’ region of the high-dimensional parameter space where a circuit displays an experimentally observed behavior. The local analysis separates the viable parameter sets in particular subsets (sensitivity, stability, etc.). The combination of those global and local analysis helps to derive properties linked to network structure.

3 Phase response curve

In mathematical biology, the phase response curve (PRC) has proven to be a useful tool to study the input-output properties of oscillators. It tabulates the steady state phase shift that results from a particular input as a function of the phase at which it is received.

Representative PRCs of circadian oscillators for light pulses exhibit delay phase shifts in the early subjective night, and advance phase shifts in the late subjective night, and little phase shifts during the subjective day.

4 Discriminating between architectures based on the PRC

We currently investigate whether the PRC can be exploited to define qualitative and quantitative measures of the entrainment and then used as a discriminant criterion for the model selection.

Our comparative analysis focuses on two moderately complex models of circadian rhythms in *Drosophila*. The simpler model contains a single negative feedback loop [3] and the more complex model describes both branches of negative feedback [4].

References

- [1] Jörg Stelling, Ernst Dieter Gilles, and Francis J Doyle III. Robustness properties of circadian clock architectures. *P Natl Acad Sci USA*, 101(36):13210–5, Sep 2004.
- [2] Neda Bagheri, Jorg Stelling, and Francis J Doyle III. Quantitative performance metrics for robustness in circadian rhythms. *Bioinformatics*, 23(3):358–364, Feb 2007.
- [3] Albert Goldbeter. A model for circadian oscillations in the *Drosophila* period protein (PER). *P Roy Soc Lond B Bio*, 261(1362):319–324, Sep 1995.
- [4] Jean-Christophe Leloup and Albert Goldbeter. A model for circadian rhythms in *Drosophila* incorporating the formation of a complex between the PER and TIM proteins. *J Biol Rhythms*, 13(1):70–87, Feb 1998.
- [5] Marc Hafner, Heinz Koepl, Martin Hasler, and Andreas Wagner. ‘Glocal’ robustness analysis and model discrimination for circadian oscillators. *PLoS Comput Biol*, 5(10):e1000534, Oct 2009.

Acknowledgements

This work was supported by the Belgian National Fund for Scientific Research (FNRS) through a Research Fellowship at the University of Liège. This paper presents research results of the Belgian Network DYSCO (Dynamical Systems, Control and Optimization), funded by the Interuniversity Attraction Poles Programme, initiated by the Belgian State, Science Policy Office. The scientific responsibility rests with its authors.

Modeling orienting eye movements

Sebastien Coppe
CESAME and IoNS

Universite catholique de Louvain (UCL)
Av. G. Lemaitre 4, 1348 Louvain la Neuve
Belgium

Email: sebastien.coppe@uclouvain.be

Gunnar Blohm

Centre for Neuroscience Studies
Queen's University

Stuart Street 18, Kingston, Ontario, K7L 3N6
Canada

Email: blohm@biomed.queensu.ca

Jean-Jacques Orban de Xivry

Biomedical Engineering Department
Johns Hopkins University
Rutland Ave 720, MD 21205 Baltimore
USA

Email: jean-jacques.orban@jhu.edu

Philippe Lefevre

CESAME and IoNS

Universite catholique de Louvain (UCL)
Av. G. Lemaitre 4, 1348 Louvain la Neuve
Belgium

Email: philippe.lefevre@uclouvain.be

The objective of this study was to implement a model which could illustrate the orienting eye movements of human subjects. This model generates the two main types of orienting eye movements, the fast movements (saccades) and the slow movements (pursuit). In the literature, there is no model illustrating the detailed interactions between those two types of eye movements, for example to determine the switch between fast and slow systems.

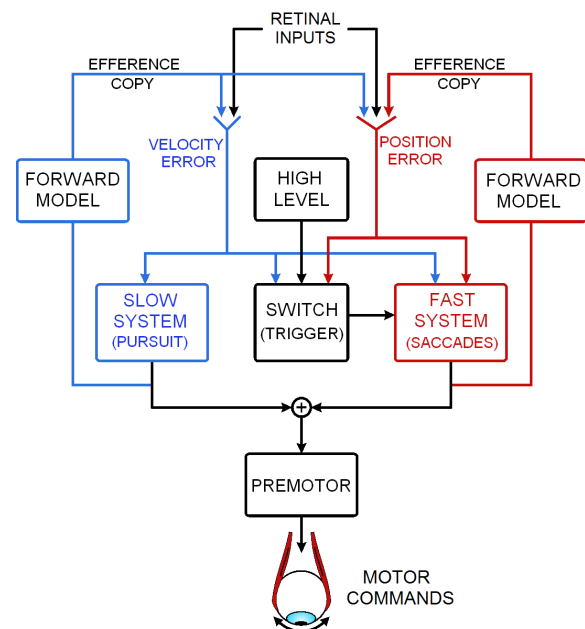
It is important to emphasize the fact that there are important delays (more than 100 ms) in visual sensory signals. One way to deal with these delays is to have a good interaction between the two systems. Another way is to use prediction to anticipate target movement. These predictive mechanisms are also used in absence of visual stimuli, for example during temporary blanking of the target, and need as well an efficient interaction between fast and slow systems.

The model proposed here takes into account recent experimental results in order to explain the behavior of a normal subject performing a visual tracking task. A major issue in the interaction between fast and slow systems is to know what triggers catch-up saccades. An important parameter for the saccade trigger is the estimation of the time at which the eye will cross the target. If this estimation of the eye-crossing time is too short or too long, the subject will execute in most of the cases a catch-up saccade.

In our model, retinal inputs are used to estimate both position error and velocity error. These two inputs do not share the same areas and the same pathways in the brain. These estimations are then processed by the fast and slow systems into motor commands. In parallel, the decision to trigger or not a saccade is taken. In addition, the predictive mechanisms are based on an internal forward model. It means that the brain can estimate the future position and veloc-

ity errors without visual stimulus, by coupling the previous movements of the eyes (obtained from an efference copy) and an estimation of the movement of the target.

This model could facilitate the interpretation of new experimental results, based on its theoretical predictions. It could also guide future experimental research.



Schema of the oculomotor system (adapted from [1])

References

- [1] Orban de Xivry JJ and Lefevre P (2007). "Saccades and pursuit: two outcomes of a single sensorimotor process". *J Physiol* 584, 11-23.

The visuomotor transformation of velocity signals in visually guided manual tracking when the eye is in motion

Guillaume Leclercq

CESAME and IoNS, Université catholique de Louvain
Avenue Georges Lemaitre 4, 1348 Louvain-la-Neuve, Belgium
Email: guillaume.leclercq@uclouvain.be

Gunnar Blohm

Centre for Neuroscience Studies, Queen's University
Stuart Street 18, Kingston, Ontario, K7L 3N6, Canada

Philippe Lefèvre

CESAME and IoNS, Université catholique de Louvain

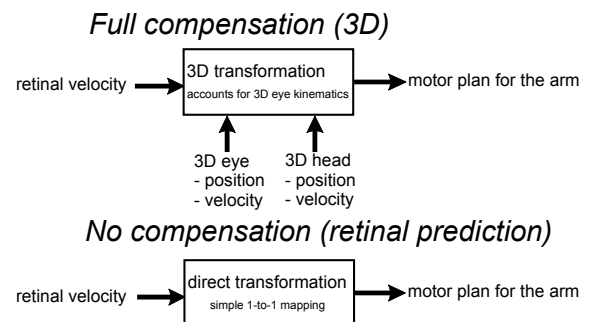
Visually guided arm movements are common actions carried out each day in our everyday life, like reaching out to our cup of coffee, playing tennis, or driving a car. When performing visually guided arm movements, the brain needs to transform the visual information (the tennis ball, an obstacle) into an appropriate motor plan for the arm [1] (i.e. a command to drive the arm's muscles). It is known that for arm movements, the brain accounts for the 3D eye-head-shoulder geometry when transforming position [2] or velocity signals [4] (knowing that position and velocity signals are processed by different neural pathways in the brain [3]). In these experiments, the eyes and head were static during the task. But new implications arise if the eye and/or head is moving during the task, which frequently happens in everyday life (for example, when walking or driving a car). Here, we investigated if the brain accounted for the 3D eye kinematics in the visuomotor transformation of velocity signals for manual tracking movements.

A visuomotor transformation model taking into account the complete 3D eye-on-head and head-on-shoulder kinematics (see figure, top panel) was developed using dual quaternions. Model predictions show that 3D eye velocity signals are needed in order to transform the retinal velocity input into a spatially accurate motor plan. Specifically, the model predicts that the brain must compensate for non-linear errors induced by differences in eye and target 1) directions and 2) velocities. The alternative model (see figure, lower panel) only uses retinal information and thus leads to errors in the predicted initial direction of the arm, which could in theory be corrected using delayed visual feedback.

To test our predictions, eight human subjects performed manual tracking movements while pursuing another target with the eyes with the head upright and fixed. We compared the arm initial direction with the predictions provided by both models.

For each subject, we performed a linear regression analysis on the observed compensation versus the predicted full compensation accounting for the eye kinematics. No com-

Visuomotor transformation model



ensation would result in a regression slope of zero. If the observed compensation was perfect, the slope of the compensation should be one. For each subject, the slope of the regression line ranged from 0.80 to 0.95 and was significantly different from 0 ($R > 0.75$). This suggests that the brain uses eye velocity and direction signals to account for the eye kinematics in the visuomotor transformation of velocity signals for manual tracking movements. Why the compensation is slightly less than 1 and how the brain implements such a transformation are to be investigated.

References

- [1] Crawford JD, Medendorp WP and Marotta JJ, Spatial transformations for eye-hand coordination, *Journal of Neurophysiology*, 92, 10-19, 2004
- [2] Blohm G and Crawford JD, Computations for geometrically accurate visually guided reaching in 3-D space. *Journal of Vision*, 7(5) :4, 1-22, 2007
- [3] Krauzlis RJ, The control of voluntary eye movements : new perspectives. *Neuroscientist* 11,124-137, 2005
- [4] Leclercq G, Blohm G and Lefèvre P, Visually-guided manual tracking requires a 3D visuomotor transformation of velocity signals. *SFN abstract*, 854.17, 2008

New model of gaze tracking in 2D: Compensation for perturbations of the head.

Pierre M. Daye
 CESAME/IoNS
 UCLouvain
 Avenue Georges Lemaitre, 4
 1348 Louvain-la-Neuve
 Belgium
 Email: pierre.daye@uclouvain.be

Lance M. Optican
 LSR, NEI
 NIH
 Building 49, Room 2A50
 49 Convent Drive
 Bethesda, Maryland 20892-4435, USA
 Email: lmo@lsr.nei.nih.gov

Gunnar Blohm
 Queen's University
 Centre for Neuroscience Studies
 Botterell Hall, Room 230
 18, Stuart Street
 Kingston, Ontario, K7L 3N6, Canada
 Email: gunnar.blohm@queensu.ca

Philippe Lefèvre
 CESAME/IoNS
 UCLouvain
 Avenue Georges Lemaitre, 4
 1348 Louvain-la-Neuve
 Belgium
 Email: philippe.lefevre@uclouvain.be

1 Abstract

During everyday life, clear vision requires compensation for any head displacement by an opposite eye movement. This stabilization process is known as the vestibulo-ocular reflex (VOR). There are numerous situations in which this reflex can be counterproductive. For example, to track a moving target with a combined eye-head movement, there is no need to compensate for the head displacement moving toward the target. However, any other head movement is a perturbation from the gaze goal, and should be negated. One can conclude that the VOR needs to discriminate between those head movements that are part of the gaze command, and those that are perturbations. Two mechanisms have been proposed to account for this behavioral dichotomy. The first assumes that an opposite signal is added to the VOR to cancel the counter-rolling of the eye that would be caused by gaze movements (VOR cancellation). The second decreases the gain of the VOR when it would be counterproductive (VOR suppression). Experiments can show either cancellation [1] or suppression [2]. In simple tracking of a moving target, gaze is not perturbed when the head is suddenly braked, implying that the effect of the VOR was cancelled by subtracting a head command signal [1]. When very large (≥ 50 [deg]) gaze movements are made, a brief acceleration of the head is not compensated during the perturbation, but the final gaze position is accurate [3, 4]. This implies that the VOR has been attenuated, but that a feedback loop has kept track of the actual movement. We developed a new model of gaze control that can simulate both types of behavior. If the VOR is attenuated, final position accuracy is guaranteed because the vestibular afferent signals are also integrated by the different controllers. Efference copies of

gaze-directed movement commands are subtracted from the sensory signals (head velocity from semi-circular canals and cervical afferents) that are fed to the VOR, allowing cancellation of the afferent signals caused by the gaze-directed head movement during tracking. Commands for voluntary head movements (other than gaze-directed movements), are not subtracted, and are thus not cancelled. In conclusion, a mixture of cancellation and feedback circuits are required to model VOR compensation during gaze movements.

References

- [1] R. J. Leigh and J. A. Sharpe and P. J. Ranalli and S. E. Thurston and M. A. Hamid Comparison of smooth pursuit and combined eye-head tracking in human subjects with deficient labyrinthine function, *Experimental Brain Research*, Vol. 66, 1987.
- [2] P. Lefèvre and I. Bottemanne and A. Roucoux Experimental study and modeling of vestibulo-ocular reflex modulation during large shifts of gaze in humans, *Experimental Brain Research*, Vol. 91, 1992.
- [3] R.D. Tomlinson and P.S. Bahra Combined eye-head gaze shifts in the primate. II. Interactions between saccades and the vestibuloocular reflex, *Journal of Neurophysiology*, Vol. 56, 1986.
- [4] D. Guitton and D.P. Munoz and H.L. Galiana Gaze Control in the Cats: Studies and Modeling of the coupling Between Orienting Eye and Head Movements in Different Behavioral Tasks, *Journal of Neurophysiology*, Vol. 64, 1990.

Dynamical modeling of alcoholic fermentation and its link with nitrogen consumption

Robert David and Denis Dochain
 CESAME
 Université catholique de Louvain
 1348 Louvain-la-Neuve Belgium
 denis.dochain@uclouvain.be

Alain Vande Wouwer
 Automatic Control Laboratory
 Université de Mons
 7000 Mons Belgium
 alain.vandewouwer@umons.ac.be

Jean-Roch Mouret and Jean-Marie Sablayrolles
 IPV - Laboratoire de Microbiologie et Technologie des Fermentations
 INRA - Montpellier SupAgro
 34060 Montpellier France
 sablayro@supagro.inra.fr

The development of paradigms in food process control is one of the issues of the EC CAFE project (www.cafe-project.org) that considers four case studies [1], and among them the bioconversion process of wine-making mainly described by the alcoholic fermentation step. The objective of the CAFE project about the wine-making fermentation is to design control tools aimed at optimising the fermentation so as to obtain a well defined aromatic profile [2]. Indeed, during the alcoholic fermentation hexoses are converted to ethanol and carbon dioxide, but many other compounds are removed from the must and a large set of by-products are formed that affect the organoleptic properties of the wine.

The mathematical modeling step requires a relevant description of the key-compounds dynamics before considering by-products like the aromatic compounds. Therefore this work proposes a dynamical mass balance model describing the main physiological phenomena observed during the batch fermentation in the wine-making process, on the basis of a set of biological reactions in which the nitrogen consumption plays a central role, in line with experimental evidence deduced from extensive experimental studies. The experimental database considered for the parameters identification has been generated by a simulator issued from a logistic model especially dedicated to the wine fermentation [3] which is a valuable representation of the process, yet with a complex formulation that appears to be not suitable for control purposes. The results of the modeling efforts performed on the basis of this model are presented, demonstrating the good predictive capability of the proposed model (Fig. 1).

Acknowledgements. This paper includes results of the CAFE project that is supported by the Food, Agriculture and Fisheries, and Biotechnology program of the European Community (Contract number KBBE-212754). It also presents research results of the Belgian Programme on Interuniversity Poles of Attraction initiated by the Belgian

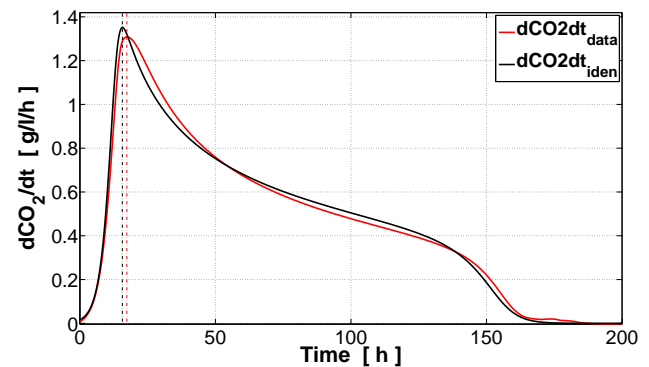


Figure 1: Evolution of the carbon dioxide production rate during a fermentation with temperature $T = 25^{\circ}\text{C}$ and initial concentration of nitrogen $N_0 = 0.17 \text{ g/l}$.

State, Prime Minister's Office, Science, Technology and Culture. The scientific responsibility rests with its authors.

References

- [1] S. Bruin and Th.R.G. Jongen (2003). Food Process Engineering: The Last 25 Years and Challenges Ahead. *Comprehensive Reviews in Food Science and Technology*, Vol 2, p 42.
- [2] B. Charnomordic, R. David, D. Dochain, N. Hilgert, J.R. Mouret, J.M. Sablayrolles and A. Vande Wouwer (2010). Two modelling approaches of wine-making : first principle and metabolic engineering. To appear in *Mathematical and Computer Modelling of Dynamical Systems*.
- [3] S. Malherbe, V. Fromion, N. Hilgert and J. M. Sablayrolles (2004). Modeling the Effects of Assimilable Nitrogen and Temperature on Fermentation Kinetics in Enological Conditions. *Biotechnology and Bioengineering*, 86(3), 261-272.

State estimation of simulated moving bed chromatographic processes (SMB)

Cristina Retamal^{a,b}, Michel Kinnaert^a

^a Control Engineering Department

Université Libre de Bruxelles (ULB)

Avenue F.D. Roosevelt 50, CP 165/55 1050 Bruxelles
Belgium

Email: cristina.retamal@umons.ac.be
michel.kinnaert@ulb.ac.be

Carlos Vilas^b, Alain Vande Wouwer^b

^b Automatic Control Laboratory

Université de Mons

31 Boulevard Dolez, 7000 Mons
Belgium

Email: carlos.vilas@umons.ac.be
Alain.VandeWouwer@umons.ac.be

Abstract

Chromatographic processes have been used for separation, extraction and purification of complex mixtures becoming notably important in the field of pharmaceuticals, biomolecules and other products. The true moving bed (TMB) and the Simulated moving bed (SMB) are continuous chromatographic processes. In the true moving bed (TMB) process a continuous counter-current chromatography is performed. However, in practice the movement of the solid is difficult to carry out. On the other hand, the SMB process simulate a counter-current movement of the solid phase. For a better understanding, the SMB system is graphically represented in the Figure (1). We can distinguish 4 zones delimited by the inlet and the outlet ports. The component A represents the component that has less affinity for the adsorbent and is withdrawn in the raffinate. The component B represents the more retained component, which is collected like extract. Each zone is composed by a given number of chromatographic columns connected in series. The simulation of the solid phase movement is achieved by periodically switching the inlet and the outlet ports in the direction of the liquid flow as indicated in the Figure (1) by the dashed arrows. The SMB process has a transient be-

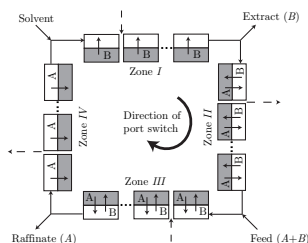


Figure 1: Scheme of the separation of a mixture in a SMB process.

haviour during one switching period, on the contrary the TMB model presents an steady state behaviour. However, one can connect the TMB and SMB models based on the assumption that the TMB model gives an approximation of the SMB profiles at 50% of the switching period [1].

These processes are described by nonlinear partial differential equations (PDEs), thus numerical techniques, as finite difference and finite element method (FEM) must be applied for finding the solution of the involved equations. These techniques are based on the approximation of the spatial operators on a spatial grid leading to a system of ordinary differential equations (ODEs). The set of ODEs resulting after the application of these techniques is, en general, very large. Hence, these approaches become unsuitable for tasks to be performed in real time like control, due to the computation load needed to solve the large number of equations. Therefore, a reducer order model technique could be useful for improving the efficiency of the simulation.

The aim of this work is to develop a state observer based on the early lumping approach. To develop this observer the TMB model is used. The main advantage of the use of the TMB is its significant reduction of the computational complexity in comparison with SMB. Moreover, the observer is constructed following the Kalman Filter design and a reducer order model technique namely Proper Orthogonal Decomposition [2] is applied, as well.

Acknowledgments

This work presents research results of the Belgian Network DYSCO, funded by the Interuniversity Attraction Poles Program, initiated by the Belgian State, Science Policy Office.

References

- [1] V. Grosfils, C. Levrie, M. Kinnaert, and A. Vande Wouwer. A systematic approach to smb processes model identification from batch experiments. *Chemical Engineering Science*, 62(15):3894–3908, 2007.
- [2] C. Vilas. *Modelling, Simulation and Robust Control of Distributed Processes: Application to Chemical and Biological Systems*. PhD thesis, University of Vigo, Spain, May 2008. Available online at <http://digital.csic.es/handle/10261/4236>.

Nonlinear model predictive control of animal cell cultures in perfusion mode

Ines Saraiva, Alain Vande Wouwer, Lino O. Santos¹

Automatic Control Laboratory

Polytechnic Faculty

University of Mons

31 Boulevard Dolez, 7000 Mons

Belgium

Ines.Saraiva@umons.ac.be, Alain.VandeWouwer@umons.ac.be

1 Introduction

The cultivation of animal cells plays an important role in the production of pharmaceuticals such as recombinant proteins or antibodies. Traditionally, the culture medium composition is *a priori* defined and includes all the necessary substrate components in large excess. Depending on the cell life cycle, some of these components are only partially consumed or in some cases, even produced, resulting in important waste and poor economical balance. It is therefore appealing to develop the concept of dynamic growth medium, in which a multivariable controller would act on the culture medium composition dynamically so as to satisfy the cell metabolism and to achieve a better economic balance.

The design of such multivariable controllers implies the derivation of adequate metabolic models, which would sustain the development of suitable optimality criteria. These models could be obtained through the reduction of detailed metabolic models as proposed in [1] and [2]. Based on these reduced-order models and optimality criteria, a natural framework for the control design would be provided by nonlinear model predictive control (NMPC), which allows an easy incorporation of various process constraints [3, 4].

2 Some preliminary results

In order to explore this approach, a relatively simple model of hybridoma cells producing monoclonal antibodies [5] is considered in this study. Based on this model, NMPC is developed and compared in simulation with previously considered control policies [6].

Several issues are investigated including the formulation of the optimality criterion and process constraints, the selection of the manipulated variables and their parameterization, the selection of the MPC parameters and the implementation of the receding-horizon optimization.

Simulation tests for cultures in a 2L bioreactor operated in perfusion mode are discussed.

3 Acknowledgments

This work presents research results of the Belgian Network DYSCO (Dynamical Systems, Control, and Optimization), funded by the Interuniversity Attraction Poles Program, initiated by the Belgian State, Science Policy Office. The scientific responsibility rests with its authors. This work is carried out in the framework of the research project OCPAM (Hainaut-Biomed) funded by FEDER.

References

- [1] A. Provost and G. Bastin. Dynamic metabolic modeling under the balanced growth condition. *Journal of Process Control*, 14:717-728, 2004.
- [2] A. Provost and G. Bastin. Metabolic design of macroscopic bioreaction models: application to Chinese hamster ovary cells. *Bioprocess and Biosystems Engineering*, 29:349-366, 2006.
- [3] J. Maciejowski. Predictive control with constraints. 1st ed., Prentice-Hall, 2002.
- [4] L. O. Santos. Multivariable Predictive Control of Chemical Processes. PhD thesis, Faculty of Sciences and Technology, University of Coimbra, Coimbra, Portugal, 2001.
- [5] M. de Tremblay, M. Perrier, C. Chavarie and J. Archambault. Optimization of fed-batch culture of hybridoma cells using dynamic programming: single and multi feed cases. *Bioprocess Engineering*, 7:229-234, 1992.
- [6] M. de Tremblay, M. Perrier, C. Chavarie and J. Archambault. Fed-batch culture of hybridoma cells: comparison of optimal control approach and closed loop strategies. *Bioprocess Engineering*, 9:13-21, 1993.

¹Lino O. Santos is currently on leave from the Chemical Engineering Department, Faculty of Sciences and Technology, University of Coimbra, Portugal. Lino@eq.uc.pt

On a Reduced Order Model for the Representation of Plant Bioprocesses

A. Delmotte, J. Mailier, A. Vande Wouwer
Automatic Control Laboratory
University of Mons (FPMs)
7000 Mons, Belgium

M. Cloutier, M. Jolicoeur
Chemical Engineering Department
École Polytechnique de Montréal
H3C 3A7 Montréal, Canada

AntoineDelmotte@hotmail.com, Johan.Mailier@umons.ac.be, Alain.VandeWouwer@umons.ac.be,
Mathieu.Cloutier@polymtl.ca, Mario.Jolicoeur@polymtl.ca

Abstract

Many valuable compounds are nowadays extracted from plants rather than being artificially synthesized, both for ease and cost reasons. Biological models have therefore been developed in the last two decades to describe and predict the nutritional state of the most encountered culture types, namely plant suspension cells and hairy roots. Among these models, the one developed by Cloutier et al. [1] is the first to describe both the extracellular and intracellular dynamics for the three major constitutive nutrients (carbon source, phosphate, and nitrogen) in both plant cells and hairy roots cultures. Although its output dynamics can accurately fit with experimental data, the high number of parameters involved by this model does not allow them to be estimated from the available datasets. Its parameter values are thus often taken directly from literature, without any mean of validation. As a consequence, its prediction ability outside the scope of the experimental datasets may turn out to be weaker. The present work suggests a simplification of Cloutier's descriptive model, so as to make it tractable for parameter identification. Moreover, the simplified model is written in the form of a macroscopic reaction scheme, for which well-established policies of monitoring and control already exist [2].

Assuming that Cloutier's model [1] is representative of the actual complexity of plant cultures, informative datasets are generated by simulation, so as to provide a solid foundation for model analysis and reduction. Firstly, a principal component analysis technique allow to reduce the complexity of the original model by determining the minimum number of reactions required to represent the data with a given accuracy [3]. Sensitivity studies are then used to progressively remove those parts of the model that have few or no influence on its output dynamics [4]. Finally, a practical structure is derived, which represents with a minimum complexity, the dynamics of plant cells and hairy roots nutritional state, as a function of the feeding concentrations in inorganic sugars, phosphate, and nitrogen.

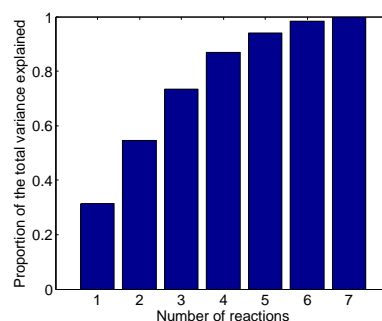


Figure 1: Explained fraction of the output variance as a function of the reaction number for cultures of *Catharanthus roseus*

Acknowledgment

This paper presents research results of the Belgian Network DYSCO (Dynamical Systems, Control, and Optimization), funded by the Interuniversity Attraction Poles Program, initiated by the Belgian State, Science Policy Office. The scientific responsibility rests with its author(s).

Johan Mailier is a Research Fellow by the FNRS (Fonds de la Recherche Scientifique), the Belgian Foundation. The authors are thus very grateful to it for its support.

References

- [1] M. Cloutier, E. Bouchard-Marchand, M. Perrier, M. Jolicoeur, "A predictive nutritional model for plant cells and hairy roots," *Biotechnology and Bioengineering* 99(1):189-200, 2008.
- [2] G. Bastin, D. Dochain, "Online estimation and adaptive control of bioreactors," Elsevier Science, 1990.
- [3] O. Bernard, G. Bastin, "On the estimation of the pseudo-stoichiometric matrix for macroscopic mass balance modelling of biotechnological processes," *Mathematical Biosciences* 193:51-77, 2005.
- [4] H. Schmidt, M. Jirstrand, "Systems biology toolbox for matlab: a computational platform for research in systems biology," *Bioinformatics* 22(4):514-515, 2006. <http://www.sbtoolbox2.org>.

Robust linearizing control of yeast and bacteria fed-batch cultures

Laurent Dewasme^a, Alain Vande Wouwer^a
^a Service d'Automatique, Université de Mons
 31 Boulevard Dolez, 7000 Mons
 Belgium
 Email: laurent.dewasme@umons.ac.be
 Alain.VandeWouwer@umons.ac.be

Daniel Coutinho^b
^b Dept. Electrical Engineering
 Pontificia Universidade do Rio Grande do Sul
 Av. Ipiranga 6681, 90619-900, Porto Alegre
 RS, Brazil
 Email: dcoutinho@pucrs.br

1 Introduction

The culture of host recombinant micro-organisms is probably the only economical way of producing pharmaceutical biochemicals. The fed-batch operation is popular in industrial practice, since it is advantageous from an operational and control point of view. In this mode of operation, the bioreactor is manipulated by controlling its feeding rate. The off-line design of the optimal feeding profile in general does not give high productivity, since in open-loop an excess of substrate leads to the accumulation of by-products (ethanol for yeast and acetate for bacteria), which in turn leads to an inhibition of the cell respiratory capacity.

To avoid high concentrations of inhibitory by-product, a closed-loop solution is in general applied leading to a wide diversity of approaches, e.g., [2, 3, 4]. Nevertheless, the closed-loop control optimization of fed-batch cultures of microorganisms exhibiting this kind of overflow metabolism is still a challenging task for two main reasons. Firstly, the process kinetics is governed by highly nonlinear functions with uncertain model parameters. Secondly, there is a lack of reliable and low cost online sensors for the measurement of key state variables.

Adaptive control is often used to cope with time-varying model uncertainties. However, the use of online adaption schemes may lead to closed-loop instability in the presence of unmodeled dynamics. In this paper, we follow a different direction by applying the robust control theory to design a nonlinear controller (with a fixed parametrization) taking model uncertainties into account. The control strategy is based on the classical feedback linearizing technique which is widely applied to fermentation process. However, feedback linearizing control schemes are very sensitive to model uncertainties. To handle the lack of robustness, the resulting linear dynamics is designed in order not only to improve the overall performance but also to achieve robustness against model uncertainties using LMI and H-infinity theory.

2 A suboptimal robust control strategy

The maximum of productivity is obtained when the quantity of by-product is constant and equal to zero ($VP = 0$ where

V is the bioreactor volume and P the byproduct concentration). Unfortunately, evaluating accurately the volume is a difficult task as it depends on the inlet and outlet flows including F_{in} but also the added base quantity for pH control and several gas flow rates. Moreover, maintaining the quantity of byproduct constant in a fed-batch process means that the byproduct concentration has to decrease while the volume increases. So, even if the volume is correctly measured, VP becomes unmeasurable once P reaches the sensitivity level of the byproduct probe. For those practical limitations, a suboptimal strategy is elaborated through the control of the byproduct concentration around a low value depending on the sensitivity of commercially available probes (for instance, a general order for ethanol probe is $0.1g/l$), and requiring only an estimation of the volume by integration of the feed rate.

The basic principle of the controller is thus to regulate the by-product at a constant low setpoint, leading to a self-optimizing control and ensuring that the culture operates in the respiro-fermentative regime (i.e., where the byproduct is produced), close to the biological optimum, i.e., close to the edge with the respirative regime (where the byproduct is consumed).

In this study, linearizing control strategies using on-line adaptation or a robust gain design using LMI [1] are compared in terms of implementation and performance, as illustrated in simulation.

Acknowledgment

This paper presents research results of the Belgian Network DYSCO (Dynamical Systems, Control, and Optimization), funded by the Interuniversity Attraction Poles Program, initiated by the Belgian State, Science Policy Office. The scientific responsibility rests with its authors.

References

- [1] D. Coutinho, L. Dewasme and A. Vande Wouwer. *Robust Control of Yeast Fed-Batch Cultures for Productivity Enhancement*. In Proceedings of the ADCHEM conference in Istanbul (2009).
- [2] Pomerleau, Y. *Modélisation et commande d'un procédé fed-batch de culture des levures à pain*. Département de génie chimique. Ecole Polytechnique de Montréal. PhD Thesis (1990).
- [3] Chen, L. and Bastin, G. and van Breusegem, V. *A case study of adaptive nonlinear regulation of fed-batch biological reactors*. *Automatica*, 31(1):55-65, 1995.
- [4] L. Dewasme, A. Richelle, P. Dehottay, P. Georges, M. Remy, Ph. Bogaerts and A. Vande Wouwer. *Linear robust control of *S. cerevisiae* fed-batch cultures at different scales*. Accepted in the *Biochemical Engineering Journal* as regular journal paper.

Microbial kinetics at the growth/inactivation interface: estimation of the maximum growth temperature

Eva Van Derlinden and Jan F. Van Impe

BioTeC - Chemical and Biochemical Process Technology and Control

Department of Chemical Engineering, Katholieke Universiteit Leuven

W. de Croylaan 46, B-3001 Leuven, Belgium

jan.vanimpe@cit.kuleuven.be - eva.vanderlinden@cit.kuleuven.be

1 Introduction

Temperature is one of the most important factors influencing the behavior of spoilage microorganisms and pathogenic bacteria in food products. Amongst the different kinetic models constructed in predictive food microbiology to describe the temperature effect on the microbial growth rate, the Cardinal Temperature Model with Inflection (CTMI) (Rosso et al. 1993) is often preferred. Previously, a framework was constructed based on optimal experiment design techniques, which resulted in reliable CTMI parameter estimates. However, a drawback was uncovered: a reliable estimate of the maximum growth temperature (T_{max}) is only obtained when temperatures at or very close to the true T_{max} are included in the optimal dynamic temperature profile. This requires a reliable initial estimate of T_{max} .

Here, the possibility to estimate T_{max} from dynamic experiments with temperatures exceeding T_{max} is tested. The temperature crosses the growth boundary and T_{max} can be determined as the temperature at which growth starts. A microbial dynamics scenario is considered where there exists a temperature range δ in which, at macroscopic level, neither growth nor inactivation is observed. The informative character of temperature profiles with the initial temperature situated between T_{max} and $T_{max} + \delta$ is evaluated.

2 Simulation study

The simulation study includes two steps. (1) Microbial dynamics as a function temperature are simulated using a growth model combined with the CTMI model. An error is added to mimic uncertainty due to experimental errors and biological variability. (2) Parameters and variances are estimated from simulated data via minimization of the sum of squared errors, using the *lsqnonlin* routine (Optimization Toolbox, Matlab, The Mathwork Inc.).

3 Results

The informative character of the dynamic experiments with respect to the estimation of T_{max} is evaluated. The temperature profiles are based on a previously designed optimal experiment, in which a phase at constant temperature is followed by a linear temperature decrease ($\approx 5^\circ\text{C}/\text{h}$) and a second phase at constant temperature (15°C). Five temperature profiles are considered with different initial tempera-

tures (45°C , 46°C , 47°C , 48°C and 49°C) with the true T_{max} equal to 46.54°C .

The results of the simulation study can be summarized as follows. (1) For T_{min} , the largest variability on the parameter estimates can be observed for a temperature profile T_1 equal to 45°C . When T_1 is increased to 46°C , the range of T_{min} estimates decreases significantly. For higher T_1 values, similar values are obtained. (2) For T_{opt} , no real trend as a function of T_1 can be observed. (3) For T_{max} , values estimated from experiments with T_1 equal to 45°C , vary enormously (45.70°C to 47.33°C). Increasing T_1 to 46°C significantly improves the estimation of T_{max} . All values are situated in a range of 0.2°C around the true T_{max} . Further increasing T_1 has a contrary effect, i.e., the variability on T_{max} is significantly enlarged and the its average deviates from the true value. The higher the initial temperature, the higher the average of the T_{max} estimates. (4) As with T_{opt} , no real trend can be observed for μ_{opt} .

4 Conclusion

It can be concluded that extending the dynamic temperature profile to temperatures above T_{max} does not increase the experimental information content. By starting the experiment at 46°C , the growth rate at this temperature can be estimated rather easily and accurately. However, by further increasing T_1 , initially no growth occurs and growth rates can only be derived during the temperature decrease. Clearly, the information with respect to growth at temperatures close to T_{max} is required for an accurate and reliable T_{max} estimate.

Acknowledgments

This research is supported in part by projects OT/09/25 and BOF EF/05/006 (OPTEC Optimization in Engineering) of the Research Council of the KULeuven, project KP/09/005 (SCORES4CHEM) of the Industrial Research Fund, and the Belgian Program on Interuniversity Poles of Attraction, initiated by the Belgian Federal Science Policy Office. J. Van Impe holds the chair Safety Engineering sponsored by the Belgian chemistry and life sciences federation essenscia.

References

- [1] Rosso, L., Lobry, J. R. & Flandrois, J. P. (1993) An unexpected correlation between cardinal temperatures of microbial growth highlighted by a new model. *J Theor Biol*, 162, 447–463.
- [2] Van Derlinden, E., Bernaerts, K. & Van Impe, J. F. (2008) Accurate estimation of cardinal temperatures of *Escherichia coli* from optimal dynamic experiments. *Int J Food Microbiol*, 128, 89–100.

Adaptive detection and isolation of sensor faults in doubly-fed induction generators for wind turbine applications

Manuel Gálvez and Michel Kinnaert

Université Libre de Bruxelles (U.L.B.)

50, Av. F.D. Roosevelt-CP 165/55, B-1050 Brussels, Belgium

mgalvezc@ulb.ac.be, michel.kinnaert@ulb.ac.be

1 Introduction

Doubly-fed induction generators (DFIG) are currently one of the most used generating units for wind turbine applications. The DFIG represents a good trade-off between power converter size (approximately 30 % of the nominal generator power), and control capability (speed variation from -40% to +30% around the synchronous speed). Nevertheless, DFIG can be subject to diverse kinds of faults, notably electrical sensor faults. In this work, a model-based fault detection and isolation (FDI) system with parameter adaptation is designed to address the issue of FDI of incipient (small magnitude) faults in the rotor current sensors.

2 DFIG model with parameter adaptation

The large range of operating conditions of a wind turbine induces electrical parameter variation in the generator unit. The stator and rotor resistance (R_s , R_r), and magnetizing inductance (L_m) can vary due to temperature changes and magnetization characteristics, respectively. This parameter variation can degrade the performance of any model-based FDI system. After a sensitivity analysis, it was concluded that variations in the rotor resistance (R_r) produce the largest impact on the magnitude of rotor currents. Therefore, a sensor model-based FDI system need to consider the adaptation of the rotor resistance.

In our approach, the dynamics of the DFIG is expressed in dq coordinates, aligned with the stator voltage vector. The considered states are the rotor current (\vec{i}_r) and the rotor flux ($\vec{\lambda}_r$) vectors, plus the rotor resistance (the parameter to be adapted). The control input is the rotor voltage vector (\vec{u}_r), and the stator voltage vector (\vec{u}_s) and the generator speed (Ω_g) are considered as measured disturbances. The measured rotor currents are expressed as abc quantities, and are considered to be subject to additive faults (offset or slow drift). Only one fault is assumed to occur at a time.

3 Residual generation and decision system

For residual generation purposes, a multi-observer approach is used, based on the Generalized Observer Scheme (GOS). In this approach, the i -th observer uses all but the i -th measurement, as shown in Fig. 1. The residual generator is actually a discrete extended Kalman filter (EKF), of which the

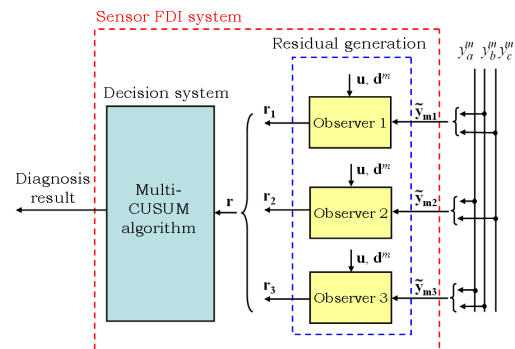


Figure 1: Scheme of FDI system

innovation is used as residual vector. For the decision system, the multi-CUSUM (Cumulative sum) [1], a statistical change detection and isolation algorithm is used. In this approach, the whole set of residuals signals r_i , for $i \in \{1, 2, 3\}$, is combined in a single residual vector. The latter is processed using as many CUSUM algorithms as the number of possible faults. Three modified CUSUM decision functions are then used to perform both detection and isolation. A given criterion, namely a required mean detection delay ($\bar{\tau}$) is used to assess the FDI performance. The FDI system has been validated for diverse magnitudes of additive (offset) faults. The faults have been properly detected and isolated within the required detection delay, even in the presence of disturbances and changes in the references, and the rotor resistance has been correctly estimated.

Acknowledgments

The work of Manuel Gálvez is supported by the ARC project 'Advanced supervision and dependability of complex processes: application to power systems'. This paper presents research results of the Belgian Network DYSCO (Dynamic Systems, Control and Optimization), funded by the Interuniversity Attraction Poles Programme, initiated by the Belgian State, Science Policy Office. The scientific responsibility rests with its authors.

References

- [1] I. Nikiforov, A simple recursive algorithm for diagnosis of abrupt changes in signals and systems, In *Proceedings of the 1998 American Control Conference*, vol. 3, pp. 1938–1942, Philadelphia, USA, 1998.

Active damping in precision equipment using piezo

Bayan Babakhani, Theo de Vries

Control Engineering group, Faculty of EEMCS, University of Twente

Email: b.babakhani@ewi.utwente.nl, t.j.a.devries@imotec.nl

1 Introduction

In this paper, the rotational vibration in the linearly actuated precision machines with low damping is discussed. This so called Rocking mode is e.g. caused by the compliance in the guiding system of a linear actuator and leads to a long settling time of the end-effector. Another problem occurs when a feedback motion controller is applied to the plant. Complex poles present in the loop transfer that are close to the imaginary axis due to low damping, are destabilized by a relatively small gain. A possible solution is actively damping the resonance frequencies. By flattening the resonance peaks, the bandwidth of the system can increase without the danger of instability. In turn, this allows for higher integral gain in the motion control algorithm.

2 Active damping in simulation

Figure 1 shows a 1-Dimensional model of the Rocking mode and the corresponding transfer function. The actuator force F initiates a translational movement and at the same time, a rocking mode around the COM, due to the present compliance, c . This causes a ripple on the measured position, x .

The plant consists of three main parts; the actuator, the

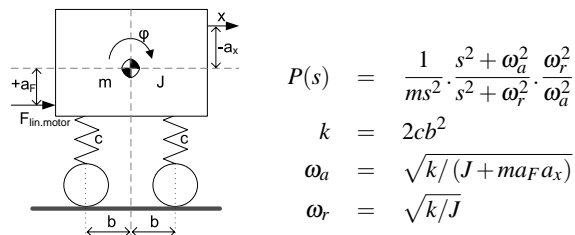


Figure 1: 1D model of a plant with rocking mode

guiding system and a moving part. The damping should be applied between the moving part and the guiding system of the actuator, where the compliance causing the rocking mode is located. A platform on which the Active Vibration Control device (AVC) can be mounted, can be created by dividing the moving part into two parts: a lightweight carriage and the rest (containing the end-effector) called the head (see Figure 2). The resonance frequency of the carriage is relatively high due to its light weight and is thus negligible. The plant model now consists of a linear actuator, the carriage (translational mass), AVC and the head (mass and inertia). AVC loop operates in parallel with the motion control loop. The implemented AVC algorithm is a Leaking Integral

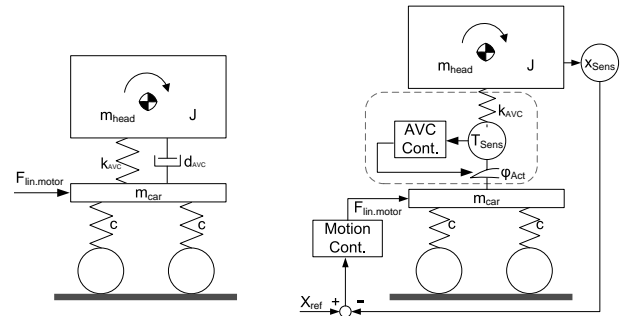


Figure 2: Active damping

Force Feedback, as described by [2]. The transfer function of this intrinsically passive controller is $C_{AVC}(s) = \frac{K_{LIFF}}{s + p_{LIFF}}$, where $d_{AVC} = K_{LIFF}^{-1}$ and $k_{AVC} = p_{LIFF} \cdot d_{AVC}$. For motion control, a PID controller with high frequency roll-off is used, which is tuned based on the moving mass transfer function, according to [1]. Adding this controller to the plant without AVC results in an unstable system. The pole-zero plots (Fig. 3) show that by adding active damping, the closed-loop system remains stable over a wider gain range.

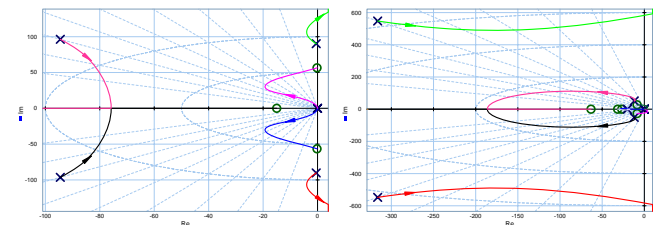


Figure 3: Plant with motion control; left: no AVC, right: with AVC

3 Conclusion

The effect of active damping on a plant with Rocking mode has been investigated in simulation. This results in a stable closed-loop system with high bandwidth, which allows for fast response, low settling-time and low steady-state error.

References

- [1] H.J. Coelingh, "Design support for motion control systems", University of Twente, The Netherlands, 2000
- [2] J. Holterman, "Vibration control of high-precision machines with active structural elements", University of Twente, The Netherlands, 2002

Experimental synchronization of Hindmarsh-Rose neurons

Erik Steur, Patrick Neefs, Henk Nijmeijer

Department of Mechanical Engineering

Eindhoven University of Technology

P.O. Box 513, 5600 MB, Eindhoven, The Netherlands

Email: (e.steur,h.nijmeijer)@tue.nl, p.j.neefs@student.tue.nl

1 Introduction

It is well known that neurons synchronize their behavior to each other. Examples include synchronous oscillations in the visual cortex and the olfactory bulb. It is also believed that synchronization plays a role in diseases like epilepsy. We present results on experimental synchronization of Hindmarsh-Rose (HR) neurons.

2 The experimental setup

We have realized eighteen electronic HR neurons which are given by the equations

$$\begin{aligned}\dot{v}_i(t) &= -v_i^3(t) + 3v_i(t) - 4.75 + 5w_{1,i}(t) - w_{2,i}(t) + u_i(t), \\ \dot{w}_{1,i}(t) &= -v_i^2(t) - 2v_i(t) - w_{1,i}(t), \\ \dot{w}_{2,i}(t) &= 0.005(4v_i(t) + 4.472 - w_{2,i}(t)),\end{aligned}\quad (1)$$

where $\dot{\cdot} := \frac{d}{dt^*}$, $t^* = 1000t$, $i = 1, 2, \dots, k$, membrane potential (output) $v_i(t)$, synaptic input $u_i(t)$ and internal variables $w_{1,i}(t)$, $w_{2,i}(t)$. The electronic equivalent is depicted in Figure 1(a).

The electronic HR neurons interact via the coupling interface which is shown in Figure 1(b). The interface allows to couple up to eighteen systems. Here, we used diffusive coupling functions of the form

$$u_i(t) = \gamma \sum_{j=1, j \neq i}^k a_{ij}(v_j(t - \tau) - v_i(t - \tau)), \quad (2)$$

where $\gamma > 0$ denotes the coupling strength, $\tau \geq 0$ is a time delay, and $a_{ij} = a_{ji} = 1$ if system i connects to system j and is zero otherwise.

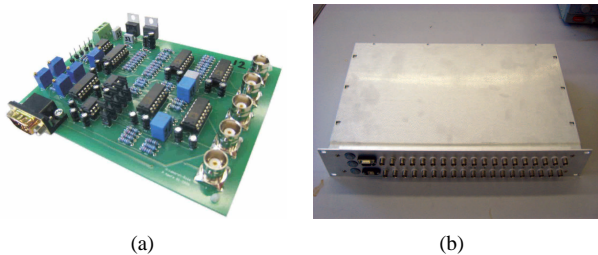


Figure 1: (a) An electronic HR neuron. (b) The interface.

3 Results

Since the systems in the experimental setup do not have exactly identical dynamics, we cannot expect them to synchronize perfectly, i.e. the state variables of all systems asymptotically match. We have to introduce a slightly weaker notion of synchronization:

Definition 3.1 (Practical synchronization). *The neurons are called practically synchronized, if for any initial function segment the following limiting relation holds*

$$\limsup_{t \rightarrow \infty} \|\text{col}(v_i, w_i)(t) - \text{col}(v_j, w_j)(t)\| \leq \varepsilon, \quad (3)$$

for all $i, j = 1, 2, \dots, k$ and sufficiently small constant $\varepsilon > 0$.

Experiments have been performed in network with delay ($\tau > 0$) and without delay ($\tau = 0$). The results for the networks depicted in Figure 2(a) in presence of delays are shown in Figure 2(b). The region enclosed by the curves and the γ -axis corresponds to the region of practical synchronization for the specific network topology. Remarkably the shapes of the curves are all similar, and after a scaling of the γ -axis some of these curves even coincide, see Figure 2(c).

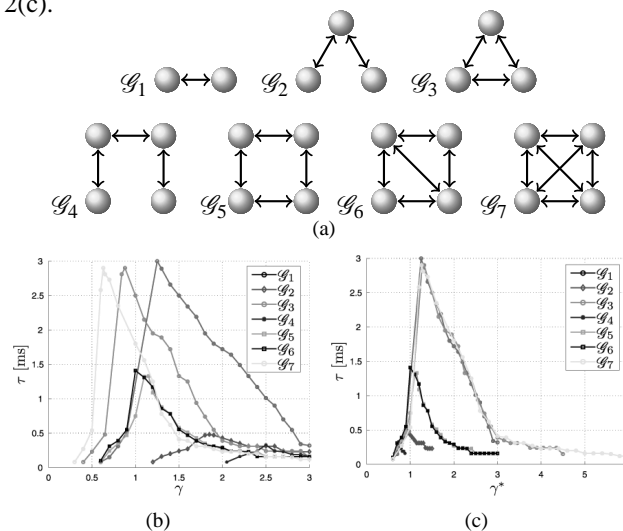


Figure 2: (a) The networks. (b) The regions of practical synchronization. (c) The scaled results.

References

- [1] P.J. Neefs, E. Steur and H. Nijmeijer, *Network complexity and synchronous behavior: an experimental approach*, (submitted for publication), 2009

Over-actuation to compensate for static deformation

J. Achterberg, C.M.M. van Lierop, P.P.J. van den Bosch
Control Systems, department of Electrical Engineering
Eindhoven University of Technology
P.O. Box 513, 5600 MB Eindhoven, The Netherlands
Email: j.achterberg@tue.nl

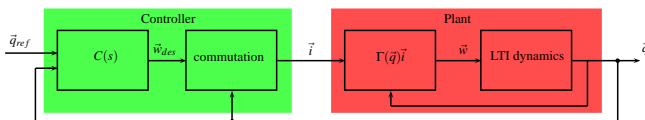


Figure 1: control scheme

1 Introduction

Conventional waferstages have xy -drives that consist of multiple actuators in a configuration which allows planar movement. To achieve high accuracy it needs a fast long stroke stage and an accurate short stroke stage to compensate for the long stroke errors. The need for higher accuracies, a faster operation and the ability to operate in a vacuum environment initiated the research of electromagnetic planar actuators for this type of application. They can be divided into a moving-magnet versus a moving-coil topology. The latter needs cables and hoses to power and cool the moving coils, which introduces non repetitive disturbances and is, therefore, undesired. The moving-magnet, however, demands a more complex decoupling of the dynamics and position dependence.

2 Decoupling dynamics and position dependence

A previous model-based method of decoupling dynamics and position dependence for this application, uses a first order harmonic approximation of the coupling between coil currents and the force and torque components acting on the mass centre point of the translator. This is evaluated each sample time and stored in a matrix. A weighted generalised inverse of this matrix can be calculated and is used to determine the coilcurrents that are needed for exciting a desired force and torque. After decoupling the dynamics that is observed is that of a mass and three inertias around each axis, which is position independ. The control scheme is depicted in Figure 1.

For a smooth transition in long-stroke operation there are far more coils active than the amount needed for controlling all six degrees of freedom of the translator. Therefore, since the decoupling of position dependence and dynamics is not unique, the generalised inverse is applied resulting in an energy optimal solution. To make better use of this freedom a

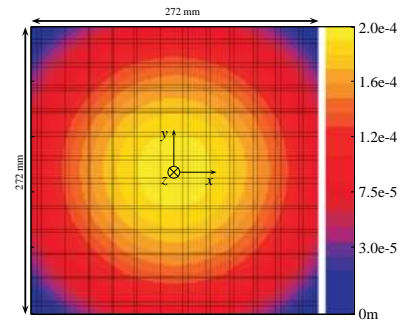


Figure 2: Static deformation of a Halbach array

method is investigated to actively compensate flexible deformations of the translator. This requires a method that considers force distributions on the translator instead of a single force and torque acting on the centre of mass. Therefore, the model is extended to the coupling between coilcurrents and forces on the individual magnets of the magnet array.

3 Static compensation

The magnet array has a Halbach configuration to focus its field to one side of the magnet array. Due to this configuration, it also experiences large internal forces, that statically deform the magnet array [1]. This is shown in Figure 2. By using a novel decoupling it is possible to create a force distribution to compensate for this static deformation.

4 Conclusion

Using models that describe the coupling between forces on individual magnets and coil currents, the position dependence and dynamics of the moving magnet planar actuator can be decoupled. Furthermore it allows for using force distributions as an input to a flexible system instead of forces and torques to a rigid system. By exciting suitable force distributions one can compensate static deformations, caused by the Halbach configuration of the magnet array.

References

- [1] J.M.M. Rovers, J.W. Jansen, E.A. Lomonova, and M.J.C. Ronde, Calculation of the Static Forces Among the Permanent Magnets in a Halbach Array, IEEE Transactions on Magnetics, vol.45, no. 10, pp. 4372-4375, 2009.

Tracking periodic signals for simple hysteretic mechanical systems using repetitive internal model

Robert Huisman and Bayu Jayawardhana¹

1 Introduction

During the past decade, there have been significant research advancements in the nonlinear regulation problem. The tracking and/or disturbance rejection problem is one of the central topics in nonlinear control theory, and control systems that are designed to solve this problem for certain reference and disturbance signals are usually referred to as servo systems. For the case when the reference signals are generated by a finite-dimensional exosystem, the solvability of the Byrnes-Isidori equation [1, 2] is required for the solvability of the regulation problem. Based on the solution of the Byrnes-Isidori equation, many techniques have been proposed to design a local, a semi-global or a global output regulator for various classes of nonlinear systems. These typically use internal-model based principle [2, 6] which borrows the internal-model concept by Francis and Wonham [4] in linear systems theory. The internal model principle for LTI systems, which is also adopted in the nonlinear systems, suggests that a copy of the exosystem must be included in the controller. Hence, for finite-dimensional linear exosystem, the controller uses also an internal model which is based on a finite dimensional linear system.

The drawback of using finite-dimensional servo systems is that they can only deal with a finite number of frequencies and, in particular, they are not suited for tracking general periodic signals. In this case, an infinite-dimensional internal model is needed since the periodic signals can be generated by an infinite-dimensional exosystem.

In linear systems, repetitive internal models have been proposed and used in the controller for tracking periodic signals and it is based on an infinite-dimensional internal model [7, 9]. It has been shown in [7, 8] that the repetitive internal-models are effective in dealing with periodic signals.

In our works, we will present the controller design methodology using repetitive internal model for a simple hysteretic mechanical system. The mechanical system is based on the HIFI chopper mechanism which is developed at the Netherlands Institute for Space Research (SRON) and is used in the HIFI instrument of Herschel space telescope. The method is developed based on the work by Jayawardhana *et.al.* in [5].

References

- [1] C.I. Byrnes, F.D. Priscoli, A. Isidori, *Output Regulation of Uncertain Nonlinear Systems*, Birkhäuser, Boston, 1997.
- [2] C.I. Byrnes, A. Isidori, "Limit sets, zero dynamics, and internal models in the problem of nonlinear output regulation," *IEEE Trans. Automatic Control*, vol. 48, pp. 1712–1723, 2003.
- [3] Z. Ding, "Global stabilization and disturbance suppression of a class of nonlinear systems with uncertain internal model," *Automatica*, vol. 39, pp. 471–479, 2003.
- [4] B.A. Francis, W.M. Wonham, "The internal model principle for linear multivariable regulators," *Applied Mathematics and Optimization*, vol. 2, pp. 170–194, 1975.
- [5] B. Jayawardhana, H. Logemann, E.P. Ryan, "Infinite-dimensional feedback systems: the circle criterion and input-to-state stability," *Communications in Information and Systems, special issue on the Roger Brockett's legacy* (Guest editors: J. Baillieul, J.S. Baras, A. Bloch, P.S. Krishnaprasad, J.C. Willems), vol. 8, no. 4, 2009.
- [6] F.D. Priscoli, "Output regulation with nonlinear internal models," *Systems & Control Letters*, vol. 53, pp. 177–185, 2004.
- [7] G. Weiss, M. Häfele, "Repetitive control of MIMO systems using H^∞ design," *Automatica*, vol. 35, pp. 1185–1199, 1999.
- [8] G. Weiss, Q.C. Zhong, T. Green and J. Liang, " H^∞ repetitive control of DC-AC converters in micro-grids," *IEEE Trans. on Power Electronics*, vol. 19, pp. 219–230, 2004.
- [9] Y. Yamamoto, "Learning control and related problems in infinite-dimensional systems," In H. Trentelman and J. Willems (Eds.), *Essays on Control: Perspectives in the Theory and Its Applications*, pp. 191–222, Birkhäuser, Boston, 1993.

¹B. Jayawardhana and R. Huisman are with the Faculty of Mathematics and Natural Sciences, University of Groningen, 9747 AG Groningen, The Netherlands.
E-mail: r.huisman@sron.nl, b.jayawardhana@rug.nl

Adaptive Controller Design for Automatic Micro-assembly Systems under the Influence of Surface Forces

Ruiyue Ouyang and Bayu Jayawardhana¹

1 Introduction

In the current state-of-art technology of automatic micro-assembly, micro-mechanical manipulator are widely used to handle the object. In practice, the application of mechanical manipulator in micro-assembly encounters several problems: the presence of surface forces during the manipulation of micro/nano parts and the difficulty in sensing whether the object is in contact with or is released by the manipulator.

The papers [3, 8] present an overview of the significance of van der Waals and capillary forces when the manipulated objects have dimensions less than one millimeter. Due to these surface forces, the micro/nano components can stick to the handling tools and become difficult to handle. However, it has been shown that it is also possible to exploit the surface forces for micro-assembly [2, 4, 6], with the expense of losing the deterministic control over the object's movement. Several strategies have been proposed in [1, 5, 10] to minimize the detrimental effect of these forces.

In order to overcome these problems, non-contact manipulation systems using electromagnetic forces is studied in this paper. The electromagnetic force is applied to the object by manipulating the magnetic field through the control of electrical current in electromagnets.

In the magnetic levitation systems for large objects, it is known that the coils' inductance is influenced by the position of the ferromagnetic object. Thus the interaction between the applied voltage and the object position can be simply described by Euler-Lagrange formalisms [9]. When the aspect ratio between the object and the coil size is large, the influence of the object distance to the inductance value becomes negligible. In this case, the applied electromagnetic force is computed based on the magnetic field gradient in the neighborhood of the object. This mechanism was used in the magnetic levitation system for a small robot in [7] and corresponds to the setup considered in this paper. In this paper, we focus on the design of adaptive nonlinear controller for regulating the position of micro object using the electromagnetic force.

In our work we will discuss the modeling of the magnetic levitation system which incorporates the model of various surface forces: capillary forces and van der Waals forces.

The adaptive property of the controller is designed appropriately in order to compensate for the parameter uncertainties in the model of surface forces. The controller design will be given as well and Monte Carlo simulation results will be presented in order to evaluate the behavior and performance of the controlled system under uncertainties in the parameters.

References

- [1] F. Arai, D. Andou, and T. Fukuda, "Adhesion Forces Reduction for Micro Manipulation Based on Micro Physics," IEEE Int. Workshop MEMS, 1996.
- [2] N. Boufercha, J. Sgebarth, and H. Sandmaier, "Assembly of Micro Components by a Fluidic-based Method," 19th MicroMechanics Europe Workshop, Aachen, Germany, 2008.
- [3] R. S. Fearing, "Survey of sticking effects for micro parts handling," International Conference on Intelligent Robots and Systems, 1995.
- [4] J. T. Feddema, P. Xavier, and R. Brown, "Micro-assembly Planning with van der Waals Force," IEEE Int. Symp. Assembly and Task Planning, Porto, Portugal, 1999.
- [5] M. Gauthier, S. Rgnier, B. Lopez-Walle, E. Gibeau, P. Rougeot, D. Hriban, and N. Chaillet, "Micro-assembly and modeling of the liquid microworld: the PRONOMIA project," IEEE/RSJ Int. Conf. Int. Robots and Systems Workshop, San Diego, USA, 2007.
- [6] D. S. Haliyo, Y. Rollot, and S. Rgnier, "Manipulation of micro-objects using adhesion forces and dynamical effects," IEEE ICRA, Washington DC, USA, 2002.
- [7] M. B. Khamese, N. Kato, Y. Nomura, and T. Nakamura, "Design and control of a microrobotic system using magnetic levitation," IEEE/ASME Trans. Mechatronics, vol. 7, pp. 1-14, 2002.
- [8] A. Menciassi, A. Eisinger, I. Izzo, and P. Dario, "From Macro to Micro manipulation: Models and Experiments," IEEE/ASME Trans. Mechatronics, vol. 9, pp. 311-320, 2004.
- [9] R. Ortega, A. Loría, P.J. Nicklasson, H. Sira-Ramírez, *Passivity-Based Control of Euler-Lagrange Systems*, Springer-Verlag, London, 1998.
- [10] Q. Zhou, V. Sariola, and H. N. Koivo, "Microhandling strategies for automation," IEEE/RSJ Int. Conf. Int. Robots and Systems Workshop, San Diego, USA, 2007.

¹B. Jayawardhana and R. Ouyang are with the Faculty of Mathematics and Natural Sciences, University of Groningen, 9747 AG Groningen, The Netherlands.

E-mail: b.jayawardhana, r.ouyang@rug.nl

Estimation of the probability of stable operation over a given time interval for discrete-time nonlinear state-space models

Laurent Vanbeylen, Anne Van Mulders and Johan Schoukens
Vrije Universiteit Brussel, Dept. ELEC, Pleinlaan 2, 1050 Brussel
Email: laurent.vanbeylen@vub.ac.be

1 Problem statement

This work is concerned with determining the (un)stable behaviour of discrete-time nonlinear *state-space models when excited with a random input signal*. For this kind of models, it may happen that the (in)stability properties depend on the stochastic nature of the random input. E.g. the system can show a stable behaviour at low amplitudes (variance), and an unstable behaviour at high amplitudes. In between, there can be a transition zone between low and high probabilities of instability. In the phase plane, this can be interpreted as a stable equilibrium in the neighbourhood of the origin (i.e. a bounded *Region Of Attraction* [ROA]) and the input disturbing the state in a random way. A low input amplitude causes the states to stay inside the ROA with high probability, while a large one may be more likely to push the state out of the ROA, and hence cause unstable operation with much higher probability. This idea is illustrated in Figure 1.

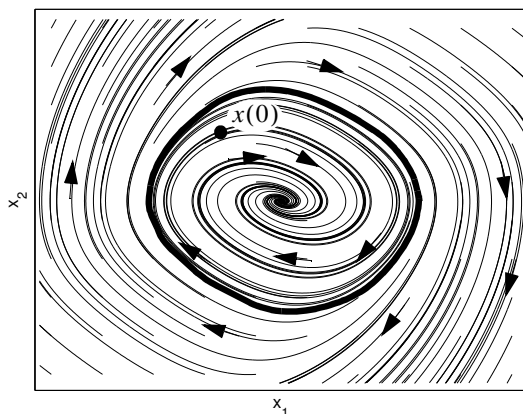


Figure 1: Instability: interpretation based on a Region Of Attraction (boundary shown in black) in the state space.

In this context, the question whether *the given model will be likely to behave stably or not* for a given class of input signals on a certain time interval $t = 0, \dots, \tau$, and starting at a given initial state $x(0)$ becomes relevant. This work allows to answer this question, in the case of a normally distributed input with a small variance and with a power spectrum determined by the user, viz. the k th frequency component's variance is specified as

$$U_k \sim N_C(0, \sigma_k^2) \quad (1)$$

with $\sigma_k^2 > 0$. The state transition function, of the form

$$x(t+1) = f(x(t), u(t)) \quad (2)$$

and its derivatives are assumed to be known.

2 Suggested approach

The probability density function (pdf) $p_{x(\tau)}(x(\tau))$ of the state $x(\tau) \in \mathbb{R}^n$ at the provided time instant τ , can be calculated as the integrated form of a higher-dimensional joint pdf based on all states and inputs:

$$p_{x(\tau)}(x(\tau)) = \int_{\mathbb{R}^{(\tau-1)n+\tau}} p_{X,x(\tau),U}(X, x(\tau), U) dX dU \quad (3)$$

with $X^T = [x(1)^T \dots x(\tau-1)^T] \in \mathbb{R}^{(\tau-1)n}$ and $U^T = [u(0) \dots u(\tau-1)] \in \mathbb{R}^\tau$; the integrand can be rewritten as $p_U(U) p_{X,x(\tau)|U}(X, x(\tau), U)$ with p_U a known Gaussian pdf based on (1), and $p_{X,x(\tau)|U}$ a known Dirac delta distribution imposing each state evolution equation (2) at $t = 0 \dots \tau-1$. If the input variance is small, the (very high dimensional) integral can be well approximated at any point of the state space via the Laplace integration method. This, in turn, requires the solution of a constrained optimization problem. After integration of the state pdf over a domain, one obtains the probability that the state has remained inside this domain. Taking the domain equal to the ROA yields the probability of stable operation until time instant τ .

3 Simulation example

The method is illustrated by means of a 2-dimensional example in Figure 2.

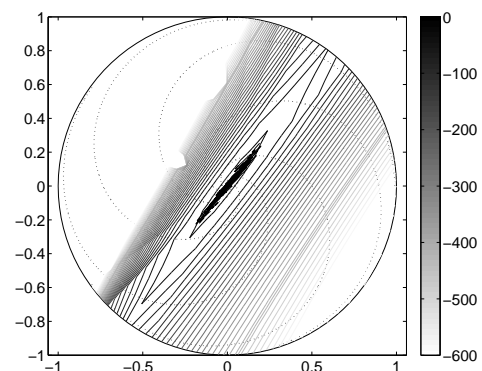


Figure 2: Contour lines of the estimated $\log p_{x(\tau)}(x(\tau))$; it is seen that random realizations stay in the high pdf region.

Numerical Solutions to Noisy Systems

Sanja Živanović

Centrum voor Wiskunde en Informatica
Amsterdam, 1098 XG, The Netherlands
Sanja.Zivanovic@cwi.nl

Pieter Collins

Centrum voor Wiskunde en Informatica
Amsterdam, 1098 XG, The Netherlands
Pieter.Collins@cwi.nl

1 Introduction

In this paper, we study systems of the form

$$\dot{x}(t) = f(x(t), u(t)), \quad u(t) \in U,$$

where $u(t)$ is bounded measurable function known as admissible control input. The main aim is to compute rigorous over-approximations to the set of reachable points at a given time T . By rewriting equation in the form

$$\dot{x}(t) \in F(x(t), U) = F(x(t)),$$

we obtain a differential inclusion describing the evolution. Differential inclusions are a generalization of differential equations with continuous or discontinuous right-hand sides with applications in many areas of science, such as mechanics, electrical engineering, the theory of automatic control, economical, biological, and social macrosystems, see [2], [5].

2 Objective

Some different techniques and various types of numerical approximations have been proposed in order for one to obtain approximations to the solution set of a differential inclusion. For example, ellipsoidal calculus was used by Valyi and Kurzanski [3], Lohner-type algorithm by Zgliczynski and Kapela [6], metric approximations by Puri and Varaiya [4]. However, these algorithms, either do not give rigorous over-approximations, or refer to linear systems, and mostly, approximations are of low-order (Euler approximations). We are interested in algorithms that give rigorous over-approximations to the solution set of a differential inclusion using high-order schemes.

3 What we do

In this paper, we present an algorithm for rigorous over-approximation of the solution set of control-affine systems

$$\dot{x}(t) = f(x(t)) + \sum_{i=0}^{N-1} g_i(x(t))u_i(t),$$

with inputs $u_i(t) \in [-1, 1]$. This corresponds to $F(x, U)$, a zonotope with N generators.

We make an approximation

$$\dot{x}(t) = f(x(t)) + \sum_{i=0}^{N-1} g_i(x(t))w_i(t),$$

where $w(t)$ is a finitely parametrised approximation to $u(t)$, and compute the uniform error if the time of computation is *a priori* known by taking w_i to be the average value \bar{u} of $u(t)$ over $[t, t+h]$. We obtain a first-order approximation. Currently, we are investigating the possibility of obtaining higher order accuracy, by taking a linear approximation to $u(t)$, $w(t) = a_0 + a_1 t$.

The algorithm for computation of the solution set consists of the following: we compute the flow of $\dot{x}(t) = f(x(t)) + \sum_{i=0}^{N-1} g_i(x(t))w_i$, taking (w_0, \dots, w_{N-1}) as parameters, and giving uniform bounds for the errors. We look at the possible reduction of parameters, e.g. using orthogonalization, and we split the new domain (if necessary) before returning to the first step.

To test our algorithms, we use tool Ariadne (a general-purpose reachability tool for computation and verification of hybrid systems, based on set-valued analysis of dynamical and control systems, see [1]).

References

- [1] Ariadne. <http://trac.parades.rm.cnr.it/ariadne/>
- [2] Filippov, A. F. Differential equations with discontinuous righthand sides. Translated from the Russian. Mathematics and its Applications (Soviet Series), 18. Kluwer Academic Publishers Group, Dordrecht, 1988.
- [3] Kurzanski, A.; Valyi, I. Ellipsoidal calculus for estimation and control. (English summary) Systems and Control: Foundations and Applications. Birkhuser Boston, Inc., Boston, MA; International Institute for Applied Systems Analysis, Laxenburg, 1997.
- [4] Puri, A.; Borkar, V. and Varaiya, P. ϵ -approximation of differential inclusions, Proc. of the 34th IEEE Conference on Decision and Control (1995), pp. 2892-2897.
- [5] Smirnov, G. V. Introduction to the theory of differential inclusions. Graduate Studies in Mathematics, 41. American Mathematical Society, Providence, RI, 2002.
- [6] Zgliczynski, P.; Kapela, T. A Lohner algorithm for perturbation of ODEs and differential inclusions. Discrete Contin. Dyn. Syst. Ser. B 11 (2009), no. 2, 365–385.

Smooth adaptive compensation of the input hysteresis

A. Katalenic, C.M.M. van Lierop
 Department of Electrical Engineering
 Eindhoven University of Technology
 P.O. Box 513, 5600 MB Eindhoven
 The Netherlands
 Email: a.katalenic@tue.nl

1 Introduction

Hysteretic systems are systems that produce different steady-state outputs for the same steady-state input value depending on the input history. Dependence of the output on the input signal history means that those systems have memory. In many applications hysteretic behavior can be neglected and expressed as random noise, but as expectations on precision and bandwidth rise, its effects have to be compensated. Hysteresis is usually present in the actuator and such systems can be modeled as a series connection of a hysteresis operator and some usually linear dynamics. The most generic approach in controlling such systems is to construct an inverse compensator for input hysteresis which will cancel its effects and then synthesize a controller for the remaining part using conventional techniques. The layout of such an approach is shown on figure 1. A survey of past attempts to control hysteretic systems with inverse compensation is given in [1]. Usually a *Preisach model* is fitted to the hysteretic nonlinearity and its inverse is then numerically implemented. Such a model is hard to identify and its inverse is computationally complex which means that it is not suited for systems where the hysteresis curve is unknown or not measurable with enough accuracy and precision. A solution to this problem was introduced in [2] where adaptive piecewise affine hysteresis inverse was constructed for known and unknown hysteretic plants. Here we introduce an adaptive hysteresis inverse that is *much smoother* than in [2] and fits practical problems more accurately without losing its adaptive nature.

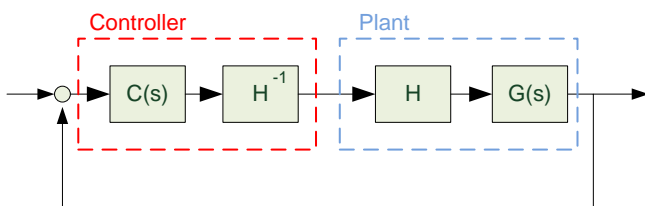


Figure 1: Generic approach in controlling systems with input hysteresis.

2 Smooth Hysteresis Inverse Compensator

The major hysteresis loop is approximated with two first order polynomials δ_1 and δ_2 , while transition curves inside the major loop are described with the smooth functions γ_1 and γ_2 which mimic transients observed in many applications. The given inverse model is described with only three parameters: k_1 , k_2 and k_3 which have a clear geometric meaning.

$$\begin{aligned}\delta_1(u(t)) &= k_3 \cdot u(t) + \frac{k_2}{2} \\ \delta_2(u(t)) &= k_3 \cdot u(t) - \frac{k_2}{2} \\ \gamma_1(u(t)) &= k_1 \left(1 - e^{-k_2(u(t)-u_{ch})} \right) + k_3(u(t) - u_{ch}) + v_{ch} \\ \gamma_2(u(t)) &= -k_1 \left(1 - e^{k_2(u(t)-u_{ch})} \right) + k_3(u(t) - u_{ch}) + v_{ch}\end{aligned}$$

Variables u_{ch} and v_{ch} represent the values of the input and output signals at the instant of the last input signal direction change. The output signal of the compensator is then constructed as follows:

$$v(t) = \begin{cases} \min(\gamma_1, \delta_1) & \dot{u}(t) \geq 0 \\ \max(\gamma_2, \delta_2) & \dot{u}(t) < 0 \end{cases} \quad (1)$$

3 Parameter adaptation

Inverse compensator (1) can be rewritten in the form of a *linear parametric model* where the smooth nonlinear functions γ_1 and γ_2 require prior linearization. Such a model can then be used in many adaptive schemes described in [3] resulting in adaptive compensation of input hysteresis that fits practical problems better than the piecewise affine compensator and is simpler and faster than compensators based on the Preisach model.

References

- [1] Ram V. Iyer, Xiaobo Tan, "Control of Hysteretic Systems Through Inverse Compensation," *IEEE Control Syst. Mag.*, vol. 29, no. 1, pp. 83-99, Feb. 2009.
- [2] Gang Tao, Petar V. Kokotovic, "Adaptive Control of Plants with Unknown Hystereses," *IEEE Transactions on Automatic Control*, vol. 40, no. 2, Feb. 1995.
- [3] Petros A. Ioannou, Jing Sun, "Robust Adaptive Control," Prentice Hall PTR, September 1, 1995.

Predictor based control of a mobile robot subject to a bilateral delay

Alejandro Alvarez-Aguirre*, Henk Nijmeijer
 Department of Mechanical Engineering
 Eindhoven University of Technology
 P.O. Box 513, 5600 MB Eindhoven
 The Netherlands
 Email: *a.a.alvarez@tue.nl

Toshiki Oguchi
 Department of Mechanical Engineering
 Tokyo Metropolitan University
 192-0397 Tokyo
 Japan

Introduction

In a setting where a robotic system and its controller are linked via a delayed communication channel, such as in Networked Control Systems (NCS), performance and stability are compromised. To compensate these negative effects, a state predictor based on synchronization is proposed.

State predictor based on synchronization

A state predictor was proposed in [1] inspired by the anticipating synchronization exhibited by some coupled chaotic systems. The same concept has been applied to a unicycle-type mobile robot subject to an input delay, and extended in order to cope with constant bilateral delays (cf. Fig. 1).

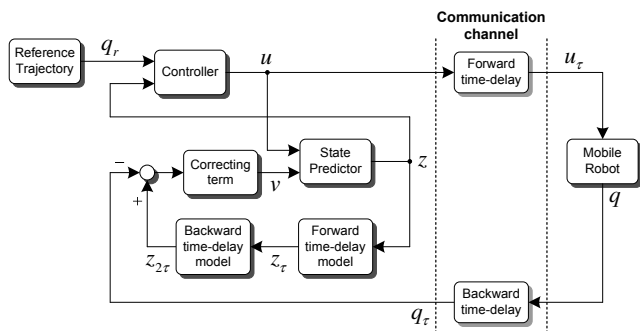


Figure 1: Bilateral predictor block diagram representation.

Consider the delay-free posture kinematic model of a unicycle-type mobile robot,

$$\dot{x} = v \cos \theta, \quad \dot{y} = v \sin \theta, \quad \dot{\theta} = \omega.$$

with the forward and angular velocities, v and ω , denoting the system's control inputs. Based on the robot's model, the following synchronizing state predictor is proposed,

$$\dot{z}_1 = v \cos z_3 + v_x, \quad \dot{z}_2 = v \sin z_3 + v_y, \quad \dot{z}_3 = \omega + v_\theta.$$

Given a reference trajectory which satisfies the kinematic model, two sets of error coordinates, z_e relating the reference and the predictor, and p_e relating the delayed predictor and the system, are used to define the correcting terms v ,

$$v_x = -K_x p_{1e} \cos z_3 + K_x p_{2e} \sin z_3,$$

$$v_y = -K_x p_{1e} \sin z_3 - K_y p_{2e} \cos z_3,$$

$$v_\theta = -K_\theta \sin p_{3e},$$

and the system's input velocities,

$$v = v_r + c_2 z_{1e} - c_3 \omega_r z_{2e}, \quad \omega = \omega_r + c_1 \sin z_{3e}.$$

Experimental results

The predictor-control scheme has been validated using the experimental setups for multi-robot systems available at TU/e and at Tokyo Metropolitan University (TMU). Data is exchanged between them by means of a TCP socket via a Virtual Private Network (VPN), inducing a round trip time-delay of approximately 265 ms. A mobile robot at TMU has been successfully controlled from TU/e (cf. Fig. 2).

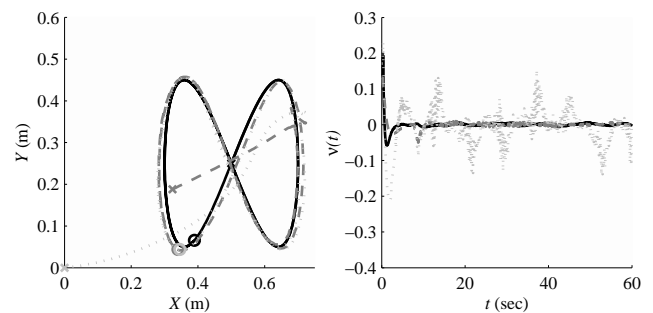


Figure 2: Workspace trajectories and correcting terms plots.

The left hand plot shows the reference (solid), mobile robot (dashed) and state predictor (dotted) trajectories in the X-Y plane, while the right hand one shows how the correcting terms v_x (solid), v_y (dashed) and v_θ (dotted) practically converge to zero. Under the assumption that the reference is not known a priori, the predictor-control scheme ensures that the system tracks a delayed version of the reference.

Conclusions and future work

The proposed state predictor and tracking controller combination are capable of coping with bilateral time-delays even if a small delay model mismatch exists. Future work includes increasing the predictor's robustness, integrating the concept with notions related to the long distance synchronization of robotic networks, and extending the predictor-control scheme to a more general setting.

References

- [1] T. Oguchi and H. Nijmeijer. Control of nonlinear systems with time-delay using state prediction based on synchronization. In *ENOC 2005*, pages 1150-1156, Eindhoven, The Netherlands, August 7-12, 2005.

Synchronization of diffusively coupled systems with time delayed interaction: a passivity based approach

Erik Steur, Henk Nijmeijer

Department of Mechanical Engineering
Eindhoven University of Technology

P.O. Box 513, 5600 MB, Eindhoven, The Netherlands

Email: (e.steur,h.nijmeijer)@tue.nl

1 Introduction

We discuss synchronization of a general class of nonlinear dynamical systems in networks with arbitrary network topology and time-delayed interactions. The systems will be called synchronized if the state variables of all systems asymptotically match.

In particular, we consider a network of k identical systems

$$\begin{aligned} \dot{y}_j(t) &= \alpha(y_j(t), z_j(t)) + u_j(t), \\ \dot{z}_j(t) &= \beta(z_j(t), y_j(t)), \end{aligned} \quad (1)$$

where $j = 1, 2, \dots, k$, output $y_j(t) \in \mathcal{Y} \subset \mathbb{R}^m$, input $u_j(t) \in \mathcal{U} \subset \mathbb{R}^m$, internal variables $z_j \in \mathcal{Z} \subset \mathbb{R}^p$. The network is represented by a (directed) graph $\mathcal{G} = (\mathcal{V}, \mathcal{E})$, where \mathcal{V} denotes the set of vertices (or nodes) and \mathcal{E} is the set of edges. We allow a general network topology. However, we will assume that

(A1) the graph \mathcal{G} is strongly connected.

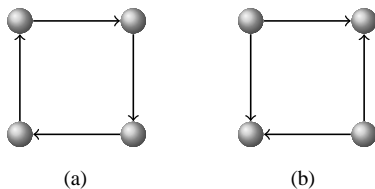


Figure 1: (a) A graph satisfying assumption (A1). (b) A graph that is not strongly connected since there is no directed path from the vertices in the bottom left and top right to the other vertices.

The systems (1) will interact via coupling of the form

$$u_j(t) = \sigma \sum_{\mathcal{E}_j} a_{ji} (y_i(t - \tau) - y_j(t - \tau)), \quad (2)$$

or

$$u_j(t) = \sigma \sum_{\mathcal{E}_j} a_{ji} (y_i(t - \tau) - y_j(t)), \quad (3)$$

where $\sigma \in \mathbb{R}_{>0}$ denotes the overall coupling strength, $\tau \in \mathbb{R}_{>0}$ is the time delay and $a_{ji} \in [0, 1]$. In addition, in case of coupling (3), to guarantee the existence of the linear invariant manifold

$$\mathcal{M} = \left\{ y \in \mathcal{Y}^k, z \in \mathcal{Z}^k : y_i = y_j, z_i = z_j, \forall i, j = 1, 2, \dots, k \right\}$$

it is assumed that

$$(A2) \sum_{\mathcal{E}_j} a_{ji} = 1 \text{ for all } j = 1, \dots, k.$$

2 Main result

Assume that each system (1) is strictly semi-passive, that is, each system has a limited amount of “free energy” available. Then, under assumption (A1) (and (A2)) the solutions of the closed-loop system (1), (2) (or (1), (3)) are *ultimately bounded*, i.e. all solutions enter a compact set in finite time and remain there as time increases. If in addition each subsystem $\dot{z}_j(t) = \beta(z_j(t), y_j(t))$ is minimum phase, then there exist constants $\bar{\sigma}$ and $\bar{\gamma}$ such that if the coupling strength $\sigma \geq \bar{\sigma}$ and $\sigma\tau \leq \bar{\gamma}$, the coupled systems always end up in synchrony. All formal statements, technical details and proofs can be found in [1]. In particular, there always exists a region in the σ - τ space, indicated in gray in Figure 2, such that if the time delay τ and the coupling strength σ belong to this region the coupled systems are guaranteed to synchronize.

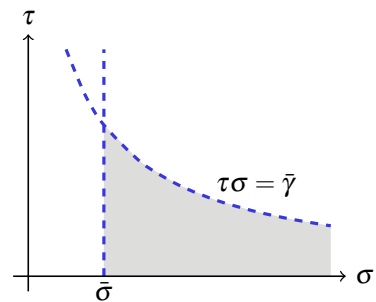


Figure 2: The curves $\tau\sigma = \bar{\gamma}$ and $\sigma = \bar{\sigma}$ in the σ - τ plane. The gray area indicates the region of synchronization.

3 Conclusions

Our results show that k strictly semipassive systems (1) with minimum phase internal dynamics, coupled via (3) or (2), will always synchronize given that the coupling is sufficiently large and the time delay sufficiently low. The result holds for general network topology under the connectivity assumption (A1).

References

- [1] Erik Steur and Henk Nijmeijer, *Synchronization in networks of linearly time-delay coupled systems: a passivity based approach*, (submitted for publication), 2009

Lyapunov theory for delay difference inclusions

Rob Gielen and Mircea Lazar

Electrical Engineering, Eindhoven University of Technology

P.O. Box 513, 5600 MB, Eindhoven

The Netherlands

Email: {r.h.gielen,m.lazar}@tue.nl

Ilya Kolmanovsky

Ford Motor Company

Dearborn, Michigan

United States of America

Email: ikolmano@ford.com

1 Abstract

In this talk we will discuss systems affected by time-delays. Comprehensive overviews of various types of time-delay systems are given in [1] and [2]. Motivated by developments in the field of networked control systems (NCS), we focus on delay discrete-time systems. Recently, polytopic delay difference inclusions emerged as a natural, adequate modeling framework for NCS, see, e.g., [3]. Therefore, we provide a complete Lyapunov framework for stability analysis and stabilization of delay difference inclusions.

However, for systems affected by delays the classical Lyapunov theory does not apply straightforwardly, as the influence of past states can cause a violation of the monotonic decrease condition that a standard Lyapunov function (LF) obeys. Therefore, two relaxations of Lyapunov theory were proposed to deal with this issue. The first relaxation [4] allows the function, called Lyapunov-Krasovskii function (LKF), to use additional information, i.e. an LKF depends on both the current state and the entire past state trajectory. The second relaxation [1] allows the function, called Lyapunov-Razumikhin function (LRF), to be non-monotonic, i.e. an LRF is required to decrease only if a certain condition on the past state trajectory and current state holds. In [2] it was proven that LRFs form a particular case of LKFs, when only stability of the origin rather than asymptotic stability, is of concern.

All of the above-mentioned results hold for systems described by differential equations. When stability of discrete-time systems affected by delay is analyzed, one of the most commonly used approaches [5] is to augment the state vector with the past states to obtain a larger dimension system. A classical LF can then be used to establish stability of this system with augmented state vector. Recently, in [6] it was pointed out that such an LF for the augmented state system provides an LKF for the original system affected by time-delay. As such, an equivalent notion of LKFs for discrete-time systems was obtained. However, for LRFs the situation is more complicated. The exact translation of this approach for discrete-time systems yields a non-causal constraint. An alternative, Razumikhin-like condition for discrete-time systems was proposed in [7], where the LRF was required to be less than the maximum over its past values within some time window. To the best of our knowledge, a result on the con-

nection between LKFs and LRFs for discrete-time systems is missing.

In this talk we first present a stability theorem based on the Krasovskii and Razumikhin approach, respectively, that extends the above results for delay difference equations to delay difference *inclusions*, which form a relevant modeling class for NCS. Then, we provide a novel result that reveals the existence of an LRF as a sufficient condition for the existence of an LKF and thus, shows that LRFs as defined in this paper form a particular type of LKFs. This result confirms the continuous-time result of [2]. For polytopic delay difference inclusions and quadratic or infinity norm based Lyapunov function candidates we provide constructive methods for analysis and synthesis, in terms of both LKFs and LRFs, respectively.

References

- [1] J. Hale, *Theory of functional differential equations*. Springer-Verlag, New York, 1977.
- [2] V. Kolmanovskii and A. Myshkis, *Introduction to the theory and applications of functional differential equations*. Kluwer Academic Publishers, 1999.
- [3] R. H. Gielen, S. Oлару, and M. Lazar, "On polytopic approximations of systems with time-varying input delays," in *Nonlinear Model Predictive Control: Towards new challenging applications*, ser. Lecture Notes in Control and Information Sciences, vol. 384. Springer, 2009, pp. 225–233.
- [4] N. N. Krasovskii, *Stability of motion*. Stanford University Press, 1963.
- [5] K. J. Åström and B. Wittenmark, *Computer controlled systems, theory and design*. Englewood Cliffs, NJ: Prentice Hall International, Inc., 1990.
- [6] L. Hetel, J. Daafouz, and C. Iung, "Equivalence between the Lyapunov-Krasovskii functionals approach for discrete delay systems and that of the stability conditions for switched systems," *Nonlinear Analysis: Hybrid Systems*, vol. 2, no. 3, pp. 697–705, 2008.
- [7] B. Liu and H. J. Marquez, "Uniform stability of discrete delay systems and synchronization of discrete delay dynamical networks via Razumikhin technique," *IEEE Transactions on Circuits and Systems*, vol. 55, no. 9, pp. 2795–2805, 2008.

A comparison of approximation algorithms for the joint spectral radius

Chia-Tche Chang and Vincent D. Blondel

Department of Applied Mathematics

Université catholique de Louvain

Avenue Georges Lemaître, 4, B-1348 Louvain-la-Neuve, Belgium

Email: {chia-tche.chang, vincent.blondel}@uclouvain.be

Abstract

Let Σ be a set of $n \times n$ matrices and let us consider the following linear iteration:

$$x(t+1) = A_t x(t), \quad A_t \in \Sigma \text{ for all } t.$$

These kinds of *switched linear systems* arise in many applications such as asynchronous systems, hybrid systems, switching control, ...

The stability under arbitrary switchings of this system depends on a quantity called the *joint spectral radius (JSR)*, which represents the maximal growth rate of such a discrete linear system. More precisely, the JSR of a set Σ of matrices is defined by the following expression:

$$\rho(\Sigma) = \lim_{k \rightarrow \infty} \max \{ \|A_{i_1} \dots A_{i_k}\|^{1/k} \mid A_i \in \Sigma \},$$

independently of the matrix norm used. For bounded sets Σ , the JSR is also equal to the so-called generalized spectral radius $\bar{\rho}$, defined by the following equation:

$$\bar{\rho}(\Sigma) = \limsup_{k \rightarrow \infty} \max \{ \rho(A_{i_1} \dots A_{i_k})^{1/k} \mid A_i \in \Sigma \}.$$

For the linear iterations we consider, all trajectories converge thus to the origin if and only if the JSR of the corresponding set of matrices is strictly less than 1.

Another quantity of interest is the *joint spectral subradius (JSS)*, also called lower spectral radius, which represents the minimal achievable growth rate:

$$\check{\rho}(\Sigma) = \lim_{k \rightarrow \infty} \min \{ \|A_{i_1} \dots A_{i_k}\|^{1/k} \mid A_i \in \Sigma \}.$$

The JSS is related to the mortality problem, where we ask if the zero matrix can be expressed as a finite product of matrices in Σ .

The joint spectral quantities are notoriously difficult to compute. Indeed, it is NP-Hard to approximate the JSR ; moreover, the problem of checking whether $\rho \leq 1$ is undecidable, and the decidability of the question $\rho < 1$ is currently unknown. Furthermore, the problem of approximating the JSS is undecidable in the general case (see [1] for a survey on

the joint spectral quantities). Despite these negative theoretical results, several algorithms have been designed in order to approximate the JSR. Indeed, in the case of the JSR, the following easy property holds:

$$\rho(\Sigma) = \inf_{\|\cdot\|} \max \{ \|A\| \mid A \in \Sigma \}.$$

Thus, one way to compute the JSR is to try to find a norm such that $\rho(\Sigma) = \max \{ \|A\| \mid A \in \Sigma \}$, i.e., an *extremal* norm. Several methods have been designed using this fact (see for example [2], [3], [4]). In this paper, we will study and compare several techniques for the computation of the joint spectral quantities, such as semidefinite programming that computes the infimum on a class of norms, or geometric algorithms that tries to approximate the unit ball of an extremal norm using polytopes.

Acknowledgements

This paper presents research results of the Belgian Network DYSCO (Dynamical Systems, Control, and Optimization), funded by the Interuniversity Attraction Poles Programme, initiated by the Belgian State, Science Policy Office. The scientific responsibility rests with the authors. Chia-Tche Chang is a Research Fellow of the *Fonds National de la Recherche Scientifique (F.R.S.-FNRS)*.

References

- [1] Raphaël M. Jungers, “The joint spectral radius, theory and applications”, *Lecture Notes in Control and Information Sciences*, Springer-Verlag, Berlin, 2009.
- [2] Vincent D. Blondel, Yurii Nesterov and Jacques Theys, “On the accuracy of the ellipsoid norm approximation of the joint spectral radius”, *Linear Algebra and its Applications*, 394(1):91–107, 2005.
- [3] Nicola Guglielmi, Marino Zennaro, “Finding extremal complex polytope norms for families of real matrices”, *SIAM Journal of Matrix Analysis and Applications*, 31(2):602–620, 2009.
- [4] Vladimir Protasov, Raphaël M. Jungers, Vincent D. Blondel, “Joint spectral characteristics of matrices: a conic programming approach”, *SIAM Journal of Matrix Analysis and Applications*, to appear.

Fixed-order Robust Controller and Time Domain Response Improvement

Keivan Zavari¹, Hamid Khatibi², Jan Swevers¹

¹ Department of Mechanical Engineering, Katholieke Universiteit Leuven, Belgium

² Electrical Engineering Department, Sharif University of Technology, Tehran, Iran

Email: keivan.zavari@student.kuleuven.be

1 Introduction

Modern controller design techniques such as \mathcal{H}_∞ and LQG, result in controllers of order at least equal to that of the plant, and usually higher because of the inclusion of weight functions. On the other hand, in the implementation phase, high-order controllers will lead to some problems both in software and hardware. Low-order controllers are always welcomed because of simplicity and hence their industrial usage such as embedded control systems for the space and aeronautics industry is more prevalent.

2 Fixed-order controller parameterization

Overshoot reduction of the step response in fixed-order controller design for polytopic systems is considered. A recent convex parameterization for fixed-order stabilizing controllers using polynomial approach based on KYP lemma is used [1]. This parameterization for discrete-time systems is equivalent to the existence of a positive definite matrix $P_i = P_i^T > 0$ for each vertex of a polytope which satisfies:

$$\begin{bmatrix} A^T P_i A - P_i & A^T P_i B - C_i^T \\ B^T P_i A - C_i & B^T P_i B - D_i - D_i^T \end{bmatrix} < 0, \quad (1)$$

where (A, B, C_i, D_i) is the controllable canonical realization form of a SPRness transfer function $H(z) = \frac{c^i(z)}{d(z)}$. The numerator $c^i(z)$ is the closed-loop characteristic polynomial for each vertex of a polytopic system and $d(z)$ is a predetermined polynomial called *central polynomial*. Note that the parameterization for continuous-time systems is very similar to 1.

3 Time-domain response improvement

Fixed-order controller parameterization of [1] is employed and three approaches are derived to place additional convex constraints in the optimization problem for minimizing the overshoot of the closed-loop step response. In addition, they can be easily extended to polytopic systems which is one of the most common ways to present structured uncertainty.

The first approach is based on the peak-to-peak gain performance formulation provided in [2, 3] for continuous and discrete-time systems respectively. The performance is not a convex constraint for fixed-order controller design problem

and hence the criterion is modified and used for minimizing the peak value of the step response.

In the next proposed method, it is shown that Markov parameters and pole assignment method can be employed to formulate a new cost function for the optimization problem. As soon as we fix the denominator by the stated pole assignment method, the problem comes linear with respect to the design parameters. Moreover, since the error signal is minimized, the rise-time of the closed-loop step response is reduced as well as the overshoot.

The third method is similar to the second method in continuous-time systems i.e. using the time-domain signal to improve the transient response. Inverse Laplace transform helps to derive a constraint via the Residue theorem. Due to the non-convexity of the constraint, a pole assignment is applied to the closed-loop system as well as the previous method.

Simulation results illustrate how these methods effectively reduce the overshoot of the closed-loop step response. A third order discrete-time polytopic system is used to compare the first method which is the modified peak-to-peak gain method, to the Markov parameters and \mathcal{H}_2 norm method. The key in \mathcal{H}_2 method is that the 2-norm of a transfer function and time-domain signal are related via Parseval's theorem. The last method is also compared to another existing approach for transient response improvement.

References

- [1] H. Khatibi, A. Karimi, and R. Longchamp, *Fixed-order controller design for systems with polytopic uncertainty using LMIs*, IEEE Transactions on Automatic Control **53** (2008), no. 1, 428–434.
- [2] J. M. Rieber, C. W. Scherer, , and F. Allgower, *Robust L_1 performance analysis for linear systems with parametric uncertainties*, International Journal of Control **81** (2008), no. 5, 851–864.
- [3] C. Scherer, P. Gahinet, and M. Chilali, *Multiobjective output-feedback control via LMI optimization*, IEEE Transactions on Automatic Control **42** (1997), no. 7, 896–911.

On Algebraic Riccati Equations Whose Coefficient Matrices Depend Periodically on a Single State Variable

S. Muhammad

Delft Institute of Applied Mathematics (DIAM), Delft University of Technology,
Mekelweg 4, 2628 CD, Delft, The Netherlands.
s.muhammad@tudelft.nl

J. van der Woude

Delft Institute of Applied Mathematics (DIAM), Delft University of Technology,
Mekelweg 4, 2628 CD, Delft, The Netherlands.
j.w.vanderwoude@tudelft.nl

1 Introduction

Use of the state dependent algebraic Riccati equations is very popular in control design and estimation problems, [1], [2], [3] etc. We study a type of state dependent algebraic Riccati equations in which the state dependency of the coefficient matrices is of periodic nature. In particular, the system matrix depends on a single state component in a periodic way. Specifically, we study the following SDARE

$$\Pi(x_1)A(x_1) + A^T(x_1)\Pi(x_1) - \Pi(x_1)BR^{-1}B^T\Pi(x_1) + Q = 0,$$

where $x_1 \in \mathbb{R}$, without loss of generality, is the first component of the state vector $\boldsymbol{x} \in \mathbb{R}^n$, $A(x_1) \in \mathbb{R}^{n \times n}$, $\Pi(x_1) \in \mathbb{R}^{n \times n}$, $B \in \mathbb{R}^{n \times m}$, $R \in \mathbb{R}^{m \times m}$, and $Q \in \mathbb{R}^{n \times n}$.

We assume that the system matrix $A(x_1)$ is piecewise smooth and θ -periodic which means that the solution matrix, $\Pi(x_1)$ is also piecewise smooth and θ -periodic. Therefore, we can introduce an interpolation method based on the Fourier series to approximate the solution of the state dependent algebraic Riccati equations of this type. i.e, we write

$$\Pi(x_1) = \frac{a_0}{2} + \sum_{k=1}^{\infty} \left(a_k \cos \frac{2k\pi x_1}{\theta} + b_k \sin \frac{2k\pi x_1}{\theta} \right).$$

The Fourier coefficients a_0 , $a_k \in \mathbb{R}^{n \times n}$ and $b_k \in \mathbb{R}^{n \times n}$ for $k = 1, 2, 3, \dots$ are constant symmetric matrices.

The Fourier coefficients are then computed by using interpolation technique. The details of the computations are omitted because of the space limitations. The advantage of this approach lies in the offline computations of the Fourier coefficients therein. This in turn results in significant reduction in the online computations of the solution of the state dependent algebraic Riccati equations. We elaborate our approach and prove its utility by using it for a physical model [4] of a ship's motion with 3 degrees of freedom (surge, sway, and yaw).

We made a quantitative comparison of two solution methods for the solution of the state dependent algebraic equation;

the Fourier series interpolation method and the solution obtained from the MATLAB routine "care" (which uses the Schur decomposition method). We noticed that the online computation time of the state dependent algebraic Riccati equation, for the particular example, has been reduced 10 times as compared with "care". Simulation results also reveals that the Fourier series based approximation of the solution converges quickly, in terms of the number of the Fourier coefficients, to the exact solution of the state dependent algebraic Riccati equation.

References

- [1] Banks, H. T., B. M. Lewis, and H. T. Tran. Nonlinear feedback controllers and compensators: a state dependent Riccati equation approach. *Computational Optimization and Applications*, 37(2):177-218, June 2007.
- [2] Çimen, T. State dependent Riccati equation control: a survey. *Proceedings of the International Federation of Automatic Control (IFAC'08) Conference*, pages:3761-3775, July 2008.
- [3] Menon, P. K., T. M. Lam, L. S. Crawford, and V. H. L. Chang. Real time computational methods for SDRE nonlinear control of missiles. *Proceedings of the American Control Conference Workshop*, 2002.
- [4] Snijder, J. Master thesis, *Wave Filtering and Thruster Allocation for Dynamic Positioned Ships*. Mathematical Systems Theory Group, Delft Institute of Applied Mathematics (DIAM), EWI Faculty, TU Delft, 2005.

Solving systems of polynomial equations: from algebraic geometry to linear algebra

Philippe Dreesen Kim Batselier Bart De Moor
Katholieke Universiteit Leuven

Department of Electrical Engineering ESAT/SCD (SISTA)
Kasteelpark Arenberg 10/2446, B-3000 Leuven, Belgium.

{philippe.dreesen, kim.batselier, bart.demoor}@esat.kuleuven.be

1 Introduction

The task of finding the solutions of a system of polynomial equations is a fundamental problem in mathematics which arises at the core of many applications in science and engineering. Recent years have witnessed a large increase in the interest in finding efficient algorithms for solving polynomial systems. On the one hand, the ever increasing availability of computing power has given rise to the successful application of algorithms from algebraic geometry to real-world problems. On the other hand, by taking into consideration the algebraic nature of the task, one is able to tackle the problem in a more thorough fashion, aiming to find all solutions.

Although there exists a huge body of knowledge in algebraic geometry research [1], there is quite a large gap between research results in this field, and their applicability. A lot of literature on algebraic geometry is available, which is generally expressed in an abstract mathematical language and mainly cast into an exact arithmetic framework. However, there is a lack of useful numerical algorithms taking into account the limited accuracy of the data measured, and the machine precision of the required calculations (i.e., floating point arithmetic instead of infinite precision (integer) calculations) implementing these deep results.

2 From Algebraic Geometry to Linear Algebra

The works of Sylvester and Macaulay [5, 8] have established a deep link between polynomial system solving and linear algebra (which has been rediscovered many times ever since [7]). The method we will discuss phrases the task at hand as a problem in (numerical) linear algebra by considering a matrix containing the coefficients multiplied with a vector containing monomials [2]. The application of realization theory in the kernel of the coefficient matrix leads to the surprising result that all solutions can be found from the solution of a generalized eigenvalue problem. (Note that also polynomial optimization problems can be tackled in the same way; the optimal solution can be found from applying the Lagrange multipliers method. Moreover, it can be shown that in the case of polynomial optimization problems, the (globally) optimal solution corresponds to an extremal eigenvalue.)

3 Applications

Although a limiting computational complexity is inherent to the problem, this approach sheds a new light on many classical problems in (applied) mathematics and engineering, and reveals several interesting links with systems theory and realization theory [3]. We will highlight a selection of possible applications in system identification [4] and algebraic statistics [6].

4 Acknowledgements

PD is supported by the Institute for the Promotion of Innovation through Science and Technology in Flanders (IWT-Vlaanderen). BDM is a full professor at Katholieke Universiteit Leuven, Belgium. Research supported by *Research Council KUL*: GOA AMBioRICS, GOA MaNet, CoE EF/05/006 Optimization in Engineering (OPTEC), IOF-SCORES4CHEM, several PhD/postdoc & fellow grants; *Flemish Government*: FWO: PhD/postdoc grants, projects G.0452.04 (new quantum algorithms), G.0499.04 (Statistics), G.0211.05 (Nonlinear), G.0226.06 (cooperative systems and optimization), G.0321.06 (Tensors), G.0302.07 (SVM/Kernel), G.0320.08 (convex MPC), G.0558.08 (Robust MHE), G.0557.08 (Glycemia2), G.0588.09 (Brain-machine) research communities (ICCoS, ANMMM, MLDM); G.0377.09 (Mechatronics MPC); IWT: PhD Grants, McKnow-E, Eureka-Flite+, SBO LeCoPro, SBO Climaqs, POM; *Belgian Federal Science Policy Office*: IUAP P6/04 (DYSCO, Dynamical systems, control and optimization, 2007-2011); *EU*: ERNSI; FP7-HD-MPC (INFOS-ICT-223854), COST intelliCIS, EMBOCOM; *Contract Research*: AMINAL; *Other*: Helmholtz: viCERP; ACCM; Bauknecht; Hoerbiger.

References

- [1] D. A. Cox, J. B. Little, and D. O'Shea. *Ideals, Varieties and Algorithms*. Springer-Verlag, third edition, 2007.
- [2] P. Dreesen and B. De Moor. Polynomial optimization problems are eigenvalue problems. In P. M. J. Van den Hof, C. Scherer, and P. S. C. Heuberger, editors, *Model-Based Control – Bridging Rigorous Theory and Advanced Technology*, pages 49–68. Springer, 2009.
- [3] B. Hanzon and M. Hazewinkel, editors. *Constructive Algebra and Systems Theory*. Royal Netherlands Academy of Arts and Sciences, 2006.
- [4] L. Ljung and T. Glad. On global identifiability for arbitrary model parametrizations. *Automatica*, 35(2):265–276, 1994.
- [5] F. S. Macaulay. On some formulae in elimination. *Proc. London Math. Soc.*, 35:3–27, 1902.
- [6] L. Pachter and B. Sturmfels. *Algebraic Statistics for Computational Biology*. Cambridge University Press, 2005.
- [7] H. J. Stetter. *Numerical Polynomial Algebra*. SIAM, 2004.
- [8] J. J. Sylvester. On a theory of syzygetic relations of two rational integral functions, comprising an application to the theory of sturms function and that of the greatest algebraical common measure. *Trans. Roy. Soc. Lond.*, 1853.

Computation of chopped system norm

Hanumant Singh Shekhawat
 Department of Applied Mathematics
 University of Twente
 P.O. Box 217, 7500 AE Enschede
 The Netherlands
 Email: h.s.s.shekhawat@utwente.nl

Gjerrit Meinsma
 Department of Applied Mathematics
 University of Twente
 P.O. Box 217, 7500 AE Enschede
 The Netherlands
 Email: g.meinsma@utwente.nl

1 Introduction

For given $\omega_N \geq 0$ and a finite dimensional system $G(s) = C(sI - A)^{-1}B$, the squared chopped norm

$$\|G\|_{\omega_N}^2 := \frac{1}{\pi} \operatorname{tr} \int_{\omega_N}^{\infty} G^{\sim}(i\omega)G(i\omega)d\omega \quad (1)$$

computation is required, e.g. in [1] for calculating the signal reconstruction error. It is a classic result that for a stable system the squared L^2 norm is given by

$$\|G\|_{L^2}^2 := \frac{1}{\pi} \operatorname{tr} \int_0^{\infty} G^{\sim}(i\omega)G(i\omega)d\omega = \operatorname{tr}(B^T P B) \quad (2)$$

where P is the unique solution of the linear Lyapunov equation

$$A^T P + P A = -C^T C. \quad (3)$$

In this paper, we are answering the question that similar to the stable system, can we express chopped norm into a single expression for a system with poles in left half plane (i.e. stable poles), or poles on imaginary axis or both (as required by [1]).

2 Chopped norm for systems with imaginary and stable poles

For a system with poles on the imaginary axis and poles in the left half plane, the squared L^2 norm (2) is not finite. On the other hand, the chopped norm (1) may be finite but requires a computation of a matrix logarithm. Now the logarithm of a matrix $X \in \mathbb{C}^{n \times n}$ itself is multivalued, but it can be made unique by requiring, for instance, that X do not have no eigenvalues on \mathbb{R}^- (closed negative real axis). In this way a unique matrix logarithm $\log(X)$ exists and it is standard in the literature, known as the *principal logarithm* [2, Theorem 1.31].

Theorem 2.1. *Suppose G is strictly proper and let $G(s) = C(sI - A)^{-1}B$ with A, B, C real matrices. Also, suppose $\operatorname{Re} \lambda_k \leq 0$ for all eigenvalues λ_k of A . Then*

$$\|G\|_{\omega_N}^2 = \frac{i}{\pi} \operatorname{tr} \{ \tilde{C} \log(\omega_N I - \tilde{A}/i) \tilde{B} \} \quad (4)$$

for $\tilde{A}, \tilde{B}, \tilde{C}$ defined as

$$\left[\begin{array}{c|c} \tilde{A} & \tilde{B} \\ \hline \tilde{C} & 0 \end{array} \right] := \left[\begin{array}{cc|c} A & 0 & B \\ -C^T C & -A^T & 0 \\ \hline 0 & B^T & 0 \end{array} \right] \quad (5)$$

and $\omega_N > \omega_{\max} = \max |\omega_k|$ where the maximum is taken over all imaginary eigenvalues $i\omega_k$ of A . \log denotes principal logarithm.

Since $\operatorname{tr} \{ \tilde{C} \tilde{B} \} = 0$, (4) is valid not only for G with poles on the imaginary axis and poles in the left half plane, but also for G with poles anywhere in complex plane. Note that the eigenvalues of matrix $\omega_N I - \tilde{A}/i$ do not lie on \mathbb{R}^- for $\omega_N > \omega_{\max}$. This is crucial for the principal logarithm to exist.

3 Chopped norm for system with stable poles

For given matrix $A \in \mathbb{R}^{n \times n}$, the chopped norm (4) requires computation of the logarithm of a $2n \times 2n$ matrix. But it can be reduced to the logarithm of a $n \times n$ matrix if the system is stable.

Theorem 3.1. *Suppose G is stable and strictly proper. Let $G(s) = C(sI - A)^{-1}B$ with A, B, C real matrices and A is asymptotically stable. Then (1) equals*

$$\|G\|_{\omega_N}^2 = -\frac{2}{\pi} \operatorname{Im} \operatorname{tr} \left\{ B^T P \log\left(\omega_N I - \frac{A}{i}\right) B \right\} \quad (6)$$

$$= \|G\|_{L^2}^2 - \frac{2}{\pi} \operatorname{Im} \operatorname{tr} \{ B^T P \log(i\omega_N I - A) B \} \quad (7)$$

where P is the unique solution of (3) and \log denotes the principal logarithm.

Theorem 3.1 can also be proved using the observability grammian in the limited frequency interval [3]. It can be shown that (6) and (7) equal the squared L^2 -norm, if $\omega_N = 0$.

References

- [1] Meinsma, G. and Mirkin, L., "System theoretic perspectives of the sampling theorem", Int. Sym. on Mathematical Theory of Networks and Systems, 24-28 July 2006, Kyoto, Japan.
- [2] Nicholas J. Higham, "Functions of Matrices: Theory and Computation", SIAM, 2008.
- [3] W. Gawronski, J.-N. Juang, "Model reduction in limited time and frequency intervals", Int. J. Systems Sciences, 349-376, 21(2), 1990.

An Approximation Method for Stochastic Max-Plus Linear Systems

Samira S. Farahani

Delft Center for Systems and Control
Delft University of Technology
Mekelweg 2, 2628 CD Delft
The Netherlands

Email: s.safaeifarahani@tudelft.nl

T. J. J. van den Boom

Delft Center for Systems and Control
Delft University of Technology
Mekelweg 2, 2628 CD Delft
The Netherlands

Email: a.j.j.vandenboom@tudelft.nl

B. De Schutter

Delft Center for Systems and Control
Delft University of Technology
Mekelweg 2, 2628 CD Delft
The Netherlands

Email: b.deschutter@tudelft.nl

1 Introduction

Due to the many attractive features of Model Predictive Control (MPC) such as handling constraints on inputs or outputs in a systematic way, it is one of the most widely used advanced control designed methods in the process industry. Besides conventional MPC, which uses linear or non-linear discrete-time models, MPC has been extended to a class of discrete-event systems, namely the max-plus linear systems. Loosely speaking, this class refers to the class of discrete event systems with synchronization but no concurrency. Such models are based on two main operations, maximization and addition. This leads to a description that is linear in max-plus algebra. One of the relevant topics that has attracted many attention recently, is the application of MPC for perturbed max-plus-linear systems in which modeling errors, noise, and/or disturbances are present. Both noise and modeling error leads to the perturbation of the system matrices; fast changes relate to noise and disturbances, while slow changes or permanent errors are considered as model mismatch.

Our focus is on the extension of the work presented in [1] where MPC for perturbed max-plus-linear system is studied in a stochastic setting. At each event step in [1], an optimization problem needs to be solved and our aim is to reduce the complexity and the computation time of it.

2 Methodology

According to the MPC methodology, the aim is to compute at each event step k an optimal input sequence that minimizes the cost criterion $J(k) = J_{\text{out}}(k) + J_{\text{in}}(k)$, which reflects the input and output cost functions over a prediction period of N_p event steps, subject to linear constraints on the inputs and outputs. Since the error is introduced as a stochastic variable, one suitable choice for the output cost

function is the sum of the expectation of the tardiness error,

$$J_{\text{out}} = \sum_{i=0}^{N_p-1} \sum_{l=1}^{n_y} E(\max(y_l(k+i) - r_l(k+i), 0)), \quad (1)$$

where $y(k+i)$ and $r(k+i)$ are the output and reference vector at event step $k+i$, respectively. However, the direct computation of the expectation is both cumbersome and time-consuming; therefore, it is desired to find an approximation method to decrease the computational complexity.

To fulfill this goal, we propose an approximation method, inspired by the inequality and limit conditions of the p -norm of vectors and matrices. In this method, instead of the direct computation of the expected value, the p -th root of the sum of the p -th moments of each value will be computed.

3 Results and Perspectives

As a first step, every element of the error vector is assumed to have a standard normal distribution. By choosing the appropriate p , the p -th moment is close enough to the exact value of the expectation of the tardiness error in (1). This results in a much more efficient computation.

The next step is to check the convexity of the approximation function. In case of the convexity, we can apply fast and efficient algorithms for convex optimization. Then the next step is to apply this approximation method for other perturbed systems such as the max-min-plus scaling perturbed systems in order to achieve new results and thus increase the computational efficiency for these systems.

References

- [1] T. van den Boom and B. De Schutter, Model predictive control for perturbed max-plus-linear systems: A stochastic approach. *International Journal of Control*, vol. 77, no. 3, pp. 302-309, February 2004.

ACADO Multi-Objective: a toolkit for multiple objective optimal control

Filip Logist, Jan Van Impe
BioTeC & OPTEC, Chemical Engineering Dept., K.U. Leuven
W. de Croylaan 46, B-3001 Leuven, Belgium.
Email: {filip.logist, jan.vanimpe}@cit.kuleuven.be

Boris Houska, Moritz Diehl
SCD & OPTEC, Electrical Engineering Dept., K.U. Leuven,
Kasteelpark Arenberg 10, 3001 Leuven, Belgium.
Email: {boris.houska, moritz.diehl}@esat.kuleuven.be

1 Introduction

Many practical engineering problems involve the determination of optimal control trajectories for given multiple and conflicting objectives. These conflicting objectives typically give rise to a set of Pareto optimal solutions. To enhance real-time decision making efficient approaches are required for determining the Pareto set in a fast and accurate way.

2 Approach

Hereto, the current paper integrates efficient multiple objective scalarisation strategies (e.g., Normal Boundary Intersection (NBI) [1] and Normalised Normal Constraint (NNC) [4]) with fast deterministic approaches for dynamic optimisation (e.g., Single and Multiple Shooting). The scalarisation methods convert the original multi-objective optimisation problem into a series of parametric single objective optimisation problems whose solution each time yields one point of the Pareto set. By consistently varying the scalarisation parameter(s) (often referred to as weight(s)) an approximation of the Pareto set is obtained.

3 ACADO Multi-Objective

Building on the proof-of-principle given in [3], all techniques have been implemented as an easy-to-use add-on module of the automatic control and dynamic optimisation toolkit ACADO [2] which are both freely available at www.acadotoolkit.org. Due to the self-contained, object-oriented, C++ implementation, the toolkit is easy-to-use, does not require third-party software, and allows a flexible control over algorithmic settings.

ACADO Multi-Objective allows an automatic generation of Pareto sets for multiple objective optimal control problems. Its features include: (i) several multiple objective optimisation methods (i.e., NBI, NNC as well as the classic weighted sum), (ii) an automatic generation of the scalarisation parameter values (or weights), (iii) different initialisa-

tion strategies for the series of single objective optimisation problems (e.g., fixed initial guess, hot-start policies), (iv) various direct optimal control approaches (currently Single Shooting and Multiple Shooting are available, while Orthogonal Collocation will be made available in the near future), (v) a Pareto filter to remove possibly generated non-Pareto optimal solutions and (vi) several visualisation and export features.

4 Results

It will be illustrated how to set up an multiple objective optimal control problem in ACADO. Several successful applications of ACADO Multi-Objective to problems from various engineering disciplines ((bio)chemical engineering, mechanical engineering,...) will be discussed.

5 Acknowledgements

This research was supported by Research Council KUL: CoE EF/05/006 Optimization in Engineering (OPTEC), OT/03/30, OT/09/025TBA, IOF - SCORES4CHEM HBKP/06/002 KP/09/005; the Flemish Government via the FWO research community ICCoS; and the Belgian Federal Science Policy Office: IUAP P6/04. J. Van Impe holds the chair Safety Engineering sponsored by the Belgian chemistry and life sciences federation essencia. The scientific responsibility is assumed by its authors.

References

- [1] I. Das and J.E. Dennis. Normal-Boundary Intersection: A new method for generating the Pareto surface in nonlinear multicriteria optimization problems. *SIAM Journal on Optimization*, 8:631–657, 1998.
- [2] B. Houska, H.J. Ferreau, and M. Diehl. ACADO Toolkit homepage. <http://www.acadotoolkit.org>, 2009.
- [3] F. Logist, P.M.M. Van Erdeghem, and J.F. Van Impe. Efficient deterministic multiple objective optimal control of (bio)chemical processes. *Chemical Engineering Science*, 64:2527–2538, 2009.
- [4] A. Messac and C.A. Mattson. Normal constraint method with guarantee of even representation of complete Pareto frontier. *AIAA Journal*, 42:2101–2111, 2004.

A solution with reduced conservatism for \mathcal{H}_2 or \mathcal{H}_∞ multi-objective output-feedback control of LTI systems

E. Simon and V. Wertz

Department of Applied Mathematics
Ecole Polytechnique de Louvain
1348 Louvain-la-Neuve
Belgium
Emile.Simon@uclouvain.be

P. Rodríguez-Ayerbe, C. Stoica and D. Dumur

Department of Automatic Control
SUPELEC
91190 Gif-sur-Yvette
France

Our work addresses the following very fundamental control problem: the design of a control structure with two degrees of freedom (d.o.f.) around a Linear Time Invariant (LTI) model of a plant such that all the three closed-loop's sensitivity functions (S , S_u and S_i , respectively the output, control and input sensitivity) are of minimal norm. Each of the norms considered here can be either \mathcal{H}_2 or \mathcal{H}_∞ . The integral action of the control is also ensured. The method can be applied both to discrete or continuous time models. A dynamic output feedback control is developed, though the procedure can be easily transposed for state feedback control (note also that the method works for Multi Input Multi Output (MIMO) systems, even non-squares). For illustration purposes, a convenient representation of a general plant is given as follows:

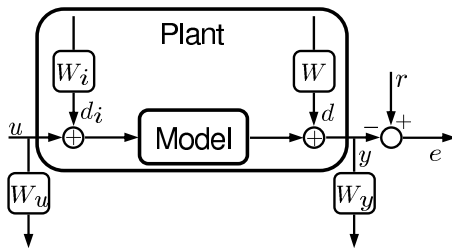


Figure 1: Classic plant representation

with u the control input, y the measured output, d the output disturbance, d_i the input disturbance, W_u, W_y, W, W_i the weighting functions associated to these signals, r the set-point and e the error. The closed-loop response is governed by the four following sensitivity functions [2]: $T = Y/R$, $S = Y/D$, $S_u = U/D$ and $S_i = Y/Di$. Thanks to the relation $S + T = I$, designing the three sensitivities S , S_u and S_i entirely shapes the closed-loop. Therefore, a possible reformulation for any optimal and/or robust control design in the \mathcal{H}_2 or \mathcal{H}_∞ sense for LTI systems is to find a control structure that minimizes the global objective o given in equation:

$$o = \|W_y S W\| + \|W_u S_u W\| + \|W_y S_i W_i\| \quad (1)$$

The norms (\mathcal{H}_2 or \mathcal{H}_∞) and the weights W s are chosen depending on user's needs.

This objective falls in the scope of multi-objectives or mixed objectives control design. Such designs are obtained in a linear, convex fashion either using Riccati [6] or Linear Matrix Inequalities (LMIs) methods [1, 4, 3], both introducing the conservatism of using a unique Lyapunov matrix for all channel objectives. This conservatism is reduced here using a 2-step LMI optimization method, which is the main contribution of this work. Note that the global solution of the minimization of a single channel's norm (e.g. $\|W_y S W\|$) is known exactly.

The second contribution of this work lies in the way the control structure is built (also used in [5]). The interest of using two d.o.f is that each of these d.o.f is used to design the behavior of the closed-loop separately for the two kinds of exogenous signals: the known reference signals and the unknown disturbances (from model unstructured uncertainties, noises, measurement errors,...).

Both of these layers are inserted using an internal model of the plant. These two d.o.f are inserted as Youla-Kučera parameters and thus span the entire range of stabilizing controllers for each d.o.f. Note that the first layer influences all three sensitivities whereas the second only changes the sensitivities from unknown disturbances, S_u and S_i .

Acknowledgments This abstract presents research results of the Belgian Network DYSCO (Dynamical Systems, Control and Optimization), funded by the Programme on Interuniversity Attraction Poles, initiated by the Belgian Federal Science Policy Office.

References

- [1] S. Boyd, L. E. Ghaoui, E. Feron, and V. Balakrishnan, *Linear matrix inequalities in system and control theory*. SIAM Publications, 1994.
- [2] G. Goodwin, S. Graebe, and M. Salgado, *Control System Design*. Prentice Hall, 2001.
- [3] C. Scherer, "An efficient solution to multi-objective control problem with lmi objectives," *Systems and Control Letters*, vol. 40, pp. 43–57, 2000.
- [4] C. Scherer, P. Gahinet, and M. Chilali, "Multi-objective output-feedback control via lmi optimization," *IEEE T. Automat. Contr.*, vol. 42, pp. 896–911, 1997.
- [5] E. Simon, C. Stoica, P. Rodríguez-Ayerbe, D. Dumur, and V. Wertz, "Robustified optimal control of a coal-fired power plant," 2010, submitted to American Control Conference, Baltimore.
- [6] K. Zhou, J. C. Doyle, and K. Glover, *Robust and Optimal Control*. Prentice Hall, 1996.

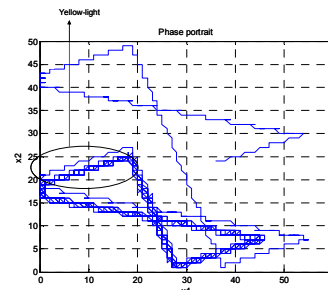
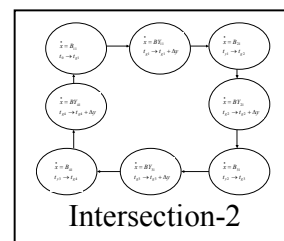
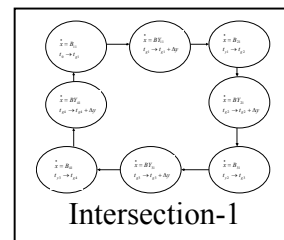
Hybrid Automata Model Approach for Coordinating Traffic Signal Control

Herman Sutarto, René Boel
 SYSTeMS Research Group, EESA Department of UGent
 {Herman.Sutarto, René.Boel}@ugent.be

This paper studies the control of urban road traffic. A network of roads with signalized intersections is considered. Coordinating control for traffic control based on hybrid automata is investigated. The coordination has hierarchical properties where low-level control action is described via the red/green switching-time and high-level action is adjusting the cycle time and the average offset, in between successive traffic light.

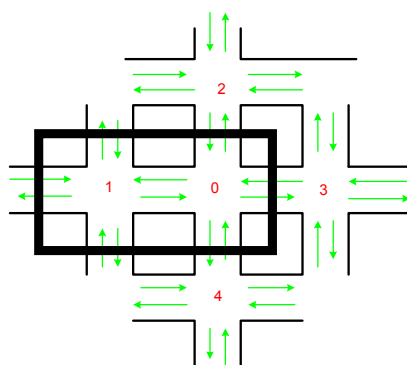
Composition of fluid-flow based hybrid automata model per intersection (a switched linear system) and a simple delay model for the connecting links is used with red-yellow-green signal transition times as control values. A traffic signal controller is designed to minimize the average delay using information on the flow of vehicles from the adjacent intersections. This information is important to determine the switching time of the traffic light of the next period and also to change the offset for coordinating.

At this time we concentrate the analysis of two intersections to develop a low-level controller but already using minimum information from the adjacent intersections. Currently we consider threshold based controllers that switch from green to red for direction 1 when the queue-length for direction 2 hit the threshold or when the queue length for direction 1 becomes 0. In the future, coordination and high-level model will be explored more rigorously.



References:

1. E.Lefeber and J.E Rooda, Controller design for switched linear systems with setups, *Physica A*,363 (2006) 48 – 61
2. Ahmet Yazici, Gangdo Seo and Umit Ozguner, Model Predictive Control Approach for decentralized traffic signal control, *Proceeding of the 17th IFAC*, July,2008
3. Thomas A Henzinger, Hybrid Automata with Finite Bisimulations, *Proceedings of the 22nd ICALP*, Lecture Notes in Computer Science 944, Springer, 1995.



Velocity Trajectory Optimization in Hybrid Electric Trucks

Thijs van Keulen, Bram de Jager, Maarten Steinbuch
 Control Systems Technology, Department of Mechanical Engineering,
 Eindhoven University of Technology
 P.O. Box 513, 5600 Eindhoven, The Netherlands
 Email: t.a.c.v.keulen@tue.nl

1 Introduction

Hybrid electric vehicles enable fuel savings by re-using kinetic and potential energy that was recovered and stored in a battery during braking or driving down hill. Besides, the vehicle itself can be seen as a storage device, where kinetic energy can be stored and retrieved by changing the forward velocity within certain constraints.

In literature several useful contributions, [1-3], can be found regarding velocity trajectory optimization in conventional vehicles. The velocity trajectory optimization problem can be defined as: finding a velocity trajectory, taking advantage of satellite navigation, providing velocity constraints, road curvature and road slope, that minimizes the fuel consumption subject to a time and distance constraint.

It is beneficial to optimize the velocity trajectory in order to minimize the fuel consumption in two ways; i) to assist the driver in tracking an optimal velocity trajectory, e.g., input to an Adaptive Cruise Controller (ACC); ii) to estimate the future power request trajectory which can be used to optimize the hybrid components use. A possible control structure is shown in Figure 1.

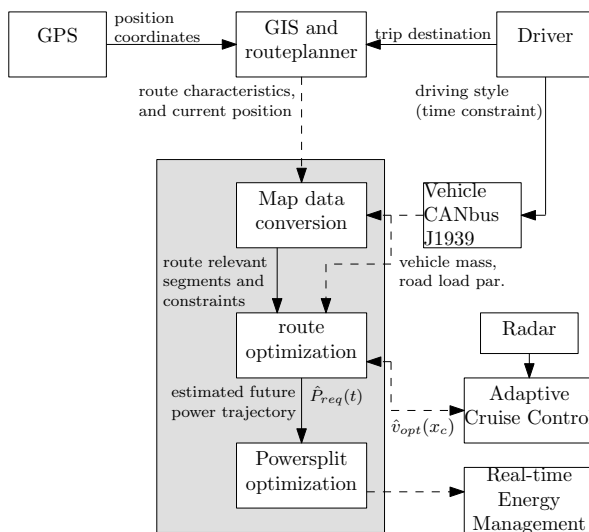


Figure 1: Topology of velocity trajectory optimization. Legend: $\hat{v}_{opt}(x_c)$ is the optimized velocity at the actual vehicle position x_c , $\hat{P}_{req}(t)$ is the estimated power trajectory.

2 Results

The benefit of route optimization is shown in a simulation example of a hybrid electric truck driving on a highway trajectory in a hilly environment, see Figure 2.

The top figure shows the height profile as function of travelled distance. The middle figure depicts the simulated velocity with constant CC setting (dashed), and the optimized ACC setting (solid). The bottom figure indicates the consumed fuel, as function of time. It can be seen that the ACC obtains a 5% fuel saving compared to a CC with constant velocity setpoint, subject to the same distance and time constraint.

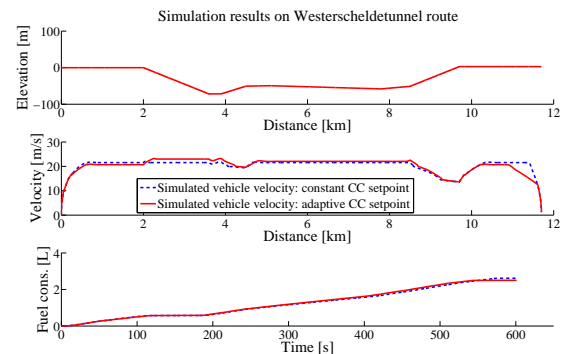


Figure 2: Simulation results for Westerscheldetunnel (N62) route from Terneuzen to Ellewoutsdijk (The Netherlands).

References

[1] E. Hellström, M. Ivarsson, J. Åslund, L. Nielsen. *Look-ahead control for heavy trucks to minimize trip time and fuel consumption*, Control Engineering Practice 17, pp. 245-254, July 2008.

[2] A.P. Stoicescu. *On Fuel-Optimal Velocity Control of a Motor Vehicle*, International Journal of Vehicle Design, Vol. 16, Nos 2/3, pp. 229-256, 1995.

[3] T. van Keulen, B. de Jager, D. Foster, M. Steinbuch, *Velocity Trajectory Optimization in Hybrid Electric Trucks*, submitted 2009.

Estimating nonlinear dynamics in nonlinear state-space models

Anna Marconato, Jonas Sjöberg, Johan Schoukens
 Dept. ELEC
 Vrije Universiteit Brussel
 Pleinlaan 2
 1050 Brussels
 Belgium
 Email: `anna.marconato@vub.ac.be`

Johan Suykens
 Dept. ESAT-SCD-SISTA
 Katholieke Universiteit Leuven
 Kasteelpark Arenberg 10
 3001 Leuven (Heverlee)
 Belgium

1 Introduction

This work aims at developing methods for estimating nonlinear state-space models of the form

$$\begin{aligned} x(t+1) &= f(x(t), u(t)) \\ y(t) &= g(x(t)) \end{aligned} \quad (1)$$

based on a combination of ideas from the statistical learning community used to solve nonlinear regression problems on one hand, see e.g. [1] and [2], and methods to handle dynamics from the system identification community on the other hand. The approach targets systems which are fairly well approximated by linear models. The proposed method consists of the following steps:

- model the dynamics of the system
- estimate the nonlinear states
- model the nonlinearities

2 Model the dynamics of the system

We start with the best linear approximation of the nonlinear system

$$\begin{aligned} x(t+1) &= Ax(t) + Bu(t) \\ y(t) &= Cx(t) \end{aligned} \quad (2)$$

which can be captured by applying classic system identification techniques. The nonlinear dynamics in Eq. (1) are then described as $f(x(t), u(t)) = Ax(t) + \tilde{f}(x(t), u(t)) + Bu(t)$ and $g(x(t)) = Cx(t) + \tilde{g}(x(t))$ so that only the deviation from the linear model needs to be modelled, which has been proposed by several authors, see e.g. [3] and [4].

3 Estimate the nonlinear states

Eq. (2) is used to generate approximate data $\{\tilde{x}(t)\}$ for the relation $\tilde{x}(t+1) = \tilde{f}(\tilde{x}(t), u(t))$ so that regression methods can be applied in the next step that models the nonlinear terms in the state-space model. These nonlinear state estimates $\tilde{x}(t)$ are obtained by a weighted fit between the linear model on the one hand and the data on the other hand. This can be formulated as a Kalman filtering problem where, in

the noise-less case, the Kalman feedback compensates for the nonlinear distortion, or it can be formulated as by the following least-squares problem

$$\min_{x(t)} \sum_t (x(t+1) - Ax(t) - Bu(t))^2 + \lambda \sum_t (y(t) - Cx(t))^2$$

4 Model the nonlinearities

Given $\{\tilde{x}(t)\}$ regression methods are employed to estimate both functions $\tilde{f}(\tilde{x}(t), u(t))$ and $\tilde{g}(\tilde{x}(t))$ using the methods of the statistical learning community. Several possibilities of nonlinear functions can be considered, such as Neural Networks or Support Vector Machines for Regression.

5 Remarks

The obtained initial estimate of the non-linear model Eq. (1) can be further fitted to data using a gradient based method which takes the dynamics into account. The described initialization procedure has several advantages, as (i) the separation between system dynamics and nonlinear terms makes it possible to identify them independently; (ii) many nonlinear estimation techniques can be tested rapidly on the obtained regression problem. In the final presentation we will also discuss results obtained by applying the proposed method on real data.

References

- [1] T. Hastie, R. Tibshirani, J. Friedman, The Elements of Statistical Learning: Data Mining, Inference, and Prediction, Springer-Verlag, 2009.
- [2] J.A.K. Suykens, T. Van Gestel, J. De Brabanter, B. De Moor, J. Vandewalle, Least Squares Support Vector Machines, World Scientific, Singapore, 2002.
- [3] J. Sjöberg, "On Estimation of Nonlinear Black-Box Models: How to Obtain a Good Initialization", IEEE Workshop on Neural Networks for Signal Processing, Amelia Island Plantation, FL, USA, 1997.
- [4] J. Paduart, Identification of Nonlinear Systems using Polynomial Nonlinear State Space Models, PhD Thesis, Vrije Universiteit Brussel, Brussels, 2008.

Assigning the Nonlinear Distortions of a Two-input Single-output System

W. D. Widanage and J. Schoukens

Department ELEC

Vrije Universiteit of Brussels

Pleinlaan 2. 1050.

Belgium

Email: wwidanag@vub.ac.be

Email: Johan.Schoukens@vub.ac.be

1 Abstract

In a multiple-input multiple-output (MIMO) nonlinear system the nonlinear distortions are composed of contributions that are either purely due to each individual input or a combination with some of the inputs. A three stage experimental design method valid for a wide range of nonlinear systems is presented that detects and classifies, in the frequency domain, the level of these nonlinear contributions. Periodic broadband excitation signals with several harmonics suppressed are used as the inputs to reduce the noise contributions and evaluate the nonlinear distortion levels present at the suppressed harmonics. Experimental results for a two-input single-output (TISO) system are presented demonstrating the effectiveness of the techniques.

2 Introduction

It is assumed that the nonlinear system can be modelled as a Volterra series in the mean square sense, with the error converging to zero as the kernel order tends to infinity. Such a description allows the nonlinear distortions to be grouped into contributions purely from each of the inputs and their combinations. In Figure 1, $D_1(k)$ is the distortion purely due to input $u(t)$, $D_2(k)$ to that of $v(t)$ and $D_3(k)$ the distortion from combinations of both inputs. To estimate D_1 , D_2

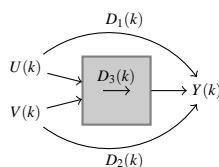


Figure 1: TISO: $D_1(k)$: Contributions from $u(t)$. $D_2(k)$: Contributions from $v(t)$. $D_3(k)$: Contributions from both inputs.

and D_3 :

- 1) Set input $v(t)$ at zero, yielding nonlinear distortions purely due to $u(t)$, $D_1(k)$.
- 2) Set input $u(t)$ at zero, yielding nonlinear distortions purely due to $v(t)$, $D_2(k)$.

- 3) Excite both inputs $u(t)$ and $v(t)$ giving rise to the total nonlinear distortions. Deduct $D_1(k) + D_2(k)$ (obtained from the previous steps) from $Y(k)$ yielding the nonlinear distortions due to the input combinations, $D_3(k)$.

3 Experimental Results

A TISO electronic filter is examined and Figure 2 illustrates that distortions which are a function of both inputs dominate, while those purely due to input $u(t)$ have a lesser magnitude and those purely due to $v(t)$ have the least.

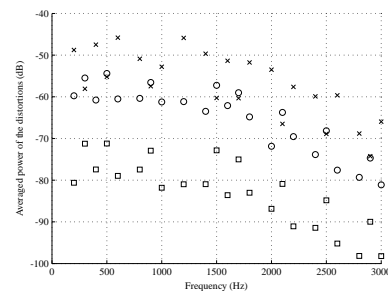


Figure 2: Power spectrum of nonlinear distortions. Circle: From $u(t)$, $D_1(k)$; Square: From $v(t)$, $D_2(k)$; Cross: From both, $D_3(k)$

4 Alternative Method

Alternatively, each input signal can be designed with a harmonic specification such that the harmonics of the output signal indicate the presence of these nonlinear contributions. However the input harmonics become sparse as the order of the nonlinearity increase that the signals becomes impractical for experimental use. [Widanage and Schoukens, 2010]

References

Widanage, W. D. and Schoukens, J. [2010], "Assigning the nonlinear distortions of a two-input single-output system", *IMAC XXVIII: A Conference and Exposition on Structural Dynamics*, Jacksonville, Florida U.S.A, February 1-4, 2010, Paper No: 56.

Using linear system estimates within LS-SVM models

Tillmann Falck, Johan A.K. Suykens, Bart De Moor

K.U. Leuven, ESAT - SCD/SISTA

Kasteelpark Arenberg 10, B-3001 Leuven

E-mail: {tillmann.falck,johan.suykens}@esat.kuleuven.be

Johan Schoukens

Vrije Universiteit Brussel, ELEC

Pleinlaan 2, B-1050 Brussel

E-mail: johan.schoukens@vub.ac.be

1 Introduction

Traditionally most nonlinear black box models rely on a NARX structure to generate predictions. This methodology does not exploit any prior information on the linear dynamics of the system as past input and output measurements are just mapped to new prediction values. For the special case of least squares support vector machines (LS-SVMs) [1] we compare different approaches to integrate prior information in terms of linear system dynamics into the nonlinear model. All approaches are based on rational orthogonal basis functions [2] which describe the dynamics of linear dynamical systems. We evaluate the use of these basis functions as inputs for the nonlinear model instead of lagged in- and outputs. Furthermore we explore the estimation of a nonlinear black box model that is orthogonal to the space spanned by this basis and models the residuals.

2 Identification scheme

2.1 Identification and modeling of linear dynamics

The rational orthogonal basis functions [2] can be constructed by concatenating sections of first and second order all pass filters. The resulting basis functions show fast convergence rates if the poles of the all pass sections are already close to ones of the true linear system. Therefore we use the best linear approximation (BLA) [3] to obtain a good estimate of the linear dynamics for the nonlinear system.

2.2 Least squares support vector machines

LS-SVMs [1] are formulated in the primal domain as a convex optimization problem

$$\begin{aligned} \min_{w,b,e_t} \quad & \frac{1}{2} w^T w + \frac{1}{2} \gamma \sum_{t=1}^N e_t^2 \\ \text{subject to} \quad & y_t = w^T \varphi(x_t) + b + e_t, \quad t = 1, \dots, N. \end{aligned} \quad (1)$$

The feature map φ is defined implicitly by a positive definite kernel function $K(x,y) = \varphi(x)^T \varphi(y)$ and can be infinite dimensional as it is the case for the popular RBF kernel $K_{\text{RBF}}(x,y) = \exp(-\|x-y\|^2/\sigma^2)$. Therefore in practice the Lagrange dual, which is finite dimensional and expressed in terms of the kernel, is solved instead of the primal problem in (1).

2.3 Integration of LS-SVMs and linear dynamics

Instead of employing the usual NARX structure for the inputs x_t , we investigate the use of inputs generated by the ba-

sis functions embedding the linear dynamics of the data. In this context the polynomial kernel $K_{\text{POLY}}(x,y) = (x^T y + c)^d$ with $c \geq 0$ and $d \in \mathbb{N}$ is interesting as its feature map corresponds to polynomials of order d in x . Thus LS-SVMs provide an efficient way to learn a polynomial combination of the basis functions with the benefit of the active regularization in LS-SVMs which limits the effective number of parameters. The RBF kernels allows even more complex combinations of the basis functions. An alternative approach is described in [4] where the basis function model is extended with a classical kernel based NARX model. In that case the kernel model is restricted such that it is orthogonal to the space spanned by the basis functions. This extends the existing set of linear orthogonal basis function by a nonparametric orthogonal model fitting the nonlinear components in the residuals.

3 Experiments

We will show results that compare the different ways of integration on the Wiener-Hammerstein benchmark data set [5]. The linear dynamics embedding via the outlined multi stage approaches are shown to improve the estimation of NARX based LS-SVM model.

Acknowledgements

B. De Moor is a full and J. Suykens is a professor at the Katholieke Universiteit Leuven, Belgium. J. Schoukens is a full professor at the Vrije Universiteit Brussel. Research supported by KUL: CoE EF/05/006 OPTeC; FWO: G.0211.05 (Nonlinear), G.0302.07 (SVM/Kernel); IUAP P6/04 (DYSCO); EU: ERNSI.

References

- [1] J. A. K. Suykens, T. Van Gestel, J. De Brabanter, B. De Moor, and J. Vandewalle, *Least Squares Support Vector Machines*. World Scientific, 2002.
- [2] P. S. Heuberger, P. M. Van Den Hof, and B. Wahlberg, *Modelling and Identification with Rational Orthogonal Basis Functions*. Springer, 2005.
- [3] J. Schoukens, J. G. Nemeth, P. Crama, Y. Rolain, and R. Pintelon, "Fast approximate identification of nonlinear systems," *Automatica*, vol. 39, 2003.
- [4] T. Falck, M. Signoretto, J. A. K. Suykens, and B. De Moor, "A two stage algorithm for kernel based partially linear modeling with orthogonality constraints," Internal Report 10-03, ESAT-SISTA, K.U. Leuven (Leuven, Belgium), 2010.
- [5] J. Schoukens, J. A. K. Suykens, and L. Ljung, "Wiener-Hammerstein benchmark," in Proc. of the 15th IFAC Symposium on System Identification (SYSID 2009), Saint-Malo, France, Jul. 2009.

Reduction of polynomial nonlinear state-space models by means of nonlinear similarity transforms

Anne Van Mulders, Laurent Vanbeylen and Johan Schoukens
 Vrije Universiteit Brussel, Department ELEC, Pleinlaan 2, B1050 Brussels, BELGIUM
 Email: Anne.Van.Mulders@vub.ac.be

1 Model structure: pros and cons

The considered models are state-space expressions in discrete time. It is known very well that state-space models are particularly well suited for multiple-input multiple-output (MIMO) systems. Let n_u and n_y represent resp. the number of input and output signals. In general, a discrete time nonlinear state-space model can be formulated as:

$$\begin{aligned} x(t+1) &= f(x(t), u(t)) \\ y(t) &= h(x(t), u(t)) \end{aligned} \quad (1)$$

Herein, $t \in \mathbb{N}$ is the discrete time instant, $x \in \mathbb{R}^n$ are the states and $u \in \mathbb{R}^{n_u}$ and $y \in \mathbb{R}^{n_y}$ are the input and output and n is the model order. When f and h are polynomial functions, the model is called a Polynomial Nonlinear State-Space (PNLSS) model [1].

The major advantage of the PNLSS model is its ability to describe *a very large class of nonlinear systems*, such as bilinear models, affine models, nonlinear models with only nonlinearities in the states, nonlinear models with only nonlinearities in the input and certain block-structured nonlinear models (Wiener, Hammerstein, Wiener-Hammerstein and nonlinear feedback). The model has been successfully applied to several examples [1]. Consequently, it can be stated that the PNLSS model is a *generic all-purpose black-box model*. When a full parameterisation (i.e. all nonlinear coefficients composing f and h are identified) is used in combination with a high nonlinear degree or a high model order n , one gets the following drawback: the *number of parameters grows very large* in a combinatorial way (e.g. $n = 6$ and powers 1, 2 and 3 in the polynomials results in 833 parameters), even if the underlying physical system has a sparse structure. In this paper, we want to retrieve this sparsity in the identified model.

2 State transformations affecting model sparsity

As any state-space model, the PNLSS model can be represented in an infinite amount of ways by means of similarity transformations on the states (2), without affecting the input-output behaviour.

$$\tilde{x} = T(x) \quad (2)$$

In contrast to linear models, in which only linear similarity transforms can keep the model type unchanged, in the

nonlinear case, *both linear and nonlinear transformations* can create a new model that fits within the same model class (i.e. preserving the same symbolic representation). In this research, we want to identify a system possessing certain internal structural properties, without knowing them in advance. E.g. a Wiener-Hammerstein system can be written in state-space form such that only the first component enters the model equations in a nonlinear way. We have observed that, using a full parameterisation of the PNLSS model, the existing identification method *destroys the sparse structure* of the model equations, creating a huge number of redundant nonzero parameters. Our goal is to take advantage of the freedom offered by these state transformations to *retrieve the original, a priori unknown, sparse representation*. Finding a good nonlinear transformation can greatly reduce the effective number of parameters, especially the number of nonlinear terms. Moreover, this could also provide extra insight in the type of nonlinear system (e.g. Wiener-Hammerstein) that was identified.

3 Achieving the goal

The goal of this research, which is to find a nonlinear transformation that manages to make the model more parsimonious, can be achieved in two ways. A first option is to keep the number of nonzero parameters small during the data fitting procedure, e.g. by means of a regularisation term. The second option is to manipulate the model obtained from an existing identification method [1, 2] applied to the data. Practically, the first step of this manipulation would be to detect the relationships that exist between the parameters. The second step is to use these relationships to transform the model to its simplest form.

References

- [1] J. Paduart. *Identification of nonlinear systems using Polynomial Nonlinear State Space models*. PhD thesis, Vrije Universiteit Brussel, 2008.
- [2] A. Van Mulders, M. Volckaert, M. Diehl, and J. Schoukens. Two nonlinear optimization methods for black box identification compared. In *15th IFAC Symposium on System Identification (SYSID 2009)*, pages 1086–1091, 2009.

Good short record confidence regions for system identification

Kurt Barbé and Johan Schoukens

Dept. ELEC, Vrije Universiteit Brussel, Pleinlaan 2, B-1050 Brussels, Belgium

Email: kurt.barbe@vub.ac.be

1. Introduction

A large field of applications like biological, biochemical and biomedical systems, deals with the problem that measurements are very expensive and hence only short records are available, see for instance [1].

The desirable properties of these statistical models often rely on asymptotic results which are only valid when the number of measurements tends to infinity. In practice, the number of measurements is fixed and hence it is important to check a method's robustness with respect to finite or short sample effects.

Similarly when looking at different estimators, we like to select the best confidence regions that capture the actual parameter values with a user-defined confidence. In this setting, the best confidence region is the smallest in size such that the number of possible false values is minimized, [2].

Interval estimation is the area of estimation or identification theory focusing on constructing good confidence regions for a given problem. The problem is well studied for large sample problems, however solutions for short record problems are more involved, [2]. We can study the robustness of the optimal "large sample"

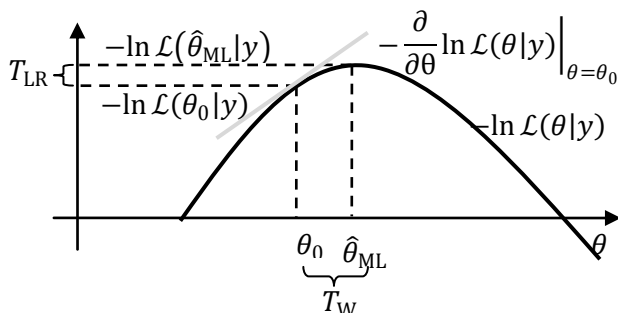


Figure 1: Geometry of the different tests: T_{LR} and T_W denote the Likelihood-ratio and the Wald test respectively and Rao's test is the slope in gray.

confidence regions with respect to short data records. To the authors best knowledge, this robustness has only been studied for very particular problems, [3], [4], and hence no practical guidelines for the user are available.

2. Three likelihood based confidence regions

A confidence region can statistically be defined as the acceptance region of a statistical test, see [2]. Since, the likelihood function captures all the information of the

observed data, likelihood based statistical tests are asymptotically optimal. Indeed, three popular statistical tests are: Wald's, Likelihood ratio and Rao's test, see [5]. The three tests are likelihood based and are asymptotically equivalent, but its finite sample behavior can be quite different. The difference between the different tests is illustrated in Figure 1.

3. Conclusion

We studied the robustness of asymptotic methods to construct confidence regions with respect to finite sample effects. The geometry of the different methods show that

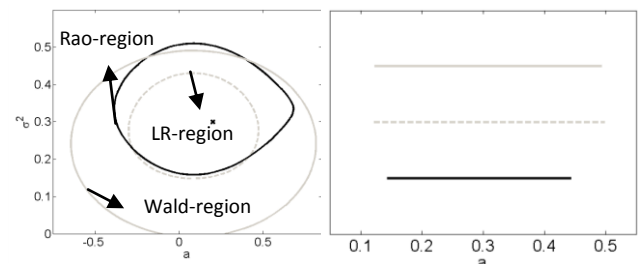


Figure 2: Left: 95% confidence interval for the parameter (a, σ^2) . Right: 95% confidence interval for the system parameter a .

one should discriminate between a confidence region of a system parameter (which is in general an internal point of the parameter space) for which the score region should be used and of an estimate of the noise variance (the noise variance has a physical bound at zero) for which the LR region should be used as illustrated in Figure 2.

References

- [1] V. Beelaerts, et al., "On the elimination of bias averaging-errors in proxy records," *Mathematical Geosciences*, vol. 41, no. 2, pp. 129-144, 2008.
- [2] M. Kendall and A. Stuart, *The advanced theory of statistics*, 4th ed. London: Griffin, 1983.
- [3] P. M. Bentler and K. H. Yuan, "Structural equation modeling with small samples: Test statistics," *Multivariate Behavioral Research*, vol. 34, no. 2, pp. 181-197, 1999.
- [4] W. E. Ferson and S. R. Foerster, "Finite sample properties of the generalized method of moments in tests of conditional asset pricing models," *Journal of Financial Economics*, vol. 36, no. 1, pp. 29-55, 1994.
- [5] A. Buse, "The likelihood ratio, Wald and Lagrange multiplier tests: An expository note," *The American Statistician*, vol. 36, no. 3, pp. 153-157, Aug. 1982.

Spectral Clustering of Time Series: Identifying Profiles in Power Load Data

Carlos Alzate, Marcelo Espinoza, Bart De Moor and Johan A. K. Suykens
K.U.Leuven, ESAT-SCD-SISTA
Kasteelpark Arenberg 10, B-3001 Leuven, Belgium
Email: carlos.alzate@esat.kuleuven.be

1 Introduction

Spectral clustering provides a powerful unsupervised learning tool to find similar patterns underlying the data. These methods use the eigenspectrum of Laplacian matrices derived from the data to find the clusters. A recent approach linking spectral clustering with a form of weighted kernel PCA has been proposed in [1]. One of the main advantages is the possibility to extend the clustering model to out-of-sample points in a learning framework. Time series data pose a challenge to standard clustering methods due mainly to the high-dimensionality. The particular dataset corresponds to readings of power load. The objective is to identify customer types using the raw time series without pre-modeling or dimensionality reduction steps.

2 Power Load Time Series

A time series dataset containing readings of the power load measured at 245 substations in the Belgian grid is used in this work. The power load was measured every hour for a period of 5 years. The dimensionality of each time series is 43,824. Figure 1 shows one time series from the dataset.

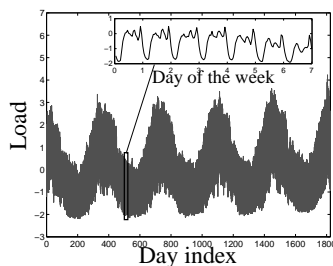


Figure 1: Example of time series from the power load dataset.

3 Spectral Clustering via Weighted Kernel PCA

The clustering formulation in the primal is [1, 2]:

$$\min_{w^{(l)}, e^{(l)}, b_l} \frac{1}{2N} \sum_{l=1}^{k-1} \gamma_l e^{(l)T} D^{-1} e^{(l)} - \frac{1}{2} \sum_{l=1}^{k-1} w^{(l)T} w^{(l)} \quad (1)$$

such that $e^{(l)} = \Phi w^{(l)} + b_l 1_N, l = 1, \dots, k-1$

where k is the number of desired clusters, $\gamma_l \in \mathbb{R}^+$ are regularization constants, $e^{(l)} = [e_1^{(l)}; \dots; e_N^{(l)}]$ are the pro-

jections representing a set of $k-1$ binary cluster indicators through: $\text{sign}(e_i^{(l)}), i, \dots, N$, b_l are bias terms, $\Phi = [\varphi(x_1)^T; \dots; \varphi(x_N)^T]$, $\varphi(\cdot) : \mathbb{R}^d \rightarrow \mathbb{R}^{m_h}$ is the mapping to a high dimensional feature space, D^{-1} is the inverse of the graph degree matrix and $l = 1, \dots, k-1$. In the dual, the formulation becomes the eigenvalue problem:

$$D^{-1} M_D \Omega \alpha^{(l)} = \lambda_l \alpha^{(l)}, l = 1, \dots, k-1$$

where $\lambda_1 \geq \dots \geq \lambda_N$ are the ordered eigenvalues, $M_D = I_N - (1/1_N^T D^{-1} 1_N) 1_N 1_N^T D^{-1}$, Ω is the $N \times N$ kernel matrix $\Omega_{ij} = \varphi(x_i)^T \varphi(x_j) = K(x_i, x_j)$ and $K(\cdot, \cdot)$ is a positive definite kernel function. From the top $k-1$ eigenvectors $\alpha^{(l)}$, a codebook can be formed containing k codewords representing the cluster encodings. The projections of any data point x can be expressed now as $z^{(l)}(x) = \sum_{i=1}^N \alpha^{(l)} K(x, x_i) + b_l, l = 1, \dots, k-1$. The cluster indicators of x can be obtained by assigning $\text{sign}(z^{(l)}(x))$ to the cluster encoding in the codebook with minimal Hamming distance.

4 Experimental Results

The RBF kernel parameter $\sigma = 200$ and the number of clusters $k = 7$ were tuned using the BLF criterion [1] on validation data. The training and validation sets were randomized 10 times. The results compare favorably with respect to an existing approach [3] using periodic autoregressions and pre-modeling.

Acknowledgments: This work was supported by grants and projects for the Research Council K.U.Leuven (GOA-Mefisto 666, GOA-Ambiorics, several PhD / Postdocs & fellow grants), the Flemish Government FWO: PhD / Postdocs grants, projects G.0240.99, G.0211.05, G.0407.02, G.0197.02, G.0080.01, G.0141.03, G.0491.03, G.0120.03, G.0452.04, G.0499.04, G.0226.06, G.0302.07, ICCoS, AN-MMM; AWI:IWT:PhD grants, GBOU (McKnow) Soft4s, the Belgian Federal Government (Belgian Federal Science Policy Office: IUAP V-22; PODO-II (CP/01/40), the EU(FP5-Quprodis, ERNSI, Eureka 2063-Impact;Eureka 2419-FLiTE) and Contracts Research/Agreements (ISMC / IPCOS, Data4s, TML,Elia, LMS, IPCOS, Mastercard). Bart De Moor and Johan Suykens are professors at the K.U.Leuven, Belgium. The scientific responsibility is assumed by its authors.

References

- [1] C. Alzate and J. A. K. Suykens, "Multiway spectral clustering with out-of-sample extensions through weighted kernel PCA," *IEEE Transactions on Pattern Analysis and Machine Intelligence*, vol. 32, no. 2, pp. 335–347, 2009.
- [2] C. Alzate, M. Espinoza, B. De Moor, and J. A. K. Suykens, "Identifying customer profiles in power load time series using spectral clustering," in *Proceedings of the 19th International Conference on Neural Networks (ICANN 2009)*, 2009, pp. 315–324.
- [3] M. Espinoza, C. Joye, R. Belmans, and B. De Moor, "Short-term load forecasting, profile identification and customer segmentation: A methodology based on periodic time series," *IEEE Transactions on Power System*, vol. 20, no. 3, pp. 1622–1630, August 2005.

Image segmentation and real-time video tracking using graph based techniques

Arnaud Browet Paul Van Dooren P.-A. Absil
arnaud.browet@uclouvain.be paul.vandooren@uclouvain.be absil@inma.ucl.ac.be

Departement of Mathematical Engineering
Université catholique de Louvain (UCL)
Bâtiment Euler - 4, Avenue G. Lemaître B-1348 Louvain-la-Neuve (Belgique)

1 Introduction

In many applications, object segmentation and video tracking are more and more used to answer specific requests of users (in aerospace, defense, surveillance or security). This information needs to be available as soon as possible, meaning that picture analysis must be done online, and must be robust and reliable even in the presence of picture degradation (noisy input camera, occlusion, etc). In the last few decades, a lot of research has been performed on this topic and various techniques have been proposed, but there are still several open questions that need to be addressed such as appearing objects detection or multi-target tracking.

In this talk, we present our recent work on segmentation and tracking techniques based on graph analysis. We show that the success of these methods often crucially depends on the choice of several parameters (definition of edges and vertices, weight of edges, etc.). A research objective is to design an adaptive algorithm capable of setting those parameters automatically, according to the type of image and without any prior knowledge on shapes, subjects, or background.

2 Graph based analysis

Based on an input image, one can define a weighted graph G as follows: each pixel becomes a vertex of the graph, (alternatively, feature extraction can be used to find representative pixels in the original image, leading to a reduction of computational complexity at the cost of some loss of information) and the weights of the edges are computed according to the attributes of the pixels (RGB, HSV, gray-scaled, etc.) and to other informations such as their distance in the picture.

Once this weighted adjacency matrix W is defined, a popular segmentation technique, allowing to find objects in the picture, is spectral clustering [1]. However, this approach involves finding eigenvectors of an n -by- n matrix, where n is the number of pixels, which is often computationally intractable in real time.

Based on the graph associated to the image, another way of looking at clustering is to consider community detection in

a large network. Communities are sets of nodes such that the intra-community edges tend to have large weights and the inter-community edges small weights. A popular measure of quality for community detection is the so-called Q -modularity [2] defined by

$$Q = \frac{1}{2m} \sum_{i,j} \left[W_{ij} - \frac{k_i k_j}{2m} \right] \delta_{c_i c_j},$$

where $m = \frac{1}{2} \sum_{i,j} W_{ij}$ is the total weight of edges, $k_i = \sum_j W_{ij}$ is the total weight of edges attached to node i , c_i represents the community of node i and δ is the Kronecker delta. Optimizing the modularity leads to good clustering but is known to be NP-hard. An efficient greedy (but sub-optimal) algorithm has been proposed by Blondel et al. [3].

However, we observed that Q -modularity does not favor picture segments with large diameter. To solve this, we propose modifications of the definition of the Q -modularity that also take into account the geometry of the elements of the graphs. For example, we add a parameter λ_{ij} depending on the distance between pixels i and j in the image:

$$Q = \frac{1}{2m} \sum_{i,j} \left[W_{ij} - \lambda_{ij} \frac{k_i k_j}{2m} \right] \delta_{c_i c_j}.$$

This modification reduces the negative component of the modularity for large segmented regions in the image. Preliminary results are promising for static pictures. We are also looking at a possible extension for video tracking by considering a larger network of consecutive "slices" for which each slice is the weighted graph of a single video frame.

References

- [1] J. Shi, and J. Malik, "Normalized cut and image segmentation," IEEE TPAMI, 2000.
- [2] M.E.J. Newman, "Finding community structure in networks," Phys. Rev. E 74, 2006.
- [3] V. Blondel, J-L. Guillaume, R. Lambiotte, and E. Lefebvre, "Fast unfolding of communities in large networks," Journal of Statistical Mechanics, 2008.

Regression on fixed-rank positive semidefinite matrices: a geometric approach

G. Meyer¹, S. Bonnabel² and R. Sepulchre¹

¹Montefiore Institute, University of Liège, Belgium

{g.meyer, r.sepulchre}@ulg.ac.be

²CAOR Mathématiques et Systèmes, Mines ParisTech, France

silvere.bonnabel@mines-paristech.fr

1 Introduction

In this paper, we adopt a differential-geometry viewpoint to tackle the problem of learning a regression model whose parameter is a fixed-rank positive semidefinite (PSD) matrix. Given data $\mathbf{x} \in \mathbf{R}^d$ and observations $y \in \mathbf{R}$, the problem amounts to solve

$$W^* = \operatorname{arg\,min}_{W \in S_+(r,d)} \mathbb{E}_{\mathbf{x},y} \{l(\hat{y}, y)\}, \quad (1)$$

where $S_+(r, d) = \{W \in \mathbf{R}^{d \times d} : W = W^T \succeq 0, \operatorname{rank}(W) = r\}$, $\hat{y} = \mathbf{x}^T W \mathbf{x}$ defines the considered quadratic regression model and l is a loss function. A standard choice for scalar observations is the quadratic loss $l(\hat{y}, y) = (\hat{y} - y)^2$.

Learning low-rank matrices is a typical solution to reduce the computational complexity of subsequent algorithms. Indeed, the complexity generally decreases from $O(d^3)$ to $O(dr^2)$ where the approximation rank r is generally much smaller than the problem size d .

Whereas efficient convex formulations exist in the full-rank case ($r = d$), the problem is no longer convex if the rank constraint is introduced. Nevertheless, the set $S_+(r, d)$ has a rich Riemannian geometry that can be exploited for algorithmic purposes [1].

2 Gradient based learning

Batch and online gradient descent algorithms are classical iterative approaches to solve problem (1). In the batch setting, the loss function $L(W) = \sum_{i=1}^n l(\hat{y}_i, y_i)$ is minimized over a finite set of observations $\{(\mathbf{x}_i, y_i)\}^n$. When the number of observations is very large, online algorithms reduce the computational load by considering the observation received at time t only, that is, $L(W) = l(\hat{y}_t, y_t)$. In both cases, the gradient iteration can be interpreted as

$$W_{t+1} = \operatorname{arg\,min}_{W \in S_+(r,d)} D(W, W_t) + \eta L(W), \quad (2)$$

where $D : S_+(r, d) \times S_+(r, d) \rightarrow \mathbf{R}$ is a well-chosen closeness measure between matrices of $S_+(r, d)$ and η is a trade-off parameter that controls the balance between the conservative term $D(W, W_t)$ and the innovation term $L(W)$.

3 Closeness between fixed-rank PSD matrices

In this paper, we discuss the choice of two particular closeness measures between fixed-rank PSD matrices and we derive the corresponding gradient descent algorithms in the framework of optimization on matrix manifolds [2]. In contrast to previous contributions in the literature, the range space of the matrix is free to evolve during the optimization process. Moreover, the proposed algorithms scale to high-dimensional problems and enjoy important invariance properties.

4 Application to the distance learning problem

An important instance of the considered regression problem is the learning of a distance function parameterized by a fixed-rank PSD matrix [3, 4]. This task is a central issue for many machine learning applications where a data-specific distance has to be constructed, or where an existing distance needs to be improved based on additional side information. The good performance of the algorithms is illustrated on several well-known classification and clustering benchmarks.

References

- [1] S. Bonnabel and R. Sepulchre. Riemannian metric and geometric mean for PSD matrices of fixed rank. *SIAM Journal on Matrix Analysis and Applications*, 31(3):1055–1070, 2009.
- [2] P.-A. Absil, R. Mahony, and R. Sepulchre. *Optimization Algorithms on Matrix Manifolds*. Princeton University Press, 2008.
- [3] K. Tsuda, G. Ratsch, and M. Warmuth. Matrix exponentiated gradient updates for on-line learning and bregman projection. *Journal of Machine Learning Research*, 6:995–1018, 2005.
- [4] J. Davis, B. Kulis, P. Jain, S. Sra, and I. Dhillon. Information-theoretic metric learning. In *Proceedings of the 24th International Conference on Machine Learning*, 2007.

Acknowledgments

This work was supported by the Belgian National Fund for Scientific Research (FNRS) through a Research Fellowship at the University of Liège. This paper presents research results of the Belgian Network DYSCO (Dynamical Systems, Control, and Optimization), funded by the Interuniversity Attraction Poles Programme, initiated by the Belgian State, Science Policy Office. The scientific responsibility rests with its author(s).

Means and medians in nonlinear spaces

Anne Collard and Rodolphe Sepulchre

Departement of Electrical Engineering and Computer Science,

University of Liège, B-4000 Liège, Belgium

Email: Anne.Collard@ulg.ac.be, R.Sepulchre@ulg.ac.be

1 Introduction

Until a few years ago, the majority of numerical techniques for optimization assumed an underlying Euclidean space. However, many of these computational problems are posed on non-Euclidean spaces. This motivates the development of new optimization methods that take into account the particular structure of the considered space. In this work, we focus on those spaces which can be seen as Riemannian manifolds. Some instances of these spaces are the space of rotation and the space of positive semidefinite matrices, for which many applications exist. An example of these applications is the new medical imaging technique called Diffusion Tensor Imaging. Some adapted tools are necessary to use this technique, as for instance methods for approximation, interpolation, filtering and estimation on this manifold. For this space as for others, one of the principal needs is to find robust statistical estimators of Riemannian data [1]. In this work, we present and study some known estimators for different spaces.

2 Statistical estimators

The mean is a natural statistical estimator of a set of data. However, as we can easily check in an Euclidean space, the mean is relatively sensible to outliers. The theory of robust estimation in Euclidean space has led to the development of numerous robust estimators, one of which is the geometric median. Since a (geodesic) distance function is chosen for a manifold, these notions of mean and geometric median on Euclidean space can easily be extended to this manifold.

The computation of these estimators implies to choose a distance function for the considered manifold and to implement an optimization algorithm on this manifold. These estimators are indeed defined as the minimum of a particular function.

Each manifold can be described in different ways. Depending upon the chosen metric, means and medians of a same set of data can be slightly different.

3 Means and medians on Riemannian manifolds

In this work, we consider four different manifolds: the group of rotations, the set of p -dimensional subspaces in \mathbf{R}^n , the set of positive definite matrices and the set of positive semidefinite

matrices of fixed rank. For each of these, many representations are studied and the resulting differences in the means and medians are analyzed. For illustrating purposes, this work focus on three dimensional spaces.

For the space of 3D-rotations (usually called $SO(3)$), we choose to represent rotations as rotations matrices. Two different distances are considered: the chordal one [2] and the geodesic one.

The space of positive definite matrices is denoted by $S_+(3)$. We use two different representations of this space: the Log-Euclidean one [3] and the affine invariant one [4]. Relations between means computed with different metrics are studied. The Grassman manifold is the set of p -dimensional linear subspaces of \mathbf{R}^n [5]. The representation used in this work enables us to compute the mean of a set of elements of this manifold using a Newton algorithm.

The space of flat ellipsoids (positive semidefinite matrices of fixed rank) is the less studied of these manifolds. The mean between two flat ellipsoids can be computed by combining results of $S_+(3)$ with results of Grassman manifolds [6].

For each computed estimators, the methods are compared in respect to the robustness to outliers and to the computational cost of the methods.

References

- [1] P.T Fletcher *et al*, *The geometric median on Riemannian manifolds with application to robust atlas estimation*, *NeuroImage* **45**, S143-S152 (2009)
- [2] A. Sarlette, *Geometry and Symmetries in Coordination Control*, PhD Thesis, ULg (2009)
- [3] V. Arsigny *et al*, *Geometric means in a novel vector space structure on symmetric positive-definite matrices*, *SIAM J. on Matrix Anal. and Appl.* **29**, 328-347 (2007)
- [4] X. Pennec *et al*, *A Riemannian framework for tensor computing*, *International Journal of Computer Vision* **66**, 41-66 (2006)
- [5] P.-A. Absil *et al*, *Riemannian geometry of Grassman manifolds with a view on algorithmic computation*, *Acta Appl. Math.* **80**, 199-220 (2004)
- [6] S. Bonnabel and R. Sepulchre, *Riemannian metric and geometric mean for positive semidefinite matrices of fixed rank*, *SIAM J. on Matrix Anal. and Appl.* **31**, 1055-1070 (2009)

On Adjoint-Based Sequential Convex Programming for Parametric Nonlinear Programming

Quoc Tran Dinh
 Department of Electrical Engineering (SCD-ESAT) and OPTEC
 Katholieke Universiteit Leuven, Kasteelpark Arenberg 10
 3001 Heverlee, Belgium

Moritz Diehl

Email: {quoc.trandinh, moritz.diehl}@esat.kuleuven.be

1 Short Introduction

Consider the following parametric nonlinear programming problem:

$$P(\xi) : \begin{cases} \min_{x \in \mathbf{R}^n} & f(x) \\ \text{s.t.} & g(x) + M\xi = 0, x \in \Omega, \end{cases}$$

where $f : \mathbf{R}^n \rightarrow \mathbf{R}$ is convex, twice continuously differentiable, $g : \mathbf{R}^n \rightarrow \mathbf{R}^m$ is nonlinear, twice continuously differentiable, $\Omega \subset \mathbf{R}^n$ is a nonempty closed convex subset, M is an $m \times p$ matrix, and $\xi \in \Gamma \subset \mathbf{R}^p$ is a parameter.

This talk deals with the efficient calculation of approximate solutions to a sequence of problems of the form $P(\xi)$, where the parameter ξ is slowly varying. In other words, for a sequence $\{\xi^k\}_{k \geq 0}$ such that $\|M(\xi^k - \xi^{k-1})\|$ is small, we want to solve the problems $P(\xi^k)$ in an efficient way without requiring too much accuracy in the result. In practice, sequences of problems of the form $P(\xi)$ must be solved in the framework of online optimization as well as nonlinear model predictive control (MPC).

Exploiting the idea of the real-time iteration from [1, 2] and the adjoint-based methods from [3] we introduce a new method for solving the parametric nonlinear programming problem $P(\xi)$, which we call the adjoint-based sequential convex programming (adjSCP). Instead of solving at each sample of parameter ξ a complete optimization problem, we only perform one step of adjoint-based sequential convex programming, which means that only one convex subproblem needs to be solve at each sample of parameter. The advantage of this approach is to exploit the convex substructure of the problem and using the rich of convex optimization methods. In particular, it can handle the cases of non-smooth and general convex constraints (e.g., convex cones, LMI).

2 Main contribution

2.1. Adjoint-based SCP algorithm. The main task of the adjoint-based SCP algorithm is to solve at each sample of parameter ξ^k a convex subproblem of the form:

$$P(x^k, \lambda^k, \xi^k) : \begin{cases} \min_{x \in \mathbf{R}^n} & f(x) + m(x^k, \lambda^k)^T (x - x^k) \\ \text{s.t.} & g(x^k) + A(x^k)^T (x - x^k) + M\xi^k = 0, \\ & x \in \Omega, \end{cases}$$

where $A(x^k)$, a given matrix at iteration k , approximates to $\nabla g(x^k)$, the Jacobian of g at x^k , and $m(x^k, \lambda^k) = [\nabla g(x^k) - A(x^k)]\lambda^k$ with $z^k := (x^k, \lambda^k)$ is a KKT point of the subproblem $P(x^{k-1}, \lambda^{k-1}; \xi^{k-1})$, the previous iteration. The term $m(x^k, \lambda^k)^T (x - x^k)$ can be considered as a correction of the inconsistency between $A(x^k)$ and $\nabla g(x^k)$.

2.2. Local contraction estimate. The main result of this talk is a local contraction estimate. Suppose that $z^*(\xi)$ is an exact KKT point of $P(\xi)$ and $\bar{z}(z^k, \xi)$ is an approximate KKT point of $P(\xi)$ obtained from the KKT system of the convex subproblem $P(x^{k-1}, \lambda^{k-1}; \xi)$, where $z^{k-1} = (x^{k-1}, \lambda^{k-1})$ is a KKT point of the convex subproblem at the previous iteration. Under mild conditions, we prove that if $M(\xi^k - \xi^{k-1})$ is sufficiently small then

$$\|z^{k+1} - z^*(\xi^k)\| \leq \omega \|z^k - z^*(\xi^{k-1})\| + C_0 \|M(\xi^k - \xi^{k-1})\|,$$

where $z^{k+1} := \bar{z}(z^k, \xi^k)$, $\omega \in (0, 1)$ and $C_0 > 0$ are two constants, which do not depend on k .

2.3. Special cases. When the set of parameters $\Gamma = \{\xi\}$, $P(\xi)$ becomes a nonlinear programming problem. The adjoint-based SCP method reduces to an adjoint-based SCP method for solving nonlinear programming. If the exact Jacobian of g at each iteration k is provided, i.e. $A(x^k) = \nabla g(x^k)$, our method collapses to an exact Jacobian real-time SCP algorithm for solving $P(\xi)$.

References

- [1] M. Diehl. *Real-Time Optimization for Large Scale Nonlinear Processes*. PhD thesis, Universität Heidelberg, 2001. <http://www.ub.uni-heidelberg.de/archiv/1659/>.
- [2] M. Diehl, H.G. Bock, J.P. Schlöder, R. Findeisen, Z. Nagy, and F. Allgöwer. Real-time optimization and Non-linear Model Predictive Control of Processes governed by differential-algebraic equations. *J. Proc. Contr.*, 12(4):577–585, 2002.
- [3] A. Griewank and A. Walther. On constrained optimization by adjoint-based quasi-newton methods. *Optim. Methods Softw.*, 17:869–889, 2002.

Synchronization Criteria for Discrete Dynamical Networks via Impulsive Couplings

Hui Liu and Ming Cao

Faculty of Mathematics and Natural Sciences
University of Groningen
Nijenborgh 4, 9747 AG, Groningen
The Netherlands

Email: Hui.Liu@rug.nl, m.cao@rug.nl

Jun-an Lu

School of Mathematics and Statistics
Wuhan University
Wuhan, 430072, Hubei
China

Email: jalu@whu.edu.cn

1 Introduction

In recent years, more and more researchers have become to be interested in the synchronization behavior in complex dynamical networks. This is because synchronization is related to various research topics in natural and man-made systems, such as animal groups, power grids, sensor networks, cellular neural networks, and so on.

In the mean time, impulsive control has been widely studied for stabilizing and synchronizing nonlinear systems. In particular, studies on synchronization of coupled oscillators through impulsive control [1] has been utilized in different applications, and thus generated great interest. In [2], continuous model with impulsive coupling was proposed and its synchronization scheme was studied, where only symmetric couplings were considered. A more complex case was considered in [3] discussing the robust impulsive synchronization of uncertain nonlinear discrete dynamical systems or networks. However, there are few results for discrete dynamical networks with impulsive couplings. It is worth pointing out that previous studies on impulsive control and synchronization for coupled systems mainly consider continuous coupling while in practice, there is great need to analyze discrete systems that are coupled only by impulsive connections at discrete time instants. Hence, in this paper, we propose a discrete dynamical network model in which the couplings occur impulsively at discrete time instants. Such a model is motivated by some natural and man-made networked systems, such as the information transfer and exchange in ant groups. For the model constructed, by making use of the multi-Lyapunov function method, both global and local stability analysis of the synchronization manifold is performed, and two synchronization criteria have been obtained.

2 Main Results

Let $X(t) = (x_1^T(t), x_2^T(t), \dots, x_N^T(t))^T$ and $F(X(t)) = (f^T(x_1(t)), f^T(x_2(t)), \dots, f^T(x_N(t)))^T$. The discrete dynamical network via impulsive couplings can be described

by

$$\begin{cases} X^-(t) = F(X^+(t-1)), & t \in \mathcal{N}, \\ X^+(t) = X^-(t), & \text{if } t \in \mathcal{N}/\mathcal{T}, \\ X^+(t) = X^-(t) + (A(t) \otimes B_k)X^-(t) & \text{if } t = t_k \in \mathcal{T}, \\ X^+(0) = X_0 = (x_1^T(0), x_2^T(0), \dots, x_N^T(0))^T, \end{cases} \quad (1)$$

where $\mathcal{N} = \{1, 2, \dots\}$, $x_i(t) \in \mathbb{R}^n$ with $i = 1, \dots, N$, $f(\cdot) : \mathbb{R}^n \rightarrow \mathbb{R}^n$, $\mathcal{T} = \{t_k, k = 1, 2, \dots\}$ is the set of given integer impulsive time instants. Here, $-A(t_k) \in \mathbb{R}^{N \times N}$ is the Laplacian matrix of the network at the impulsive coupling instant t_k , and $B_k \in \mathbb{R}^{n \times n}$ is the coupling strength matrix.

Assumption 1. Suppose there is a nonnegative constant L , such that $\|f(x_i(t)) - f(x_j(t))\| \leq L\|x_i(t) - x_j(t)\|$, for any $t \in \mathcal{N}$ and any $x_i(t) \neq x_j(t)$, where $x_i(t), x_j(t) \in \mathbb{R}^n$.

Theorem 1. Suppose Assumption 1 holds. Denote that

$$\rho(t_k) = \|(I_{(N-1)n} + \tilde{A}(t_k) \otimes B_k)\|_2.$$

Then the impulsively coupled network (1) achieves global synchronization as $t \rightarrow \infty$, if there exists a constant $\alpha > 0$ such that

$$\ln \rho(t_k) + (t_k - t_{k-1}) \ln L \leq -\alpha, \quad \text{for } k = 1, 2, \dots.$$

References

- [1] B. Liu, X. Liu, G. Chen, and H. Wang, "Robust impulsive synchronization of uncertain dynamical network," *IEEE Trans. Circuits Syst. I*, **52**(7): 1431-1441, 2005.
- [2] X.P. Han, J.A. Lu, and X.Q. Wu, "Synchronization of impulsively coupled systems," *Int. J. Bifurcation and Chaos*, **18**(5): 1539-1549, 2008.
- [3] B. Liu, and X. Liu, "Robust stability of uncertain discrete impulsive systems," *IEEE Trans. Circuits Syst. II*, **54**(5): 455-459, 2007.

An Approach to Observer-Based Decentralized Control under Periodic Protocols

N.W. Bauer, M.C.F. Donkers, W.P.M.H. Heemels, N. van de Wouw

Department of Mechanical Engineering
Eindhoven University of Technology

P.O. Box 513, 5600 MB Eindhoven, The Netherlands

{N.W.Bauer, M.C.F.Donkers, W.P.M.H.Heemels, N.v.d.Wouw}@tue.nl

1 Introduction

Recently, there has been an enormous interest in control of large-scale systems that are physically distributed over a wide area. Examples of such distributed systems are electrical power distribution networks, water distribution networks, industrial factories and energy collection networks (such as wind farms). This work considers stability analysis and controller design for this class of systems.

2 Problem Statement

The control structure we consider has a number of features that complicate the design enormously. First of all, the controller is decentralized in the sense that it consists of a number of local controllers that do not share information. Although a centralized controller can be considered, the achievable bandwidth associated with using a centralized structure would be limited by long delays from distant sensors and actuators.

Secondly, when considering control of a large-scale system, it would be unreasonable to assume that all states are measured. Therefore an observer-based design is needed to estimate the states that cannot be directly measured. Moreover, with an observer-based controller it is possible to reduce the number of sensors, which alleviates the demands on the network design. However, it has been proven that, in general, it is hard to obtain decentralized observers that will converge to the ‘true’ state estimate [3]. Despite this fact, stability of the observer-based controller can still be achieved, but design is of course challenging.

Finally, the controller needs to have certain robustness properties when we would like to use communication networks. Indeed, the advantages of using a wired/wireless network are inexpensive and easily modifiable communication links. However, the drawback is that control structure is susceptible to undesirable (possibly destabilizing) side-effects. There are five recognized side-effects: time-varying delays, packet dropouts, varying transmission intervals, quantization and communication constraints. We would like to design our feedback such that the closed-loop remains stable given bounds on the network imperfections. However, for model simplicity, we only consider varying transmission intervals and communication constraints in this work. The communication constraints impose a need for a protocol to orchestrate in what order sensor and actuator data is sent over the shared network. We assume the protocol to be periodic.

3 Decentralized Networked Control System Model

The continuous-time linear plant we consider is decomposed into N discrete-time subsystems $P^{(1)} \dots P^{(N)}$. The corresponding subsystem controllers $C^{(1)} \dots C^{(N)}$ are switched discrete-time systems consisting of a switched-observer structure to deal with the presence of communication constraints. The general setup is depicted in Fig. 1 and more details can be found in [1].

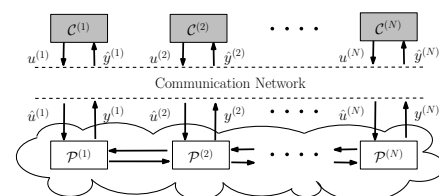


Fig. 1. Decentralized Networked Control System

4 Stability Analysis

Although transmission interval variation introduces a non-linear parameter dependency in the dynamics, robust stability of the entire closed-loop system can still be verified by proving that a convex over-approximation of the uncertain switched system is stable, e.g. using techniques of [2].

5 Design Procedure

This still leaves the difficult question of how to design the switching control gains. We propose to design the controllers by treating the global coupling between the subsystems and network imperfections as uncertainties, which require robustness properties for the decoupled dynamics. With this simplification, the closed-loop dynamics reveal a cascaded interconnection of three switched-linear systems and allows to design the observer and feedback gains independently using the tools of hybrid system theory. If the addition of the coupling terms do not destabilize the closed-loop system, which can be verified by our analysis methods, then we provide methods to calculate the amount of uncertainty in the transmission intervals that the control loop can withstand.

References

- [1] N.W. Bauer, M.C.F. Donkers, W.P.M.H. Heemels, and N. van de Wouw. An approach to observer-based decentralized control under periodic protocols. *Submitted*.
- [2] M.C.F. Donkers, W.P.M.H. Heemels, N. van de Wouw, L. Hetel, and M. Steinbuch. Stability analysis of networked control systems using a switched linear systems approach. *Submitted*.
- [3] Dragoslav D. Siljak. *Decentralized control of complex systems* / Dragoslav D. Siljak. Academic Press, Boston, 1991.

Multi-Level Model Predictive Control of Large-Scale Networks

Noortje Groot, Bart De Schutter, Hans Hellendoorn

Delft Center for Systems and Control, Delft University of Technology

Mekelweg 2, 2628 CD Delft, The Netherlands

{N.B.Groot, B.DeSchutter, J.Hellendoorn}@tudelft.nl

1 Introduction

In this presentation we provide an introduction to the intended research domain. Here Model Predictive Control (MPC) can be seen as a keyword put in the context of intelligent infrastructures, which include large-scale systems like electricity and road traffic networks that are equipped with sensors to make optimal use of control and that give rise to optimization opportunities. Rather than going into specific applications, the underlying structure of a multi-level MPC system is investigated upon. The main focus here will be on extending coordination between levels of controllers.

2 Research Framework

In large-scale intelligent networks many sub-systems can be found, each with many sensors, actuators, and different performance goals to be achieved at different levels. This obviously leads to a complex system where the coordination of actions is of paramount importance to keep the system stable and well-performing on the control objectives.

To achieve such coordinated control, at all levels of the system MPC will be used, except in the lowest levels where decisions are made on time scales below a second (there, e.g., PID control is adopted). In short, in MPC an optimization problem like the maximization of a performance function of a (sub)system is solved over a given prediction horizon, using a model of the system. Subsequently, the resulting optimal actions are implemented for the duration of the next sample period, after which an updated problem is solved.

However, comparing different versions of MPC, centralized MPC is computationally too demanding for large-scale systems, and whereas in distributed MPC controllers *do* share information, a division in different levels is not applicable. In hierarchical MPC there is such a division, but also a distinction in authority. In other words, higher-level control systems can coordinate lower-level controllers that in their turn can only send information upwards in the hierarchy.

Therefore expanding the interaction between controllers, we now look at situations where information flows in *both* directions, i.e., without information asymmetry between levels. Especially in large-scale systems it is important to design coordination mechanisms efficiently, where agents from different layers of the control system additionally can operate on different *time scales* and span different or *over-*

lapping parts of the total system under control. These are two important aspects of a system that complicate a standard MPC application and lead to what we will call coordinated or *multi-level* MPC. An initial representation of the framework of multi-level MPC is depicted in Figure 1.

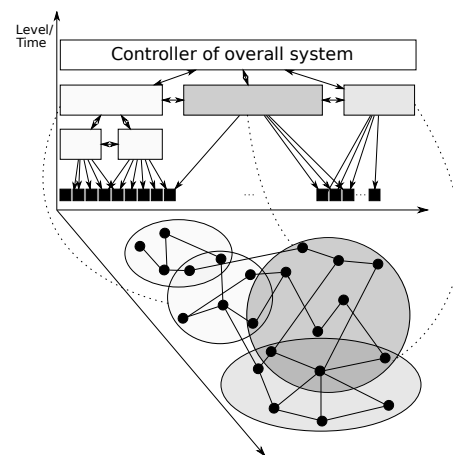


Figure 1: Schematic representation of multi-level MPC with controllers (1) operating on different time scales, (2) covering different or overlapping parts of the overall system under control, and (3) sharing information within *and* between different levels.

Finally, complexity issues or limitations are also of great importance in this context, as there is a trade-off between (near) optimality in the realization of the intended optimization goals, and computation time and overhead needed to achieve these objectives.

3 Intended Approach

All in all, the goal is to construct a more or less general way to apply multi-level MPC in large-scale intelligent infrastructures in order to arrive at a control system that operates efficiently and meets the control objectives within good margins. To develop a coherent framework, elements from game theory will be used to design the sharing of information between agents in the system and thus the coordination of controllers. Having designed such a coordinated system, algorithms can be devised to actually apply the control method and optimize the system. Examples of considerations to be made here are the timing of decisions made by several controllers and the selection of information to be shared between controllers and/or levels.

Distributed Control using Decompositions applied to a network of houses with μ CHP's.

G.K.H. Larsen
FMNS

University of Groningen
g.k.h.larsen@rug.nl

J.M.A. Scherpen
FMNS

University of Groningen
j.m.a.scherpen@rug.nl

N.D. van Foreest
FEB

University of Groningen
n.d.van.foreest@rug.nl

1 Introduction

In this project a network of households which are both producers and consumers of electricity, is assumed. We investigate how pricing mechanisms can be used to control the electricity supply of micro Combined Heat Power (μ CHP) systems to the electricity grid. Such systems produce at the same time heat and electricity, and the generated electric power can also be sold. The goal of the network is maximum energy transport at the lowest cost, while the goal of the household will be to reduce its cost. We wish to find a price mechanism that stimulates the household to a flat electricity demand.

2 Dynamic Dual Decomposition and Distributed Control

Distributed control is used when decision makers have access to different information concerning underlying dynamics and constraints. In particular each household (node in network) has different electricity demands and decides independently when to put on and off its μ CHP. Rantzer [3]



Figure 1: A house/ μ CHP is effected by nearest neighbor.

describes an approach for iterative decentralized feedback synthesis of coupled dynamic systems. The distributed performance validation is combined with control synthesis. An explicit algorithm for local update of a feedback matrix in a distributed system is given in [2]. Given the full system

$$x(\tau + 1) = Ax(\tau) + Bu(\tau) \quad (1)$$

where the A matrix will be tri-diagonal when the nodes are connected in a linear way as in figure 1. B is assumed diagonal, meaning a control signal only effects one μ CHP directly. The power usage is represented by x and u is the control variable representing the increase/decrease in electricity production/consumption. With dual decomposition and constraints relaxed by Lagrange multipliers, a controller is based on iterative solutions of a finite horizon approximation, N , of the infinite horizon cost [1]. This cost is given in

[1] by

$$V^N(\bar{x}) = \max_p \sum_i \min_{u_i, x_i, v_i} \sum_{\tau=0}^N [l_i(x_i, u_i) + p_i^T v_i - x_i^T (\sum_{j \neq i} A_{ji}^T p_j)]$$

where i is the number of houses, N is the prediction horizon, v is the expected influence from other μ CHPs, l is convex, p is the Lagrange multiplier which can be interpreted as prices. Now the first term in the equation corresponds to the local cost of the μ CHP, the second term represents what it expects to be charged by neighbors and the last term is what the μ CHP is payed by others. In each household/node of the network we then have two players. The first player chooses control inputs $u_i(0) \dots u_i(N)$ to minimize $V^N(\bar{x})$, given the prices. The second player chooses the prices $p_i(0) \dots p_i(N)$ in order to maximize $\sum_{\tau=0}^N p_i^T (\sum_{j \neq i} A_{ij} x_j - v_i)$.

3 Implementation

Earlier the scenarios of no-control and a power-balance based control in a small network of μ CHPs was investigated in the DTPA group [4]. Now the above ideas will be implemented on the same network of μ CHPs. Applications of these algorithms should enable to embed the μ CHP in our electricity system, and result in more efficient power generation.

Acknowledgments

This work is carried out in cooperation with the Flexines project.

References

- [1] P. Giselsson and A. Rantzer, "Distributed Model Predictive Control with Suboptimality Bounds", Submitted to American Control Conference, 2010.
- [2] K. Mårtensson and A. Rantzer, "Gradient Methods for Iterative Distributed Control Synthesis", CDC 2009.
- [3] A. Rantzer, "Dynamic Dual Decomposition for Distributed Control", Proceedings of American Control Conference, 2009.
- [4] J. Bakker, "The effects of different control methods on a small network of micro-CHP's", Master Thesis, 2008.

Review of Similarity Matrices and Application to Subgraph Matching

T. P. Cason P.-A. Absil P. Van Dooren

Department of Mathematical Engineering, Université catholique de Louvain
4, avenue Georges Lemaître, B-1348 Louvain-la-Neuve, Belgium

<http://www.inma.ucl.ac.be/~cason/> ([~absil/](http://www.inma.ucl.ac.be/~absil/), [~vdooren/](http://www.inma.ucl.ac.be/~vdooren/))

Introduction

Graphs are a powerful tool for many practical problems such as pattern recognition, shape analysis, image processing and data mining. Measures of graph similarity have a broad array of applications, including comparing chemical structures, navigating complex networks like the World Wide Web, and analyzing different kinds of biological data [1].

1 Node to node similarity

A node to node similarity measure can conveniently be represented in a matrix S whose (i, j) entry tells how the i^{th} node of a graph G_A is similar to the j^{th} node of a graph G_B (possibly different of G_A).

Early ideas in this context were stated in [2]. In the later, the author considers that chemical compounds are graphs, whose node and edges are respectively atoms and inter-atomic bounds, and he uses a similarity measure on this graph in order to identify isomers. Isomers are characterized by the same graph topology and this problem is equivalent to a graph matching problem.

Several similarity measures use reinforcement loops, *i.e.*, the similarity score between two nodes is computed using other similarity scores between other nodes [3, 4, 5].

2 Affine Iterations

Several existing methods can be rewritten in terms of extremal points of a scaled affine transformation

$$S^+ := \frac{\mathcal{M}(S)}{\|\mathcal{M}(S)\|}$$

where

$$[\mathcal{M}(S)]_{ij} := \sum_k \sum_l C_{ijkl} S_{lk} + D_{ij} = \text{tr}(C_{ij..} \cdot S) + D_{ij}.$$

Nevertheless, definitions of similarity available in the literature can lead to counterintuitive results. For example, Blondel *et al.* [3] state that the similarity between i and j should be large if their neighborhoods are similar, and propose to

define the similarity matrix to be the limit of the following iteration

$$\rho S_{ij}^+ := \sum_{\substack{k \text{ child of } i \\ l \text{ child of } j}} S_{kl} + \sum_{\substack{k \text{ parent of } i \\ l \text{ parent of } j}} S_{kl}, \quad (1)$$

where ρ is a normalization factor. This method gives very high similarity score to nodes that have many parents and children since their similarity score gets more contributions in (1). As a consequence, all nodes from one graph tend to have a high similarity score with the highest-degree node of the other graph. Moreover if one graph is undirected, the similarity matrix has rank 1, *i.e.*, $S = uv^T$ for some vectors u and v . This implies that $\arg \max_i S_{ij}$ (resp. $\arg \max_j S_{ij}$) is the same for all j (resp. i), *i.e.*, all nodes of one graph have the highest similarity score with one single node of the other graph.

In this research, we compare several node to node similarity measures and further test these methods on benchmark problems that reveal their key properties. We consider their capability to solve subgraph matching problems and compare their computational cost and speed of convergence.

References

- [1] L. Zager. *Graph Similarity and Matching*. PhD thesis, Massachusetts Institute of Technology, may 2005.
- [2] Jon M. Kleinberg. Authoritative sources in a hyper-linked environment. *J. ACM*, 46(5):604–632, 1999.
- [3] V. D. Blondel, A. Gajardo, M. Heymans, P. Senellart, and P. Van Dooren. A measure of similarity between graph vertices: applications to synonym extraction and Web searching. *SIAM Review*, 46(4):647–666, 2004.
- [4] E. A. Leicht, P. Holme, and Newman M. E. J. Vertex similarity in networks. *Physical Review*, (2), 2006.
- [5] S. Melnik, H. Garcia-Molina, and E. Rahm. Similarity flooding: a versatile graph matching algorithm and its application to schema matching. In *Data Engineering, 2002. Proceedings. 18th International Conference on*, pages 117–128, 2002.

Coordinate transformation as a help for controller design in walking robots

Gijs van Oort, Stefano Stramigioli
University of Twente, Faculty of EEMCS
g.vanoort@ewi.utwente.nl, s.stramigioli@utwente.nl

1 Introduction

In robotics, it is very useful to have a model describing the mechanics of a robot. The model consists of a state (configuration and velocity of each part of the robot) and equations of motion that tell how the state evolves in time. In order to do calculations, the state needs to be expressed in numbers. There is no unique way to do this, nor is there a universal ‘best’ way (it depends on what needs to be calculated).

For walking robots, the robot’s absolute position must be reflected in the state. Usually one chooses to include the pose and velocity of the torso in the state (*i.e.*, the torso is taken as the *reference body*). However, sometimes it is useful to choose a different reference body; in particular the stance foot is a good choice.

2 Equations of motion and coordinate transform

Let $Q_{(\text{tor})}$ denote the configuration of the robot with the torso as reference frame, *i.e.*, $Q_{(\text{tor})} = (H_{\text{tor}}^w, q)$, where $H_{\text{tor}}^w \in SE(3)$ is the homogeneous transformation matrix [1] representing the pose of the torso expressed in world coordinates and q is a n -element vector of all internal joint angles. Also, let $v_{(\text{tor})}$ denote the generalized velocity of the robot with the torso as reference frame, *i.e.*, $v_{(\text{tor})} = \Phi_{\bullet}(\mathcal{Q}_{(\text{tor})})\dot{\mathcal{Q}}_{(\text{tor})} = \begin{pmatrix} T_{\text{tor}}^w \\ \dot{q} \end{pmatrix}$, where $\Phi_{\bullet}(\bullet)$ is a configuration-dependent matrix, T_{tor}^w the Twist (6D ‘velocity’) of the torso relatively to the fixed world and \dot{q} are the angular velocities of all joints. Together, $Q_{(\text{tor})}$ and $v_{(\text{tor})}$ form a representation of the state of the robot. Similarly, $Q_{(\text{stf})}$ and $v_{(\text{stf})}$ can be defined, having the stance foot (*stf*) as reference body. For both representations we can write down the equations of motion:

$$\bar{P}_{(\text{tor})} = M_{(\text{tor})}v_{(\text{tor})}, \dot{\bar{P}}_{(\text{tor})} = C_{(\text{tor})}\bar{P}_{(\text{tor})} + G_{(\text{tor})} + B_{(\text{tor})}\tau; \quad (1)$$

$$\bar{P}_{(\text{stf})} = M_{(\text{stf})}v_{(\text{stf})}, \dot{\bar{P}}_{(\text{stf})} = C_{(\text{stf})}\bar{P}_{(\text{stf})} + G_{(\text{stf})} + B_{(\text{stf})}\tau. \quad (2)$$

where \bar{P}_{\bullet} is the generalized momentum, which depends on the representation. The matrices M , C and G are the well-known mass matrix, and coriolis and gravity vectors. $B_{\bullet} = [0_{n \times 6} \quad I_{n \times n}]^T$ and τ are the joint torques. Usually the equations of motion in the model are (1), where the torso is taken as the reference frame. An explicit expression for M is given in [2].

The relation between $M_{(\text{tor})}$ and $M_{(\text{stf})}$ is $M_{(\text{stf})} = E^{-T}M_{(\text{tor})}E^{-1}$. Similar relations exist for \bar{P} , C and G .

3 Applications

The stance foot reference frame vectors and matrices, $\bar{P}_{(\text{stf})}$, $M_{(\text{stf})}$, $C_{(\text{stf})}$ and $G_{(\text{stf})}$, have some nice features not found in other representations. A few of them will be listed here. The proofs are left behind in this abstract.

1. When walking, the stance foot stands still on the ground. This is reflected in the first six elements of $\bar{P}_{(\text{stf})}$ being zero.
2. It is easy to check the required joint torques to keep the robot statically stable in a certain configuration. The last n elements of $G_{(\text{stf})}$ directly reflect the actuator torques needed. Moreover, the first 6 elements give information about the COM of the robot being above the stance foot (which is needed to prevent falling over) or not.
3. $M_{(\text{stf})}$ really reflects the ratio between force and resulting acceleration accurately. This is *not* the case for any other mass matrix representation (*e.g.*, $M_{(\text{tor})}$). It can be used to do accurate feed-forward control, as well as (MIMO) P(I)D-control with well tuned controllers.

4 Conclusions and future work

In this abstract it was shown that (nonlinear) coordinate transformation may be of help in order to obtain nice expressions for the equations of motion. When well-chosen, the expressions give much insight and make the life of walking-algorithm developers easier. However, a few remarks need to be made.

- All of this is ‘just’ math. We transform one problem into another problem, which is, fortunately, easier to solve. However, this theory alone does not solve any problems, *i.e.*, this theory does not make a robot walk.
- This theory can correctly be used only when exactly one foot has contact with the ground. During double support we have an overactuated system with a diminished number of degrees of freedom, which ruins the correctness of the results presented here. Solving this is future work.

References

- [1] R. Featherstone, “Rigid body dynamics algorithms,” Springer, 2008.
- [2] S. Stramigioli, V. Duijndam, G. van Oort, and A. Goswami, “Compact analysis of 3D bipedal gait using geometric dynamics of simplified models,” in *Proceedings of ICRA 2009*, May 2009, pp. 1978–1984.

Real-Time Clustering Of Position And Omnivision Object Observations In The RoboCup Domain

Rob Janssen
 Department of Mechanical Engineering
 Eindhoven University of Technology
 P.O. Box 513
 5600 MB Eindhoven
 The Netherlands
 Email: R.J.M.Janssen@tue.nl

René van de Molengraft
 Department of Mechanical Engineering
 Eindhoven University of Technology
 P.O. Box 513
 5600 MB Eindhoven
 The Netherlands
 Email: M.J.G.v.d.Molengraft@tue.nl

1 Introduction

In the RoboCup Mid-Size league two teams of autonomous robots compete against each other in a game of soccer. One of the main issues, is for each robot to know where the peer and opponent players are located on the field. By using an omnivision camera the robot is able to obtain the position of robots in its own environment, but it cannot distinct between peer or opponent robots. Another issue is that due to resolution deterioration of the camera on larger distances ($>5\text{m}$), the robot does not know what is beyond this range. By combining the peer position and omnivision object data from all peer robots and efficiently clustering this data a unique and complete view of the field can be created. This allows the robot for instance to plan a path over the total length of the field ($>18\text{m}$), or to pass a ball to a peer robot that is actually positioned beyond the robots own field of view.

2 Observation properties

The peer position and omnivision object data are send to the other peers by WiFi. These observations have several properties.

- the observations originate from moving robots on a 2D surface,
- the observations include noise,
- the observations are sequential in time,
- the actual number of robots present is unknown.

3 Clustering the data

To extract the relevant information from the observations an hypotheses-tree based sequential clustering algorithm [1] is adopted, with some adaptations to make it run in real-time and to deal with the dynamics of the moving robots. Labeling is added to distinct between peer or opponent robot and to track an identified opponent. If one of the originating observations contains a position measurement of a peer robot, the robot is labeled as 'peer'. If the originating observations only contain position measurements obtained by the omnivision camera, the robot is labeled as 'opponent'.

For each observation the following steps are performed.

1. the hypotheses tree is expanded. Either the new observation can be classified as clutter, a new observed robot or belonging to an already observed robot. If a new robot is observed it is labeled as peer or opponent,
2. a Kalman propagation is performed for each existing object in the hypotheses tree,
3. a likelihood update is applied, based on the spatial distance of the observation and the already observed robots,
4. the hypotheses tree is pruned so that it stays maintainable,
5. the hypothesis with the highest probability is selected.

The selected hypothesis describes the total number of peer and opponent robots. From the Kalman states that belong to these robots the current position and velocity of that specific robot can be derived. A static representation of the outcome of the algorithm is depicted in Fig. 1.

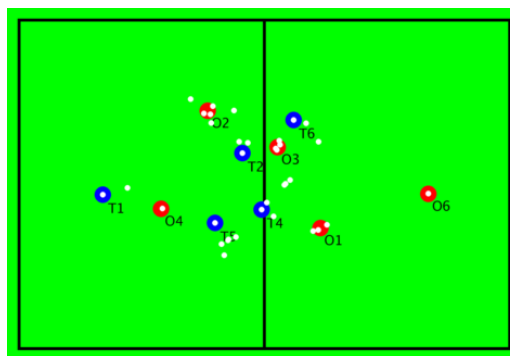


Figure 1: Observations (white), peers (blue) and opponents (red).

References

- [1] J.Schubert, H.Sidenbladh, *Sequential clustering with particle filters - Estimating the number of clusters from data*. Proc. 8th Intern.Conference on Information Fusion, 2005

Application of the IMPACT structure on bilateral teleoperation

Alper Denasi,¹ Dragan Kostić,² and Henk Nijmeijer³

Department of Mechanical Engineering

Technische Universiteit Eindhoven

P.O. Box 513, 5600 MB Eindhoven

The Netherlands

Email: {¹A.Denasi, ²D.Kostic, ³H.Nijmeijer}@tue.nl

Abstract

A common issue encountered in teleoperation systems is a time-delay in the communication channel. Depending on the type of communication protocol, the delay can be constant or time-varying. In both cases, the delay can seriously degrade performance of teleoperations or even destroy stability. The Smith predictor [1] can be used to compensate for undesirable effects of time-delays. Reference [2] addresses some issues of robustness and disturbance rejection characteristic to time-delay compensation using Smith predictors. There, a control structure is proposed to increase robustness of systems with Smith predictors. This control structure makes use of the Internal Model Principle and Control Together (IMPACT) approach.

In this work, we apply the IMPACT approach to position error (PERR) based teleoperations, where only position information is exchanged between the master and slave manipulators. Our method combines a Smith predictor with a disturbance estimator designed based on an expected class of disturbances acting at the output of the slave manipulator. The block diagram of the control structure we propose is presented in Figure 1. Here, T_d represents the forward and backward time-delays in the communication channel that are both assumed to be constant, known and identical to each other in the design and robustness analysis of the controller. The time delays used in the controller are different than the ones that exist in the communication channel and the influence of this mismatch on the robustness has been investigated. We consider 1 d.o.f. equation of motion:

$$J_i \ddot{q}_i + B_i \dot{q}_i = \tau_i, \quad (1)$$

where q_i , \dot{q}_i , and \ddot{q}_i represent the position, velocity and acceleration of the manipulators, respectively, τ_i is the control, J_i and B_i are the inertia and the viscous friction coefficient, and $i \in \{m, s\}$ identifies variables at the master or slave side. In Figure 2, we show simulation results in the case of a sinusoidal disturbance acting at the slave side. Here, both master and slave robots are commanded to follow a step reference signal. It can be observed from Figure 2 that the influence of the disturbance on the steady-state values of both master and slave manipulators is reduced reasonably fast with the help of the proposed control strategy.

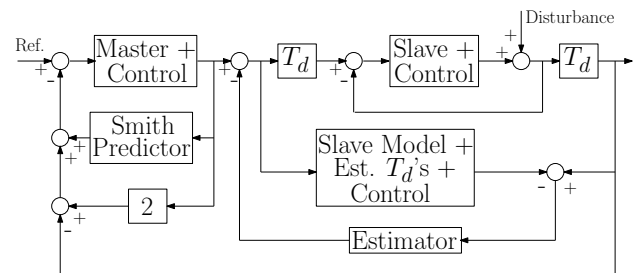


Figure 1: IMPACT structure for PERR based teleoperation

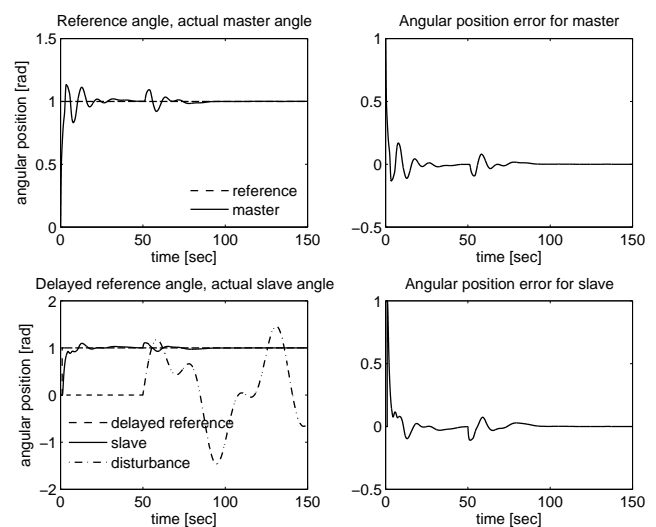


Figure 2: Disturbance absorption of a sinusoidal disturbance

The robustness of our approach is evaluated by means of the Nyquist stability criterion. In the future, we will extend our approach to manipulators with multiple d.o.f.'s and to different type of teleoperation architectures (e.g., force-position or 4-channel).

References

- [1] C. Kravaris and R.A. Wright, "Deadtime compensation for nonlinear processes," *AIChE Journal*, vol. 35, no. 9, pp. 1535-1542, Aug 1989.
- [2] M.R. Stojić, M.S. Matijević, and L.S. Draganović, "A robust Smith predictor modified by internal models for integrating process with dead time," *IEEE Trans. Automatic Control*, Vol. 46, No. 8, pp. 1293-1298, 2001.

Transparency in Force-sensorless Teleoperation Setups

Stefan Lichiardopol
Dynamics and Control Group
Department of Mechanical Engineering
Eindhoven University of Technology
5600 MB Eindhoven
The Netherlands
Email: s.lichiardopol@tue.nl

Henk Nijmeijer
Dynamics and Control Group
Department of Mechanical Engineering
Eindhoven University of Technology
5600 MB Eindhoven
The Netherlands
Email: h.nijmeijer@tue.nl

1 INTRODUCTION

In this paper, we consider the problem of bilateral teleoperation in force-sensor-less robotic setups. It is well-known that haptic robotic devices and teleoperation systems exploit information regarding the external forces (see [1] and [2], e.g. for haptic feedback). The slave robot interacts with the environment and its dynamics are dependent on external forces induced by this interaction. These forces can be contact forces (interaction forces between environmental objects and the robot) or exogenous forces induced by the environment.

In bilateral teleoperation, knowledge on the unknown environmental force applied on the slave robot is typically needed to achieve coordinated teleoperation.

Here, we present a control approach for bilateral teleoperation with an estimation strategy for external forces acting on the slave robot with a load with unknown mass. This method extends a result presented in [3], which considered human-robotic co-manipulation problem. The proposed algorithm is robust for large uncertainties in the mass of the load.

2 CONTROL DESIGN

Due to the uncertainties in the model of the slave robot we can not estimate the unknown environmental force and track the master robot position at the same time. Therefore, we are proposing a switching controller based on a cyclic algorithm (see Figure 1).

During the first phase, which last for a period of T_0

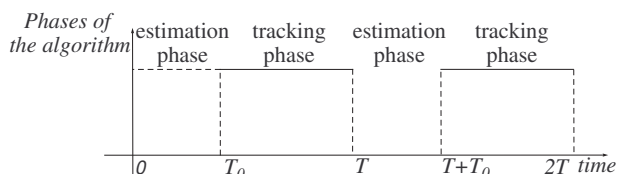


Figure 1: Temporal division of the control strategy.

($T_0 < T$), the controller will behave as a force estimator. Here we are using the force observer introduced in [3] to estimate the external force which will be used for the purpose of haptic feedback and during the second phase we are keeping the estimated force constant. In the second phase, we are using a PD controller for the slave robot to track the position of the master robot. In Figure 2, we present

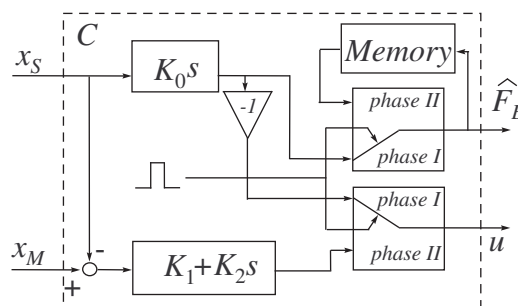


Figure 2: Controller Design.

the block diagram representation of the controller where the controller blocks are represented by their transfer functions in the Laplace domain ($s \in \mathbb{C}$) and the block called *Memory* saves the last estimate of the environmental force at the end of the first phase and provides the same constant output during the entire second phase.

3 CONCLUSIONS

In this paper, we have introduced a new control algorithm for bilateral teleoperation in force-sensorless setups using a switching strategy between a force estimating controller and a tracking controller. This switching estimation/tracking algorithm on the one hand guarantees estimation of the environmental force forces on the slave robot (to be used in haptic feedback) in the absence of force sensors, on the other hand the algorithm is shown to guarantee bounded tracking errors in the face of external perturbations.

References

- [1] D. Lawrence, "Stability and transparency in bilateral teleoperation," *IEEE Transactions on Robotics and Automation*, vol. 9, pp. 624–637, 1993.
- [2] P. F. Hokayem and M. W. Spong, "Bilateral teleoperation: A historical survey," *Automatica*, vol. 42, pp. 2035–2057, 2006.
- [3] S. Lichiardopol, N. van de Wouw, and H. Nijmeijer, "Boosting human force: A robotic enhancement of a human operator's force," *Proceedings of International Conference on Decision and Control*, pp. 4576–4581, 2008.

Stabilisation of unstable transition boiling states

R.W. van Gils^{*,1,2}, M.F.M. Speetjens² and H. Nijmeijer¹

Eindhoven University of Technology, PO Box 513, 5600 MB Eindhoven

Department of Mechanical Engineering,¹Dynamics and Control,²Energy Technology

Email: *r.w.v.gils@tue.nl

1 Introduction

The ability for massive heat removal becomes more and more relevant in further development of high-performance technologies. Cooling schemes based on boiling heat transfer can accomplish the desired heat removal rates. Pool-boiling may serve as physical system for such cooling applications. It typically consists of a heater surface submerged in a pool of boiling liquid. In the pool-boiling system, heat is extracted from the heater in a nonlinear fashion, described by the boiling curve given in Figure 1, [1]. Here q_F and T_F represents the heat flux and the temperature at the fluid-heater interface, respectively.

As a result, in a two-dimensional (2D) pool-boiling system so-called heterogeneous equilibria exist, characterised by local regions of low and high temperatures. The objective of current investigation is the stabilisation of these inherently unstable equilibria.

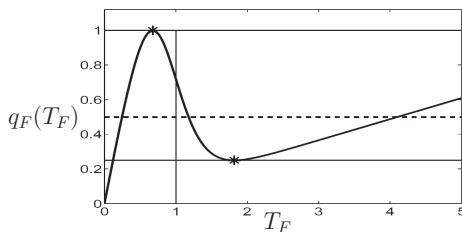


Figure 1 Nondimensional boiling curve. Nonlinear heat extraction at interface.

2 Pool boiling model description

The unstable steady states are investigated using a 2D pool-boiling model, which consists of a 2D rectangular heater only. The temperature $T(x, y, t)$ within this heater is given by the heat equation

$$\frac{\partial T}{\partial t}(x, y, t) = \kappa \nabla^2 T(x, y, t). \quad (1)$$

The boundary conditions comprise adiabatic sidewalls, a controlled heat supply at the bottom and the nonlinear heat extraction at the top of the heater, i.e.

$$\frac{\partial T}{\partial \mathbf{v}} = \begin{cases} 0, & \text{for } x = 0 \wedge x = 1, \\ \frac{1}{\Lambda} (1 + u(t)), & \text{for } y = 0, \\ -\frac{\Pi_2 q_F(T_F)}{\Lambda}, & \text{for } y = D, \end{cases} \quad (2)$$

with \mathbf{v} the outward normal on the heater boundary, Λ , Π_2 and κ positive system parameters, $q_F(T_F)$ the boiling curve and $u(t)$ the input, i.e. an additional heat supply at the bottom of the heater, see Figure 2, from [1].

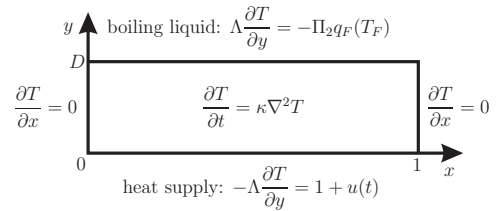


Figure 2 Two-dimensional rectangular heater.

3 Stabilisation of heterogeneous equilibria

A linear feedback controller is used to stabilise one of several heterogeneous (spatially varying) equilibria. The controller is based on the spectral coefficients obtained by spatial discretisation of the temperature profile using a Chebyshev-Fourier-cosine expansion, cf. [2].

In Figure 3 the simulated evolution of the interface temperature ($T(x, D, t)$) is shown (arrows indicate progression in time). As can be seen, the spatially varying equilibrium is stabilised. Important to note is, that this is done by a spatially uniform input (linear static feedback).

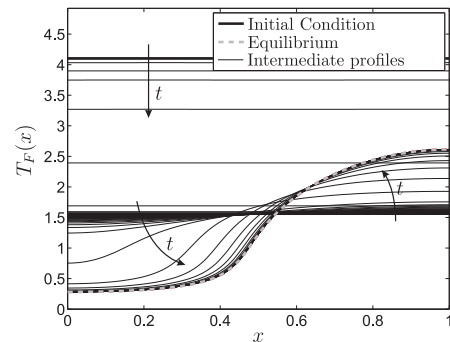


Figure 3 Evolution of the interface temperature profile.

4 Conclusion

Analyses reveal that some of the unstable equilibria of the 2D pool-boiling system can be stabilised. Especially the fact that spatially varying equilibria are stabilised by a spatially uniform input must be emphasised.

References

- [1] R. van Gils, et al. Feedback stabilisation of a pool-boiling system. *Int. J. of Heat and Mass Transfer*, 2009. Accepted.
- [2] C. Canuto, et al. *Spectral methods in fluid dynamics*, Springer, New York, third edition, 1987.

Design of optimal deterministic output estimators for distributed parameter systems

Jochem Visser

Department of Electrical Engineering
Technische Universiteit Eindhoven
P.O. Box 513, 5600 MB Eindhoven
The Netherlands
Email: j.a.w.visser@tue.nl

Siep Weiland

Department of Electrical Engineering
Technische Universiteit Eindhoven
P.O. Box 513, 5600 MB Eindhoven
The Netherlands
Email: s.weiland@tue.nl

1 Abstract

Distributed parameter systems occur in numerous engineering applications. Estimation of outputs based on measurements is necessary if a direct measurement is not available or are affected by noise. The solution to the optimal state estimation problem for distributed parameter systems is solved in a stochastic setting, for instance see [1]. We present a route for the derivation of a deterministic optimal H_2 output estimator for linear distributed parameter systems. The route avoids stochastic interpretations of variables.

2 Optimal state estimation as optimization problem

Let \mathcal{X} be a Hilbert space and let \mathcal{Y} , \mathcal{Z} , \mathcal{D}_1 and \mathcal{D}_2 be Euclidean spaces of finite dimension. Consider system Σ_p with states $x(t) \in \mathcal{X}$, outputs $z(t) \in \mathcal{Z}$, measurements $y(t) \in \mathcal{Y}$ and disturbances $d_1(t) \in \mathcal{D}_1$, $d_2(t) \in \mathcal{D}_2$, given by the abstract evolution equations:

$$\Sigma_p : \begin{cases} \dot{x} = Ax + Gd_1 \\ y = Cx + Sd_2 \\ z = Hx \end{cases} \quad (1)$$

Here $A : \mathcal{X} \rightarrow \mathcal{X}$ is a linear (possibly unbounded) operator and $G : \mathcal{D} \rightarrow \mathcal{X}$, $C : \mathcal{X} \rightarrow \mathcal{Y}$ and $H : \mathcal{X} \rightarrow \mathcal{Z}$ are bounded linear operators. Assume that the operator A is the infinitesimal generator of an exponentially stable semigroup operator $T(t) : \mathcal{X} \rightarrow \mathcal{X}$ and assume that the pair (A, C) is observable. The mild solution of this system is given by:

$$x(t) = T(t-t_0)x(t_0) + \int_{t_0}^t T(t-\tau)Gd_1(\tau)d\tau,$$

$$z(t) = Hx(t), \quad y(t) = Cx(t) + Sd_2(t),$$

where $t \in [t_0, t_e]$. We consider the problem of designing an estimator Σ_e for the outputs of Σ_p as illustrated in Figure 1. Σ_e produces estimates according to the causal relation $\hat{z}(t) =$

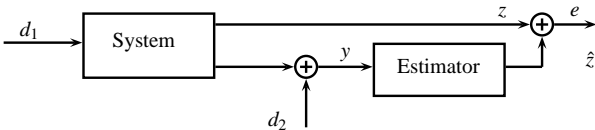


Figure 1: Estimation scheme

$(M(\cdot, t) * y(\cdot))(t) := \int_{t_0}^t M(\tau, t)y(\tau)d\tau$, where the integration

kernel $M(t, t_e)$ characterizes the estimator. The deterministic H_2 estimation problem amounts to the problem of finding M such that a given cost criterion is minimal. As design criterion we consider the functional:

$$J(M) = \|K_M\|_2^2 + \|L_M\|_2^2,$$

where $\|f\|_2 := \int_{t_0}^{t_e} \text{tr}(f^*(t)f(t))dt$, K_M is the integration kernel of the mapping $d_1 \mapsto z - \hat{z}$ and L_M is the integration kernel of the mapping $d_2 \mapsto z - \hat{z}$. Note that:

$$K_M(t) = HT(t)G - (M(\cdot, t_e) * CT(\cdot)G)(t) \quad L_M(t) = M(t, t_e)S.$$

Please note that this cost functional, in contrast to a cost functional for design in a stochastic setting and the approach followed in [1], is defined by operator norms. We show that optimization of the cost functional containing the norms of the kernels K_M and L_M over all possible operators M results in the optimal output estimator. The optimization problem will be reformulated as an optimal control problem for an artificial system and we show that the optimal estimator is characterized by $M = M_{opt}$, with:

$$M_{opt}(t, t_e) = HU(t_e, t)P(t)C^*S^{-2},$$

where $P(t)$ is the solution of the Riccati equation

$$\frac{d}{dt} \langle \phi_1, P(t)\phi_2 \rangle = \langle \phi_2, P(t)A^*\phi_1 \rangle + \langle A^*\phi_2, P(t)\phi_1 \rangle + \langle Q^*\phi_1, Q^*\phi_2 \rangle - \langle P(t)C^*S^{-2}CP(t)\phi_2, \phi_1 \rangle$$

for $\phi_1, \phi_2 \in \mathcal{X}$. and $U(t_e, t)$ is the mild solution of the artificial system.

3 Comparison of estimators

We compare three estimators for a model that represents heat diffusion in a slab of finite length. We compare the optimal estimator based on design in the infinite dimensional setting with an estimator that is an approximation of the optimal infinite dimensional estimator based on the most dominant POD basis functions and with an estimator that is optimal for a finite dimensional approximation of the problem.

References

[1] Curtain R.F. and Zwart H.J. An introduction to infinite-dimensional linear systems theory, 1995, Springer.

Cluster synchronization algorithms

Weiguo Xia, Ming Cao

University of Groningen, Faculty of Mathematics and Natural Sciences,

Nijenborgh 4, 9747 AG Groningen, The Netherlands

Email: w.xia@rug.nl, m.cao@rug.nl

1 Introduction

In recent years, the study of distributed coordination of multi-agent systems has attracted significant attention from researchers in different disciplines. Simple local coordination rules can sometimes lead to complicated collective behavior, such as synchronization that has been discovered in natural, social and engineering networks and systems. In this line of research, various algorithms have been successfully constructed to cause all the agents in a group to converge to the same value asymptotically [1]. However, there is an emerging trend to study how an interconnected group may evolve into different sub-groups called clusters [2]. In contrast to the widely studied synchronization behavior, in the cluster synchronization problem studied in this paper, we require the interconnected agents to evolve into several clusters and each agent only to synchronize within its cluster. Two approaches are presented to achieve cluster synchronization in dynamical multi-agent systems. The first approach is to add a constant forcing to the dynamics of each agent that are determined by positive diffusive couplings; and the other is to introduce both positive and negative couplings between the agents.

2 Problem formulation

Consider a dynamical system consisting of N agents with dynamics

$$\dot{x}(t) = f(x(t), t), \quad (1)$$

where $x(t) = (x_1(t), \dots, x_N(t))^T \in \mathbb{R}^N$, $x_i(t)$ is the state of the i th agent, and f is a continuous map. Let $\{C_1, C_2, \dots, C_n\}$ be a partition of the set $\mathcal{N} = \{1, 2, \dots, N\}$ into n nonempty subsets, i.e., $C_i \neq \emptyset$, $\bigcup_{i=1}^n C_i = \{1, \dots, N\}$, and l_i is the number of labels within C_i . For $i \in \{1, \dots, N\}$, let \hat{i} denote the index of the subset in which the number i lies, i.e., $i \in C_{\hat{i}}$. System (1) is said to realize n -cluster synchronization with the partition $\{C_1, C_2, \dots, C_n\}$, if $\lim_{t \rightarrow \infty} \|x_i(t) - x_j(t)\| = 0$ when $\hat{i} = \hat{j}$, and $\lim_{t \rightarrow \infty} \|x_i(t) - x_j(t)\| \neq 0$ when $\hat{i} \neq \hat{j}$.

3 Cluster synchronization with constant forcing

Consider N agents under some external constant forcing, whose dynamics are described by

$$\dot{x}_i(t) = -x_i(t) + \sum_{j=1}^N g_{ij} x_j(t) + a_{\hat{i}}, \quad (2)$$

where $1 \leq i \leq N$, $g_{ij} \geq 0$ for $i \neq j$, $\sum_{j=1}^N g_{ij} = 0$, and $a_{\hat{i}}$ are constants satisfying $a_{\hat{i}} \neq a_{\hat{j}}$ for $\hat{i} \neq \hat{j}$. Let

$$G = \begin{pmatrix} G_{11} & G_{12} & \cdots & G_{1n} \\ G_{21} & G_{22} & \cdots & G_{2n} \\ \vdots & \vdots & \ddots & \vdots \\ G_{n1} & G_{n2} & \cdots & G_{nn} \end{pmatrix}, \quad (3)$$

where $G_{ij} \in \mathbb{R}^{l_i \times l_j}$ and $\sum_{i=1}^n l_i = N$.

Theorem 1. System (2) achieves n -cluster synchronization for almost all (in the sense of Lebesgue measure) a_i ($1 \leq i \leq n$, $a_i \neq a_j$, for $i \neq j$), if block matrices G_{ij} ($1 \leq i, j \leq n, i \neq j$) have constant row sums.

4 Cluster synchronization with negative weights

Consider the linear time-invariant multi-agent system

$$\dot{x}(t) = Gx(t), \quad (4)$$

where $G \in \mathbb{R}^{N \times N}$ is in the form of (3). Suppose G satisfies the condition that the row sums of G_{ij} ($1 \leq i, j \leq n$) are 0, which implies that G has negative off-diagonal elements. Let $\eta_1 = (\underbrace{1, \dots, 1}_{l_1}, 0, \dots, 0)^T, \dots, \eta_n = (0, \dots, 0, \underbrace{1, \dots, 1}_{l_n})^T$

be n independent right eigenvectors associated with 0, and $\alpha_1, \dots, \alpha_n$ be the corresponding n left eigenvectors satisfying $\eta_i^T \alpha_j = 0$, if $i \neq j$; $\eta_i^T \alpha_j = 1$, if $i = j$.

Theorem 2. Suppose the initial values of system (4) satisfy that $\alpha_i^T x(0)$ ($1 \leq i \leq n$) are not equal to each other, then n -cluster synchronization can be achieved if and only if G has exactly n zero eigenvalues and all the other eigenvalues have negative real parts.

References

- [1] W. Ren and R. W. Beard, Consensus seeking in multiagent systems under dynamically changing interaction topologies. *IEEE Trans. Auto. Contr.*, 50, 655-661, 2005.
- [2] J. Yu and L. Wang, Group consensus of multi-agent systems with undirected communication graphs. *Proceedings of the 7th Asian Control Conference*, 105-110, Hong Kong, China, 2009.

Feedback control of the sawtooth behavior in nuclear fusion

Gert Witvoet,^{1,2} Maarten Steinbuch,¹ Egbert Westerhof,² Niek Doelman,³ Marco de Baar²

¹ Eindhoven University of Technology
Department of Mechanical Engineering
Control Systems Technology group
P.O. Box 513, 5600 MB Eindhoven
{G.Witvoet,M.Steinbuch}@tue.nl

² FOM - Institute for Plasma Physics
Association EURATOM-FOM
Trilateral Euregio Cluster
P.O. Box 1207, 3430 BE Nieuwegein
{E.Westerhof,M.deBaar}@rijnh.nl

³ TNO Science and Industry
BU Mechatronic Equipment
Precision Motion Systems department
P.O. Box 155, 2600 AD Delft
Niek.Doeleman@tno.nl

1 Introduction

In nuclear fusion research, a hot ionized plasma is confined by magnetic fields. Often these plasmas show sawtooth instabilities in the core of the plasma. Sawteeth can trigger secondary instabilities [1] and mix the fusion products in the plasma core. To optimize between these effects control of the sawtooth period is essential.

2 Sawtooth modeling

The sawtooth behavior can be modeled as an infinite dimensional impulsive dynamical system [2]:

$$\frac{\partial}{\partial t} B_\theta = \frac{\partial}{\partial r} \left(\frac{\eta}{\mu_0 r} \left(B_\theta + r \frac{\partial}{\partial r} B_\theta \right) - \eta J_{CD} \right) \quad \text{if } s_1(B_\theta) \leq s_{crit} \quad (1a)$$

$$B_\theta(r, t^+) = \begin{cases} B_\theta(r, t^-) & \text{for } r \geq r_{mix} \\ \frac{1}{R} r B_\phi & \text{for } r < r_{mix} \end{cases} \quad \text{if } s_1(B_\theta) > s_{crit} \quad (1b)$$

The sawtooth period τ_s is the time between subsequent state jumps (1b). The current drive actuator J_{CD} (characterized by total input current I_{CD} and injection angle ϑ) alters the poloidal magnetic field B_θ , which influences the magnetic shear $s_1(B_\theta)$. This advances or delays (1b), changing τ_s .

3 Nonlinear input-output behavior

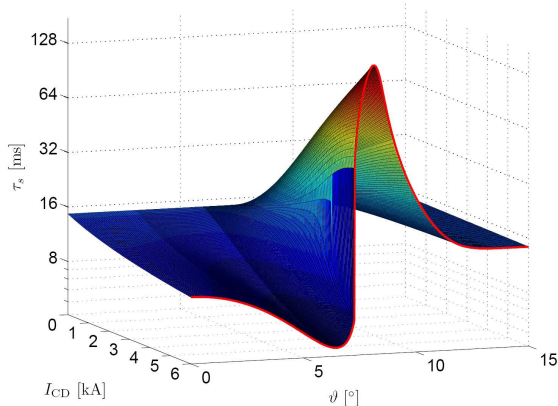


Figure 1: Steady state dependency of sawtooth period on the inputs I_{CD} (total current drive) and ϑ (injection angle)

Steady state simulations (Fig. 1) show that the sawtooth model (1) behaves highly nonlinear. The system gain, i.e.

the steady-state dependency of τ_s on I_{CD} and ϑ , depends on the operating point (I_{CD}, ϑ) . Moreover, the system output behaves event driven, i.e. the output τ_s only changes after a state jump (1b), since τ_s can only be computed when a new state jump has occurred. Hence, the signal τ_s is stair-shaped.

4 Linearization and closed loop results

Linearizations (using approximate realization) around different operating points (I_{CD}, ϑ) were carried out to obtain local LTI models of the system. These can be used to design local (PI) controllers, for which Fig. 2 shows some specific closed loop results. In these results the desired sawtooth period can be obtained without any steady-state error.

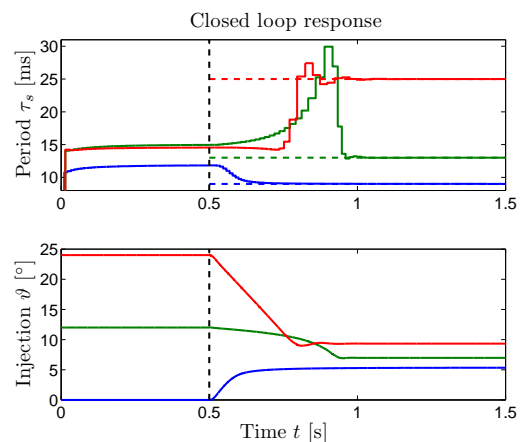


Figure 2: Closed loop simulation results

5 Conclusions

Local linearizations of the nonlinear system provide a good basis for local controller designs. Guaranteeing global stability or designing global controllers is still an important part of the current research.

References

- [1] B.A. Hennen, *et al.*, "A closed-loop control system for stabilization of MHD events on TEXTOR," *Fusion Eng. Des.*, vol. 84, pp. 928-934, 2009.
- [2] G. Witvoet, *et al.*, "Control oriented modeling and simulation of the sawtooth instability in nuclear fusion tokamak plasmas," in *Proc. 48th Conf. Decis. Contr.*, Shanghai, China, December 2009, pp. 1360-1366.

Modeling and Control of Inline Separators: An Introduction

Martijn Leskens, Adrie Huesman, Paul Van den Hof
Delft Center for Systems and Control

Delft University of Technology, Mekelweg 2, 2628 CD Delft, The Netherlands
Email: {m.leskens, a.e.m.huesman, p.m.j.vandenhof}@tudelft.nl

Stefan Belfroid, Erik Nennie

TNO Science & Industry

Stieltjesweg 1, 2628 CK Delft, The Netherlands
Email: {stefan.belfroid, erik.nennie}@tno.nl

Paul Verbeek, Ruud Henkes, Edwin van Donkelaar
Shell Global Solutions

Sir Winston Churchillaan 299, 2288 DC Rijswijk, The Netherlands /
Badhuisweg 3, 1031 CM Amsterdam, The Netherlands
Email: {paul.verbeek, ruud.henkes, edwin.vandonkelaar}@shell.com

Abstract

Hydrocarbons are increasingly difficult to find while, simultaneously, the demand is rising. This discrepancy has been leading to an increasing pressure on the oil and gas (exploration & production) industry to improve their operations all through the production chain. One part of that chain is the separation of the produced flow into separate streams, which typically are an oil, water, gas and solid stream. This separation is mostly performed by means of voluminous, high weight vessels, with the main separation mechanism being gravity. A current trend in the oil and gas industry, however, is to use compact so called inline separators (ILS), where the main separation mechanism is that of centrifugal forces, which are introduced by creating a swirl in the flow to be separated. A main motivation for using such separators is their low volume, which renders them very useful for e.g. production operations where space is limited, such as on offshore platforms. The advantage of a low volume is, however, also a disadvantage in the sense of a highly reduced capability of properly handling ILS inlet flow rate and pressure variations. These variations are commonly encountered at oil and gas production operations, in particular in the form of slug flow. The low inlet flow variation handling capacity easily leads to economic loss, in the form of production deferment, and other operational problems, which are amplified by an increasing number of production operations that encounter slug flow type of variations or growing such variations.

Optimal mitigation of ILS inlet flow variations is currently a highly relevant problem for the oil and gas industry. A considerable amount of solutions have been proposed to solve

this problem which roughly can be divided in control and non-control based ones. Here, only the first type is considered, which have the advantage of typically being much cheaper. Recently, driven by the industrial need to deliver optimal such solutions, a (post-doc) research project has been started to derive such solutions for optimal mitigation of ILS inlet flow variations. Particular problems that have to be dealt with are e.g. that, depending on the considered ILS system, (i) such solutions are either absent or (ii) the optimality of the available solution is not known. A model based approach is pursued, as a result of which the derivation of control oriented ILS models is an important research component. Particular problems that are encountered with this modeling are e.g. that, again depending on the considered ILS system, control oriented ILS models are either absent or the available one may be insufficient for deriving an optimal ILS control solution.

Here, first results from the research project on optimal ILS control are presented. More specific, the main aims are (i) to provide an introduction into the main issues involved in ILS modeling and control, through providing the state-of-the-art of these and relevant subjects, (ii) to discuss future research directions and (iii) to present some first application results.

Acknowledgements

The research presented here is performed as part of the Integrated System Approach Petroleum Production (ISAPP) programme, which is a joint TNO, Delft UT and Shell research programme that aims to increase hydrocarbon recovery through application of innovative reservoir development and management technologies.

Positivity criteria for Hilbert state-space Systems

B. Abouzaid, V. Wertz

CESAME, Department of Mathematical Engineering
 Université Catholique de Louvain
 4-6 Avenue G. Lemaitre
 B-1348, Louvain-la-Neuve, Belgium
 Email: bab@math.fundp.ac.be,
 vincent.wertz@uclouvain.be

J.J. Winkin

Department of Mathematics
 University of Namur (FUNDP)
 8, Rempart de la vierge
 B-5000, Namur, Belgium
 Email: joseph.winkin@fundp.ac.be

Positive linear systems are linear dynamical systems whose state trajectories are nonnegative for every nonnegative initial state and for all nonnegative input functions. Such systems are of great practical importance, as the nonnegativity property occurs quite frequently in practical applications, where the state variables correspond to quantities that do not have real meaning unless they are nonnegative (e.g. human population, cells number, concentration, etc). The importance of the positivity property for infinite-dimensional (state-space) systems has been recently revealed by the stocking and industrial systems which involve chemical reactions and heat exchangers, e.g. distributed parameter models of tubular reactors, see [2]. As positive linear systems are defined on cones and not on linear spaces, the theory of infinite-dimensional positive systems is more complicated (see [1], [3]). In this work, we look for an algebraic characterization of the infinitesimal generator of a positive C_0 -semigroup on the Hilbert space of square summable real sequences $l^2 := l^2(\mathbb{N})$, whose positive cone is reported to have an empty interior. More specifically, we study the positive off-diagonal property, which is known to characterize positive C_0 -semigroups for an ordered Banach space whose positive cone has a nonempty interior. This condition is also well-known as the Metzler matrix condition for finite-dimensional systems. Criteria are also reported for the positivity of controlled infinite dimensional systems on l^2 .

Let $\{e_n\}_{n \geq 1}$ be a positive Schauder basis of l^2 , i.e. each element z of l^2 has a unique representation of the form $z = \sum_{n=1}^{\infty} \alpha_n e_n$, where the coefficients α_n are the components of z in the basis $\{e_n\}_{n \geq 1}$ and will be denoted here by $\alpha_n = \langle z, e_n \rangle$. Consider the positive cone

$$l^2_+ = \{z = \sum_{n=1}^{\infty} \alpha_n e_n \mid \alpha_n \geq 0, \forall n\}.$$

Proposition 1: The interior of the positive cone of l^2 is empty, i.e. $\text{int}(l^2_+) = \emptyset$, where l^2 is equipped with the usual order, i.e. $x = (x_n)_{n \geq 1} \leq y = (y_n)_{n \geq 1}$ if $x_n \leq y_n$ for all $n \geq 1$.
 Let $A : D(A) \subset l^2 \rightarrow l^2$ be a linear operator on l^2 . We assume that $\{e_n\}_{n \geq 1} \subset D(A)$ where A is the infinitesimal generator of a C_0 -semigroup $(T_A(t))_{t \geq 0}$. Consider the infinite matrix representation of A , i.e. $A = (a_{nk})_{n,k \geq 1} = (\langle Ae_k, e_n \rangle)_{n,k \geq 1}$.

If the system $\dot{z}(t) = Az(t)$ is positive, then A is Metzler, i.e. $a_{nk} \geq 0$ for all $n \neq k$, and the converse holds whenever the interior of the positive cone is not empty (see e.g. [1]). How-

ever here, in view of Proposition 1, the converse is not necessarily true.

For a fixed integer N , let l^2_N be the finite-dimensional subspace of l^2 that is generated by the vectors e_1, e_2, \dots, e_N , i.e. $l^2_N = \text{span}\{e_1, e_2, \dots, e_N\}$. In addition, assume that the following condition holds:

l^2_N is $T_A(t)$ -invariant $\forall t \geq 0$, i.e. $T_A(t)l^2_N \subset l^2_N, \forall t \geq 0$.

Theorem 1: If A is Metzler, then the system $\dot{z}(t) = Az(t)$ is positive on l^2_N , i.e. $T_A(t)(l^2_N)^+ \subset (l^2_N)^+, \forall t \geq 0$, where $(l^2_N)^+$ is the positive cone of l^2_N . \square

Let us now consider the controlled system $\Sigma(A, B)$ which is described by $\dot{z}(t) = Az(t) + Bu(t)$, where B is a bounded linear operator from \mathcal{U} to Z , and $\mathcal{U} = \{u : \mathbb{R}^+ \rightarrow U, \text{continuous}\}$, where U is the control space with a positive cone U^+ .

Theorem 2: The system $\Sigma(A, B)$ is positive if and only if A is the infinitesimal generator of a positive C_0 -semigroup and B is a positive operator. \square

Now consider $U = \mathbb{R}^m$ and the bounded linear operator B given by $Bu = \sum_{i=1}^m b_i u_i$, where $u = [u_1, u_2, \dots, u_m]^T$ and $b_i \in l^2_N$ for $i = 1, \dots, m$.

Corollary: Assume that A is Metzler, l^2_N is $T_A(t)$ -invariant for all $t \geq 0$ and B is a positive operator. Then, for every initial state $z_0 \in (l^2_N)^+$ and for every control u such that $\text{Im}(u) \subset \mathbb{R}^m_+$, the corresponding state trajectory $z(t)$ of the controlled system $\Sigma(A, B)$ is positive, i.e. $z(t) \in (l^2_N)^+, \forall t \geq 0$. \square

Acknowledgement This paper presents research results of the Belgian network DYSCO (Dynamical Systems, Control and Optimization), funded by the Interuniversity Attraction Poles Programme, initiated by the Belgian state, Science Policy Office (BELSPO). The scientific responsibility rests with its authors. The work of B. Abouzaid is supported by a BELSPO (FUNDP-CERUNA, respectively) post-doctoral research grant at the Université Catholique de Louvain (University of Namur, respectively), during the year 2009 (2010, respectively).

References

- [1] Ph. Clément, H.J.A.M Heijmans et al., "One-parameter semigroups," CWI Monographs 5, North-Holland, Amsterdam-New York-Oxford-Tokyo, 1987.
- [2] M. Laabissi, M. E. Achhab, J. Winkin and D. Dochain, "Trajectory analysis of nonisothermal tubular reactor nonlinear models," Systems and Control Letters, Vol. 42, pp. 169-184, 2001.
- [3] R. Nagel et al., "One-Parameter Semigroups of Positive operators," Lecture Notes in Mathematics, Springer-Verlag, 1986.

Almost Decentralized Lyapunov-based Model Predictive Control

Ralph Hermans, Mircea Lazar, Andrej Jokić
 Department of Electrical Engineering
 Eindhoven University of Technology
 P.O. Box 513, 5600 MB Eindhoven, The Netherlands
 Emails: {r.m.hermans, m.lazar, a.jokic}@tue.nl

1 Introduction

Over the last few years control of networks of interacting dynamical systems has gained a continuously increasing attention from the systems and control community. Examples of such networked dynamical systems (NDS) are electrical power networks, automated highways with formation control of autonomous vehicles, and urban water supply networks. The large size and complexity of NDS generally hamper the application of centralized control laws, which is the main reason for which the non-centralized implementation of controllers for NDS has become of major concern.

The design of non-centralized control laws for NDS is not straightforward, as these systems are often subject to strong coupling between local dynamics, hard and possibly coupled constraints on the control actions and states, and communication restrictions. Roughly speaking, we can divide non-centralized control schemes into two categories: *decentralized* techniques, in which local controllers operate without communication, and *distributed* techniques that exploit mutual exchange of information over a usually predefined structured communication network to compute the control action. Although solutions to specific varieties of structured control problems exist, a general theory for synthesizing stabilizing control laws under arbitrary system and information constraints is still lacking.

2 Lyapunov-based Model Predictive Control

Recently, a lot of research has been dedicated to model predictive control (MPC) as a tool for setting up non-centralized control algorithms. When stability is the main focus, a successful technique within MPC is the so-called Lyapunov-based MPC (L-MPC) approach [1]. L-MPC, which makes use of an explicit control Lyapunov function (CLF) to achieve stability, was already successfully applied to networked control systems, see [2]. Therein the focus is more on communication network effects such as time delays and packet dropouts, rather than decentralized stabilization of large-scale networks.

3 Almost Decentralized Stabilization

In this talk, we propose a non-centralized L-MPC scheme for discrete-time nonlinear NDS that are subject to separable

constraints. The key ingredient of the approach is a set of structured CLFs with a particular type of convergence condition, which provides a novel alternative to the method defined recently in [3]. While the convergence condition does not impose that each of these functions should be monotonously decreasing, as typically required for a CLF, we show that the maximum over all the functions in the set is a CLF for the overall network. Still, these convergence conditions might be too conservative. As such, we provide a solution for relaxing the temporal monotonicity of the global CLF based on an adaptation of the Lyapunov-Razumikhin (LR) technique [4], which was originally meant for systems with time delays. An attractive feature of the proposed L-MPC method is that it can be implemented in an almost decentralized fashion. By this we mean that the scheme only requires one run of information exchange between direct neighbors per sampling instant. This is in contrast to many of the existing non-centralized MPC schemes, which either require iterative computations or global information, or employ contractive constraints or small gain conditions to guarantee stability.

For systems that are affine in the control input, we show that by employing infinity-norm based structured CLFs, the proposed L-MPC setup can be implemented by solving a single linear problem per sampling instant and node. A non-trivial example is worked out in which the performance of the proposed scheme matches that of existing state-of-the-art schemes, despite its much lower complexity.

References

- [1] A. Bemporad, "A predictive controller with artificial Lyapunov function for linear systems with input/state constraints," *Automatica*, vol. 34, no. 10, pp. 1255–1260, 1998.
- [2] J. Liu, D. Muñoz de la Peña, P. D. Christofides, and J. F. Davis, "Lyapunov-based model predictive control of nonlinear systems subject to time-varying measurement delays," *International Journal of Adaptive Control and Signal Processing*, vol. 23, no. 8, pp. 788–807, 2009.
- [3] A. Jokić and M. Lazar, "On decentralized stabilization of discrete-time nonlinear systems," *28th American Control Conference*, pp. 5777–5782, 2009.
- [4] J. Hale, *Theory of functional differential equations*. Berlin, Germany: Springer, 1977.

Time optimal MPC for mechatronic systems

Lieboud Van den Broeck, Moritz Diehl, Jan Swevers

Katholieke Universiteit Leuven

Celestijnenlaan 300c, 3000 Leuven, Belgium

Email: lieboud.vandenbroeck@mech.kuleuven.be

1 Introduction

Model predictive control (MPC) [?] is an advanced control methodology that determines the control action by solving on-line, at every discrete time step, an open-loop optimal control problem taking into account bounds on system variables such as input, outputs and internal state variables. MPC is applied mainly to slow processes, such as chemical and oil refinement plants, where minimizing input costs is usually one of the main control objectives. The application of MPC to fast systems such as mechatronic systems is emerging due to improved computing power and the development of fast numerical optimization algorithms [?]. For these systems, achieving minimal settling time is often the main concern, while the input cost is usually of less importance. Hence, this talk presents a new type of MPC; time optimal MPC (TOMPC) which minimizes the settling time of the system.

2 Time Optimal MPC

TOMPC is developed for point-to-point motion, i.e. a desired endpoint of motion is defined but no intermediate trajectory. Hence, TOMPC has to define the trajectory with the lowest settling time, i.e. deadbeat behavior, while respecting all constraints on inputs and outputs. Hence, the following two layer optimization problem is proposed: a traditional MPC problem with endpoint constraints is formulated, of which the length N has to be optimized, taking into account a minimal length N_{\min} , to avoid deadbeat behavior on noise corrupted measurements close to the endpoint.

Low level Problem A:

$$V_A^*(\bar{x}_l, N) = \min_{\substack{x_0, \dots, x_N \\ u_0, \dots, u_{N-1}}} \sum_{k=0}^{N-1} \|u_k - u_{\text{ref}}\|_R^2 + \|x_k - x_{\text{ref}}\|_Q^2,$$

subject to the constraints:

$$\begin{aligned} x_0 &= \bar{x}_l, \\ x_{k+1} &= f(x_k, u_k), \\ g(x_k, u_k) &\geq 0 \quad k \in [0, N-1], \\ x_N &= x_{\text{ref}} \end{aligned}$$

Then, an admissible set $\mathbb{X}(N)$ is defined as:

$$\mathbb{X}(N) = \{\bar{x}_l | P_A(\bar{x}_l, N) \text{ is feasible}\}$$

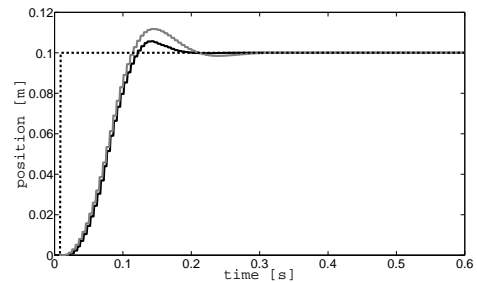


Figure 1: System output with TOMPC (black line) and traditional MPC (grey line) for a given reference (dashed line)

This admissible set allows to define high level Problem B:

$$V_B^*(\bar{x}_l) = \min_{N \in \mathbb{N}} N$$

subject to the constraints:

$$\begin{aligned} N &\geq N_{\min}, \\ N &\leq N_{\max}, \\ \bar{x}_l &\in \mathbb{X}(N). \end{aligned}$$

3 Results

TOMPC is numerically and experimentally validated on a linear motor drive, with a sampling period of 5ms, and compared with regular MPC. In order to achieve this sampling rate, similarities between subsequent optimization problems are fully exploited. Figure ?? demonstrates the benefits of TOMPC with respect to regular MPC: the settling time with TOMPC is considerably lower.

Acknowledgment

Lieboud Van den Broeck is funded by a Ph.D. fellowship of the Research Foundation - Flanders (FWO - Vlaanderen). This work benefits from K.U.Leuven-BOF EF/05/006 Center-of-Excellence Optimization in Engineering, the Belgian Programme on Interuniversity Attraction Poles, initiated by the Belgian Federal Science Policy Office (DYSCO), research project FP7-HD-MPC, and FWO research projects G.0377.09, G0.0320.08 and G.0558.08. Also, ETEL is gratefully acknowledged for their support.

References

- [1] J.M. Maciejowski, "Predictive control with constraints," Prentice Hall, 2000.
- [2] H.J. Ferreau, H.G. Bock and M.Diehl, "An online active set strategy to overcome the limitations of explicit MPC," International Journal of Robust and Nonlinear Control

Constrained predictive control of fast-sampling linear systems: An inversion-based algebraic approach

Jean-François Stumper and Ralph Kennel
 Department of Electrical Engineering and Information Technology
 Technische Universität München
 D-80333 Munich, Germany
 Email: jean-francois.stumper@tum.de

1 Introduction

Predictive control is of increasing interest in modern control systems. Especially for systems with constraints, a prediction-based approach can be very helpful in terms of optimal control. However, the established constrained predictive control schemes are hard to implement on fast-sampling systems. The known algorithms come along with high computational requirements, as they are based on iterative numerical procedures. Furthermore, wide parameter ranges and mixed state constraints represent obstacles to efficient and reliable numerical solutions.

This work represents an extension of the combination of system inversion and the Ritz-Galerkin method to constrained systems. Algebraic methods are proposed to transform the constrained predictive control problem to a finite-parameter optimization problem, solvable in finite time.

2 Inversion-based Predictive Control

An inversion-based control scheme applies a so-called inverse system model, which is essentially the (inverted) controller canonical form of the system [1], [2]. If the controller canonical form output $y_{opt}(t)$ is given, along with a finite number of its derivatives, the corresponding state trajectories \mathbf{x}_{opt} and the control input u_{opt} can be computed without solving differential equations. The controller setup is shown in Figure 1. Thus, through the use of an inverse system model, the predictive control problem reduces to optimizing an output trajectory.

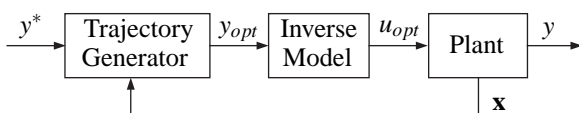


Figure 1: Inversion-based predictive controller

3 Transformation to Finite-Parameter Optimization

A linear system with a quadratic cost function and linear state and input constraints is considered. The output trajectory is defined as the power series

$$y(t) = \sum_{i=0}^N \alpha_i t^i, \quad t \in [t_0, t_f],$$

with the undetermined coefficients α_i to be found by optimization. In optimal control theory, this is known as the Ritz-Galerkin method, or basis function approach [1].

This definition, together with the inverse model, transforms the cost function into a quadratic cost function in the parameters α_i . It will be shown that it is also possible to transform equality and inequality constraints on the system variables to affine constraints on the parameters, independent of t .

The constrained output trajectory optimization can thus be reduced to a simple quadratic programming problem (QP), which is known to be computationally efficient and convergent within finite time.

An algebraic transformation of the constraints is the only possibility to obtain this result. In contrast, using i.e. penalty functions or nonlinear coordinate transformations turns the quite simple linear-quadratic problem into a hard to solve nonlinear programming problem (NP-hard), where convergence within a given time interval cannot be guaranteed.

4 Acknowledgments

This work was supported by the National Research Funds of Luxembourg under grant PhD-08-070.

References

- [1] M. Guay and J. Forbes, "Real-time Dynamic Optimization of Controllable Linear Systems," *J. of Guidance, Control and Dynamics*, Vol. 29, No. 4, pp. 929-935, 2006.
- [2] M.B. Milam, K. Mushambi and R.M. Murray, "A New Computational Approach to Real-Time Trajectory Generation for Constrained Mechanical Systems," *Proc. of the 39th IEEE Conf. on Decision and Control*, pp. 845-851, 2000.

Predictive control for non-strictly proper and non-causal systems

Abhishek Dutta, Bart Wyns, Clara Ionescu, Robin De Keyser
Electrical Energy, Systems and Automation, Ghent University

Email: {dutta.abhishek,bart.wyns,claramihaela.ionescu,robain.dekeyser}@UGent.be

1 Introduction

Model Predictive Control (MPC) optimizes the future control actions to bend the future model behavior towards desired plant target, while simultaneously obeying the system constraints. It is interesting to note that this widely successful MPC technology is yet to be generalized for non-strictly proper (NSP) and non-causal systems (NCS), an attempt towards it is made in this paper. NCS are important for two reasons. Firstly, the ideal system for a given application could often belong to the family of NSP or NCS, which although not physically possible, can give insight into the design of a derived strictly proper or causal system to accomplish a similar purpose. Secondly, there are instances when a system does not operate in pseudo-real time but is rather simulated offline, such as post-processing an audio or video recording. The state space variant of MPC cannot be used jointly with NSP causal state space models due to the generation of an algebraic loop. Therefore, the Extended Prediction Self-Adaptive Control (EPSAC) approach to MPC is used as a proof of concept [1].

2 Methodology

The EPSAC scheme considers the following process model:

$$y(t) = x(t) + n(t) \quad (1)$$

where $y(t), x(t)$ are the process and model outputs respectively and $n(t)$ is model/process disturbance. The model is assumed to be strictly proper i.e.:

$$x(t) = f[x(t-1), x(t-2), \dots, u(t-1), u(t-2), \dots] \quad (2)$$

The postulated response $\hat{y}(t+k/t)$ made at the end of prediction horizon $k = N_2$, with the linear system being at time t is given by the superposition:

$$\hat{y}(t+k/t) = \hat{y}_b(t+k/t) + \Delta u(t/t)H(k) + \dots + \Delta u(t+N_u-1/k)S(k-N_u+1) \quad (3)$$

where $\hat{y}_b(t+k/t)$ is the base response computed by holding the subsequent inputs to u_b (chosen a priori), H and S are impulse and step responses, N_u the control horizon, with $\Delta u(k/t)$ as the control difference at k with u_b . The response Y and its optimal input U^* in matrix form are given by:

$$Y = \bar{Y} + G.U$$

$$U^* = (G^T G)^{-1} G^T (R - \bar{Y}) \quad (4)$$

which is derived by minimizing the norm of difference in future response to reference trajectory R . R is vector of $r(k/t)$ which is defined over set points $s(t)$. \bar{Y} is base response vector. G is concatenation of impulse and step responses. Note that only the first control input is applied to plant.

Proposition 1 For NSP i.e. $x(t) = f[x(t-1), x(t-$

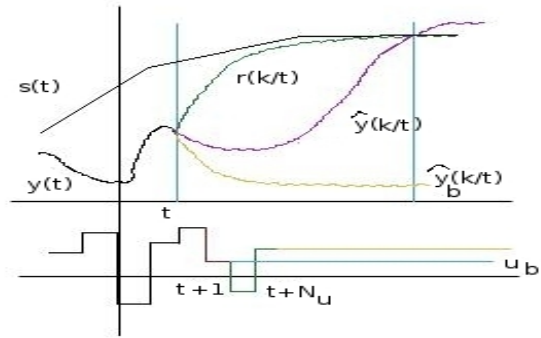


Figure 1: NSP-EPSAC (control horizon = 1)

2), ..., u(t), u(t-1), ...], the prediction takes the form:

$$\hat{y}(t+k/t) = \hat{y}_b(t+k/t) + \Delta u(t+1/t)H(k-1) + \dots + \Delta u(t+N_u/t)S(k-N_u) \quad (5)$$

The proof follows from the discrete time convolution which is now starting with a change in the input at $t+1$ and continuing to $t+N_u$, i.e. a shift of one time step from (3).

Corollary 1 This is the usual case in MPC with $N_u = 1$ (refer fig. 1):

$$\hat{y}(t+k/t) = \hat{y}_b(t+k/t) + \Delta u(t+1/t)H(k-1) \quad (6)$$

Proposition 2 For NCS with non-causality order = nc i.e. $x(t) = f[x(t-1), x(t-2), \dots, u(t+nc), u(t+nc-1), \dots, u(t), u(t-1), \dots]$, the following Universal Predictive Control (UPC) formulation of (3) can be used:

$$\hat{y}(t+k/t) = \hat{y}_b(t+k/t) + \Delta u(t+nc+1/t)H(k-nc-1) + \dots + \Delta u(t+N_u+nc/t)S(k-N_u-nc) \quad (7)$$

The proof is along the lines of proposition 1 by extending the convolution to accommodate the effects of future inputs. The optimal control sequence is computed in similar fashion as EPSAC, however $u(t+nc+1)$ is applied to the system.

3 Discussion

The above formulations can be applied to non-causal systems, operating in pseudo real time by introducing a lag i.e. if a system depends on input for 1 second in future, it can process in real time with 1 second lag.

4 Acknowledgement

This research is supported by IWT-SBO project LeCoPro (grant nr. 80032).

References

- [1] R. De Keyser, "Model Based Predictive Control," Invited chapter in UNESCO EoLSS, Article contribution 6.43.16.1, Oxford, ISBN 0 9542 989 18-26-34, 30p, 2003.

Is there free lunch in control? An adaptive disturbance model for MPC.

XU Zuhua¹, ZHU Yucui^{2*}, HAN Kai¹, ZHAO Jun¹ QIAN Jixin¹

¹State Key Laboratory of Industrial Control Technology,
Zhejiang University Hangzhou 310027, China

²Faculty of Electrical Engineering, Eindhoven University of Technology,
PO Box 513, 5600 MB Eindhoven, The Netherlands.

* Also at: Tai-Ji Control BV, Grensheuvel 10, 5685 AG Best, The Netherlands

1 Abstract

Normally control performance and robustness are two conflicting requirements; and one needs to strive a good trade-off between the two. This observation is often nicknamed no-free-lunch theorem. This paper proposes an MPC method that uses an adaptive disturbance model to improve the accuracy of prediction. In unmeasured disturbance model identification, a novel multi-iteration pseudo-linear regression (MIPLR) method is used which is more accurate and has faster convergence than traditional recursive identification methods. The adaptive disturbance model is used in an MPC scheme for improved performance in disturbance rejection. The method is demonstrated by the simulation of a distillation column and also tested on the real process. The test results show that the proposed MPC scheme can not only increase control performance, but also increase robustness. Is this not a free lunch?

Keywords

model predictive control, disturbance model, time series, recursive estimation, multi-iteration

References

- [1] Ljung L. and T. Sderstrm. Theory and practice of recursive identification. The MIT press: 1983
- [2] Zhu, Y.C. Multivariable System Identification for Process Control. Elsevier Science: Oxford, 2001.
- [3] XU Zuhua, ZHU Yucui, HAN Kai, ZHAO Jun and QIAN Jixin (2010). A multi-iteration pseudo-linear regression method and an adaptive disturbance model for MPC. Submitted to Journal of Process Control.

Robust Feedforward Control For a DoD Inkjet Printhead

Amol A. Khalate, Xavier Bombois, Robert Babuška

Delft Center for Systems and Control

Delft University of Technology, Delft, The Netherlands

Email: {a.a.khalate, x.j.a.bombois, r.babuska}@tudelft.nl

R. Waarsing, W. de Zeeuw, P. Klerken

Océ-Technologies B.V.

5900 MA, Venlo, The Netherlands

1 Abstract

The ability of Inkjet technology to deposit materials with diverse chemical and physical properties on a substrate has made it an important technology for both industry and home use. Apart from conventional document printing, the inkjet technology has been successfully applied in the areas of electronics, mechanical engineering, and life sciences. The success of Inkjet technology in all these application is mainly due to its low operational costs.

A typical a Drop-on-Demand (DoD) inkjet printhead consists of several ink channels in parallel. Each channel is provided with a piezo-actuator, which on application of a standard actuation voltage pulse generates pressure oscillations inside the ink channel. These pressure oscillations push the ink drop out of the nozzle. The print quality delivered by an inkjet printhead depends on the properties of the jetted drop i.e., the drop velocity, the jetting directionality and the drop volume. To meet the challenging performance requirements posed by new applications, these drop properties have to be tightly controlled.

The performance of the inkjet printhead is limited by two operational issues. The first issue is the *residual pressure oscillation*. The actuation pulses are designed to provide an ink drop of a specified volume and velocity under the assumption that the ink channel is in steady state. Once the ink drop is jetted the pressure oscillations inside the ink channel take several micro-seconds to decay. If the next ink drop is jetted before settling of these residual pressure oscillations, the resulting drop properties will be different from the ones of the previous drop. This can degrade the printhead performance. The second operational issue is the *cross-talk*. The drop properties through an ink channel are affected when its neighboring channels are actuated simultaneously. The drop velocity variation caused by the cross-talk is much less significant than the one caused by the residual oscillations. A consequence of the residual oscillations in the ink channel is that the velocity of the drops will only be constant if these drops are jetted at a low frequency.

It is possible to tackle these operational issues with a systems and control approach. The possibility to use feedback control for damping the residual oscillations is ruled out due to the limited control capabilities of the actuation system [1]. Given the fact that printhead dynamics is very predictable and that the bitmaps to be printed are priori known, feedfor-

ward control can be used to improve the performance of the DoD inkjet printhead.

The feedforward control action is constrained in practice, as the driving electronics limit the range of actuation pulses to pulses with a trapezoidal shape. In such scenario, the residual oscillations can be damped by means of the trapezoidal actuation pulse designed using an optimization-based feedforward control proposed in [1]. However, the performance of this feedforward controller degrades considerably in presence of modeling uncertainty. Therefore, we will attempt to improve the robustness of the optimization-based feedforward control.

We have the plant transfer function $H(z)$ between the actuation pulse and the pressure in the ink channel. It is observed that the parameters of the transfer function $H(z)$ are likely to change during the operation of the inkjet printhead. We can bound the deviation of the parameters from their nominal values by a polytopic uncertainty $\Delta \in U$. Further, we design a template $y_{ref}(t)$ for the channel pressure which is desired as the output i.e. a pressure profile with fast decaying oscillations. Based on this template $y_{ref}(t)$ and the plant model $H(z, \Delta)$ the robust actuation pulse $u(t)$ will be determined as the one minimizing the following objective function

$$\mathcal{J} = \max_{\Delta \in U} \|y_{ref}(t) - H(z, \Delta)u(t)\|_2, \quad (1)$$

which is the guaranteed H_2 norm of the tracking error. As the system dynamics depends affinely on the polytopic uncertainty Δ , we can efficiently compute the objective function using the LMI-based H_2 performance evaluation criteria presented in [2]. In this optimization problem, the class of input signals is limited to trapezoidal actuation pulses since these are the pulses that can be generated in practice.

References

- [1] Amol A. Khalate, Xavier Bombois, Robert Babuška, "Optimization-Based feedforward Control for a DoD Inkjet Printhead," submitted to *ACC2010*.
- [2] L. Xie, L. Lu, D. Zhang, H. Zhang, "Improved robust H_2 and H_∞ filtering for uncertain discrete-time systems" *Automatica*, vol. 40, pp. 873–880, 2004.

Acknowledgements : This work has been carried out as part of the Octopus project with Océ Technologies B.V. under the responsibility of the Embedded Systems Institute. This project is partially supported by the Netherlands Ministry of Economic Affairs under the Bsik program.

Global analysis of pulse-coupled oscillators: discrete and continuous models

Alexandre Mauroy and Rodolphe Sepulchre

Department of Electrical Engineering and Computer Science,

University of Liège, B-4000 Liège, Belgium

Email: alexandre.mauroy@ulg.ac.be, r.sepulchre@ulg.ac.be

1 Pulse-coupled firing oscillators

The Peskin model [1] is a simple but seminal model to study networks of interacting agents, such as pacemaker cells of the heart or neurons. Each agent corresponds to an oscillator whose state variable x_i evolves according to the dynamics $\dot{x}_i = F(x_i) > 0$ between two threshold values. Upon reaching the upper threshold, the state is reset to the lower threshold — the oscillator is said to fire. The coupling is defined as follows: whenever an oscillator fires, it emits a pulse which instantaneously increases by $\varepsilon > 0$ the state of every other oscillators.

When considering standard leaky integrate-and-fire (LIF) oscillators, i.e. characterized by $F(x_i) = S + \gamma x_i$, the behavior of the network is strongly dichotomic: according to the curvature of their time evolution, identical oscillators either achieve perfect synchrony [2] or aggregate in a phase-locked clustering configuration [3]. In both situations, global convergence is established, which reinforces the evidence of dichotomy in the model. Using an appropriate 1-norm, we prove that the “distance” between two different configurations strictly increases (synchronization) or decreases (clustering) from one firing to the next one.

2 Global analysis of the continuous model

In order to investigate the case of a (very) large number of agents, the population of oscillators is approximated by a density function (mean-field approximation) which evolves according to a partial differential equation (PDE). The PDE is a standard transport equation with an additional coupling term, interpreted as a “feedback” term providing the system with stability properties. For LIF oscillators, the previous 1-norm is generalized and adapted to this infinite-dimensional case. It leads to the development of a Lyapunov functional, which is helpful and relevant for the study of the considered PDE. In particular, one shows that it is linked to the total variation distance often used to compare probability measures.

3 Extension of the LIF model

We next consider other dynamics $\dot{x}_i = F(x_i)$ characterized by even positive functions $F(x)$ verifying $F'(x) > 0$ for

$x > 0$. For instance, such a model is the well-known quadratic integrate-and-fire (QIF) model, which corresponds to $F(x_i) = S + x_i^2$. In some cases, the local stability of the equilibrium configuration is proved. However, the global convergence appears to be more difficult to establish and, in particular cases, the dichotomy prevailing in the LIF model is no longer observed. We currently investigate sufficient conditions for the dichotomy to exist.

We will report on global stability results for both discrete and continuous LIF models and on preliminary results concerning the extension to more general models.

References

- [1] C. S. Peskin, *Mathematical aspects of heart physiology*, Courant Institute of Mathematical Sciences, New York University, New York, pp. 268-278, 1975
- [2] R. E. Mirollo and S. H. Strogatz, *Synchronization of pulse-coupled biological oscillators*, *Siam J. Appl. Math.*, Vol. 50, No. 6, pp. 1645-1662, December 1990
- [3] A. Mauroy and R. Sepulchre, *Clustering behaviors in networks of integrate-and-fire oscillators*, *Chaos*, 18, 037122 (2008)

Acknowledgments

This work was supported by the Belgian National Fund for Scientific Research (FNRS) through a Research Fellowship at the University of Liège. This paper presents research results of the Belgian Network DYSCO (Dynamical Systems, Control, and Optimization), funded by the Interuniversity Attraction Poles Programme, initiated by the Belgian State, Science Policy Office. The scientific responsibility rests with its author(s).

Identification of biochemical reaction systems using semi-definite programming

Dirk Fey
Systems & Modelling
Institute Montefiore
University of Liege
Belgium
fey@montefiore.ulg.ac.be

Eric Bullinger
Systems & Modelling
Institute Montefiore
University of Liege
Belgium
e.bullinger@montefiore.ulg.ac.be

1 Introduction

Modelling biological systems on the intracellular level has been a research topic for over half a century. For example, Hodgkin and Huxley [1] explained the neuron function by means of a mathematical model of different ion channels. Hodgkin and Huxley were able to estimate the model parameters from experimental data, a challenging task still today in most biological systems. Nowadays, ever improving developments of experimental techniques provide more and more high quality experimental data, putting the task of identification into reachable scope. However, the straight forward application of systems theoretical methods to biology is impaired by certain particularities of biological systems [2].

Biochemical systems have peculiar system properties such as for example positivity and monotonicity. Exploiting these properties has the potential of enhancing current identification techniques [3, 4, 5]. Here we present two complementary methods which explicitly take into account particular structure and dynamics of biological models as arising from mass action, Michaelis-Menten and Hill kinetics.

2 Limiting the parameter search space

The first approach proves inconsistency of entire parameter regions for a given model structure and data set, by formulating a semi-definite feasibility problem. The feasibility problem is only feasible for parameter regions that contain consistent parameter values. Thus, checking feasibility for different upper and lower bounds on the parameter values using semi-definite programming identifies inconsistent parameter regions. This drastically reduces the parameter search space, such that subsequent parameter estimation methods can disregard the inconsistent parameter regions. In contrast to similar approaches in the literature, the here presented approach does not require a steady state assumption, nor a discretisation of the system. Measurement uncertainties are dealt with using upper and lower bounds and regular sampling times are not required.

3 Estimating the parameter values

The second approach estimates the kinetic parameters using a nonlinear observer, i.e. a mathematical system that feeds back the error of prediction and measurement. The approach relies on a nonlinear state space extension transforming the system into a parameter-independent form. This state space representation facilitates the design of a nonlinear observer based on a dissipativity arguments using linear matrix inequalities. An observer is a dynamical system performing the actual estimation by feeding back the error of prediction and measurement. To ensure the convergence of the estimate, certain observability conditions must hold. These are related to the identifiability of model and data, i.e. the existence of a unique solution for the parameter estimate.

4 Conclusions

The presented approaches show that systems theoretical tools and semidefinite programming can be used to develop parameter estimation methods that are particularly tailored to biological systems. The mathematical rigour of systems theory enables us to give exact statements in the form of guarantees, even in the presence of uncertainties. Both methods are illustrated using simple, yet biological significant examples.

References

- [1] Hodgkin, A. L. & Huxley, A. F. *J Physiol*, 1952, 117, 500-544.
- [2] Wellstead, P.; Bullinger, E.; Kalamatianos, D.; Mason, O. & Verwoerd, M. *Annual Reviews in Control*, 2008, 32, 33-47.
- [3] Fey, D.; Findeisen, R. & Bullinger E. *Control Theory and Systems Biology E*. Iglesias, P. A. & Ingalls, B. (ed.), MIT press, 2009, 297-316.
- [4] Fey, D. & Bullinger, E. 15th IFAC SYSID, Saint Malo, France, 2009, 1259-1264.
- [5] Fey, D.; Findeisen, R. & Bullinger, E. 17th IFAC World Congress, Seoul, Korea, 2008, 313-318.

Performance and robustness of bistable systems

Laura Trotta
L.Trotta@ulg.ac.be

Eric Bullinger
E.Bullinger@ulg.ac.be

Rodolphe Sepulchre
R.Sepulchre@ulg.ac.be

Department of Electrical Engineering and Computer Science.
University of Liège, Belgium.

1 Introduction

Biological systems are complex networks involving many reactions, feedback loops and connections. Using engineering tools, some design principles have been identified. Among these, one can cite clocks and switches found in several cellular processes [1]. The study focuses on biological switches and properties of bistable models.

2 The model of Griffith

Bistable models have been used to describe several physiological decision-making processes including cell cycle progression, apoptosis and development [1]. One simple bistable model is the model of genetic control proposed by Griffith [2] which presents two stable steady states (unexcited and excited states) and a saddle point. This model was used as a toy to define performance criteria of bistable systems.

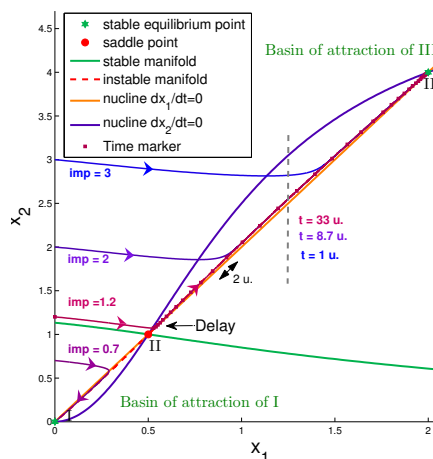


Fig 1: Model of Griffith - Trajectories for increasing impulse inputs.

The system was characterized as an input-output system.

$$\begin{cases} \dot{x}_1 = -ax_1 + x_2 & a, b, \text{ parameters,} \\ \dot{x}_2 = \frac{x_1^2}{1+x_1^2} - bx_2 + u(t) & u(t), \text{ input (impulse or step)} \end{cases}$$

Performance was then defined as the capacity of the system to present a typical response to a signal input while robustness was related to its capacity to preserve this response in the face of perturbations. Results showed that performance of bistable systems is linked to properties of their saddle point. Especially, this point plays an important role in the transient response of the system.

3 Models of apoptosis

Apoptosis is the programmed cell death used by multicellular organisms to remove unwanted, damaged or potentially harmful cells. The apoptotic process can be modelled as a bistable system where the cell switches between two states, the survival and the death. Two bistable models describing the apoptotic switch were investigated [3], [4]. Although these systems are much more complex, it seems that the saddle point keeps a significant role in the dynamics of transition between states.

4 Results and Conclusion

The study of the three models reveals that they share specific features in common. They all present a saddle point with only one positive eigenvalue. This eigenvalue is real and has the smallest absolute value of all the eigenvalues of the point. Moreover, in all the models, the transition time between the unexcited and the excited state depends on the strength of the input signal. The transition is delayed close to the saddle point. We called this kind of bistable systems, *Retarding Switch Systems* (RSS).

Performance and robustness of bistable systems were investigated. In all the studied models, the saddle point plays a role in performance of the switch. In addition, the analysis shed light on a mechanism that retard the switch in particular bistable systems.

References

- [1] J. Tyson, R. Albert, A. Goldbeter, P. Ruoff and J. Sible, *Biological switches and clocks*, J. R. Soc. Interface, 2008.
- [2] J. S. Griffith, *Mathematical Neurobiology* Academic Press, New York, 1971.
- [3] T. Eißing, H. Conzelmann, E. Gilles, F. Allgöwer and E. Bullinger, *Bistability Analyses of a Caspase Activation Model for Receptor-induced Apoptosis*, The Journal of Biological Chemistry, 2004.
- [4] M. Schliemann, T. Eißing, P. Scheurich, and E. Bullinger, *Mathematical modelling of TNF- α induced anti-apoptotic signalling pathways in mammalian cells based on dynamic and quantitative experiments*, Proceedings of the 2nd Foundations of Systems Biology in Engineering FOSBE, 2007.

Modeling of the interaction force between the instrument and the trocar in minimally invasive surgery

J. Verspecht, T. Delwiche, A. Buttafuoco, L. Catoire, S. Torfs and M. Kinnaert
Control Engineering and System Analysis Department
Université libre de Bruxelles (U.L.B.)
jonathan.verspecht@ulb.ac.be

1 Introduction

Modeling the forces between two bodies in contact has been the object of a huge number of papers on friction modeling. Numerous models exist in the literature, the static friction models (Coulomb model and Stribeck model) and the dynamical models (Dahl Model, LuGre Model, Leuven Model and the Maxwell-Slip model) [2]. The dynamical friction models deal with asperities deformation. Asperities are microscopical irregularities present on every surface. The Maxwell-Slip model [1] has been used as a source of inspiration in our work. However, as the seals used in trocars are subject to large deformation ($\approx 1cm$), the hypothesis of microscopic deformation does not hold. Hence a specific hybrid model, the Extended Maxwell Slip (EMS) model, has been developed and validated experimentally for our application.

2 Friction model of the trocar

Considering an axial symmetry of the medical device and of the seal, the contact between these two bodies can be depicted by the left part of figure 1. During the motion of the medical device, two situations can appear. First, the seal may stick to the medical device. Secondly, the medical device may slide on the seal. These two situations lead to the two operating modes of the EMS model, the deformation mode which replaces the sticking mode of the GMS model, and the sliding mode. In the deformation mode the friction force F_f corresponds to the force required to deform the seal. In sliding mode the friction force corresponds to the sliding force between the seal and the instrument.

In figure 1, O is a fixed reference, A is the contact point between the medical device and the seal of the trocar and B an arbitrary fixed point on the medical device. An EMS element is defined by the right part of figure 1 and is characterized by three variables, the spring deformation amplitude z_{def} , the spring deformation velocity \dot{z}_{def} and the relative velocity between the instrument and the seal v_{sl} . The medical device velocity v_d does not correspond to the sliding velocity v_{sl} . The deformation force F_{def} is assumed to be modeled by :

$$F_{def} = k(z_{def})z_{def} + \sigma(\dot{z}_{def})\dot{z}_{def} \quad (1)$$

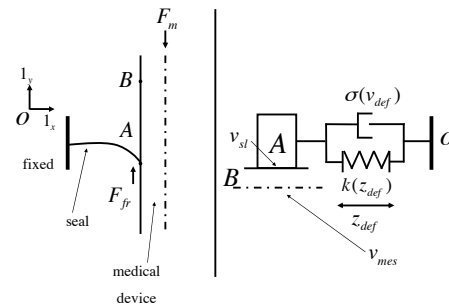


Figure 1: Schematic drawing of one stage of the trocar sealing mechanism and definition on an EMS elements

The variable stiffness of the spring is modeled by a function of the amplitude of deformation only $k(z_{def})$. The viscoelastic part is modeled by a damping function $\sigma(\dot{z}_{def})$ which depends only on the deformation velocity. The sliding force is modeled by a Stribeck model.

The model of an *AutoSuture* Thoracoport 10.5mm* trocar has been identified. The comparison between the simulator based on this model and the experimental results leads to a RMS error approximately equal to 0.17N which corresponds to 5% of the friction amplitude.

Acknowledgments

The work of Jonathan Verspecht is supported by a FRIA grant. The experimental setup is financed by the FNRS. This paper presents research results of the Belgian Network DYSCO (Dynamical Systems, Control and Optimization) funded by the Interuniversity Attraction Poles Program, initiated by the Belgian State, Science Policy Office. The scientific responsibility rests with its authors

References

- [1] Farid Al-Bender, V. Lampaert, and J. Swevers. The generalized maxwell-slip model: a novel model for friction simulation and compensation. *IEEE transactions on automatic control*, 50(11):1883:1887, 2005.
- [2] B. Bona and M. Indri. Friction compensation in robotics: an overview. *IEEE conference on decision and control, and the European control conference, Seville*, 2005.

Robust patterning in Arabidopsis flowers

S. van Mourik¹, G.H. Immink¹, R.H Merks², and J. Molenaar¹

1: Plant Sciences Group, Wageningen University and Research Center, The Netherlands.

email: simon.vanmourik@wur.nl.

2: Netherlands Institute for Systems Biology and Centrum Wiskunde Informatica, Amsterdam, The Netherlands.

1 Abstract

In the plant *Arabidopsis Thaliana*, the flowers consist of four types of organs, that grow in four concentric whorls on the florescence meristem. In each whorl, the cells attain a different identity, that is determined by the concentrations of five types of proteins.

We propose an ODE model that describes the gene expression dynamics of a representative gene regulatory network. The network consists of six genes that regulate each other's expression. For example, proteins that are formed by gene A can attach themselves to gene B and accelerate or slow down the production of gene B. The model incorporates transcription regulation via Michaelis-Menten kinetics, decay, dimer formation, trigger mechanisms that lead to cell differentiation, and a mass balance [1]. These triggers result in a short pulse of specific proteins at specific places, leading to four steady states of protein concentrations in the four different whorls.

In [2] it was shown that the proteins can easily travel through cell membranes, giving rise to a large diffusive effect. The question is: how can the cells in the different whorls have different protein levels with such a large diffusion. Or, more mathematically: is the stability of the network robust against the large disturbances caused by protein diffusion?

References

[1] Continuous-time modeling of cell fate determination in *Arabidopsis* flowers. Simon van Mourik, Aalt-Jan van Dijk, Maarten de Gee, Richard Immink, Kerstin Kaufmann, Gerco Angenent, Roeland van Ham and Jaap Molenaar. Submitted 2009.

[2] Intercellular transport of epidermis-expressed MADS domain transcription factors and their effect on plant morphology and floral transition. Susan L. Urbanus, Adriana P. Martinelli, Q.D. (Peter) Dinh, Lilian C.B. Aizza, Marcelo C. Dornelas, Gerco C. Angenent, and Richard G.H. Immink. Submitted 2009.

SK Channels as Regulators of Synaptically Induced Bursting and Neural Synchrony

Guillaume Drion^{1,2}, Anne Collard¹, Vincent Seutin² and Rodolphe Sepulchre¹

¹Department of Electrical Engineering and Computer Science

²Laboratory of Pharmacology, GIGA Neurosciences

University of Liège, 9 Place du 20-Août, Liège, Belgium

Email: gdrion@ulg.ac.be

Intracellular calcium is a universal second messenger which has been shown to be a critical component of cell signaling. Among others, it plays important roles in neurotransmitter release, cell migration and muscle contraction [1]. On the other hand, long lasting accumulation of calcium in the cytoplasm is known to induce cell death, suggesting the necessity of a tight regulation.

In neurons, as in other cells, the relative variations of the intracellular calcium concentration ($[Ca^{2+}]_{in}$), although tightly regulated, are much larger than those of all other ions. Moreover, a number of ion channels are calcium-regulated, which suggests a major role for this ion in the firing regulation of excitable cells.

The present study focuses on the role of small-conductance calcium-activated potassium (SK) channels. Remarkably, these channels are totally insensitive to the variations of membrane potential, which makes their activity an image of the intracellular calcium concentration. These channels are important and prevalent in a large set of neurons (for a recent review, see e.g. [2]). In hippocampal CA1 pyramidal cells, these channels are located close to NMDA receptors and mediate a negative feedback loop by hyperpolarizing the membrane when calcium flows through NMDA channels. This hyperpolarization in turn reduces the NMDA conductance [3]. For many other neurons, an inhibition of the SK current affects both the excitability and the firing pattern (see e.g. [4]). *In vitro*, SK channel blockade usually induces irregularities in the firing and potentiates the response of the cell to excitatory stimuli. *In vivo*, the blockade also strongly affects the firing pattern. In particular, it causes several of those neurons to switch from low-frequency single spike firing to bursting, with a high intra-burst firing frequency (see e.g. [5]).

To date, the mechanisms allowing synaptic afferents to modulate the firing pattern of pacemaker neurons and its regulation are poorly understood.

We propose a one-compartmental model endowed with a minimal set of conductances that reproduces these experimental observations, regardless of the specifics of each neuron. This simple model is useful to understand essential mechanisms of firing pattern and regulation of synchroniza-

tion of pacemaker neurons. The model is composed of fast Na-K dynamics, which are responsible for the generation of action potentials, and slow calcium dynamics involving L-type calcium channels and calcium pumps, which control the low frequency firing mode.

In addition, stochastic activation of excitatory synaptic inputs is used to model the afferences. The amplitude of this external noise is the only parameter that we used to differentiate *in vitro* and *in vivo* conditions in the model.

At the single cell level, we show that, in the absence of SK channels, the *in vivo* bursting behavior is mainly underlain by the coupling of excitatory synaptic inputs and the calcium-regulation of calcium channels. SK channels, when present, attenuate the effect of these inputs on the firing of the cell. In that sense, they are shown to act as a “filter” against external excitatory noise.

At the population level, we demonstrate that they critically interfere with synchronization of neuronal firing. Namely, SK channels oppose synaptically-induced synchronization of neurons with different endogenous rhythms.

References

- [1] Berridge MJ (2004) Calcium signal transduction and cellular control mechanisms. *Biochim. Biophys. Acta.* 1742:3-7.
- [2] Vogalis F, Storm JF, Lancaster B (2003) SK channels and the varieties of slow after-hyperpolarizations in neurons. *Eur J Neurosci.* 18:3155-66.
- [3] Ngo-Anh TJ, Bloodgood BL, Lin M, Sabatini BL, Maylie J, Adelman, JP (2005) SK channels and NMDA receptors form a Ca²⁺-mediated feedback loop in dendritic spines. *Nat Neurosci.* 8:550.
- [4] Bond CT, Maylie J, Adelman JP (2005) SK channels in excitability, pacemaking and synaptic integration. *Curr Opin Neurobiol.* 15:305-11.
- [5] Rouchet N, Waroux O, Lamy C, Massotte L, Scuvée-Moreau J, Liégeois JF, Seutin V (2008) SK channel blockade promotes burst firing in dorsal raphe serotonergic neurons. *Eur J Neurosci.* 28:1108-15.

Metabolic Flux Analysis of an Underdetermined Network of CHO Cells Considering Measurement Errors

Francisca Zamorano, Alain Vande Wouwer
Service d'Automatique, FPMs
Université de Mons
Boulevard Dolez 31, B-7000 Mons
Belgium

Email: francisca.zamorano, alain.vandewouwer@umons.ac.be

Georges Bastin
CESAME
Université Catholique de Louvain
Avenue Georges Lemaitre 4, B-1348 Louvain-La-Neuve
Belgium
Email: bastin@inma.ac.be

In this work, the flux distribution in a detailed metabolic network of CHO-320 cells is evaluated using Metabolic Flux Analysis, in particular, the algorithm METATOOL [2]. As in many practical situations, the available information is not sufficient to completely define the metabolic fluxes, and so, the mass balance system of equations is underdetermined. However, the measurements of the time evolution of a number of extracellular components can provide a set of constraints on the metabolic network, so that a range of possible (non-negative) solutions for each metabolic reaction can be computed instead. In this way, metabolic flux intervals can be established for each intra-extracellular flux in the metabolic network. Moreover, the incorporation of simple theoretical assumptions or the addition of further extracellular measurements, result in the determination of certain metabolic fluxes and the delimitation of quite narrow intervals for the others, so providing a good guess of the real flux distribution in CHO-320 cells. A unique flux distribution can also be computed through linear optimization and the definition of some optimality criteria [1, 4].

In this presentation, several of the above-mentioned situations are discussed, highlighting the importance of specific measurements and comparing the flux intervals under some particular assumptions such as optimal biomass growth or no Threonine catabolism. In addition, the influence of the measurement accuracy on the numerical results is explored using Monte Carlo techniques [3], showing a remarkable consistency of the metabolic flux analysis.

Acknowledgments This work presents research results of the Belgian Network DYSCO (Dynamical Systems, Control, and Optimization), funded by the Interuniversity Attraction Poles Programme, initiated by the Belgian State, Science Policy Office.

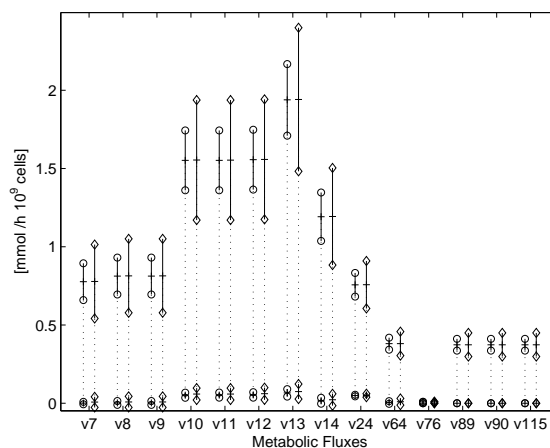


Figure 1: Flux Distribution Intervals for the TCA cycle considering measurement errors. (○) 5% error; (◇) 10% error. 95% confidence intervals for the maximal and minimal bounds.

References

- [1] Hendrik P. J. Bonarius, Georg Schmid, and Johannes Tramper. Flux analysis of underdetermined metabolic networks: the quest for the missing constraints. *TIBTECH*, 15:308–314, August 1997.
- [2] T. Pfeiffer, I. Sánchez-Valdenebro, J.C. Nuño, F. Montero, and S. Schuster. METATOOL: for studying metabolic networks. *Bioinformatics*, 15(3):251–257, Mar 1999.
- [3] Reuven Y. Rubinstein and Dirk P. Kroese. *Simulation and the monte carlo method*. Wiley series in probability and statistics, 2008.
- [4] G. N. Stephanopoulos, A. A. Aristidou, and J. Nielsen. *Metabolic Engineering: Principles and Methodologies*. 1998.

The production of food for manned space missions - Simple mass balance models for plant growth

Heather Maclean¹, Denis Dochain¹, Geoff Waters², Mike Dixon²

Laury Chaerle³, Dominique Van Der Straeten³

¹ Université catholique de Louvain, CESAME, 1348 Louvain-la-Neuve
heather.macleaen@uclouvain.be, denis.dochain@uclouvain.be

² CESRF, University of Guelph, 50 Stone Road East, Guelph, Canada

³ Unit Plant Hormone Signaling and Bio-Imaging, Ghent University, 9000 Gent

1 Abstract

A simple mass balance model for plant growth is presented. This work is a first step in the development of a model intended to enable the prediction and control of a plant production chamber for MELiSSA, a regenerative life support system project developed by the ESA. The model is required to be robust, so that the results of failures or stress conditions are predictable.

Photosynthesis and respiration were selected as key reactions for biomass production. Considering these reactions, the model was developed using a mass balance approach. It was assumed that the gas concentrations in the leaves would be approximately equal to their concentrations in the atmosphere of the plant chamber.

$$\begin{aligned} \frac{dXV}{dt} &= Y_1 r \\ \frac{dC_i}{dt} = \frac{dC_a}{dt} &= \frac{-r}{V_{chamber}} + \frac{u_1}{V_{chamber}} \\ \frac{dO_i}{dt} = \frac{dO_a}{dt} &= \frac{Y_2 r}{V_{chamber}} \end{aligned}$$

where XV is biomass (g), C_i and O_i are CO_2 and O_2 concentrations in the leaves (g m^{-3}), C_a and O_a are CO_2 and O_2 concentrations in the atmosphere of the chamber (g m^{-3}), Y_i are the yields (g g^{-1}), $V_{chamber}$ is the volume of the plant growth chamber (29 m^3), u_1 is the rate of CO_2 addition to the chamber for control ($\text{g CO}_2/\text{s}$), and r is the rate equation to be defined ($\text{g CO}_2 \text{ s}^{-1}$) assuming photosynthesis and respiration can be treated as a single stoichiometrically reversible reaction.

Reaction kinetics were chosen based on plant physiology and standard biochemical reaction knowledge. The kinetic model includes a term for the photosynthesis reaction and a term for respiration. Monod kinetics were chosen to represent the rate of photosynthesis. The respiration equation has been divided into two parts, a growth respiration component which is proportional to the photosynthetic rate, and a maintenance respiration component proportional to the to-

tal biomass [1].

$$r = \frac{v_1 C_i \text{Light}}{K_C + C_i} - (v_2 r_{ps, \text{daily avg}} + v_3 XV)$$

In the above equation v_i are the three rate constants (v_1 ($\text{m}^2 \text{ s} \mu\text{mol PAR}^{-1}$), v_2 and v_3 (s^{-1})) required to be identified, K_C is a Michaelis-Menten constant for carbon dioxide (g m^{-3}), and $r_{ps, \text{daily avg}}$ represents the average value of r_{ps} over the previous day (g s^{-1}).

The identification and validation of yield and kinetic parameters were performed using data from lettuce experiments in a closed plant chamber (Figure 1). Biomass production is accurately predicted for full experiments. Some discrepancies remain in the prediction of gas concentrations. Future work will include testing the model on different plants and under different environmental conditions in order to improve robustness.

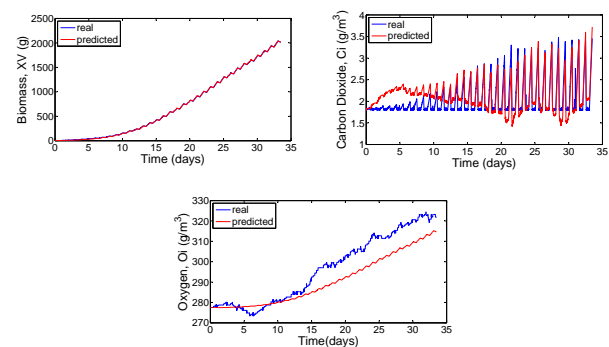


Figure 1: Validation of kinetic model identification over full experiment, showing predicted and real (a) biomass (b) CO_2 and (c) O_2 versus time.

References

- [1] Thornley J.H.M. and M.G.R. Cannell (2000). Modelling the Components of Plant Respiration: Representation and Realism, *Annals of Botany*, Vol. 85, pp 55-67.

Data reconciliation from an electrochemical biosensor to measure toxicity in water

STEIN Nienke^{1,2,3}, KEESMAN Karel², HAMELERS Hubertus³, BUISMAN Cees^{1,3}

¹Wetsus, centre of excellence for sustainable water technology

²Systems and control group, Wageningen University

³Subdepartment of Environmental Technology, Wageningen University

Keywords: biosensor, on-line estimation, electrochemically active bacteria

It is of crucial importance that drinking water is safe to drink. A fast and economical way to monitor the water quality is through on-line continuous sensing. The current on-line toxicity sensors have some limitations, e.g. low number of individuals, a complicated metabolism or a loss in accuracy due to a two-step translation of the signal. A better sensor is required to overcome these limitations (Hasan *et al.*, 2005)

The overall goal of our research is to develop a robust, continuous sensor for the integral determination of (toxic) changes in water quality using electricity producing bacteria. Electrochemically active bacteria produce electrical current dependent on their metabolic state. This current therefore represents the quality of the water and can be directly measured. (Kim *et al.*, 2007). Fluctuations in the water composition will lead to fluctuations in electrical current. These fluctuations can be due to changes in organic composition of the water or due to the presence of toxic components.

The aim of the current research is to reconstruct unmeasured process data and parameters from noisy measurements. Therefore we need a model that can reconcile process data from the electrical current measurements and relate this to substrate consumption. Using observer theory allows us to reconstruct the process data.

Furthermore, a model is being developed that connects biochemical metabolism of the bacteria with the electrochemical reactions on the electrode and with the electrical current

measurements. The next step is to identify parameters that indicate the presence of a toxic component in the water. Again observer theory could be used to identify changes in these parameters.

The system is complicated due to non-linear behavior in the bacterial metabolism. However, it appears that these non-linearities can be described by rational biokinetic functions, for which recently effective estimation algorithms have been developed. (Doeswijk and Keesman, 2009; Keesman and Doeswijk, 2009)

References

Hasan, J., D. Goldbloom-Helzner, et al. (2005). Technologies and Techniques for Early Warning Systems to Monitor and Evaluate Drinking Water Quality: A State-of-the-Art Review

Kim, M., M. S. Hyun, et al. (2007). A novel biomonitoring system using microbial fuel cells. *Journal of environmental monitoring* **9**: 1323-1328.

Doeswijk, T.G. and Keesman, K.J. (2009). Linear Parameter Estimation of Rational Biokinetic Functions. *Water Research* **43**(1), 107-116,

Keesman, K.J. and Doeswijk, T.G. (2009) Direct Least-squares Estimation and Prediction of Rational Systems: Application to Food Storage. *Journal of Process Control* **19**, 340–348,

Combined online quality prediction and critical vs. non-critical process disturbance discrimination in (bio-)chemical batch processes

G. Gins, J. Vanlaer, J.F.M. Van Impe

BioTeC - Chemical and Biochemical Process Technology and Control
Department of Chemical Engineering, Katholieke Universiteit Leuven,
W. de Croylaan 46, B-3001 Leuven, Belgium.
{geert.gins, jef.vanlaer, jan.vanimpe}@cit.kuleuven.be

1 Introduction

In the (bio-)chemical process industry, *Statistical Process Control* (SPC [2]) is used for monitoring (fed-)batch processes. This is required to achieve a constant and satisfactory final product quality. Most research effort has been directed towards fault detection (e.g., [3, 5]). These methods detect deviations from the nominal behavior by comparing the measured process behavior with an empirical model identified from periods of normal operation [5]. However, they are unable to estimate the batch-end quality.

Multiway Partial Least Squares models (MPLS [4]) are capable of making these batch-end quality predictions [3, 5]. While Nomikos and MacGregor combine batch-end quality prediction and fault detection [5], they use a suboptimal online procedure [3]. García-Munoz *et al.* only focus on batch-end quality prediction, and ignore fault detection [3].

This work proposes a novel methodology for true online combined prediction of batch-end quality and discrimination between critical and non-critical process disturbances. In addition to traditional fault detection, where all process disturbances are treated equally, the presented methodology is capable of discriminating between critical and non-critical disturbances with respect to the batch-end product quality. This is achieved by coupling a *Multiway Partial Least Squares* (MPLS) model using all available measurements is with an MPLS model utilizing only those measurements influencing the final product quality. The approach is illustrated on a simulated industrial-scale fermentation process for penicillin production.

2 Model structure

Using a *bottom-up branch and bound* selection procedure, the measurements which influence the final product quality (i.e., the critical measurements) are selected. Next, two MPLS are constructed: one with only the critical measurements as inputs, and one with all available measurements. The first model provides the online estimate of the batch-end quality, and detects process disturbances influencing the final product quality. The second model detects all possible process upsets, even those not (yet) influencing the quality.

Combining the information from these two models, a discrimination can be made between critical and non-critical process disturbances.

3 Results

The proposed methodology is illustrated on a simulated industrial-scale fermentation process for penicillin production [1]. It is shown that the proposed multi-model approach is capable of providing accurate estimates of the final quality. In addition, disturbances can be successfully classified as either critical or non-critical.

Acknowledgements. Work supported in part by Projects OT/09/25/TBA and EF/05/006 (Center-of-Excellence Optimization in Engineering) of the Research Council of the Katholieke Universiteit Leuven, Project KP/09/005 (SCORES4CHEM) of the Industrial Research Council of the Katholieke Universiteit Leuven, and the Belgian Program on Interuniversity Poles of Attraction initiated by the Belgian Federal Science Policy Office. J. Vanlaer has a Ph.D grant of the Institute for the Promotion of Innovation through Science and Technology in Flanders (IWT-Vlaanderen). J. Van Impe holds the chair Safety Engineering sponsored by the Belgian chemistry and life sciences federation *essenscia*. The scientific responsibility is assumed by its authors.

References

- [1] G. Birol, C. Ündey, and A. Çinar. A modular simulation package for fed-batch fermentation: penicillin production. *Comput. Chem. Eng.*, 26:1553-1565, 2002.
- [2] L. Eriksson, E. Johansson, N. Kettaneh, and S. Wold. *Multi- and Megavariate Data Analysis: Principles and Applications* Umetrics Academy, 91-973730-1-X, 2002.
- [3] S. García-Munoz, T. Kourti, and J.F. MacGregor. Model predictive monitoring for batch processes. *Ind. Eng. Chem. Res.*, 43:5929-5941, 2004.
- [4] P. Geladi and B.R. Kowalski. Partial least-squares regression: a tutorial. *Anal. Chim. Acta*, 185:1-17, 1986.
- [5] P. Nomikos and J.F. MacGregor. Multivariate SPC charts for monitoring batch processes. *Technom.*, 37(1):41-59, 1995.

Online fault detection and diagnosis of (bio)chemical batch processes

P. Van den Kerkhof, G. Gins, J. Vanlaer, J.F.M. Van Impe
 BioTeC, Department of Chemical Engineering, Katholieke Universiteit Leuven,
 W. de Croylaan 46, B-3001 Leuven, Belgium.
 {pieter.vandenkerkhof, geert.gins, jef.vanlaer, jan.vanimpe}@cit.kuleuven.be

1 Introduction

Due to their high flexibility, batch processes play an important role in the (bio)chemical industry. However, batch processes are affected by many disturbances (e.g., operator faults, sensor failures). Online monitoring of the current process run allows for (i) timely interventions to adjust the final product quality or (ii) saving valuable production time by aborting the process. As process plants nowadays dispose of extensive databases containing the frequent measurements on hundreds of variables, the application of statistical methods to fault detection and diagnosis is a promising combination.

2 Statistical Process Monitoring

The basic principle of Statistical Process Monitoring is identifying abnormal process behavior by referencing the current measurements against a reference dataset obtained under nominal operating conditions. This comparison is greatly simplified by applying a data reduction technique (e.g., Principal Component Analysis (PCA) [1], Partial Least Squares (PLS) [2]). In this way, the monitoring of the process is reduced to monitoring a few so-called latent variables.

Fault detection is carried out by calculating fault detection statistics (e.g., Hotelling's T^2 statistic, Squared Prediction Error statistic). Control limits are calculated based on the properties of the reference set. If a statistic exceeds its control limits, the current process behaviour is characterized as abnormal.

Upon detection of an abnormal situation, information about the cause of the disturbance is obtained by examining the contribution of each variable to the out-of-control statistic on contribution plots. High contributions indicate a problem with this variable or group of variables and thereby greatly narrow the search for the cause of abnormal behavior [3].

3 Conclusions & Future work

Statistical data-driven methods are among the best performing techniques for fault detection. In the area of fault diagnosis however, further research is needed. In most cases, a disturbance in one variable has an influence on other variables. As a consequence, multiple variables will show a significant contribution, which hinders the interpretation of

contribution plots. Moreover, in industrial processes with many (possibly redundant) sensors, interpretation of contribution plots becomes cumbersome.

Future research will consist of developing an online classification scheme to automatically assign the correct diagnosis to a detected fault, based on the contribution pattern in the contribution plot. With this information, operators will be able to take quick corrective actions. For most industrial applications, few fault samples are available to train a classifier, therefore Support Vector Machines (SVMs) will be used for classification. SVMs are a family of classification algorithms originating from the machine learning research area which show good generalization performance when samples are few [4].

Acknowledgements

Work supported in part by Projects OT/09/25/TBA and EF/05/006 (Center-of-Excellence Optimization in Engineering) of the Research Council of the Katholieke Universiteit Leuven, Project KP/09/005 (SCORES4CHEM) of the Industrial Research Council of the Katholieke Universiteit Leuven, and the Belgian Program on Interuniversity Poles of Attraction initiated by the Belgian Federal Science Policy Office. J. Vanlaer and P. Van den Kerkhof are funded by a Ph.D grant of the Institute for the Promotion of Innovation through Science and Technology in Flanders (IWT-Vlaanderen). J. Van Impe holds the chair Safety Engineering sponsored by the Belgian chemistry and life sciences federation *essenscia*. The scientific responsibility is assumed by its authors.

References

- [1] P. Nomikos, and J.F. MacGregor. Monitoring batch processes using multiway principal component analysis. *AIChE J*, 40(8):1361-1375, 1994.
- [2] P. Nomikos, and J.F. MacGregor. Multi-way partial least squares in monitoring batch processes. *Chemom Intell Lab Syst*, 30:97-108, 1995.
- [3] J.A. Westerhuis, S.P. Gurden, and A.K. Smilde. Generalized contribution plots in multivariate statistical process monitoring. *Chemom Intell Lab Syst*, 51:95-114, 2000.
- [4] C.J.C. Burges. A tutorial on Support Vector Machines for pattern recognition. *Data Min Knowl Discov*, 2:121-167, 1998.

The influence of measurement noise on PLS-based data mining techniques

J. Vanlaer, G. Gins and J.F.M. Van Impe
BioTeC - Chemical and Biochemical Process Technology and Control
Department of Chemical Engineering, Katholieke Universiteit Leuven,
W. de Croylaan 46, B-3001 Leuven, Belgium.
{jef.vanlaer, geert.gins, jan.vanimpe}@cit.kuleuven.be

1 Introduction

Data mining techniques such as Principal Component Analysis (PCA) and Partial Least Squares (PLS) are generally considered valuable tools for on-line monitoring of (bio)chemical processes. These techniques are frequently investigated for use in fault detection applications (e.g., [4]) or for batch-end quality prediction purposes (e.g., [3]), often employing data from computer simulators such as Pensim [1] or the Tennessee Eastman Process simulator [2]. However, techniques that perform really well with simulated data often lead to much poorer results when tested on real industrial data.

One possible reason for this discrepancy might be the measurement noise in the data. If the noise that is added to the simulated data does not correspond to the noise level present in the industrial process data, this could explain the performance differences. In this work, the influence of measurement noise on data mining techniques, more specifically on batch-end quality prediction using Multi-way PLS with Variable-wise unfolding (MPLSV), is investigated.

2 Problem statement and methodology

Earlier work of the authors has shown that Multi-way PLS-models with Batch-wise unfolding (MPLSB) yield good results for batch-end quality prediction using both simulated and real industrial data [3]. However, employing batch-wise unfolding makes it necessary to compensate for unknown future data using *Trimmed Scores Regression (TSR)*. In a variable-wise unfolding approach no knowledge about future data is needed, making the prediction a lot more straight-forward. Performing MPLSV on data simulated by Pensim yields very good prediction results, comparable to those in [3]. With real industrial data from a batch polymerization process however, no adequate quality prediction is achieved. A difference in the noise level present in both datasets is assumed to cause this discrepancy.

To investigate the influence of measurement noise on the prediction capability of the MPLSV models, Gaussian noise of different levels is added to simulated data of 200 batches for penicillin production. Model inputs are selected using a branch-and-bound leave-one-out crossvalidation methodology, retaining the next input only if it improves the prediction with more than 1 percent. The leave-one-out cross-

validation Sum of Squared Errors (SSE) over all batches and measurement samples is used to compare the batch-end quality prediction for different noise levels.

3 Results and discussion

Adding extra noise to the simulated data has a profound effect on the number of selected model inputs. A higher noise level results in the selection of more (correlated) input variables while keeping the model order low in an attempt to filter the noise from the data. However, even with more inputs the prediction capability of the models decreases when more noise is added, resulting in much higher SSE values. Consequently, the noise level is definitely one of the reasons for the discrepancy between simulations and industrial applications, but also other factors (e.g., absence of sensors for certain variables, sample interval) might be important.

Acknowledgements. Work supported in part by Projects OT/09/25/TBA and EF/05/006 (Center-of-Excellence Optimization in Engineering) of the Research Council of the Katholieke Universiteit Leuven, Project KP/09/005 (SCORES4CHEM) of the Industrial Research Council of the Katholieke Universiteit Leuven, and the Belgian Program on Interuniversity Poles of Attraction initiated by the Belgian Federal Science Policy Office. J. Vanlaer is funded by a Ph.D grant of the Institute for the Promotion of Innovation through Science and Technology in Flanders (IWT-Vlaanderen). J. Van Impe holds the chair Safety Engineering sponsored by the Belgian chemistry and life sciences federation *essencia*. The scientific responsibility is assumed by its authors. The authors thank J. De Wilde of CYTEC (Drogenbos, Belgium) for the industrial polymerization data set provided for this study.

References

- [1] G. Birol, C. Ündey, and A. Çinar. A modular simulation package for fed-batch fermentation: penicillin production. *Comput Chem Eng*, 26:1553–1565, 2002.
- [2] J.J. Downs and E.F. Vogel. A plant-wide industrial process control problem. *Comput Chem Eng*, 17(3):245255, 1993.
- [3] G. Gins, J. Vanlaer, and J.F.M. Van Impe. Online batch-end quality estimation: does laziness pay off? Proceedings of the 7th IFAC International Symposium on Fault Detection, Supervision and Safety of Technical Processes (SafeProcess2009), Barcelona (Spain), 1246-1251, 2009.
- [4] P. Nomikos and J.F. MacGregor. Monitoring batch processes using multiway principal component analysis. *AIChE J*, 40(8):1361-1375, 1994.

Stress driven security analysis of power systems

Florence Fonteneau-Belmudes
University of Liège
Florence.Belmudes@ulg.ac.be

Damien Ernst
University of Liège
dernst@ulg.ac.be

Louis Wehenkel
University of Liège
L.Wehenkel@ulg.ac.be

This paper presents an approach for assessing the security of a power system based on the decomposition of power system security along the structural weak points of the system given in the form of a set of critical transmission elements or subsystems whose failure induced directly or indirectly by the occurrence of a hazard (e.g. a multiple contingency) would subsequently lead to system wide instabilities. Contrary to existing approaches that decompose security assessment according to the contingencies initiated by hazards (i.e. combinations of primary line outages, short-circuits, variations of power injections) whose likelihood to happen is strongly influenced by highly volatile environmental effects (primarily power markets and meteorological conditions), our approach decomposes the problem according to the critical elements of the transmission system itself. Thereby, this approach may take advantage of existing prior knowledge of power system engineers in charge of the security management of the system, who generally know the main structural weaknesses of their system and the possible ways to counter the instabilities induced by their solicitation.

From an algorithmic point of view, rather than trying to identify for each hazardous combination of contingencies the elements of the system whose failure would be induced by that combination of contingencies, we develop tools that for each vulnerable system element try to identify which hazardous combination of contingencies might induce their failure. Given the nature of electric power systems, this approach might reveal more efficient in the context where it is desirable to identify multiple contingencies that could threaten the system integrity and is also possibly in a better synergy with the way experts address the problem.

In this context, we define a contingency as being a combination {initial Configuration, hazardous Event, corrective Action}, also denoted by {C, E, A}, whose elements are described hereafter. The initial configuration C corresponds to the generation and load patterns of the system (at a specific moment). The event E refers to the tripping of one or several transmission lines. Even if the triggering event is limited to the tripping of one transmission line, the cascading contingencies are covered by this framework since we consider the trajectory followed by the system after the occurrence of the triggering event (and such trajectories include the eventual tripping of other transmission lines, e.g. due to cascading overloads). The corrective action A can be any decision taken by a system operator, immediately after the considered triggering event or later on, in order to miti-

gate its consequences. These three features (initial configuration, event and corrective action) determine the trajectory that will be followed by the state of the system over time, i.e. the sequence of steady-state configurations reached by the system starting from the instant at which the triggering event occurs.

The objective of this research is to identify, among all possible combinations {C, E, A}, those for which the trajectory of the system will reach a configuration C' in which the considered transmission line or corridor will subsequently trip. The output of this approach is a list of combinations {C,E,A} considered as dangerous since they could lead to the cascading tripping of a critical transmission element. It is interesting to notice that the list of {C, E, A} combinations identified as dangerous with respect to the "element specific" criterion considered would be much shorter, and therefore much easier to exploit, than a list of dangerous contingencies according to a "system wide" criterion as usually used for $N - k$ security analyses.

In such a context, the dangerous {C, E, A} combinations are typically very rare with respect to the non-dangerous ones. For instance, it is obvious that it is less probable that a contingency leads to the cascading tripping of a specific transmission line than to the overload of any transmission line of the system. At the same time, the subset of combinations that would appear as dangerous for a specific "target" element of the system will in most cases be locally concentrated in an area constrained by geographical or electrical distances around the target element.

Based on these rarity and localization properties, we use in this work some methods derived from the rare-event simulation theory, as done in [1, 2], to identify the dangerous {C, E, A} combinations for a given target element. The developed framework will be illustrated on data related to the Belgian transmission system.

References

- [1] F. Fonteneau-Belmudes, D. Ernst, and L. Wehenkel. A rare event approach to build security analysis tools when $N - k$ ($k > 1$) analyses are needed (as they are in large scale power systems). In *Proceedings of the 2009 IEEE Bucharest PowerTech Conference, Bucharest, Romania, 28 June - 2 July, 2009*. 8 pages.
- [2] F. Belmudes, D. Ernst, and L. Wehenkel. Cross-entropy based rare-event simulation for the identification of dangerous events in power systems. In *Proceedings of the 10th International Conference on Probabilistic Methods Applied to Power Systems (PMAPS-08)*, Rincon, Puerto Rico, 2008. 8 pages.

Coordinated Voltage Control in Electrical Power Systems

Mohammad Moradzadeh
 SYSTeMS Research Group
 Departement of EESA
 University of Ghent
 Technologiepark - Zwijnaarde 914
 B-9052 Zwijnaarde, Belgium
 Email: Mohammad.Moradzadeh@UGent.be

René Boel
 SYSTeMS Research Group
 Departement of EESA
 University of Ghent
 Technologiepark - Zwijnaarde 914
 B-9052 Zwijnaarde, Belgium
 Email: René.Boel@UGent.be

Abstract

Over the last two decades power systems have been operated under much more stressed conditions than were usual in the past due to environmental pressures on generation and transmission expansion, competitive markets, and unpredictability of renewable energy sources. Under these stressed conditions, voltage instabilities result from the attempt of loads to draw more power than can be delivered by the transmission and generation system. Components such as generators and loads drive the continuous dynamic behavior. On the other hand, discrete events such as threshold reached by over excitation limiters (OXLs) and logical controllers such as load tap-changing transformers (LTCs) and switched capacitor banks (CBs) actions lead to discrete state dynamics. So, the behavior of power systems is characterized by the complex interactions between continuous dynamics of the power system and many hybrid automata representing the logical controllers, i.e. power systems exhibit complex hybrid behavior.

LTCs and CBs can locally maintain the voltage but many voltage collapse incidents have been caused by uncoordinated interactions of LTCs following a major disturbance that locally causes a strong decrease in the voltages. Current practice disables some of those controllers such as LTCs in order to prevent additional problems resulting from their interaction and up to now there has been relatively little attention paid to devising a true coordinated voltage control using message exchange between discrete event controllers by applying distributed control theory and taking discrete events into account.

So, we aim at voltage stability enhancement by using coordinated control actions of the discrete event controllers by using message exchange between the different local control agents (e.g. one control agent per bus). A hybrid system model for investigating the quality of these distributed controllers has been implemented in Simulink using also (SymPowerSystem & Stateflow) which allows reliable simulation of the behavior of both the continuous and the logical components of 12 bus power system with 3 LTCs and 3 CBs. Various approaches for coordinating local controllers (e.g. distributed model predictive controllers) can be investigated using this simulator.

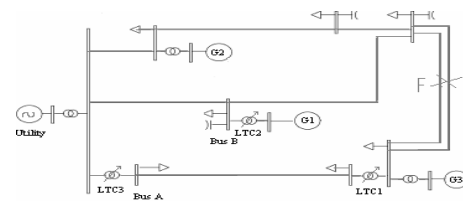


Figure 1: 12-bus IEEE standard power system.

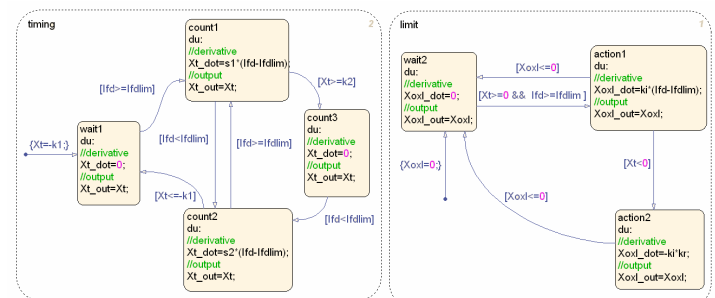


Figure 2: Hybrid system model for OXL.

References

- [1] Van Cutsem, T, and Vournas, C, Voltage stability of electric power systems. Power electronics and power systems series, Kluwer academic publisher, 1998.
- [2] Larsson, M, Coordinated voltage control in electric power systems. Ph.D. thesis, Industrial electrical engineering and automation, Lund university, Sweden, 2000a.
- [3] Ian A. Hiskens, Power system modeling for inverse problems, IEEE transaction on circuits and systems, Vol. 51, No. 3, March 2004.

Visual Feature-Based Motion Control

Jeroen de Best, René van de Molengraft and Maarten Steinbuch

Department of Mechanical Engineering

Technische Universiteit Eindhoven

P.O. Box 513, 5600 MB Eindhoven

The Netherlands

Email: J.J.T.H.d.Best@tue.nl

1 Abstract

The research described here focusses on control design for planar production processes of repetitive structures consisting of identical features. The goal is to move the tool between arbitrary features with velocities of up to 1 m/s and with an accuracy in the order of 1-10 μm . The key idea in this work is to use a camera to directly measure the relative position between the tool and the feature. Moreover, we exploit feature based control, in which the position measurement is based on the interpolation of feature labels instead of their real physical distance.

2 Feature Based Measurement

In many production processes the position of the feature and the tool are often measured separately leading to an indirect relative position measurement between the tool and feature. For a task where the tool should move towards an arbitrary feature assumptions about the pitch between features should be made since they are not measurable using classical encoders for example. Variations in the pitch make this assumption incorrect. In feature based control we overcome these difficulties by observing the repetitive structure with a camera, and introducing a new position measurement that takes values in the feature domain. The concept, first described in [1], is extended to two dimensions in this work. It will be explained using Fig. 1. A part of a pitch varying repetitive pattern is shown, where the dots represent the features. Only a part of the structure is within the field of view. The center of the image, indicated by the cross, is enclosed by four features, labeled (i, j) , through $(i+1, j+1)$, $i, j \in \mathbb{Z}$. The feature based position of this point is related to the en-

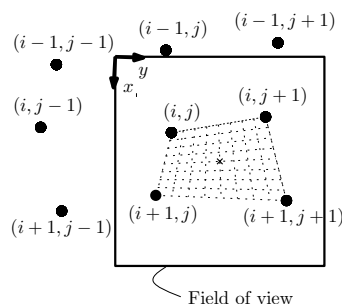


Figure 1: Position in the feature domain.

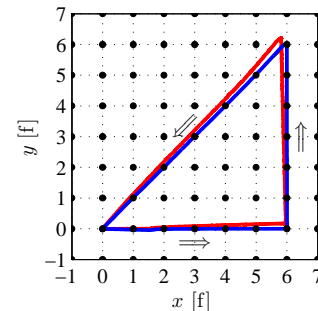


Figure 2: Measured position in the feature domain (visual encoder, motor encoder).

closing point by the interpolation as shown in Fig. 1. In this case the feature based position is given by $(i+0.5, j+0.5)$. The advantage of this position measurement is that the positions of the features in the feature domain are known exactly, i.e., $i = 1, 2, \dots, j = 1, 2, \dots$, even if structure variations are present. In the absence of pitch variations the feature based position and the physical position is identical up to a scaling with the pitch.

3 Results

The feature based position measurement is used in a closed loop visual servoing setup capable of sampling at 1 kHz, with a measurement resolution of 2 μm . An experiment is done, where the center of the camera is to be moved to feature $(6,0)$, then towards feature $(6,6)$ and finally back to feature $(0,0)$ again. In Fig. 2 the blue line shows the results using the feature based position. During the experiment, where a structure with a pitch of 4 ± 0.06 mm and dots with a diameter of 2 mm was used, the maximum error was 80 μm . The red line shows the results using the motor encoders, which are clearly less accurate.

References

- [1] J. de Best, R. van de Molengraft and M. Steinbuch, "Direct Dynamic Visual Servoing at 1 kHz by Using the Product As 1.5D Encoder", Control and Automation, IEEE Int. Conf., Christchurch, New Zealand, December 2009.

Real-time control of magnetic islands in a fusion plasma

Bart Hennen, Egbert Westerhof, Marco de Baar
FOM-Institute for Plasma Physics Rijnhuizen
Email: B.A.Hennen@tue.nl

Pieter Nuij, Maarten Steinbuch, TU Eindhoven
and the TEXTOR team,
Forschungszentrum Jülich GmbH

Introduction

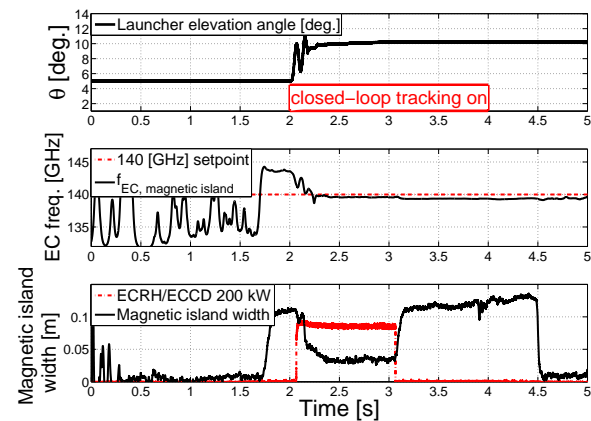
In nuclear fusion research, a hot, fully ionised plasma is confined by magnetic fields in a 'tokamak' reactor. A tokamak plasma is prone to instabilities such as magnetic islands, which harm the operational stability and performance. Real-time control of magnetic islands is in demand and has been demonstrated experimentally in the TEXTOR tokamak.

Real-time control of magnetic islands

The formation of magnetic islands is triggered by perturbation of the magnetic field and current distribution, which disturbs a plasma and its magnetic topology locally. Localized injection of high power microwaves or electron cyclotron waves (i.e. Electron Cyclotron Resonance Heating and Current Drive, ECRH/ECCD) via a steer-able mirror into the plasma induces a local heating and current drive mechanism, which suppresses the island width w . Magnetic islands cause a local flattening in the electron temperature profile of a plasma. A so-called Electron Cyclotron Emission (ECE) diagnostic measures the electron temperature and is applicable as a feedback sensor to monitor magnetic islands (typically a detection within 10 [ms] is required). For effective suppression, a magnetic island control system must direct the ECRH/ECCD beam precisely and fast at the center of the magnetic island. A maximum steady-state positioning error of 1-2 [cm] and a settling time of 100 [ms] are allowed. The settling time is limited by the dynamics of the steer-able mirror (launcher). In addition, feedback controlled on/off modulation of the ECRH/ECCD beam is required to synchronize the microwave injection with the rotation of the magnetic island. The islands pass the ECRH/ECCD beam with rotation frequencies up to 5 [kHz].

The real-time control system, used in the TEXTOR experiments, measures electron temperature fluctuations at a 100 [kHz] sampling rate at 6 radial coordinates. The ECE channels are distributed equally around the ECRH/ECCD deposition location (corresponding to an EC frequency $f = 140$ [GHz]). The radial mode location $f_{EC, magnetic\ island}$ is determined in real-time from the fluctuations and specified as a frequency in the ECE spectrum (in [GHz]). The magnetic island identification algorithm runs at a 16 [μ s] clock rate on a Field Programmable Gate Array (FPGA).

A tracking loop minimizes the control error: $e = 140 - f_{EC, magnetic\ island}$, to align the 140 [GHz] ECRH/ECCD deposition and the island center. A standard feedback con-



troller $C_{magnetic\ island} = \frac{K_p}{s}$ is applied as tracking filter. A second feedback loop with additional feed-forward (BW: 12 [Hz], 5 [kHz] sampling rate) controls the angular position θ of the steer-able mirror. This controller is designed based on dynamical analysis of the steer-able mirror. Both feedback control loops are operated in cascade on the FPGA. Finally, an analog phase-locked loop is added to synchronize the ECRH/ECCD modulation with the island rotation (monitored by a single ECE channel). The figure shows an experimental result. A magnetic island appears in the time frame $t = 1.7-4.5$ [s]. The launcher is actively controlled in the time interval $t = 2 - 4$ [s] ($\theta_{initial} = 5^\circ$) and alignment is achieved within 100 [ms] when $e = 140 - f_{EC, magnetic\ island} < 0.5$ [GHz] ~ 1 [cm]. ECRH/ECCD (200 [kW]) is applied continuously from $t = 2.1-3.1$ [s] and the island is suppressed to a constant width.

Conclusion and outlook

The TEXTOR experiments demonstrate successful real-time controlled stabilisation of magnetic islands. A simulation model is currently developed to analyse the dynamics and to design more advanced controllers. The model includes magnetic island and plasma dynamics, models for the actuators, diagnostics, data-processing and control algorithms. Simulations will be performed for typical TEXTOR conditions and validated with experimental results.

Acknowledgements This work was performed in the framework of the NWO-RFBR Centre of Excellence (grant 047.018.002) on Fusion Physics and Technology and within the framework of the European Fusion Programme under the contract of the Association EURATOM/FOM. The views and opinions expressed herein do not necessarily reflect those of the European Commission.

Overactuated feedback control using a decoupling approach

Michael Ronde*, Maurice Schneiders, René van de Molengraft, Maarten Steinbuch
 Department of Mechanical Engineering, Control Systems Technology
 Eindhoven University of Technology
 Email: * m.j.c.ronde@tue.nl

1 Introduction

In (semiconductor)industry it is desired to obtain higher throughput speeds. To achieve this goal, higher bandwidths of the feedback controllers are required, whereas a consequence a system with a higher stiffness is necessary. This results in a heavier system with larger required actuators and hence more power dissipation. To break this trend, mass and thus stiffness should be decreased, which puts a limit on the achievable bandwidth of the feedback system and the mechanical flexibilities can not be neglected anymore.

Since such machines typically contain more actuators (and sensors) than rigid-body modes, additional design freedom is left. Employing more actuators and sensors than rigid-body modes is called *overactuated control* [1]. The additional actuators can be used to provide artificial stiffness and dampen internal vibrations. In this paper overactuated control is considered from a feedback point of view.

2 Experimental setup and modal decoupling

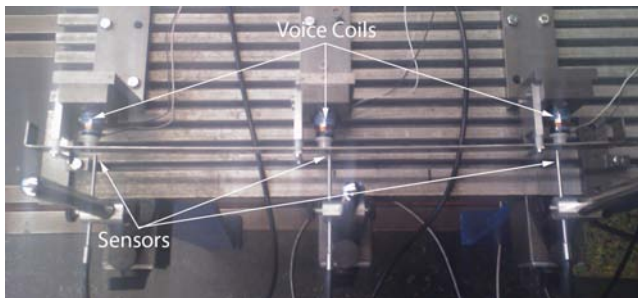


Figure 1: The experimental (3 inputs, 3 outputs) setup

The experimental setup as shown in Fig. 1 is a slender steel beam, where its motion has been constrained to the translation and rotation by wire springs. Using three voice coils the beam can be positioned over approximately 6 mm stroke, which is done by contactless using fiberoptic sensors. A nonparametric MIMO model of the experimental setup has been identified by subsequently exciting each channel with a Schroeder multisine.

For mechanical systems it is known that they (approximately) satisfy the properties of a *dyadic system* if the internal flexibilities are not dominant, such that it can be trans-

formed such that

$$G(s) = U\Sigma(s)V^T, \quad (1)$$

where U and V^T are constant matrices and $\Sigma(s)$ is a diagonal matrix containing all rational transfer functions. Using this property the system can be (approximately) decoupled [2] using $G_{dec} = T_y G(s) T_u$, $T_y = U^{-1}$, $T_u = V^{-T}$.

For the overactuated setup in Fig. 1, which is not exactly dyadic, this results in an approximate diagonal plant. The diagonal terms contain the two rigid-body modes and the first flexible mode. Due to the approximate decoupling, the higher order modes are still present and the off-diagonal parts are nonzero, but sufficiently small. Using the decou-

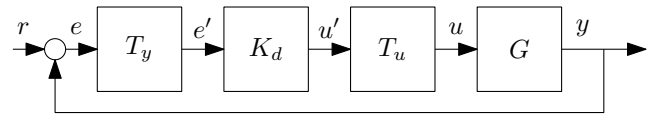


Figure 2: Proposed (decoupling) control scheme

pled plant G_{dec} , a decentralized controller K_d is designed based on manual loopshaping. This controller is used in the proposed control schematic of Fig. 2.

3 Conclusions and future work

Using the additional design freedom from the extra actuator/sensor pair compared to traditionally actuated system, a controller is designed which explicitly takes care of the first non-rigid body mode. With this controller, the two rigid-body modes and the first flexible mode can be controlled independently. The extension to overactuated feedforward and experimental validation remain points of future research.

References

- [1] M. G. E. Schneiders, "Overactuated motion control, a modal approach," Ph.D. dissertation, Eindhoven University of Technology, to appear in 2010.
- [2] M. Boerlage, M. Steinbuch, and G. Angelis, "Frequency response based multivariable control design for motion systems," in *Conference on Control Applications*, 2005, pp. 980–985.

Two-phase Anti-lock Braking System using Force Measurement

Mathieu Gerard ^{*}, Michel Verhaegen ^{*}, Edward Holweg ^{*,^o}

^{*} Delft Center for Systems and Control, Delft University of Technology, Delft, The Netherlands

^o SKF Automotive Division, Nieuwegein, The Netherlands

e-mail: m.p.gerard@tudelft.nl

1 Abstract

Anti-lock Braking System (ABS) is the most important active safety system for passenger cars. Thanks to force measurement, provided for example by the new SKF Load Sensing Hub Bearing Units, hybrid algorithms can be made much simpler and robust than when only using wheel acceleration measurement. A two-phase algorithm is presented, where the wheel acceleration is controlled in closed-loop and the force measurement is used to fire phase switching. Realistic simulations shows that this simple algorithm can handle changes in velocity and friction without extra logic or adaptation of the controller parameters. Finally the algorithm is validated on a tyre-in-the-loop experimental facility.

2 The algorithm

The algorithm consist of 2 phases and a switching mechanism. During each phase, the wheel acceleration is controlled in closed loop. The reference acceleration is either higher or lower than the vehicle acceleration ensuring that the slip will respectively decrease or increase. The switching, implemented looking at the brake force measurement, will take place when the tyre is on the other side of the maximum of the characteristic compared to the start of the phase. This back and forth process will ensure that the system is cycling around the optimal point.

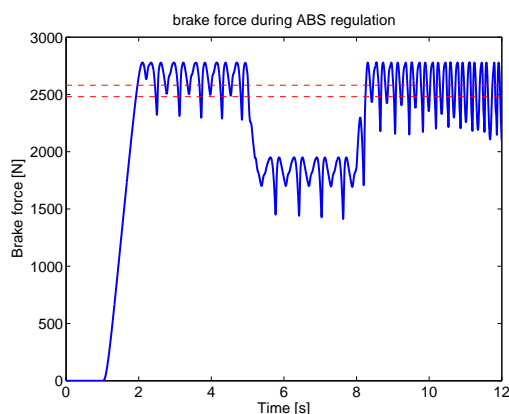


Figure 1: Simulation - Brake force during ABS regulation. The algorithm can deal with friction drop.

3 Simulation

The algorithm is simulated using a realistic model. The relaxation effect of the tyre as well as the delays in measurement and actuation are taken into account. In the simulation presented on figure 1, the car starts braking at 55 m/s and goes nearly until a full stop. The algorithm has no difficulty at all to handle the friction drop between $t=5$ and $t=9$.

4 Experimental validation

The proposed algorithm has been tested in practice on the tyre-in-the-loop experimental facility of Delft University of Technology. The test bench consists of a large drum of 2.5 meter diameter on top of which the tyre is rolling. An illustration can be seen on Figure 12.6 of [2]. The controller is tuned exactly like in simulation. A test performed at 18 m/s is shown on Figure 2. The algorithm works precisely like expected from the simulation. The brake force remains really close to the maximum of 2800 N.

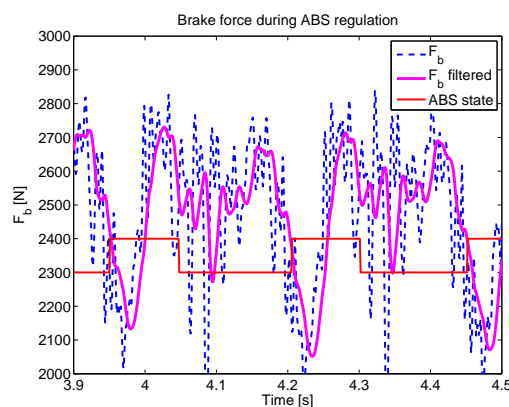


Figure 2: Experiment - Brake force during ABS regulation.

References

- [1] P. W. A. Zegelaar, The dynamic Response of Tyres to Brake Torque Variations and Road Unevenness, PhD Thesis, Delft University of Technology, 1998.
- [2] Hans B. Pacejka, Tyre and Vehicle Dynamics, Butterworths-Heinemann, 2006.
- [3] W. Pasillas-Lépine, Hybrid modeling and limit cycle analysis for a class of five-phase anti-lock brake algorithms, Vehicle System Dynamics, vol 44, num 2, pg 173-188, 2006.

Nonsmooth bifurcations of equilibria in planar continuous systems

J.J. Benjamin Biemond, Nathan van de Wouw, and Henk Nijmeijer

Eindhoven University of Technology

P.O. Box 513

5600 MB Eindhoven

The Netherlands

Email: {j.j.b.biemond, n.v.d.wouw, h.nijmeijer}@tue.nl

1 Introduction

In this work, bifurcations are studied in planar piecewise smooth dynamic systems that are described by a continuous, though nonsmooth, differential equation. Such dynamics can arise due to nonsmooth elements such as actuator saturation, one-sided mechanical contact or a switching controller. We develop a procedure to find all limit sets that appear or disappear during a bifurcation of an equilibrium in planar continuous piecewise smooth systems.

2 Approach

Under certain conditions, the neighbourhood of an equilibrium in a piecewise smooth planar system can locally be approximated with a conewise affine system:

$$\dot{\mathbf{x}} = A_i \mathbf{x} + \mu \mathbf{b}, \mathbf{x} \in S_i, i = 1, \dots, m, \quad (1)$$

with state $\mathbf{x} \in \mathbb{R}^2$, bifurcation parameter $\mu \in \mathbb{R}$, and domains $S_i \subset \mathbb{R}^2$, that are cones, covering the complete state space.

When $\varphi_a(t)$ is a trajectory of (1) with $\mu = \mu_a$, then $\varphi_b(t) := c\varphi_a(t)$, $c > 0$ is a trajectory of (1) with $\mu = c\mu_a$. Therefore, all bifurcations of the system can be identified by studying the system (1) for an arbitrarily chosen positive and negative μ , and $\mu = 0$. At $\mu = 0$, the systems contains an equilibrium point at the origin.

The following procedure is presented to study the bifurcations of continuous systems (1), cf. [1]:

1. Identify equilibria for varying μ .
2. Study the stability of the equilibrium point for $\mu = 0$.
3. For an arbitrarily chosen positive and negative μ :
 - a. Compute -trajectories through the origin and through points, where the trajectory is tangent to the boundaries between the cones S_i .
-stable and unstable manifolds of nodes and saddles; check for homoclinic and heteroclinic tangles.
 - b. Using these trajectories, identify what sequences of boundaries and cones can be traversed by periodic orbits.
 - c. Using the method developed in [1], find a circle that contains all limit cycles in its interior.
 - d. Compute the return maps for the sequences of boundaries and domains obtained in step 3.b. From these

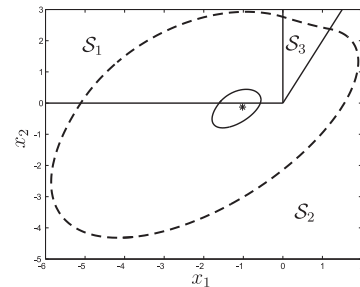


Figure 1: Limit sets of the system for $\mu = 1$. The asterisk depicts the position of a stable focus. The dashed limit cycle is stable, the solid limit cycle is unstable.

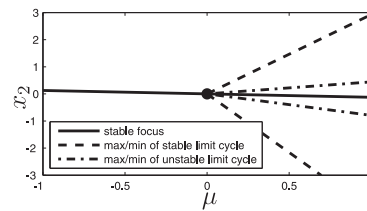


Figure 2: Bifurcation diagram of the exemplary system.

maps, identify all closed orbits, including limit cycles, and their stability.

4. Identify what limit sets appear, disappear or change stability for changing μ .

3 Example

In [1], an exemplary system is analysed with the given procedure. For $\mu \leq 0$, the limit set of the system consists of a single equilibrium point in S_2 . This equilibrium persists for $\mu > 0$, and is encircled by two limit cycles, c.f. Figure 1. This bifurcation, depicted in Figure 2, is not possible in smooth systems.

4 Conclusion

Multiple limit sets can appear or disappear at nonsmooth bifurcations of equilibria in piecewise smooth systems. With the presented procedure, all these limit sets and their stability can be identified. For example, this can be used to assess the parameter robustness of a nonsmooth control system.

References

- [1] J.J.B. Biemond, N. van de Wouw, H. Nijmeijer, Nonsmooth bifurcations of equilibria in planar continuous systems, to appear in Nonlinear Analysis: Hybrid Systems (2010).

The logarithmic quantiser is not optimal for LQ control

Jean-Charles Delvenne¹

University of Namur,

Department of Mathematics, 8, Rempart de la Vierge, 5000 Namur, Belgium

jean-charles.delvenne@math.fundp.ac.be

Control with a communication constraint

Imagine a plant that communicates with a physically distant controller through communication channels. The limited capacity of communication lines makes the design of controller able to stabilise the plant a more difficult, and sometimes impossible, task. This family of problems, acutely useful with the generalisation of digital communication technologies, leads to a dialogue between control theory and information theory which has essentially started with [2], and has been pursued actively in the last decade (see, e.g., [4, 5, 6]).

In this paper, we consider the simplest such problem: stabilising the discrete-time scalar linear system $x_{t+1} = ax_t + u_t$, with $|a| > 1$. We know that the initial state is distributed uniformly in the interval $[-1, 1]$. The controller receives the state x_t through a communication channel, with a capacity limited to R bits per channel use (see Fig. 1). An energy function on the state space $x \mapsto E(x)$, typically $E(x) = x^2$, is given. Our task is to design a coding/decoding strategy for the communication channel and a controller in order to make the closed-loop system stable and minimise the cost defined as follows. The cost of such a control strategy is defined as $\mathbb{E} \sum_{t \geq 0} E(x_t)$, where \mathbb{E} denotes the expected value over all initial states. For $E(x) = x^2$, we therefore solve an LQ optimal control problem. This problem is a generalisation of the one considered in [5, 3]. Note that $\mathbb{E} \sum_{t \geq 0} E(x_t)$ can be written as $\mathbb{E}(E(x_0))\tau$, where τ is a time, loosely interpreted as the average time taken by a piece of energy to leave the system.

The logarithmic strategy

A popular strategy to solve the problem is to quantise the state, i.e., partition the state space $[-1, 1]$ into countably many intervals, and to replace the state x_t by the centre of the interval, $q(x_t)$ to which it belongs. As there are only countably many so quantised values of the state, it takes finitely many bits to transmit that value through the channel. The controller then acts as if the state was actually $q(x_t)$.

One particular such strategy, based on the so-called log-

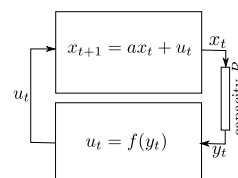


Figure 1: A channel of capacity R restricts the communication between the plant and the controller. We look for the controller that will minimise a quadratic cost. The logarithmic strategy, which discretises x_t with a logarithmic quantiser, is shown to be optimal only in the low capacity limit.

arithmic quantiser, was proved by Elia and Mitter [4] to the least sense (in a certain sense) to achieve stabilization of the system.

In this contribution, we show that if we are interested in minimising the cost, not only stabilising the system, then the logarithmic strategy is not optimal any more. The optimality only holds in the low capacity limit. We show that in the high capacity limit, a modification of the logarithmic quantiser called the nested uniform quantiser achieves optimality.

References

- [1] D. Delchamps. Stabilizing a linear system with quantized state feedback. *IEEE Transactions on Automatic Control*, AC-35:916–924, 1990.
- [2] J.-Ch. Delvenne. An optimal quantized feedback strategy for scalar linear systems. *IEEE Transactions on Automatic Control*, 51(2):298–303, 2006.
- [3] N. Elia and S.K. Mitter. Stabilization of linear systems with limited information. *IEEE Transactions on Automatic Control*, AC-46:1384–1400, 2001.
- [4] F. Fagnani and S. Zampieri. Stability analysis and synthesis for scalar linear systems with a quantized feedback. *IEEE Transactions on automatic control*, 48(9):1569–1584, 2003.
- [5] S. Tatikonda and S. K. Mitter. Control under communication constraints. *IEEE Transactions on Automatic Control*, 49(7):1056–1068, 2004.

¹This extended abstract presents research results of the Belgian Programme on Interuniversity Attraction Poles, initiated by the Belgian Federal Science Policy Office.

Quantized Continuous-Time Average Consensus

F. Ceragioli

Dipartimento di Matematica

Politecnico di Torino

10129 Torino, Italy

francesca.ceragioli@polito.it

C. De Persis

Lab. Mechanical Automation and Mechatronics

University of Twente

7500 AE Enschede, Netherlands

c.depersis@ctw.utwente.nl

P. Frasca

Istituto per le Applicazioni del Calcolo - C.N.R.

00161 Roma, Italy

paolo.frasca@gmail.com

1 Introduction

A group of interconnected dynamical systems is said to reach consensus when their internal states converge to a common value. Typically this common value is a function (e.g. the arithmetic mean) of the systems' initial conditions. Communication constraints play a major role in consensus and related problems of distributed computation and control. Such constraints can be represented by a graph of available communication links among agents, together with further restrictions on what information can be exchanged across such links. Over the last few years, the constraint of quantization, that is of communication restricted to a discrete set of symbols, has received significant attention. Although most of to-date works have dealt with discrete-time dynamics (see e.g. [5] and references therein), it is very important to consider the same restrictions in the context of continuous-time dynamics, as recently done in [4]. In this way, it is possible to study the effect of quantization on continuous-time systems without necessarily considering their discretized or sampled-data model. This may be interesting in particular for applications to robotic networks.

2 Quantized consensus and solutions

Besides discussing the general issues of quantization in consensus dynamics, we aim at giving a rigorous treatment of continuous-time average consensus dynamics with uniform quantization in communications. It is well-known that consensus problems can be thought in terms of feedback control systems: As expected, when quantization enters the loop, the stabilization problem becomes more challenging. From the mathematical point of view, a consequence of quantization is that we obtain a system with discontinuous righthand side, whose solutions have to be intended in some generalized sense. In fact we prove by means of an example that classical or Carathéodory solutions actually may not exist. In the literature one can find different approaches to the technical problem of having a system with discontinuous righthand side (see e.g. [3] for a review on these topics). Here we focus on Krasowskii solutions essentially for two rea-

sons. First, there are many handy results concerning existence and continuation of Krasowskii solutions, as well as a complete Lyapunov theory [1, 2]. Second, since the set of Krasowskii solutions includes Filippov and Carathéodory solutions, then results about Krasowskii solutions also hold for Filippov and Carathéodory solutions, in case they exist. On the other hand, the set of Krasowskii solutions may be "too large". In particular, it may contain sliding modes which, from a practical point of view, induce chattering phenomena. To cope with those issues, we propose the use of a quantizer endowed with an hysteretic mechanism, and study the resulting dynamics by a hybrid system approach. Convergence results are given for both the Krasowskii and the hysteretic dynamics: Note that due to the constraint of static uniform quantization we can not precisely obtain consensus. Nevertheless we obtain approximations of the consensus condition we informally refer to as "practical consensus".

References

- [1] J.P. Aubin and A. Cellina. *Differential inclusions*, volume 264 of *Grundlehren der Mathematischen Wissenschaften*. Springer, Berlin, 1984.
- [2] A. Bacciotti and F. Ceragioli. Stability and stabilization of discontinuous systems and nonsmooth Liapunov functions. *ESAIM: Control, Optimisation & Calculus of Variations*, 4:361–376, 1999.
- [3] J. Cortés. Discontinuous dynamical systems – a tutorial on solutions, nonsmooth analysis, and stability. *IEEE Control Systems Magazine*, 28(3):36–73, 2008.
- [4] D. V. Dimarogonas and K. H. Johansson. Quantized agreement under time-varying communication topology. In *American Control Conference*, pages 4376–4381, June 2008.
- [5] P. Frasca, R. Carli, F. Fagnani, and S. Zampieri. Average consensus on networks with quantized communication. *International Journal of Robust and Nonlinear Control*, 19(16):1787–1816, 2009.

Adaptive control of port-Hamiltonian systems

D.A. Dirksz

Faculty of Mathematics and Natural Sciences
University of Groningen
9747 AG Groningen
The Netherlands
Email: d.a.dirksz@rug.nl

J.M.A. Scherpen

Faculty of Mathematics and Natural Sciences
University of Groningen
9747 AG Groningen
The Netherlands
Email: j.m.a.scherpen@rug.nl

Abstract

Adaptive control is an alternative approach for controlling systems which are sensitive to parameter uncertainty. With adaptive control it is possible to estimate parameter errors and to compensate for those errors. This can result in a better performance of the controlled system. Some techniques and results in adaptive control are described in [7] for linear, nonlinear, single-input and multi-input systems. Adaptive control for stabilization and tracking control of Euler-Lagrange (EL) systems is described in [5]. More recent results in the field of nonlinear applied adaptive control are presented in [1], which rely on the notions of *immersion and invariance*.

For adaptive control of port-Hamiltonian (PH) systems with uncertain parameters little is known. PH systems were introduced for modeling of a large class of physical systems [4]. They describe a large class of (nonlinear) systems including passive mechanical systems, electrical systems, electromechanical systems and mechanical systems with nonholonomic constraints [6]. For PH systems [2] presented the use of an adaptive internal model to overcome sinusoidal disturbances, but system parameters were assumed to be known. In [8] adaptive control was applied to simultaneously stabilize PH systems. However, the results hold only for time-invariant systems and the assumptions limit the class of systems to which the results can be applied. Here we introduce an adaptive control scheme for general PH systems. The adaptive control compensates for input errors caused by not exactly knowing the value of the necessary system parameters. Compared to [8] we have weaker assumptions, deal also with time-varying systems and do not require the system to already have reached the desired equilibrium points. The requirement of the closed-loop system to also have a skew-symmetric interconnection matrix (which is so for all PH systems) directly provides the estimation law for the unknown system errors. It can then be proven for a class of systems that the error estimations converges to the real errors and that the system is asymptotically stabilized.

The general results are used to apply adaptive tracking control of fully actuated standard PH systems. Tracking control is realized by transforming a system into an error system and then asymptotically stabilizing the error system. We ex-

tend results presented in [3] for tracking control to realize adaptive tracking control. The adaptive tracking methods presented in [7] and [5] for EL systems have the disadvantage of losing structure: the error system is passive but is not an EL system. These methods also require a redefinition of the error signal and additional tuning. With the proposed PH adaptive control scheme the PH structure is preserved and a redefinition of the error signal is not necessary. In the near future we plan to verify the adaptive scheme by experiments applied on a planar manipulator system. We also want to investigate how performance is affected when bounds on the parameter errors are available.

References

- [1] A. Astolfi, D. Karagiannis, R. Ortega, 2008, Towards applied nonlinear adaptive control, *Annual Reviews in Control* Vol. 32, No. 2, 136-148
- [2] C. Bonivento, L. Gentili, A. Paoli, 2004, Internal model based fault tolerant control of a robot manipulator, *Proceedings IEEE Conference on Decision and Control*, Atlantis, Bahamas
- [3] K. Fujimoto, K. Sakurama, T. Sugie, 2003, Trajectory tracking of port-controlled Hamiltonian systems via generalized canonical transformations, *Automatica*, Vol. 39, No. 12, 2059-2069
- [4] B.J.M. Maschke, A.J. van der Schaft, 1992, Port-controlled Hamiltonian systems: modeling origins and system-theoretic properties, *IFAC symposium on Nonlinear Control Systems*, Borbeaux, France, 282-288
- [5] R. Ortega, A. Loria, P.J. Nicklasson, H. Sira-Ramírez, 1998, Passivity-based control of Euler-Lagrange systems: mechanical, electrical and electromechanical applications, London, Springer
- [6] A.J. van der Schaft, 2000, L_2 -gain and passivity techniques in nonlinear control, London, Springer
- [7] J.J.E. Slotine, W. Li, 1991, Applied Nonlinear Control, Prentice Hall, New Jersey
- [8] Y. Wang, G. Feng, D. Cheng, 2007, Simultaneous stabilization of a set of nonlinear port-controlled Hamiltonian systems, *Automatica*, Vol. 43, No. 3, 403-415

A Cyclo-dissipativity Condition for Power Factor Improvement in Nonsinusoidal Systems with Significant Source Impedance

Dunstano del Puerto-Flores, and
 Jacquelin M.A. Scherpen
 Dept. of Discrete Technology and Automatization
 Universiteit Groningen
 Nijenborgh 4, 9747 AG Groningen
 The Netherlands
 Emails: d.del.puerto.flores@rug.nl,
 j.m.a.scherpen@rug.nl

Romeo Ortega
 Laboratoire des Signaux et Systèmes,
 Plateau de Moulon, 91192, Gif-sur-Yvette,
 France
 Email: ortega@lss.supelec.fr

Abstract

Recently, in [1] it has been established that the classical problem in electrical engineering of optimizing energy transfer from an alternating current (ac) source to a load with non-sinusoidal source (but periodic) voltage is equivalent to imposing the property of cyclo-dissipativity to the source terminals. Since this framework is based on the cyclo-dissipativity property, see [2], the improvement of the power factor is done independent of the reactive power definition, which is a matter of discussions in the power community, see [3].

Using the cyclo-dissipativity framework the classical capacitor and inductor compensators were interpreted in terms of energy equalization, see [1] for more details. And we have presented an extension of this result in [4] where we considered arbitrary LTI lossless filters, and proved that for general lossless LTI filters the PF is reduced if and only if a certain equalization condition between the weighted powers of inductors and capacitors of the load is ensured. Although the aforementioned results were obtained by considering non-linear loads, the generator was assumed to be ideal, that is, with negligible impedance. However, there are some practical cases where the source impedance becomes significant.

We consider the energy transfer from a known voltage source v_s to a given a fixed load i_ℓ , see Figure 1. The standard approach to improve the PF is to place a lossless compensator, Y_c , between the source and the load. The PF compensation configuration considered here is depicted in Figure 2.

In this work, we formulate the power factor compensation problem in a way that the explicitly accounts for the effects of a non-negligible source impedance, Z_s , on the load voltage and current. We prove in this way that cyclo-dissipativity provides a rigorous mathematical framework useful to analyze and design power factor compensators for general non-linear loads operating in nonsinusoidal regimes with significant source impedance.

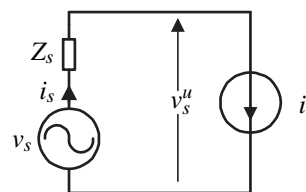


Figure 1: Uncompensated power delivery system

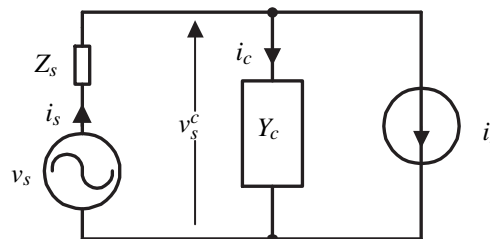


Figure 2: Load Compensation in a power delivery system

References

- [1] E. Garcia-Canseco, R. Grino, R. Ortega, M. Salichs, and A. Stankovic, "Power-factor compensation of electrical circuits," *Control Systems Magazine, IEEE*, vol. 27, pp. 46–59, April 2007.
- [2] D. J. Hill and P. J. Moylan, "Dissipative dynamical systems: Basic Input-Output and State Properties," *The Franklin Institute*, vol. 309, pp. 327–357, May 1990.
- [3] L. S. Czarnecki, "Budeanu and Fryze: Two frameworks for interpreting power properties of circuits with nonsinusoidal voltages and currents," *Electrical Engineering*, vol. 80, pp. 359–367, 1997.
- [4] D. del Puerto-Flores, R. Ortega and J. M. A. Scherpen, "Power factor compensation with lossless linear filters is equivalent to (weighted) power equalization and a new cyclo-dissipativity characterization," *Conference on Decision and Control, 2009. CDC'09*, Dec 2009.

Computing the Evolution of Hybrid Systems with Ariadne

Pieter Collins, Ivan Zapreev
Centrum Wiskunde en Informatica
Amsterdam, The Netherlands
{collins, zapreev}@cwi.nl

Luca Benvenuti
Università di Roma La Sapienza, Italy
luca.benvenuti@uniroma1.it

Davide Bresolin, Luca Geretti, Tiziano Villa
Università di Verona
Verona, Italy
{bresolin, geretti, villa}@sci.univr.it

Alberto Ferrari, Christos Sofronis
PARADES, Roma, Italy
{aferrari, cstofonis}@parades.rm.cnr.it

1 Hybrid Systems

Ariadne [1] is a software tool for analysis and verification of the evolution of hybrid systems, which are dynamic systems comprising both discrete and continuous evolution. The discrete evolution is given by a finite automaton with transition law $q' = \gamma(q, e)$, and the continuous evolution is governed by the equations

$$\dot{x} = f_q(x); \quad x' = r_{q,e}(x); \quad c_{q,e}(x) = 0, \quad (1)$$

where $c_{q,e}$ is the *guard* condition for event e to occur in mode q , and $r_{q,e}$ the corresponding *reset-map*. The main functionality of the tool is to compute the *reachable set* of the system evolution from the initial set X_0 .

2 Functional Calculus

At the core of Ariadne's implementation is a calculus for the manipulation of functions. Given a function $f: R^n \rightarrow R$, a *model* of f is a triple $\hat{f} = (D, p, e)$ such that p is a uniform approximation for f on D with error e :

$$\sup_{x \in D} |p(x) - f(x)| \leq e. \quad (2)$$

The function models used in Ariadne are known as *Taylor models* [2] which are approximations by scaled polynomials with floating-point coefficients on coordinate-aligned boxes. Taylor models support basic operations of arithmetic, composition and antidifferentiation with guaranteed bounds on the errors introduced by the approximation. Numerical roundoff error is handled using interval arithmetic.

3 Computation of the evolution

The intermediate sets reached during the evolution are described as *constrained image sets* of the form

$$S = h(D \cap g^{-1}(C)) = \{f(x) \mid x \in D \wedge g(x) \in C\}. \quad (3)$$

The set S is approximated using function models \hat{h} and \hat{g} , yielding an *enclosure* for the true evolved set. Previous versions of Ariadne used *image sets* $S = f(D)$ and *zonotopes* as enclosures, but these were found to be too restrictive.

The reset map r can be computed by function composition,

$$r(S) = r \circ h(D \cap g^{-1}(C)). \quad (4)$$

A function model $\hat{\phi}$ approximating the flow ϕ of $\dot{x} = f(x)$ is

computed using a rigorous version of Picard iteration:

$$\phi_{n+1}(x, t) = x + \int_0^t f(\phi_n(x, \tau)) d\tau. \quad (5)$$

The guard sets are handled by computing the *crossing time* $\gamma(x)$ satisfying

$$c(\phi(x, \gamma(x))) = 0 \quad (6)$$

using an interval Newton method. This is not possible in the case of tangential crossings, so the constraints are introduced explicitly.

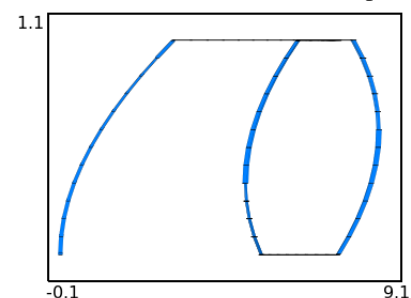
The global evolution of a hybrid system is computed by gridding the state space into a union of boxes, computing the evolution for each box over a given time interval $[0, T]$, and finally over-approximating the reached and evolved sets on the grid. The resulting computation requires testing whether an enclosure intersects a given box B , resulting in a nonlinear feasibility problem

$$\text{find } x \in D \text{ such that } f(x) \in B \text{ and } g(x) \in C, \quad (7)$$

which is solved using a rigorous primal-dual interior-point method.

4 Example

As an example of the capabilities of the tool, we display the reachable set for a watertank benchmark problem:



References

- [1] L. Benvenuti, D. Bresolin, A. Casagrande, P. Collins, A. Ferrari, E. Mazzi, A. Sangiovanni-Vincentelli and T. Villa, "Reachability computation for hybrid systems with Ariadne", *Proc. 17th IFAC World Congress*, 2008.
- [2] M. Berz and K. Makino, "Verified Integration of ODEs and Flows Using Differential Algebraic Methods on High-Order Taylor Models", *Reliable Computing* **4** (1998).

Issues on global stabilization of linear systems subject to actuator saturation

Tao Yang

School of Electrical Engineering and Computer Science,
Washington State University,
Pullman, WA 99164-2752, U.S.A.
E-mail: tyang1@eecs.wsu.edu

Anton A. Stoorvogel

Department of Electrical Engineering, Mathematics and Computer Science,
University of Twente,
P.O. Box 217, Enschede, The Netherlands
E-mail: A.A.Stoorvogel@utwente.nl

Ali Saberi

School of Electrical Engineering and Computer Science,
Washington State University,
Pullman, WA 99164-2752, U.S.A.
E-mail: saberi@eecs.wsu.edu

1 Abstract

Linear systems subject to actuator saturation are ubiquitous and have been the subject of extensive study. Internal stabilization for this class of systems has a long history. Fuller's paper [?] established that a chain of integrators with order greater or equal to three cannot be globally stabilized by any saturating linear static state feedback law with only one input channel. Sontag and Sussmann [?] established that, global stabilization of continuous-time linear systems with bounded input can be achieved if and only if the linear system in the absence of actuator saturation is stabilizable and critically unstable (equivalently, *asymptotically null controllable with bounded control*(ANCBC)). In general, this requires a nonlinear feedback laws. However, for certain cases, the global stabilization can be achieved by linear control laws. More precisely, the paper [?] noted that systems which are asymptotically null controllable with bounded inputs can be globally stabilized by linear static state feedback control laws if all non-zero eigenvalues on the imaginary axis are semi-simple (geometric and algebraic multiplicities are equal) while zero is allowed to be an eigenvalue whose Jordan blocks can be at most of size 2×2 (which are associated with double integrators). The quoted paper [?] does not give a full proof of this result. In this paper we prove this result. Moreover, this proof is constructive.

Another issue is that in the literature, there is this general belief that if there are Jordan blocks of size greater or equal to three associated to an eigenvalue in zero then we need nonlinear controllers. This is a misconception. Such a mis-

conception is possibly based on a misreading of the result of [?]. One should emphasize that the beautiful result of Fuller does not claim anything beyond static state feedback controllers for chains of integrators. In this paper we illustrate this issue by showing that a triple-integrator with multiple inputs subject to actuator saturation can be globally stabilized by a linear static state feedback. This is clearly a first step towards a better understanding when nonlinear static state feedbacks are needed.

Two general open problems are still unresolved; (1) under what conditions one can utilize a linear *static* state feedback control law to globally stabilize a linear system subject to actuator saturation?, and (2) under what conditions one can utilize a linear *dynamic* state feedback control law to globally stabilize a linear system subject to actuator saturation?

References

- [1] A.T. FULLER, "In-the-large stability of relay and saturating control systems with linear controller", *Int. J. Contr.*, 10(4), 1969, pp. 457–480.
- [2] E.D. SONTAG AND H.J. SUSSMANN, "Nonlinear output feedback design for linear systems with saturating controls", in *Proc. 29th CDC*, Honolulu, 1990, pp. 3414–3416.
- [3] F. TYAN AND D.S. BERNSTEIN, "Global stabilization of systems containing a double integrator using a saturated linear controller", *Int. J. Robust & Nonlinear Control*, 9(15), 1999, pp. 1143–1156.

Stability criteria for planar linear systems with state reset

Svetlana Polenkova
 Department of Applied Mathematics
 University of Twente
 P.O. Box 217
 7500 AE Enschede, The Netherlands
 Email: s.v.polenkova@ewi.utwente.nl

Jan Willem Polderman
 Department of Applied Mathematics
 University of Twente
 P.O. Box 217
 7500 AE Enschede, The Netherlands
 Email: j.w.polderman@math.utwente.nl

Rom Langerak
 Department of Computer Science
 University of Twente
 P.O. Box 217
 7500 AE Enschede, The Netherlands
 Email: langerak@cs.utwente.nl

1 Abstract

Stability analysis for hybrid systems is a much harder problem than for smooth systems. The reason appears to be the interplay between continuous time driven dynamics and discrete event driven dynamics. See [1, 2, 3, 4] and the references therein.

In this paper we study a seemingly simple situation: a single linear planar system with a state reset. We derive a complete characterization and an algorithm to determine stability. The class of systems that we study can conveniently be modelled as a hybrid automaton and is depicted in Figure 1.

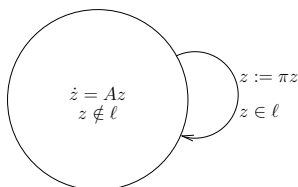


Figure 1: Linear planar system with state reset

Here π is the orthogonal projection on the x -axis. The matrix A is Hurwitz and the state is reset by orthogonal projection on the x -axis whenever the state trajectory crosses the line $l : y = kx$. Although A is Hurwitz, the state reset may lead to instability. The problem is particularly interesting for systems with oscillatory behavior, therefore we restrict the attention to matrices with complex conjugate eigenvalues:

$$\lambda = \alpha \pm \beta i, \alpha < 0, \beta \neq 0 \quad (1.1)$$

For ease of reference we define

$$\mathcal{A} = \{A \in \mathbb{R}^{2 \times 2} \mid \text{spec}(A) = \alpha \pm \beta i, \alpha < 0, \beta \neq 0\}.$$

The following problems are treated:

1. Find a criterion that for a given pair (A, ℓ) determines its stability properties.
2. For a given matrix A , find all switching lines ℓ for which the system is (asymptotically) stable.
3. For a given switching line ℓ , find all matrices A for which the system is (asymptotically) stable;

2 Conclusions

We have derived necessary and sufficient conditions for stability of planar linear systems with state reset. A geometry driven parametrization of all systems with given spectrum enabled an analysis on the flow of the system rather than on the equations making the approach to a large extent behavioral in nature.

The ideas sketched here can be extended to higher dimensions at the cost of a considerable more involved analysis.

References

- [1] Michael S. Branicky. Stability of switched and hybrid systems. In *Proc. 33rd IEEE Conf. Decision and Control*, pages 3498-3503, Orlando, FL, 1994.
- [2] J.P. Hespanha and A. S. Morse. Stability of switched systems with average dwell-time. In *Proceedings of 38-th IEEE Conference on Decision and Control*, 2655-2660, December 1999.
- [3] R.Langerak and J.W. Polderman. Tools for Stability of Switching Linear Systems: Gain Automata and Delay Compensation. In *44th IEEE Conference on Decision and Control and European Control Conference ECC*, 2005, Sevilla, Spain. pages 4867-4872.
- [4] D. Liberzon. *Switching in Systems and Control*. Birkhäuser, Boston, 2003.

On existence and uniqueness of solutions for bimodal piecewise affine systems

Le Quang Thuan
 Department of Mathematics
 University of Groningen
 P.O. Box 800, 9700 AV Groningen
 The Netherlands
 Email: t.q.le@rug.nl

M. K. Camlibel
 Department of Mathematics
 University of Groningen
 P.O. Box 800, 9700 AV Groningen
 The Netherlands
 Email: m.k.camlibel@rug.nl

1 Introduction

Piecewise affine dynamical models arise in various contexts of system and control theory. When these models are given by differential equations with discontinuous right hand sides [1], existence and uniqueness of solutions become a nontrivial issue. Such models are typically studied in the framework of differential inclusions with the so-called Filippov solution concept. Existence of Filippov solutions require very mild conditions in general. Applied to piecewise affine systems, one can readily guarantee existence of solutions. However, conditions guaranteeing uniqueness (e.g. one-sided Lipschitzian property or monotonicity-type conditions) for general differential inclusions impose quite strong requirements for piecewise affine systems. In this paper, we introduce less restrictive conditions that guarantee uniqueness of solutions.

2 Bimodal piecewise affine systems

For given matrices $(A_1, e_1), (A_2, e_2) \in \mathbb{R}^{n \times n} \times \mathbb{R}^n$ and $(c, f) \in \mathbb{R}^n \times \mathbb{R}, c \neq 0$, define the set-valued functions $F, G : \mathbb{R}^n \rightrightarrows \mathbb{R}^n$ as

$$F(x) = \begin{cases} \{A_1x + e_1\} & \text{if } y < 0 \\ \{A_1x + e_1, A_2x + e_2\} & \text{if } y = 0 \\ \{A_2x + e_2\} & \text{if } y > 0 \end{cases}$$

and $G(x) = \text{conv}(F(x))$ where $y = c^T x + f$ and $\text{conv}(S)$ denotes the convex hull of the set S . Consider the bimodal piecewise affine system given by the differential inclusion

$$\dot{x}(t) \in F(x(t)) \quad (1)$$

where $x \in \mathbb{R}^n$ is the state. In case, the implication

$$c^T x + f = 0 \implies A_1x + e_1 = A_2x + e_2 \quad (2)$$

holds, the set-valued maps F and G boil down to single-valued Lipschitz continuous functions. In this paper, we study the general case where (2) may not hold. Various solution concepts exist for differential inclusions (see e.g. [2, 3]).

This paper focuses on *Carathéodory* and *Filippov* solutions to the system (1).

An absolutely continuous function $x : \mathbb{R} \rightarrow \mathbb{R}^n$ is said to be a solution of the bimodal system (1) for the initial state x_0 in the sense of: *Carathéodory* if $x(0) = x_0$ and the differential inclusion (1) is satisfied for almost all $t \in \mathbb{R}$; *Filippov* if $x(0) = x_0$ and the differential inclusion $\dot{x}(t) \in G(x(t))$ is satisfied for almost all $t \in \mathbb{R}$.

The main goal of the paper is to investigate uniqueness of Filippov solutions to the differential inclusion (1) and its consequences. We will present a set of necessary and a set of sufficient conditions for uniqueness of Filippov solutions. Also we will derive conditions under which every Filippov solution is a Carathéodory solution. These conditions will be shown to be sufficient to rule out the so-called Zeno (chattering) behavior. Finally, the paper closes with a comparison of the presented results to those obtained in [4] for linear relay systems and to those obtained in [5] and [6] for piecewise linear bimodal systems.

References

- [1] A. F. Filippov, "Differential equations with discontinuous righthand sides", Mathematics and Its applications, Prentice-Hall, Dordrecht, The Netherlands, 1988.
- [2] A. Bacciotti, "On several notions of generalized solutions for discontinuous differential equations and their relationships", Preprint of ICTP, Trieste, 2003.
- [3] J. Cortes, "Discontinuous dynamical systems-A tutorial on solutions, nonsmooth analysis and stability", IEEE Control Systems Magazine, 36-73, 2008.
- [4] A.Yu. Pogromsky, W.P.M.H. Heemels and H. Nijmeijer, "On solution concepts and well-posedness of linear relay systems", Automatica, 39, 2139-2147, 2003.
- [5] J. Imura and A.J. van der Schaft, "Characterization of well-posedness of piecewise linear systems", IEEE Transactions on Automatic Control, Vol. 45, No. 9, 1600-1619, 2000.
- [6] M.K. Camlibel, "Well-posed bimodal piecewise linear systems do not exhibit Zeno behavior", Proc. of the 17th IFAC World Congress on Automatic Control, Seoul, South Korea, 2008.

Compositional analysis for linear control systems

Florian Kerber, Arjan van der Schaft
 Institute for Mathematics and Computing Science
 University of Groningen
 P.O. Box 407
 9700 AK Groningen
 The Netherlands

Email: {f.j.kerber, A.J.van.der.Schaft}@rug.nl

1 Introduction

Complexity issues play an important role in many areas of science and engineering. Within computer science, the problem of verifying properties of programs involving concurrent processes is known to be computationally challenging due to the problem of state explosion. As a result, straightforward approaches to formal verification such as simulating all possible executions of a program usually fail. To deal with the inherent complexity, simulation relations were introduced by Milner [6]. Expressing both the program and the property in the same language – in the area of verification mostly as labeled transition systems – and then relating them by constructing a simulation relation ensures that the given system behavior matches the desired specification. To reduce the complex verification task for the overall system, compositional analysis techniques can be employed. The main idea of compositional reasoning is to decompose proof obligations for the whole interconnected system into obligations for components which computationally are more efficiently solvable. Complementary to compositionality is the idea of assume-guarantee reasoning which can be used when properties of individual components can not be verified directly ([7]). The key principle is to restrict the behavior of a subsystem to a specific environment by interconnecting it with a subsystem representing parts of the specification. Examples of compositional and assume-guarantee reasoning for labeled transition systems and hybrid systems can be found in the computer science literature, see e. g. [2] and [3].

The goal of the current research is to make compositional techniques applicable to analyze linear continuous-time systems. This is motivated by the fact that models of engineering systems have similar features as models of concurrent processes. Firstly, the number of state components is often large, e.g. for chemical plants, mechatronic systems or discretized PDE models. Secondly, interaction between subprocesses is characteristic for various control problems such as decentralized control where a global control target is solved by the interplay of local controllers and plant subsystems. Simulation relations for continuous-time systems can be described using geometric control theory, see [1], [8] and [10]. Moreover, they are used to abstract a system by a

lower-dimensional one, generally exhibiting nondeterministic behavior ([9]). In this work, simulations relate the given with the desired system model, both expressed as interconnections of linear continuous-time systems. Compositional and assume-guarantee reasoning then allows to replace the simulation relation of the interconnections by relations involving only less complex components of the overall system. Thus, properties can be checked with less computational effort. This theory extends results previously obtained for linear ([5]) and hybrid systems ([4]).

References

- [1] R. Alur, T. A. Henzinger, G. Lafferriere, and G. J. Pappas. Discrete abstractions of hybrid systems. *Proceedings of the IEEE*, 88:971–984, 2000.
- [2] G. Frehse. *Compositional Verification of Hybrid Systems using Simulation Relations*. PhD thesis, Radboud Universiteit Nijmegen, 2005.
- [3] T. A. Henzinger, S. Qadeer, and S. K. Rajamani. You Assume, We Guarantee: Methodology and Case Studies. In *CAV 1998*, pages 440–451, 1998.
- [4] F. Kerber and A. van der Schaft. Compositional and assume-guarantee reasoning for switching linear systems. In *Preprints of the Conference on Analysis and Design of Hybrid Systems*, pages 328 – 333, 2009.
- [5] F. Kerber and A. J. van der Schaft. Assume-guarantee reasoning for linear dynamical systems. In *European Control Conference*, August 2009.
- [6] R. Milner. *Communication and Concurrency*. Prentice Hall, 1989.
- [7] J. Misra and K. M. Chandy. Proofs of networks of processes. *IEEE Trans. Softw. Eng.*, 7(4):417–426, 1981.
- [8] G. J. Pappas. Bisimilar linear systems. *Automatica*, 39:2035–2047, 2003.
- [9] G. J. Pappas, G. Lafferriere, and S. Sastry. Hierarchically consistent control systems. *IEEE Transactions on Automatic Control*, 45(6):1144–1160, 2000.
- [10] A. J. van der Schaft. Equivalence of dynamical systems by bisimulation. *IEEE Transactions on Automatic Control*, 49(12):2160–2172, 2004.

Biological implications of global bifurcations

George A.K. van Voorn
 PRI Biometris,
 Droevendaalsesteeg 1, Building 107,
 6708 PB Wageningen
 george.vanvoorn@wur.nl

Bob W. Kooi
 Department of Theoretical Biology,
 Faculty of Earth & Life Sciences,
 Vrije Universiteit (A'dam)

1 Abstract

Bifurcation analysis is a powerful tool for the analysis of ODE-models with limited variables. Typically, a few parameters are selected for variation (so-called bifurcation parameters), after which it is evaluated how the qualitative behaviour of the system changes under these parameter variations (e.g. from stable steady state to limit cycle). Thusfar, these analyses have mostly been focussed on local phenomena, where the qualitative behavioural changes are coupled to bifurcations that can be found by evaluating the local state space (i.e. *Jacobian* matrix and its eigenvalues), so steady states and limit cycles.

In this research we have shifted the attention to bifurcations of orbits through state space, that cannot be found by means of the *Jacobian* matrix. Such orbits connect saddle equilibria and/or saddle cycles, known as *homo-* and *heteroclinic* orbits. The bifurcations of such orbits are named global bifurcations. Although their existence has been known for several decades already, the numerical techniques to actually detect and continue them as functions of parameters have only been developed quite recently, among them Beyn (1994), Champneys and Kuznetsov (1994), Dieci and Rebaza (2004). In collaboration with others we have developed new techniques, based on the adjoint *Jacobian* matrix, for the detection and continuation of point-to-cycle and cycle-to-cycle connecting orbits (Doedel et al., 2008, 2009). These techniques have been incorporated as extensions of the well-known bifurcation software package AUTO (Doedel et al., Concordia University).

With the coming of the technique, there is also room for interpretation of the obtained results of the application. In the presentation I will focus mainly on some ecological examples of the application of the newly developed techniques. It is found that these techniques give robust results, and give rise to re-interpretation of old model analyses. One specific and simple example is the Allee-model, where it is found that a limit cycle, in contrast to earlier claims, does exist, but is almost immediately destroyed again by a homoclinic bifurcation (Van Voorn et al., 2007). Finally, despite the ecological context, there is room for a broad application of the discussed techniques, for instance in Systems Biology.

References

- [1] W.-J. Beyn, On well-posed problems for connecting orbits in dynamical systems, In: *Chaotic Numerics (Geelong, 1993)*, volume 172 of *Contemp. Math.*, 131–168. Amer. Math. Soc., Providence, RI, 1994.
- [2] A. R. Champneys, Yu. A. Kuznetsov, Numerical detection and continuation of codimension-two homoclinic bifurcations. *Int. J. Bifur. Chaos*, 4:785–822, 1994.
- [3] L. Dieci and J. Rebaza, Point-to-periodic and periodic-to-periodic connections, *BIT Numerical Mathematics*, 44:41–62, 2004a.
- [4] E. J. Doedel, B. Oldeman, AUTO07P: *Continuation and Bifurcation software for ordinary differential equations*, Concordia University, Montreal, Canada, 2009.
- [5] E. J. Doedel, B. W. Kooi, G. A. K. van Voorn, Yu. A. Kuznetsov, Continuation of connecting orbits in 3D-ODE's: (I) Point-to-cycle connections. *Int. J. Bif. Chaos*, 18:1889–1903, 2008.
- [6] E. J. Doedel, B. W. Kooi, G. A. K. van Voorn, Yu. A. Kuznetsov, Continuation of connecting orbits in 3D-ODE's: (II) Cycle-to-cycle connections, *Int. J. Bif. Chaos*, 19:159–169, 2009.
- [7] G. A. K. van Voorn, L. Hemerik, M. P. Boer, B. W. Kooi, Heteroclinic orbits indicate overexploitation in predator-prey systems with a strong Allee effect, *Math. Biosci.*, 209:451–469, 2007.

Switch model ILC

Gang Xu

Tongji University, Shanghai, 201804
wolfgang.xu@gmail.com

Marnix Volckaert, Jan Swevers

PMA, KU Leuven, Celestijnenlaan 300B, 3001
marnix.volckaert, jan.swevers@mech.kuleuven.be

1 Introduction

Service load simulation are widely used in automotive engineering for durability test, NVH test and etc. The key technique behind is the road profile development, namely given the response signals at different reference points on the vehicle body, to derive the road profile input at the tire patch on the testrig, such that the outputs at the reference points match the response signals measured from track test drive as close as possible. This technique is often termed as RPC (Remote Parameter Control) or TWR (Time Waveform Replication), which employs ILC (Iterative Learning Control) in frequency domain[1] to accomplish the job.

$$U_{k+1}(j\omega) = U_k(j\omega) + G^{-1}(j\omega)E_k(j\omega) \quad (1)$$

with k the iteration index, $U_k(j\omega)$ the DFT of k^{th} iteration's input, $G(j\omega)$ the FRF matrix of the system and $E_k(j\omega)$ the DFT of k^{th} iteration's tracking error ($e_k = y_r - y_k$).

A new model inversion approach based on numerical optimization in time domain was developed for the system with a sudden change of the dynamics. Assuming the system before and after the switch time are both linear respectively, and of course results in two different linear models. The proposed method can switch the model properly for each part during the process of inversion. The following time domain ILC update law is used to refine the input signal.

$$u_{k+1}(t) = u_k(t) + Q_k[G^{-1}(y_r(t)) - G^{-1}(y_k(t))] \quad (2)$$

with $y_r(t)$, $y_k(t)$ the reference signal and the k^{th} iteration's output respectively, Q_k the k^{th} iteration's update scaling factor, G the model of the system (possibly nonlinear, or different linear models), the latter is the case that this paper mainly deals with.

2 Problem Formulation

Consider the following discrete time model of the system

$$\begin{cases} x(t+1) = f(x(t), u(t)) \\ y(t) = h(x(t), u(t)) \end{cases} \quad (3)$$

The inversion problem can be formulated as the following least square form

$$\min_{x,u} \|h(x,u) - y\|_Q + \|u(t+1) - u(t)\|_R \quad (4a)$$

s.t.

$$f(x(t), u(t)) - x(t+1) = 0 \quad \text{for } t = 0, 1, \dots, N-1 \quad (4b)$$

with Q and R the weighting matrix on the predict tracking error and the change of input respectively.

The Problem (4) can be solved by constrained Gauss-Newton methods[2]. Note that the design variable also include the states variable x of the system, which means it already contains an observer. This enable us to switch the model during the process of model inversion. In order to cope with two different models in the whole trajectory, we borrow the idea of moving horizon from MPC to split the whole trajectory into pieces (whose length is equal to the predicted horizon N_h), and solve each piece using the states information from the previous piece separately. Let's denote the change moment t_s , the system's model before t_s as *Model 1*, and after t_s as *Model 2* respectively, the whole process was depicted in Figure 1.

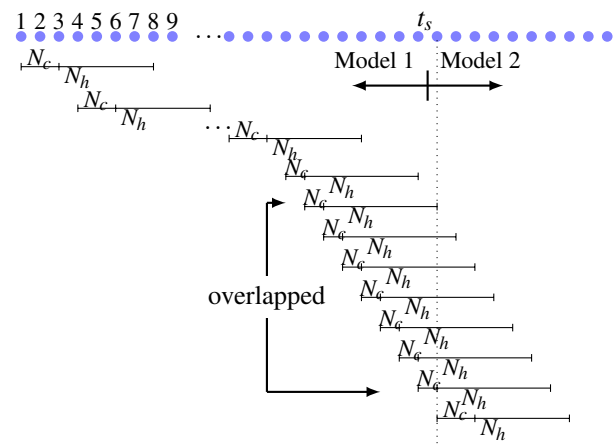


Figure 1: Moving horizon technique

3 Numerical and experimental validation

The proposed approach was validated numerically, the experimental validation is an ongoing programme. The results will be available in the near future.

References

- [1] Cryer B W, Nawrocki P E, Lund R A. A road simulation system for heavy duty vehicles. SAE 760361, 1976.
- [2] Nocedal J, Wright S J. Numerical Optimization. 2nd ed., New York, USA: Springer, 2006.

Xtreme Motion: Control of non-rigid body dynamics of a high precision positioning stage

R. Hoogendijk

Eindhoven University of Technology, Whoog -1.126

r.hoogendijk@tue.nl

Introduction

The trend in the semi-conductor industry is still prescribed by Moore's law which states that the resolution of chips will increase while the costs per functionality will decrease. To comply with this law, positioning systems of lithography machines need to become faster and more accurate. To make the system faster, higher accelerations are required. Newton's Laws prescribe that this can either be done by applying higher forces, or by reducing the weight of the system. The first option is less favorable, since stronger actuators consume more power and produce more heat, which deteriorates the performance of the system. An alternative to increase productivity of lithography machines is to increase the standard wafer diameter from the current 300 mm to 450 mm. But, both larger and lighter stages will be more flexible, which can interfere with the accuracy of the positioning system. This motivates research on the control of high precision flexible motion stages. This abstract discusses some of the challenges that will be faced in this research area.

1 Conventional controllers

Currently, most high precision motion systems are controlled using geometric decoupling and single-input-single-output (SISO) controllers. Assume that the goal of the controller is to achieve good performance at a certain point on the system, denoted by z . The measurement of the position of the system y is typically not performed at the location z , but since it is assumed that the system is rigid, a simple geometric transformation can be used to compute z from y . Moreover, by using geometric decoupling, it is even possible to compute z for all axes in the system separately.

2 Control of flexible motion stages

The approach of the previous section cannot be followed if the system is not rigid, but flexible. In flexible systems the performance z and the measurement y are no longer related via a static, but a dynamic relation. The control problem is visualized clearly by the standard plant formulation, as depicted in Figure 1. It shows that $y \neq z$. The derivation of a control signal to get performance at z using an input u based on a measurement y will be topic of research. Different control strategies such as inferential control modal control, H_∞ control will be investigated.

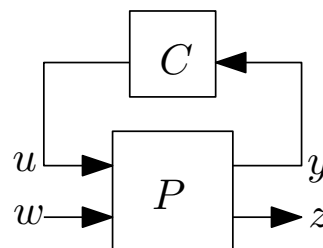


Figure 1: Standard plant system representation. The plant P is controlled with controller C , by applying an input u based on a measurement y . Note that the disturbances w and performance z are different from u and y .

Conventionally, there will be as much actuators in the system as there are rigid body modes. But the extra dynamics in the system will probably require more actuators than rigid body modes to suppress the internal dynamics. In this research, it will be studied, whether extra actuators can be used to improve the performance of the system. When the number of actuators is larger than the number of rigid body modes, the terminology *overactuated* or *non-rigid body control* is used.

The term *performance* has been mentioned a few times now, but presently it is even not clear yet what the performance needs to be for this system. This also depends on the chosen strategy. One approach could be to damp all internal dynamics. This would give a spatially distributed performance specification. An other approach could be to position the point of interest very accurately while the rest of the system is allowed to be in motion. This leads to a performance specification at a certain point on the geometry.

3 Conclusion

A few issues regarding the control of flexible high precision motion stages have been discussed. The key feature of these systems is that the control can no longer be done with decoupling and SISO controllers. The spatial distribution of the system and its internal dynamics have to be taken into account when the system is flexible.

Optimal Regenerative Braking with a Pushbelt CVT: an Experimental Study

Koos van Berkel¹, Theo Hofman¹, Bas Vroemen², Maarten Steinbuch¹

¹Department of Mechanical Engineering, Eindhoven University of Technology, Den Dolech 2, 5600 MB Eindhoven, The Netherlands.

²DriveTrain Innovations, Croy 46, 5653 LD Eindhoven, The Netherlands.

Email: (k.v.berkel, t.hofman, m.steinbuch)@tue.nl, vroemen@dtinnovations.nl

1 Introduction

Hybrid transmissions give a significant improvement in fuel economy as shown in many vehicles. However, current battery-based systems are relatively expensive, due to large battery packs and additional motor/generator(s). As a low-cost alternative, the "mecHybrid" project was initiated to develop a mechanical hybrid module using a flywheel system and a pushbelt Continuously Variable Transmission (CVT) instead. The topology is shown in Figure 1.

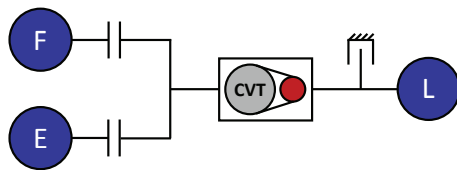


Figure 1: Hybrid topology with flywheel (F), engine (E), wheel load (L), CVT, clutches and brake.

This concept uses the CVT to energize the flywheel (F) with wheel load (L) during regenerative braking and to retrieve energy during flywheel driving. To make maximum use of the recuperation energy, the CVT should be controlled by changing the speed ratio such that the hybrid system is operated at the most efficient points [1].

2 Problem formulation

This study focuses on the approach and results of efficiency experiments on the CVT, under regenerative braking and flywheel driving conditions. The experimental results form a solid basis for future work on an efficiency model of the CVT, which is valuable for an Energy Management Strategy that makes optimal use of the recuperation energy.

3 Approach

Experiments are performed on a test rig with two electric motor/generators tracking prescribed speed and torque set-points, representing the flywheel and wheel load, see Figure 2. For the CVT, a controller is designed to track the prescribed speed ratio under flywheel conditions, i.e., with pos-

itive and negative powerflows. A velocity profile is chosen with constant velocities (30 and 50 km/h) and accelerations ($\pm 0.8 \text{ m/s}^2$) that are common in drive cycles, see Figure 3.

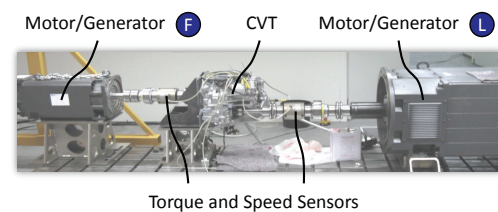


Figure 2: Test setup.

4 Experimental results and conclusions

The experimental results are shown in Figure 3. Observe that the CVT can be used very efficiently for regenerative braking, as the efficiency is relative very high during acceleration, medium vehicle velocity and deceleration. Based on these results it can be concluded that "mecHybrid" can be a promising design solution for efficient hybrid vehicle propulsion, which will be the focus for future research.

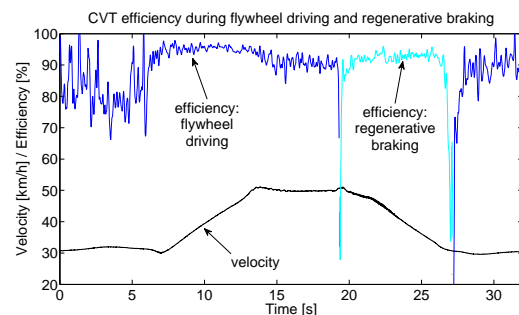


Figure 3: Transmission efficiency of a CVT during flywheel driving and regenerative braking.

References

- [1] Yeo, H., Wang, S., Kim, H., "Regenerative Braking Algorithm for a Hybrid Electric Vehicle with CVT Ratio Control," Proc. Inst. of Mech. Eng., Part D., Vol. 220, No.11, 2006, pp. 1589-1600.

Real-time Control of Industrial Batch Crystallizers: A Model-based Control Approach

Ali Mesbah

Delft Center for Systems and Control
Delft University of Technology
Mekelweg 2, 2628 CD Delft
The Netherlands

Email: ali.mesbah@tudelft.nl

Herman J.M. Kramer

Process and Energy Laboratory
Delft University of Technology
Leeghwaterstraat 44, 2628 CA Delft
The Netherlands

Email: h.j.m.kramer@tudelft.nl

Adrie E.M. Huesman

Delft Center for Systems and Control
Delft University of Technology
Mekelweg 2, 2628 CD Delft
The Netherlands

Email: a.e.m.Huesman@tudelft.nl

Paul M.J. Van den Hof

Delft Center for Systems and Control
Delft University of Technology
Mekelweg 2, 2628 CD Delft
The Netherlands

Email: p.m.j.vandenhof@tudelft.nl

Batch crystallization is a key separation and purification step in the pharmaceutical, food, and fine chemical industries, with a significant impact on the efficiency and profitability of the overall process. In view of the fierce economic competition between the companies manufacturing high value-added crystalline products, there is an ever-increasing interest in optimal operation of batch crystallization processes in order to boost the process productivity, while satisfying the stringent market-driven product quality requirements.

In recent years, the advent of process analytical technology in addition to the development of computationally powerful modeling and optimization tools have paved the way for on-line model-based control of batch crystallizers. The model-based control approach allows seeking a trade-off between the conflicting product quality and process productivity considerations, while honoring various operational constraints.

This work presents a generic nonlinear model-based control approach for optimal operation of industrial seeded batch crystallizers. As the cornerstone of the control approach, the population balance modeling framework in its most general form enables the application of the controller to a wide range of industrial batch crystallization systems. In order to ensure the viability of the model-based controller for real-time implementations, the direct multiple shooting optimization strategy is adopted to transform the optimal control problem into a nonlinear programming problem with special structure that can be efficiently solved by state-of-the-art large-scale nonlinear optimization solvers. The underlying population balance model is solved by a high order finite volume method in combination with a flux limiting function. While possessing a relatively low computational burden, the numerical scheme is well capable of resolving the sharp discontinuities and steep moving fronts commonly encountered in simulation of seeded batch crystallization processes.

The model-based control approach has been applied to a semi-industrial fed-batch evaporative crystallizer. Simulation results reveal that the performance of the controller is largely dependent on the coarseness of the finite volume grid mesh adopted for discretization of the population balance equation. A coarse grid mesh typically gives rise to structural plant-model mismatch that may significantly deteriorate the effectiveness of the controller in terms of the reference trajectory tracking. In order to eliminate the adverse effect of the structural model imperfection, the performance objective function of the optimal control problem has been modified such that the discrepancy between the predicted value of the controlled process variable, i.e. crystal growth rate, and its measured value inferred from the concentration measurements is accounted for. This in turn avoids product quality degradation, as well as loss in the batch productivity. Furthermore, to be able to effectively diminish the detrimental effects of parametric model imperfection and process uncertainties on the performance of the model-based control approach, the controller has been implemented in an output feedback fashion where a moving horizon estimator is utilized to recursively estimate the system states based on the available on-line measurements. The simulation results clearly show that the output feedback application of the control approach restores the efficacy of the optimal profiles in the presence of process uncertainties. Effective fulfillment of the crystal growth rate constraint in the latter case leads to increased production of larger crystals with the desired product quality attributes. The performance of the model-based control approach has also been experimentally validated on the semi-industrial fed-batch evaporative crystallizer. It is shown that that real-time application of the control architecture leads to a substantial increase in the batch productivity, while preserving the product quality requirements.

Badminton playing robot - a multidisciplinary test case in mechatronics

Julian Stoev PhD.

Email: julian.stoev@fmtc.be

Steven Gillijns PhD.

Email: steven.gillijns@fmtc.be

Andrei Bartic PhD.

Email: Andrei.Bartic@fmtc.be

Wim Symens PhD.

Email: Wim.Symens@fmtc.be

Flanders Mechatronics Technology Centre (FMTC)
Celestijnenlaan 300d - bus 4027, 3001 Heverlee, Belgium

1 Introduction

A particular challenge in the Mechatronics is the integration of diverse technologies from different areas of engineering and science.

We present a design of a badminton playing robot. The robot integrates several distinct and inter-operating sub-systems. The subsystems in question are dealing with visual recognition of the flying shuttle, estimation of its trajectory and possible interception points, moving the robot to the interception point and performing the interception hit.

Mechanical design of the robot and embedded hard real-time and soft real-time system programming on distributed computing platforms are also an important part of the realization.

2 The visual system

The visual system has two high-definition black and white cameras with sampling rate of 100Hz. These cameras provide sufficient resolution and information to detect the probable locations of the flying shuttle. The related optical distortions are compensated and the cameras are calibrated to measure accurately the positions of objects. A visual detection algorithm was designed, which is able to localize the fast moving shuttle.

3 The trajectory estimation and interception system

Using the data from the visual system, the probable trajectory is estimated and a point on the trajectory is chosen where the interception should occur. The estimation of the trajectory is performed using an extended Kalman filter which is based on a simplified analytical model of shuttlecock motion that includes drag, but neglects lift and spin. The initial estimates are approximate, but converge rapidly and can be used to predict the motion of the shuttlecock with the required accuracy. This prediction is used to analyze and propose reachable interception points taking into account the current coordinates of the robot and its acceleration and speed limitations.

4 Actuation system

The actuation system receives the target coordinates of the interception point and positions the robot at the location where the hit motion should happen. The main challenge is due to the very limited time for this move and the high degree of uncertainty especially at the beginning of the move when the shuttle trajectory is not known well. Thus the motion trajectory should be time-optimal, but in the same time it should be computed on the fly, as the motion occurs and should be able to accommodate the latest information propagated through the visual, trajectory estimation and interception parts. The motion controller should be able to take into account and compensate disturbances that are due to nonlinear coupling between axes and the approximate modeling of mechanical parts. In the same time it is required to be sufficiently simple to be implementable to the real hardware in real time.

5 Mechanical design

The mechanical design of the robot was very challenging due to the extremely high acceleration requirements. Several alternative mechanical configurations were analyzed during the concept phase. Some of them were rejected, some of them may be implemented on the later stages of the project.

6 Software

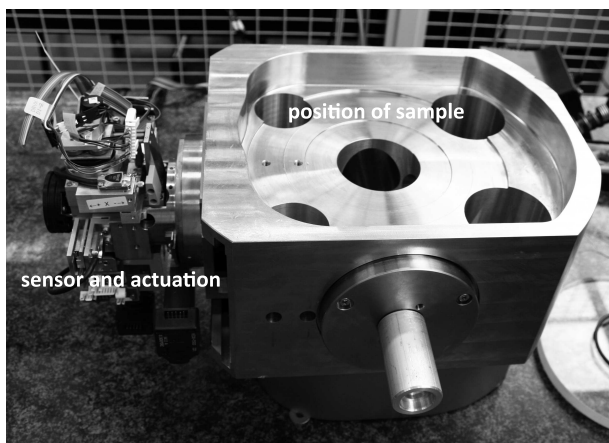
The diversity of sub-systems is reflected in the soft-wares used. It is very difficult to find a single vendor, who can provide end-to-end solutions for all the requirements set forward by the different tasks. Also, the computational load is quite significant. Thus the system is divided on several computing platforms. Special effort is made to keep the costs low, while extracting maximum performance.

Detection of Nonlinearities in Industrial Motion Stages

David Rijlaarsdam^{*†}, Pieter Nuij^{*} and Maarten Steinbuch^{*}
^{*} dept. Mechanical Eng. (Eindhoven University of Technology)
[†] dept. ELEC (Free University of Brussels)
 Den Dolech 2, P.O. Box 513
 5612 AZ Eindhoven, The Netherlands
 Email: d.j.rijlaarsdam@tue.nl

1 Introduction

Detection and classification of nonlinearities in motion systems becomes of increasing importance with high demands on (closed loop) performance. This contribution¹ illustrates and compares two methods used to detect and classify nonlinearities. The results are illustrated by utilizing the discussed methods to identify the dynamics of a high precision industrial motion stage as depicted below.



2 Abstract

In this contribution two methods are compared that aim to measure both the linearized dynamics and the influence of nonlinearities. First, a broadband signal is used to measure a linear approximation of the systems dynamics. This method uses multisine signals [3] with identical amplitude spectrum, but randomly distributed phases [4]. Averaging over multiple periodic responses to the same signal and over multiple realizations of the random phase multisine allows the computation of the level of nonlinearities and external disturbances separately. This yields both a linear approximation of the systems dynamics and the amount of nonlinear 'disturbance' as a function of frequency. Second, single sine based measurements are used to measure the Higher Order Sinusoidal Input Describing Functions (HOSIDF) [1, 2] of

the system under test. HOSIDFs describe the response of the system by describing not only the 'direct' response (gain and phase shift) of the system at the input frequency, but by describing the response at higher harmonics of the input frequency as well. This yields a quantitative measure of the power generated by nonlinearities at harmonics of the input frequency as a function of this frequency and the signal amplitude. In this contribution these methods are utilized to acquire a non-parametric model for an industrial high precision stage. The effects of and sources for nonlinear influences are discussed for this particular case as well.

References

- [1] Nuij, P.W.J.M., O.H. Bosgra, M. Steinbuch (2006). Higher-order sinusoidal input describing functions for the analysis of non-linear systems with harmonic responses, *Mechanical Systems and Signal Processing*, vol. 20, pp. 1833–1904.
- [2] Nuij, P.W.J.M., M. Steinbuch, O.H. Bosgra (2008). Measuring the higher order sinusoidal input describing functions of a non-linear plant operating in feedback, *Control Engineering in Practice*, vol. 16, pp. 101–113.
- [3] Pintelon, R., J. Schoukens (2001). *System identification: a frequency domain approach*, IEEE Press Piscataway, NJ, (ISBN 0-7803-6000-1).
- [4] Pintelon, R., G. Vandersteen, L. De Locht, Y. Rolain, J. Schoukens (2004). Experimental characterization of operational amplifiers: a system identification approach, *IEEE Trans. Meas. Instr.*, vol. 53, no. 3, pp. 854–867.

¹This work is carried out as part of the Condor project, a project under the supervision of the Embedded Systems Institute (ESI) and with FEI company as the industrial partner. This project is partially supported by the Dutch Ministry of Economic Affairs under the BSIK program.

Identification of Linear, Periodically Time-Varying Systems

Ebrahim Louarroudi*, John Lataire* and Rik Pintelon*

*Department ELEC, Vrije Universiteit Brussel, Belgium, e-mail: elouarro@vub.ac.be

1 Introduction

In some applications the considered real-life systems do not satisfy the time invariant condition. For that reason it is convenient to extent the framework of LTI-systems to systems that might evolve over time. There exist a wide range of applications where the treatment of time-varying systems is indispensable (e.g. flight flutter analysis, pitting corrosion in metals, periodically time-varying robot, etc.). When the time variation is forced experimentally one can choose between periodically, arbitrary (non-periodically) or hold (piecewise constant variation) configurations for the external (scheduling) parameter(s). This article deals only with imposed external scheduling parameters that are periodically varying over time; we talk about Linear Periodically Time-Varying (LPTV) systems. These kinds of systems that will be discussed in this paper can be described by linear, SISO (single-Input, Single-Output), lumped, continuous time, ordinary differential equation with periodically time dependent parameters:

$$\sum_{n=0}^{N_a} a_n(t) \frac{d^n y_o(t)}{dt^n} = \sum_{n=0}^{N_b} b_n(t) \frac{d^n u_o(t)}{dt^n} \quad (1)$$

with $u_o(t)$ & $y_o(t) \in \mathbb{R}$ respectively the undisturbed input and output time signals. The periodically time-varying parameters $a_n(t)$ & $b_n(t)$ in eq. (1) are approximated by means of Fourier series (multisines, [1]).

2 Frequency Domain Description

Contrary to most current identification methods that are yet available [2], the identification will be performed in the frequency domain (as in [1]). During the experiment design we assume that the excitation signal and the periodically scheduling parameters are synchronized such that the transformation to the frequency domain can be done without leakage and aliasing errors. If this assumption is made, then eq. (1) could be transformed by Fourier transform properties and hence eq. (1) becomes:

$$\begin{aligned} \sum_{n=0}^{N_a} \sum_{k=-N_{k_a}}^{+N_{k_a}} A_{n,k}(\Omega_l - k\Omega_0)^n Y_T(\Omega_l - k\Omega_0) \\ = \sum_{n=0}^{N_b} \sum_{k=-N_{k_b}}^{+N_{k_b}} B_{n,k}(\Omega_l - k\Omega_0)^n U_T(\Omega_l - k\Omega_0) \end{aligned} \quad (2)$$

where $U_T(\Omega_l)$ & $Y_T(\Omega_l)$ denotes respectively the windowed, sampled input-output spectra defined at the discrete frequencies $\Omega_l = j \frac{2\pi(l+1)}{T}$ with T the length of the (measured) rectangle time window. The spectra in eq. (2) can exactly be replaced by the Discrete Fourier Transform (DFT) if the assumption mentioned above is valid. The time-invariant system parameters $A_{n,k}$ & $B_{n,k}$ in eq. (2), which appear in their

Fourier series representations, are the periodic coefficients of the periodically time-varying parameters $a_n(t)$ & $b_n(t)$.

3 System Response

From eq. (2) the system response can easily be obtained if the system parameters ($A_{n,k}$ & $B_{n,k}$) and the excitation spectrum $U_T(\Omega_l)$ (multisine, [1]) are known. A simulation example of how the response of a LPTV-system in the frequency domain looks like, is depicted in Fig. 1.

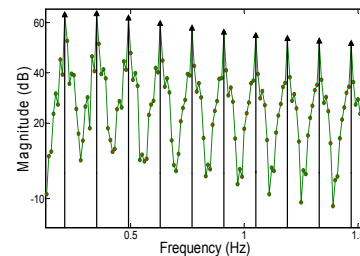


Fig. 1. This figure shows the output spectrum of a LPTV-system. The excited lines are indicated by the black arrows.

As we can see from Fig. 1, the main contribution of the spectrum is concentrated around the excited lines, but there is still energy present between the adjacent lines. These *skirt-like* signals are due to the (shifted) periodic coefficients ($A_{n,k}$ & $B_{n,k}$) (i.e. normalized spectrum of the system parameters) in eq. (2).

4 Goal

The identification will be done in the frequency domain within an errors-in-variables framework. One attempts to find the periodic coefficients ($A_{n,k}$ & $B_{n,k}$) in such way that model (2) matches the deterministic part of the system as well as possible, so that the noise is eliminated as much as possible. A frequency domain simulator will also be built to solve the model (2) efficiently without making any use of time integration solvers. The simulator will be used to validate the estimated model. The identification algorithms will be applied later on simulations and real-life systems.

References

- [1] Lataire J. en Pintelon R., 2008, Frequency Domain Identification of Linear, Deterministically Time-Varying Systems, Proceed IFAC, World Congress, pp. 11474-11479.
- [2] Niedzwiecki M. (2000) – *Identification of Time-varying Processes* – J. Willey & Sons.

Frequency Domain Total Least Squares Estimator of Time-Varying Systems

John Lataire and Rik Pintelon

Vrije Universiteit Brussel, Pleinlaan 2, 1050 Brussels, Belgium, e-mail: jlataire@vub.ac.be

1 Introduction

In many engineering applications the assumption of time invariance is not fulfilled. Consider for instance the identification of the resonance frequency and the damping of the wings of a plane. These are functions of the flight speed and the height and, thus, are time-varying while flying. The ability of identifying time-varying models on these kinds of systems is more than welcome.

Contrary to most previous works (e.g. [3]), frequency domain methods are used. These have proven their usefulness in system identification for the efficient selection of a desired frequency band of interest and the immediate identification of continuous-time linear models from sampled data in a band-limited measurement setup [1].

2 Problem formulation

The considered systems are assumed to fulfil a linear ordinary differential equation (ODE) with time-varying coefficients:

$$\sum_{n=0}^{N_\alpha} \alpha_n(t) \frac{d^n y(t)}{dt^n} = \sum_{n=0}^{N_\beta} \beta_n(t) \frac{d^n u(t)}{dt^n} \quad (1)$$

where $u(t)$ and $y(t)$ are the input and output signals respectively. Both $\alpha_n(t)$ and $\beta_n(t)$ are real valued piecewise polynomials in the time t and are responsible for the time varying character of the system. They are modelled as linear combinations of Legendre polynomials in t . The dynamics of the system are modelled as linear combinations of Legendre polynomials in s (the Laplace variable).

The identification problem consists of estimating the system parameters, namely the coefficients of these Legendre polynomials. The cost function chosen is the sum of the squared absolute values of the difference between the left hand side and the right hand side of (1), after conversion to the frequency domain. It will be shown how the regression matrix of the resulting linear total least squares (TLS) cost function can be computed very

easily by using discrete Fourier transform algorithms. The resulting leakage errors are taken care of.

The advantage of using Legendre polynomials instead of modelling the dynamics as combinations of simple monomials in s is that the energy of the first is nicely spread over the whole frequency band. This circumvents the drawback that higher weights are given to the higher frequency bands when using simple monomials as basis functions [2] and, thus, usually gives better estimates. This is illustrated on a simulation example in Fig. 1. The mean error on the estimated instantaneous transfer function when using Legendre polynomials (black dashed line) is about 15 dB smaller than the error when using monomials (grey dashed line), especially at the low frequencies. Before running the estimator, both the input and the output signals were corrupted by coloured noise. The signal-to-noise ratio was 25dB.

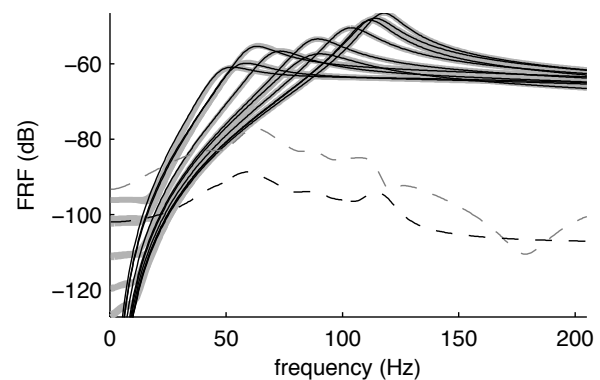


Figure 1: Simulation Results. Full thin black line: *actual* instantaneous transfer function. Full thick grey line: *estimated* instantaneous transfer function. Black dashed line: mean error when using Legendre polynomials as basis functions. Grey dashed line: mean error when using simple monomials as basis functions.

References

- [1] Hugues Garnier and L. Wang. *Identification of Continuous-time Models from Sampled Data*. Springer, London, 2008.
- [2] R. Pintelon and J. Schoukens. *System Identification – A frequency domain approach*. IEEE Press, Piscataway, 2001.
- [3] R. Toth, P.S.C. Heuberger, and P.M.J. Van den Hof. Asymptotically optimal orthonormal basis functions for LPV system identification. *Automatica*, 45(6):1359–70, June 2009.

Acknowledgement - This work was supported in part by the Fund for Scientific Research (FWO-Vlaanderen), by the Flemish Government (Methusalem Fund, METH1), and by the Belgian Federal Government (IUAP VI/4). J. Lataire's work was supported by the Research Foundation – Flanders (FWO) under a Ph. D. fellowship.

Frequency domain identification of Output Error models in Matrix Fraction Description

R. S. Blom ^{a,b,*}(r.s.blom@tudelft.nl), P. M.J. Van den Hof ^a, H.H. Langen ^b, R.H. Munnig Schmidt ^b

^a Delft Center for Systems and Control, ^b Precision and Microsystems Engineering

Delft University of Technology

1 Introduction

In this presentation, we will address the following MIMO identification problem. The objective is to identify an Output Error (OE) model in matrix fraction description (MFD) for a MIMO plant. This plant is unstable and has high order dynamics, including very lightly damped resonances. Excitation signals must be kept small to avoid non-linear distortions. Consequently, the signal-to-noise ratio (SNR) is limited.

From the characteristics of the problem, we derive the following constraints for the identification approach. First, due to the unstable nature of the plant, the identification experiments need to be performed in a stabilizing closed-loop. Second, in order to compensate for the limited SNR, large data sets need to be created. Careful experiment design is needed to allow data set reduction while achieving optimal noise reduction. Last, the model set selection results in a high-order non-linear optimization problem. An iterative scheme is needed that ensures optimality upon convergence.

2 A two-step frequency domain approach

A two-stage frequency domain approach to this problem will be presented. In the first stage, the objectives are to deal with the closed-loop nature and to achieve a large reduction of the data set. This is realized by non-parametric estimation of the multivariable Frequency Response Function (FRF) of the open-loop plant. Hereto the closed-loop is excited with orthogonal random-phase multisine signals, which results in estimates of the FRF with least variance compared to other common excitation signals [1]. Using the excitation as instrumental variable, an estimate of the FRF can be obtained that is asymptotically unbiased.

Let $\{G(j\omega_k)\}$, $k = 1..N$ denote the estimated FRF of the open-loop plant. The objective in the second step is to find the parameter vector θ minimizing the OE cost criterion

$$V(\theta) = \sum_{k=1}^N \|W(\omega_k) * (G(j\omega_k) - B(j\omega_k, \theta)A^{-1}(j\omega_k, \theta))\|_F^2$$

Here, the model is represented in right-MFD; a similar expression can be given for model representations in left-

This research is supported by MicroNed and the Delft Center for Mechatronics and Microsystems.

MFD. The cost is Schur-weighted with weighting function $W(\omega_k)$. For the weighting, estimates of the variance of the FRF are used, which can be computed using the periodic nature of the excitation. The frequency grid $\{\omega_k\}$, $k = 1..N$ is chosen such to have high density at the relevant frequency ranges.

A well-known iterative approach to minimize the nonlinear cost function $V(\theta)$ was first formulated by Sanathanan and Koerner [2]. A disadvantage of this approach is that in general convergence of the iterations does not imply minimization of $V(\theta)$, which inevitably leads to modeling errors. To overcome this, an alternative procedure is used, which ensures optimality upon convergence. This algorithm is known for time-domain identification (SRIV), and was formulated for frequency domain identification in [3]. Here we generalized this formulation to MIMO identification of models in matrix fraction description. The iterative algorithm involves computation of a linearization of $\frac{\partial}{\partial \theta} V(\theta)$ at estimate θ_k , which is equated to zero to find θ_{k+1} .

3 Results

This approach is applied to a high-speed micro-milling AMB spindle yielding favorable results. A total number of ± 126 mln samples is measured in step 1, and used to compute an estimate of the 4×4 open-loop FRF matrix at 858 frequencies. A total number of 288 parameters is estimated in step 2, yielding a parametric model that has very good correspondence to the estimated non-parametric FRF in all relevant frequency areas. Comparison of the pole locations of the estimated model to those of a first principles model reveals a similar structure, indicating the validness of the approach.

References

- [1] T. Dobrowiecki, J. Schoukens, P. Guillaume (2006). Optimized Excitation Signals for MIMO Frequency Response Function Measurements. *IEEE Trans. Instrum. Meas.*, Vol. 55, No. 6, 2072-2079.
- [2] C. Sanathanan, and J. Koerner (1963). Transfer function synthesis as a ratio of two complex polynomials. *IEEE Trans. Autom. Control*, AC-8, 56-58.
- [3] P. M. J. Van den Hof, and S. G. Douma (2008). An IV-based iterative linear regression algorithm with optimal output error properties. *DCSC Technical report* nr. 09-018, Delft University of Technology.

Higher Order Cumulant Based Blind Channel Identification: Enhanced Line Search Solutions

I.Yu. Domanov

Group Science, Engineering and Technology, KULeuven Campus Kortrijk, Belgium
Department of Electrical Engineering ESAT/SCD, KULeuven, Belgium
ignat.domanov@kuleuven-kortrijk.be, ignat.domanov@esat.kuleuven.be

L. De Lathauwer

Group Science, Engineering and Technology, KULeuven Campus Kortrijk, Belgium
Department of Electrical Engineering ESAT/SCD, KULeuven, Belgium
lieven.delathauwer@kuleuven-kortrijk.be, lieven.delathauwer@esat.kuleuven.be

1 Abstract

Numerous Finite Impulse Response (FIR) system identification methods have been proposed in the literature on blind system identification. These methods are widely used in many signal processing applications such as channel equalization in data communication, time delay estimation, array processing, source separation, etc. An important family of blind equalization algorithms identify a communication channel model based on fitting higher order cumulants. An interesting property of high order statistics (HOS) techniques is that they are insensitive to additive colored Gaussian noise. HOS based methods are very useful in dealing with non-Gaussian and/or nonminimum phase linear systems. HOS-based methods pose a nonlinear optimization problem that can be reformulated [1] in terms of the computation of the Canonical or Parallel Factor Decomposition (CANDECOMP/PARAFAC) of a 3rd-order tensor composed of 4th-order output cumulant values.

This 3rd-order tensor has certain symmetry properties, and its factors in the PARAFAC decomposition have a Hankel structure.

The algorithms used to find the PARAFAC decomposition are most often based on alternating least squares (ALS) initialized by either random values or values calculated by a direct trilinear decomposition based on the generalized eigenvalue problem. ALS has two main drawbacks. First, ALS may take a long time to converge. Second, ALS does not preserve the symmetry properties of the original tensor.

Recently, it has been shown [2, 3] that ALS-based PARAFAC algorithms can be significantly improved by applying an enhanced line search (ELS) procedure. Namely, new ELS algorithms are less sensitive to local optima and have higher convergence speed. Furthermore, ELS can be combined with any search direction (not necessarily the ALS direction).

On the other hand, a single-step least-squares (SS-LS) al-

gorithm has recently been proposed [1] to solve the problem. This algorithm preserves the symmetry of the tensor that we need to decompose but it does not necessarily converge monotonically.

We compute the PARAFAC decomposition by means of an ELS algorithm. This method converges monotonically. It preserves the symmetry and the Hankel structure. We derive an explicit solution for the optimal complex step. We compare the computation of the optimal complex step with alternating between updates of the real and imaginary part of the step. Our new algorithm is more accurate and more stable than the SS-LS algorithm.

References

- [1] Fernandes Carlos Estêvão R.; Favier Gérard; Mota João Cesar M. Blind channel identification algorithms based on the Parafac decomposition of cumulant tensors: The single and multiuser cases. *Signal Processing*, Volume 88, Issue 6 (2008), 1382-1401.
- [2] Nion Dimitri; De Lathauwer Lieven. An enhanced line search scheme for complex-valued tensor decompositions. Application in DS-CDMA. *Signal Processing*, Volume 88 (2008), Issue 3, 749-755.
- [3] Rajih, Myriam; Comon, Pierre; Harshman, Richard A. Enhanced line search: a novel method to accelerate PARAFAC. *SIAM J. Matrix Anal. Appl.* 30 (2008), no. 3, 1128–1147.

Model reduction as an identification problem

S.K.Wattamwar¹Siep Weiland¹Ton Backx¹

Many large scale (chemical) processes which are function of more than one independent variable (e.g. space and time) are modeled by Partial Differential Equations (PDE). These (full order) process models are solved by different numerical tools (often, CFD) which rely on discretization of the underlying spatial and the temporal domain. Such solution technique inherently lead to a large number of Ordinary Differential Equations (ODEs) (sometimes upto 10^{6-8}) which need to be solved at each time instance. The full order process models are reliable representation of the underlying process, but their large state dimension makes it difficult to simulate them by using ordinarily configured PC in real time. Therefore model reduction or model approximation is a necessary step. Model approximation is motivated by the possibility to get rid of the (full order) modeling redundancy. There are different objectives which are aimed at determining an approximate process model, e.g. reduction of complexity and the state dimension, maintaining the accuracy, approximation of process nonlinearity, preserving the invariant system properties, possibility of the extension of the notions from the linear system theory to the resulting model, applicability to be used in closed loop with a controller and an optimizer, applicability of the methods to different physical processes without much insight into the underlying physics, usability of the model approximation techniques in the form of generic toolbox, etc.

Among different model approximation techniques, identification type of model approximation techniques hold lot of promises. Some of the identification based model approximation methods are presented in [1] and the references therein. The identification based approximation methods extensively use the availability of the states of the full order model to infer the data based approximate models. The methods proposed there rely on the full order model as a simulator. Process simulators which are based on first principle (conservation laws) models, are often used in the chemical process industry. Such process simulators give dynamic evolution of the states but do not give access to the governing model equations. The identification methods are based on the separation of the fast from the slow dynamic patterns and subsequent identification of the lower dimensional models to approximate the dynamic evolutions of the dominant temporal patterns. The method of spectral decompositions can be used to infer separate the spatio-temporal patterns.

The identification based methods treats the full order model

¹Department of Electrical Engineering, Eindhoven University of Technology, P.O. Box 513, 5600 MB Eindhoven, The Netherlands, E-mail: s.wattamwar@tue.nl.

as the plant and use the notions from the field of system identification to identify the reduced order models. Notions from the system identification field like design of input signals, design of experiments, parameter estimations, form of a model structure etc. are very useful to infer computationally efficient reduced order models. In particular, approximate models of structure- LTI, LPV and tensorial (multi-variable polynomial) are proposed. The resulting models are validated on large scale benchmark examples of industrial tubular reactor and glass manufacturing process. The possibility to approximate the process nonlinearities makes the method attractive. The proposed idea should be able to apply to other applications from the chemical process industry.

The identification approach to model reduction is relatively new and many things still need to be done in coming future. For example, the model quality assessment, minimization of the mismatch between the actual process and the reduced model, validation of the proposed methods on different processes belonging to different model class needs to be carefully analyzed.

Acknowledgement

This work has been supported by the Eindhoven University of Technology and the European union within the Marie-Curie Training Network PROMATCH under the grant number MRTN-CT-2004-512441.

References

- [1] S. Wattamwar, "Identification of low order models for large scale processes", PhD thesis, Eindhoven University of Technology, 2010.

POD model reduction of multi-variable distributed systems

Femke van Belzen

Department of Electrical Engineering
 Eindhoven University of Technology
 P.O. Box 513, 5600 MB Eindhoven
 The Netherlands
 Email: f.v.belzen@tue.nl

Siep Weiland

Department of Electrical Engineering
 Eindhoven University of Technology
 P.O. Box 513, 5600 MB Eindhoven
 The Netherlands
 Email: s.weiland@tue.nl

Multi-variable distributed systems are described by sets of coupled Partial Differential Equations (PDEs) in several scalar- and vector-valued physical variables. Systems like these occur frequently in different fields of science and engineering, including fluid dynamics, electromagnetics and chemistry. Trajectories of these kinds of systems can usually only be obtained using Finite Element Methods on fine grids, leading to models that have very large simulation times. To reduce the simulation times a model reduction strategy can be used.

Model Reduction

Proper Orthogonal Decompositions (POD) is the only model reduction technique that is suitable for the class of systems under consideration in this abstract. When using POD model reduction for multivariable systems there is freedom in the choice of spectral expansion [1]. One can use single-variable expansions, where every physical signal has its own spectral expansion and set of basis functions. Alternatively, one can use lumped-variable expansions where the physical variables are stacked into a vector giving one set of vector-valued basis functions. For a vector of physical variables $\underline{s}(x, t) \in \mathbb{R}^n$ at position $x \in \{x_1, \dots, x_{N_X}\}$ and time t the expansions are

$$\begin{aligned} s_1(t) &= \sum_{k=1}^{N_X} a_k^{(1)}(t) \varphi_k^{(1)} \\ &\vdots \\ s_n(t) &= \sum_{k=1}^{N_X} a_k^{(n)}(t) \varphi_k^{(n)} \end{aligned} \quad \underline{s}(t) = \begin{pmatrix} s_1(t) \\ \vdots \\ s_n(t) \end{pmatrix} = \sum_{k=1}^{n \cdot N_X} b_k(t) \xi_k \quad (1)$$

where $\{\varphi_1^{(\ell)}, \dots, \varphi_{N_X}^{(\ell)}\}$ forms an orthonormal basis for \mathbb{R}^{N_X} for $1 \leq \ell \leq n$ and $\{\xi_1, \dots, \xi_{n \cdot N_X}\}$ forms an orthonormal basis for $\mathbb{R}^{n \cdot N_X}$. In the single-variable case, basis functions are computed through the SVD of a snapshot matrix for each of the physical variables separately, see Fig. 1 (left). In a lumped-variable approach, the basis functions are computed through a SVD of a large matrix in which the snapshot data for each of the physical variables has been stacked, see Fig. 1 (middle).

We propose an alternative to these spectral expansions by placing the snapshot data in a multidimensional array and using a tensor SVD to compute basis functions, see Fig. 1

(right). The spectral expansion becomes

$$\underline{s}(t) = \sum_{k=1}^{N_X} \begin{bmatrix} c_k^{(1)}(t) \\ \vdots \\ c_k^{(n)}(t) \end{bmatrix} \varphi_k. \quad (2)$$

where $\{\varphi_1, \dots, \varphi_{N_X}\}$ again forms an orthonormal basis for \mathbb{R}^{N_X} . This orthonormal basis can be computed using a tensor SVD [2].

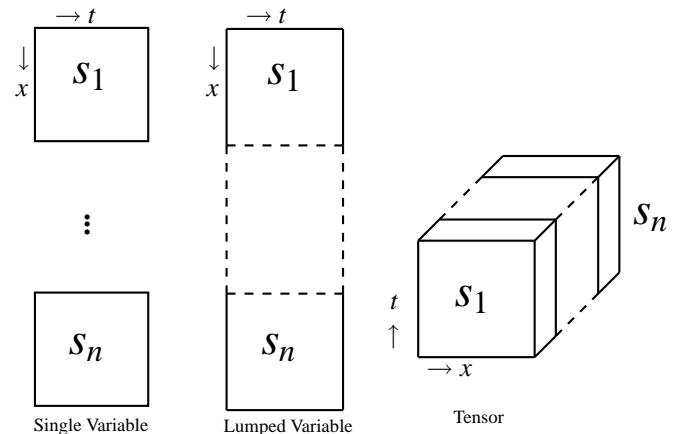


Figure 1: Overview of different approaches, t denotes time and x denotes position.

Conclusions

In the presentation the techniques discussed in this abstract will be applied to a benchmark example to examine their performance. The different strategies will be compared with respect to robustness, computational efficiency and sensitivity to scaling of the physical variables.

References

- [1] C.W.Rowley et al., “Model reduction for compressible flows using POD and Galerkin projection,” *Physica D*, 2004.
- [2] L. De Lathauwer et al., “A multilinear singular value decomposition,” *SIAM J. Matrix Anal.Appl.*, 2000.

Closed-loop Model Reduction for Controller- and Observer Design

Mark Mutsaers

Department of Electrical Engineering
Eindhoven University of Technology
P.O. Box 513, 5600MB Eindhoven
The Netherlands

E-mail: M.E.C.Mutsaers@tue.nl

Siep Weiland

Department of Electrical Engineering
Eindhoven University of Technology
P.O. Box 513, 5600MB Eindhoven
The Netherlands

E-mail: S.Weiland@tue.nl

1 Motivation

The synthesis of low-order controllers or low-order observers that are designed from models often follow either of the following two popular design strategies, as illustrated in Figure 1:

1. A controller or observer synthesis on the basis of a low-order plant that is obtained by applying a popular model reduction technique on the plant model.
2. A controller or observer synthesis on the basis of the full-order plant followed by a popular model reduction technique on the controller.

We refer to these as “reduce-then-optimize” and “optimize-then-reduce” strategies, respectively. Although both techniques lead to low-order controllers and observers, a major disadvantage is the lack of guarantees that can be given on closed-loop performance, stability and robustness.

Indeed, the apparent disconnect between model reduction strategies and optimal synthesis procedures may actually cause control relevant dynamics to be discarded in the model reduction process of either plant or controller. Therefore we propose to use a “direct” approach, which preserves these desired closed-loop properties.

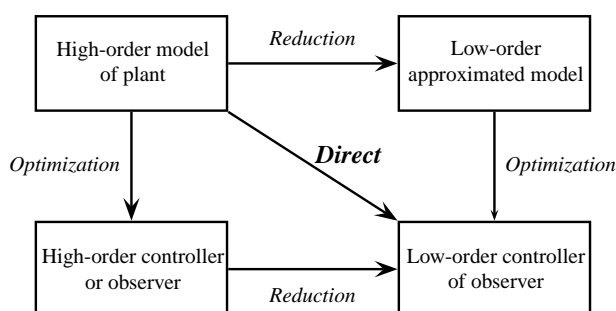


Figure 1: Motivation for closed-loop model reduction.

2 Proposed MPC approach

We consider the reduced order control and observer synthesis problems in which the desired specifications are given in terms of \mathcal{H}_∞ performance criteria. Using duality and variational analysis, we derive a Hamiltonian system, which outputs the optimal control trajectory u^* or the optimal observer impulse response ρ^* . A direct model reduction technique on this Hamiltonian system is proposed to generate optimal control inputs or optimal estimator impulse responses directly from a low order Hamiltonian system.

In this presentation, we will focus on the design of Kalman and \mathcal{H}_∞ observers using the introduced “direct” approach. Performance levels will be compared with the other two strategies. We will illustrate this observer design technique in an application of MPC design, as illustrated in Figure 2, using a controller designed with the same Lagrangian approach.

References

- [1] Siep Weiland, Jochem Wildenberg, Leyla Ozkan, and Jobert Ludlage, *A Lagrangian Method for Model Reduction of Controlled Systems*, Proceedings of the 17th IFAC World Congress, pp. 13402-13407, Seoul, Korea, 2008.
- [2] Mark Mutsaers, Siep Weiland and Richard Engelaar, *Reduced Order Observer Design using a Lagrangian Method*, Proceedings of the Joint 48th IEEE Conference on Decision and Control and 28th Chinese Control Conference, Shanghai, China, 2009.

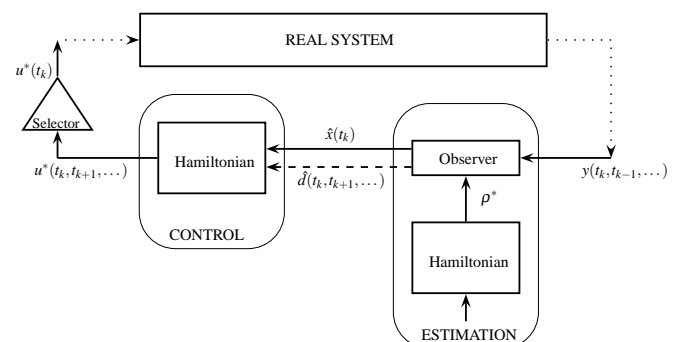


Figure 2: Modeling Predictive Control scheme.

A small-gain theorem for input-to-state convergent systems

Bart Besselink, Nathan van de Wouw, Henk Nijmeijer
 Department of Mechanical Engineering, Eindhoven University of Technology
 P.O. Box 513, 5600 MB Eindhoven, The Netherlands
 Email: b.besselink@tue.nl

1 Introduction

Convergent systems form a relevant class of nonlinear systems and exhibit a unique, global asymptotically stable (steady-state) solution that is bounded on the entire time axis. The convergence property has been shown to be highly instrumental in solving many control problems such as output regulation, tracking observer design and synchronization [1].

In this work, coupled convergent systems are of interest. More specifically, a small-gain condition under which the interconnection of two input-to-state convergent systems is itself input-to-state convergent is presented.

2 Convergent systems

Consider the nonlinear system

$$\dot{x} = f(x, u) \quad (1)$$

with $x \in \mathbb{R}^n$, $u \in \mathbb{R}^m$.

Definition 1. A system (1) is said to be (uniformly, exponentially) convergent for a class of inputs if, for each input $u(t)$ in that class, there exists a solution $\bar{x}_u(t)$ such that

1. $\bar{x}_u(t)$ is defined and bounded for all $t \in \mathbb{R}$,
2. $\bar{x}_u(t)$ is globally (uniformly asymptotically, exponentially) stable.

Here, $\bar{x}_u(t)$ is called the steady-state solution for the corresponding input u . A stronger stability property is the input-to-state convergence property, which is defined as follows:

Definition 2. A system (1) is said to be input-to-state convergent if it is globally uniformly convergent and for every input $u(\cdot)$ system (1) is input-to-state stable (ISS) with respect to the steady-state solution $\bar{x}_u(t)$, i.e. there exist a class \mathcal{KL} -function $\beta(r, s)$ and a class \mathcal{K}_∞ -function $\gamma(r)$ such that any solution $x(t)$ of (1) corresponding to some input $\tilde{u}(t)$ satisfies

$$|x(t) - \bar{x}_u(t)| \leq \beta(|x(0) - \bar{x}_u(0)|, t) + \gamma\left(\sup_{0 \leq s \leq t} |\tilde{u}(s) - u(s)|\right). \quad (2)$$

3 Small-gain theorem

The configuration of Fig. 1 is considered with

$$\Sigma_x : \dot{x} = f(x, z, u), \quad (3)$$

$$\Sigma_z : \dot{z} = g(z, x, v), \quad (4)$$

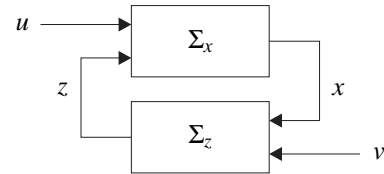


Figure 1: Coupled input-to-state convergent systems

where Σ_x and Σ_z are assumed to be input-to-state convergent with respect to the inputs z , u and x , v , respectively. Then, a small-gain condition for the input-to-state convergence of the interconnected system is given by the following theorem:

Theorem 1. Given Σ_x and Σ_z with gain functions $\gamma_{xz}(r)$ and $\gamma_{zx}(r)$, respectively. Then, the interconnected system (3), (4) is input-to-state convergent if there exist class \mathcal{K}_∞ -functions $\rho_1(r)$ and $\rho_2(r)$ such that

$$(\text{id} + \rho_1) \circ \gamma_{xz} \circ (\text{id} + \rho_2) \circ \gamma_{zx}(s) \leq s \quad \forall s \geq 0, \quad (5)$$

where id denotes the identity function, i.e. $\text{id}(r) = r$.

The proof of the small-gain theorem consists of two parts, which are based on results in [2] and [3], respectively:

1. The existence of a unique and bounded on \mathbb{R} steady-state solution $[\bar{x}_{u,v}^T, \bar{z}_{u,v}^T]^T$ for every external input signal u, v is proven.
2. Input-to-state stability of the coupled system with respect to the steady-state solution, i.e. input-to-state convergence, is proven.

4 Conclusions

A small-gain condition for input-to-state convergent systems is presented. The result provides an analysis tool for coupled input-to-state convergent systems and will be used in error analysis for model reduction of coupled nonlinear systems.

References

- [1] A. Pavlov, N. van de Wouw and H. Nijmeijer. Uniform output regulation of nonlinear systems: a convergent dynamics approach, Birkhäuser, 2006.
- [2] A. Pavlov and K.Y. Pettersen. Stable inversion of nonminimum phase nonlinear systems: a convergent systems approach, Proc. 46th IEEE CDC, pp. 3995-4000, 2007
- [3] Z.-P. Jiang, A.R. Teel and L. Praly. Small-gain theorem for ISS systems and applications, Math. Control Signals Systems 7(2): 95-120, 1994

Selection and Grouping with Multiple Graphs

Marco Signoretto and Johan A.K. Suykens

K.U. Leuven, ESAT-SCD

Kasteelpark Arenberg 10 B-3001 Leuven, Belgium

marco.signoretto@esat.kuleuven.be and johan.suykens@esat.kuleuven.be

Introduction

A common problem in learning from observational data consists in estimating a high dimensional coefficient vector $\beta \in \mathbb{R}^p$ based on a sample of n input-output pairs where, possibly, $n \ll p$. A general approach prescribes to use penalized empirical risk minimization to find an estimate $\hat{\beta}$. From a theoretical standpoint, consistency can be usually proved based on certain structural assumptions on the generative model β^* . In particular, the error $\hat{\beta} - \beta^*$ can be related to how well the underlying structure is captured by the penalty function $r(\beta)$ (see e.g. [1] and references therein). When p is large, a popular example of structural assumption is *sparsity* and the corresponding choice of the penalty is $r(\beta) = \|\beta\|_1$. More recently, structure-inducing norms have been proposed as a promising alternative [7],[8],[9]. The general idea is to convey structural assumption on the problem, such as grouping or hierarchies over the set of input variables, by suitably crafting the penalty.

Conveying Structural Information with Graphs

A different but related method requires to endow the set of covariates with a graph structure [5]. In this case nodes are variables, edges represent interactions and groups naturally emerge as connected components of the graph. Given the graph Laplacian L one then uses the composite penalty

$$r_\alpha(\beta) = (1 - \alpha)\langle \beta, L\beta \rangle + \alpha\|\beta\|_1$$

for some user-defined $0 < \alpha < 1$. The idea extends the elastic-net [6] to endow prior information synthesized in the graph Laplacian. The first term in the penalty enforces smooth profile of coefficients associated to neighboring nodes. The second term ensures that coefficients with small contribution would shrink to exact zero.

The m-NET Approach

In this work we illustrate a recently proposed extension [3] which allows to combine structural information coming from multiple sources. This is important as the graph topology is also estimated from data and the use of multiple graphs has the potential to improve results. In bioinformatics, for example, multiple independent databases such as miRNAmap [10] or microRNA.org [11] can be used to synthesize transcription factor networks. The approach we propose permits to integrate them both in the learning process and find predictive groups of functionally related genes.

Our contribution is threefold. We first highlight the relation between the model assumptions and the spectral properties of the network prior. We then formulate Multiple NET (simply referred to as m-NET), a convex optimization problem that generalizes the problem in [5] to any differentiable loss function and permits to integrate multiple graph priors. As a third contribution, we propose an algorithm which is suitable to large scale problems and conclude with examples.

Acknowledgments

Research supported by Research Council KUL: GOA AM-BioRICS, GOA MaNet, CoE EF/05/006 Optimization in Engineering(OPTEC), IOF-SCORES4CHEM; Flemish Government: FWO: PhD/postdoc grants, G.0499.04 (Statistics), G.0211.05 (Nonlinear), G.0302.07 (SVM/Kernel); IWT: PhD Grants, McKnow-E, Eureka-Flite+, SBO LeCoPro, SBO Climaqs, POM Belgian Federal Science Policy Office: IUAP P6/04.

References

- [1] S. Negahban, P. Ravikumar, M.J. Wainwright and B. Yu. A unified framework for high-dimensional analysis of M-estimators with decomposable regularizers. *Advances in Neural Information Processing Systems*, 2009.
- [2] F.R.K. Chung. *Spectral graph theory*. American Mathematical Society, 1997.
- [3] M. Signoretto, A. Daemen, C. Savorgnan, J.A.K. Suykens. Variable Selection and Grouping with Multiple Graph Priors. NIPS Workshop on Optimization for Machine Learning, 2009.
- [4] E. D. Kolaczyk. *Statistical Analysis of Network Data: Methods and Models*. Springer, 2009.
- [5] C. Li and H. Li. Network-constrained regularization and variable selection for analysis of genomic data. *Bioinformatics*, 24(9):1175-1182, 2008.
- [6] H. Zou and T. Hastie. Regularization and variable selection via the elastic net. *J. Roy. Stat. Soc. Ser. B*, 67(2):301-320, 2005.
- [7] P. Zhao, G. Rocha, B. Yu. The composite absolute penalties family for grouped and hierarchical variable selection. *Annals of Statistics*, 37:3468-3497, 2009.
- [8] M. Yuan and Y. Lin. Model selection and estimation in regression with grouped variables. *J. Roy. Stat. Soc. Ser. B*, 68(1):49-67, 2006.
- [9] R. Jenatton, J.Y. Audibert, F. Bach. Structured variable selection with sparsity-inducing norms. *Technical report*, arXiv:0904.3523, 2009.
- [10] S.D. Hsu *et al.* miRNAmap 2.0: genomic maps of microRNAs in metazoan genomes. *Nucleic Acids Research*, 36:D165-D169, 2008.
- [11] D. Betel *et al.* The microRNA.org resource: targets and expression. *Nucleic Acids Research*, 36:D149-D153, 2007.

Very fast temperature pulsing: first results

Jasper Stolte
Postbus 513
5600 MB Eindhoven
J.Stolte@tue.nl

Ton Backx
Postbus 513
5600 MB Eindhoven
A.C.P.M.Backx@tue.nl

1 Introduction

Chemical reaction systems are commonly operated under steady state conditions. They are nonlinear, and portrait complex behaviour when driven away from the steady state. Including certain non-steady reaction conditions provides additional freedom which can be used to optimize the reaction. Specifically, literature suggests it can be profitable to do fast temperature cycling. However, the typically high thermal inertia in reactors has prevented any research into fast temperature variation. This work presents a prototype setup which is capable of very fast temperature variations at a catalytic surface. Measurement results will be presented.

2 Setup

An experimental setup has been built which combines mass flow controllers, a pressure controller, valves, integrated heating, temperature pulsing and a mass spectrometer. All these devices are centrally controlled and automatised using LabVIEW. Figure 1 shows a photograph of the reactor.

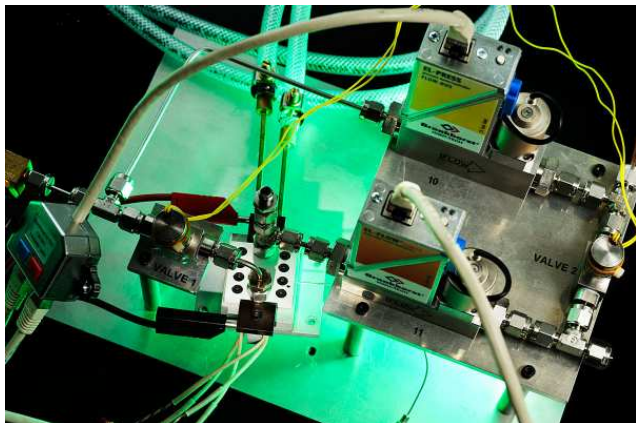


Figure 1: Photograph of the chemical reactor.

3 Simulation

A simulation was created to inspect the heat distribution throughout the reactor when the catalytic layer is subjected to a current pulse. Figure 2 shows the simulated catalytic surface temperature for this design. Pulses of hundreds of Kelvin in tens of microseconds are feasible using this design [1]. The temperature gradients are orders of magnitude higher than any result known from literature.

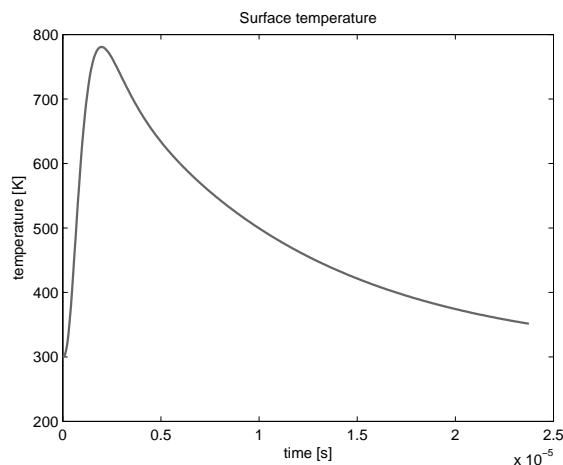


Figure 2: Simulation of the temperature at the catalytic surface. The peak is hundreds of K which is reached in approximately 20 μ s.

4 Test Reaction

As test reaction the oxidation of carbon monoxide to carbon dioxide over a platinum catalyst has been chosen. Many prior studies have been reported for this reaction system, such that the influence of the temperature pulsing can be properly studied. Measurements of the influence of temperature pulses on this reaction will be presented at the meeting.

5 Conclusion

A prototype reactor capable of very fast temperature pulsing has been constructed. Results are available on the catalytic oxidation of carbon monoxide over platinum.

References

- [1] J. Stolte, A.C.P. Backx, and O.H. Bosgra. Very fast temperature pulsing: catalytic reactor design. In *Benelux Meeting Systems and Control*, 2009.

Stability Analysis of Stochastic Networked Control Systems

M.C.F. Donkers¹, W.P.M.H. Heemels¹, D. Bernardini², A. Bemporad²

¹Department of Mechanical Engineering
Eindhoven University of Technology

P.O.Box 513, 5600 MB Eindhoven, The Netherlands
{m.c.f.donkers,w.p.m.h.heemels}@tue.nl

²Department of Information Engineering
University of Siena

Via Roma 56, 53100 Siena, Italy
{bernardini,bemporad}@unisi.it

1 Introduction

A Networked Control System (NCS) is a control system wherein the control loops are closed through a real-time network. The presence of the network introduces the following communication imperfections (see, e.g., [1]):

- (i) quantisation of the signals;
- (ii) possible loss of transmitted data;
- (iii) time-varying transmission delays;
- (iv) non-equidistant sampling;
- (v) communication constraints, i.e., not all sensors and actuators can be accessed simultaneously.

Basically one can either adopt a deterministic modelling approach imposing upper and lower bounds on the sampling intervals, the transmission delays, and the maximal number of subsequent dropouts, or one can use stochastic information of these phenomena. In this work, we will consider the latter for the network imperfections of type (ii)-(v). A deterministic approach can be found in [5].

2 NCS Model

Consider the NCS as given in Fig. 1. Because of the network, the actual input of the plant \hat{u} and the controller \hat{y} are not equal to u and y , respectively. By combining the plant, controller and the network effects, we obtain an uncertain switched closed-loop system of the following form:

$$\bar{x}_{k+1} = \tilde{A}_{\sigma_k, h_k, \tau_k} \bar{x}_k, \quad (1)$$

where \bar{x}_k denotes the state of the NCS, h_k the sampling interval, τ_k the delay, and σ_k the scheduling protocol that determines which data is sent at a sampling instant. Since analysing stability of (1) for all $(h, \tau) \in \Theta$, where $\Theta \subset \mathbb{R}^2$, would require to verify stability for infinitely many possible sequences $\{(h_k, \tau_k)\}_{k \in \mathbb{N}}$, we approximate (1) by a polytopic system. This approximation is such that for each $\sigma \in \{1, \dots, n_y + n_u\}$, and $\mathcal{S}_m \subseteq \Theta$, $m \in \{1, \dots, s\}$, it holds that

$$\{\tilde{A}_{\sigma, h, \tau} | (h, \tau) \in \mathcal{S}_m\} \subseteq \text{co}\{\bar{A}_{\sigma, 1}, \dots, \bar{A}_{\sigma, M}\}.$$

Stability of polytopic systems can be analysed using a finite number of LMIs. A thorough comparison between the existing approximation techniques is given in [2].

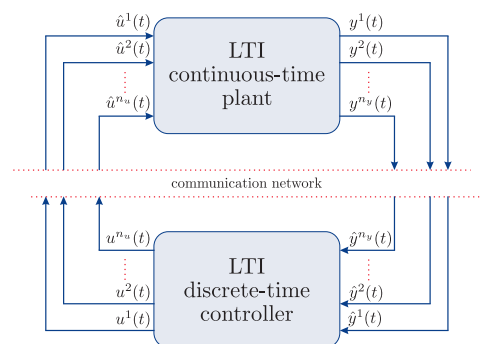


Fig. 1 Networked Control System block diagram

3 Illustrative Example

To illustrate the theory, we consider a benchmark example of a batch reactor (see [3-6]). The results are shown in Table 1 (for $\tau_k = 0$ for all $k \in \mathbb{N}$).

Table. 1 Allowable Range of Sampling Intervals

Method	Range
Constant sampling times, as in [3]	$h \in (0, 0.08]$
Deterministic bound, as in [3]	$h \in (0, 10^{-5}]$
Deterministic bound, as in [4]	$h \in (0, 0.0108]$
Deterministic bound, as in [5]	$h \in [10^{-4}, 0.068]$
Using a Uniform Distribution, as in [6]	$h \in (0, 0.11]$

References

- [1] W.Zhang, M.S. Branicky, S.M. Phillips: Stability of Networked Control Systems. *IEEE Control Systems Magazine*, 2001.
- [2] W.P.M.H. Heemels, N. van de Wouw, R.H. Gielen, M.C.F. Donkers, L. Hetel, M. Lazar, J. Daafouz, S. Oлару, S. Niculescu: Comparison of Overapproximation Methods for Stability Analysis of Networked Control Systems. *To be presented at the 2010 HSCC*.
- [3] G.C. Walsh, H. Ye, L.G. Bushnell: Stability analysis of networked control systems. *IEEE Trans. on Control Systems Technology*, 2002.
- [4] D. Carnevale, A.R. Teel, D. Nešić: A Lyapunov proof of improved maximum allowable transfer interval for networked control systems. *IEEE Trans. on Autom. Control*, 2007.
- [5] M.C.F. Donkers, W.P.M.H. Heemels, N.v.d. Wouw, L. Hetel: Stability Analysis of Networked Control Systems Using a Switched Linear Systems Approach. *Submitted*.
- [6] M.C.F. Donkers, W.P.M.H. Heemels, D. Bernardini, A. Bemporad: Stability Analysis of Stochastic Networked Control. *To be presented at the 2010 ACC*.

Modelling a hysteretic relay in a self-oscillating loop

Paul van der Hulst
Piak electronic design b.v.
Markt 49
4101 BW Culemborg
The Netherlands

Email: p.v.d.hulst@tue.nl

André Veltman
Piak electronic design b.v.
Markt 49
4101 BW Culemborg
The Netherlands

Email: a.veltman@piak.nl

P.P.J. van den Bosch
Department of Electrical Engineering
Eindhoven University of Technology
Postbus 513
5600 MB Eindhoven
The Netherlands
Email: p.p.j.v.d.bosch@tue.nl

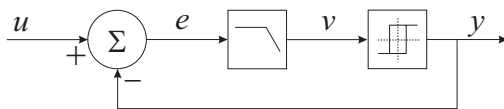


Figure 1: Self-oscillating loop with hysteretic relay

1 Abstract

The hysteretic relay is a key non-linear element. It is typically applied as a bang-bang controller. Although bang bang control seems to be very crude at first sight, it is applied in some of the best (class-D) audio amplifiers ([1][2]). However, no theoretical framework exists for the design and optimisation of these amplifiers.

A bang-bang controlled system contains a feedback loop which is in limit-cycling modus. A general example of such a system is shown in figure 1. The system consists of a summation, a low-pass loop filter and a hysteretic relay. The loop will exhibit oscillation at a frequency determined by the transfer of the low-pass loop filter and the hysteresis width of the relay. The oscillation criterion for linear systems is inaccurate for this system because of the non-sinusoidal wave forms. An exact oscillation criterion can be derived and is given in eq. (1)

$$h = -\frac{4}{\pi} \left(\sum_{n=1}^{\infty} \frac{1}{n} \sin^2(nk\pi) \Im(H_{lpf}(nj\omega_{sw})) \right) \quad (1)$$

where h is the hysteresis, ω_{sw} is the switching frequency and k is the duty-cycle of the PWM output signal y .

Because of the non-linearity of the relay, the system has a non-linear transfer from input u to output y . However, as the application in class-D amplifiers suggests, this non-linearity can be very small within the signal bandwidth. Most notably

the switching frequency is modulated by the input signal, which also follows from eq. (1). The switching frequency components in the output signal can however usually be ignored.

In order to minimise output signal distortion caused by the non-linear signal transfer, it is necessary to identify the input-output closed-loop system transfer function $H_{u \rightarrow y}$ of the system. It turns out that the relay transfer function $H_{v \rightarrow y}$ and thus also $H_{u \rightarrow y}$ is largely determined by the transfer function of the loop filter. For DC input signals, the DC (average) input of the relay can be calculated to be equal to:

$$\bar{v} = \frac{2}{\pi} \left(\sum_{n=1}^{\infty} \frac{1}{n} \sin(2nk\pi) \Re(H_{lpf}(nj\omega_{sw})) \right) \quad (2)$$

From this result, the DC relay gain can numerically be calculated as $g_{relay} = \frac{\bar{v}}{v} = \frac{2k-1}{v}$.

The expressions in eq. (1) and (2) are not very convenient due to the sum for $n \rightarrow \infty$, and need to be calculated numerically. For simple 1st order loop filters they can however very accurately be approximated with a 2nd or 3rd order polynomial respectively. This close equivalence needs further examination. Also, although DC analysis is sufficient for thermostats, typical switching frequencies for class-D are only 10 to 15 times higher than the highest signal frequency. Simulations show that a ‘quasi DC’ assumption is inaccurate.

References

- [1] A. Veltman, H.J.J. Domensino, Amplifier circuit having output filter capacitance current feedback, US patent no. 6552606, 2003
- [2] Bruno Putzeys, Globally modulated self-oscillating amplifier with improved linearity, AES 37th international conference, Hillerød, 2009

Friction Based Actuation and Control Systems in CVT Applications

Irmak Aladagli, Theo Hofman, Maarten Steinbuch
Control Systems Technology Group
Eindhoven University of Technology
The Netherlands
Email: i.aladagli@tue.nl

Roell van Druten
Drivetrain Innovations
Croy 46, 5653 LD Eindhoven
The Netherlands
Email: druten@dtinnovations.nl

1 Background

The reduction of fuel consumption and pollution by transportation trucks is desired regarding ecological and economical concerns. Within the sector of road transportation, electrical auxiliaries that are used to condition the freight are a major source of fuel consumption. In most trucks, these auxiliaries are driven by an additional diesel generator. However; there are a many of disadvantages of using such an additional diesel generator: relatively high fuel consumption (thus pollution) compared to the main drive of the truck; the weight of the additional diesel generator and its fuel tank; and high noise produced by such diesel generators, see [2].

An alternative to minimize such disadvantages is to drive the auxiliaries by the internal combustion engine (ICE) of the truck through a generator. In this case, continuously variable transmission (CVT) is required to produce constant voltage and frequency, from varying speed of the truck engine. Govers e.t., DTI Advanced Technologies BV (DTI-AT) and Eindhoven University of Technology (TU/e) are developing such a constant speed power take-off (CS-PTO) CVT topology, to deliver power from the truck engine working at variable speeds to the generator that requires constant speed, to power the refrigeration unit of the refrigeration trucks in particular. The CVT application in consideration has a friction based actuations system. Due to their non-linear and time varying characteristics, the control of such friction based systems are quite challenging. However; if successfully integrated, the efficiency of the trucks with auxiliaries can be greatly increased.

2 Goal and Approach

The main goal of the CS-PTO project by Govers and DTI-AT is to design and realize a feasible CVT system to power the auxiliaries of the truck by its ICE and attain 15% fuel reduction compared to the trucks with a traditional diesel generator. A CS-PTO CVT system has already been designed by DTI-AT. This existing CVT topology under research is composed of four different components: shafts, torque cams (torque sensors), a metal push-belt variator and a electro-mechanical actuation clutch. This topology with two torque cams and the continuously slipping actuation clutch on the output side to control the transmission ratio of the variator is a novel design. Optimized control of the metal push-belt CVT for high efficiencies, with the friction elements of this novel design is a challenging problem, see [1].

Modeling, model verification, design and realization of an efficient control strategy and integration within a truck are

some of steps to be taken in this project in order to obtain such a feasible and efficient CVT system based on the topology devised by DTI-AT. With the modeling step it is aimed to find out if the system is controllable and to determine the requirements for the friction surfaces and the actuator.

The initial model being built is a semi-dynamic multi-body model with some assumptions like: no slip between the belt and the pulleys, no friction in various components like bearings, linear springs, rigid body behavior for the gears and bearings, etc. The elements of the driveline like shafts gears, bearings, etc. are modeled with first principles modeling, as mass-spring-damper systems, using the above assumptions where appropriate. The Ide model is used to model the transient behavior of the variator. After this model is completed to represent various phenomena observed in the actual setup, model verification will follow next.

3 Conclusions and Looking Forward

The universal goal in many modern automotive researches, is increasing *drivability* and decreasing *fuel consumption* and *pollution*. This project aims to attain this goal by using an highly efficient CVT system and power the auxiliaries of transportation trucks using the main ICE. Design and control optimization of the existing CVT topology are the main challenges to be faced. Nonlinear and time-varying characteristics of the CVT and the friction based actuations system require a robust control strategy to be applied.

Moreover, it is possible to add energy management strategies, involving the route information and using the cooled unit as an energy storage system to attain the universal goals mentioned above. Optimization and regulation of such a system, see [3], might be of interest future in the research.

References

- [1] B. Bonsen, T.W.G.L. Klaassen, K.G.O. van de Meerakke, P.A. Veenhuizen, and M. Steinbuch. Measurement and control of slip in a continuously variable transmission. In *Mechatronics*, 2004.
- [2] Daniel Jehudi de Cloe. The constant speed power take off. Master's thesis, Eindhoven University of Technology, 2002.
- [3] T. Hofman, D. Hoekstra, R. M. van Druten, and M. Steinbuch. Optimal design of energy storage systems for hybrid vehicle drivetrains. In *Proc. IEEE Conference Vehicle Power and Propulsion*, page 5, 7–9 Sept. 2005.

The C–Lever Project: Haptics for Automotive Applications

E. García–Canseco, A. Ayemlong–Fokem, M. Steinbuch

Eindhoven University of Technology, Fac. Mechanical Eng.

Control Systems Technology Group

PO Box 513, 5600 MB Eindhoven, The Netherlands.

E.Garcia.Canseco@tue.nl

M.Steinbuch@tue.nl

A.Ayemlong.Foken@student.tue.nl

serrarens@dtinnovations.nl

A. Serrarens

Drivetrain Innovations BV

Croy 46, 5653 LD Eindhoven,

The Netherlands

1 Introduction

The automotive industry is experiencing not only a strong enhancement of automation in primary driving tasks, e.g., automated gear shifting, lane-keeping systems, adaptive cruise control, park-assists, automatic hill-hold, brake-by-wire, etc, but also, the introduction of more auxiliaries and interior functions, e.g., USB-connectors, mp3 players, navigation, among others. These trends lower the driver's workload significantly, and draw the driver's attention more and more to the interior functions of the car. Adding more functionality to vehicles increases driver satisfaction or pleasure, however, it can also lead to a significant increase of driver distraction. Haptic cues might offer a promising and relatively unexplored alternative to give warnings and other messages to the driver, and also to aid drivers in the execution of their driving tasks. In the recent years, the automotive industry has been taking a keen interest in haptics [1]. Car makers such as BMW, Audi, Lexus, Nissan and many more have already installed haptic interfaces in their automobiles.

The goal of this project is to research the effectiveness of a controlled haptic force feedback shift lever that can accurately reproduce the behavior of either an automatic or a manual gear shift during driving, and that might also be used to control interior and comfort functions in the car (Fig. 1).

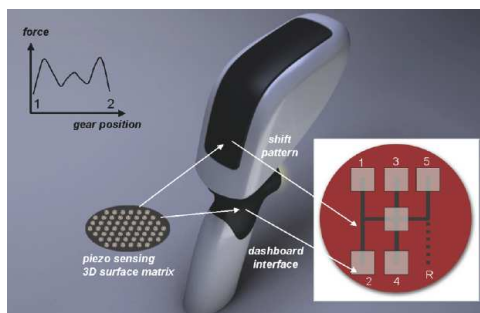


Figure 1: Haptic gearshift interface concept.

Our haptic interface, as depicted in Fig. 2, is a two degrees-of-freedom mechatronic device, whose working principle is based on the self-locking property of a worm pair transmission [2]. Without actuation, it is therefore impossible to force the worm to rotate by applying a force to the lever mounted on the worm gear. Vice versa, the actuator is able to move the worm gear and lever around their rotation axis rather easily. One advantage of this worm pair transmission

is the low power consumption, more feedback force requires less power and there is no consumption at all when the lever is kept at its rest position [3].

To implement model-based control strategies on the system, the dynamical model of the haptic interface has been obtained using the Euler–Lagrange methodology. Friction phenomena has been also incorporated via a static friction model with Stribeck velocity [4]. Borrowing some inspiration from [5], we have proposed force profiles that mimic the behavior of automatic and manual gearshifts.

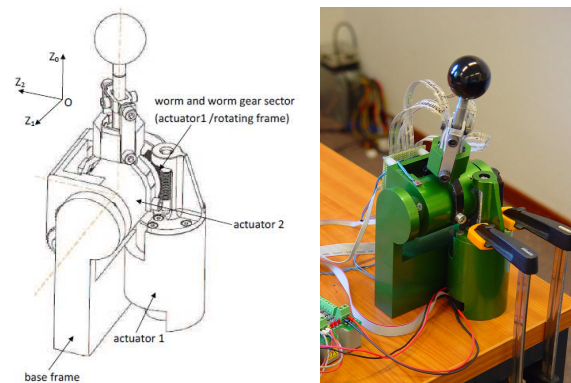


Figure 2: Two degrees-of-freedom haptic gearshift device.

2 Acknowledgments

This research is supported by the SenterNovem IOP Man–Machine Interaction Project MMI07105 “Control solutions for human-in-the-loop user interfaces” and by DTI Automotive Mechatronics BV.

References

- [1] S. J. Bigelow. Haptics make it happen. *Smart Computing*, 2004.
- [2] A. Serrarens. Gear changing device for automotive applications. Patent AF16H5904FI, 2005.
- [3] K. van Diepen. Dynamic haptic control for a 1-dof shift-by-wire system. Confidential DCT 2008.71, Eindhoven University of Technology, Eindhoven, The Netherlands, July 2008.
- [4] H. Olsson, K.J. Astrom, C. Canudas de Wit, M. Gafvert, and P. Lischinsky. Friction models and friction compensation. *European Journal of Control*, 4(3), 1998.
- [5] J. Ren, K. A. McIssaac, R. V. Patel, and T. M. Peters. A potential field model using generalized sigmoid functions. *IEEE Transactions on Systems, Man and Cybernetics—Part B: Cybernetics*, 37(2):477–484, April 2007.

Comparison of Decentralized Kalman Filters for Heated Plates

Z. Hidayat, R. Babuška, and B. De Schutter

Delft Center for Systems and Control

Delft University of Technology, The Netherlands

Email: z.hidayat@tudelft.nl

1 Introduction

Current technological advances enable the design of spatially distributed sensing systems. These systems consist of sensors that are equipped with embedded computing and communication modules. The communication modules allow sensors to form networks called sensor networks. The computation and communication capabilities of sensor networks open new challenges in state estimation problems, namely decentralized state estimation.

The Kalman filter is a common state estimation method. Widely used for many applications in a centralized way, the Kalman filter and its variants are also used in a decentralized way, e.g., in sensor network applications. Some approaches of the decentralized Kalman filter are [2]: Parallel Information Filter (PIF), Distributed Information Filter (DIF), Decoupled Hierarchical Kalman Filter (DHKF), Distributed Kalman Filter with Consensus Filter (DKFCF), and Distributed Kalman Filter with Bipartite Fusion Graph (DKFBFG). In this paper, the above decentralized approaches are compared in the estimation state of the discretized temperature of a heated plate in simulation.

2 Heated Plate Model and Simulation Setup

The model of the heated plate is formulated based on an energy balance and can be written as [1]

$$\frac{\partial T}{\partial t} = \frac{1}{\rho C_p} \left[\kappa \frac{\partial^2 T}{\partial x^2} + \kappa \frac{\partial^2 T}{\partial y^2} + \frac{\dot{Q}_s(x,y,t)}{\partial z} + \frac{h}{\partial z} (T_{\text{env}} - T) \right]$$

where T is the temperature of the plate, T_{env} the temperature of the environment, ρ the density of the plate, C_p the heat capacity per unit mass, κ the thermal conductivity, \dot{Q}_s the heater power per unit area, h the convection coefficient, x , y , z are spatial coordinates of length, width, and height and the height of the plate is much smaller than the length and width.

For the simulation, a 1.5 m by 1 m plate is modeled and divided into a 10-by-15 grid. The plate is heated only at one element. The plate is discretized spatially using the first and second order of forward, backward, and central approximations. The forward and backward approximations are used for elements on the edge and the central approximation for elements between the edges. The model is then discretized in time with a sampling period of 0.2 s and simulated for 20

min. Six sensors are placed in the intersection of row 3 and 8 and column 3, 8, and 13 to measure the temperature.

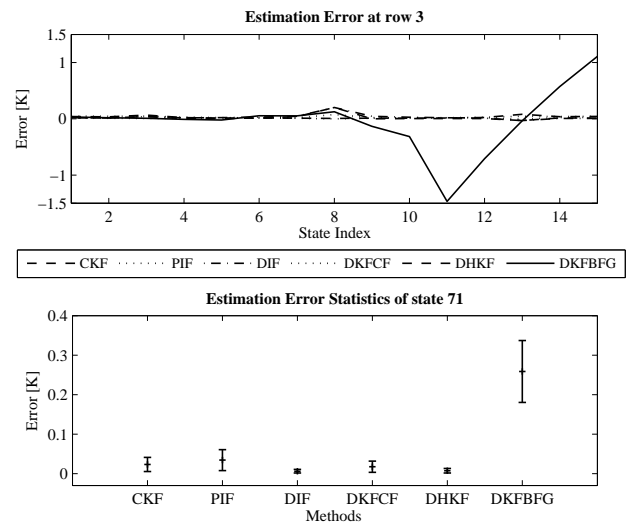


Figure 1: Estimation errors of the compared methods

3 Results

Figure 1 shows the estimation errors at the final time of the simulation for row 3 of the grid (upper) and the statistics of the estimation error for state 71 (lower) from 5 experiments and computed over time. In the figure, the errors from the Centralized Kalman Filter (CKF) are also shown as a comparison to the decentralized approach.

In the figure, it can be seen that for the all methods have relatively small errors except the DKFBFG. This means that most of the decentralized Kalman filter is comparable with the centralized one. With respect to the error variation, the figure shows that the DIF has the smallest error and variation compared to the other methods, including the CKF. The small error variation implies that the estimates of the DIF are better for each time instant.

References

- [1] J.P. Holman, *Heat Transfer*, McGraw-Hill Higher Education, 10thEd., 2008
- [2] J. Sijts, M. Lazar, P.P.J. van den Bosch, and Z. Papp, An overview of non-centralized Kalman filters. *In Proceedings of IEEE International Conference on Control Applications (CCA 2008)*, pp. 739–744, San Antonio USA, Sep. 2008.

Distributed Estimation for Domestic Mobile Robots: an experimental setup

Andrea Simonetto

Tamás Keviczky

Delft Center for Systems and Control, Delft University of Technology

Mekelweg 2, 2628CD, Delft, The Netherlands

Email: {a.simonetto, t.keviczky}@tudelft.nl

1 Introduction

The near future will witness the design of fully automated houses where everyday chores, such as vacuum cleaning, will be performed by small and inexpensive mobile robots. The state estimation of these robots, namely position and orientation, will be the duty of a sensor network integrated in the house itself. Most likely, these sensors will be capable of range-only measurements and the network will work in a distributed way, to decrease the computation load of the single units. A reliable, real-time and distributed solution of this estimation problem is still not available although it has received increased attention from the research community in the past years.

2 Problem Formulation

With reference to Figure 1, let (x, y) be the position of a mobile robot on the floor, let θ be its orientation and let its Nonlinear Time-Invariant dynamical model with state $\mathbf{x} = \{x, y, \theta\}^T \in \mathbf{R}^3$ be:

$$\begin{aligned} x(k+1) &= x(k) + \frac{v(k)}{\omega(k)} (\sin(\theta(k) + \omega(k)\Delta t) - \sin \theta(k)) \\ y(k+1) &= y(k) - \frac{v(k)}{\omega(k)} (\cos(\theta(k) + \omega(k)\Delta t) - \cos \theta(k)) \\ \theta(k+1) &= \theta(k) + \omega(k)\Delta t \end{aligned}$$

here v and ω are the velocity and the angular velocity respectively and they are the control inputs. Δt is the sampling time and $k \in \mathbf{Z}$ is the discrete time instant. Let the robot be observed by N sensors, labeled $i = 1, \dots, N$ and placed at a specified height h , each with some processing and communication capability. The sensor can measure the distance between them and beacons on the robot. Let the robot have two beacons and let the two (range-only) measurement equations for each sensor $z_{\pm, i}(k)$ be:

$$z_{\pm, i}(k) = \left\| \begin{Bmatrix} x(k) \pm L \cos \theta(k) - \ell_{x_i} \\ y(k) \pm L \sin \theta(k) - \ell_{y_i} \\ h \end{Bmatrix} \right\|_2 + \mu_{\pm, i}(k)$$

where $(\ell_{x_i}, \ell_{y_i}, h)$ is the position of the sensor, $2L$ is the distance between the beacons and $\mu_{\pm, i}(k)$ is a Gaussian noise term. In the distributed setting each sensor estimates the state, and $\hat{\mathbf{x}}_i(k)$ denotes the estimate of sensor i at time k .

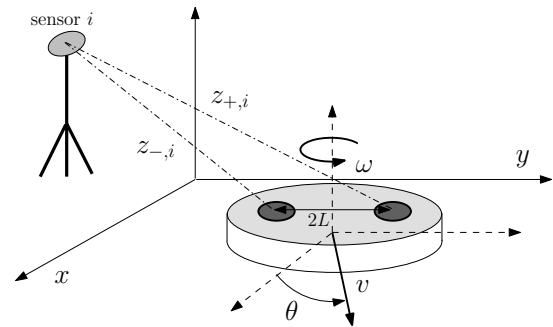


Figure 1: Problem Formulation

The distributed estimation problem can be formulated as follows. Allowing only local communication among the sensors, estimate N different copies of the state so that 1) each $\hat{\mathbf{x}}_i(k)$ is an unbiased estimate of $\mathbf{x}(k)$ at each time step k , 2) for $k \rightarrow \infty$, all the $\hat{\mathbf{x}}_i(k)$'s have the same value.

3 Experimental Setup

The experimental setup consists of a mobile robot, iRobot Create, which is allowed to move in a playground of approx. 3×2 m, 6 range-only sensors (the MIT Cricket sensors) are placed on tripods, $h = 1.5$ m, along the border of the playground. They can communicate with a central PC, where the distributed estimation schemes are simulated. Two beacons are placed on the robot and $L = 13$ cm. The sampling time is 1 s. A camera is mounted on the ceiling for validation; the accuracy of the camera is around 1 cm on the position and < 1 deg on the orientation.

4 Discussion

Table 1: Simulation tests

	Raw triangulation	DUKF	DPF
Average Error [cm]	6.4 ± 2.8	3.8 ± 2.2	1.7 ± 1.4
Normalized comp. time	$\sim 10^{-2}$	$\sim 10^{-1}$	1

Simulation tests (Table 1) show that a distributed version of the Unscented Kalman Filter (DUKF) could be the best for this specific problem in term of accuracy versus computation time. At this moment, experimental validations are being performed to test this solution along with distributed Particle Filters (DPF) and Moving Horizon Estimation.

Nonlinear non-Gaussian state estimation using a land surface model and the particle filter

Plaza D., De Lannoy G. J. M., Pauwels V. R. N.
 Laboratory of Hydrology and Water Management
 University of Ghent
 Coupure Links 653, B-9000 Gent
 Belgium
 Email: Douglas.PlazaGuingla@UGent.be

Robin De Keyser
 Department of Electrical energy, Systems and
 Automation - University of Ghent
 Technologiepark 913, B-9052 Gent
 Belgium
 Email: rdk@autoctrl.UGent.be

1 Introduction

Land Surface Models (LSM) represent the physical processes of the hydrologic cycle such as runoff, infiltration, evapotranspiration, soil-water content, discharge. These processes are interdependent, making the construction of hydrologic models very complex. The volumetric soil moisture and temperature profiles define the state of the LSM. State estimation is used in order to adapt the results of model simulations using external observations. The state estimation using land observations is also known as Land Data Assimilation. Data assimilation (DA) is used in many different disciplines such as earth sciences, space sciences, computer graphics, and industrial applications.

Evensen [1] presents the Ensemble Kalman Filter (EnKF) as a Monte Carlo approach to the nonlinear filtering problem. Recently, the Particle Filter (PF), which is a sequential Monte Carlo method for state estimation, has been widely applied in mobile robot localization with promising results [3]. The goal of this study is to evaluate the performance of the PF as a DA method. Further research will include a comparative study between the EnKF and the PF.

2 The study area and the land surface model

The study area is the Alzette watershed, which is located in Luxembourg and the area of the catchment is 356 km². Measurements of volumetric soil moisture content and discharge of water to the river are recorded every one hour. Atmospheric forcings such as precipitation, air humidity, wind speed and air temperature are obtained from a meteorological station.

The hydrologic model chosen for this study is the Community Land Model (CLM) [2], CLM is a global LSM. Surface heterogeneity is represented through different land cover types: glacier, vegetation, urban and wetlands. The vertical structure is represented by one vegetation layer, 10 soil layers and up to 5 snow layers.

3 The state estimation technique

The Sequential Importance Resampling (SIR) particle filter is used in this study. The SIR method is based on the Se-

quential Importance Sampling (SIS) approach plus a resampling step which is used in order to avoid the degeneracy problem. Artificial soil moisture data is assimilated and the particle set size is 64.

4 Preliminary results

Figure 1 presents the performance of the PF when volumetric soil moisture state is estimated using the soil moisture measurement corresponding to julian day 46. The benefit of updating soil moisture at one day seems to persist for a number of days. Further validation of the method will involve a comparative study of the PF and the EnKF and to assess the impact of soil moisture assimilation on the generation of the discharge.

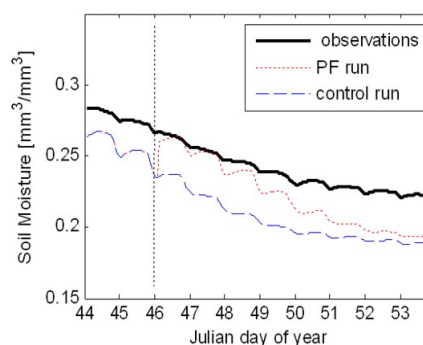


Figure 1: Surface soil moisture

References

- [1] G. Evensen, "Sequential data assimilation with a nonlinear quasi-geostrophic model using Monte Carlo methods to forecast error statistics." *J. Geophys. Res.*, 99, 10 143-10 162, 1994.
- [2] K. Oleson, Y. Dai, G. Bonan, M., Dickinson. "Technical description of the Community Land Model (CLM) (Tech. Rep)." NCAR, Boulder, CO. 2004.
- [3] M. Arulampalam, S. Maskell, and N. Gordon, "A tutorial on particle filters for online nonlinear/non-gaussian bayesian tracking." *IEEE Transactions on Signal Processing*, vol. 50, pp. 174-188, 2002.

A filtering technique on the Grassmann manifold

Quentin Rentmeesters P.-A. Absil Paul Van Dooren
 quentin.rentmeesters@uclouvain.be absil@inma.ucl.ac.be vdooren@csam.ucl.ac.be
 Department of Mathematical Engineering
 Université catholique de Louvain (UCL)
 Bâtiment Euler, Avenue Georges Lemaître 4, B-1348 Louvain-la-Neuve, Belgium

1 Introduction

In many applications related to signal processing and image processing, it is necessary to filter measurements that belong to the Grassmann manifold, i.e., the set of p -dimensional subspaces of \mathbb{R}^n or \mathbb{C}^n denoted by $\text{Grass}(p, n)$. This appears for instance in the direction of arrival tracking problem in antenna array processing when a time division multiple access technique is applied to increase the capacity of the antenna array, see [1]. In this case, the measurements are estimations of the signal subspace, which can be used to recover the directions of arrival. In object tracking problems on a video sequence, the tracked object can be represented by the dominant subspace of a covariance matrix, see [3]. To deal with deformations and illumination variations, this subspace must be updated. A filtering technique is then required to update this subspace using the subspaces representing the object at the previous time steps.

In this talk, we present a Luenberger-like observer based on a constant velocity dynamical model on the Grassmann manifold. This model is used to reduce the influence of high frequency noises or outliers in the measurements, i.e., subspaces in this case. This method does not work with particles and is then cheaper to compute than the particle filtering technique introduced in [2]. It has also a lower numerical cost than [3] due to an efficient representation of points and velocities on $\text{Grass}(p, n)$. The following section gives more details on this approach.

2 Our approach

Let us assume that we measure corrupted data $Y_k \in \text{Grass}(p, n)$ for $1 \leq k \leq T$. The goal is to filter recursively these data to reduce the influence of the noise and the outliers. To achieve this goal, we assume that the data Y_k are the outputs of the following discrete-time dynamical system whose state is composed of the position (a subspace X_k) and the velocity (a tangent vector V_k at X_k):

$$X_{k+1} = \exp_{X_k}(V_k), \quad V_{k+1} = \Gamma_{X_k \rightarrow X_{k+1}}(V_k), \quad Y_k = \exp_{X_k}(U_k),$$

where \exp_{X_k} stands for the exponential map, $\Gamma_{X_k \rightarrow X_{k+1}}$ denotes the parallel transport along the geodesic curve joining X_k to X_{k+1} and U_k is an i.i.d. Gaussian vector of mean 0 and variance σ^2 that belongs to the tangent space at X_k . This

constant velocity model, i.e., a geodesic model, for the dynamic of the subspaces is chosen to act as a smoother on the subspace trajectory to reduce the influence of the noise.

Our filtering method is based on the design of a Luenberger observer for this dynamical system. A Luenberger observer on Riemannian manifolds has been introduced in [4] to observe the state (position and velocity) of a class of nonlinear mechanical systems. In this talk, we follow the same idea except that we work in the discrete-time domain. Our observer is the following:

$$\begin{aligned} \hat{X}_{k+1} &= \exp_{\hat{X}_k}(\hat{V}_k + \alpha \exp_{\hat{X}_k}^{-1}(Y_k)) \\ \hat{V}_{k+1} &= \Gamma_{\hat{X}_k \rightarrow \hat{X}_{k+1}}(\hat{V}_k + \beta \exp_{\hat{X}_k}^{-1}(Y_k)) \end{aligned}$$

where \hat{X}_k denotes the estimated state, \hat{V}_k the estimated velocity and α, β are two tunable real parameters. This observer can be implemented efficiently using two n -by- p matrices: one whose column space represents the subspace and another one that represents the velocity of the subspace, i.e., a tangent vector. In fact, there exists formulas to compute the parallel transport, the exponential map and its inverse in $O(np^2)$ operations on $\text{Grass}(p, n)$ using this representation.

We compare this technique to the particle filtering technique of [2] and the filter of [3]. On some tracking problems, we observe results that are similar to those obtained with the particle filtering technique, and better than those obtained with the filter of [3].

References

- [1] R. Weber. Subspace Tracking for Mobile Communications. Techn. Univ. München, Munich, Germany, Tech. Rep. TUM-LNS-TR-97-7, 1997.
- [2] Anuj Srivastava and Eric Klassen. Bayesian and geometric subspace tracking. *Adv. in Appl. Probab.*, 36(1):43–56, 2004.
- [3] Tiesheng Wang, Andrew Backhouse, and Irene Y.H. Gu. Online subspace learning in Grassmann manifold for moving object tracking in video. In *Proceedings of IEEE international conf. Acoustics, Speech, and Signal Processing (ICASSP'08)*, pages 969–972, 2008.
- [4] Nasradine Aghannan and Pierre Rouchon. An intrinsic observer for a class of Lagrangian systems. *IEEE Trans. Automat. Control*, 48(6):936–945, 2003.

A Comparison of Spacecraft Attitude Estimation Filters

Jeroen Vandersteen^{1,2}, Jan Swevers², Conny Aerts¹

¹Institute for Astronomy, ²Department of Mechanical Engineering
K.U.Leuven, Belgium

jeroen@ster.kuleuven.be, jan.swevers@mech.kuleuven.be, conny.aerts@ster.kuleuven.be

1 Abstract

The application of moving horizon estimators (MHE) and particles filters (PF) for spacecraft attitude estimation is investigated. Their performance is compared to the extended Kalman filter (EKF) and the unscented Kalman filter (UKF) through simulations. Due to the nonlinear spacecraft dynamics, the EKF and the UKF are suboptimal. Recently, Moving Horizon Estimators (MHE) and Particle Filters (PF) have been introduced in the process industry and in tracking applications. We show that these new filters can cope better with the nonlinear system dynamics, and result in a higher accuracy.

2 Introduction

For high-performance and high-accuracy spacecraft, the pointing error is dominated by the sensor noise. In order to reduce the effect of sensor noise, the information from different attitude sensors, such as sun sensors, star trackers, inertial measurement units and magnetometers, is combined in an attitude estimation filter. The implementation of this filter in the onboard software requires a low computational cost. In this article, several different filters are implemented, and their performance is compared through simulations. The EKF will serve as the reference filter to which all other filters are compared, as this filter has been the standard attitude filter on spacecraft for many years in the industry.

The spacecraft kinematics and dynamics are described by a nonlinear, discrete-time state-space model. The onboard angular position sensor is corrupted by Gaussian, zero-mean, additive white noise. The angular velocity sensor is corrupted by Gaussian, additive white noise with an unknown bias. This bias vector is appended to the true state vector, to enable joint state and bias estimation.

3 Classical Methods

For linear systems, the Kalman filter is the optimal state observer. The extended Kalman filter was developed for nonlinear systems. The EKF uses a linearization of the system dynamics about its last estimated state. By taking only first-order terms into account, this results in a suboptimal solution. Recently, the unscented Kalman filter was introduced [1]. By making use of the unscented transform, the UKF is able to capture the first and second order terms of the nonlin-

ear system, thereby achieving better estimation performance than the EKF.

4 Moving Horizon Estimation

The state estimation problem can be formulated as an optimization problem, with the estimated states over a finite horizon as optimization variables [2]. By linearizing the system dynamics around the last estimated trajectory, the optimization problem becomes an unconstrained linear quadratic problem, which can be solved efficiently in one step. This algorithm is implemented as a moving horizon estimator. As a further improvement on this basic moving horizon estimator, a second MHE implementation iterates a finite number of times over this reference trajectory. This will lead to only a mild improvement in accuracy, but implies a significant increase in computational cost.

5 Particle Filters

An additionally considered filter is an implementation of a particle filter. This filter will propagate a large number of particles through the spacecraft model, each with artificial random noise added [3]. In order to avoid particle degeneracy, systematic importance resampling is performed at every time step [4]. The *a posteriori* probability density of these particles will approach the real *a posteriori* probability density for larger numbers of particles, yielding a very accurate filter. Due to the fact that the plant model has to be propagated many times, the computational cost of this filter is high.

References

- [1] J.L. Crassidis, F.L. Markley, Unscented Filtering for Spacecraft Attitude Estimation, *Journal of Guidance, Control and Dynamics*, vol. 26, July-August 2003
- [2] J. M. Maciejowski, Predictive Control with Constraints, *Pearson Education Limited*, 2002
- [3] B. Ristic, S. Arulampalam, N. Gordon, Beyond the Kalman Filter - Particle Filters for Tracking Applications, *Artech House*, 2004
- [4] G. Kitagawa, Monte Carlo filter and smoother for non-Gaussian non-linear state space models, *Journal of Computational and Graphical Statistics*, vol. 5, no. 1, pp. 1-25, 1996

Part 3

Plenary Lectures

Acknowledgements

- Former PhD-students: Kristian Lindqvist, Henrik Jansson, Jonas Mårtensson, Märta Barenthin
- Collaborators: Xavier Bombois, László Gerencsér, Michel Gevers, Roland Hildebrand, Lennart Ljung, Brett Ninness, Cristian Rojas, Bo Wahlberg, James Welsh

Part I: Coping with complexity – Concepts

Introduction

- Complexity of a system
- Experiment design
- Is complexity a problem?

Cost of complexity

- Introduction
- Cost of complexity and stochastic identification
- An alternative formulation
- Application to output error models

The impact of optimal experiments on the identification problem

- The Izzy and Ozzy problems
- Optimal experiments and model selection

Summary

SYSTEM IDENTIFICATION
OF
COMPLEX AND STRUCTURED
SYSTEMS

Håkan Hjalmarsson

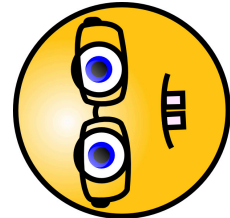
ACCESS Linnaeus Center, School of Electrical Engineering
KTH - Royal Institute of Technology, Stockholm

29th Benelux Meeting on Systems and Control
March 30–April 1, 2009



My assistants

Please say hi to



Izzy

and



Ozzy

Part II: Coping with complexity – Practice

Numerical computation
Introduction

Implementation of experiment designs
Introduction
The chicken-and-egg problem
Adaptive input design

Application examples
Non-minimum phase zero estimation
Zero estimation of Hammerstein system

Summary

Part III: Identification of structured systems

Structural limitations on modeling accuracy
MIMO identification
Multisensor identification
A closer look at the asymptotic covariance matrix
Multisensor identification cont'd

An example of decentralized identification
The problem
Centralized vs decentralized identification
Decentralized id with limited information exchange

Summary

Outline

Introduction

Complexity of a system
Experiment design
Is complexity a problem?

Cost of complexity
Introduction

Cost of complexity and stochastic identification
An alternative formulation
Application to output error models

The impact of optimal experiments on the identification problem
The Izzy and Ozzy problems
Optimal experiments and model selection

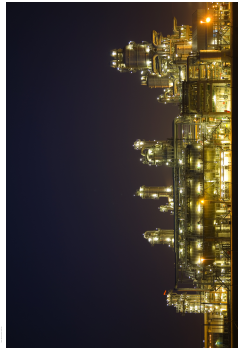
Summary

Part I

Coping with complexity: Concepts

What do we mean by complexity?

- Computer science: Computational complexity (Turing, Church, ...)
- Systems and control:
 - ▶ Computational complexity (see survey by Blondel and Tsitsiklis)
 - ▶ Feedback control under uncertainty (Zames; Egerstedt and Brockett; Delvenne and Blondel; Zhang and Guo)
- System identification:



???

Complexity in system identification



- Kolmogorov n -width (Zames)
- VC-dimension and PAC-learning (Vapnik-Chervonenkis, Vidyasagar)
- The minimum cost required to get within a given accuracy
- The minimum *experimental* cost
- Example: Time complexity of worst-case system identification (Poolla and Tikku)
- Here: *The minimum experimental cost required to achieve a certain performance in the application*

Outline

Introduction

Complexity of a system

Experiment design

Is complexity a problem?

Cost of complexity

Introduction

Cost of complexity and stochastic identification

An alternative formulation

Application to output error models

The impact of optimal experiments on the identification problem

The Izzy and Ozzy problems

Optimal experiments and model selection

Summary

Experiment design for system identification

- Much work in 1970's: (Mehra; Goodwin and Payne; Ng, Goodwin and Söderström; Zarrop)
 - ▶ Scalar criteria, often not involving the application directly
 - ▶ All covariance matrices can be generated by sinusoidal inputs
- Renewed interest in mid 1980's:
 - ▶ Use of high order variance expressions (Gevers and Ljung)
 - ▶ Design tied to the application (e.g. minimum variance control)
- Revival in 2000's:
 - ▶ *Least-costly identification for robust control* (Bombois, Scorletti, Van den Hof, Gevers and Hildebrand)
 - ▶ Semi-definite programming (Cooley, Lee and Boyd; Lindqvist; Jansson)
 - ▶ Robust stability and robust performance criteria (Hildebrand and Gevers; Jansson)
 - ▶ Nonlinear systems (Mårtensson; Novara, Vincent and Poolla)
 - ▶ Robust input design (Mårtensson; Rojas, Welsh, Goodwin, Feuer)
 - ▶ Plant-friendly design (Rivera, Lee, Mittelmann and Braun)

Outline

Introduction

Complexity of a system
Experiment design

Is complexity a problem?

Cost of complexity
Introduction

Cost of complexity and stochastic identification
An alternative formulation
Application to output error models

The impact of optimal experiments on the identification problem

The Izzy and Ozzy problems
Optimal experiments and model selection

Summary

Is there a problem?

The water-bed effect (Rojas, Welsh and Agüero):

$$\frac{1}{2\pi} \int_{-\pi}^{\pi} \underbrace{N \Phi_u^{id}(e^{j\omega})}_{\text{Input energy density}} \text{Var}[\hat{G}(e^{j\omega})] d\omega = \underbrace{n}_{\text{\# parameters}} \underbrace{\lambda_e}_{\text{noise variance}}$$

(output error models)

A fundamental limitation

YES, there is a problem!

Outline

Introduction

Complexity of a system
Experiment design
Is complexity a problem?

Cost of complexity
Introduction

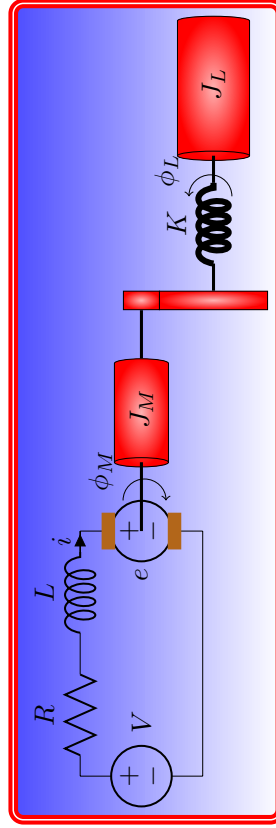
Cost of complexity and stochastic identification
An alternative formulation
Application to output error models

The impact of optimal experiments on the identification problem

The Izzy and Ozzy problems
Optimal experiments and model selection

Summary

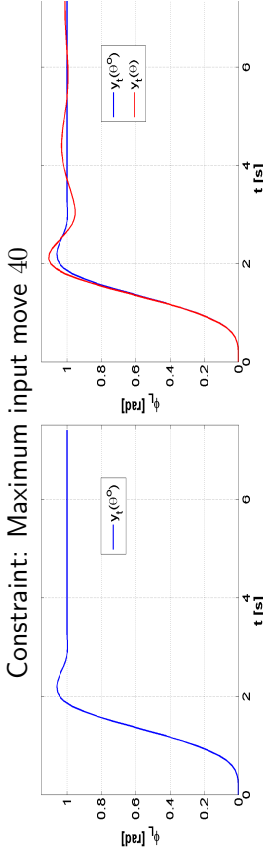
An application example: MPC of a DC-motor



- Input: Voltage V
- Output: Angle ϕ_L
- Model parameters θ : Resistance R , Moment of inertia J_L , Elasticity K , ...
- True parameters: θ^o

An application example: MPC of a DC-motor

- Ideal response: $y_t(\theta^o)$ - true parameters used in MPC
- Actual response: $y_t(\theta)$ - parameter θ used in MPC



Performance degradation / Set of acceptable models

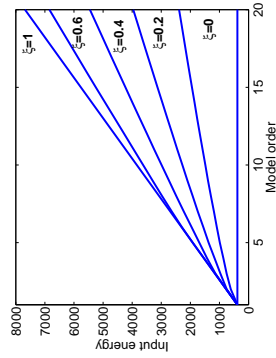
$$V_{app}(\theta) = \frac{1}{N} \sum_{t=1}^N (y_t(\theta^o) - y_t(\theta))^2$$

$$\mathcal{E}_{app} = \left\{ \theta : V_{app}(\theta) \leq \frac{1}{\gamma} \right\} \quad (\gamma = \text{accuracy})$$

Frequency function estimation

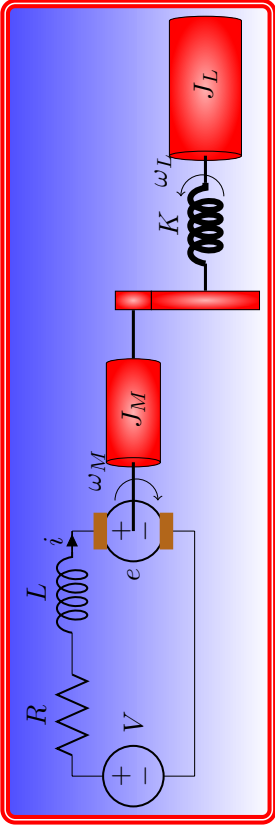
- FIR system: $y(t) = \sum_{k=0}^n \theta_k^o q^{-k} u(t) + e(t)$, $\mathbb{E}e^2(t) = \sigma_e^2$
- Application: $|G(e^{j\omega}, \hat{\theta}_N) - G(e^{j\omega}, \theta^o)|^2 \leq \frac{1}{\gamma}$ $|\omega| \leq \xi \pi$

Cost of complexity

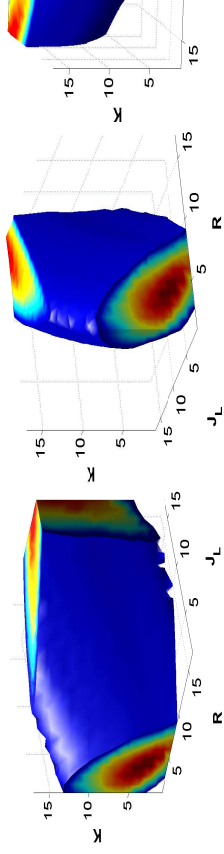


- Cost of complexity: $Q \approx \lambda_e \gamma n \xi$
- Rojas, Barentin and Welsh

An application example: MPC of a DC-motor



Set of acceptable models \mathcal{E}_{app} : (Maximum move size 3)



Summary of concepts

- Performance degradation for application: $V_{app}(\theta)$
- Set of acceptable models: $\mathcal{E}_{app} = \left\{ \theta : V_{app}(\theta) \leq \frac{1}{\gamma} \right\}$
- Identification: Produce $\hat{\theta}_N \in \mathcal{E}_{app} \subset \mathbb{R}^n$ (N = sample size)
- **Cost of complexity Q**
= Minimum possible experimental cost required for $\hat{\theta}_N \in \mathcal{E}_{app}$
- Least-costly identification
- **Quantification of Q**
- Here: Experimental cost = input energy

Cost of complexity

$$Q := \min_{NE} [u_t^2] \quad \text{s.t. } \hat{\theta}_N \in \mathcal{E}_{app} \subset \mathbb{R}^n$$

An optimal experiment design problem

Outline

Introduction

- Complexity of a system
- Experiment design
- Is complexity a problem?

Cost of complexity

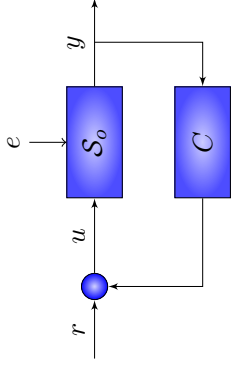
- Introduction
- Cost of complexity and stochastic identification
- An alternative formulation
- Application to output error models

The impact of optimal experiments on the identification problem

- The Izzy and Ozzy problems
- Optimal experiments and model selection

Summary

Identification recap



- Prediction error identification:
 - ▶ Prediction error: $\varepsilon_t(\theta)$
 - ▶ $\hat{\theta}_N = \arg \min \sum_{t=1}^N \varepsilon_t^2(\theta)$, $V_{id}(\theta) = \mathbf{E}[\varepsilon_t^2(\theta)] - \lambda_e \geq 0$
- Random noise (innovations (noise) variance λ_e)
- Stationary signals
- True system in the model set: $S_0 \Leftrightarrow \theta^o$ (to be relaxed later)
- High accuracy γ (implies large sample size N)
- $\sqrt{N} (\hat{\theta}_N - \theta^o) \sim \text{AsN} (0, 2\lambda_e V_{id}''(\theta^o)^{-1})$

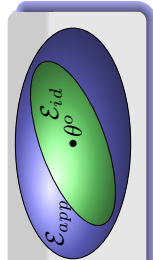
The cost of complexity

- Random noise $\Rightarrow \hat{\theta}_N$ random variable
- Cannot guarantee $\hat{\theta}_N \in \mathcal{E}_{app}$
- Relaxation: **Probability** ($\hat{\theta}_N \in \mathcal{E}_{app}$) = α (= 99% e.g.)
- In general difficult to compute
- Use standard asymptotic confidence ellipsoids:

Probability ($\hat{\theta}_N \in \mathcal{E}_{id}$) $\approx \alpha$, where

Cost of complexity

$$Q := \min \text{NE}[u_t^2] \\ \text{s.t. } \mathcal{E}_{id} \subseteq \mathcal{E}_{app} \subset \mathbb{R}^n$$



Outline

Introduction

- Complexity of a system
- Experiment design
- Is complexity a problem?

Cost of complexity

- Introduction
- Cost of complexity and stochastic identification
- An alternative formulation
- Application to output error models

The impact of optimal experiments on the identification problem

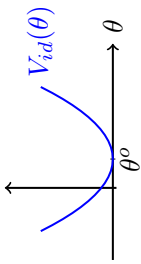
- The Izzy and Ozzy problems
- Optimal experiments and model selection

Summary

An alternative expression for the confidence ellipsoid

$$\mathcal{E}_{id} = \left\{ \theta : \frac{N}{2} (\theta - \theta^o)^T V_{id}''(\theta^o) (\theta - \theta^o) \leq \lambda_e n \right\}$$

Recall: $V_{id}(\theta) = E[\varepsilon_t^2(\theta)] - \lambda_e$. High accuracy γ , i.e. \mathcal{E}_{app} small



$$\Rightarrow V_{id}(\theta) \approx \frac{1}{2} (\theta - \theta^o)^T V_{id}''(\theta^o) (\theta - \theta^o)$$

$$\Rightarrow \mathcal{E}_{id} = \{ \theta : NV_{id}(\theta) \leq \lambda_e n \}$$

Confidence ellipsoid = Level set for identification criterion!

An alternative formulation of cost of complexity

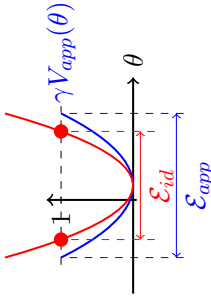
An alternative formulation of cost of complexity

Level sets:

$$\mathcal{E}_{app} = \left\{ \theta : V_{app}(\theta) \leq \frac{1}{\gamma} \right\} = \left\{ \theta : \gamma V_{app}(\theta) \leq 1 \right\}$$

$$\mathcal{E}_{id} = \left\{ \theta : NV_{id}(\theta) \leq \lambda_e n \right\} = \left\{ \theta : \frac{N}{\lambda_e n} V_{id}(\theta) \leq 1 \right\}$$

Recall: High accuracy $\gamma \Rightarrow \mathcal{E}_{app}$ small $\Rightarrow V_{id}$ and V_{app} quadratic:



$$\mathcal{E}_{id} \subseteq \mathcal{E}_{app} \Leftrightarrow \frac{N}{\lambda_e n} V_{id}(\theta) \geq \gamma V_{app}(\theta) \quad \forall \theta \in \mathcal{E}_{app}$$

$$\Leftrightarrow NV_{id}(\theta) \geq \lambda_e \gamma n V_{app}(\theta) \quad \forall \theta \in \mathcal{E}_{app}$$

A generalized version

General case:

$n_{app} = \#$ non-singular directions of V_{app} (= rank V_{app}'')

Cost of complexity

$$Q := \min NE[u_t^2]$$

$$s.t. NV_{id}(\theta) \geq \lambda_e \gamma n_{app} V_{app}(\theta), \quad \forall \theta \in \mathcal{E}_{app}$$

Example (Estimation of an impulse response coefficient)

- Model: $y_t = \sum_{k=1}^n \theta_k u_{t-k} + e_t$
- Objective: Estimate θ_1
- $V_{app}(\theta) = (\theta_1^o - \theta_1)^2$
- Only one parameter matters!
- but our confidence ellipsoid includes all n parameters
- Use a confidence ellipsoid for that parameter only: $n \Rightarrow 1$

Cost of complexity

$$Q := \min NE[u_t^2]$$

$$s.t. NV_{id}(\theta) \geq \lambda_e \gamma n_{app} V_{app}(\theta), \quad \forall \theta \in \mathcal{E}_{app}$$

Outline

Introduction

- Complexity of a system
- Experiment design
- Is complexity a problem?

Cost of complexity

- Introduction
- Cost of complexity and stochastic identification
- An alternative formulation

Application to output error models

- The impact of optimal experiments on the identification problem
- The Izzy and Ozzy problems
- Optimal experiments and model selection

Summary

Output error models

True system: $y_t = G_o(q)u_t + e_t$

Model: $y_t = G(q, \theta)u_t + e_t$

PE: $\varepsilon_t(\theta) = y_t - G(q, \theta)u_t = (G_o(q) - G(q, \theta))u_t + e_t$

$$V_{id}(\theta) = E[\varepsilon_t^2(\theta)] - \lambda_e = \frac{1}{2\pi} \int_{-\pi}^{\pi} \Phi_u^{id}(e^{j\omega}) |G(e^{j\omega}, \theta) - G_o(e^{j\omega})|^2 d\omega$$

Output error models

Output error models: Influence of $\lambda_e \gamma n_{app}$

$$Q := \frac{1}{2\pi} \int_{-\pi}^{\pi} N \Phi_u^{id}(e^{j\omega}) d\omega$$

$$s.t. \quad \frac{1}{2\pi} \int_{-\pi}^{\pi} N \Phi_u^{id}(e^{j\omega}) |G(e^{j\omega}, \theta) - G_o(e^{j\omega})|^2 d\omega \geq \lambda_e \gamma n_{app} V_{app}(\theta)$$

- Cost & constraint linear in $N \Phi_u^{id}$
 - ⇒ Problem scales with $\lambda_e \gamma n_{app}$
 - ⇒ **Cost of complexity: $Q = \lambda_e \gamma n_{app} \tilde{Q}$**
 - Optimal energy density: $N \Phi_u^{id} = \lambda_e \gamma n_{app} \tilde{\Phi}_u$**
- where $\tilde{\Phi}_u$ the solution to

$$\tilde{Q} := \min E[u^2(t)]$$

$$s.t. \quad V_{id}(\theta) \geq V_{app}(\theta)$$

- Independent of sample size, noise variance, accuracy, # of parameters
- Normalized problem

Cost of complexity

$$Q := \min N E[u_t^2] = \frac{1}{2\pi} \int_{-\pi}^{\pi} N \Phi_u^{id}(e^{j\omega}) d\omega$$

$$s.t. \quad \underbrace{N V_{id}(\theta)}_{\frac{1}{2\pi} \int_{-\pi}^{\pi} N \Phi_u^{id}(e^{j\omega}) |G(e^{j\omega}, \theta) - G_o(e^{j\omega})|^2 d\omega} \geq \lambda_e \gamma n_{app} V_{app}(\theta)$$

- Minimization with respect to energy density spectrum $N \Phi_u^{id}$
- Optimization tries to achieve

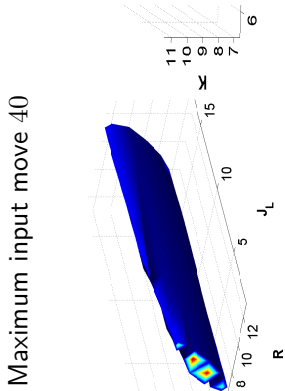
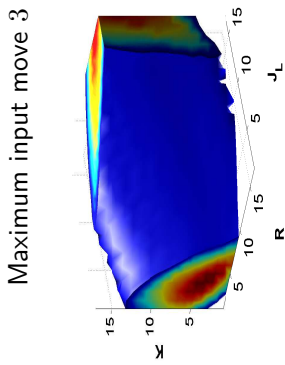
$$N V_{id}(\theta) = \lambda_e \gamma n_{app} V_{app}(\theta)$$

Identification cost matched to performance degradation

The normalized problem - Insights

$$\tilde{Q} := \min E[u^2(t)]$$

$$s.t. V_{id}(\theta) \geq V_{app}(\theta)$$

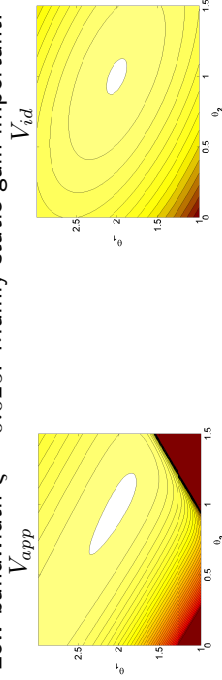


- Performance specifications determine the shape of $V_{app}(\theta)$
 - Curvature of $V_{app}(\theta)$ increases when specs. are tightened
- $\Rightarrow \tilde{Q}$ reflects performance specifications in the application
We will use $0 \leq \xi \leq 1$ to indicate specs. i.e. $\tilde{Q}(\xi)$

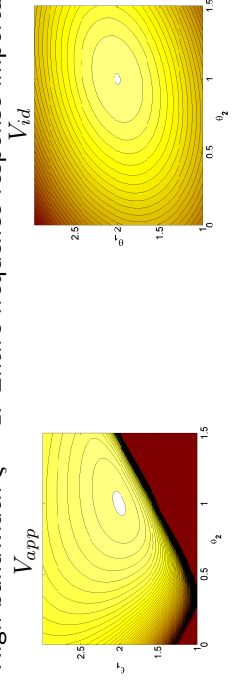
MRC: The impact of the performance specs.

$$y_t = G_o(q)u_t + e_t = \theta_1 u_t + \theta_2 u_{t-1} + e_t$$

- Low bandwidth $\xi = 0.025$. Mainly static gain important:

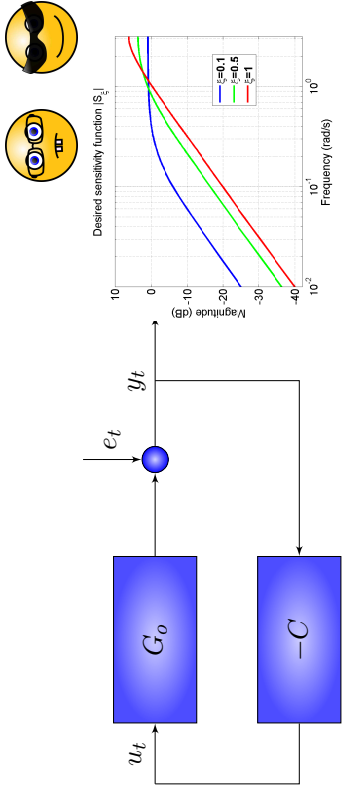


- High bandwidth $\xi = 1$. Entire frequency response important:



- How does ξ influence the cost of complexity?

Izzy and Ozzy goes to MRC (model reference control)



- Controller $C = C(G)$, G output error model
- Desired sensitivity function: S_ξ
- Achieved sensitivity function: $S(G) = \frac{1}{1+C(G)G_o}$
- Performance degradation: $V_{app}(G) := \left\| \frac{S(G) - S_\xi}{S_\xi} \right\|_2^2$

MRC: Cost of complexity

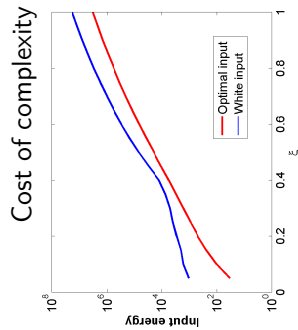
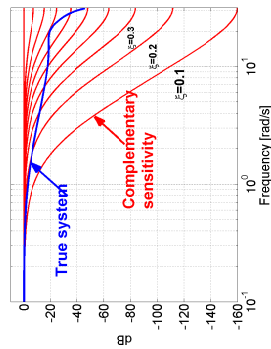
$$\tilde{Q} := \min E[u^2(t)]$$

$$s.t. V_{id}(\theta) \geq V_{app}(\theta)$$

- Matching condition: $V_{id}(\theta) = V_{app}(\theta)$
- Output error: $V_{id}(\theta) = \frac{1}{2\pi} \int_{-\pi}^{\pi} \tilde{\Phi}_u(e^{j\omega}) |G(e^{j\omega}, \theta) - G_o(e^{j\omega})|^2 d\omega$
- MRC: $V_{app}(G) := \left\| \frac{S(G) - S_\xi}{S_\xi} \right\|_2^2 \approx \frac{1}{2\pi} \int_{-\pi}^{\pi} \frac{\Phi_u^{desired}(e^{j\omega})}{\lambda_e} |G - G_o|^2 d\omega$
- Take $\tilde{\Phi}_u = \Phi_u^{desired} / \lambda_e \Rightarrow N \Phi_u^{id} = \gamma m \Phi_u^{desired}$
Scaled version of desired operating conditions!
- Upper bound: $Q \leq \gamma m \|\Phi_u^{desired}\|_1$

MRC: Cost of complexity

- $Q \leq \gamma n \|\Phi_u^{desired}\|_1 = \lambda_e \gamma n \left\| \frac{1-S\xi}{G_o} \right\|_2^2$
 - Allows user to make informed trade-offs:
 - Performance specs. vs experimental cost
 - Time vs excitation: $N\Phi_u^{id} = \gamma n \Phi_u^{desired}$.
 - Minimum time stealth id.: $E[u_t^2] \leq \lambda_u^{max}$
- $$\Rightarrow \min N = \gamma n \frac{E[u_{max}^2]}{\lambda_u^{max}}$$



Output error models: Cost of complexity - Summary

Cost of complexity

$$Q \approx \lambda_e \gamma n_{app} \tilde{Q}(\xi)$$

- λ_e : noise level
- γ : accuracy
- n_{app} : # of non-singular directions in the parameter space
- $\tilde{Q}(\xi)$: normalized cost

Implications:

- System complexity not important
- Performance specs of application determine cost
- Allows user to make informed trade-offs: specs. vs cost, time vs excitation

Some connections to the past

- Identification experiment = desired closed loop operating conditions:
- Random errors
 - ▶ Minimum variance control (Gevers and Ljung 1986, Hjalmarsson, Gevers and De Bruyne 1996, Hildebrand and Solari 2007, Mårtensson, Rojas and Hjalmarsson 2009)
 - Bias errors
 - ▶ Many contributions in the 1990s to identification for control, e.g.:
 - ▶ Control-relevant prefiltering (Rivera, Pollard, Garcia 1992)
 - ▶ Iterative identification and control (Schrama 1992, Zang, Bitmead and Gevers 1995)
 - ▶ Virtual feedback reference tuning (Campi, Lecchini, Savaresi 2002)
 - Contributions here:
 - ▶ Results above different sides of the same coin (matching V_{id} and V_{app})
 - ▶ Matching not enough. Sufficient input energy required. ($N\Phi_u^{id} = \lambda_e \gamma n \Phi_u^{desired}$)

Outline

- Introduction
 - Complexity of a system
 - Experiment design
 - Is complexity a problem?
- Cost of complexity
 - Introduction
 - Cost of complexity and stochastic identification
 - An alternative formulation
 - Application to output error models
- The impact of optimal experiments on the identification problem
 - The Izzy and Ozzy problems
 - Optimal experiments and model selection
- Summary

The Izzy and Ozzy problems



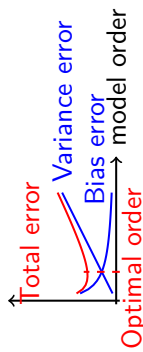
Izzy and Ozzy

Static gain estimate

Model order:	very low	true	very high
Constant input	good	good	good

Impulse response coefficient estimate

Model order:	very low	true	very high
White input	fair	good	good



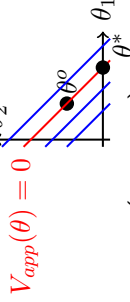
Robustness against choice of model order. Why?

The Izzy & Ozzy problems: Static gain estimation

Model order:	low	true	high
Constant input	good	good	good

$$y_t = \sum_{k=1}^n \theta_k u_{t-k} + e_t$$

Performance degradation: $V_{app}(\theta) = (\sum \theta_k - \sum \theta_k^o)^2$

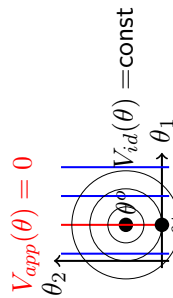


- Optimal input: $u_t = u$ (constant) $\Rightarrow y_t = \sum_k \theta_k^o u + e_t$
- Property of interest visible
- No other system property visible (due to min energy crit.)
- \Rightarrow Perfect match $V_{id}(\theta) \propto V_{app}(\theta)$
- Same input optimal for high order system \Rightarrow high order ok
- $V_{id}(\theta) \propto V_{app}(\theta) \Rightarrow$ Bias minimized!
- $V_{id}(\theta^*) = 0 \Rightarrow$ no unmodelled dynamics \Rightarrow low order optimal

The Izzy & Ozzy problems: Impulse response

Model order:	low	true	high
White input	fair	good	good

Performance degradation: $V_{app}(\theta) = (\theta_1 - \theta_1^o)^2$



- Optimal input: white
- Property of interest visible
- All system properties visible (V_{id} cannot be shaped arbitrarily)
- \Rightarrow No match $V_{id}(\theta) \propto V_{app}(\theta)$
- Same input optimal for high order system \Rightarrow high order ok
- V_{id} aligned to $V_{app} \Rightarrow$ Bias minimized!
- $V_{id}(\theta^*) > 0 \Rightarrow$ unmodelled dynamics \Rightarrow low order not optimal
- NMP-zero estimation another example

Outline

Introduction
Complexity of a system
Experiment design
Is complexity a problem?

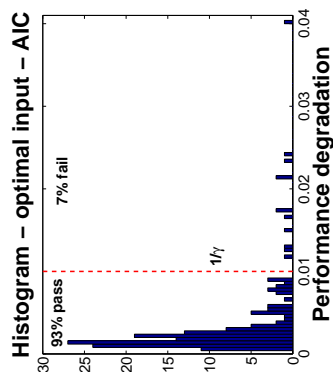
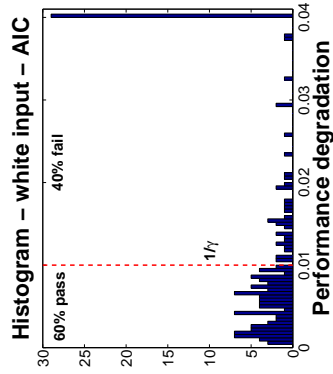
Cost of complexity
Introduction
Cost of complexity and stochastic identification
An alternative formulation
Application to output error models

The impact of optimal experiments on the identification problem
The Izzy and Ozzy problems
Optimal experiments and model selection

Summary

MRC: Model selection using AIC

- AIC unbiased estimate of $E[V_{id}(\hat{\theta}_N)]$
- Optimal experiment design: $V_{id} \propto V_{app}$
- Use AIC to estimate $E[V_{app}(\hat{\theta}_N)]$
- Model order selection with the application in mind
- MRC example revisited:



Outline

- Introduction
 - Complexity of a system
 - Experiment design
 - Is complexity a problem?
- Cost of complexity
 - Introduction
 - Cost of complexity and stochastic identification
 - An alternative formulation
 - Application to output error models
- The impact of optimal experiments on the identification problem
 - The Izzy and Ozzy problems
 - Optimal experiments and model selection
- Summary

Identification of complex systems: Concepts

Optimal experiment

Aims at achieving

$$NV_{id}(\theta) = \lambda_e \gamma n_{app} V_{app}(\theta)$$

using minimum energy

- To achieve this requires **parsimonious excitation**:
 - System properties important to the application should be visible in the data
 - System properties not important to the application should not be visible in the data, unless necessary for i).
(The let sleeping dogs lie paradigm)
- As a result, the entire system may not have to be identified!
 - ▶ Choice of model structure less critical
 - ▶ Advice: Don't use too low order (c.f. impulse response). Use model reduction instead (c.f. the ASYM method by Zhu).

Part II

Coping with complexity: Practice

Outline

Numerical computation
Introduction

Implementation of experiment designs
Introduction
The chicken-and-egg problem
Adaptive input design

Application examples

Non-minimum phase zero estimation
Zero estimation of Hammerstein system

Summary

Numerical computation

Cost of complexity

$$Q := \min NE[u^2(t)]$$

$$s.t. NV_{id}(\theta) \geq \lambda_e \gamma n_{app} V_{app}(\theta)$$

Recall: Output error models

$$NV_{id}(\theta) = \frac{1}{2\pi} \int_{-\pi}^{\pi} N\Phi_u^{id}(e^{j\omega}) |G(e^{j\omega}, \theta) - G_o(e^{j\omega})|^2 d\omega$$

$$NE[u^2(t)] = \frac{1}{2\pi} \int_{-\pi}^{\pi} N\Phi_u^{id}(e^{j\omega}) d\omega$$

- Use finite dimensional parametrization of $N\Phi_u^{id}$
- ⇒ Semi-definite program!
- Generalizes to other model structures

Outline

Numerical computation
Introduction

Implementation of experiment designs
Introduction
The chicken-and-egg problem
Adaptive input design

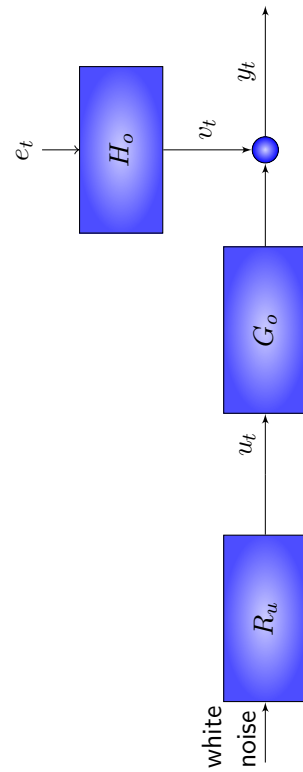
Application examples

Non-minimum phase zero estimation
Zero estimation of Hammerstein system

Summary

Implementation

- Optimal experiment design ⇒ Input spectrum Φ_u^{id}
- Spectral factorization: $\Phi_u^{id}(e^{j\omega}) = |R_u(e^{j\omega})|^2$



Outline

Numerical computation
Introduction

Implementation of experiment designs
Introduction

The chicken-and-egg problem
Adaptive input design

Application examples

Non-minimum phase zero estimation
Zero estimation of Hammerstein system

Summary

Implementation

Cost of complexity

$$Q := \min NE[u^2(t)]$$

$$s.t. NV_{id}(\theta) \geq \lambda_e \gamma n_{app} V_{app}(\theta)$$

- Optimization problem depends on the unknown system!
- Major obstacle
- Solutions:
 - ▶ Robust experiment design (e.g. Rojas, Welsh, Goodwin, Feuer 2007)
 - ▶ Adaptive (sequential) experiment design

Outline

Numerical computation
Introduction

Implementation of experiment designs
Introduction

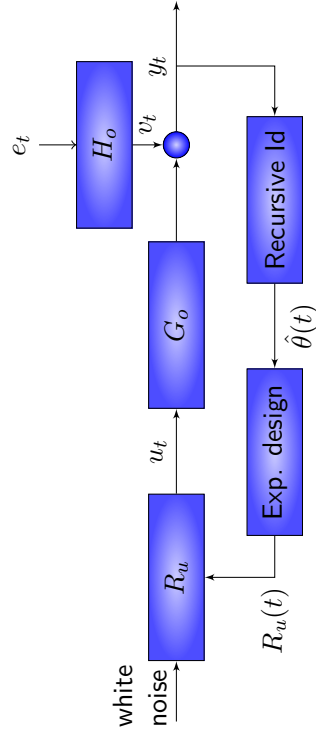
The chicken-and-egg problem
Adaptive input design

Application examples

Non-minimum phase zero estimation
Zero estimation of Hammerstein system

Summary

Adaptive input design



- An adaptive feedback system
- But measured signal not fed back directly
- Exp. design limits input power \Rightarrow Stability when G_o stable

Key questions:

- Convergence?
- Accuracy?

Adaptive input design

Key questions:

- Convergence?
- Accuracy?

Theorem (Gerencsér's free lunch theorem for ARX-models)

- True system in the model set
 - System stable
- ⇒ Optimal accuracy when sample size grows

Gerencsér

Adaptive input design

What happens when true system is not in the model set?

Example

NMP-zero estimation

- Quantity of interest: $z_o: G_o(z_o) = 0, |z_o| > 1$
- Optimal input: $u_t = \frac{c}{z^{-1}-z_o} u_t$
- V_{id} and V_{app} not matched (c.f. impulse response problem)
- Still $y_t = \theta_1 u_t + \theta_2 u_{t-1} \Rightarrow$ consistent estimate

Outline

Numerical computation

Introduction

Implementation of experiment designs

Introduction

The chicken-and-egg problem

Adaptive input design

Application examples

Non-minimum phase zero estimation

Zero estimation of Hammerstein system

Summary

Non-minimum phase zero estimation

- Objective: Estimate NMP zero: $G_o(z_o) = 0, |z_o| > 1$
- $V_{app}(\theta) = (z_o - z(\theta))^2$
- $n_{app} = 1!$ (only the zero matters)
- Optimal input: $u_t = z_o^{-1} u_{t-1} + c e_t, e_t$ white noise
- V_{id} and V_{app} not matched!

Summary

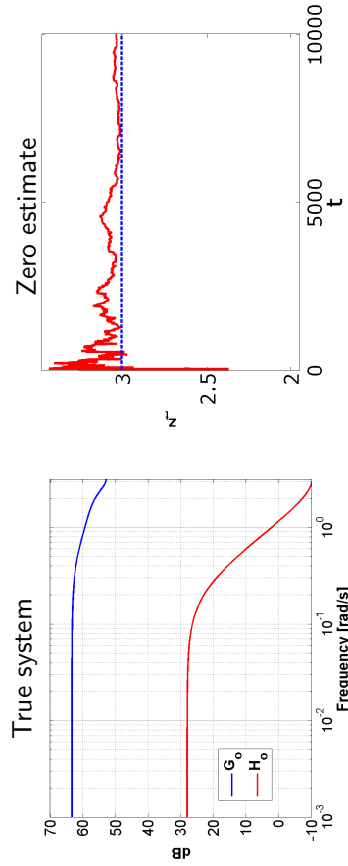
- Important properties visible
- Other prop. need not be visible
- Model set less critical
- $n_{app} = 1$

NMP estimation

- Input spectrum has a pole at $z_o!$
- Input persistently exciting
- $y_t = \theta_1 u_t + \theta_2 u_{t-1} \Rightarrow$ consistent estimate
- Energy/input independent of system complexity

Non-minimum phase zero estimation

True system: $y_t = \frac{(q-3)(q-0.1)(q-0.2)(q+0.3)}{q^4(q-0.5)}u_t + \frac{q}{q-0.8}e_t^o$
 Model: $y_t = \hat{g}_1 \frac{q-\hat{z}}{q^2}u_t + e_t$, Input: $u_t = \hat{z}_t u_{t-1} + c_t e_t$



Example: Non-minimum phase zero estimation

Theorem (Rojas and Gerencsér)

True system: $y_t = G_o(q)u_t + H_o(q)e_t^o$
 Model: $y_t = \hat{g}_1 \frac{q-\hat{z}}{q^2}u_t + e_t$
 Input: $u_t = \hat{z}_t u_{t-1} + c_t e_t$

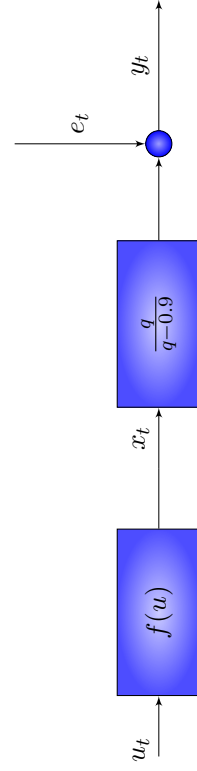
with G_o and H_o stable and rational.
 $\hat{z}_t \rightarrow$ largest NMP-zero of system w.p.1

Outline

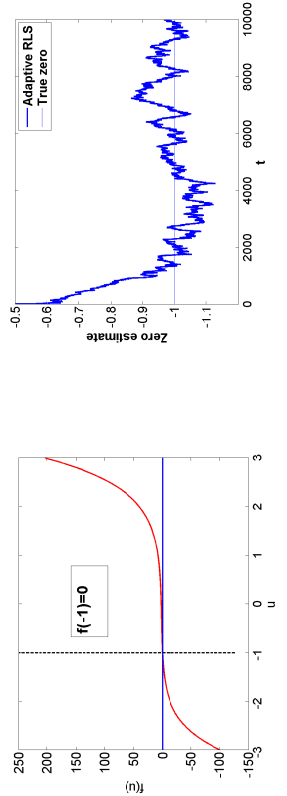
- Numerical computation
 - Introduction
- Implementation of experiment designs
 - Introduction
 - The chicken-and-egg problem
 - Adaptive input design
- Application examples
 - Non-minimum phase zero estimation
 - Zero estimation of Hammerstein system

Summary

Example: Zero estimation of Hammerstein system



Model: $y_t = u_t + \theta u_{t-1}$ (1 parameter only)



Outline

Numerical computation
Introduction

Implementation of experiment designs
Introduction
The chicken-and-egg problem
Adaptive input design

Application examples

Non-minimum phase zero estimation
Zero estimation of Hammerstein system

Summary

What have we learnt?

- A framework for quantification of the experimental cost where the application is taken into account
 - Allows the user to make trade-offs
 - The optimal experiment matches the identification criterion to the performance degradation using parsimonious excitation (The let sleeping dogs lie paradigm)
 - Simplifies the identification problem
 - Adaptive input design practical implementation
 - Focus on the application!
- Future directions:
- Nonlinear systems
 - Communication systems
 - Adaptive control
 - Structured systems (e.g. decentralized and networked)
A lot of exciting problems remain!!

Outline

Structural limitations on modeling accuracy

MIMO identification

Multisensor identification

A closer look at the asymptotic covariance matrix

Multisensor identification cont'd

An example of decentralized identification

The problem

Centralized vs decentralized identification

Decentralized id with limited information exchange

Summary

Part III

Identification of structured systems

MIMO identification

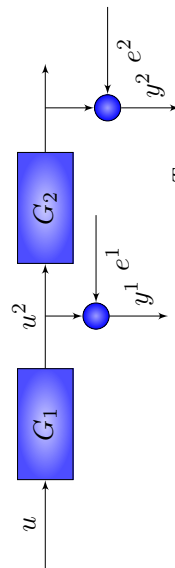
- Significant progress in regards to computation (subspace id, overparametrized state-space models)
- Asymptotic theory (convergence, normality, ...) well understood (since long)
- e.g. formula for Fisher information matrix
- but
- so far relatively little work on structural properties
- MISO (Gevers, Miskovic, Bonvin and Karimi 2006)

Outline

- Structural limitations on modeling accuracy
- MIMO identification
- Multisensor identification**
- A closer look at the asymptotic covariance matrix
- Multisensor identification cont'd
- An example of decentralized identification
- The problem
- Centralized vs decentralized identification
- Decentralized id with limited information exchange

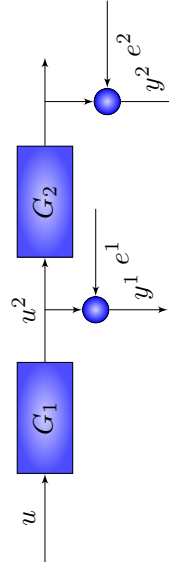
Summary

Multisensor identification (cascade systems)

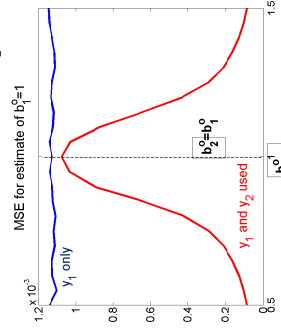


- $y_t^i = u_t^i + b_i^o u_{t-1}^i + e_t^i$, $\theta = [b_1 \ b_2]^T$
- Input u white noise. Variance λ_u
- y^1 low quality (Noise variance $\lambda_{e^1} = \lambda_u$)
- y^2 high quality (Noise variance $\lambda_{e^2} = 0.1\lambda_{e^1}$)
- b_1^o parameter of interest
- u but not u^2 available

Multisensor identification

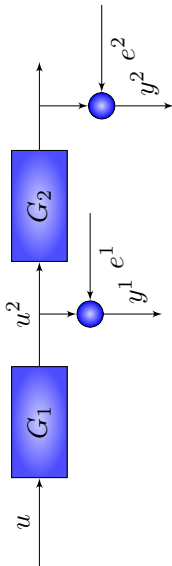


$$y_t^i = u_t^i + b_i^o u_{t-1}^i + e_t^i, \quad \theta = [b_1 \ b_2]^T$$



Despite y^2 being high quality, almost no improvement when $b_2^o \approx b_1^o$
Why?

A simpler case



- Model set: $G_i(q) = b_i q^{-1}$, $i = 1, 2$
- $y^1(t) = b_1^0 u_{t-1} + e_t^1$
- Gives us b_1^0 with poor accuracy
- $y^2(t) = b_1^0 b_2^0 u_{t-2} + e_t^2$
- Gives us $b_1^0 b_2^0$ with high accuracy
- Does not add to the information regarding b_1^0 !
- Structural property
- To be continued ...

The asymptotic covariance matrix: Pandora's (black) box

A lot of model error information hidden in P :

- System properties
 - ▶ Frequency function
 - ▶ Impulse response coefficients
 - ▶ Gains
 - ▶ Poles and zeros
 - ▶ Control applications
- Structural
 - ▶ Model structure (ARX, ARMAX, Box-Jenkins, non-linear,...)
 - ▶ Model order
 - ▶ Open vs closed loop
 - ▶ Input channels and input excitation
 - ▶ Sensor channels
 - ▶ Noise

Many have contributed to revealing its secrets!

Outline

Structural limitations on modeling accuracy
 MIMO identification
 Multisensor identification
A closer look at the asymptotic covariance matrix
 Multisensor identification cont'd

An example of decentralized identification
 The problem
 Centralized vs decentralized identification
 Decentralized id with limited information exchange

Summary

The asymptotic variance for a quantity of interest

$$\sqrt{N} (\hat{\theta}_N - \theta^o) \sim \text{AsN}(0, P)$$

Quantity of interest: $\mathcal{J}(\theta^o)$

$$\sqrt{N} (\mathcal{J}(\hat{\theta}_N) - \mathcal{J}(\theta^o)) \sim \text{AsN}(0, \mathcal{J}'(\theta^o)^T P \mathcal{J}'(\theta^o))$$

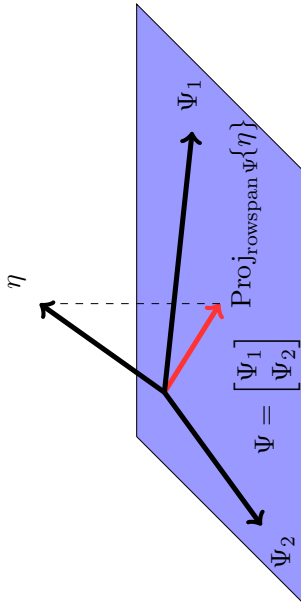
$$\mathcal{J}'(\theta^o)^T P \mathcal{J}'(\theta^o) = \mathcal{J}'(\theta^o)^T \langle \Psi, \Psi \rangle^{-1} \mathcal{J}'(\theta^o)$$

$$\Psi(e^{j\omega}) = \text{Model sensitivity} \times \text{SNR}$$

Meaning what???

A geometric interpretation

Projection of a (row) vector on a subspace:



$$\text{Proj}_{\text{rowspan } \Psi} \{\eta\} = \eta \Psi^T (\Psi \Psi^T)^{-1} \Psi = \langle \eta, \Psi \rangle \langle \Psi, \Psi \rangle^{-1}$$

where $\langle X, Y \rangle = XY^T$

$$\|\text{Proj}_{\text{rowspan } \Psi} \{\eta\}\|^2 = \langle \eta, \Psi \rangle \langle \Psi, \Psi \rangle^{-1} \langle \Psi, \eta \rangle$$

A geometric interpretation

$$\|\text{Proj}_{\text{rowspan } \Psi} \{\eta\}\|^2 = \langle \eta, \Psi \rangle \langle \Psi, \Psi \rangle^{-1} \langle \Psi, \eta \rangle$$

$$\mathcal{J}'(\theta^0)^T P \mathcal{J}'(\theta^0) = \mathcal{J}'(\theta^0)^T \langle \Psi, \Psi \rangle^{-1} \mathcal{J}'(\theta^0)$$

Suppose we had η such that $\langle \Psi, \eta \rangle = \mathcal{J}'(\theta^0)$

$$\Rightarrow \mathcal{J}'(\theta^0)^T P \mathcal{J}'(\theta^0) = \|\text{Proj}_{\text{rowspan } \Psi} \{\eta\}\|^2$$

$$\Psi(e^{j\omega}) = \text{Model sensitivity} \times \text{SNR}$$

- Geometric interpretation of asymptotic variance
- Rowspace of Ψ depends on model structure and experiment
- η exists and often same η for different structures
- ⇒ Comparisons using rowspace of Ψ only

Outline

Structural limitations on modeling accuracy
 MIMO identification
 Multisensor identification
 A closer look at the asymptotic covariance matrix
Multisensor identification cont'd

An example of decentralized identification

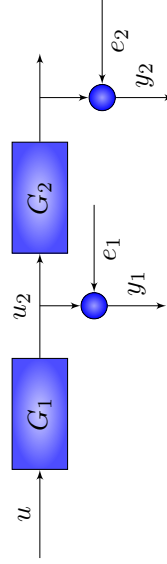
The problem

Centralized vs decentralized identification

Decentralized id with limited information exchange

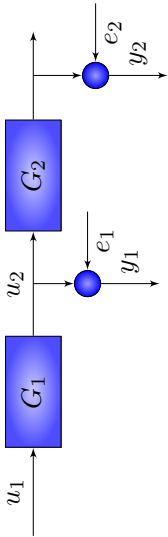
Summary

Application: Multisensor identification



- $G_i(\theta_i)$ (independent parametrizations)
- y^1 only: $\Psi^{y^1, y^2}(z) = [G_1'(\theta_1^0) \ 0]$
- y^1 and y^2 : $\Psi^{y^1, y^2}(z) = \begin{bmatrix} G_1'(\theta^0) & \alpha G_2(\theta_2^0) G_1'(\theta_1^0) \\ 0 & \alpha G_1(\theta_1^0) G_2'(\theta_2^0) \end{bmatrix}$
- Same $\eta(z) = [f(z) \ 0]$ works for one and two sensor cases
- Suppose **rowspan $G_2(\theta_2^0) G_1'(\theta_1^0) \subseteq \text{rowspan } G_1(\theta_1^0) G_2'(\theta_2^0)$**
- ⇒ $\text{rowspan } \Psi^{y^1, y^2}(z) = \text{rowspan } \Psi^{y^1}(z) \oplus [0 \ G_1(\theta_1^0) G_2'(\theta_2^0)]^{\perp \eta}$
- ⇒ $\|\text{Proj}_{\text{rowspan } \Psi^{y^1, y^2}} \{\eta\}\|^2 = \|\text{Proj}_{\text{rowspan } \Psi^{y^1}} \{\eta\}\|^2$
- ⇒ **Same variance for θ_1^0 estimate!**

Application: Multisensor identification (Simple case)

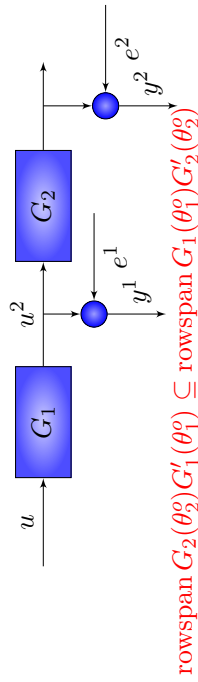


- u_1 white noise. Variance λ_u
- Quantity of interest: $\mathcal{J}(\theta^0) = b_1^0$.
- Variance of \hat{b}_1 : $\|\text{Proj}_{\text{rowspan } \Psi}\{\eta\}\|^2$

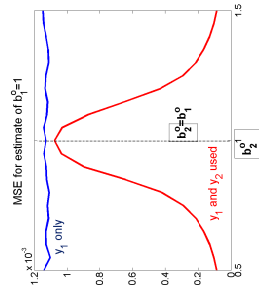
y_1 only:

- $y_1(t) = b_1 u(t-1) + e_1(t)$
- $\Psi^{y_1}(z) = \left[\left(\frac{\lambda_u}{\lambda_{e_1}}\right)^{1/2} z^{-1} \quad 0 \right]$
- $\gamma = \left(\frac{\lambda_{e_1}}{\lambda_u}\right)^{1/2} [z^{-1} \quad 0] \Rightarrow \langle \gamma, \Psi^{y_1} \rangle = 1$

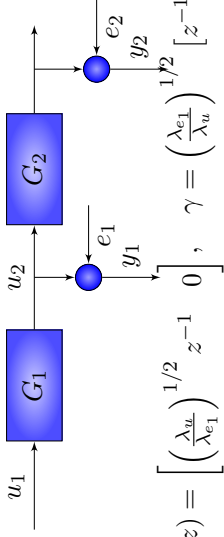
Application: Multisensor identification (Less simple case)



- G_1 and G_2 same structure and $\theta_1^0 = \theta_2^0$
- $\Rightarrow G_2(\theta_2^0)G_1'(\theta_1^0) = G_1(\theta_1^0)G_2'(\theta_2^0)$



Application: Multisensor identification (Simple case)



y_1 only:

- $\Psi^{y_1}(z) = \left[\left(\frac{\lambda_u}{\lambda_{e_1}}\right)^{1/2} z^{-1} \quad 0 \right]$, $\gamma = \left(\frac{\lambda_{e_1}}{\lambda_u}\right)^{1/2} [z^{-1} \quad 0]$

y_1 and y_2 :

- $y_2(t) = b_1 b_2 u(t-2) + e_2(t)$
- $\Psi^{y_1, y_2}(z) = \begin{bmatrix} \left(\frac{\lambda_u}{\lambda_{e_1}}\right)^{1/2} z^{-1} & \left(\frac{\lambda_u}{\lambda_{e_2}}\right)^{1/2} b_2^0 z^{-2} \\ 0 & \left(\frac{\lambda_u}{\lambda_{e_2}}\right)^{1/2} b_1^0 z^{-2} \end{bmatrix}$
- $\langle \gamma, \Psi^{y_1, y_2} \rangle = [1 \quad 0]$. Same γ works!
- $\text{rowspan } \Psi^{y_1, y_2} = \text{rowspan } \Psi^{y_1}(z) \oplus \left[0 \quad \left(\frac{\lambda_u}{\lambda_{e_2}}\right)^{1/2} b_1^0 z^{-2} \right]$

$\Rightarrow \|\text{Proj}_{\text{rowspan } \Psi^{y_1, y_2}}\{\eta\}\|^2 = \|\text{Proj}_{\text{rowspan } \Psi^{y_1}}\{\eta\}\|^2$
 \Rightarrow Same variance for \hat{b}_1^0 estimate!

Outline

- Structural limitations on modeling accuracy
- MIMO identification
- Multisensor identification
- A closer look at the asymptotic covariance matrix
- Multisensor identification cont'd

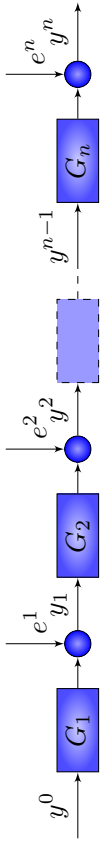
An example of decentralized identification

The problem

- Centralized vs decentralized identification
- Decentralized id with limited information exchange

Summary

Decentralized identification



- $G_i = b_i^o z^{-1}$
- Correlated noise: $e^1 = e^2 = \dots = e^n =: e$ (prior knowledge)
- Objective: Estimate $\sum_{i=1}^n b_i$
- Scenarios:
 - ▶ Centralized: Use y^0, \dots, y^n to estimate all parameters
 - ▶ Decentralized: Use y^{i-1}, y^i to estimate b_i^o .
- Accuracy of $\sum_{i=1}^n \hat{b}_i$?

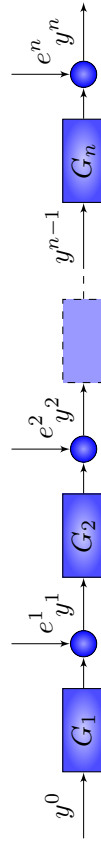
Outline

Structural limitations on modeling accuracy
 MIMO identification
 Multisensor identification
 A closer look at the asymptotic covariance matrix
 Multisensor identification cont'd

An example of decentralized identification
 The problem
 Centralized vs decentralized identification
 Decentralized id with limited information exchange

Summary

Centralized vs decentralized identification



Centralized:

- $y_t^i = b_i y_{t-1}^{i-1} + e_t$
- $e_t = y_t^i - b_i y_{t-1}^{i-1}$
- $y_t^{i+1} = b_{i+1} y_{t-1}^i + e(t) = b_{i+1} y_{t-1}^i + y_t^i - b_i y_{t-1}^{i-1}$
- Noise free relationship! \Rightarrow Exact estimates of all b_i !

Decentralized:

- $y_t^i = b_i y_{t-1}^{i-1} + e_t$
- LS-estimate: $\hat{b}_i = b_i^o + w$, where $w = \frac{1}{N} \sum_{i=1}^N e_t$
- $\sum_{i=1}^n \hat{b}_i = \sum_{i=1}^n b_i^o + nw$
- Variance $= n^2 E[w^2] = n^2 \lambda_e / N$

Can we improve on the decentralized estimate?

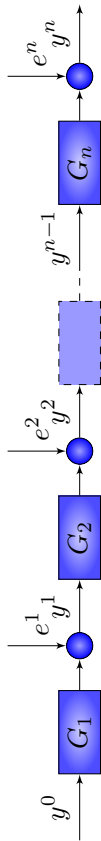
Outline

Structural limitations on modeling accuracy
 MIMO identification
 Multisensor identification
 A closer look at the asymptotic covariance matrix
 Multisensor identification cont'd

An example of decentralized identification
 The problem
 Centralized vs decentralized identification
 Decentralized id with limited information exchange

Summary

Decentralized estimation with information exchange



- $y_t^{i+1} = b_{i+1}y_t^i + y_t^i - b_i y_t^{i-1}$
- Neighbor i passes a few samples of its input y^{i-1} to the next node $i + 1$
- Exact estimates obtained in decentralized identification

Identification of structured systems

- MIMO systems is a very rich family of systems
- Geometric approach (an alternative to matrix algebra)
- Only at the beginning of decentralized identification

Outline

Structural limitations on modeling accuracy
 MIMO identification
 Multisensor identification
 A closer look at the asymptotic covariance matrix
 Multisensor identification cont'd

An example of decentralized identification
 The problem
 Centralized vs decentralized identification
 Decentralized id with limited information exchange

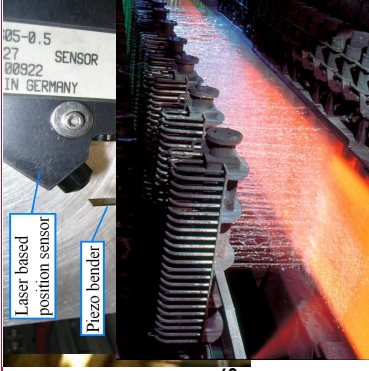
Summary

Control of PDEs: Trajectory Planning and Feedforward Control (Part I)

Andreas KUGI and Thomas MEURER

29th Benelux Meeting on Systems and Control
Heeze, The Netherlands
March 30–April 1, 2010

Tracking Control Problems for DPS



- Piezoelectric actuators and piezoactuated adaptive structures
- Adaptive optics
- Tubular, fixed-bed reactors in chemical engineering and 3-way catalytic converters
- Reheating and cooling processes in steel industry

Characteristics: Modeling leads to a description in terms of PDEs

Consequence: The DPS character has to be taken into account for trajectory planning, feedforward and feedback control

Early Lumping: "First approximate, then design..."

- **Advantage:** Well-known design methods of linear and nonlinear control theory for finite-dimensional systems can be applied
- **But:**
 - Structure of the physical system is not fully exploited
 - In general, this results in high-dimensional feedback laws
 - The neglected dynamics may degrade the control performance (spillover)
 - Systematic proof of the stability of the closed-loop system is often not possible

Late Lumping: "First design, then approximate (if necessary)..."

Flatness for Finite-Dimensional Systems

- The notion of flatness [Fliess et al. '95, Rudolph '03]

The system $\frac{d}{dt}x = f(x, u), \quad x(0) = x_0$

with the state $x \in \mathbb{R}^n$ and the input $u \in \mathbb{R}^m$ is said to be (differentially) **flat**, if there exists a set of m differentially independent variables (the **flat output**)

$$y = [y_1, \dots, y_m] \quad y = \psi(x, u, \dot{u}, \dots, u^{(n)})$$

s.t.

$$\begin{cases} x = \phi_1(y, \dot{y}, \dots, y^{(x)}) \\ u = \phi_2(y, \dot{y}, \dots, y^{(x+1)}) \end{cases}$$



A. Kugi and T. Meurer
31.03.2010



Gruppe für Komplexe
Dynamische Systeme (CDS)

5

Agenda: Feedforward Controller Design

- Operator based design (Euler-Bernoulli beam, piezoelectric stack actuator, linear heavy chain system)
- Spectrum based design (MFC actuated beam)
- Power series based design (DCR system and semilinear heavy chain example)
- Recursion based design (DCR system on higher dimensional domains)



A. Kugi and T. Meurer
31.03.2010



Gruppe für Komplexe
Dynamische Systeme (CDS)

7

Agenda: Feedforward Controller Design

- Operator based design (Euler-Bernoulli beam, piezoelectric stack actuator, linear heavy chain system)
- Spectrum based design (MFC actuated beam)
- Power series based design (DCR system and semilinear heavy chain example)
- Recursion based design (DCR system on higher dimensional domains)



A. Kugi and T. Meurer
31.03.2010

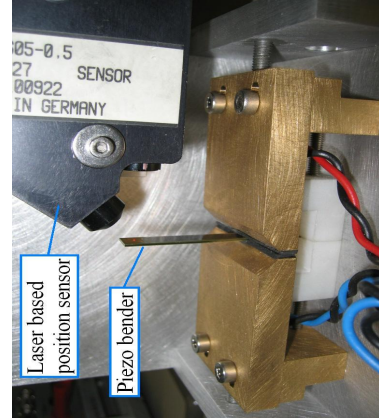


Gruppe für Komplexe
Dynamische Systeme (CDS)

6

Tracking Control of a Piezoelectric Bender

Micro-positioning device: piezoelectric trimorph bender



- carbonfiber VIBRIT 1100
- dimensions: 40 x 7,2 x 0,75 mm
- supply voltage: +/- 100 V
- 1st resonance frequency: 298,6 Hz



A. Kugi and T. Meurer
31.03.2010

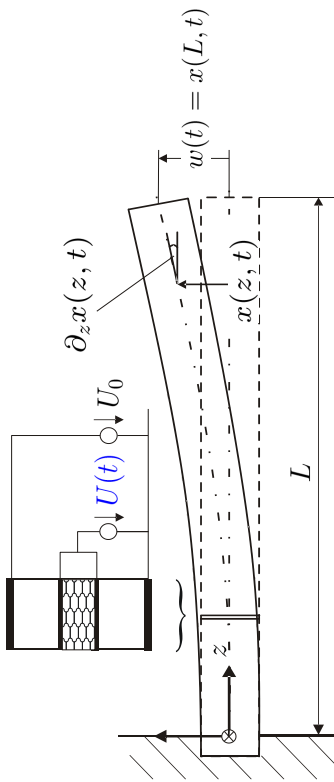


Gruppe für Komplexe
Dynamische Systeme (CDS)

8

Tracking Control of a Piezoelectric Bender

Micro-positioning device: piezoelectric trimorph bender



Goal: design of a high-dynamic tracking control for the beam's tip position



A. Kugi and T. Meurer
31.03.2010



Gruppe für Komplexe
Dynamische Systeme (CDS)

9



A. Kugi and T. Meurer
31.03.2010

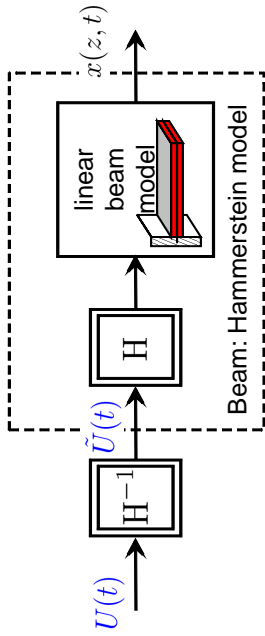


Gruppe für Komplexe
Dynamische Systeme (CDS)

10

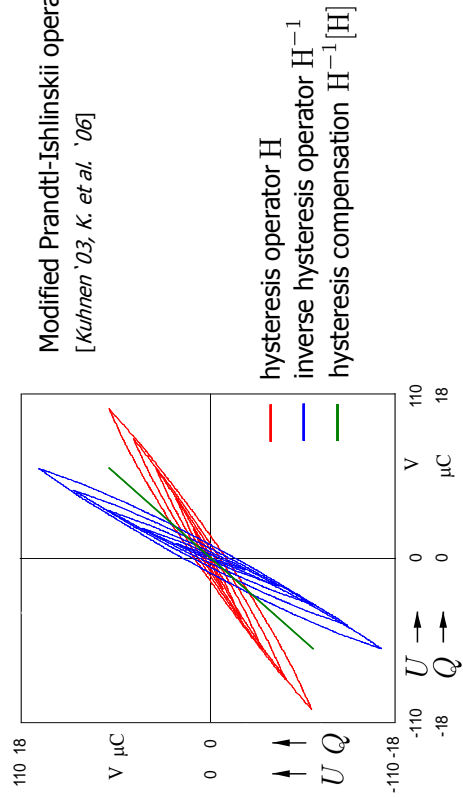
Tracking Control of a Piezoelectric Bender

Assumption: linear constitutive piezoelectric relation
(hysteresis compensation)



Tracking Control of a Piezoelectric Bender

Assumption: linear constitutive piezoelectric relation
(hysteresis compensation)



Modified Prandtl-Ishlinskii operator
[Kühnen '03, K. et al. '06]

hysteresis operator H
inverse hysteresis operator H^{-1}
hysteresis compensation $H^{-1}[H]$



A. Kugi and T. Meurer
31.03.2010



Gruppe für Komplexe
Dynamische Systeme (CDS)

11



A. Kugi and T. Meurer
31.03.2010



Gruppe für Komplexe
Dynamische Systeme (CDS)

12

Tracking Control of a Piezoelectric Bender

Further assumption: Bernoulli-Euler theory with viscous damping $\beta > 0$

Equations of motion (scaled):

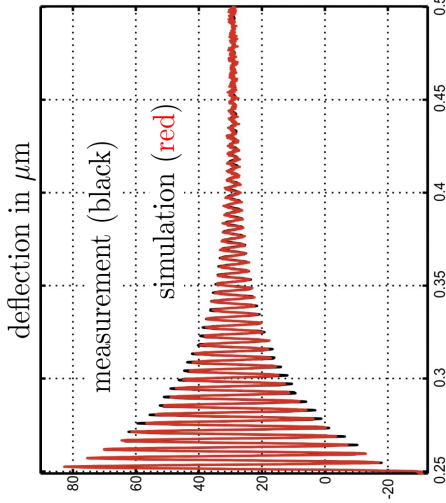
$$\text{PDE: } \partial_t^2 x(z, t) + \beta \partial_t x(z, t) + \partial_z^4 x(z, t) = 0, \quad t > 0, \quad z \in (0, 1)$$

$$\text{BC: } x(0, t) = 0, \quad \partial_z x(0, t) = 0$$

$$\partial_z^2 x(1, t) = u(t), \quad \partial_z^3 x(1, t) = 0$$

$$\text{IC: } x(z, 0) = \partial_t x(z, 0) = 0$$

Tracking Control of a Piezoelectric Bender



Tracking Control of a Piezoelectric Bender

- Idea of **differential flatness**: parametrize $x(z, t)$ and $u(t)$ in terms of a **basic (flat) output** $y(t)$ and its time derivatives $y^{(n)}(t)$, $n \in \mathbb{N}$ [Fliess et al. '95, Acoustin et al. '97, Rudolph et al. '02f, K. et al. '05f]
- Application of operational calculus \Rightarrow BVP

$$\frac{d^4 \hat{x}(z, s)}{dz^4} - q^4(s) \hat{x}(z, s) = 0, \quad z \in (0, 1), \quad q^4(s) = -(s^2 + \beta s)$$

$$\hat{x}(0, s) = 0, \quad \frac{d\hat{x}}{dz}(0, s) = 0, \quad \frac{d^2 \hat{x}}{dz^2}(1, s) = \hat{u}(s), \quad \frac{d^3 \hat{x}}{dz^3}(1, s) = 0$$

- General solution of the BVP:

$$\hat{x}(z, s) = \hat{\chi}_1(s) \hat{C}_1(z, s) + \hat{\chi}_2(s) \hat{S}_1(z, s) + \hat{\chi}_3(s) \hat{C}_2(z, s) + \hat{\chi}_4(s) \hat{S}_2(z, s)$$

$$\hat{C}_1(z, s) = \frac{\cosh(q(s)z) + \cos(q(s)z)}{2}, \quad \hat{C}_2(z, s) = \frac{\cosh(q(s)z) - \cos(q(s)z)}{2q^2(s)},$$

$$\hat{S}_1(z, s) = \frac{\sinh(q(s)z) + \sin(q(s)z)}{2q(s)}, \quad \hat{S}_2(z, s) = \frac{\sinh(q(s)z) - \sin(q(s)z)}{2q^3(s)}$$



A. Kugi and T. Meurer
31.03.2010
Gruppe für Komplexe
Dynamische Systeme (CDS)

13



A. Kugi and T. Meurer
31.03.2010
Gruppe für Komplexe
Dynamische Systeme (CDS)

14

Tracking Control of a Piezoelectric Bender

- General solution of the BVP:

$$\hat{x}(z, s) = \underbrace{\hat{\chi}_1(s) \hat{C}_1(z, s) + \hat{\chi}_2(s) \hat{S}_1(z, s)}_{\text{clamped end}} + \underbrace{\hat{\chi}_3(s) \hat{C}_2(z, s) + \hat{\chi}_4(s) \hat{S}_2(z, s)}_{\text{free end}}$$

$$\hat{R}(s) \begin{bmatrix} \hat{\chi}_3(s) \\ \hat{\chi}_4(s) \end{bmatrix} = \begin{bmatrix} \hat{u}(s) \\ 0 \end{bmatrix}$$

$$\hat{R}(s) = \begin{bmatrix} \hat{C}_1(1, s) & \hat{S}_1(1, s) \\ q^4(s) \hat{S}_2(1, s) & \hat{C}_1(1, s) \end{bmatrix}$$

- Introduction of the **basic output** $y(t)$

$$\begin{bmatrix} \hat{\chi}_3(s) \\ \hat{\chi}_4(s) \end{bmatrix} = \frac{\text{adj} \hat{R}(s)}{\det \hat{R}(s)} \begin{bmatrix} \hat{u}(s) \\ 0 \end{bmatrix}$$

$$\hat{u}(s) = \det \hat{R}(s) \hat{y}(s)$$

$$\downarrow =$$

$$\text{adj} \hat{R}(s) \begin{bmatrix} \hat{y}(s) \\ 0 \end{bmatrix}$$



A. Kugi and T. Meurer
31.03.2010
Gruppe für Komplexe
Dynamische Systeme (CDS)

15



A. Kugi and T. Meurer
31.03.2010
Gruppe für Komplexe
Dynamische Systeme (CDS)

16

Tracking Control of a Piezoelectric Bender

- Parametrization in the operator domain

input $\hat{u}(s) = \det \hat{R}(s) \hat{y}(s) = (\hat{C}_1^2(1, s) - q^4(s) \hat{S}_1(1, s) \hat{S}_2(1, s)) \hat{y}(s)$

state $\hat{x}(z, s) = (\hat{C}_1(1, s) \hat{C}_2(z, s) - q^4(s) \hat{S}_2(1, s) \hat{S}_2(z, s)) \hat{y}(s)$

output $\hat{w}(s) = \hat{x}(1, s) = (\hat{C}_1(1, s) \hat{C}_2(1, s) - q^4(s) \hat{S}_2^2(1, s)) \hat{y}(s)$

- Idea of feedforward control

$$t \mapsto y^*(t) \circ \bullet \hat{y}^*(s) \Rightarrow \hat{u}^*(s), \hat{x}^*(z, s), \hat{w}^*(s)$$

- Transformation to the time domain (series representation)

$$s \circ \bullet \frac{d}{dt}$$



A. Kugi and T. Meurer
31.03.2010
Gruppe für Komplexe
Dynamische Systeme (CDS)

15



A. Kugi and T. Meurer
31.03.2010
Gruppe für Komplexe
Dynamische Systeme (CDS)

16

Tracking Control of a Piezoelectric Bender

- Parametrization in the time domain

$$\text{input } u(t) = y(t) + \sum_{n=1}^{\infty} \frac{2^{2n-1}}{(4n)!} \sum_{k=0}^n \binom{n}{k} \beta^{n-k} \frac{d^{k+n} y(t)}{dt^{k+n}}$$

$$\text{state } x(z, t) = \frac{z^2}{2} y(t) + \sum_{n=1}^{\infty} \left(\sum_{k=0}^n \frac{z^{4k+2}}{(4k+2)!(4(n-k))!} - \sum_{k=0}^{n-1} \frac{z^{4k+3}}{(4k+3)!(4(n-k)-1)!} \right) \times \sum_{j=0}^n (-1)^j \binom{n}{j} \beta^{n-j} \frac{d^{j+n} y(t)}{dt^{j+n}}$$

- Series convergence is ensured by appropriate **trajectory planning** [Austin et al. '97, Fliess et al. '97, Rudolph et al. '02]

Let $y(t)$ be a Gevrey function of order $1 < \alpha < 2$, i.e. $y(t) \in C^\infty$ and $\exists M, R > 0$ s.t.

$$\sup_t \left| \frac{d^k y(t)}{dt^k} \right| \leq \frac{M}{R^k} (k!)^\alpha, \quad k \in \mathbb{N}$$

then the series parametrizations of $u(t), x(z, t)$ **converge absolutely**.



A. Kugi and T. Meurer
31.03.2010



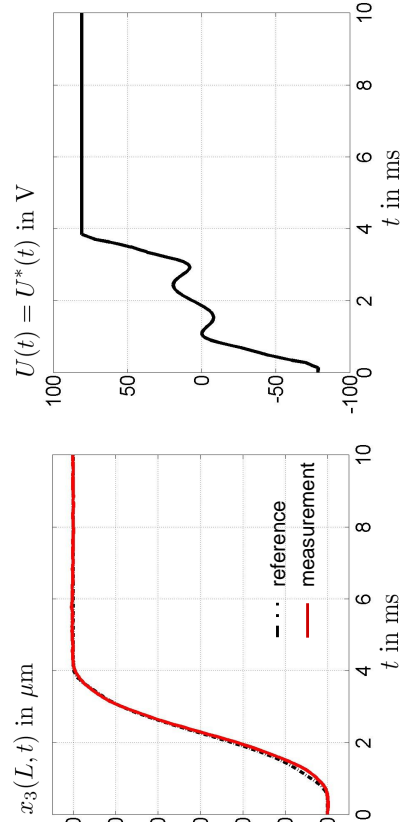
Gruppe für Komplexe
Dynamische Systeme (CDS)

17

Tracking Control of a Piezoelectric Bender

Experimental setup: (dSpace implementation, sampling time 70 μ s)

Measurement results: **feedforward control**



A. Kugi and T. Meurer
31.03.2010

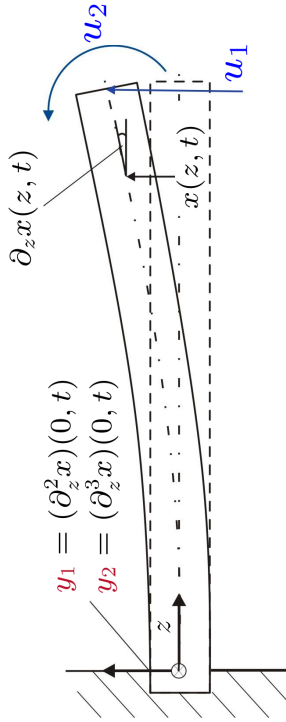


Gruppe für Komplexe
Dynamische Systeme (CDS)

19

Physical Interpretation of Basic Output

- Up to the author's knowledge, there is **no physical interpretation** of the basic output in the case of the Euler-Bernoulli beam
- With two inputs u_1 and u_2 the quantities $y_1 = (\partial_z^2 x)(0, t)$ and $y_2 = (\partial_z^3 x)(0, t)$ serve as possible **basic outputs**.



A. Kugi and T. Meurer
31.03.2010



Gruppe für Komplexe
Dynamische Systeme (CDS)



A. Kugi and T. Meurer
31.03.2010

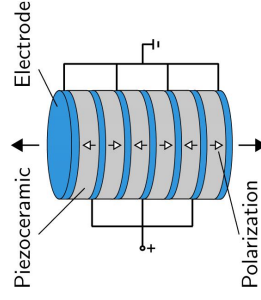


Gruppe für Komplexe
Dynamische Systeme (CDS)

18

Piezoelectric Stack Actuator (PSA)

- PSAs are used in a wide field of applications:
 - Highly dynamical **fuel injectors** and valves to reduce consumption and emissions
 - **Positioning systems**, e.g., in AFMs or optical systems to realize fast and accurate positioning



Goal: exact and highly-dynamic transient tracking of the position of a device connected to the PSA



A. Kugi and T. Meurer
31.03.2010



Gruppe für Komplexe
Dynamische Systeme (CDS)

19



A. Kugi and T. Meurer
31.03.2010

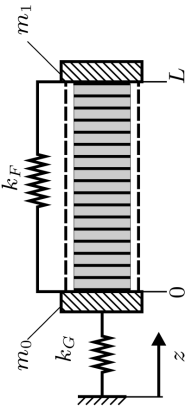


Gruppe für Komplexe
Dynamische Systeme (CDS)

20

Piezoelectric Stack Actuator (PSA)

■ Energy-based modeling



Modeling assumptions

Small strain, linear piezoelectric material, 11-mode, charge control $Q(t) = -N/au(t)$

Notation

Y Young's modulus, a inv. piezoelectric charge coeff., N number of PZT layers, ρ mean density, F cross sectional area

■ Kinetic energy

$$W_k(t) = \frac{F\rho}{2} \int_0^L (\partial_t x(z,t))^2 dz + \frac{m_0}{2} (\partial_t x(0,t))^2 + \frac{m_1}{2} (\partial_t x(L,t))^2$$

■ Potential energy

$$W_p(t) = \frac{1}{2} \int_0^L (FY (\partial_z x(z,t))^2 + 2u(t) \partial_z x(z,t)) dz + \frac{k_G}{2} (x(L,t) - x(0,t))^2 + \frac{k_F}{2} x^2(0,t)$$



A. Kugi and T. Meurer
31.03.2010



Gruppe für Komplexe
Dynamische Systeme (CDS)

21

Piezoelectric Stack Actuator (PSA)

■ Flatness-based trajectory planning [MK '10]

■ Operational calculus

$$\begin{aligned} \text{ODE: } & \partial_z^2 \hat{x}(z,s) = \frac{s^2}{c^2} \hat{x}(z,s), \quad z \in (0,L) \\ \text{BCs: } & a_0 \partial_z \hat{x}(0,s) + a_1 (\hat{x}(L,s) - \hat{x}(0,s)) - (a_2 + m_0 s^2) \hat{x}(0,s) + \hat{u}(s) = 0 \\ & a_0 \partial_z \hat{x}(L,s) + a_1 (\hat{x}(L,s) - \hat{x}(0,s)) + m_1 s^2 \hat{x}(L,s) + \hat{u}(s) = 0 \end{aligned}$$

■ General solution

$$\hat{x}(z,s) = \hat{\chi}_1 e^{\mu(s)z} + \hat{\chi}_2 e^{-\mu(s)z}, \quad \mu(s) = \frac{s}{c}$$

■ Substitution in BCs

$$\hat{R}(s) \begin{bmatrix} \hat{\chi}_1(s) \\ \hat{\chi}_2(s) \end{bmatrix} = - \begin{bmatrix} 1 \\ 1 \end{bmatrix} \hat{u}(s) \Rightarrow \begin{bmatrix} \hat{\chi}_1(s) \\ \hat{\chi}_2(s) \end{bmatrix} = - \frac{\text{adj}(\hat{R}(s))}{\det(\hat{R}(s))} \begin{bmatrix} 1 \\ 1 \end{bmatrix} \hat{u}(s)$$

basic output \Rightarrow

$$\hat{u}(s) = e^{-\mu(s)L} \det(\hat{R}(s)) \hat{y}(s)$$

$$\Rightarrow \hat{x}(z,s) = -e^{-\mu(s)L} \begin{bmatrix} e^{\mu(s)z} & e^{-\mu(s)z} \end{bmatrix} \text{adj}(\hat{R}(s)) \begin{bmatrix} 1 \\ 1 \end{bmatrix} \hat{y}(s)$$



A. Kugi and T. Meurer
31.03.2010

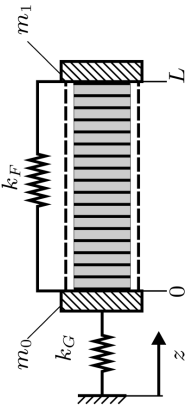


Gruppe für Komplexe
Dynamische Systeme (CDS)

23

Piezoelectric Stack Actuator (PSA)

■ Energy-based modeling



Modeling assumptions

Small strain, linear piezoelectric material, 11-mode, charge control $Q(t) = -N/au(t)$

Notation

Y Young's modulus, a inv. piezoelectric charge coeff., N number of PZT layers, ρ mean density, F cross sectional area

■ Equations of motion from Hamilton's principle

$$\text{PDE: } \partial_t^2 x(z,t) = c^2 \partial_z^2 x(z,t), \quad c = \sqrt{Y/\rho}, \quad z \in (0,L), \quad t > 0$$

$$\text{BCs: } m_0 \partial_t^2 x(0,t) = a_0 \partial_z x(0,t) + a_1 (x(L,t) - x(0,t)) - a_2 x(0,t) + u(t)$$

$$m_1 \partial_t^2 x(L,t) = -a_0 \partial_z x(L,t) - a_1 (x(L,t) - x(0,t)) - u(t)$$

$$\text{ICs: } x(z,0) = \partial_t x(z,0) = 0$$

Output: $w(t) = x(L,t) \rightarrow w^*(t)$

\Rightarrow Tracking controller design



A. Kugi and T. Meurer
31.03.2010



Gruppe für Komplexe
Dynamische Systeme (CDS)

22

Piezoelectric Stack Actuator (PSA)

■ State and input parametrization in the time domain

$$\begin{aligned} x(z,t) &= \frac{1}{2} \left(-m_0 \delta_{L-z}^2 \{y(t)\} + m_1 \delta_z^2 \{y(t)\} - \frac{a_0}{c} \left[\delta_{L-z}^1 \{y(t)\} - \delta_z^1 \{y(t)\} \right] + a_2 \delta_{L-z}^0 \{y(t)\} \right) \\ u(t) &= \frac{1}{2} \left(m_0 m_1 \delta_0^4 \{y(t)\} + \frac{a_0(m_0 + m_1)}{c} \delta_0^3 \{y(t)\} + \left[a_2 m_1 + \frac{a_0^2}{c^2} + a_1(m_0 + m_1) \right] \delta_0^2 \{y(t)\} \right) \\ &\quad + \frac{a_0}{c} (2a_1 + a_2) \delta_0^1 \{y(t)\} + a_1 a_2 \delta_0^0 \{y(t)\} - \frac{4}{c} a_0 a_1 \partial_t y \left(t - \frac{L}{c} \right) h \left(t - \frac{L}{c} \right) \\ w(t) &= x(L,t) = \frac{1}{2} \left(-m_0 \delta_0^2 \{y(t)\} - \frac{a_0}{c} \left[\delta_0^1 \{y(t)\} - \delta_L^1 \{y(t)\} \right] + a_2 \delta_{2L}^0 \{y(t)\} \right) \end{aligned}$$

$$\delta_\alpha^n \{y(t)\} := \partial_t^n y \left(t - \frac{\alpha}{c} \right) h \left(t - \frac{\alpha}{c} \right) + (-1)^{n+1} \partial_t^n y \left(t - \frac{2L-\alpha}{c} \right) h \left(t - \frac{2L-\alpha}{c} \right)$$

■ The quantity $y(t)$ is a flat or basic output

■ Any desired trajectory $t \mapsto y^*(t) \in C^4(\mathbb{R}^+)$ has to take into account the minimal transition time

$$T_{\min} = \frac{2L}{c} \Rightarrow x^*(z,t), u^*(t), w^*(t)$$



A. Kugi and T. Meurer
31.03.2010



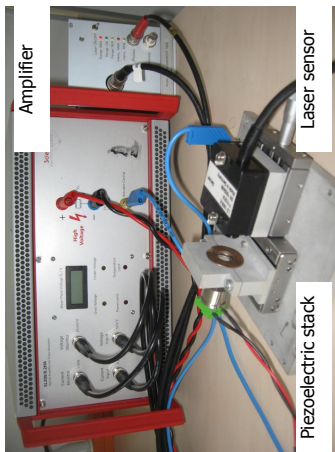
Gruppe für Komplexe
Dynamische Systeme (CDS)

24

Piezoelectric Stack Actuator (PSA)

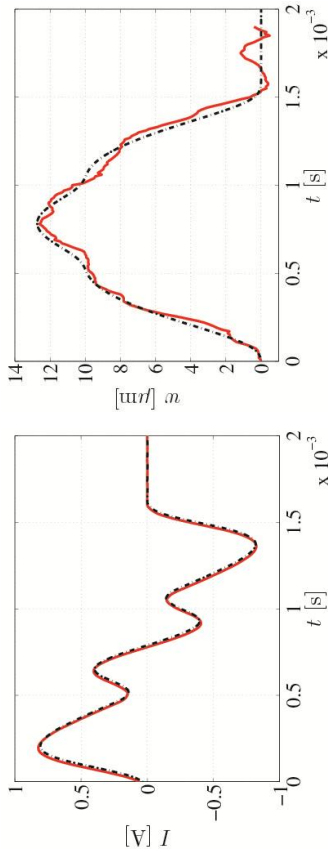
Piezoelectric Stack Actuator (PSA)

Experimental set-up



- Implementation in dSpace DS1103
- Sampling time 100 μ s
- Charge control using hybrid amplifier (ScienLab)
- Laser-based position measurement (μ e)

Measurement results: feedforward control



A. Kugi and T. Meurer
31.03.2010



Gruppe für Komplexe
Dynamische Systeme (CDS)

25



A. Kugi and T. Meurer
31.03.2010



Gruppe für Komplexe
Dynamische Systeme (CDS)

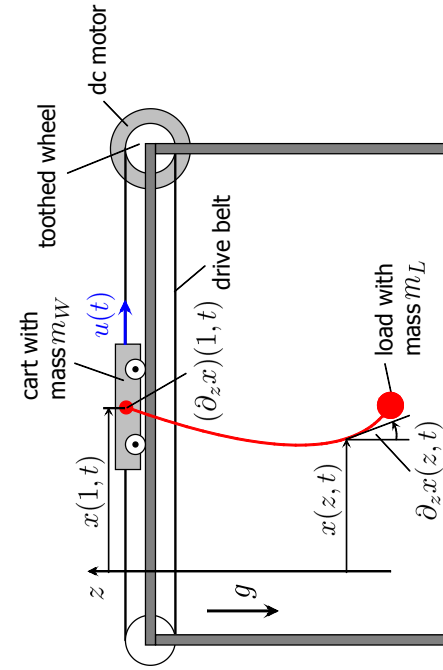
26

Gantry Crane with Heavy Chains

Gantry Crane with Heavy Chains



- chain length $L = 1$ m
- chain line density $\rho = 2.7$ kg m $^{-1}$
- mass of load $m_L = 0.22$ kg
- mass of cart $m_W = 1.2$ kg
- maximum force on the cart $|u(t)| < 18$ N



Goal: design of a **high-dynamic** tracking controller for the load position



A. Kugi and T. Meurer
31.03.2010



Gruppe für Komplexe
Dynamische Systeme (CDS)

27



A. Kugi and T. Meurer
31.03.2010



Gruppe für Komplexe
Dynamische Systeme (CDS)

28

Gantry Crane with Heavy Chains

- Equations of motion with $P(z) = g\left(\rho z + \frac{m_L}{2}\right)$

$$\text{PDE: } \rho \partial_t^2 x(z, t) = \partial_z [P(z) \partial_z x(z, t)], \quad z \in (0, 1), t > 0$$

$$\text{BCs: } m_L \partial_t^2 x(0, t) = 2P(0) \partial_z x(0, t), \quad t > 0$$

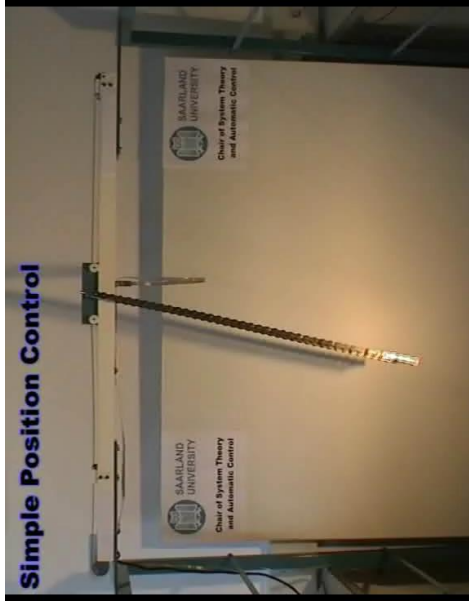
$$m_W \partial_t^2 x(1, t) = -P(1) \partial_z x(1, t) + u(t), \quad t > 0$$

$$\text{ICs: } x(z, 0) = 0, \partial_t x(z, 0) = 0, \quad z \in [0, 1]$$

- Position of the load is a **basic output**: $y(t) = x(0, t)$
[Petit/Rouchon '04]

Gantry Crane with Heavy Chains

- Movie



A. Kugi and T. Meurer
31.03.2010



Gruppe für Komplexe
Dynamische Systeme (CDS)

29



A. Kugi and T. Meurer
31.03.2010

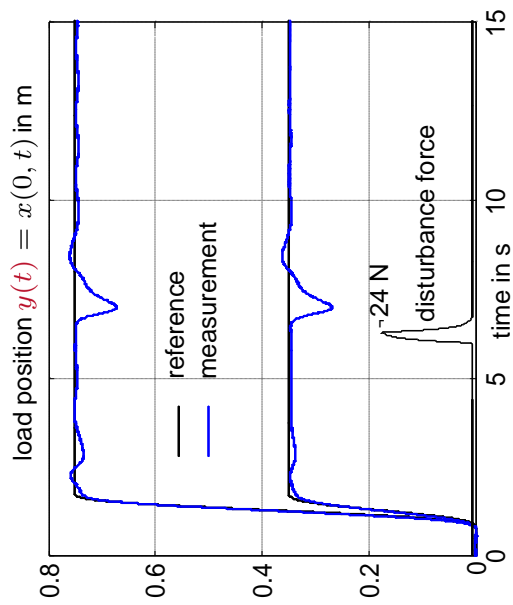


Gruppe für Komplexe
Dynamische Systeme (CDS)

30

Gantry Crane with Heavy Chains

- Measurement result [Thull/Wild/K. '06]



A. Kugi and T. Meurer
31.03.2010



Gruppe für Komplexe
Dynamische Systeme (CDS)

31



A. Kugi and T. Meurer
31.03.2010

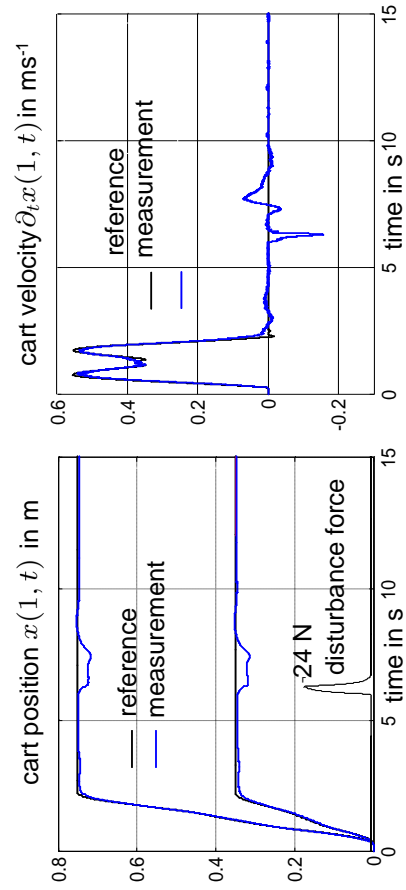


Gruppe für Komplexe
Dynamische Systeme (CDS)

32

Gantry Crane with Heavy Chains

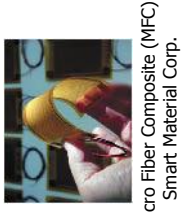
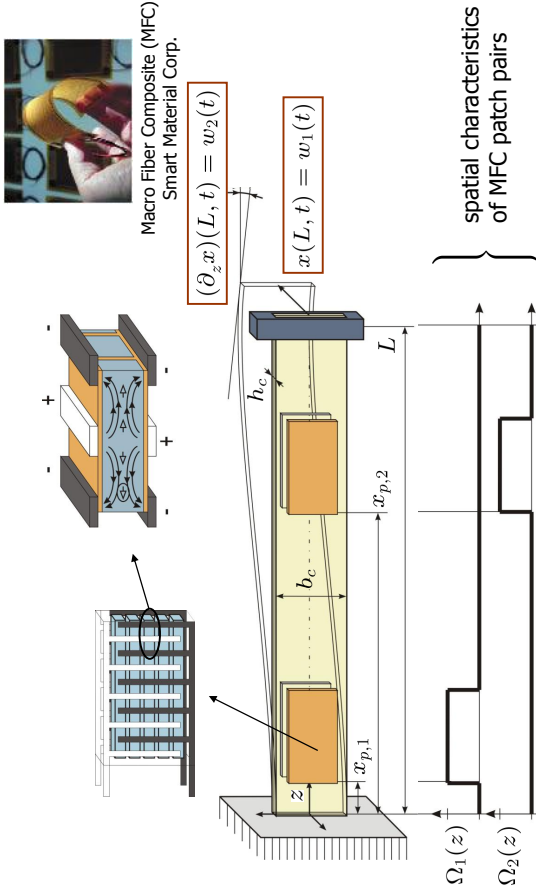
- Measurement result [Thull/Wild/K. '06]



Agenda: Feedforward Controller Design

- Operator based design (Euler-Bernoulli beam, piezoelectric stack actuator, linear heavy chain system)
- Spectrum based design (MFC actuated beam)
- Power series based design (DCR system and semilinear heavy chain example)
- Recursion based design (DCR system on higher dimensional domains)

MFC-actuated Flexible Beam



A. Kugi and T. Meurer
31.03.2010



Gruppe für Komplexe
Dynamische Systeme (CDS)

33

MFC-actuated Flexible Beam

- Equations of motion [Schrück/M/K '09]

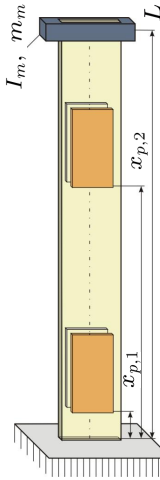
PDE: $\mu(z)\partial_t^2 x + \gamma^e(z)\partial_t x + \gamma^i(z)\partial_t \partial_z^2 x + \partial_z^2 (\Lambda(z)\partial_z^2 x + \partial_z^2 (\Lambda(z)\partial_z^2 x + \gamma^i(z)\partial_t \partial_z^2 x) = -2 \sum_{j=1}^2 u_j \Gamma_p \partial_z^2 \Omega_j(z)$

output: $w(t) = \begin{bmatrix} w_1(t) \\ w_2(t) \end{bmatrix} = \begin{bmatrix} x(L, t) \\ (\partial_z x)(L, t) \end{bmatrix}$

$\Omega_j(z) \notin C^2([0, L])$
Unbounded operator

BCs: $\left. \begin{aligned} x = 0, \partial_z x = 0 & \text{ for } z = 0 \\ \Lambda_c \partial_z^2 x + \gamma_c^i \partial_t \partial_z^2 x + I_m \partial_t^2 \partial_z x = 0 \\ \Lambda_c \partial_z^3 x + \gamma_c^i \partial_t \partial_z^3 x - m_m \partial_t^2 x = 0 \end{aligned} \right\} \text{ for } z = L$

ICs: $\left. \begin{aligned} x(z, 0) = x_0(z) = 0 \\ (\partial_t x)(z, 0) = x_1(z) = 0 \end{aligned} \right\}$



A. Kugi and T. Meurer
31.03.2010



Gruppe für Komplexe
Dynamische Systeme (CDS)

34

MFC-actuated Flexible Beam

- Weak form

$$\int_0^L \mu(z) \partial_t^2 x \xi dz + \sigma_1(x, \xi) + \sigma_2(x, \xi) = -2 \sum_{j=1}^2 \Gamma_p u_j \int_{\Omega_j} \partial_z^2 \xi dz$$

with the positive sesquilinear forms, $\xi \in H_0^2$

$$\sigma_1(x, \xi) = \int_0^L \Lambda(z) \partial_z^2 x \partial_z^2 \xi dz$$

$$\sigma_2(x, \xi) = \int_0^L \gamma^e(z) x \xi dz + \int_0^L \gamma^i(z) \partial_z x \partial_z^2 \xi dz$$

- Series expansion

$$x(z, t) = \sum_{k=1}^n q_k(t) \phi_k(z)$$

with ϕ_k chosen as the eigenfunctions of the undamped (spatially constant) clamped-free Euler-Bernoulli beam

$$\partial_z^4 \phi_k = \lambda \phi_k$$

- Test function $\xi(z) = \phi_k(z)$, $k = 1, \dots, n$



A. Kugi and T. Meurer
31.03.2010



Gruppe für Komplexe
Dynamische Systeme (CDS)

35



A. Kugi and T. Meurer
31.03.2010



Gruppe für Komplexe
Dynamische Systeme (CDS)

36

MFC-actuated Flexible Beam

- Resulting system of ODEs

$$M\partial_t^2 \mathbf{q} + D\partial_t \mathbf{q} + K\mathbf{q} = B\mathbf{u},$$

$$\mathbf{w} = C\mathbf{q}$$
- Solution of the generalized eigenvalue problem of the system

$$\widetilde{M}\partial_t \boldsymbol{\eta} + \widetilde{K}\boldsymbol{\eta} = \widetilde{B}\mathbf{u}, \quad \boldsymbol{\eta} = [\mathbf{q}, \partial_t \mathbf{q}]^T$$

$$\mathbf{w} = \widetilde{C}\boldsymbol{\eta}$$
- Modal transformation

$$\partial_t \zeta_i - \lambda_i \zeta_i = \boldsymbol{\psi}_i^T \widetilde{B}\mathbf{u}, \quad i \in \mathbb{Z}_n = \{-n, \dots, n\} \setminus \{0\}$$

$$\mathbf{w} = \sum_{i \in \mathbb{Z}_n} \widetilde{C}\boldsymbol{\psi}_i \zeta_i \quad \rightarrow \lambda_i = \bar{\lambda}_{-i}, \quad \boldsymbol{\psi}_i = \overline{\boldsymbol{\psi}_{-i}}$$
- Application of Laplace transform

$$\zeta_i = \frac{\boldsymbol{\psi}_i^T \widetilde{B} \prod_{k \in \mathbb{Z}_n \setminus \{i\}} (s - \lambda_k)}{(s - \lambda_i) \prod_{k \in \mathbb{Z}_n \setminus \{i\}} (s - \lambda_k)} \hat{\mathbf{u}}, \quad i \in \mathbb{Z}_n$$



A. Kugi and T. Meurer
31.03.2010



Gruppe für Komplexe
Dynamische Systeme (CDS)

37

MFC-actuated Flexible Beam

- $$\hat{\zeta}_i = \frac{D_\zeta^i(s)}{D_u(s)} \hat{\mathbf{u}},$$

$$D_\zeta^i(s) = -\alpha_i \prod_{k \neq |i|}^{k=1} \left(1 - s \left(\frac{1}{\lambda_k} + \frac{1}{\lambda_k}\right) + \frac{s^2}{\lambda_k \lambda_k}\right),$$

$$D_u(s) = \prod_{k=1}^n \left(1 - s \left(\frac{1}{\lambda_k} + \frac{1}{\lambda_k}\right) + \frac{s^2}{\lambda_k \lambda_k}\right), \quad \alpha_i = \frac{1}{\lambda_i} \boldsymbol{\psi}_i^T \widetilde{B} \left(1 - \frac{s}{\lambda_i}\right)$$
- Introduction of **basic output** $\mathbf{y}(t)$

$$\hat{\mathbf{u}} = D_u(s) \hat{\mathbf{y}} \quad \downarrow = \quad D_\zeta^i(s) \hat{\mathbf{y}}$$
- Transformation to the time domain

$$\zeta_i(t) = (D_\zeta^i(s))|_{s^k = \partial_t^k}, \quad k=0, 1, \dots, 2n-1 \quad \mathbf{y}(t)$$

$$\mathbf{u}(t) = (D_u(s))|_{s^k = \partial_t^k}, \quad k=0, 1, \dots, 2n \quad \mathbf{y}(t)$$



A. Kugi and T. Meurer
31.03.2010



Gruppe für Komplexe
Dynamische Systeme (CDS)

38

MFC-actuated Flexible Beam

- Rest-to-rest motion** from $w^*(t=0)$ to $w^*(t=T)$, $T < \infty$
Calculate the corresponding stationary values of $\mathbf{y}^*(0)$, $\mathbf{y}^*(T)$ from

$$\mathbf{w}^*(0) = \sum_{i \in \mathbb{Z}_n} \widetilde{C}\boldsymbol{\psi}_i D_\zeta^i(0) \mathbf{y}^*(0)$$

$$\mathbf{w}^*(T) = \sum_{i \in \mathbb{Z}_n} \widetilde{C}\boldsymbol{\psi}_i D_\zeta^i(0) \mathbf{y}^*(T)$$
- Design of feedforward controller $\mathbf{y}^*(t) \in C^{2n}(\mathbb{R}^+)$



A. Kugi and T. Meurer
31.03.2010



Gruppe für Komplexe
Dynamische Systeme (CDS)

39

MFC-actuated Flexible Beam

- Numerical convergence** $x(z, t) = \sum_{k=1}^n q_k(t) \phi_k(z)$, $n \in \{5, 10, 15, 20\}$



A. Kugi and T. Meurer
31.03.2010



Gruppe für Komplexe
Dynamische Systeme (CDS)

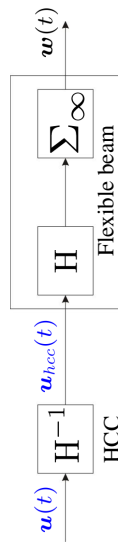
40

MFC-actuated Flexible Beam



- > Carrier layer
 - $L = 0.406$ m
 - $b_c = 0.045$ m
 - $h_c = 7.5 \times 10^{-4}$ m
- > End mass
 - $m_m = 0.0126$ kg
 - $I_m = 0.0$ kg m²
- > 2 pairs of MFC patches
 - $x_{p,1} = 0.031$ m
 - $x_{p,2} = 0.246$ m
- > 2 laser sensors
 - $x_{l,1} = 0.357$ m
 - $x_{l,2} = 0.383$ m

Hysteresis- and creep-compensation (HCC)

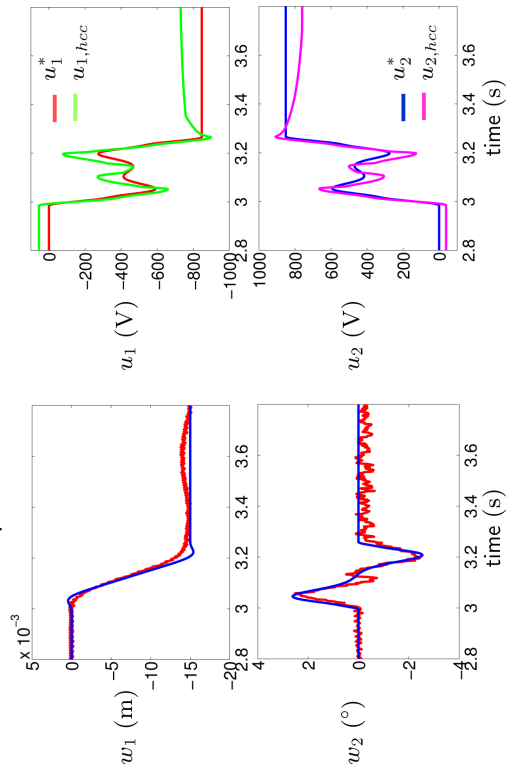


A. Kugi and T. Meurer
31.03.2010
ACIN
Gruppe für Komplexe
Dynamische Systeme (CDS)

41

MFC-actuated Flexible Beam

■ Scenario I: beam tip deflection - detail

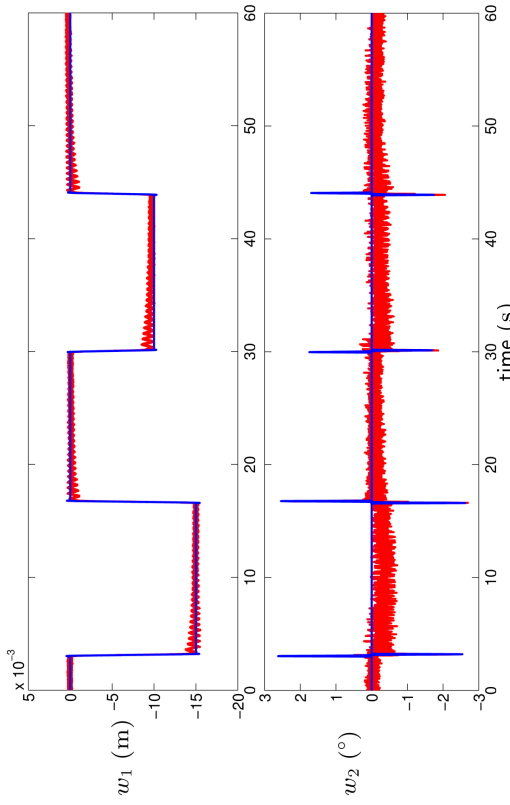


A. Kugi and T. Meurer
31.03.2010
ACIN
Gruppe für Komplexe
Dynamische Systeme (CDS)

43

MFC-actuated Flexible Beam

■ Scenario I: beam tip deflection

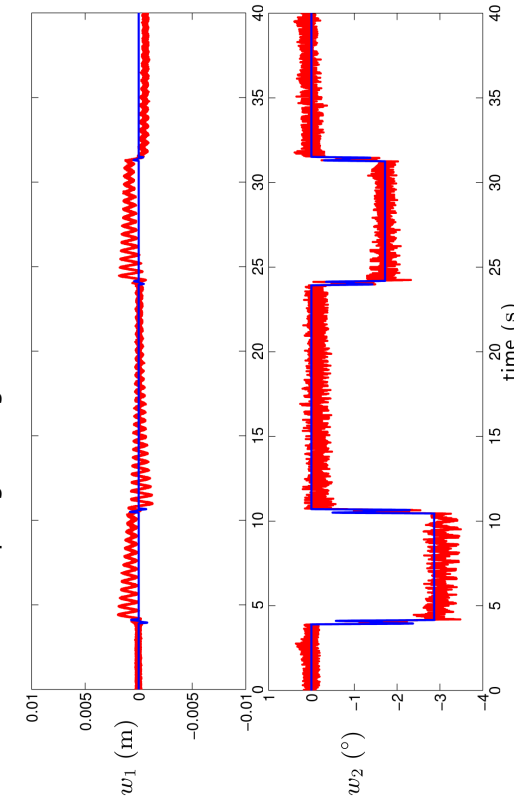


A. Kugi and T. Meurer
31.03.2010
ACIN
Gruppe für Komplexe
Dynamische Systeme (CDS)

42

MFC-actuated Flexible Beam

■ Scenario II: beam tip angle change

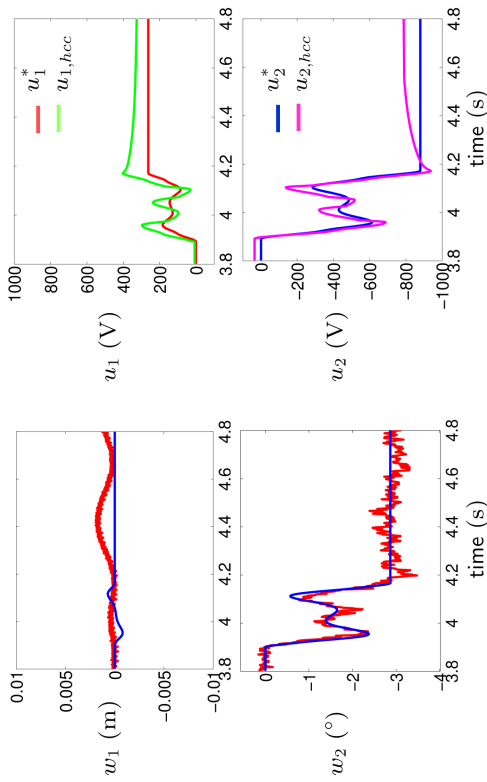


A. Kugi and T. Meurer
31.03.2010
ACIN
Gruppe für Komplexe
Dynamische Systeme (CDS)

44

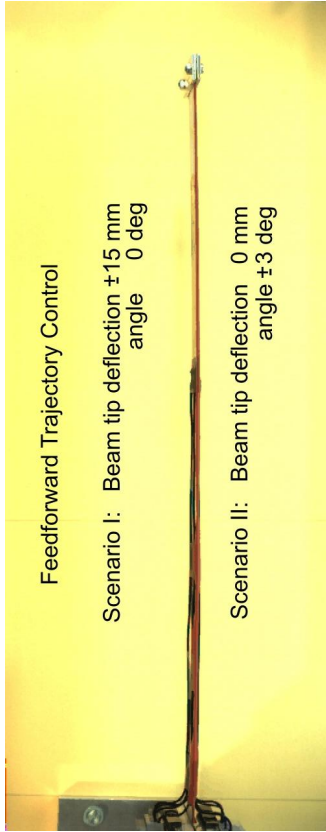
MFC-actuated Flexible Beam

- Scenario II: beam tip angle change - detail



MFC-actuated Flexible Beam

- Movie



A. Kugi and T. Meurer
31.03.2010



Gruppe für Komplexe
Dynamische Systeme (CDS)

45



A. Kugi and T. Meurer
31.03.2010



Gruppe für Komplexe
Dynamische Systeme (CDS)

46

Agenda: Feedforward Controller Design

- Operator based design (Euler-Bernoulli beam, piezoelectric stack actuator, linear heavy chain system)
- Spectrum based design (MFC actuated beam)
- Power series based design (DCR system and semilinear heavy chain example)
- Recursion based design (DCR system on higher dimensional domains)

Power Series based Feedforward Control Design

- Motivation: Linear boundary controlled DR equation [Fliess et al. '98a,b, Larochte et al. '98f, Rudolph et al. '02, Meurer et al. '03f]

$$\text{PDE : } \partial_t x(z, t) = \partial_z^2 x(z, t) + cx(z, t), \quad z \in (0, 1), t > 0$$

$$\text{BCs : } \partial_z x(0, t) = 0, \quad t > 0$$

$$x(1, t) = u(t), \quad t > 0$$

$$\text{IC : } x(z, 0) = x_0(z), \quad z \in [0, 1]$$

- Substitution of $x(z, t) \rightarrow \hat{x}(z, t) = \sum_{n=0}^{\infty} \hat{x}_n(t) \frac{z^n}{n!}$

$$\text{PDE} \Rightarrow \hat{x}_{n+2}(t) = \partial_t \hat{x}_n(t) - c \hat{x}_n(t), \quad n \geq 0$$

$$\text{BC}(z=0) \Rightarrow \hat{x}_1(t) = 0$$

$$\text{Choice} \Rightarrow \hat{x}_0(t) = y(t)$$

Differential recursion for
 $\hat{x}_n(y(t), \partial_t y(t), \dots)$



A. Kugi and T. Meurer
31.03.2010



Gruppe für Komplexe
Dynamische Systeme (CDS)

47



A. Kugi and T. Meurer
31.03.2010



Gruppe für Komplexe
Dynamische Systeme (CDS)

48

Power Series based Feedforward Control Design

- Motivation:** Linear boundary controlled DR equation [Fliess et al. '98a,b, Larache et al. '98f, Rudolph et al. '02, Meurer et al. '03f]

$$\text{PDE : } \partial_t x(z, t) = \partial_z^2 x(z, t) + cx(z, t), \quad z \in (0, 1), \quad t > 0$$

$$\text{BCs : } \partial_z x(0, t) = 0, \quad t > 0$$

$$x(1, t) = u(t), \quad t > 0$$

$$\text{IC : } x(z, 0) = x_0(z), \quad z \in [0, 1]$$
- Basic output:** $y(t) = x(0, t)$

$$x(z, t) = \sum_{n=0}^{\infty} \mathcal{D}^n \{y(t)\} \frac{z^{2n}}{(2n)!}$$

$$u(t) = \sum_{n=0}^{\infty} \mathcal{D}^n \{y(t)\} \frac{1}{(2n)!}$$
- Uniform series convergence** with infinite radius of convergence if $y(t)$ is a Gevrey function of order $\alpha < 2$



A. Kugi and T. Meurer
31.03.2010



Gruppe für Komplexe
Dynamische Systeme (CDS)

49

Extensions of the Formal Power Series Approach

- Certain examples of quasilinear boundary controlled DCR equations [Lynch/Rudolph '02, Meurer/Zeitz '05f]
 - Systematic approach** also applicable to **systems of DCR equations**
 - Analytic nonlinearities** which can be represented as series in the system states
 - Complex differential recursions** for the computation of the parametrized series coefficients
 - Restrictive convergence** results combining system parameters and trajectory planning for the basic output
- One way to overcome the convergence restrictions is given by the incorporation of so-called **summability methods**, which allow to accelerate the convergence of slowly converging series and to sum certain divergent series to a meaningful limit [Wagner et al. '04, Meurer/Zeitz '05f]



A. Kugi and T. Meurer
31.03.2010

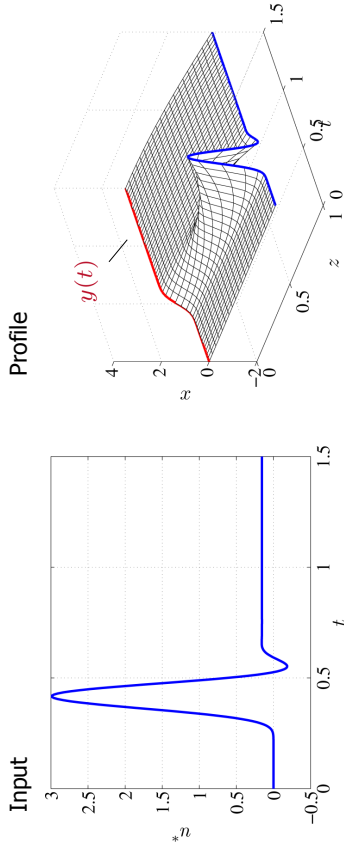


Gruppe für Komplexe
Dynamische Systeme (CDS)

51

Power Series based Feedforward Control Design

- Simulation result** ($c = 2$)



A. Kugi and T. Meurer
31.03.2010



Gruppe für Komplexe
Dynamische Systeme (CDS)

50

Towards Nonlinear Hyperbolic PDEs

Assumption: cart is ideally position controlled, i.e. $x(1, t) = u(t)$

$$P(z) = g \left(\rho z + \frac{m_L}{2} \right)$$

- Equations of motion** (including nonlinear damping term $\alpha > 0$)

$$\text{PDE : } \rho \partial_t^2 x(z, t) = \partial_z [P(z) \partial_z x(z, t)] - \alpha \partial_t x(z, t)$$
- BCs :** $m_L \partial_t^2 x(0, t) = 2P(0) \partial_z x(0, t), \quad t > 0$
 $x(1, t) = u(t), \quad t > 0$
- ICs :** $x(z, 0) = 0, \quad \partial_t x(z, 0) = 0, \quad z \in [0, 1]$



A. Kugi and T. Meurer
31.03.2010



Gruppe für Komplexe
Dynamische Systeme (CDS)

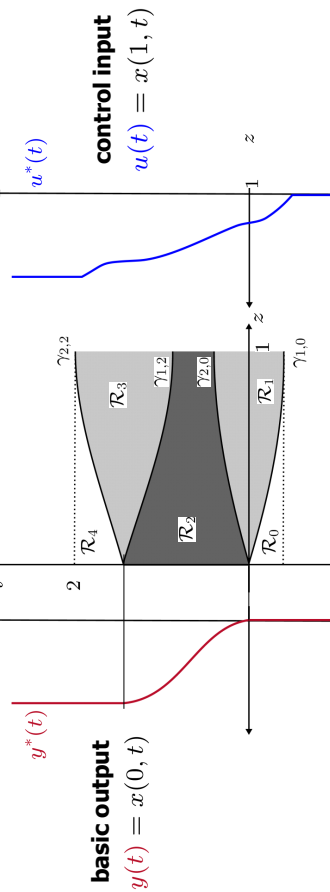
52

Towards Nonlinear Hyperbolic PDEs

- Trajectory planning for a semilinear heavy chain system

- Approach [Wagner/M/K '08]

a) Split the domain into regions according to the characteristic curves



b) Formal power series solution on each region \mathcal{R}_i

c) Compatibility conditions along characteristic curves $\gamma_{1,j}, \gamma_{2,j}$



A. Kugi and T. Meurer
31.03.2010



Gruppe für Komplexe
Dynamische Systeme (CDS)

53



A. Kugi and T. Meurer
31.03.2010

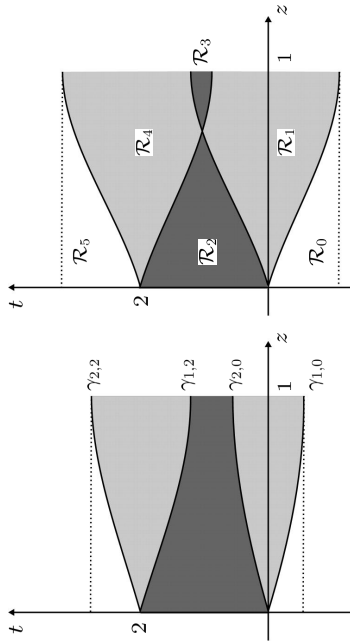


Gruppe für Komplexe
Dynamische Systeme (CDS)

54

Towards Nonlinear Hyperbolic PDEs

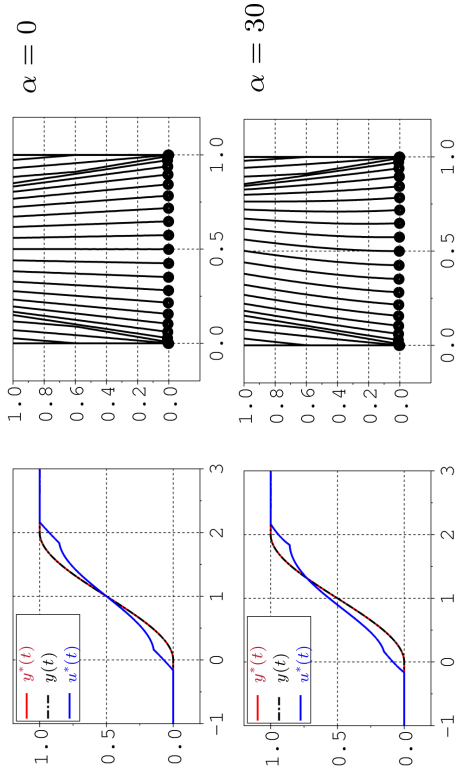
- Depending on the system parameters the characteristic curves may intersect



Towards Nonlinear Hyperbolic PDEs

- Trajectory planning for a semilinear heavy chain system

- Simulation result $m_L = 10$



A. Kugi and T. Meurer
31.03.2010



Gruppe für Komplexe
Dynamische Systeme (CDS)

55



A. Kugi and T. Meurer
31.03.2010



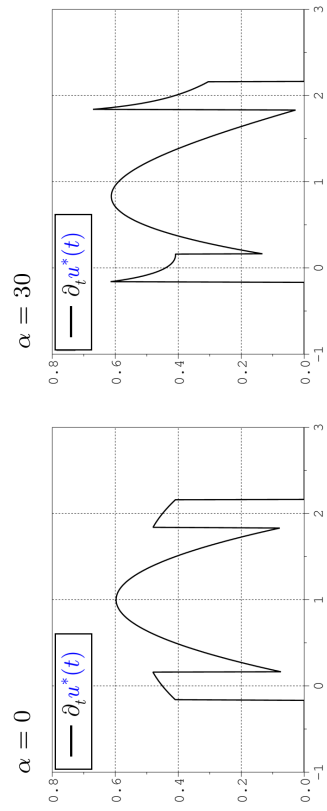
Gruppe für Komplexe
Dynamische Systeme (CDS)

56

Towards Nonlinear Hyperbolic PDEs

- Trajectory planning for a semilinear heavy chain system

- Simulation result $m_L = 10$



Agenda: Feedforward Controller Design

- Operator based design (Euler-Bernoulli beam, piezoelectric stack actuator, linear heavy chain system)
- Spectrum based design (MFC actuated beam)
- Power series based design (DCR system and semilinear heavy chain example)
- Recursion based design (DCR system on higher dimensional domains)



A. Kugi and T. Meurer
31.03.2010

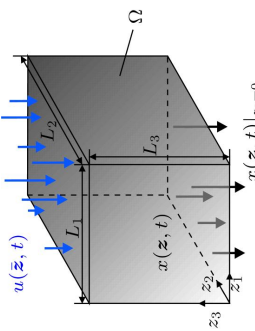


Gruppe für Komplexe
Dynamische Systeme (CDS)

57

Extensions to Higher-dimensional Domains

- Trajectory planning problem



$$\begin{aligned} \text{PDE: } & \partial_t x(z, t) = \sum_{j=1}^3 \partial_{z_j}^2 x(z, t) + c(z, t)x(z, t), \quad (z, t) \in \Omega \times \mathbb{R}_0^+, \\ \text{BCs: } & p_j^0 \partial_{z_j} x(z, t) + p_j^1 x(z, t) = 0, \quad z_j = 0, \quad j \in 1, 2, 3, \quad t > t_0 \\ & -q_j^0 \partial_{z_j} x(z, t) + q_j^1 x(z, t) = 0, \quad z_j = L_j, \quad j \in 1, 2, \quad t > t_0 \\ & \psi(x(z, t), \partial_{z_3} x(z, t)) = u(\bar{z}, t), \quad z_3 = L_3, \quad t > t_0 \\ \text{IC: } & x(z, t_0) = x_0(z), \quad z \in \bar{\Omega} \end{aligned}$$

$$z = (z_1, z_2, z_3) \quad \text{and} \quad \bar{z} = (z_1, z_2)$$

- **Explicit computation** of the necessary $u(\bar{z}, t)$ for a boundary controlled diffusion-reaction system (DRS)
- Take into account **spatially and time-varying** reaction parameters



A. Kugi and T. Meurer
31.03.2010

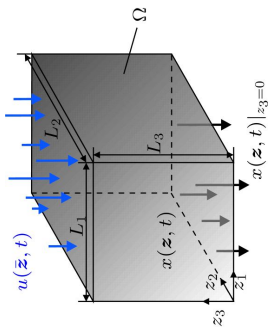


Gruppe für Komplexe
Dynamische Systeme (CDS)

58

Extensions to Higher-dimensional Domains

- Trajectory planning problem



$$z = (z_1, z_2, z_3) \quad \text{and} \quad \bar{z} = (z_1, z_2)$$

- **Explicit computation** of the necessary $u(\bar{z}, t)$ for a boundary controlled diffusion-reaction system (DRS)
- Take into account **spatially and time-varying** reaction parameters

$$x(z, t_0) \Big|_{z_3=0} \xrightarrow[t \in [t_0, t_0+T]]{u(\bar{z}, t)} x(z, t_0 + T) \Big|_{z_3=0} \quad \text{along} \quad x^*(z, t) \Big|_{z_3=0}$$

Recursion based Feedforward Control Design

- Implicit parametrization

- Formal integration with respect to z_3

$$\begin{aligned} \partial_t x(z, t) &= \sum_{j=1}^3 \partial_{z_j}^2 x(z, t) + c(z, t)x(z, t) \\ \Rightarrow \partial_{z_3}^2 x(z, t) &= \partial_t x(z, t) - c(z, t)x(z, t) - \sum_{j=1}^2 \partial_{z_j}^2 x(z, t) \end{aligned}$$

$$\begin{aligned} \Rightarrow x(z, t) &= x(z, t) \Big|_{z_3=0} + z_3 \partial_{z_3} x(z, t) \Big|_{z_3=0} \\ &+ \int_0^{z_3} \left(\partial_t x(z, t) - c(z, t)x(z, t) - \sum_{j=1}^2 \partial_{z_j}^2 x(z, t) \right) \Big|_{z_3=\sigma} d\sigma \end{aligned}$$

- Determine $x(z, t) \Big|_{z_3=0}$ and $\partial_{z_3} x(z, t) \Big|_{z_3=0}$ from

$$\text{BC } (z_3 = 0) \quad p_3^0 \partial_{z_3} x(z, t) \Big|_{z_3=0} + p_3^1 x(z, t) \Big|_{z_3=0} = 0$$

$$\text{Choice} \quad r_3^0 \partial_{z_3} x(z, t) \Big|_{z_3=0} + r_3^1 x(z, t) \Big|_{z_3=0} = y(\bar{z}, t)$$



A. Kugi and T. Meurer
31.03.2010



Gruppe für Komplexe
Dynamische Systeme (CDS)

59



A. Kugi and T. Meurer
31.03.2010



Gruppe für Komplexe
Dynamische Systeme (CDS)

60

Recursion based Feedforward Control Design

- Parametrization of initial conditions

$$x(z, t)|_{z_3=0} = s_3^1 y(\bar{z}, t), \partial_{z_3} x(z, t)|_{z_3=0} = s_3^0 y(\bar{z}, t).$$

- Implicit formal state and input parametrization

$$x(z, t) = (s_3^1 + z_3 s_3^0) y(\bar{z}, t) + \int_0^{z_3} \left(\partial_z x(z, t) - c(z, t)x(z, t) - \sum_{j=1}^2 \partial_{z_j}^2 x(z, t) \right) \Big|_{z_3=\sigma} d\sigma d\eta$$

$$u(\bar{z}, t; y(\bar{z}, t)) = \psi \left(x(z, t; y(\bar{z}, t)), \partial_{z_3} x(z, t; y(\bar{z}, t)) \right) \Big|_{z_3=L_3}$$

Volterra-type integral equation with operator kernel (IEOK)

- Explicit series solution $x(z, t) = \sum_{n=0}^{\infty} x_n(z, t)$ with coefficients from

$$x_0(z, t) = (s_3^1 + z_3 s_3^0) y(\bar{z}, t)$$

$$x_n(z, t) = \int_0^{z_3} \int_0^{\eta} \left(\partial_z x_{n-1}(z, t) - c(z, t)x_{n-1}(z, t) - \sum_{j=1}^2 \partial_{z_j}^2 x_{n-1}(z, t) \right) \Big|_{z_3=\sigma} d\sigma d\eta, \quad n \geq 1$$

$y(\bar{z}, t)$ is a basic (flat) output

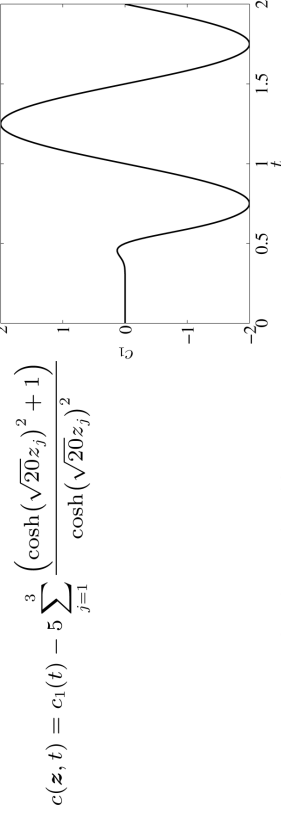


A. Kugi and T. Meurer
31.03.2010
Gruppe für Komplexe
Dynamische Systeme (CDS)

61

Recursion based Feedforward Control Design

- Simulation scenario
 - Homogeneous Neumann BCs and Dirichlet input $x(z, t) = u(\bar{z}, t)$, $z_3 = L_3$
 - Spatially and time-varying reaction parameter



- Basic output $y(\bar{z}, t) = x(z, t)|_{z_3=0}$
- Trajectory planning problem $0 = y(\bar{z}, t = 0) \rightarrow y(\bar{z}, t \geq 2) = 1$ along a prescribed spatio-temporal transition path



A. Kugi and T. Meurer
31.03.2010
Gruppe für Komplexe
Dynamische Systeme (CDS)

63

Recursion based Feedforward Control Design

- Convergence analysis and feedforward control

- Bound the growth of $c(z, t)$ and $y(\bar{z}, t)$, which yields the

absolute and uniform convergence with finite radius of convergence for $c(z, t) \in G_{D_c}^{1,\beta}(\Omega \times \mathbb{R}_{t_0}^+)$ and $y(\bar{z}, t) \in G_{D_y}^{1,\beta}(\Omega_3 \times \mathbb{R}_{t_0}^+)$ with $1 < \beta \leq 2$

Proof: by induction [MK 09b]

- Feedforward tracking control by evaluating the input parametrization

$$u(\bar{z}, t; y(\bar{z}, t)) = \psi \left(x(z, t; y(\bar{z}, t)), \partial_{z_3} x(z, t; y(\bar{z}, t)) \right)$$

with a desired trajectory $y(\bar{z}, t) = y^*(\bar{z}, t)$ satisfying the **convergence conditions** and additional **compatibility requirements**

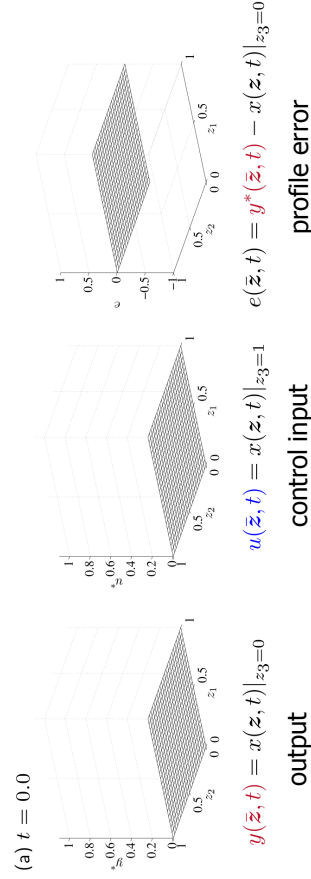


A. Kugi and T. Meurer
31.03.2010
Gruppe für Komplexe
Dynamische Systeme (CDS)

62

Recursion based Feedforward Control Design

- Simulation results
 - Numerical solution using a Crank-Nicholson approach
 - Profile, input, and tracking error at $t \in \{0.0, 1.0, 2.0\}$



$y(\bar{z}, t) = x(z, t)|_{z_3=0}$ output
 $u(\bar{z}, t) = x(z, t)|_{z_3=1}$ control input
 $e(\bar{z}, t) = y^*(\bar{z}, t) - x(z, t)|_{z_3=0}$ profile error

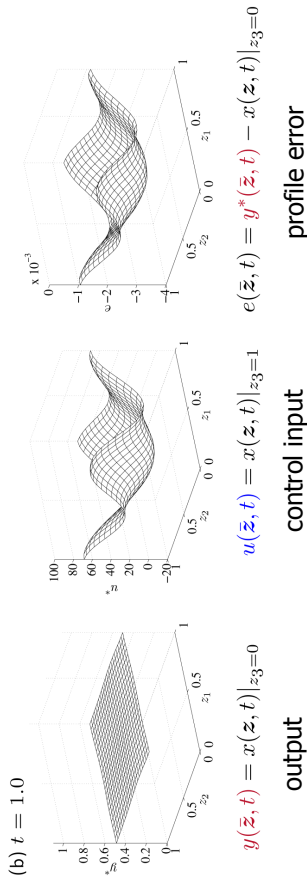


A. Kugi and T. Meurer
31.03.2010
Gruppe für Komplexe
Dynamische Systeme (CDS)

64

Recursion based Feedforward Control Design

- Simulation results
 - Numerical solution using a Crank-Nicholson approach
 - Profile, input, and tracking error at $t \in \{0.0, 1.0, 2.0\}$



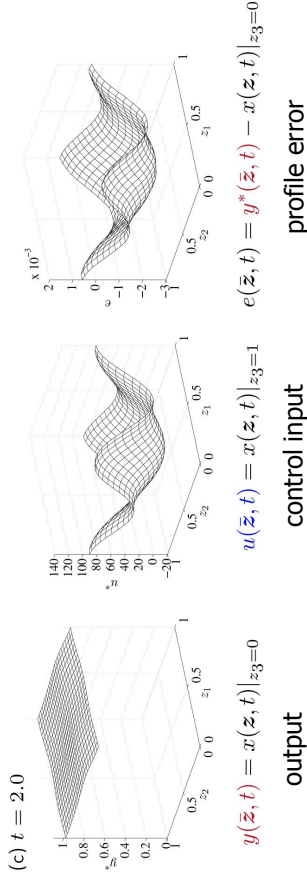
A. Kugi and T. Meurer
31.03.2010



Gruppe für Komplexe
Dynamische Systeme (CDS)

Recursion based Feedforward Control Design

- Simulation results
 - Numerical solution using a Crank-Nicholson approach
 - Profile, input, and tracking error at $t \in \{0.0, 1.0, 2.0\}$



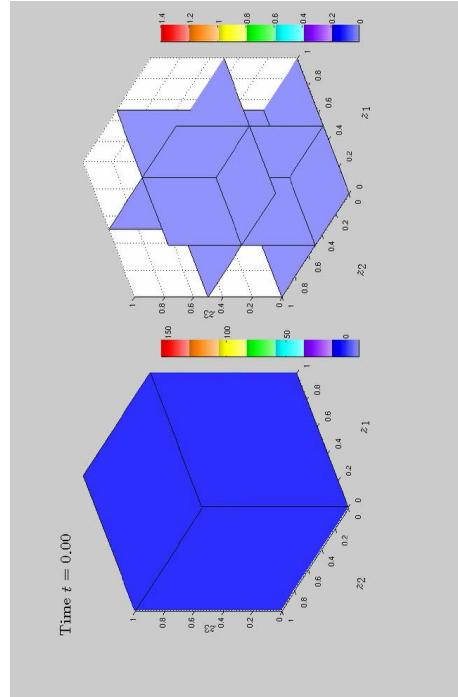
A. Kugi and T. Meurer
31.03.2010



Gruppe für Komplexe
Dynamische Systeme (CDS)

Recursion based Feedforward Control Design

- Movie



A. Kugi and T. Meurer
31.03.2010



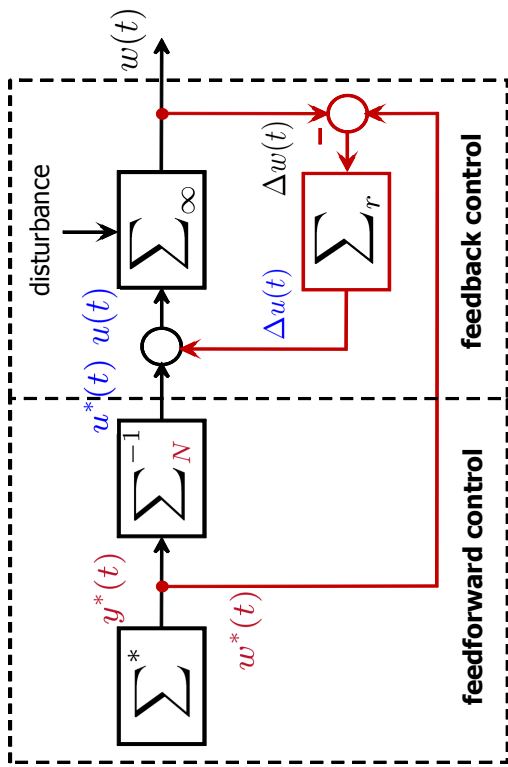
Gruppe für Komplexe
Dynamische Systeme (CDS)

Control of PDEs: Feedback and Tracking Control (Part II)

Andreas KUGI and Thomas MEURER

29th Benelux Meeting on Systems and Control
Heeze, The Netherlands
March 30-April 1, 2010

Two-Degrees-of-Freedom Control



Agenda: Feedback Controller Design

- Passivity based design (Euler-Bernoulli beam)
- Integrator Backstepping design (linear heavy chain system)
- PDE backstepping (DCR system)

Agenda: Feedback Controller Design

- Passivity based design (Euler-Bernoulli beam)
- Integrator Backstepping design (linear heavy chain system)
- PDE backstepping (DCR system)

Tracking Control of a Piezoelectric Bender (cont'd)

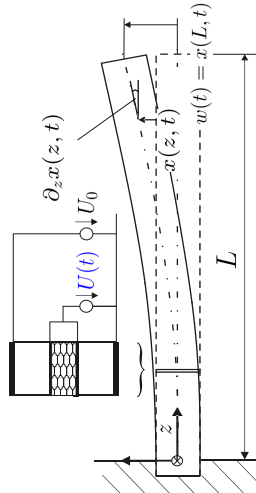
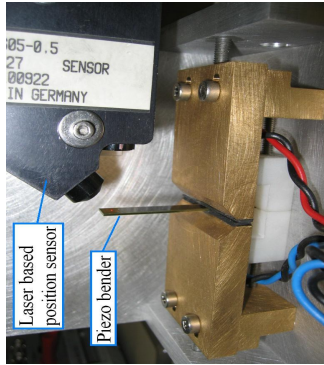
Equations of motion (scaled):

PDE: $\partial_t^2 x(z, t) + \beta \partial_t x(z, t) + \partial_z^4 x(z, t) = 0, \quad t > 0, z \in (0, 1)$

BC: $x(0, t) = 0, \quad \partial_z x(0, t) = 0$

$\partial_z^2 x(1, t) = u(t), \quad \partial_z^3 x(1, t) = 0$

IC: $x(z, 0) = \partial_t x(z, 0) = 0$



A. Kugi and T. Meurer
31.03.2010



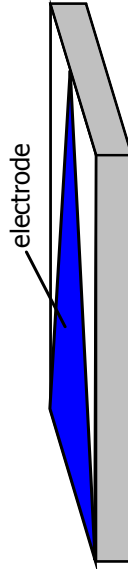
Gruppe für Komplexe
Dynamische Systeme (CDS)

72

Tracking Control of a Piezoelectric Bender (cont'd)

- Change of the energy $E = \frac{1}{2} \int_0^1 (\partial_t e(z, t))^2 + (\partial_z^2 e(z, t))^2 dz$
- $\frac{d}{dt} E = \Delta u(t) \partial_t \partial_z e(1, t) - \beta \int_0^1 (\partial_t e(z, t))^2 dz$

- Enforce collocation by **static shape control**
[Jrščik et al. '02f, K.'01f, Schlaicher/K. '99]



Cantilever: voltage applied to a triangular-shaped electrode acts in the same way on the beam as a tip force



A. Kugi and T. Meurer
31.03.2010



Gruppe für Komplexe
Dynamische Systeme (CDS)

74

Tracking Control of a Piezoelectric Bender (cont'd)

- $u^*(t)$ and $x^*(z, t)$ satisfy the PDE and BCs
- Introduction of the deflection error $e(z, t) = x(z, t) - x^*(z, t)$ and of the additional control input $\Delta u(t) = u(t) - u^*(t)$
- Tracking error system

$\partial_t^2 e(z, t) + \beta \partial_t e(z, t) + \partial_z^4 e(z, t) = 0, \quad t > 0, z \in (0, 1)$

$e(0, t) = 0, \quad \partial_z e(0, t) = 0$
sensor output error (tip position error)

$\partial_z^2 e(1, t) = \Delta u(t) \quad \partial_z^3 e(1, t) = 0$
 $\Delta w(t) = w(t) - w^*(t)$

non-collocated actuator/sensor pairing



A. Kugi and T. Meurer
31.03.2010



Gruppe für Komplexe
Dynamische Systeme (CDS)

73

Tracking Control of a Piezoelectric Bender (cont'd)

Collocated case: Let $\Delta u(t)$ be the control input and $\partial_t \Delta w(t)$ the sensor output

tip force tip position
bending moment at the tip tip angle

The control law [Morgül '01f, Luo et al. '99, K. et al. '05]

$\partial_t v = Av + b \partial_t \Delta w$ **P-controller**
 $\Delta u = c^T v + d \partial_t \Delta w + k \Delta w$ **I-controller**

asymptotically stabilizes the tracking error system for $k > 0$ and (A, b, c, d) be the minimal realization of a SPR transfer function

- A is Hurwitz and $G(s) = c^T (sI - A)^{-1} b + d$
- $\text{Re}(G(j\omega)) \geq d > 0$ for all $\omega \in \mathbb{R}$



A. Kugi and T. Meurer
31.03.2010



Gruppe für Komplexe
Dynamische Systeme (CDS)

75

Tracking Control of a Piezoelectric Bender (cont'd)

Kalman-Yakubovich-Popov lemma: Since $G(s)$ is SPR there exist $P > 0$, q and $\epsilon > 0$ s.t.

$$PA + A^T P = -q q^T - \epsilon P$$

$$Pb = c - q \sqrt{2(d - \delta)}$$

Closed-loop system as a first order evolution equation $\partial_t \mathbf{h} = \mathcal{F} \mathbf{h}$ with the linear operator $\mathcal{F} : D(\mathcal{F}) \subset \mathcal{H} \rightarrow \mathcal{H}$ and

$$\mathcal{H} = \left\{ \mathbf{h} = (e, e_t, v) : e \in H_0^2(0, 1), e_t \in L^2(0, 1), v \in \mathbb{R}^n \right\}$$

and the (energy) inner product

$$\langle \mathbf{h}, \mathbf{h} \rangle_{\mathcal{H}} = \|\mathbf{h}\|_{\mathcal{H}}^2 = \frac{1}{2} \int_0^1 e_t^2 + (\partial_z^2 e)^2 dz + \frac{1}{2} k (\Delta w)^2 + \frac{1}{2} v^T P v$$



A. Kugi and T. Meurer
31.03.2010



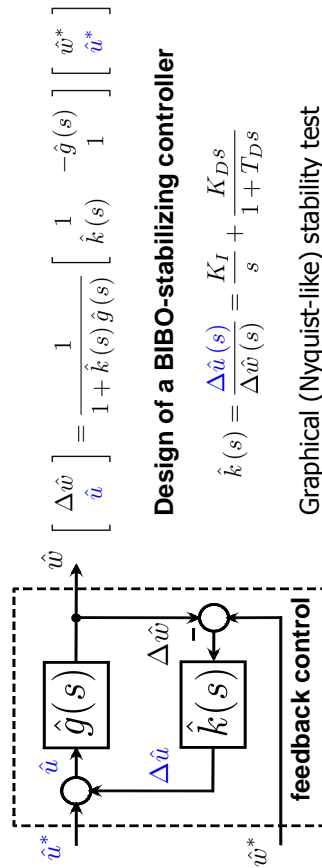
Gruppe für Komplexe
Dynamische Systeme (CDS)

76

Tracking Control of a Piezoelectric Bender (cont'd)

Non-collocated case: I/O-representation of the tracking error system (input: bending moment at the tip $\Delta u(t)$; output: tip position $\Delta w(t)$)

$$\hat{g}(s) = \frac{\hat{w}(s)}{\hat{u}(s)} = \frac{\sin(q(s)) \sinh(q(s))}{q^2(s) [1 + \cos(q(s)) \cosh(q(s))]}, \quad q(s) = -(s^2 + \beta s)$$



Design of a BIBO-stabilizing controller

$$\hat{k}(s) = \frac{\Delta \hat{u}(s)}{\Delta \hat{w}(s)} = \frac{K_I}{s} + \frac{K_D s}{1 + T_D s}$$

Graphical (Nyquist-like) stability test
[Willems '69, Callier/Desoer '72f]



A. Kugi and T. Meurer
31.03.2010



Gruppe für Komplexe
Dynamische Systeme (CDS)

78

Tracking Control of a Piezoelectric Bender (cont'd)

■ Sketch of the proof

- (a) \mathcal{F} is the infinitesimal generator of a C_0 -semigroup of contractions on \mathcal{H}
 - $\langle \mathcal{F} \mathbf{h}, \mathbf{h} \rangle_{\mathcal{H}} \leq 0 \rightarrow \mathcal{F}$ is dissipative
 - \mathcal{F}^{-1} exists and is bounded $\rightarrow 0 \in \rho(\mathcal{F})$ (resolvent set of \mathcal{F})
- (b) By LaSalle's Invariance Principle all solutions of the closed-loop system asymptotically tend to the maximal invariant subset of $\mathcal{Z} = \{ \mathbf{h} \in \mathcal{H} \mid \partial_t V(t) = 0 \}$ with $V(t) = \|\mathbf{h}\|_{\mathcal{H}}^2$
 - $(\lambda I - \mathcal{F})^{-1}$ is compact for some $\lambda > 0$
 - $\mathcal{Z} = \{0\}$ by direct computation



A. Kugi and T. Meurer
31.03.2010



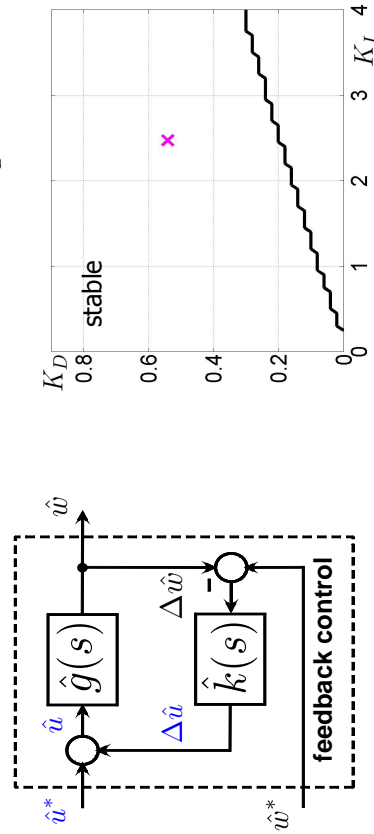
Gruppe für Komplexe
Dynamische Systeme (CDS)

77

Tracking Control of a Piezoelectric Bender (cont'd)

I-DT1 controller: **stability region**
[M/Thull/K.'08]

$$\hat{k}(s) = \frac{K_I}{s} + \frac{K_D s}{1 + T_D s}, \quad T_D \ll 1$$



A. Kugi and T. Meurer
31.03.2010



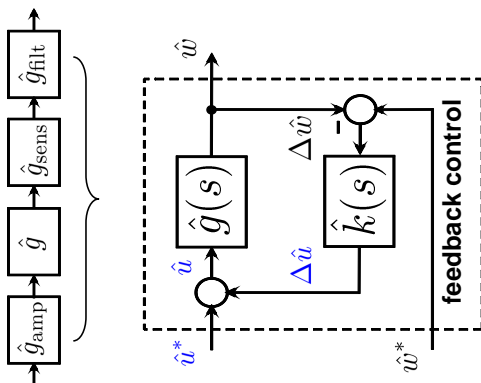
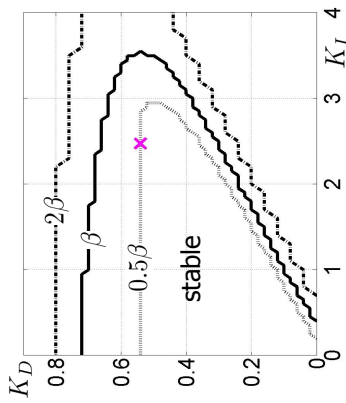
Gruppe für Komplexe
Dynamische Systeme (CDS)

79

Tracking Control of a Piezoelectric Bender (cont'd)

I-DT1 controller: **stability region**
 $[M/Thull/K \cdot 08]$

$$\hat{k}(s) = \frac{K_I}{s} + \frac{K_D s}{1 + T_D s}, \quad T_D \ll$$



A. Kugi and T. Meurer
31.03.2010



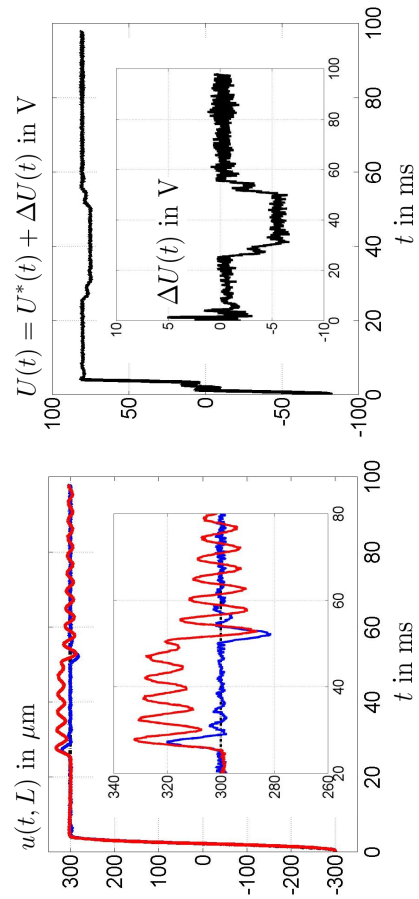
Gruppe für Komplexe
Dynamische Systeme (CDS)

80

Tracking Control of a Piezoelectric Bender (cont'd)

Experimental setup: (dSpace implementation, sampling time 70 μs)

Measurement results: **feedforward and feedback control**



A. Kugi and T. Meurer
31.03.2010



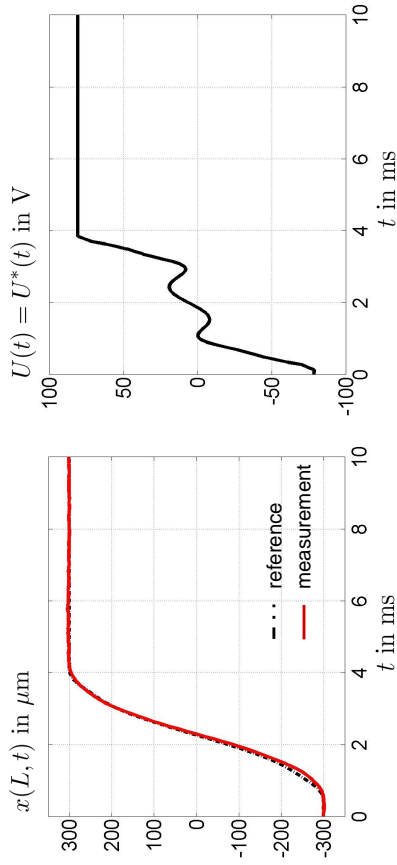
Gruppe für Komplexe
Dynamische Systeme (CDS)

82

Tracking Control of a Piezoelectric Bender (cont'd)

Experimental setup: (dSpace implementation, sampling time 70 μs)

Measurement results: **feedforward control**



A. Kugi and T. Meurer
31.03.2010



Gruppe für Komplexe
Dynamische Systeme (CDS)

81

Agenda: Feedback Controller Design

- Passivity based design (Euler-Bernoulli beam)
- Integrator Backstepping design (linear heavy chain system)
- PDE backstepping (DCR system)



A. Kugi and T. Meurer
31.03.2010

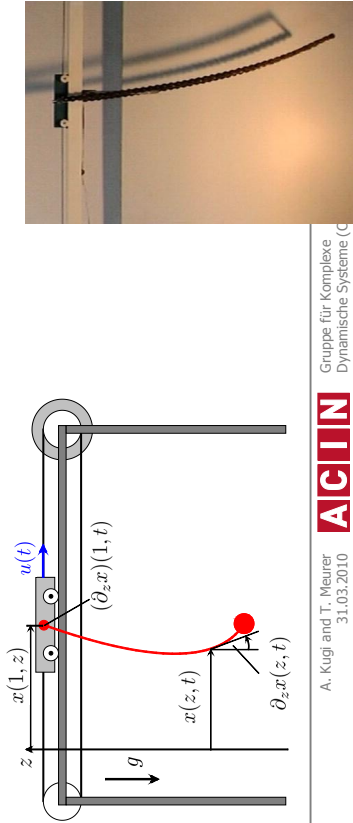


Gruppe für Komplexe
Dynamische Systeme (CDS)

83

Gantry Crane with Heavy Chains (cont'd)

- Tracking error system $e(z, t) = x(z, t) - x^*(z, t)$, $\Delta u(t) = u(t) - u^*(t)$
 $z \in (0, 1)$, $t > 0$
- PDE: $\rho \partial_t^2 e(z, t) = \partial_z [P(z) \partial_z e(z, t)]$, $z \in (0, 1)$, $t > 0$
- BCs: $m_L \partial_t^2 e(0, t) = 2P(0) \partial_z e(0, t)$, $t > 0$
- $m_W \partial_t^2 e(1, t) = -P(1) \partial_z e(1, t) + \Delta u$, $t > 0$
- ICs: $e(z, 0) = 0$, $\partial_t e(z, 0) = 0$, $z \in [0, 1]$



A. Kugi and T. Meurer
31.03.2010



Gruppe für Komplexe
Dynamische Systeme (CDS)



Gantry Crane with Heavy Chains (cont'd)

- Investigating the energy flow between the cart and the chain
- Change of \bar{E} along a solution curve, with

$$\bar{E} = \int_0^1 P(z) (\partial_z e(z, t))^2 + \rho (\partial_t e(z, t))^2 dz + \frac{m_W}{2} ((\partial_t e)(1, t))^2 + \frac{m_L}{2} ((\partial_t e)(0, t))^2$$

yields $\frac{d}{dt} \bar{E} = -\Delta f_i(t) \partial_t e(1, t)$

virtual control input

$$\partial_t e(1, t) = k \Delta f_i(t), \quad k > 0$$

is a good candidate for the asymptotic stabilization of the error dynamics



$$\Delta f_i(t) = -2P(1) \partial_z e(1, t)$$

Gantry Crane with Heavy Chains (cont'd)

- Simple damping injection: change of the total energy E along a solution with $P(z) = g \left(\rho z + \frac{m_L}{2} \right)$

$$E = \int_0^1 P(z) (\partial_z e(z, t))^2 + \rho (\partial_t e(z, t))^2 dz + \frac{m_W}{2} ((\partial_t e)(1, t))^2 + \frac{m_L}{2} ((\partial_t e)(0, t))^2$$

reads as

$$\frac{d}{dt} E = \Delta u(t) \partial_t e(1, t)$$

- The control law $\Delta u(t) = -k \partial_t e(1, t)$, $k > 0$ yields

$$\frac{d}{dt} E = -k (\partial_t e(1, t))^2$$

Problem: stick-slip effects



A. Kugi and T. Meurer
31.03.2010



Gruppe für Komplexe
Dynamische Systeme (CDS)

Gantry Crane with Heavy Chains (cont'd)

- BC for the cart: $m_W \partial_t^2 e(1, t) + 2P(1) \partial_z e(1, t) = \Delta u(t)$

$$\text{control law } \Delta u(t) = 2P(1) \partial_z e(1, t) + m_W \Delta \tilde{u}(t)$$

leads to $\partial_t e(1, t) = e_t(1, t)$

$$\partial_t e_t(1, t) = \Delta \tilde{u}(t)$$

virtual control input

- Simple integrator backstepping on the boundary

$$V = \alpha_1 \bar{E} + \frac{\alpha_2}{2} [e_t(1, t) - \Delta f_i(t)]^2 \quad \alpha_1, \alpha_2 > 0$$

$$\frac{d}{dt} V = -\alpha_1 \Delta f_i^2(t) + [e_t(1, t) - \Delta f_i(t)] [-\alpha_1 \Delta f_i(t) + \alpha_2 \Delta \tilde{u}(t) - \alpha_2 \partial_t \Delta f_i(t)]$$

design $\Delta \tilde{u}(t)$, s.t. $= -\beta [e_t(1, t) - \Delta f_i(t)]$, $\beta > 0$



A. Kugi and T. Meurer
31.03.2010



Gruppe für Komplexe
Dynamische Systeme (CDS)



A. Kugi and T. Meurer
31.03.2010



Gruppe für Komplexe
Dynamische Systeme (CDS)

Gantry Crane with Heavy Chains (cont'd)

- Consideration of the deviation of the cart position is possible by adding the term $\alpha_3(e(1,t))^2$ to \bar{E} and repeating the procedure
- Structure of the control law

$$\Delta \ddot{u}(t) = \theta_1 e(1,t) + \theta_2 \partial_z e(1,t) + \theta_3 e_t(1,t) + \theta_4 \partial_z e_t(1,t)$$
- Hilbert space

$$\mathcal{H} = \{h = (e, e_t, \xi, \psi) : e \in H^2(0,1), e_t \in H^1(0,1), \xi \in m_L e_t(0) \in \mathbb{R}, \psi \in m_W e_t(1) \in \mathbb{R}\}$$
- Evolution equation $\partial_t h = \mathcal{F}h$

$$\mathcal{F} : \begin{bmatrix} e \\ e_t \\ \xi \\ \psi \end{bmatrix} \rightarrow \begin{bmatrix} e_t \\ \frac{1}{\rho} \partial_z (P \partial_z x) \\ 2P(0) \partial_z x \\ \theta_1 e(1) + \theta_2 \partial_z e(1) + \theta_3 e_t(1) + \theta_4 \partial_z e_t(1) \end{bmatrix}$$



A. Kugi and T. Meurer
31.03.2010



Gruppe für Komplexe
Dynamische Systeme (CDS)

88

Agenda: Feedback Controller Design

- Passivity based design (Euler-Bernoulli beam)
- Integrator Backstepping design (linear heavy chain system)
- PDE backstepping (DCR system)



A. Kugi and T. Meurer
31.03.2010



Gruppe für Komplexe
Dynamische Systeme (CDS)

90

Gantry Crane with Heavy Chains (cont'd)

with inner product $\alpha_1, \alpha_2, \alpha_3, \gamma > 0$

$$\langle h, \check{h} \rangle_{\mathcal{H}} = \alpha_1 \int_0^1 P(z) \partial_z e \partial_z \check{e} + \rho e_t \check{e}_t dz + \frac{\alpha_1}{2m_L} \xi \check{\xi} + \frac{\alpha_2}{2} \left(\frac{\psi}{m_W} + 2P(1) \partial_z e(1) + \alpha_3 e(1) \right) \left(\frac{\check{\psi}}{m_W} + 2P(1) \partial_z \check{e}(1) + \alpha_3 \check{e}(1) \right) + \gamma \left(\alpha_1 \int_0^1 \frac{1}{\rho} \partial_z (P \partial_z e) \partial_z (P \partial_z \check{e}) + P \partial_z e_t \partial_z \check{e}_t dz + \frac{2\alpha_1 P^2(0)}{m_L} \partial_z e(0) \partial_z \check{e}(0) + \frac{\alpha_3}{2m_W} \psi \check{\psi} \right)$$

Let there be constants $a, b > 0$ satisfying $(a + b - 1)^2 < 4ab$, s.t.

$$\theta_3 = \frac{\theta_1}{b} - m_W a \quad \text{and} \quad \theta_4 = \frac{\theta_2}{b},$$

and $\theta_1, \dots, \theta_4 < 0$, then \mathcal{F} is the infinitesimal generator of a C_0 -semigroup of contractions and the system is **asymptotically stable**.

Proof: [Stürzer/Arnold'09]



A. Kugi and T. Meurer
31.03.2010



Gruppe für Komplexe
Dynamische Systeme (CDS)

89

PDE Backstepping

- Idea [Boskovic/Balogh/Krstic '02f, Krstic/Smyshlyaev/Vazquez '04f]

PDE : $\partial_t x(z,t) = \partial_z^2 x(z,t) + cx(z,t), \quad z \in (0,1), t > 0$

BCs : $x(0,t) = 0, \quad t > 0$
 $x(1,t) = u(t), \quad t > 0$

IC : $x(z,0) = x_0(z), \quad z \in [0,1]$

- Semi-discretization \Rightarrow finite-dimensional system in **strict-feedback form**

$$x_0(t) = 0$$

$$\partial_t x_n(t) = \frac{(c(\Delta z)^2 - 2)x_n(t) + x_{n-1}(t)}{(\Delta z)^2} + \frac{x_{n+1}(t)}{(\Delta z)^2}, \quad \Delta z = \frac{1}{N+1}, \quad n = 1, \dots, N$$

$$x_{N+1}(t) = u(t) = \beta_N((x_1(t), x_2(t), \dots, x_N(t)))$$

Apply finite-dimensional backstepping-style transformation



A. Kugi and T. Meurer
31.03.2010



Gruppe für Komplexe
Dynamische Systeme (CDS)

91

PDE Backstepping

- Idea [Boskovic/Balogh/Krstic '02f, Krstic et al. 04f]

- Backstepping-style transformation

$$x_0(t) = 0$$

$$\partial_t x_n(t) = \frac{c(\Delta z)^2 - 2x_n(t) + x_{n-1}(t)}{(\Delta z)^2} + \frac{x_{n+1}(t)}{(\Delta z)^2}, \quad n = 1, \dots, N$$

Possibly unstable

$$x_{N+1}(t) = u(t) = \beta_N(x_1(t), x_2(t), \dots, x_N(t))$$

$$\zeta_0(t) = x_0(t) = 0$$

$$\zeta_n(t) = x_n(t) - \beta_{n-1}(x_1(t), \dots, x_{n-1}(t)) \quad \beta_n = \sum_{j=1}^n k_{n,j} x_j, \quad n = 1, \dots, N$$

$$\zeta_{N+1}(t) = 0, \quad \beta_0 = 0, \quad n = 1, \dots, N$$



$$\zeta_0(t) = 0$$

$$\partial_t \zeta_n(t) = \frac{-\mu(\Delta z)^2 - 2\zeta_n(t) + \zeta_{n-1}(t)}{(\Delta z)^2} + \frac{\zeta_{n+1}(t)}{(\Delta z)^2}, \quad n = 1, \dots, N$$

Exp. stable

$$\zeta_{N+1}(t) = 0$$



A. Kugi and T. Meurer
31.03.2010
ACIN
Gruppe für Komplexe Dynamische Systeme (CDS)

92

PDE Backstepping

- Extension to PDEs with spatially and time varying parameters [M/K '09]

$$\text{PDE: } \partial_t x(z, t) = \partial_z^2 x(z, t) + c(z, t)x(z, t), \quad z \in (0, 1), \quad t > t_0$$

$$\text{BCs: } -p_0 \partial_z x(0, t) + p_1 x(0, t) = 0, \quad t > t_0$$

$$\psi(x(1, t), \partial_z x(1, t)) = u(t), \quad t > t_0$$

$$\text{IC: } x(z, t_0) = x_0(z), \quad z \in [0, 1]$$



$$\zeta(z, t) = x(z, t) - \int_0^z k(z, \xi, t)x(\xi, t)d\xi \Rightarrow u(t)$$



$$\text{PDE: } \partial_t \zeta(z, t) = \partial_z^2 \zeta(z, t) - \mu(t)\zeta(z, t), \quad z \in (0, 1), \quad t > t_0$$

- The PDE is **exponentially stable** if $\mu(t) + \lambda_{\min} > \epsilon > 0$
- in L^2 -norm for Dirichlet/Neumann/mixed BCs
 - in H^1 - and sup-norms for Dirichlet/Neumann BCs



A. Kugi and T. Meurer
31.03.2010
ACIN
Gruppe für Komplexe Dynamische Systeme (CDS)

94

PDE Backstepping

- Idea [Boskovic/Balogh/Krstic '02f, Krstic et al. 04f]

- Limit as $N \rightarrow \infty$

$$x_0(t) = 0$$

$$\partial_t x_n(t) = \frac{c(\Delta z)^2 - 2x_n(t) + x_{n-1}(t)}{(\Delta z)^2} + \frac{x_{n+1}(t)}{(\Delta z)^2}$$

$$x_{N+1}(t) = u(t) = \beta_N(x_1(t), x_2(t), \dots, x_N(t))$$



$$\zeta_0(t) = x_0(t) = 0$$

$$\zeta_n(t) = x_n(t) - \sum_{j=1}^{n-1} k_{n-1,j} x_j, \quad n = 1, \dots, N$$

$$\zeta_{N+1}(t) = 0$$



$$\zeta_0(t) = 0$$

$$\partial_t \zeta_n(t) = \frac{-\mu(\Delta z)^2 - 2\zeta_n(t) + \zeta_{n-1}(t)}{(\Delta z)^2} + \frac{\zeta_{n+1}(t)}{(\Delta z)^2}$$

$$\zeta_{N+1}(t) = 0$$

Exp. stable, parabolic target DRS

Volterra integral transformation [Colton '77]

$$\zeta(z, t) = x(z, t) - \int_0^z k(z, \xi)x(\xi, t)d\xi$$



$$\partial_t \zeta(z, t) = \partial_z^2 \zeta(z, t) - \mu \zeta(z, t)$$

$$\zeta(0, t) = 0, \quad \zeta(1, t) = 0$$

Exp. stable, parabolic target DRS



A. Kugi and T. Meurer
31.03.2010
ACIN
Gruppe für Komplexe Dynamische Systeme (CDS)

93

PDE Backstepping

- Kernel $k(z, \xi, t)$ has to satisfy the kernel-PDE

$$\text{PDE: } \partial_t k(z, \xi, t) = \partial_z^2 k(z, \xi, t) - \partial_\xi^2 k(z, \xi, t) - (c(\xi, t) + \mu(t))k(z, \xi, t)$$

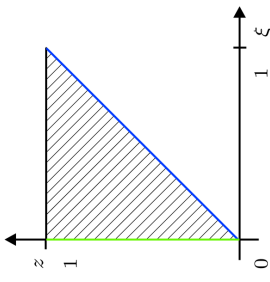
$$=: \gamma(\xi, t)$$

$$\text{BCs: } \gamma(z, t) + 2\partial_z k(z, z, t) = 0, \quad \partial_z k(z, z, t) = \partial_z k(z, z, t) + \partial_z^2 k(z, z, t)$$

$$-\partial_\xi k(z, 0, t) + \bar{p}_1 k(z, 0, t) = 0, \quad \bar{p}_1 = p_1/p_0 \quad (p_0 \neq 0)$$

$$k(0, 0, t) = \bar{p}_1 - \frac{p_1^w}{p_0^w}, \quad (p_1^w > 0, \quad p_0^w \geq 0)$$

$$\text{IC: } k(z, \xi, t_0) = 0, \quad (x_0(z) = \zeta_0(z))$$



Solution by means of the **method of integral operators** and **successive approximation** [Colton '77]



A. Kugi and T. Meurer
31.03.2010
ACIN
Gruppe für Komplexe Dynamische Systeme (CDS)

94

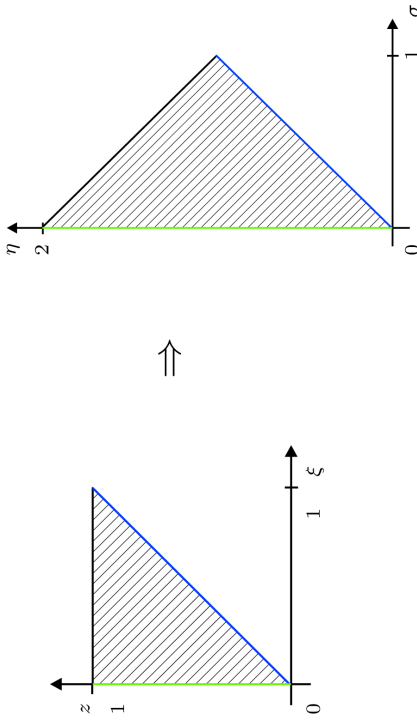
A. Kugi and T. Meurer
31.03.2010
ACIN
Gruppe für Komplexe Dynamische Systeme (CDS)

95

PDE Backstepping

- Sketch of the solution approach

■ Scattering coordinates $\eta = z + \xi$
 $\sigma = z - \xi \Rightarrow k(z, \xi, t) = \bar{k}(\eta(z, \xi), \sigma(z, \xi), t)$



PDE Backstepping

- Sketch of the solution approach

- Formal implicit solution (method of integral operators)

$$\bar{k}(\eta, \sigma, t) = A(\eta, \sigma, t) + \int_0^\sigma [B_{\bar{k}}(\sigma, s, t) + \frac{1}{4} \int_\sigma^{r-s} (\partial_r \bar{k}(r, s, t) + \gamma(\frac{r-s}{2}, t) \bar{k}(r, s, t)) dr] ds$$

$$\bar{k}(\eta, \sigma, t) = \sum_{n=1}^{\infty} \bar{K}^n(\eta, \sigma, t)$$

- Successive approximation \Rightarrow

$$\bar{K}^1(\eta, \sigma, t) = A(\eta, \sigma, t)$$

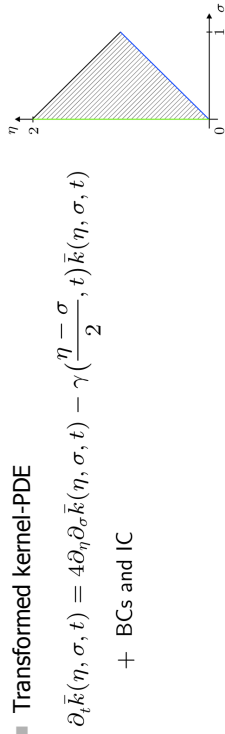
$$\bar{K}^n(\eta, \sigma, t) = \int_0^\sigma [B_{\bar{K}^{n-1}}(\sigma, s, t) + \frac{1}{4} \int_\sigma^{r-s} (\partial_r \bar{K}^{n-1}(r, s, t) + \gamma(\frac{r-s}{2}, t) \bar{K}^{n-1}(r, s, t)) dr] ds, \quad n \geq 2$$

- Convergence must be investigated

PDE Backstepping

- Sketch of the solution approach

■ Scattering coordinates $\eta = z + \xi$
 $\sigma = z - \xi \Rightarrow k(z, \xi, t) = \bar{k}(\eta(z, \xi), \sigma(z, \xi), t)$



- Transformed kernel-PDE

$$\partial_r \bar{k}(\eta, \sigma, t) = 4\partial_\eta \partial_\sigma \bar{k}(\eta, \sigma, t) - \gamma(\frac{\eta - \sigma}{2}, t) \bar{k}(\eta, \sigma, t) + \text{BCs and IC}$$

- Formal integration w.r.t. to η and σ

$$\bar{k}(\eta, \sigma, t) = \frac{1}{4} \int_\sigma^\eta \int_0^\sigma \partial_r \bar{k}(\eta, \sigma, t) + \gamma(\frac{\eta - \sigma}{2}, t) \bar{k}(\eta, \sigma, t) ds dr + \text{BCs}$$

PDE Backstepping

- Convergence

■ If $\sup_{t \in \mathbb{R}^+} |\partial_t^l [c(z, t) + \mu(t)]| \leq D^{l+1}(t)^\alpha \quad \forall z \in [0, 1]$ with $\alpha \in [1, 2)$

then $\bar{k}(\eta, \sigma, t) = \sum_{n=1}^{\infty} \bar{K}^n(\eta, \sigma, t)$ converges **absolutely and uniformly** for all $\sigma \in [0, 1], \eta \in [\sigma, 2 - \sigma]$ independent of D

- Proof: [M/K 09a] providing also a strong solution to the kernel-PDE

- State feedback control (Neumann boundary condition of the target system at $z = 1 : \partial_z \zeta(1, t) = 0$)

$$\zeta(z, t) = x(z, t) - \int_0^z k(z, \xi, t) x(\xi, t) d\xi \Rightarrow u(t)$$

$$\text{BC at } z = 0 : \psi(x(1, t), \partial_z x(1, t)) = u(t)$$

$$u(t) = \psi(x(1, t), k(1, 1, t)x(1, t) + \int_0^1 \partial_z k(1, \xi, t)x(\xi, t) d\xi)$$

PDE Backstepping

■ Summary

The application of the determined state feedback control **exponentially stabilizes** the original system in the L^2 -norm as well as for all combinations of Dirichlet and Neumann BCs in the target system in the H^1 - and sup-norms.

- Implications of this result towards tracking control are twofold
 - Exponentially stabilizing tracking control within the **two-degrees-of-freedom control** concept
 - **Integrated approach** for the exponentially stabilizing tracking control



A. Kugi and T. Meurer
31.03.2010



Gruppe für Komplexe
Dynamische Systeme (CDS)

100

Two-degrees-of-freedom Control for Semilinear DCRS

■ Linear tracking error dynamics

$$\text{PDE: } \partial_t e(z, t) = \bar{a}(z)\partial_z^2 e(z, t) + \bar{b}(z)\partial_z e(z, t) + \bar{c}(z,t)e(z, t) + \bar{e}(z,t)e(z, t), \quad z \in (0, 1), \quad t > 0$$

$$\text{BCs: } -\bar{p}_0\partial_z e(0, t) + \bar{p}_1 e(0, t) = 0, \quad t > 0$$

$$\bar{q}_0\partial_z e(1, t) + \bar{q}_1 e(1, t) = \Delta u(t), \quad t > 0$$

$$\text{IC: } e(z, 0) = e_0(z), \quad z \in [0, 1]$$

■ Gauge transformation

$$\text{PDE: } \partial_t e(z, t) = \partial_z^2 e(z, t) + c(z, t)e(z, t), \quad z \in (0, 1), \quad t > 0$$

$$\text{BCs: } -p_0\partial_z e(0, t) + p_1 e(0, t) = 0, \quad t > 0$$

$$q_0\partial_z e(1, t) + q_1 e(1, t) = \Delta u(t), \quad t > 0$$

$$\text{IC: } e(z, 0) = e_0(z), \quad z \in [0, 1]$$

Starting point for the backstepping approach above



A. Kugi and T. Meurer
31.03.2010



Gruppe für Komplexe
Dynamische Systeme (CDS)

102

Two-degrees-of-freedom Control for Semilinear DCRS

■ Consider the semilinear DCR system [MK'07]

$$\text{PDE: } \partial_t x(z, t) = \bar{a}(z)\partial_z^2 x(z, t) + \bar{b}(z)\partial_z x(z, t) + f(z, t, x), \quad z \in (0, 1), \quad t > 0$$

$$\text{BCs: } -\bar{p}_0\partial_z x(0, t) + \bar{p}_1 x(0, t) = 0, \quad t > 0$$

$$\bar{q}_0\partial_z x(1, t) + \bar{q}_1 x(1, t) = u(t), \quad t > 0$$

$$\text{IC: } x(z, 0) = x_0(z), \quad z \in [0, 1]$$

- Assume system is **flat** with basic output $y(t) \rightarrow y^*(t)$
- State and input parametrizations $x^*(z, t), u^*(t)$ satisfy PDE+BCs+IC
- Introduce the **tracking error system** in $e(z, t) = x(z, t) - x^*(z, t)$ with the new input $\Delta u = u(t) - u^*(t)$
 - ⇒ Semilinear time-varying DCR system
- **Linearization** with respect to desired state $x^*(z, t), u^*(t)$ yields

Linear DCR system with spatially and time-varying parameters



A. Kugi and T. Meurer
31.03.2010



Gruppe für Komplexe
Dynamische Systeme (CDS)

101

Two-degrees-of-freedom Control for Semilinear DCRS

■ Simulation result

- **System:** $\bar{a} = 1, \bar{b} = 3, f(x) = 3(x+x^3), \partial_z x(0, t) = 0, \frac{\partial}{\partial t}\partial_z x(1, t) + x(1, t) = u(t)$

- **Basic output:** $y(t) = x(0, t)$

- State and input parametr. using formal power series and summability methods

- **Target system:** $\mu(t) = \mu \in \{5, 10\}, \partial_z \zeta(0, t) = 0, \partial_z \zeta(1, t) + \frac{3}{2}\zeta(1, t) = 0$

- Tracking controller

$$u(t) = u^*(t) + k(1, 1, t) + \int_0^1 e^{2\xi} \left[\frac{\bar{a}}{b} \partial_z k(1, \xi, t) + \frac{1}{2} k(1, \xi, t) \right] (x(z, t) - x^*(z, t)) d\xi$$

$\Delta u(t)$



A. Kugi and T. Meurer
31.03.2010

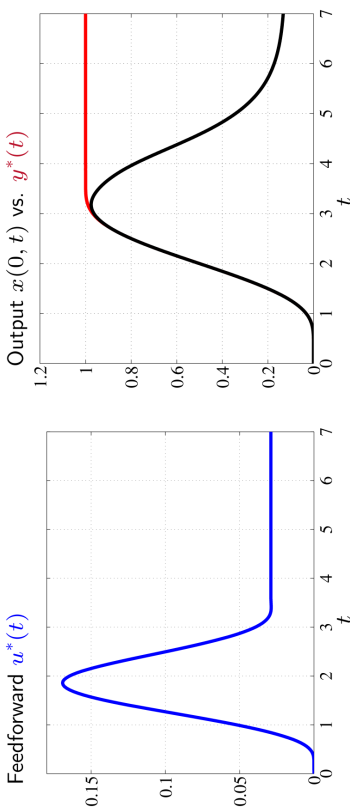


Gruppe für Komplexe
Dynamische Systeme (CDS)

103

Two-degrees-of-freedom Control for Semilinear DCRS

- Simulation result: feedforward control



A. Kugi and T. Meurer
31.03.2010

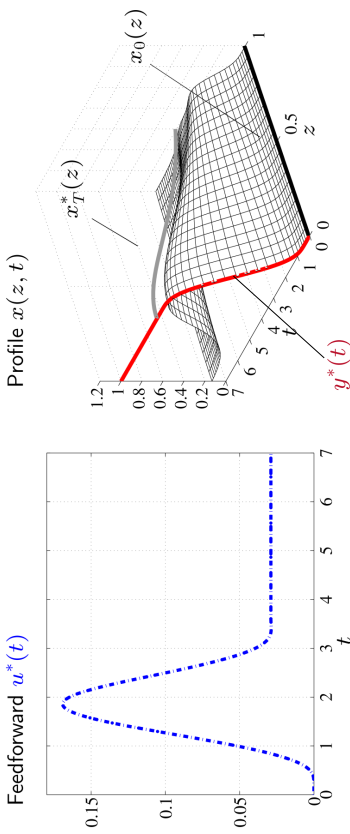


Gruppe für Komplexe
Dynamische Systeme (CDS)

104

Two-degrees-of-freedom Control for Semilinear DCRS

- Simulation result: feedforward control



Unstable desired final profile $x_T^*(z)$



A. Kugi and T. Meurer
31.03.2010

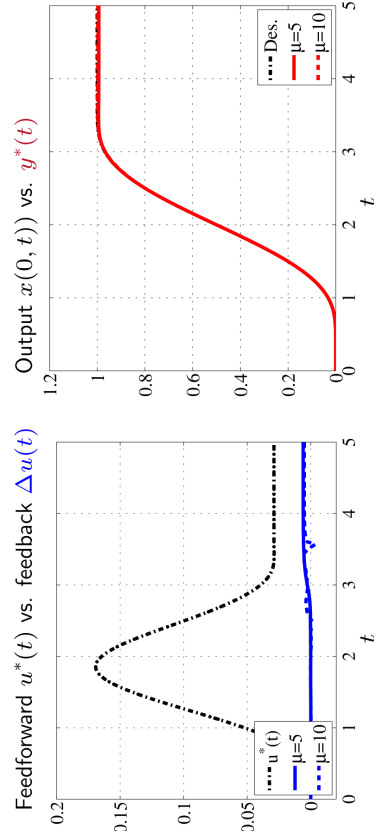


Gruppe für Komplexe
Dynamische Systeme (CDS)

105

Two-degrees-of-freedom Control for Semilinear DCRS

- Simulation result: backstepping-based tracking control



A. Kugi and T. Meurer
31.03.2010

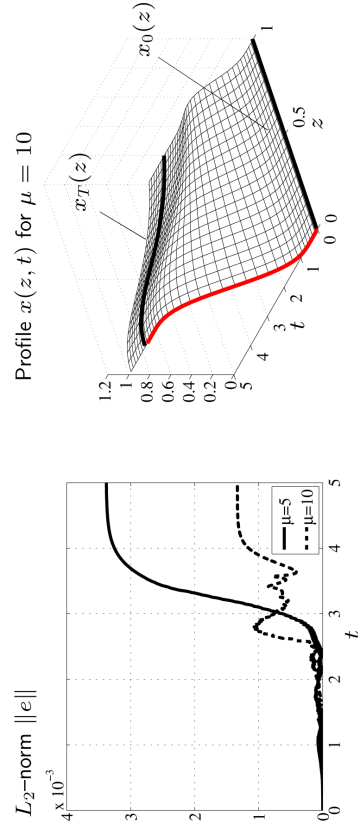


Gruppe für Komplexe
Dynamische Systeme (CDS)

106

Two-degrees-of-freedom Control for Semilinear DCRS

- Simulation result: backstepping-based tracking control



Profile $x(z, t)$ for $\mu = 10$



A. Kugi and T. Meurer
31.03.2010



Gruppe für Komplexe
Dynamische Systeme (CDS)

106



A. Kugi and T. Meurer
31.03.2010



Gruppe für Komplexe
Dynamische Systeme (CDS)

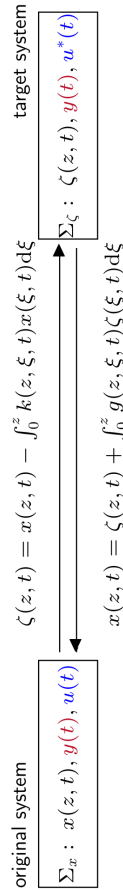
107

Integrated Exponentially Stabilizing Tracking Control

- Idea: Introduce a degree-of-freedom in the target system [M/K 09a]

PDE: $\partial_t \zeta(z, t) = \partial_z^2 \zeta(z, t) - \mu(t) \zeta(z, t)$, $z \in (0, 1)$, $t > t_0$
 mit $\mu(t) \geq \epsilon > 0$
 BCs: $-p_0^w \partial_z \zeta(0, t) + p_1^w \zeta(0, t) = 0$, $t > t_0$
 $q_0^w \partial_z \zeta(1, t) + q_1^w \zeta(1, t) = u^*(t)$, $t > t_0$
 IC: $\zeta(z, t_0) = \zeta_0(z)$, $z \in [0, 1]$

Trajectory planning



Flatness-based trajectory planning may be performed for the target system instead of the original system



A. Kugi and T. Meurer
31.03.2010



Gruppe für Komplexe
Dynamische Systeme (CDS)

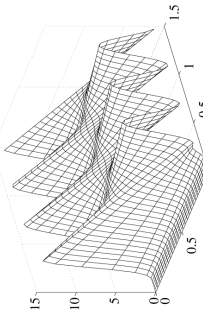
108

Integrated Exponentially Stabilizing Tracking Control

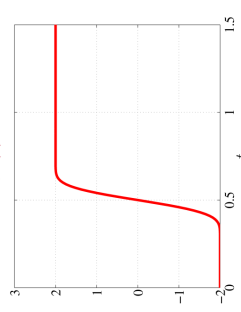
- Simulation results

- DR system ($z \in (0, 1)$, $t_0 = 0$)
 - PDE: $\partial_t x(z, t) = \partial_z^2 x(z, t) + c(z, t)x(z, t)$
 with $c(z, 0) = 0$, $\partial_z^n c(z, t) = 0$, $n \geq 1$, $t = 0$
 - BCs: $-\partial_z x(0, t) + x(0, t) = 0$
 $\partial_z x(1, t) + \sinh(x(1, t)) = u(t)$
 - IC: $x(z, t_0) = x_0(z)$
 - output: $y(t) = x(0, t)$
- Target system ($\mu = 10$)
 - PDE: $\partial_t \zeta(z, t) = \partial_z^2 \zeta(z, t) - \mu \zeta(z, t)$
 - BC: $\partial_z \zeta(0, t) = 0$
 $\partial_z \zeta(1, t) = u^*(t)$
 - IC: $\zeta(z, t_0) = \zeta_0(z)$
 - output: $y(t) = \zeta(0, t)$

Parameter $c(z, t)$



Desired output $y^*(t)$



A. Kugi and T. Meurer
31.03.2010



Gruppe für Komplexe
Dynamische Systeme (CDS)

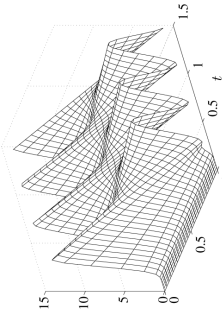
109

Integrated Exponentially Stabilizing Tracking Control

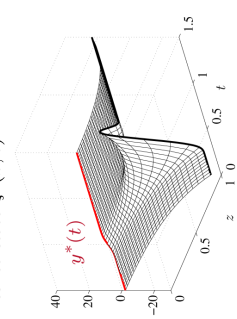
- Simulation results

- DR system ($z \in (0, 1)$, $t_0 = 0$)
 - PDE: $\partial_t x(z, t) = \partial_z^2 x(z, t) + c(z, t)x(z, t)$
 with $c(z, 0) = 0$, $\partial_z^n c(z, t) = 0$, $n \geq 1$, $t = 0$
 - BCs: $-\partial_z x(0, t) + x(0, t) = 0$
 $\partial_z x(1, t) + \sinh(x(1, t)) = u(t)$
 - IC: $x(z, t_0) = x_0(z)$
 - output: $y(t) = x(0, t)$
- Target system ($\mu = 10$)
 - PDE: $\partial_t \zeta(z, t) = \partial_z^2 \zeta(z, t) - \mu \zeta(z, t)$
 - BC: $\partial_z \zeta(0, t) = 0$
 $\partial_z \zeta(1, t) = u^*(t)$
 - IC: $\zeta(z, t_0) = \zeta_0(z)$
 - output: $y(t) = \zeta(0, t)$

Parameter $c(z, t)$



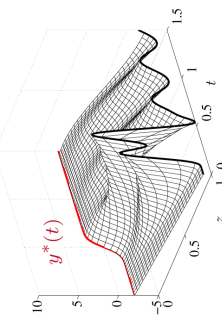
Desired state $\zeta^*(z, t)$



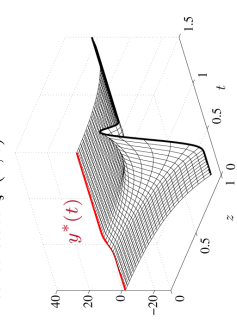
- Simulation results

- DR system ($z \in (0, 1)$, $t_0 = 0$)
 - PDE: $\partial_t x(z, t) = \partial_z^2 x(z, t) + c(z, t)x(z, t)$
 with $c(z, 0) = 0$, $\partial_z^n c(z, t) = 0$, $n \geq 1$, $t = 0$
 - BCs: $-\partial_z x(0, t) + x(0, t) = 0$
 $\partial_z x(1, t) + \sinh(x(1, t)) = u(t)$
 - IC: $x(z, t_0) = x_0(z)$
 - output: $y(t) = x(0, t)$
- Target system ($\mu = 10$)
 - PDE: $\partial_t \zeta(z, t) = \partial_z^2 \zeta(z, t) - \mu \zeta(z, t)$
 - BC: $\partial_z \zeta(0, t) = 0$
 $\partial_z \zeta(1, t) = u^*(t)$
 - IC: $\zeta(z, t_0) = \zeta_0(z)$
 - output: $y(t) = \zeta(0, t)$

Desired state $x^*(z, t)$



Desired state $\zeta^*(z, t)$



A. Kugi and T. Meurer
31.03.2010



Gruppe für Komplexe
Dynamische Systeme (CDS)

110



A. Kugi and T. Meurer
31.03.2010



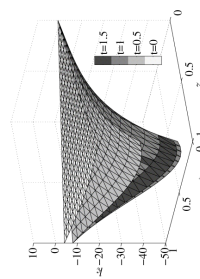
Gruppe für Komplexe
Dynamische Systeme (CDS)

111

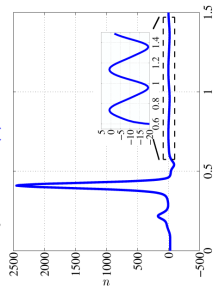
Integrated Exponentially Stabilizing Tracking Control

■ Simulation results

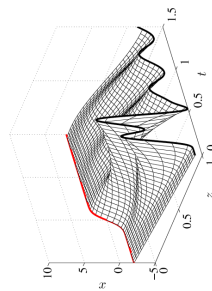
Kernel $k(z, \xi, t)$



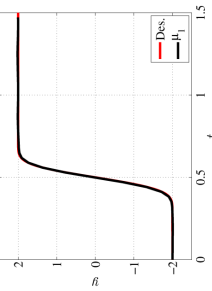
Boundary control $u(t)$



Profile $x(z, t)$



Output $x(0, t), y^*(t)$



Conclusions

- Methods for the design of flatness based **feedforward controllers** for certain classes of PDEs (operator based approach, series based approach, recursion based approach)
- **Feedback design** was based on passivity methods and on the PDE backstepping strategy
- Combination of these concepts for tracking control in a **two-degrees-of-freedom control structure**
- Similar design strategies can be applied to the **observer design** (passivity based Luenberger observer, backstepping observer)
- **Future work:** Extension of the concepts to certain types of quasilinear PDEs and incorporation of geometrically more complex domains



A. Kugi and T. Meurer
31.03.2010



Gruppe für Komplexe
Dynamische Systeme (CDS)

112

Bibliography

- [Aoustin et al (1997)] Y. Aoustin, M. Fliess, H. Mounier, P. Rouchon, and J. Rudolph. Theory and practice in the motion planning and control of a flexible robot arm using Mikusiński operators. In *Proc. 5th IFAC Symposium on Robot Control*, pages 287–293, Nantes (F), 1997.
- [Becker and Meurer(2007)] J. Becker and T. Meurer. Feedforward Tracking Control for Non-Uniform Timoshenko Beam Models: Combining Differential Flatness, Modal Analysis and FEM. *ZAMM*, 87(1): 37–58, 2007.
- [Bošković and Krstić(2002)] D.M. Bošković and M. Krstić. Backstepping control of chemical tubular reactors. *Comp. Chem. Eng.*, 26:1077–1085, 2002.
- [Bošković et al.(2003)] D.M. Bošković, A. Balogh, and M. Krstić. Backstepping in infinite dimension for a class of parabolic distributed parameter systems. *Mathematics of Control, Signals, and Systems*, 16: 44–75, 2003.
- [Callier and Desoer(1972)] F.M. Callier and C.A. Desoer. A graphical test for checking the stability of a linear time-invariant feedback system. *IEEE Trans. Automat. Control*, 17:773–780, 1972.
- [Callier and Desoer(1978)] F.M. Callier and C.A. Desoer. An Algebra of Transfer Functions for Distributed Linear Time-Invariant Systems. *IEEE Trans. Circuits. Syst.*, 25(9):651–662, 1978.



A. Kugi and T. Meurer
31.03.2010



Gruppe für Komplexe
Dynamische Systeme (CDS)

114



A. Kugi and T. Meurer
31.03.2010



Gruppe für Komplexe
Dynamische Systeme (CDS)

113

Bibliography

- [Colton(1977)] D. Colton. The Solution of Initial–Boundary Value Problems for Parabolic Equations by the Method of Integral Operators. *J. Diff. Eqns.*, 26:181–190, 1977.
- [Fliess et al.(1995)] M. Fliess, J. Lévine, P. Martin, and P. Rouchon. Flatness and defect of non-linear systems: introductory theory and examples. *Int. J. Control*, 61:1327–1361, 1995.
- [Fliess et al.(1997)] M. Fliess, H. Mounier, P. Rouchon, J. Rudolph. Systèmes linéaires sur les opérateurs de Mikusiński et commande d’une poutre flexible. *ESAIM Proceedings*, 2:183–193, 1997.
- [Fliess et al.(1998a)] M. Fliess, H. Mounier, P. Rouchon, and J. Rudolph. Controlling the transient of a chemical reactor: a distributed parameter approach. In *Proc. Computational Engineering in Systems Application IMACS Multiconference (CESA’98)*, Hammamet, Tunisia, 1998a.
- [Fliess et al.(1998b)] M. Fliess, H. Mounier, P. Rouchon, and J. Rudolph. A distributed parameter approach to the control of a tubular reactor: a multi-variable case. In *Proc. 37th Conference on Decision and Control*, pages 439–442, Tampa, FL, USA, 1998b.
- [Grabowski(2008)] P. Grabowski. The motion planning problem and exponential stabilization of a heavy chain. Part II. *Opuscula Mathematica*, 28:481–505, 2008.
- [Grabowski(2009)] P. Grabowski. The motion planning problem and exponential stabilization of a heavy chain. Part I. *Int. J. Contr.*, 82:1539–1563, 2009.



A. Kugi and T. Meurer
31.03.2010



Gruppe für Komplexe
Dynamische Systeme (CDS)

115

Bibliography

- [Irschik(2002)] H. Irschik. A review on static and dynamic shape control of structures by piezoelectric actuation. *Eng. Struct.*, 24(1):5–11, 2002.
- [Kstic and Smyshlyayev(2008)] M. Kstic and A. Smyshlyayev. *Boundary Control of PDEs: A Course on Backstepping Designs*. SIAM, 2008.
- [Kugi(2001)] A. Kugi. *Non-linear Control Based on Physical Models*, volume 260 of *LNCIS*. Springer-Verlag, London, 2001.
- [Kugi and Thull(2005)] A. Kugi and D. Thull. Infinite-Dimensional Decoupling Control of the Tip Position and the Tip Angle of a Composite Piezoelectric Beam with Tip Mass. In T. Meurer et al., editors, *Control and Observer Design for Nonlinear Finite and Infinite Dimensional Systems*, volume 322 of *LNCIS*, pages 351–368. Springer-Verlag, Berlin, 2005.
- [Kugi et al.(2006)] A. Kugi, D. Thull, and K. Kuhnen. An infinite-dimensional control concept for piezoelectric structures with complex hysteresis. *Struct. Control Health Monit.*, 13(6):1099–1119, 2006.
- [Kuhnen(2003)] K. Kuhnen. Modeling, Identification and Compensation of Complex Hysteretic Nonlinearities - A modified Prandtl-Ishlinskii approach. *European Journal of Control*, 9(4):407–418, 2003.



A. Kugi and T. Meurer
31.03.2010



Gruppe für Komplexe
Dynamische Systeme (CDS)

116

Bibliography

- [Meurer(2005)] T. Meurer. *Feedforward and Feedback Tracking Control of Diffusion-Convection-Reaction Systems using Summability Methods*. Fortschr.-Ber. VDI Reihe 8 Nr. 1081. VDI Verlag, Düsseldorf, 2005.
- [Meurer and Kugi(2009a)] T. Meurer and A. Kugi. Tracking control for boundary controlled parabolic PDEs with varying parameters: combining backstepping and flatness. *Automatica*, 45(5):1182–1194, 2009a.
- [Meurer and Kugi(2010)] T. Meurer and A. Kugi. Tracking control design for a wave equation with dynamic boundary conditions modeling a piezoelectric stack actuator. *Int. J. Robust Nonlinear Control*, 2010. Accepted for publication.
- [Meurer and Kugi(2007)] T. Meurer and A. Kugi. Tracking control for a diffusion-convection-reaction system: combining flatness and backstepping. In *Proc. 7th IFAC Symposium "Nonlinear Control Systems"* (NOLCOS 2007), pages 583–588, Pretoria (SA), Aug. 21–24 2007.
- [Meurer and Kugi(2009b)] T. Meurer and A. Kugi. Trajectory planning for boundary controlled parabolic PDEs with varying parameters on higher-dimensional spatial domains. *IEEE Trans. Automat. Control*, 54(6):1854–1868, 2009b.
- [Meurer and Zeitz(2005)] T. Meurer and M. Zeitz. Feedforward and feedback tracking control of nonlinear diffusion-convection-reaction systems using summability methods. *Ind. Eng. Chem. Res.*, 44:2532–2548, 2005.



A. Kugi and T. Meurer
31.03.2010



Gruppe für Komplexe
Dynamische Systeme (CDS)

118

Bibliography

- [Laroche and Martin(2000)] B. Laroche and P. Martin. Motion planning for a 1-D diffusion equation using brunovsky-like decomposition. In *Proc. 14th Int. Symposium on Mathematical Theory of Networks and Systems (MTNS)*, Perpignan, France, 2000.
- [Laroche et al.(1998)] Laroche, Martin, and Rouchon] B. Laroche, P. Martin, and P. Rouchon. Motion planning for a class of partial differential equations with boundary control. In *Proc. 37th Conference on Decision and Control*, pages 3494–3497, Tampa, FL, USA, 1998.
- [Laroche et al.(2000)] Laroche, Martin, and Rouchon] B. Laroche, P. Martin, and P. Rouchon. Motion planning for the heat equation. *Int. J. Robust Nonlinear Control*, 10:629–643, 2000.
- [Luo and Guo(1995)] Z.H. Luo and B. Guo. Further Theoretical Results on Direct Strain Feedback Control of Flexible Robot Arms. *IEEE Trans. Automat. Control*, 40(4):747–751, 1995.
- [Luo et al.(1999)] Z.H. Luo, B.Z. Guo, and O. Morgül. *Stability and Stabilization of Infinite Dimensional Systems with Applications*. Springer-Verlag, London, 1999.
- [Lynch and Rudolph(2002)] A.F. Lynch and J. Rudolph. Flatness-based boundary control of a class of quasilinear parabolic distributed parameter systems. *Int. J. Control*, 75(15):1219–1230, 2002.



A. Kugi and T. Meurer
31.03.2010



Gruppe für Komplexe
Dynamische Systeme (CDS)

117

Bibliography

- [Meurer and Zeitz(2008)] T. Meurer and M. Zeitz. Model inversion of boundary controlled parabolic partial differential equations using summability methods. *Math. Comp. Model. Dyn. Sys. (MCMDS)*, 14(3): 213–230, 2008.
- [Meurer and Zeitz(2003)] T. Meurer and M. Zeitz. A Novel Design Approach to Flatness-Based Feedback Boundary Control of Nonlinear Reaction-Diffusion Systems with Distributed Parameters. In W. Kang et al., editors, *New Trends in Nonlinear Dynamics and Control*, volume 295 of *LNCIS*, pages 221–236. Springer-Verlag, 2003.
- [Meurer et al.(2008)] T. Meurer, D. Thull, and A. Kugi. Flatness-based tracking control of a piezoactuated Euler-Bernoulli beam with non-collocated output feedback: theory and experiments. *Int. J. Control*, 81(3):475–493, 2008.
- [Morgül(2001)] O. Morgül. Stabilization and Disturbance Rejection for the Beam Equation. *IEEE Trans. Automat. Control*, 46(12):1913–1918, 2001.
- [Petit and Rouchon(2001)] N. Petit and P. Rouchon. Flatness of Heavy Chain Systems. *SIAM J. of Control and Optimization*, 40(2):475–495, 2001.
- [Rudolph(2003)] J. Rudolph. *Flatness Based Control of Distributed Parameter Systems*. Shaker-Verlag, Aachen, 2003.
- [Rudolph and Woittennek(2002)] J. Rudolph and F. Woittennek. Flachheitsbasierte Randsteuerung von elastischen Balken mit Piezoaktuatoren. *at-Automatisierungstechnik*, 50:412–421, 2002.



A. Kugi and T. Meurer
31.03.2010



Gruppe für Komplexe
Dynamische Systeme (CDS)

119

Bibliography

- [Schlacher and Kugi(1999)] K. Schlacher and A. Kugi. Control of Mechanical Structures by Piezoelectric Actuators and Sensors. In D. Aeyels, F. Lamnabhi-Lagarrigue, and A. van der Schaft, editors. *Stability and Stabilization of Nonlinear Systems*, volume 246 of *LNCIS*, pages 275–291. Springer-Verlag, London, 1999.
- [Schröck et al.(2009)] J. Schröck, T. Meurer, and A. Kugi. Motion planning for a flexible beam structure with macro-fiber composite actuators. In *Proc. (CD-ROM) European Control Conference (ECC)*, pages 2193–2198, Budapest (H), Aug. 23-26 2009.
- [Smyshlyayev and Krstic(2005a)] A. Smyshlyayev and M. Krstic. On control design for PDEs with space-dependent diffusivity or time-dependent reactivity. *Automatica*, 41:1601–1608, 2005a.
- [Smyshlyayev and Krstic(2004)] A. Smyshlyayev and M. Krstic. Closed-Form Boundary State Feedbacks for a Class of 1-D Partial Integro-Differential Equations. *IEEE Trans. Automat. Control*, 49(12):2185–2202, 2004.
- [Smyshlyayev and Krstic(2005b)] A. Smyshlyayev and M. Krstic. Backstepping observers for a class of parabolic PDEs. *Systems & Control Letters*, 54:613–625, 2005b.
- [Stuerzer and Arnold (2009)] D. Stürzer, and A. Arnold. Asymptotic Stability of a Closed-loop Control System Applied to a Gantry Crane with Heavy Chains. In *Internal Report of the Institute for Analysis and Scientific Computing, TU Vienna*, 2009.



A. Kugi and T. Meurer
31.03.2010



Gruppe für Komplexe
Dynamische Systeme (CDS)

120

Bibliography

- [Thull et al.(2006)] D. Thull, D. Wild, and A. Kugi. Application of a Combined Flatness- and Passivity-based Control Concept to a Crane with Heavy Chains and Payload. In *Proc. (CD-ROM) IEEE Int. Conf. Control Appl. (CCA)*, pages 656–661, Munich, Germany, Oct. 4–6 2006.
- [Vazquez and Krstic(2008a)] R. Vazquez and M. Krstic. Control of 1-D parabolic PDEs with Volterra nonlinearities Part I: Design. *Automatica*, 44:2778–2790, 2008a.
- [Vazquez and Krstic(2008b)] R. Vazquez and M. Krstic. Control of 1-D parabolic PDEs with Volterra nonlinearities Part II: Analysis. *Automatica*, 44:2791–2803, 2008b.
- [Wagner et al.(2004)] M.O. Wagner, T. Meurer, and M. Zeitz. K -summable power series as a design tool for feedforward control of diffusion-convection-reaction systems. In *Proc. 6th IFAC Symposium "Nonlinear Control Systems" (NOLCOS 2004)*, pages 149–154, Stuttgart (D), 2004.
- [Wagner et al.(2008)] M.O. Wagner, T. Meurer, and A. Kugi. Feedforward control design for the wave equation with nonlinear boundary conditions modelling a torsional rod. In *Proc. (CD-ROM) IEEE Conference on Decision and Control (CDC)*, pages 1459–1464, Cancun (MX), Dec. 9–11 2008.
- [Willems(1969)] J.C. Willems. Stability, Invertibility and Causality. *SIAM J. Control*, 7(4): 645–671, 1969.
- [Woittennek and Rudolph(2003)] F. Woittennek and J. Rudolph. Motion planning for a class of boundary controlled linear hyperbolic PDE's involving finite distributed delays. *ESAIM: Control, Optimisation and Calculus of Variations*, 9:419–435, 2003.



A. Kugi and T. Meurer
31.03.2010



Gruppe für Komplexe
Dynamische Systeme (CDS)

121

Where innovation starts

Networked Control Systems

Part I: Introduction and overview

Maurice Heemels & Nathan van de Wouw



Technische Universiteit
Eindhoven
University of Technology

Benelux Meeting on Systems and Control, 2010, Heeze, Netherlands

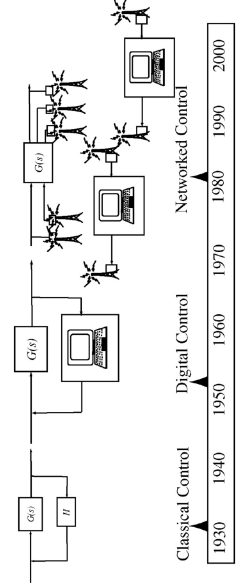
Outline

- History of control
- Motivation for networked control systems (NCS)
- Challenges in NCS
- Overview minicourse




Technische Universiteit
Eindhoven
University of Technology

History of control



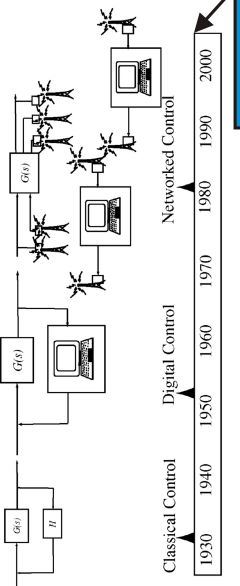
- Classical control: Nyquist, Bode, Nichols, etc.
- Digital control: advent of digital computers and microprocessors
- Networked control: CAN (1986) & decentralized control

J.J. Baillieul & P.J. Antsaklis, Control and Communication Challenges in Networked Real-Time Systems, Proc. IEEE, 2007



Technische Universiteit
Eindhoven
University of Technology


History of control



Two major trends:

- Increasing complexity and scale of professional systems, and distribution, manufacturing & chemical plants → systematic control solutions!
- Enabling technologies
 - low-cost processing power at remote locations via microprocessors
 - reliable transmittal of information via digital and wireless networks

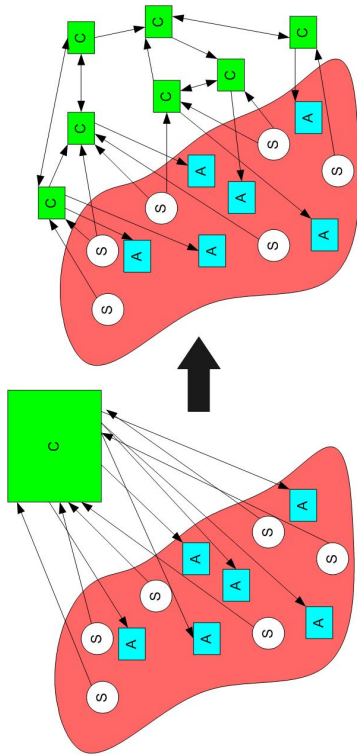
push for **wireless & distributed control** = “modern” **networked control**



Technische Universiteit
Eindhoven
University of Technology

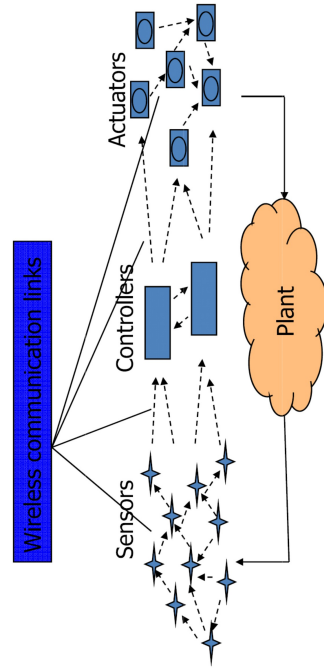
Networked control systems

Paradigm shift: from centralized to distributed and wireless



Wireless control systems

How to control a plant when sensor, actuator and controller nodes are wireless network devices?



Todo:

- Control over (wireless) networks
- Distributed control to handle large scale



[K.H. Johansson, DISC summer school 2009]

Wealth of applications

Great potential for wireless links and low-cost microprocessors

★ Industrial automation & High-tech systems:



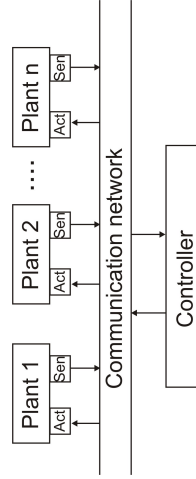
★ Manufacturing and process industries (Large-scale systems):



★ Transportation and distribution networks:



Control over networks

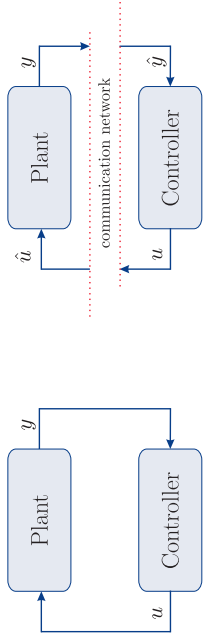


To network ...

- Ease of installation and maintenance
- Large flexibility (especially with Wireless Sensor Net (WSN))
- Deployment in harsh environments
- Enabler for distributed control
- Lower costs
- Less wires (less wear, less disturbances, less weight) in case of WSN



Control over networks



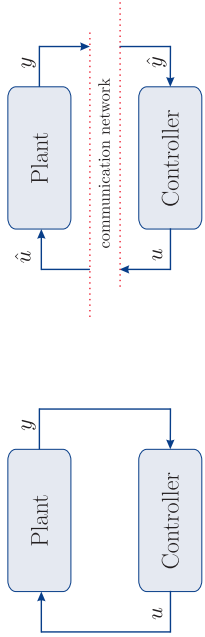
To network ... or not to network:

- (i) Varying sampling/transmission interval
- (ii) Varying communication delays
- (iii) Packet loss
- (iv) Communication constraints through shared network
- (v) Quantization

Question: Is this really an issue?



Control over networks



To network ... or not to network:

- (i) Varying sampling/transmission interval
- (ii) Varying communication delays
- (iii) Packet loss
- (iv) Communication constraints through shared network
- (v) Quantization

These (uncertain) effects influence stability and performance



Motivating example

The influence of **time-varying delays** on stability ...

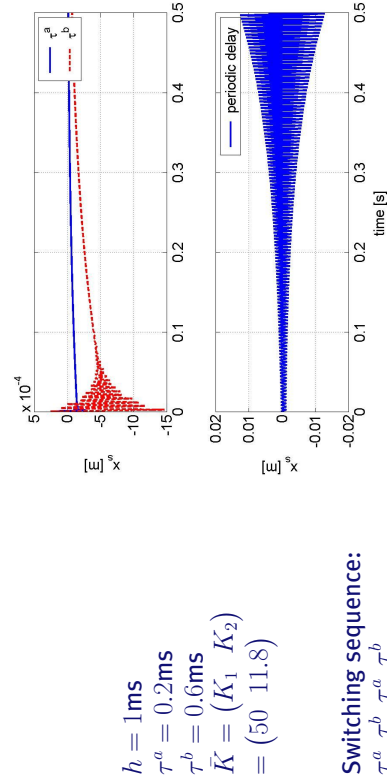
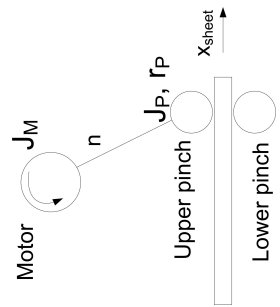
$$\dot{x}(t) = Ax(t) + Bu^*(t)$$

$$u^*(t) = u_k, \text{ for } t \in [s_k + \tau_k, s_{k+1} + \tau_{k+1})$$

$$A = \begin{pmatrix} 0 & 1 \\ 0 & 0 \end{pmatrix}, B = \begin{pmatrix} 0 \\ \frac{1}{J_M + \tau^2 J_P} \end{pmatrix}$$

$$x(t) = \begin{pmatrix} x_s(t) \\ \dot{x}_s(t) \end{pmatrix}$$

$$u_k = -\bar{K}x_k$$



$$h_s = 1 \text{ ms}$$

$$\tau^a = 0.2 \text{ ms}$$

$$\tau^b = 0.6 \text{ ms}$$

$$\bar{K} = (K_1 \quad K_2)$$

$$= (50 \quad 11.8)$$

Switching sequence:
 $\tau^a, \tau^b, \tau^a, \tau^b, \dots$

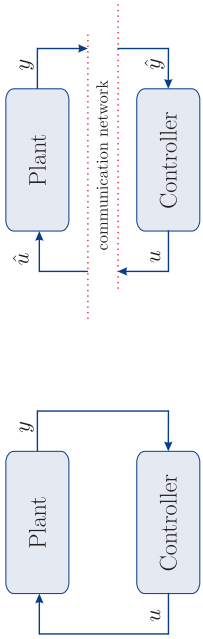
• Also varying sampling intervals h_k might show similar (destabilizing) effects



[Cloosterman et al, CDC 2006, IEEE Trans. Aut. Control, 2009]

Control over networks

12



To network ... or not to network:

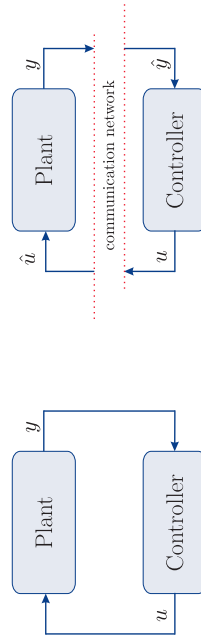
- (i) Varying sampling/transmission interval
- (ii) Varying communication delays
- (iii) Packet loss
- (iv) Communication constraints through shared network
- (v) Quantization

Goal: Quantitative understanding of effects on stability & performance



Control over networks

14



To network ... or not to network:

- (i) Varying sampling/transmission interval
- (ii) Varying communication delays
- (iii) Packet loss
- (iv) **Communication constraints through shared network**
- (v) Quantization

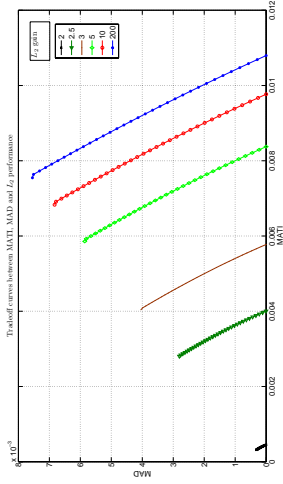
Goal: Quantitative understanding of effects on stability & performance



Tradeoffs in NCS

13

$$L_2 \text{ gain: } \int_0^\infty \|w(t)\|^2 dt \leq \gamma^2 \int_0^\infty \|d(t)\|^2 dt.$$



Tradeoffs between network and control properties

- MATI: maximal allowable transmission interval
- MAD: maximal allowable delay
- \mathcal{L}_2 performance



Communication Constraints

15

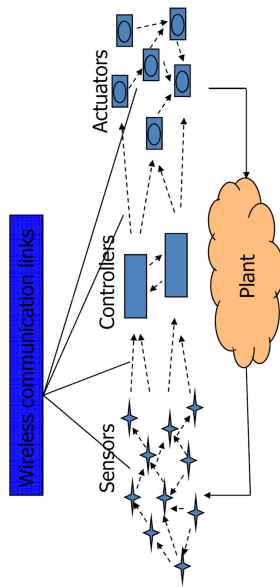
- Network is divided into sensor and actuator nodes
- Only one node can access the network simultaneously
- This gives rise to the problem of scheduling: protocols



Overview of minicourse

16

- Part I: Introduction and overview
- Part II: NCS without communication constraints (Nathan)
- Part III: NCS with communication constraints (Maurice)



Networked Control Systems: Part II: Without Communication Constraints

Nathan van de Wouw & Maurice Heemels
*Department of Mechanical Engineering,
 Eindhoven University of Technology,
 the Netherlands*

Benelux Meeting, April 1, 2010

1/48

Network Control Systems: Different Approaches TU/e

- ▶ Existing approaches towards modelling/stability analysis:
 1. **Emulation approach (Nešić, Teel, Carnevale, Tabarra, Heemels):**
 - Time-varying sampling intervals, SMALL delays
 - Communication constraints, general classes of scheduling protocols
 - Nonlinear systems
 - Continuous-time control synthesis based on continuous-time model

Contents of this part of the mini-course TU/e

- ▶ Different Approaches in Modelling and Stability Analysis of Networked Control Systems
- ▶ Problem Setting
- ▶ Discrete-time Modelling of Linear Networked Control Systems with time-varying sampling intervals, delays and packet dropout
- ▶ Stability analysis of linear NCS (Robustness with respect to communication-induced uncertainties)
- ▶ Illustrative Examples
- ▶ Conclusions & Outlook on Future Work

2/48

Network Control Systems: Different Approaches TU/e

- ▶ Existing approaches towards modelling/stability analysis:
 1. **Emulation approach (Nešić, Teel, Carnevale, Tabarra, Heemels):**
 - Time-varying sampling intervals, SMALL delays
 - Communication constraints, general classes of scheduling protocols
 - Nonlinear systems
 - Continuous-time control synthesis based on continuous-time model
 2. **Modelling in terms of delay(-impulsive) differential equations (Naghsthabrizi, Hespanha, Gao, Fridman, Michiels, van de Wouw):**
 - Time-varying sampling intervals, LARGE delays
 - Linear systems
 - LMI-based stability and controller synthesis

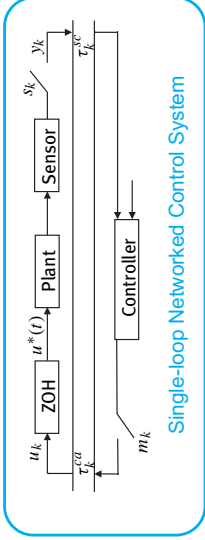
3/48

3/48

Existing approaches towards modelling/stability analysis:

1. **Emulation approach** (Nešić, Teel, Carnevale, Tabarra, Heemels):
 - Time-varying sampling intervals, SMALL delays
 - Communication constraints, general classes of scheduling protocols
 - Nonlinear systems
 - Continuous-time control synthesis based on continuous-time model
2. **Modelling in terms of delay(-impulsive) differential equations** (Nagsthabrizi, Hespanha, Gao, Fridman, Michiels, van de Wouw):
 - Time-varying sampling intervals, LARGE delays
 - Linear systems
 - LMI-based stability and controller synthesis
3. **Discrete-time modelling** (Zhang, Hetel, Fujioka, Garcia, Cloosterman, van de Wouw, Heemels, Donkers, Gielen):
 - Time-varying sampling intervals, LARGE delays, packet dropouts
 - Communication constraints, particular classes of scheduling protocols
 - Linear systems
 - LMI-based stability and controller synthesis

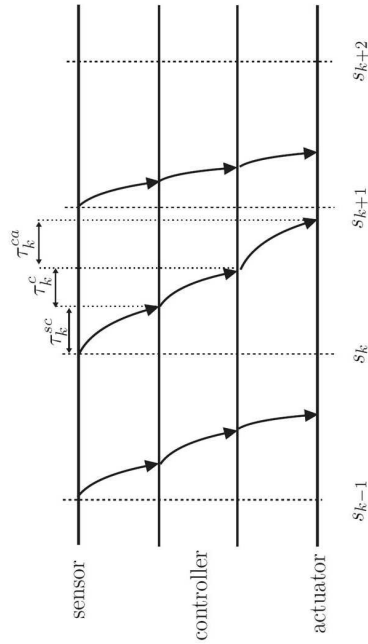
3/48



Assumptions:

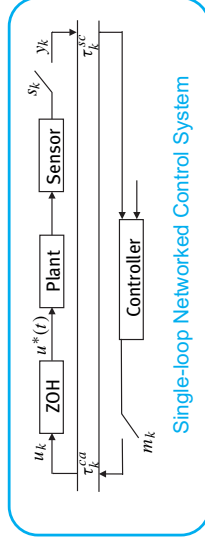
- ▶ Time-driven sensor (sampling times: s_k)
 - ▶ Event-driven controller
 - ▶ Event-driven actuator
- Time-delays:
- ▶ Sensor-to-controller $\tau_{s,c,k}$
 - ▶ Controller-to-actuator $\tau_{c,a,k}$
 - ▶ Computational delay $\tau_{c,k}$
 - ▶ $\tau_k = \tau_{s,c,k} + \tau_{c,a,k} + \tau_{c,k}$

4/48



- ▶ Value of output at k th sensor moment: $y_k := y(s_k)$
- ▶ u_k is control value computed on the basis of y_k
- ▶ We will assume $y_k = x_k$ (full state measurements)

5/48



Network-induced uncertainties:

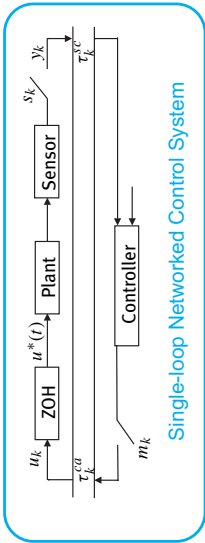
- ▶ Time-varying delays: $\tau_k \in [\tau_{min}, \tau_{max}]$
- ▶ Time-varying sampling intervals: $h_k = s_{k+1} - s_k \in [h_{min}, h_{max}]$
- ▶ Packet dropouts:

$$m_k = \begin{cases} 1, & u_k \text{ is dropped} \\ 0, & u_k \text{ is not dropped} \end{cases}$$

$$\sum_{v=k-\bar{\delta}}^k m_v \leq \bar{\delta}$$

- ▶ Maximum of $\bar{\delta}$ subsequent dropouts:

6/48



Assumptions:

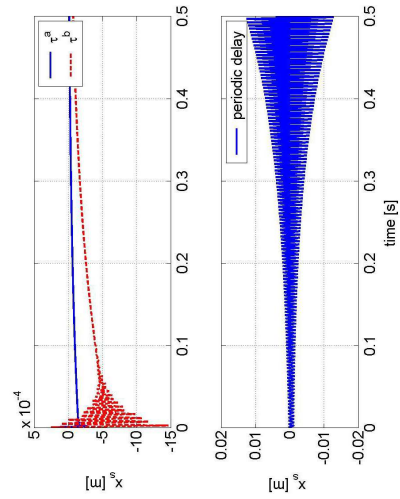
- ▶ **Time-varying delays:** $\tau_k \in [\tau_{min}, \tau_{max}]$
- ▶ **Time-varying sampling intervals:**
 $h_k = s_{k+1} - s_k \in [h_{min}, h_{max}]$
- ▶ **Packet dropouts:**
 $m_k = \begin{cases} 1, & u_k \text{ is dropped} \\ 0, & u_k \text{ is not dropped} \end{cases}$

Problem:
How to guarantee stability in the face of these network-induced uncertainties

6/48

Example with periodic delays

- ▶ Constant sampling interval: $h = 1 \text{ ms}$
- ▶ Periodically varying delays: $\tau_a, \tau_b, \tau_c, \dots$ ($\tau_a = 0.2h, \tau_b = 0.6h$)
- ▶ $\bar{K} = [50 \quad 1.18]$



- ▶ Similarly destabilising effects can occur for varying sampling intervals h_k

8/48

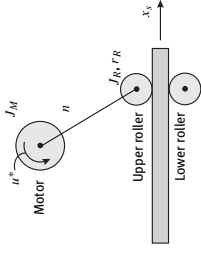
- ▶ Example to motivate the importance of investigating the influence of time-varying delays on stability (Cloosterman, CDC2006, TAC2009)

- ▶ Continuous-time dynamics:

$$\dot{x} = Ax + Bu^*(t), A = \begin{bmatrix} 0 & 1 \\ 0 & 0 \end{bmatrix}, B = \begin{bmatrix} 0 \\ b \end{bmatrix},$$

$$\text{with } b := \frac{mR}{J_M + n^2 J_R}, x = [x_s(t) \quad \dot{x}_s(t)]^T$$

- ▶ State-feedback $u_k = -\bar{K}x_k$



7/48

Network Control Systems: Problem Setting

PROBLEM SETTING:
How to guarantee the robust stability of Networked Control Systems with

- uncertain time-varying sampling intervals
- uncertain time-varying delays
- packet dropouts

9/48

- ▶ Discrete-time approach for stability analysis has received wide attention in the literature:

- Wittenmark, et. al. ACC1995
- Zhang, et. al. CSM2001
- Sala, Automatica2005
- Zhang, et. al. TAC2005
- Pan et. al. IJC2006
- Garcia-Rivera et. al. Automatica2007
- Hetel et. al. TAC2006, IJC2008
- Fujioka, ACC2008
- Dritsas et. al. IJC2009
- Cloosterman et. al. TAC2009, Automatica2010 (Submitted)
- Gielen et. al. Automatica2010
- etc. etc.

- ▶ Results typically applicable for a subset of the network-induced uncertainties

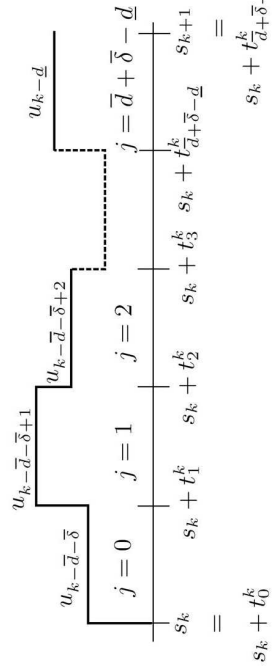
- ▶ Synthesis problem less well-studied

10/48

- ▶ Continuous-time (sampled-data) dynamics of the linear plant:

$$\begin{aligned} \dot{x}(t) &= Ax(t) + Bu^*(t) \\ u^*(t) &= u_{k+j-\bar{d}-\bar{\delta}}^k \quad \text{for } t \in [s_k + t_j^k, s_k + t_{j+1}^k), \end{aligned}$$

where $\underline{d} := \lfloor \frac{\tau_{\min}}{h_{\max}} \rfloor, \bar{d} := \lceil \frac{\tau_{\max}}{h_{\min}} \rceil$ and $t_j^k \in [0, h_k]$ the actuation update instants



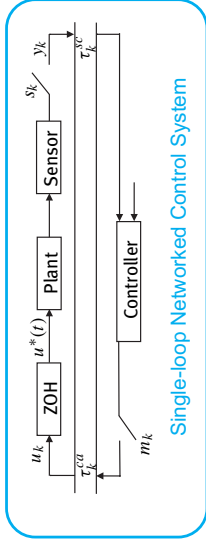
12/48

- ▶ Continuous-time (sampled-data) dynamics of the linear plant:

$$\begin{aligned} \dot{x}(t) &= Ax(t) + Bu^*(t) \\ u^*(t) &= u_{k^*}^*(t) \end{aligned}$$

- ▶ Parameter $k^*(t)$ that denotes the index of the most recent control input that is available at time t as

$$k^*(t) := \max\{k \in \mathbb{N} \mid s_k + \tau_k \leq t \wedge m_k = 0\}$$



11/48

- ▶ Continuous-time (sampled-data) dynamics of the linear plant:

$$\begin{aligned} \dot{x}(t) &= Ax(t) + Bu^*(t) \\ u^*(t) &= u_{k+j-\bar{d}-\bar{\delta}}^k \quad \text{for } t \in [s_k + t_j^k, s_k + t_{j+1}^k), \end{aligned}$$

where $\underline{d} := \lfloor \frac{\tau_{\min}}{h_{\max}} \rfloor, \bar{d} := \lceil \frac{\tau_{\max}}{h_{\min}} \rceil$ and $t_j^k \in [0, h_k]$ the actuation update instants

- ▶ Explicit expressions for $t_j^k = t_j^k(h_k, \tau_k, m_k, h_{k-1}, \tau_{k-1}, m_{k-1}, \dots)$ exist
- ▶ Bounds h_{\min}, h_{\max} on sampling intervals
- ▶ Bounds τ_{\min}, τ_{\max} on the delays
- ▶ Bound $\bar{\delta}$ on subsequent packet dropouts
- ▶ Upper and lower bounds on t_j^k

12/48

- ▶ Use an augmented state vector: $\xi_k = (x_k^T \ u_{k-1}^T \ \dots \ u_{k-\bar{d}-\bar{\delta}}^T)^T$
- ▶ Uncertain parameters: $\theta_k := (h_k, t_1^k, \dots, t_{\bar{d}+\bar{\delta}-\underline{d}}^k)$
- ▶ Discrete-time uncertain NCS model:

$$\xi_{k+1} = F(\theta_k)\xi_k + G(\theta_k)u_k,$$

where

$$F(\theta_k) = \begin{pmatrix} \Lambda(\theta_k) & M_{\bar{d}+\bar{\delta}-1}(\theta_k) & M_{\bar{d}+\bar{\delta}-2}(\theta_k) & \dots & M_1(\theta_k) & M_0(\theta_k) \\ 0 & I & 0 & \dots & 0 & 0 \\ \vdots & \vdots & \vdots & \ddots & \vdots & \vdots \\ 0 & \dots & \dots & \dots & 0 & I \end{pmatrix}$$

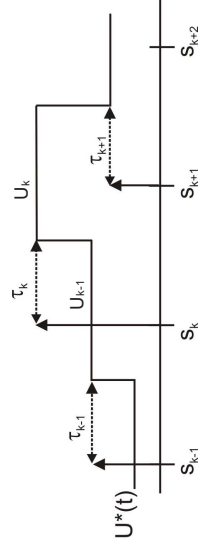
and

$$\Lambda(\theta_k) = e^{A h_k}, \quad G(\theta_k) = \begin{pmatrix} M_{\bar{d}+\bar{\delta}}(\theta_k) \\ 0 \\ \vdots \\ 0 \end{pmatrix}, \quad M_j(\theta_k) = \begin{cases} \int_{h_k-t_j^k}^{h_k-t_{j+1}^k} e^{A_s} ds B & \text{if } 0 \leq j \leq \bar{d} + \bar{\delta} - \underline{d} \\ 0 & \text{if } \bar{d} + \bar{\delta} - \underline{d} < j \leq \bar{d} + \bar{\delta} \end{cases}$$

- ▶ Continuous-time (sampled-data) dynamics of the linear plant:

$$\dot{x}(t) = Ax(t) + Bu^*(t)$$

$$u^*(t) = u_k \quad \text{for } t \in [s_k + \tau_k, s_{k+1} + \tau_{k+1})$$



- ▶ Uncertain parameters: $\theta_k := (h_k, t_1^k, \dots, t_{\bar{d}+\bar{\delta}-\underline{d}}^k)$

- ▶ Exact discretisation of the sampled-data NCS dynamics at the sampling instants:

$$\begin{aligned} x_{k+1} &= \Lambda(\theta_k)x_k \\ &+ M_{\bar{d}+\bar{\delta}-1}(\theta_k)u_{k-1} + \dots + M_0(\theta_k)u_{k-\bar{d}-\bar{\delta}} \\ &+ M_{\bar{d}+\bar{\delta}}(\theta_k)u_k \end{aligned}$$

Current state
Past Control Inputs
Current Control Input

where

$$\Lambda(\theta_k) = e^{A h_k}, \quad M_j(\theta_k) = \begin{cases} \int_{h_k-t_j^k}^{h_k-t_{j+1}^k} e^{A_s} ds B & \text{if } 0 \leq j \leq \bar{d} + \bar{\delta} - \underline{d} \\ 0 & \text{if } \bar{d} + \bar{\delta} - \underline{d} < j \leq \bar{d} + \bar{\delta} \end{cases}$$

BUT.....LET'S KEEP IT SIMPLE...
Consider the small-delay case, with a constant sampling interval and no packet dropouts

- ▶ Use a lifted state vector: $\xi_k = (x_k^T \ u_{k-1}^T)^T$
- ▶ Uncertain parameters: $\theta_k := \tau_k$
- ▶ Discrete-time uncertain NCS model:

$$\xi_{k+1} = F(\tau_k)\xi_k + G(\tau_k)u_k$$

where

$$F(\tau_k) = \begin{pmatrix} e^{Ah} & \int_{h-\tau_k}^h e^{As} ds B \\ 0 & 0 \end{pmatrix}, \quad G(\tau_k) = \begin{pmatrix} \int_0^{h-\tau_k} e^{As} ds B \\ I \end{pmatrix}$$

- ▶ Example with continuous-time plant dynamics:

$$\dot{x} = Ax + Bu^*(t), \quad A = \begin{bmatrix} 0 & 1 \\ 0 & 0 \end{bmatrix}, \quad B = \begin{bmatrix} 0 \\ b \end{bmatrix}$$

- ▶ Discrete-time uncertain NCS model:

$$\xi_{k+1} = F(\tau_k)\xi_k + G(\tau_k)u_k$$

where

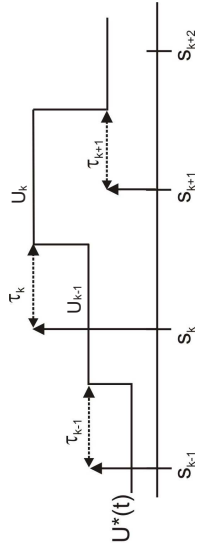
$$F(\tau_k) = \begin{pmatrix} e^{Ah} & \int_{h-\tau_k}^h e^{As} ds B \\ 0 & 0 \end{pmatrix}, \quad G(\tau_k) = \begin{pmatrix} \int_0^{h-\tau_k} e^{As} ds B \\ I \end{pmatrix}$$

$$F(\tau_k) = \begin{pmatrix} 1 & h & \frac{b}{2}(h^2 - (h - \tau_k)^2) \\ 0 & 1 & b(h - (h - \tau_k)) \\ 0 & 0 & 0 \end{pmatrix}, \quad G(\tau_k) = \begin{pmatrix} \frac{1}{2}b(h - \tau_k)^2 \\ b(h - \tau_k) \\ 1 \end{pmatrix}$$

- ▶ Uncertain parameters: $\theta_k := \tau_k$ (Only delay!)
- ▶ Exact discretisation of the sampled-data NCS dynamics at the sampling instants:

$$x_{k+1} = e^{Ah} x_k + \int_{\tau_k}^h e^{A(h-s)} ds B u_k + \int_0^{\tau_k} e^{A(h-s)} ds B u_{k-1}$$

$$x_{k+1} = e^{Ah} x_k + \int_0^{h-\tau_k} e^{As} ds B u_k + \int_{h-\tau_k}^h e^{As} ds B u_{k-1}$$



- ▶ Example with continuous-time plant dynamics:

$$\dot{x} = Ax + Bu^*(t), \quad A = \begin{bmatrix} 0 & 1 \\ 0 & 0 \end{bmatrix}, \quad B = \begin{bmatrix} 0 \\ b \end{bmatrix}$$

- ▶ Discrete-time uncertain NCS model:

$$\xi_{k+1} = F(\tau_k)\xi_k + G(\tau_k)u_k$$

where

$$F(\tau_k) = \begin{pmatrix} e^{Ah} & \int_{h-\tau_k}^h e^{As} ds B \\ 0 & 0 \end{pmatrix}, \quad G(\tau_k) = \begin{pmatrix} \int_0^{h-\tau_k} e^{As} ds B \\ I \end{pmatrix}$$

- ▶ Discrete-time uncertain NCS model:

$$\xi_{k+1} = F(\tau_k)\xi_k + G(\tau_k)u_k$$

- ▶ In closed-loop with the static discrete-time extended-state feedback controller $u_k = -\bar{K}\xi_k = -\bar{K}x_k - \bar{K}_u u_{k-1}$:

$$\begin{aligned} \xi_{k+1} &= (F(\tau_k) - G(\tau_k)K)\xi_k \\ &= \begin{bmatrix} e^{Ah} - \int_0^h e^{As} ds B \bar{K} & \int_{h-\tau_k}^h e^{As} ds B \\ -\bar{K}_u & -\bar{K} \end{bmatrix} \xi_k \end{aligned}$$

- ▶ Discrete-time linear system with exponential uncertainty : varying delay τ_k

- ▶ Note that the model is a parameter-varying system but the parameters appear in a nonlinear (exponential) fashion

20/48

- ▶ Discrete-time uncertain NCS model:

$$\xi_{k+1} = F(\tau_k)\xi_k + G(\tau_k)u_k$$

- ▶ In closed-loop with the static discrete-time extended-state feedback controller $u_k = -\bar{K}\xi_k = -\bar{K}x_k - \bar{K}_u u_{k-1}$:

$$\begin{aligned} \xi_{k+1} &= (F(\tau_k) - G(\tau_k)K)\xi_k \\ &= \begin{bmatrix} e^{Ah} - \int_0^h e^{As} ds B \bar{K} & \int_{h-\tau_k}^h e^{As} ds B \\ -\bar{K}_u & -\bar{K} \end{bmatrix} \xi_k \end{aligned}$$

- ▶ Discrete-time linear system with exponential uncertainty : varying delay τ_k

20/48

- ▶ Discrete-time uncertain closed-loop NCS model:

$$\xi_{k+1} = (F(\tau_k) - G(\tau_k)K)\xi_k =: H(\tau_k)\xi_k$$

- ▶ A first approach using a common quadratic Lyapunov function:

$$V(\xi) = \xi^T P \xi, \quad P = P^T > 0$$

- ▶ Closed-loop NCS is globally asymptotically stable if there exists $P = P^T > 0, 0 < \gamma < 1$ such that

$$H^T(\tau)PH(\tau) - P \leq -\gamma P, \quad \forall \tau \in [\tau_{min}, \tau_{max}]$$

21/48

- ▶ Discrete-time uncertain closed-loop NCS model:

$$\xi_{k+1} = (F(\tau_k) - G(\tau_k)K)\xi_k =: H(\tau_k)\xi_k$$

- ▶ A first approach using a common quadratic Lyapunov function:

$$V(\xi) = \xi^T P \xi, \quad P = P^T > 0$$

- ▶ Closed-loop NCS is globally asymptotically stable if there exists $P = P^T > 0, 0 < \gamma < 1$ such that

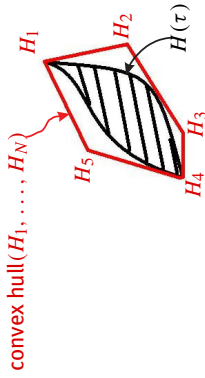
$$H^T(\tau)PH(\tau) - P \leq -\gamma P, \quad \forall \tau \in [\tau_{min}, \tau_{max}]$$

- ▶ Stability characterisations using parameter-dependent Lyapunov functions exist and can be shown to be less conservative than discrete-time Lyapunov-Krasovskii methods (Cloosterman Automatica 2010 (Submitted), Hetel CDC2009)

21/48

- ▶ **Basic idea:** embed the uncertainty matrix set $H(\tau)$, $\tau \in [\tau_{min}, \tau_{max}]$ in a polytopic set with generators (vertices) H_i , $i = 1, \dots, N$:

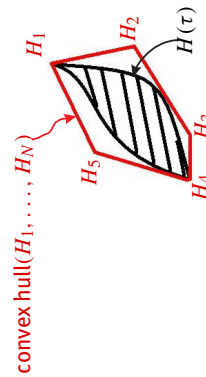
$$\{H(\tau) \mid \tau \in [\tau_{min}, \tau_{max}]\} \subseteq \text{convex hull}(H_1, \dots, H_N)$$



- ▶ Discrete-time uncertain closed-loop NCS model:
 $\xi_{k+1} = (F(\tau_k) - G(\tau_k)K)\xi_k =: H(\tau_k)\xi_k$
- ▶ A first approach using a common quadratic Lyapunov function:
 $V(\xi) = \xi^T P \xi, P = P^T > 0$
- ▶ Closed-loop NCS is globally asymptotically stable if there exists $P = P^T > 0, 0 < \gamma < 1$ such that
 $H^T(\tau)PH(\tau) - P \leq -\gamma P, \forall \tau \in [\tau_{min}, \tau_{max}]$
- ▶ **PROBLEM:** Infinite set of Linear Matrix Inequalities (LMIs)
⇒ Recognised in the literature as a tough problem (see e.g. Hespanha, Proc. IEEE2007)
- ▶ **How to arrive at a finite number of LMIs?**

- ▶ **Basic idea:** embed the uncertainty matrix set $H(\tau)$, $\tau \in [\tau_{min}, \tau_{max}]$ in a polytopic set with generators (vertices) H_i , $i = 1, \dots, N$:

$$\{H(\tau) \mid \tau \in [\tau_{min}, \tau_{max}]\} \subseteq \text{convex hull}(H_1, \dots, H_N)$$



- ▶ Polytopic overapproximation gives rise to a polytopic model:
 $\xi_{k+1} = \left(\sum_{i=1}^N \delta_i H_i\right)\xi_k, 0 \leq \delta_i \leq 1, i = 1, \dots, N, \text{ and } \sum_{i=1}^N \delta_i = 1$

- ▶ Polytopic model

$$\xi_{k+1} = \left(\sum_{i=1}^N \delta_i H_i\right)\xi_k, 0 \leq \delta_i \leq 1, i = 1, \dots, N, \text{ and } \sum_{i=1}^N \delta_i = 1$$

is globally asymptotically stable if there exist $P = P^T > 0, 0 < \gamma < 1$ such that the following finite set of LMIs are satisfied:

$$H_i^T P H_i - P \leq -\gamma P, \forall i = 1, \dots, N$$

- ▶ Discrete-time uncertain closed-loop NCS model

$$\xi_{k+1} = H(\tau_k)\xi_k$$

is globally asymptotically stable if the polytopic model is globally asymptotically stable

- ▶ Now, we only need to check N LMIs for which efficient numerical tools exist

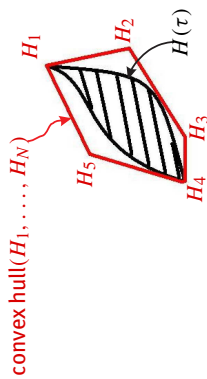
Extensions & Remarks	TU/e	Extensions & Remarks	TU/e
<ul style="list-style-type: none"> ▶ Stability of the intersample behavior (and therefore the sampled-data NCS) is also guaranteed (Cloosterman et al., CDC 2007) 	24/48	<ul style="list-style-type: none"> ▶ Stability of the intersample behavior (and therefore the sampled-data NCS) is also guaranteed (Cloosterman et al., CDC 2007) ▶ Approach for stability analysis also applicable for the case with (Cloosterman et al., TAC2009, Automatica2010 (Submitted)) <ul style="list-style-type: none"> • Variations in the sampling interval $h_k \in [h_{min}, h_{max}]$ • Large delays $\tau_k > h_k$ • Packet dropouts 	24/48
<ul style="list-style-type: none"> ▶ Stability of the intersample behavior (and therefore the sampled-data NCS) is also guaranteed (Cloosterman et al., CDC 2007) 	24/48	<ul style="list-style-type: none"> ▶ Other approaches towards modelling packet dropouts: <ul style="list-style-type: none"> • Modelled as prolongation of maximal sampling interval (Garcia-Rivera, Automatica2007) • Modelled using a separate (hybrid) model (van Schendel et.al., ACC2010) ▶ Usage of parameter-dependent Lyapunov functions, which can be proven to be more general than discrete-time Lyapunov-Krasovskii methods (Hetel et. al., CDC2009, Cloosterman et al., Automatica2010 (Submitted)) 	25/48

Polytopic overapproximation

TU/e

- ▶ **Basic idea:** embed the uncertainty matrix set $H(\tau)$, $\tau \in [\tau_{min}, \tau_{max}]$ in a polytopic set with generators (vertices) H_i , $i = 1, \dots, N$:

$$\{H(\tau) \mid \tau \in [\tau_{min}, \tau_{max}]\} \subseteq \text{convex hull}(H_1, \dots, H_N)$$



- ▶ **How to get such a polytopic overapproximation?**

26/48

251

Polytopic overapproximation

TU/e

- ▶ Important criteria for methods of over approximation:

- **Accuracy/conservatism:**

How 'tight' is the overapproximation?

- **Computational complexity:**

How many vertices do we need (number of LMIs to be solved)?

- ▶ A comparative study on the different approaches for overapproximation can be found in Heemels et. al., HSCC2010

28/48

Polytopic overapproximation

TU/e

- ▶ Methods for obtaining polytopic overapproximations based on

- **Interval matrices**
(Cloosterman, van de Wouw, Heemels, Nijmeijer, CDC 2006)
- **Taylor series**
(Hetel, Daafouz, Jung, TAC 2007)
- **Real Jordan form**
(Cloosterman, van de Wouw, Heemels, Nijmeijer, CDC 2007, ACC 2008, TAC 2009)
- **Gridding (and norm bounding of approximation error)**
(Fujioka, ACC 2008), (Suh, Automatica 2008), (Donkers, Hetel, Heemels, van de Wouw, Steinbuch, HSCC 2009), (Skaf, Boyd, TAC 2009)
- **Cayley-Hamilton theorem**
(Gielen, et. al., NMPC 2008, Automatica 2010)

27/48

Polytopic overapproximation

TU/e

- ▶ Polytopic overapproximation of the discrete-time uncertain NCS dynamics is an essential step in the stability analysis of the NCS

- ▶ Let us illustrate one approach using the real Jordan form of the continuous-time system matrix

- ▶ The overapproximation consists of the following steps:

1. the closed-loop discrete-time NCS dynamics is rewritten such that the (nonlinear functions of the) uncertainties appear in the dynamics in an affine fashion
2. the uncertain NCS dynamics is overapproximated by a polytopic model

29/48

Polytopic overapproximation using real Jordan form TU/e

- ▶ For the exponential of $A = QJQ^{-1}$ with $J = \text{diag}(J_1, \dots, J_p)$ it holds that:

$$e^{As} = Qe^{Js}Q^{-1} = Q \text{diag}(e^{J_1s}, \dots, e^{J_ps}) Q^{-1} \quad \text{with}$$

$$e^{J_i s} = e^{\lambda_i s}, e^{\lambda_i s} \begin{pmatrix} 1 & s & \frac{s^2}{2!} & \dots & \frac{s^{k-1}}{(k-1)!} \\ 0 & 1 & s & \dots & \frac{s^{k-2}}{(k-2)!} \\ \vdots & \vdots & \ddots & \ddots & \vdots \\ 0 & 0 & 0 & \dots & 1 \\ 0 & 0 & 0 & \dots & 0 \end{pmatrix},$$

$$\text{when } J_i = \lambda_i, \begin{pmatrix} \lambda_i & 1 \\ 0 & \lambda_i \end{pmatrix}, \begin{pmatrix} \lambda_i & 1 & 0 \\ 0 & \lambda_i & 1 \\ 0 & 0 & \lambda_i \end{pmatrix}, \dots, \begin{pmatrix} \lambda_i & 1 & 0 & \dots & 0 \\ 0 & \lambda_i & 1 & \dots & 0 \\ \vdots & \vdots & \ddots & \ddots & \vdots \\ 0 & 0 & \dots & \lambda_i & 1 \\ 0 & 0 & \dots & 0 & \lambda_i \end{pmatrix}$$

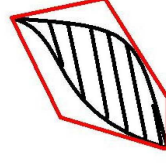
31/48

Polytopic overapproximation using real Jordan form TU/e

- ▶ Uncertainty sets for the systems matrices:

$$\mathcal{F} = \left\{ F_0 + \sum_{i=1}^{\nu} \alpha_i(\tau) F_i \mid \tau \in [\tau_{\min}, \tau_{\max}] \right\}$$

$$\mathcal{G} = \left\{ G_0 + \sum_{i=1}^{\nu} \alpha_i(\tau) G_i \mid \tau \in [\tau_{\min}, \tau_{\max}] \right\}$$



- ▶ Use $\bar{\alpha}_i = \max_{\tau \in [\tau_{\min}, \tau_{\max}]} \alpha_i(\tau)$ and $\underline{\alpha}_i = \min_{\tau \in [\tau_{\min}, \tau_{\max}]} \alpha_i(\tau)$ to obtain the overapproximation: $\mathcal{F} \subseteq \bar{\mathcal{F}}$ and $\mathcal{G} \subseteq \bar{\mathcal{G}}$

$$\bar{\mathcal{F}} = \left\{ F_0 + \sum_{i=1}^{\nu} \delta_i F_i \mid \delta_i \in [\underline{\alpha}_i, \bar{\alpha}_i], i = 1, 2, \dots, \nu \right\},$$

$$\bar{\mathcal{G}} = \left\{ G_0 + \sum_{i=1}^{\nu} \delta_i G_i \mid \delta_i \in [\underline{\alpha}_i, \bar{\alpha}_i], i = 1, 2, \dots, \nu \right\},$$

33/48

Polytopic overapproximation using real Jordan form TU/e

- ▶ Discrete-time uncertain NCS model (small delays, constant sampling interval, no packet dropouts):

$$\xi_{k+1} = (F(\tau_k) - G(\tau_k)K)\xi_k,$$

$$\text{with } F(\tau_k) = \begin{pmatrix} e^{Ah} & \int_{h-\tau_k}^h e^{As} ds B \\ 0 & I \end{pmatrix}, G(\tau_k) = \begin{pmatrix} \int_0^{h-\tau_k} e^{As} ds B \\ I \end{pmatrix}$$

- ▶ For the overapproximation of $F(\tau)$ and $G(\tau)$, consider the (real) Jordan form:

$$A = QJQ^{-1}$$

with $Q \in \mathbb{R}^{n \times n}$ a matrix that contains the generalized eigenvectors of A and

$$J = \text{diag}(J_1, \dots, J_p) \text{ with } J_i = \lambda_i, \begin{pmatrix} \lambda_i & 1 \\ 0 & \lambda_i \end{pmatrix}, \begin{pmatrix} \lambda_i & 1 & 0 \\ 0 & \lambda_i & 1 \\ 0 & 0 & \lambda_i \end{pmatrix}, \dots, \begin{pmatrix} \lambda_i & 1 & 0 & \dots & 0 \\ 0 & \lambda_i & 1 & \dots & 0 \\ \vdots & \vdots & \ddots & \ddots & \vdots \\ 0 & 0 & \dots & \lambda_i & 1 \\ 0 & 0 & \dots & 0 & \lambda_i \end{pmatrix}$$

30/48

Polytopic overapproximation using real Jordan form TU/e

- ▶ Jordan form (for the case of real eigenvalues):

$$e^{As} = Qe^{Js}Q^{-1} = Q \left(\sum_{i=1}^p \sum_{j=0}^{q_i-1} \frac{s^j}{j!} e^{\lambda_i s} S_{i,j} \right) Q^{-1},$$

- ▶ Using this and its integrated version in

$$\xi_{k+1} = \begin{pmatrix} e^{Ah} & \int_{h-\tau_k}^h e^{As} ds B \\ 0 & I \end{pmatrix} \xi_k + \begin{pmatrix} \int_0^{h-\tau_k} e^{As} ds B \\ I \end{pmatrix} u_k$$

is rewritten as

$$\xi_{k+1} = \left(F_0 + \sum_{i=1}^{\nu} \alpha_i(\tau_k) F_i \right) \xi_k + \left(G_0 + \sum_{i=1}^{\nu} \alpha_i(\tau_k) G_i \right) u_k$$

- ▶ Nonlinear functions $\alpha_i(\tau_k) = \frac{(h-\tau_k)^j}{j!} e^{\lambda_i(h-\tau_k)}$ of the uncertainties now appear in an affine fashion

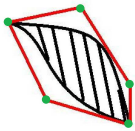
32/48

- ▶ Uncertain discrete-time NCS model: $\xi_{k+1} = (F(\tau) - G(\tau)K)\xi_k$
- ▶ For all $\tau \in [\tau_{min}, \tau_{max}]$ we have $F(\tau) \in \mathcal{F} \subset \overline{\mathcal{F}} = \text{co}(\mathcal{H}_F)$ and $G(\tau) \in \mathcal{G} \subset \overline{\mathcal{G}} = \text{co}(\mathcal{H}_G)$.

where the generators/vertices of $\overline{\mathcal{F}}$ and $\overline{\mathcal{G}}$ are given by:

$$\mathcal{H}_{\mathcal{F}} = \left\{ f_0 + \sum_{i=1}^v \delta_i F_i \mid \delta_i \in [\underline{\alpha}_i, \overline{\alpha}_i], i = 1, 2, \dots, v \right\},$$

$$\mathcal{H}_{\mathcal{G}} = \left\{ g_0 + \sum_{i=1}^v \delta_i G_i \mid \delta_i \in [\underline{\alpha}_i, \overline{\alpha}_i], i = 1, 2, \dots, v \right\}.$$



- ▶ Global exponential stability of NCS, when

$$P = P^T > 0$$

$$(H_{F,j} - H_{G,j}K)^T P (H_{F,j} - H_{G,j}K) - P \leq -\gamma P, \quad (2^v + 1 \text{ LMIs})$$

for all $(H_{F,j}, H_{G,j}) \in \mathcal{H}_{\mathcal{F}} \times \mathcal{H}_{\mathcal{G}}$

34/48

- ▶ Discrete-time uncertain NCS model:

$$\xi_{k+1} = F(\tau_k)\xi_k + G(\tau_k)u_k$$

- ▶ Using the Jordan form approach we can write

$$F(\tau_k) = \begin{pmatrix} e^{Ah} & \int_{h-\tau_k}^h e^{As} ds B \\ 0 & 1 \\ 0 & 0 \end{pmatrix} = \begin{pmatrix} 1 & h & \frac{1}{2}(h^2 - (h - \tau_k)^2) \\ 0 & 1 & b(h - (h - \tau_k)) \\ 0 & 0 & 0 \end{pmatrix}$$

$$G(\tau_k) = \begin{pmatrix} \int_0^{h-\tau_k} e^{As} ds B \\ I \end{pmatrix} = \begin{pmatrix} \frac{1}{2}b(h - \tau_k)^2 \\ b(h - \tau_k) \\ 1 \end{pmatrix}$$

36/48

- ▶ Example with continuous-time plant dynamics:

$$\dot{x} = Ax + Bu^*(t), \quad A = \begin{bmatrix} 0 & 1 \\ 0 & 0 \end{bmatrix}, \quad B = \begin{bmatrix} 0 \\ b \end{bmatrix}$$

- ▶ Discrete-time uncertain NCS model:

$$\xi_{k+1} = F(\tau_k)\xi_k + G(\tau_k)u_k$$

where

$$F(\tau_k) = \begin{pmatrix} e^{Ah} & \int_{h-\tau_k}^h e^{As} ds B \\ 0 & 1 \end{pmatrix}, \quad G(\tau_k) = \begin{pmatrix} \int_0^{h-\tau_k} e^{As} ds B \\ I \end{pmatrix}$$

35/48

- ▶ Discrete-time uncertain NCS model:

$$\xi_{k+1} = F(\tau_k)\xi_k + G(\tau_k)u_k$$

- ▶ Using the Jordan form approach we can write

$$F(\tau_k) = \begin{pmatrix} 1 & h & \frac{1}{2}(h^2 - (h - \tau_k)^2) \\ 0 & 1 & b(h - (h - \tau_k)) \\ 0 & 0 & 0 \end{pmatrix} = F_0 + \alpha_1(\tau_k)F_1 + \alpha_2(\tau_k)F_2$$

$$G(\tau_k) = \begin{pmatrix} \frac{1}{2}b(h - \tau_k)^2 \\ b(h - \tau_k) \\ 1 \end{pmatrix} = G_0 + \alpha_1(\tau_k)G_1 + \alpha_2(\tau_k)G_2$$

36/48

Discrete-time Model: an Example

TU/e

- ▶ Discrete-time uncertain NCS model:

$$\xi_{k+1} = F(\tau_k)\xi_k + G(\tau_k)u_k$$
- ▶ Using the Jordan form approach we can write

$$F(\tau_k) = \begin{pmatrix} 1 & h & \frac{1}{2}(h^2 - (h - \tau_k)^2) \\ 0 & 1 & b(h - (h - \tau_k)) \\ 0 & 0 & 0 \end{pmatrix} = F_0 + \alpha_1(\tau_k)F_1 + \alpha_2(\tau_k)F_2$$

$$G(\tau_k) = \begin{pmatrix} \frac{1}{2}b(h - \tau_k)^2 \\ b(h - \tau_k) \\ 1 \end{pmatrix} = G_0 + \alpha_1(\tau_k)G_1 + \alpha_2(\tau_k)G_2$$

with

$$F_0 = \begin{bmatrix} 1 & h & \frac{1}{2}bh^2 \\ 0 & 1 & bh \\ 0 & 0 & 0 \end{bmatrix}, \quad F_1 = \begin{bmatrix} 0 & 0 & 0 \\ 0 & 0 & -b \\ 0 & 0 & 0 \end{bmatrix}, \quad F_2 = \begin{bmatrix} 0 & 0 & -\frac{1}{2}b \\ 0 & 0 & 0 \\ 0 & 0 & 0 \end{bmatrix}$$

$$G_0 = \begin{bmatrix} 0 \\ 0 \\ 1 \end{bmatrix}, \quad G_1 = \begin{bmatrix} 0 \\ b \\ 0 \end{bmatrix}, \quad G_2 = \begin{bmatrix} \frac{1}{2}b \\ 0 \\ 0 \end{bmatrix}$$

$$\alpha_1(\tau_k) = h - \tau_k, \quad \text{and} \quad \alpha_2(\tau_k) = (h - \tau_k)^2$$

36/48

Discrete-time Model: an Example

TU/e

- ▶ Using these 4 vertices one can formulate 4 stability LMIs ($0 < \gamma < 1$):

$$(H_{F,j} - H_{G,j}K)^T P (H_{F,j} - H_{G,j}K) - P \leq -\gamma P, \quad \forall j \in \{1, 2, 3, 4\}$$

$$P = P^T > 0$$
- ▶ These LMI guarantee stability of the polytopic system
- ▶ Polytopic system is stable \Rightarrow Uncertain discrete-time NCS is stable
- ▶ With these LMIs one can check for which combinations of τ_{min} and τ_{max} stability can be guaranteed
- ▶ For simple examples one can derive these vertices manually
- ▶ We are developing a Matlab Toolbox in which overapproximation methods based on the Jordan form, the Cayley-Hamilton theorem and gridding are implemented

38/48

Discrete-time Model: an Example

TU/e

- ▶ Discrete-time uncertain NCS model:

$$\xi_{k+1} = F(\tau_k)\xi_k + G(\tau_k)u_k$$
- ▶ Using the Jordan form approach we can write

$$F(\tau_k) = \begin{pmatrix} e^{Ah} & e^{As}dsB \\ 0 & 0 \end{pmatrix} = F_0 + \alpha_1(\tau_k)F_1 + \alpha_2(\tau_k)F_2$$
- ▶ Polytopic overapproximation of $F(\tau)$ by a polytopic set with $2^v = 4$ vertices:

$$H_{F,1} = F_0 + \underline{\alpha}_1 F_1 + \underline{\alpha}_2 F_2, \quad H_{F,2} = F_0 + \underline{\alpha}_1 F_1 + \bar{\alpha}_2 F_2$$

$$H_{F,3} = F_0 + \bar{\alpha}_1 F_1 + \underline{\alpha}_2 F_2, \quad H_{F,4} = F_0 + \bar{\alpha}_1 F_1 + \bar{\alpha}_2 F_2$$

with

$$\underline{\alpha}_1 = \min \alpha_1(\tau) = h - \tau_{max}, \quad \bar{\alpha}_1 = \max \alpha_1(\tau) = h - \tau_{min}$$

$$\underline{\alpha}_2 = \min \alpha_2(\tau) = (h - \tau_{max})^2, \quad \bar{\alpha}_2 = \max \alpha_2(\tau) = (h - \tau_{min})^2$$
- ▶ And, ... similar expressions for $H_{G,i}$

37/48

Controller Synthesis

TU/e

- ▶ Controller Synthesis Problem:
 - Given a discrete-time uncertain NCS closed-loop model

$$\xi_{k+1} = F(\tau_k)\xi_k + G(\tau_k)u_k$$
 - Given a static extended state feedback controller $u_k = -K\xi_k$
 - How to design the feedback gain matrix K such that the closed-loop NCS system is globally asymptotically stable?

39/48

- ▶ Augmented state feedback controller $u_k = -\bar{K}\xi_k$
- ▶ The following linear matrix inequality can be used to design stabilising controllers ($0 < \gamma < 1$):

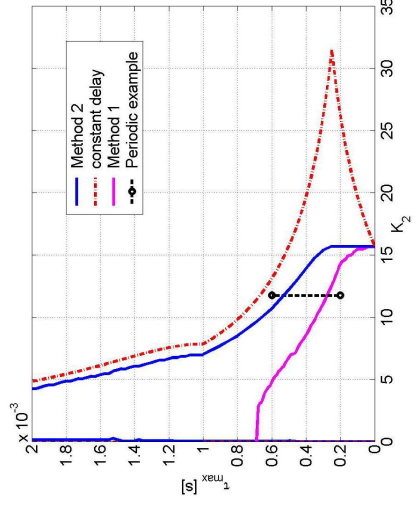
$$\begin{pmatrix} (1-\gamma)Y & YH_{F,j}^T - Z^T H_{G,j}^T \\ H_{F,j}Y - H_{G,j}Z & Y \end{pmatrix} > 0$$

- ▶ $\forall H_{F,j} \in \mathcal{H}_F, \forall H_{G,j} \in \mathcal{H}_G$
- ▶ The controller gain is given by:
 $K = ZY^{-1}$

- ▶ Design of a pure state feedback $u_k = \bar{K}x_k$ is more involved due to structure in $K = [\bar{K} \ 0]$ (Cloosterman et. al., Automatica2010 (Submitted))

Example with large delays

- ▶ Constant sampling interval: $h = 1 \text{ ms}$
- ▶ $\tau_{min} = 0, \bar{K} = [50 \ K_2]$
- ▶ Two methods for polytopic overapproximation:
 - Method 1: based on interval matrices
 - Method 2: based on the Jordan form approach



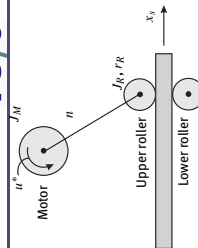
- ▶ Augmented state feedback controller $u_k = -\bar{K}\xi_k$
- ▶ Controller is stabilising if there exists a $P = P^T > 0$ and $0 < \gamma < 1$

$$(H_{F,j} - H_{G,j}K)^T P (H_{F,j} - H_{G,j}K) - P \leq -\gamma P$$

for all $(H_{F,j}, H_{G,j}) \in \mathcal{H}_F \times \mathcal{H}_G$

- ▶ Above matrix inequalities are not linear in P and K

Illustrative Example



- ▶ Example with continuous-time dynamics:

$$\dot{x} = Ax + Bu^*(t), \quad A = \begin{bmatrix} 0 & 1 \\ 0 & 0 \end{bmatrix}, \quad B = \begin{bmatrix} 0 \\ b \end{bmatrix},$$

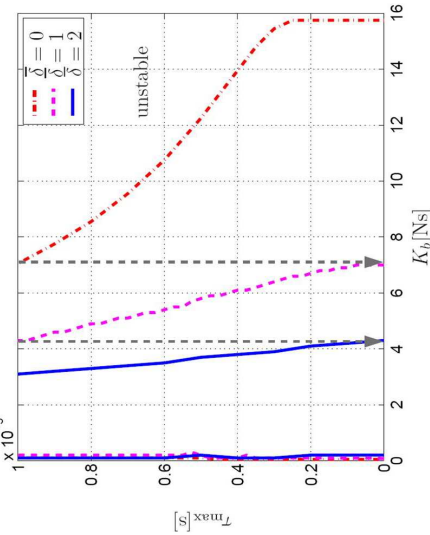
$$\text{with } b := \frac{nJ_R}{J_M + n^2 J_R}, \quad x = [x_s(t) \quad \dot{x}_s(t)]^T$$

- ▶ State-feedback $u_k = -\bar{K}x_k$

Example with delays and packet dropouts

TU/e

- ▶ Constant sampling interval: $h = 1$ ms, small delays with $\tau_{min} = 0$
- ▶ $\bar{K} = [50 \quad K_b]$
- ▶ Packet dropouts, with the maximum number of subsequent dropouts $\delta = 0, 1, 2$



44/48

Summary

TU/e

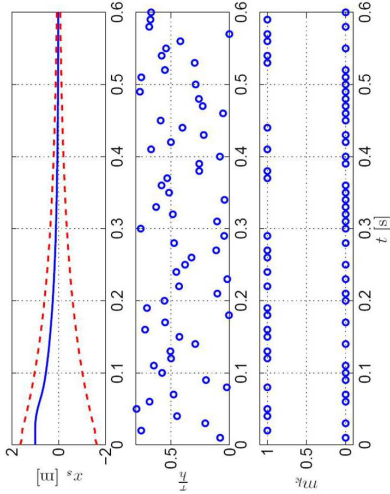
- ▶ Discrete-time modelling framework for linear networked control systems with
 - time-varying sampling intervals
 - time-varying delays
 - packet dropouts
- ▶ LMI-based conditions for stability and controller synthesis
- ▶ Polytopic overapproximation of the uncertain discrete NCS is an essential step in formulating these LMI-based conditions
- ▶ Approach is tailored to linear systems, discrete-time controller design, particular protocols and can provide less conservative results than the emulation approach by Nešić, Teel
- ▶ Results less generic than emulation framework (applicable to nonlinear systems)

46/48

Simulation example

TU/e

- ▶ Sampling interval constant $h = 0.01$ s
- ▶ Delay bounds $\tau_{min} = 0, \tau_{max} = 0.8h$
- ▶ Maximum number of subsequent packet dropouts $\delta = 2$
- ▶ Transient decay rate $\gamma = 0.1$
- ▶ Augmented state feedback controller synthesized using LMI-based conditions



45/48

Topics not covered and Future Work


TU/e

- ▶ What about performance? Results on transient performance and sensitivity to perturbations available (see e.g. van de Wouw, IJRNCS2010)
- ▶ What about other control problems, such as e.g. the tracking problem (see e.g. van de Wouw, IJRNCS2010)
- ▶ What about dynamic (and observer-based) discrete-time controllers
- ▶ What about the discrete-time approach for nonlinear NCS?
- ▶ Including communication constraints and quantisation in the discrete-time framework

47/48

- ▶ Decentralised/distributed controllers in a networked setting (EU-Project WIDE)
- ▶ Application areas:
 - Project 'Connect & Drive' on the Cooperative Adaptive Cruise Control
 - EU-project WIDE: wireless control of the water distribution network of Barcelona
- ▶ Work on a Matlab Toolbox for Networked Control Systems

48/48



technische universiteit eindhoven

Networked Control Systems


Part III: Communication constraints

Maurice Heemels & Nathan van de Wouw

Benelux Meeting on Systems and Control, 2010, Heeze, Netherlands

1/56

/department of mechanical engineering




technische universiteit eindhoven

Outline part III

- Networked control systems (NCS) and Communication imperfections:
 - (i) Varying sampling/transmission interval
 - (ii) Varying communication delays
 - (iii) Packet loss
 - (iv) **Communication constraints through shared network**
 - (v) Quantization
- Two approaches:
 - Continuous-time modeling approach (emulation)
 - Discrete-time modeling approach
- Summary of Part III
- Overall summary
- Literature list

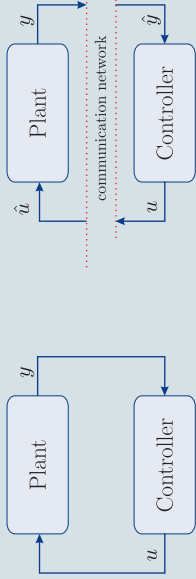
2/56

/department of mechanical engineering



technische universiteit eindhoven

Control over networks




To network ... or not to network:

- (i) Varying sampling/transmission interval
- (ii) Varying communication delays
- (iii) Packet loss
- (iv) Communication constraints through shared network
- (v) Quantization

Goal: **Quantitative understanding of effects on stability & performance**

3/56

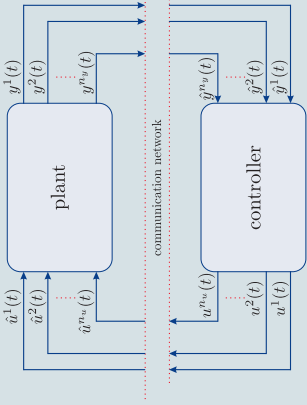
/department of mechanical engineering



technische universiteit eindhoven


Communication constraints in NCS

- Communication constraints:
 - Network is divided into sensor and actuator nodes
 - Only one node can access the network simultaneously
 - This gives rise to the problem of scheduling



4/56

/department of mechanical engineering




technische universiteit eindhoven

6/56

With constraints, no delay, no quantization

- t_k are transmission times
- $z = (u, y)$ and $\hat{z} = (\hat{u}, \hat{y})$ 'networked version' of z
- $\hat{z}(t_k^+) = z(t_k)$
- $\hat{z}(t_k^+) = \Gamma_{\sigma_k} z(t_k) + (I - \Gamma_{\sigma_k}) \hat{z}(t_k)$
- A protocol orchestrates that node $\sigma_k \in \{1, \dots, l\}$ gets access to network



technische universiteit eindhoven

/department of mechanical engineering



technische universiteit eindhoven

5/56


No constraints, no delay, no quantization

- t_k are transmission times
- $z = (u, y)$ and $\hat{z} = (\hat{u}, \hat{y})$ 'networked version' of z
- $\hat{z}(t_k^+) = z(t_k)$



technische universiteit eindhoven

/department of mechanical engineering




technische universiteit eindhoven

8/56


With constraints, with delay, no quantization

- t_k are transmission times
- $z = (u, y)$ and $\hat{z} = (\hat{u}, \hat{y})$ 'networked version' of z
- $\hat{z}(t_k^+) = z(t_k)$
- $\hat{z}(t_k^+) = \Gamma_{\sigma_k} z(t_k) + (I - \Gamma_{\sigma_k}) \hat{z}(t_k)$
- $\hat{z}((t_k + \tau_k)^+) = \Gamma_{\sigma_k} z(t_k) + (I - \Gamma_{\sigma_k}) \hat{z}(t_k + \tau_k)$



technische universiteit eindhoven

/department of mechanical engineering



technische universiteit eindhoven

7/56

With constraints, no delay, no quantization


- t_k are transmission times
- $z = (u, y)$ and $\hat{z} = (\hat{u}, \hat{y})$ 'networked version' of z
- $\hat{z}(t_k^+) = z(t_k)$
- $\hat{z}(t_k^+) = \Gamma_{\sigma_k} z(t_k) + (I - \Gamma_{\sigma_k}) \hat{z}(t_k)$
- A protocol orchestrates that node $\sigma_k \in \{1, \dots, l\}$ gets access to network

Example: Two sensors use network $z_1 = y_1$ and $z_2 = y_2$.

- if node 1 communicates at t_k ($\sigma_k = 1$):


$$\hat{z}(t_k^+) = \begin{pmatrix} z_1(t_k) \\ \hat{z}_2(t_k) \end{pmatrix} = \begin{pmatrix} 1 & 0 \\ 0 & 0 \end{pmatrix} z(t_k) + \begin{pmatrix} 0 & 0 \\ 0 & 1 \end{pmatrix} \hat{z}(t_k)$$

$$= \Gamma_{\sigma_k} z(t_k) + (I - \Gamma_{\sigma_k}) \hat{z}(t_k)$$



technische universiteit eindhoven

/department of mechanical engineering



technische universiteit eindhoven

9/56


/department of mechanical engineering

With constraints, with delay, with quantization

- t_k are transmission times
- $z = (u, y)$ and $\hat{z} = (\hat{u}, \hat{y})$ 'networked version' of z
- $\hat{z}(t_k^+) = z(t_k)$
- $\hat{z}(t_k^+) = \Gamma_{\sigma_k} z(t_k) + (I - \Gamma_{\sigma_k}) \hat{z}(t_k)$
- $\hat{z}((t_k + \tau_k)^+) = \Gamma_{\sigma_k} z(t_k) + (I - \Gamma_{\sigma_k}) \hat{z}(t_k + \tau_k)$
- $\hat{z}((t_k + \tau_k)^+) = \Gamma_{\sigma_k} q(z(t_k)) + (I - \Gamma_{\sigma_k}) \hat{z}(t_k + \tau_k)$

→ We will ignore quantization.
 → One attempt including all 5 network-induced imperfections:


[Heemels, Nesić, Teel, vdWouw, IEEE CDC / CCC 2009]



technische universiteit eindhoven

9/56

/department of mechanical engineering




technische universiteit eindhoven

10/56

/department of mechanical engineering

With constraints, with delay, no quantization


- t_k are transmission times
- $z = (u, y)$ and $\hat{z} = (\hat{u}, \hat{y})$ 'networked version' of z
- $\hat{z}(t_k^+) = z(t_k)$
- $\hat{z}(t_k^+) = \Gamma_{\sigma_k} z(t_k) + (I - \Gamma_{\sigma_k}) \hat{z}(t_k)$
- $\hat{z}((t_k + \tau_k)^+) = \Gamma_{\sigma_k} z(t_k) + (I - \Gamma_{\sigma_k}) \hat{z}(t_k + \tau_k)$
- Transmission intervals $h_k = t_{k+1} - t_k$ are time-varying
- Delays τ_k are time-varying



technische universiteit eindhoven

10/56

/department of mechanical engineering

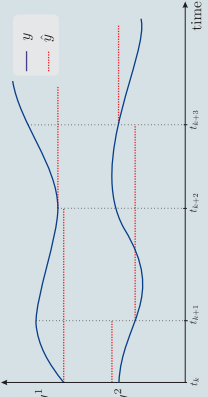


technische universiteit eindhoven

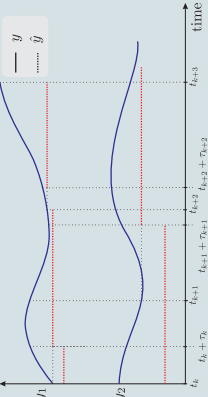
11/56


/department of mechanical engineering

With constraints, without delay: graphical illustration



With constraints, with delay: graphical illustration






technische universiteit eindhoven

11/56

/department of mechanical engineering




technische universiteit eindhoven

12/56

/department of mechanical engineering

Problem Formulation

- Given a plant, a controller, and a network protocol,
 - for what transmission intervals $h_k \in [\underline{L}, \bar{h}]$ and delays $\tau_k \in [\underline{\tau}, \bar{\tau}]$ is the NCS *globally asymptotically stable* or *certain \mathcal{L}_p gain*?



technische universiteit eindhoven

12/56

/department of mechanical engineering

TU/e
technische universiteit eindhoven

Continuous-time approach

- Initiated by [Walsh et al, TAC'01, TCST'02]
- Further developed by [Nešić, Teel, TAC'04, Aut.'04]&[Carnevale et al, TAC'07] without delays
- Including delays [Heemels et al, ECC'09, TAC'10]
- Including quantization [Nešić, Liberzon, TAC'09]
- Including delays & quantization [Heemels, Nešić, Teel, vd Wouw, CDC/CCC 2009]

What is presented here based on [Heemels et al, ECC'09, TAC'10]

◀◀◀▶▶▶ /department of mechanical engineering 14/56

TU/e
technische universiteit eindhoven

Two approaches

Comm. constraints, varying delays & transmission intervals

- **Continuous-time approach (emulation)**
 - General nonlinear plants and (UGES) protocols
 - Continuous-time controllers
 - $\underline{h} = \underline{\tau} = 0$
- **Discrete-time approach**
 - Exploits linearity of plants and controllers
 - Both continuous-time and discrete-time controllers
 - $h_k \in [\underline{h}, \bar{h}]$ and $\tau_k \in [\underline{\tau}, \bar{\tau}]$ with $\underline{h} \neq 0$ and $\underline{\tau} \neq 0$.
 - Specific protocols

◀◀◀▶▶▶ /department of mechanical engineering 13/56

TU/e
technische universiteit eindhoven

Round Robin protocol

$\hat{z}((t_k + \tau_k)^+) = z(t_k) + h(k, e(t_k))$

- Round Robin (RR) protocol in case of 2 nodes:

$$h(k, e) = \begin{cases} \begin{pmatrix} 0 \\ e^2 \end{pmatrix}, & \text{if } k = 0, 2, 4, 6, \dots \\ \begin{pmatrix} e^1 \\ 0 \end{pmatrix}, & \text{if } k = 1, 3, 5, 7, \dots \end{cases}$$

Note that in case of 1 node $h_i(k, e) = 0$

in which we get sampled-data system with delays/sampling interval variation only!

◀◀◀▶▶▶ /department of mechanical engineering 16/56

TU/e
technische universiteit eindhoven

Communication constraints and scheduling protocols

Communication constraints, varying delays and transmission intervals:

$$\hat{z}((t_k + \tau_k)^+) = \Gamma_{\sigma_k} z(t_k) + (I - \Gamma_{\sigma_k}) \hat{z}(t_k + \tau_k)$$

Or:


$$\hat{z}^i((t_k + \tau_k)^+) = \begin{cases} z^i(t_k), & \text{when node } i \text{ transmits data} \\ \hat{z}^i(t_k) = z^i(t_k) + e^i(t_k), & \text{when node } i \text{ does not transmit} \end{cases}$$

where $e^i = \hat{z}^i - z^i$ is the network-induced error for node i

In general for some h related to protocol:

$$\hat{z}^i((t_k + \tau_k)^+) = z(t_k) + h(k, e(t_k))$$

◀◀◀▶▶▶ /department of mechanical engineering 15/56



technische universiteit eindhoven

17/56


/department of mechanical engineering

Try-Once-Discard protocol

$$\hat{z}((t_k + \tau_k)^+) = z(t_k) + h(k, e(t_k))$$

- Try-Once-Discard (TOD) protocol in case of 2 nodes:

$$h(k, e) = \begin{cases} \begin{pmatrix} 0 \\ e^2 \end{pmatrix}, & \text{if } |e^1| \geq |e^2| \\ \begin{pmatrix} e^1 \\ 0 \end{pmatrix}, & \text{if } |e^2| > |e^1| \end{cases}$$



technische universiteit eindhoven

18/56

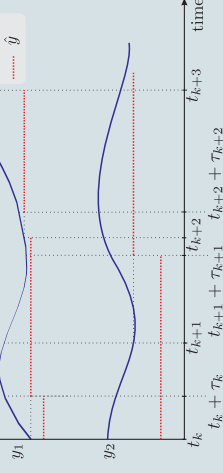
/department of mechanical engineering


Protocol rewritten $\hat{z}((t_k + \tau_k)^+) = z(t_k) + h(k, e(t_k))$

Error at the update time:

$$\begin{aligned} e((t_k + \tau_k)^+) &= \hat{z}((t_k + \tau_k)^+) - z((t_k + \tau_k)^+) \\ &= z(t_k) + h(k, e(t_k)) - z(t_k + \tau_k) \\ &= h(k, e(t_k)) + \underbrace{z(t_k) - \hat{z}(t_k + \tau_k)}_{-e(t_k)} + \underbrace{\hat{z}(t_k + \tau_k) - z(t_k + \tau_k)}_{e(t_k + \tau_k)} \\ &= h(k, e(t_k)) - e(t_k) + e(t_k + \tau_k) \end{aligned}$$

Zero-order hold assumption between updates: $\dot{\hat{z}} = 0$



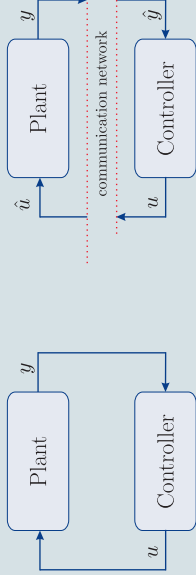


technische universiteit eindhoven

19/56

/department of mechanical engineering

Continuous-time modelling approach



Plant:


$$\begin{aligned} \dot{x}_p &= f_p(x_p, \hat{u}) \\ y &= g_p(x_p) \end{aligned}$$

Continuous-time controller

$$\begin{aligned} \dot{x}_c &= f_c(x_c, \hat{y}) \\ u &= g_c(x_c) \end{aligned}$$

Combined with protocol characterized by h

$$e((t_k + \tau_k)^+) = h(k, e(t_k)) - e(t_k) + e(t_k + \tau_k)$$



technische universiteit eindhoven

20/56

/department of mechanical engineering

Hybrid systems model formulation

Plant:

$$\begin{aligned} \dot{x}_p &= f_p(x_p, \hat{u}) \\ y &= g_p(x_p) \end{aligned}$$

Controller:

$$\begin{aligned} \dot{x}_c &= f_c(x_c, \hat{y}) \\ u &= g_c(x_c) \end{aligned}$$

$\Downarrow x = (x_p, x_c)$

ZOH:


$$\begin{aligned} \dot{\hat{y}} &= 0, \\ \hat{u} &= 0 \end{aligned}$$

Continuous-time NCS model: $(e = z - \hat{z}$ and $z = (u, y)$)

$$\begin{aligned} \dot{x}(t) &= f(x(t), e(t)) \\ \dot{e}(t) &= g(x(t), e(t)) \\ e((t_k + \tau_k)^+) &= h(\hat{u}, e(t_k)) - e(t_k) + e(t_k + \tau_k), \\ x((t_k + \tau_k)^+) &= x(t_k + \tau_k) \end{aligned}$$

Hybrid model with $\xi = (x, e)$ [Goebel, Sanfelice, Teel, CSM 2009]:

$$\begin{aligned} \dot{\xi} &= F(\xi) \\ \xi^+ &= G(\xi) \end{aligned}$$

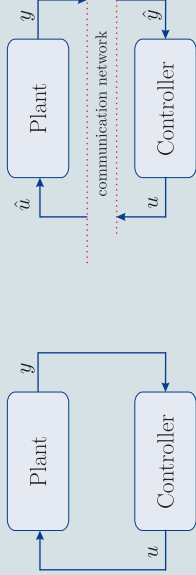


technische universiteit eindhoven

19/56

/department of mechanical engineering

Continuous-time modelling approach



Plant:


$$\begin{aligned} \dot{x}_p &= f_p(x_p, \hat{u}) \\ y &= g_p(x_p) \end{aligned}$$

Continuous-time controller

$$\begin{aligned} \dot{x}_c &= f_c(x_c, \hat{y}) \\ u &= g_c(x_c) \end{aligned}$$

Combined with protocol characterized by h

$$e((t_k + \tau_k)^+) = h(k, e(t_k)) - e(t_k) + e(t_k + \tau_k)$$



technische universiteit eindhoven

20/56

/department of mechanical engineering

TU/e
technische universiteit eindhoven

Stability analysis for the NCS

Hybrid NCS model:

$$\begin{aligned} \dot{\xi} &= F(\xi), & \text{when } \xi \in C & \quad (\text{flow}) \\ \xi^+ &= G(\xi), & \text{when } \xi \in D & \quad (\text{reset}) \end{aligned}$$

Lyapunov function $U(\xi)$ s.t.

- $\langle \nabla U(\xi), F(\xi) \rangle < 0$ for $\xi \in C$
- $U(\xi^+) \leq U(\xi)$ for $\xi \in D$

Requires Lyapunov-based conditions on protocols (resets) and closed-loop dynamics (flow)

TU/e / department of mechanical engineering 22/56

TU/e
technische universiteit eindhoven

Analysis of controller designed using emulation approach

Step 1 : Given plant: design controller ignoring the network
 Step 2a : Implement the same controller over network with a given protocol
 Step 2b : Find suff. small MATI and MAD s.t. closed loop **asympt. stable**

Maximal allowable transmission interval (MATI):
 $0 < h_k := t_{k+1} - t_k < \text{MATI}$

Maximal allowable delay (MAD):
 $0 \leq \tau_k \leq \min\{\text{MAD}, t_{k+1} - t_k\}$

TU/e / department of mechanical engineering 21/56

TU/e
technische universiteit eindhoven

Example: Try-Once-Discard protocol

$$\hat{z}((t_k + \tau_k)^+) = z(t_k) + h(k, e(t_k))$$

For two nodes: $h(k, e) = \begin{cases} \begin{pmatrix} 0 \\ e^2 \end{pmatrix}, & \text{if } |e^1| \geq |e^2| \\ \begin{pmatrix} e^1 \\ 0 \end{pmatrix}, & \text{if } |e^2| > |e^1| \end{cases}$

In case $|e^1| \geq |e^2|$

$$W(\kappa, e) = |e| = \sqrt{(e^1)^2 + (e^2)^2}$$

$$\sqrt{W(\kappa + 1, h(\kappa, e))} = \sqrt{(e^2)^2} \leq \sqrt{\frac{1}{2}(e^1)^2 + \frac{1}{2}(e^2)^2} = \sqrt{\frac{l-1}{l}} |e|$$

Hence, $W(\kappa + 1, h(\kappa, e)) \leq \lambda W(\kappa, e)$ with $\lambda = \sqrt{\frac{l-1}{l}}$

TU/e / department of mechanical engineering 24/56

TU/e
technische universiteit eindhoven

Constructing Lyapunov functions

$$e((t_k + \tau_k)^+) = h(k, e(t_k)) - e(t_k) + e(t_k + \tau_k) \xrightarrow{\text{no delay}} e(t_k^+) = h(k, e(t_k))$$

Conditions on protocols (resets) :


- The protocol given by h is UGES: there exists a function W s.t.

$$W(\kappa + 1, h(\kappa, e)) \leq \lambda W(\kappa, e)$$

$$\underline{\alpha}_W |e| \leq \overline{W}(\kappa, e) \leq \overline{\alpha}_W |e|$$
 for constants $0 < \underline{\alpha}_W \leq \overline{\alpha}_W$ and $0 < \lambda < 1$.
- for some $\lambda_W \geq 1$

$$W(\kappa + 1, e) \leq \lambda_W W(\kappa, e)$$

TU/e / department of mechanical engineering 23/56



technische universiteit eindhoven

25/56

/department of mechanical engineering

Conditions

Flow:

$$\begin{aligned} \dot{x} &= f(x, e) \\ \dot{e} &= g(x, e) \end{aligned}$$

Reset: $e((t_k + \tau_k)^+) = h(k, e(t_k)) - e(t_k) + e(t_k + \tau_k)$

- **Conditions on growth e using W**


$$\left| \frac{\partial W}{\partial e}(\kappa, e) \right| \leq M_1$$

and

$$|g(x, e)| \leq m_x(x) + M_e|e|$$

- **Conditions on growth x :** L_2 gain $< \gamma$ from $W(\kappa, e)$ to $m_x(x)$


$$\langle \nabla V(x), f(x, e) \rangle \leq -m_x^2(x) - \rho(|x|) + (\gamma^2 - \varepsilon)W^2(\kappa, e)$$



technische universiteit eindhoven

25/56

/department of mechanical engineering



technische universiteit eindhoven

26/56

/department of mechanical engineering


Stability

$$\begin{aligned} \underline{\alpha}_W|e| \leq W(\kappa, e) &\leq \bar{\alpha}_W|e| & \left| \frac{\partial W}{\partial e}(\kappa, e) \right| &\leq M_1 \\ W(\kappa + 1, h(\kappa, e)) \leq \lambda W(\kappa, e) & & |g(x, e)| &\leq m_x(x) + M_e|e| \\ W(\kappa + 1, e) \leq \lambda_W W(\kappa, e) & & \langle \nabla V(x), f(x, e) \rangle &\leq -m_x^2(x) - \rho(|x|) + (\gamma^2 - \varepsilon)W^2(\kappa, e) \end{aligned}$$

\Downarrow

$$L_0 = \frac{M_1 M_e}{\underline{\alpha}_W}; \quad L_1 = \frac{M_1 M_e \lambda_W}{\lambda \underline{\alpha}_W}$$


$$\gamma_0 = M_1 \gamma; \quad \gamma_1 = \frac{M_1 \gamma \lambda_W}{\lambda}$$



technische universiteit eindhoven

26/56

/department of mechanical engineering



technische universiteit eindhoven

27/56

/department of mechanical engineering

Main results for stability: a race between diff. eqs.

Consider differential eqs. for initial conditions $\phi_0(0)$ and $\phi_1(0)$:


$$\begin{aligned} \dot{\phi}_0 &= -2L_0\phi_0 - \gamma_0(\phi_0^2 + 1) \\ \dot{\phi}_1 &= -2L_1\phi_1 - \gamma_0(\phi_1^2 + \frac{\gamma_1^2}{\gamma_0^2}) \end{aligned}$$

Theorem: Take $MATI \geq MAD \geq 0$ such that

$$\begin{aligned} \phi_0(\tau) \geq \lambda^2 \phi_1(0) &\text{ for all } 0 \leq \tau \leq MATI \\ \phi_1(\tau) \geq \phi_0(\tau) &\text{ for all } 0 \leq \tau \leq MAD \end{aligned}$$

Then NCS is globally asymptotically stable for


- Delays $\tau_k \in [0, MAD]$
- Transmission intervals $h_k \in [0, MATI]$



technische universiteit eindhoven

27/56

/department of mechanical engineering



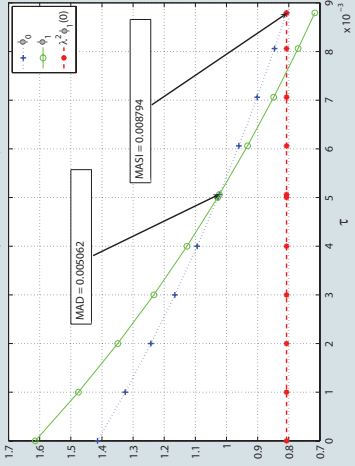
technische universiteit eindhoven

28/56


/department of mechanical engineering

Interpretation

$\phi_0(\tau) \geq \lambda^2 \phi_1(0)$ for all $0 \leq \tau \leq MATI$
 $\phi_1(\tau) \geq \phi_0(\tau)$ for all $0 \leq \tau \leq MAD$




By shifting initial conditions $\phi_0(0)$ and $\phi_1(0)$ tradeoffs!



technische universiteit eindhoven

28/56

/department of mechanical engineering



technische universiteit eindhoven

29/56

/department of mechanical engineering

The delay-free case (MAD=0)

- **Conditions on protocol h :** there exist a function W and $0 \leq \lambda < 1$ s.t.

$$W(\kappa + 1, h(\kappa, e)) \leq \lambda W(\kappa, e)$$

$$\underline{\alpha}_W |e| \leq W(\kappa, e) \leq \bar{\alpha}_W |e|$$
- **Conditions on growth e :**


$$\langle \nabla W(\kappa, e), g(x, e) \rangle \leq LW(\kappa, e) + m_x(x)$$
- **Conditions on growth x :** L_2 gain $< \gamma$ from $W(\kappa, e)$ to $m_x(x)$

$$\langle \nabla V(x), f(x, e) \rangle \leq -m_x^2(x) - \rho(|x|) + (\gamma^2 - \varepsilon)W^2(\kappa, e)$$

The NCS is globally asymptotic stable, if MAD = 0 and

$$\text{MATI} \leq \frac{1}{L} \ln \left(1 + \frac{1 - \lambda}{\gamma + \lambda} \right)$$


[Nešić, Teel TAC '04] + improved in [Carnevale, Teel, Nešić TAC '07]



technische universiteit eindhoven

29/56

/department of mechanical engineering



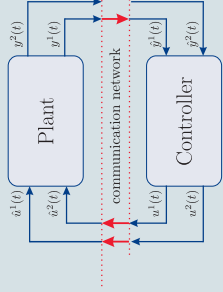
technische universiteit eindhoven


30/56

/department of mechanical engineering

Benchmark example of batch reactor

- Model of an unstable chemical batch reactor: linear plant
- Benchmark example in NCS literature
- Some features:
 - 2 inputs and 2 outputs, 4 plant and 2 controller states
 - Controlled by a linear continuous-time controller
 - Only the outputs of the plant squabble for network access






technische universiteit eindhoven

30/56

/department of mechanical engineering

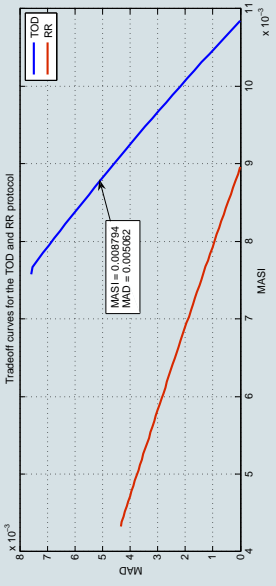


technische universiteit eindhoven

31/56


/department of mechanical engineering

Numerical results



Tradeoffs between


- MATI and MAD
- Protocols



technische universiteit eindhoven

31/56

/department of mechanical engineering



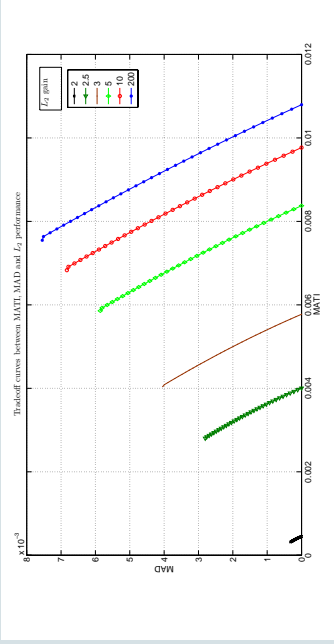
technische universiteit eindhoven

32/56

/department of mechanical engineering


Tradeoffs in NCS

L_2 gain: $\int_0^\infty \|w(t)\|^2 dt \leq \gamma^2 \int_0^\infty \|d(t)\|^2 dt$.



Tradeoffs between

- MATI, MAD & performance: control and network properties!
- Protocols



technische universiteit eindhoven

32/56

/department of mechanical engineering

TU/e
technische universiteit eindhoven

Discrete-time approach

- [Donkers, Hetel, Heemels, vdWouw, Steinbuch, HSCC 2009]

/department of mechanical engineering 34/56

TU/e
technische universiteit eindhoven

Conclusions continuous-time approach

- Systematic procedure to obtain tradeoffs between
 - Network properties (MAD, MATI, type protocol)
 - Control properties (stability and \mathcal{L}_p gains)
- All 5 network-induced phenomena: inclusion quantization & dropouts possible [Heemels, Nešić, Teel, vd Wouw, CDC/CCC 2009]
- General nonlinear plants and (UGES) protocols
- Continuous-time controllers
- $\underline{h} = \underline{\tau} = 0$
- Can only exploit linearity to some extent ...

... discrete-time approach overcomes latter issues ...

/department of mechanical engineering 33/56

TU/e
technische universiteit eindhoven

System Description

- Plant and controller are given by

$$\begin{cases} \frac{d}{dt}x^p(t) = A^p x^p(t) + B^p \hat{u}(t), & \hat{u}(t) = \hat{u}_k := \hat{u}(t_k) \quad \forall t \in [t_k, t_{k+1}) \\ y(t) = C^p x^p(t) \\ x_{k+1}^c = A^c x_k^c + B^c \hat{y}_k \\ u_k = C^c x_k^c + D^c \hat{y}_{k-1} \end{cases}$$
- Transmission intervals $h_k := t_{k+1} - t_k$ in $[\underline{h}, \bar{h}]$
- Data exchange is constrained, i.e.,

$$\hat{y}_k^i = \begin{cases} y^i(t_k), & \text{if node } i \text{ gets access } (\sigma_k = i) \\ \hat{y}_{k-1}^i, & \text{if node } i \text{ no access } (\sigma_k \neq i) \end{cases}$$
- Using diagonal matrix $\Gamma_{\sigma_k}^y = \text{diag}(1, 0, \dots, 0)$ when $\sigma_k = 1$:

$$\hat{y}_k = \Gamma_{\sigma_k}^y y_k + (I - \Gamma_{\sigma_k}^y) \hat{y}_{k-1}$$

/department of mechanical engineering 35/56

TU/e
technische universiteit eindhoven


Networked control systems

- Communication constraints
- Varying transmission intervals
- Delays

But now plant and controller linear ...

... for ease of exposition: only varying transmission intervals (no delays)

/department of mechanical engineering 35/56



technische universiteit eindhoven

37/56

/ department of mechanical engineering


System Description

- Plant and controller are given by

$$\begin{cases} \frac{d}{dt} x^p(t) = A^p x^p(t) + B^p \hat{u}(t), & \hat{u}(t) = \hat{u}_k := \hat{u}(t_k) \quad \forall t \in [t_k, t_{k+1}) \\ y(t) = C^p x^p(t) \\ x_{k+1}^c = A^c x_k^c + B^c \hat{y}_k \\ u_k = C^c x_k^c + D^c \hat{y}_{k-1} \end{cases}$$
- Transmission intervals $h_k := t_{k+1} - t_k$ in $[h, \bar{h}]$
- Data exchange is constrained, i.e.,

$$\begin{cases} \hat{y}_k = \Gamma_{\sigma_k}^y y_k + (I - \Gamma_{\sigma_k}^y) \hat{y}_{k-1} \\ \hat{u}_k = \Gamma_{\sigma_k}^u u_k + (I - \Gamma_{\sigma_k}^u) \hat{u}_{k-1} \end{cases}$$


where $\Gamma_{\sigma_k} = \text{diag}(\Gamma_{\sigma_k}^y, \Gamma_{\sigma_k}^u)$ is a diagonal matrix that determines which sensors and actuators access the network



technische universiteit eindhoven

37/56

/ department of mechanical engineering



technische universiteit eindhoven

38/56

/ department of mechanical engineering

Discrete-time NCS model


- Exact discretisation results in a *switched linear uncertain system*

$$\tilde{A}_{\sigma_k, h_k} = \tilde{A}_{\sigma_k, h_k} \tilde{x}_k \quad \text{with}$$

$$\tilde{A}_{\sigma_k, h_k} = \begin{bmatrix} e^{A^p h_k} + \frac{E_{h_k}^{p, B^p D^c}}{B^{p C^p}} & \frac{E_{h_k}^{p, B^p D^c}}{B^{p C^p}} & E_{h_k}^{p, B^p D^c} \\ C^p (I - e^{A^p h_k} - \frac{E_{h_k}^{p, B^p D^c}}{B^{p C^p}}) & -C^p \frac{E_{h_k}^{p, B^p D^c}}{B^{p C^p}} & -C^p \frac{E_{h_k}^{p, B^p D^c}}{B^{p C^p}} \\ -C^c B^{c C^p} & D^{c T} \Gamma_{\sigma_k}^y - C^c B^c (I - \Gamma_{\sigma_k}^y) & I - \Gamma_{\sigma_k}^y - C^p \frac{E_{h_k}^{p, B^p D^c}}{B^{p C^p}} - C^p \frac{E_{h_k}^{p, B^p D^c}}{B^{p C^p}} \\ & & I - \Gamma_{\sigma_k}^u \end{bmatrix}$$

where $E_{h_k}^p = \int_0^{h_k} e^{A^p s} ds$ and $\tilde{x} = (x_p, x_c, e_{u_s}, e_{y_s})$


- Uncertainty: **unknown time-varying transmission intervals**
- Switching: **communication constraints: RR & TOD protocols**



technische universiteit eindhoven

38/56

/ department of mechanical engineering



technische universiteit eindhoven

39/56

/ department of mechanical engineering

Discrete-time NCS model

- Exact discretisation results in a *switched linear uncertain system*

$$\tilde{A}_{\sigma_k, h_k} = \tilde{A}_{\sigma_k, h_k} \tilde{x}_k \quad \text{with}$$


$$\tilde{A}_{\sigma_k, h_k} = \begin{bmatrix} e^{A^p h_k} + \frac{E_{h_k}^{p, B^p D^c}}{B^{p C^p}} & \frac{E_{h_k}^{p, B^p D^c}}{B^{p C^p}} & E_{h_k}^{p, B^p D^c} \\ C^p (I - e^{A^p h_k} - \frac{E_{h_k}^{p, B^p D^c}}{B^{p C^p}}) & -C^p \frac{E_{h_k}^{p, B^p D^c}}{B^{p C^p}} & -C^p \frac{E_{h_k}^{p, B^p D^c}}{B^{p C^p}} \\ -C^c B^{c C^p} & D^{c T} \Gamma_{\sigma_k}^y - C^c B^c (I - \Gamma_{\sigma_k}^y) & I - \Gamma_{\sigma_k}^y - C^p \frac{E_{h_k}^{p, B^p D^c}}{B^{p C^p}} - C^p \frac{E_{h_k}^{p, B^p D^c}}{B^{p C^p}} \\ & & I - \Gamma_{\sigma_k}^u \end{bmatrix}$$

where $E_{h_k}^p = \int_0^{h_k} e^{A^p s} ds$ and $\tilde{x} = (x_p, x_c, e_{u_s}, e_{y_s})$

- Uncertainty: **unknown time-varying transmission intervals**
- Switching: **communication constraints: RR & TOD protocols**

After some work (polytopic overapproximations, reformulating protocols):


- Arbitrarily tight LMI conditions for existence of parameter-dependent quadratic Lyapunov functions.



technische universiteit eindhoven

39/56

/ department of mechanical engineering



technische universiteit eindhoven

40/56


/ department of mechanical engineering

Illustrative Example (batch reactor without delays)

- Results on bounds on the transmission interval (given for TOD protocol only)

Method	Range
Simulation based, obtained in [1]	$h_k \in (\varepsilon, 0.07]$
Theoretical, obtained in [1]	$h_k \in (\varepsilon, 10^{-5}]$
Theoretical, obtained in [2]	$h_k \in (\varepsilon, 0.01]$
Theoretical, obtained in [3]	$h_k \in (\varepsilon, 0.0108]$
Newly obtained theoretical bound	$h_k \in [10^{-4}, 0.066]$

[1] Walsh, *et al.*, Trans. CST '02
 [2] Nešić & Teel, TAC '04
 [3] Carnevale, *et al.*, TAC '07



technische universiteit eindhoven

40/56

/ department of mechanical engineering

TU/e
technische universiteit eindhoven

Summary Part III

- Presented two approaches for stability analysis of NCS
 - Varying delays
 - Varying transmission intervals
 - Communication constraints & protocols
- Hybrid modelling approaches
 - Continuous-time approach: hybrid inclusions (jumps & flows)
 - Discrete-time approach: switched linear uncertain systems

◀◀◀▶▶▶▶▶ /department of mechanical engineering 42/56

TU/e
technische universiteit eindhoven

Illustrative Example (batch reactor with delays)

Now: varying delays, varying transmission intervals & comm. constraints:

[17] [Heemeis, Teel, vdWouw, Nešić, ECC'09 & TAC'10]

◀◀◀▶▶▶▶▶ /department of mechanical engineering 41/56

TU/e
technische universiteit eindhoven

Overall summary

- Stability and performance analysis of NCS with
 - Varying sampling/transmission interval
 - Varying communication delays
 - Packet loss
 - Communication constraints through shared network
 - Quantization
- Part II: discrete-time approach for “linear” NCS with (i), (ii) and (iii)
 - Discretization leading to uncertain discrete-time model
 - Uncertainties (e.g. delays) appear exponentially
 - Polytopic overapproximation methods: polytopic/LPV-like systems
 - Robust stability analysis and controller synthesis using LMIs

◀◀◀▶▶▶▶▶ /department of mechanical engineering 44/56

TU/e
technische universiteit eindhoven

Summary Part III

- Presented two approaches for stability analysis of NCS
 - Varying delays
 - Varying transmission intervals
 - Communication constraints & protocols
- Hybrid modelling approaches
 - Continuous-time approach: hybrid inclusions (jumps & flows)
 - Discrete-time approach: switched linear uncertain systems
- Both methods have pros and cons:
 - Continuous-time: general NL (continuous-time) plants/controllers and protocols
 - Discrete-time: discrete and continuous-time controllers (but linear and TOD/RR-like protocols)
 - Discrete-time: less conservative in linear context
 - Discrete-time can have non-zero lower bounds on transmission intervals/delays, while continuous-time only zero!
 - Continuous-time includes L_p performance & (some) quantization

◀◀◀▶▶▶▶▶ /department of mechanical engineering 43/56

technische universiteit eindhoven

TU/e

Future work on control over networks

- Large-delay case (now only small-delay case) with communication constraints
- Include dropouts in a less conservative manner
- Extend work to include different “quantization protocols”
- Stochastic communication models (see below)
- Control and protocol (co-)design methods
- Complete the framework & numerical tools (EU project WIDE)

[Antunes et al, ACC 2009 & 2010, CDC 2009]
[Donkers et al, ACC 2010]

◀◀ ◀ ▶▶ ▶▶

/department of mechanical engineering

46/56

technische universiteit eindhoven

TU/e

Overall summary

- Part II: including communication constraints & protocols
- Hybrid models:
 - Continuous-time approach: jump-flow systems
 - Discrete-time approach: switched linear systems
- Tradeoffs between
 - Network properties (MATI, MAD, type of protocol)
 - Control properties (stability, performance)

◀◀ ◀ ▶▶ ▶▶

/department of mechanical engineering

45/56

technische universiteit eindhoven

TU/e

Literature list

For related papers: Google “Maurice Heemels” or “Nathan van de Wouw” or remember

http://www.dct.tue.nl/New/Heemels/Webpage_Heemels.html

or

http://www.dct.tue.nl/New/Wouw/Webpage_NvdWouw_new.html

Comprehensive overview of this minicourse can be found in:
W.P.M.H. Heemels and N. van de Wouw, *Stability and stabilization of networked control systems, which will appear in the book:*
A. Bemporad, W.P.M.H. Heemels and M. Johansson (Eds.), *Networked control systems*, Springer, to appear in 2010.

◀◀ ◀ ▶▶ ▶▶

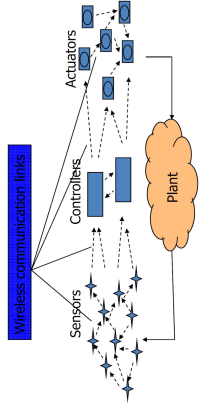
/department of mechanical engineering

48/56





technische universiteit eindhoven

TU/e

“Big goal”



→ Industrial automation & Large-scale systems:


→ Distributed and wireless control for large-scale systems


- Combine the ideas of minicourse with distributed control
- Make it work in applications!


◀◀ ◀ ▶▶ ▶▶


/department of mechanical engineering

47/56

 technische universiteit eindhoven	Continuous-time approaches	50/56 /department of mechanical engineering
<p>D. Carnevale, A.R. Teel, and D. Nešić. A Lyapunov proof of improved maximum allowable transfer interval for networked control systems. <i>IEEE Trans. Autom. Control</i>, 52:892–897, 2007.</p> <p>A. Chaillet and A. Bicchi. Delay compensation in packet-switching networked controlled systems. In <i>IEEE Conf. Decision and Control</i>, pages 3620–3625, 2008.</p> <p>Heemels, A.R. Teel, N. van de Wouw and D. Nešić. Networked Control Systems with Communication Constraints: Tradeoffs between Transmission Intervals, Delays and Performance. <i>IEEE Transactions on Automatic Control</i>, August 2010.</p> <p>Heemels, A.R. Teel, N. van de Wouw and D. Nešić. Networked control systems with communication constraints: Tradeoffs between transmission intervals and delays. <i>European Control Conference 2009</i>, Hungary, Budapest.</p> <p>Heemels, D. Nešić, A.R. Teel and N. van de Wouw. Networked and Quantized Control Systems with Communication Delays. <i>Proc. Joint 48th IEEE Conference on Decision and Control (CDC) and 28th Chinese Control Conference</i>, Shanghai, China, p. 7929-7935 (2009)</p> <p>P. Naghshtabrizi and J.P. Hespanha. Stability of network control systems with variable sampling and delays. In <i>Proc. Annual Allerton Conf. Communication, Control, and Computing</i>, 2006.</p> <p>P. Naghshtabrizi, J.P. Hespanha, and A.R. Teel. Stability of delay impulsive systems with application to networked control systems. In <i>Proc. American Control Conference</i>, pages 4899–4904, New York, USA, 2007.</p>		

 technische universiteit eindhoven	Surveys on NCS	49/56 /department of mechanical engineering
<p>W. Zhang, M.S. Branicky, and S.M. Phillips. Stability of networked control systems. <i>IEEE Control Systems Magazine</i>, 21(1):84–99, 2001.</p> <p>Y. Tipsuwan and M.-Y. Chow. Control methodologies in networked control systems. <i>Control Engineering Practice</i>, 11:1099–1111, 2003.</p> <p>Antsaklis, P. and Baillieul, J., Guest Editorial Special Issue on Networked Control Systems <i>Automatic Control</i>, <i>IEEE Transactions on</i> Volume 49, Issue 9, Sept. 2004.</p> <p>T. C. Yang. Networked control system: a brief survey. <i>IEE Proc.-Control Theory Appl.</i>, 153(4):403–412, July 2006.</p> <p>J.P. Hespanha, P. Naghshtabrizi, and Y. Xu. A survey of recent results in networked control systems. <i>Proc. of the IEEE</i>, pages 138–162, 2007.</p> <p>Baillieul, J. and Antsaklis, P., Control and Communication Challenges in Networked Real-Time Systems, <i>Proc. of the IEEE</i>, pages 9-28, vol. 95, no. 1, 2007.</p>		

 technische universiteit eindhoven	Discrete-time approaches	51/56 /department of mechanical engineering
<p>N.W. Batur, M.C.F. Donkers, W.P.M.H. Heemels, N. van De Wouw, An Approach to Observer-Based Decentralized Control under Periodic Protocols, <i>American Control Conference 2010</i>, Baltimore, USA</p> <p>M.B.G., Cloosterman, N. van de Wouw, W.P.M.H. Heemels, H. Nijmeijer, "Stability of Networked Control Systems with Uncertain Time-varying Delays", <i>IEEE Transactions on Automatic Control</i>, 54(7), pp. 1575 - 1580, 2009.</p> <p>M. Cloosterman, N. van de Wouw, W.P.M.H. Heemels, and H. Nijmeijer. Robust stability of networked control systems with time-varying network-induced delays. In <i>Proc. Conf. on Decision and Control</i>, pages 4980–4985, San Diego, USA, 2006.</p> <p>M.B.G. Cloosterman, N. van de Wouw, W.P.M.H. Heemels, and H. Nijmeijer. Stabilization of networked control systems with large delays and packet dropouts. In <i>Proc. of the American Control Conf.</i>, pages 4991–4996, 2008.</p> <p>Cloosterman, M., van de Wouw, N., Heemels, W., Nijmeijer, H.: Stability of networked control systems with large delays. In: 46th IEEE Conference on Decision and Control, pp. 5017- 5022 (2007)</p> <p>M.B.G. Cloosterman, L.Hetel, N. van de Wouw, W.P.M.H. Heemels, J. Daafouz and H. Nijmeijer, Controller synthesis for networked control systems, submitted to <i>Automatica</i>.</p> <p>M.C.F. Donkers, L. Hetel, W.P.M.H. Heemels, N. van de Wouw, and M. Steinbuch. Stability analysis of networked control systems using a switched linear systems approach. In <i>Hybrid Systems: Computation and Control</i>, Lecture Notes in Computer Science, pages 150–164. Springer Verlag, 2009.</p>		

 technische universiteit eindhoven	Continuous-time approaches - continued	51/56 /department of mechanical engineering
<p>D. Nešić and D. Liberzon. A unified framework for design and analysis of networked and quantized control systems. <i>IEEE Trans. Autom. Control</i>, 2009.</p> <p>D. Nešić and A.R. Teel. Input-output stability properties of networked control systems. <i>IEEE Trans. Autom. Control</i>, 49(10):1650–1667, 2004.</p> <p>D. Nešić and A.R. Teel. Input-to-state stability of networked control systems. <i>Automatica</i>, 40:2121–2128, 2004.</p> <p>G.C. Walsh, O. Belidman, and L.G. Bushnell. Asymptotic behavior of nonlinear networked control systems. <i>IEEE Trans. Autom. Contr.</i>, 46:1093–1097, 2001.</p> <p>G.C. Walsh, O. Belidman, and L.G. Bushnell. Stability analysis of networked control systems. <i>IEEE Trans. Control Syst. Techn.</i>, 10:438–446, 2002.</p>		

<p style="text-align: right;">technische universiteit eindhoven</p> <p style="text-align: center;">TU/e</p> <p>Discrete-time approaches</p> <p>L. Dritsas and A. Tzes. Robust stability analysis of networked systems with varying delays. <i>International Journal of Control</i>, 2009. DOI 10.1080/00207179093061705.</p> <p>H. Fujioka. Stability analysis for a class of networked/embedded control systems: A discrete-time approach. In <i>Proc. of the American Control Conf.</i>, pages 4997–5002, 2008.</p> <p>M. Garcia-Rivera, A. Barreiro, Analysis of networked control systems with drops and variable delays, <i>Automatica</i> 43 (2007) 2054–2059.</p> <p>Gielen, R., Oлару, S., Lazar, M., Heemels, W.P.M.H., van de Wouw, N., Niculescu, S., On Polytopic Inclusions as a Modeling Framework for Systems with Time-Varying Delays, <i>Automatica</i>, to appear in 2010</p> <p>R. Gielen, S. Oлару, and M. Lazar. On polytopic embeddings as a modeling framework for networked control systems. In <i>Proc. 3rd Int. Workshop on Assessment and Future Directions of Nonlinear Model Predictive Control</i>, Pavia, Italy, 2008.</p> <p>W.P.M.H. Heemels, N. van de Wouw, R.H. Gielen, M.C.F. Donkers, L. Hetel, S. Oлару, M. Lazar, J. Daafouz and S.-I. Niculescu, Comparison of Overapproximation Methods for Stability Analysis of Networked Control Systems, <i>Hybrid Systems: Computation and Control</i> 2010, Stockholm, Sweden.</p> <p>L. Hetel, M.B.G. Cloosterman, N. van de Wouw, W.P.M.H. Heemels, J. Daafouz and H. Nijmeijer, Comparison of Stability Characteristics for Networked Control Systems. <i>Proc. Joint 48th IEEE Conference on Decision and Control (CDC) and 28th Chinese Control Conference</i>, Shanghai, China, p. 7911-7916 (2009).</p> <p style="text-align: right;">◀◀◀▶▶▶ /department of mechanical engineering 53/56</p>	<p style="text-align: right;">technische universiteit eindhoven</p> <p style="text-align: center;">TU/e</p> <p>Discrete-time approaches - continued</p> <p>L. Hetel, J. Daafouz, and C. Iung. Stabilization of arbitrary switched linear systems with unknown time-varying delays. <i>IEEE Trans. Autom. Control</i>, 51(10): 1668-1674, 2006.</p> <p>L. Hetel, J. Daafouz, and C. Iung. Analysis and control of LTI and switched systems in digital loops via an event-based modeling. <i>International Journal of Control</i>, 2008.</p> <p>Kao, C.Y., Lincoln, B.: Simple stability criteria for systems with time-varying delays. <i>Automatica</i> 40, 1429-1434 (2004)</p> <p>Pan, Y.J., Marquez, H.J., Chen, T.: Stabilization of remote control systems with unknown time varying delays by LMI techniques. <i>Int. Journal of Control</i> 79(7), 732-763 (2006)</p> <p>Sala, A.: Computer control under time-varying sampling period: An LMI gridding approach, <i>Automatica</i> 41(12), 2077-2082 (2005)</p> <p>Young Soo Suh, Stability and stabilization of nonuniform sampling systems, <i>Automatica</i> 44 (2008) 3222–3226</p> <p>J. Skaf and S. Boyd, Analysis and Synthesis of State-Feedback Controllers With Timing Jitter, <i>IEEE Transactions on Automatic Control</i>, Vol. 54, No. 3, p. 652-657.</p> <p>J. van Schendel, M.C.F. Donkers, W.P.M.H. Heemels, and N. Van De Wouw, On Dropout Modelling for Stability Analysis of Networked Control Systems, <i>American Control Conference</i> 2010, Baltimore, USA</p> <p style="text-align: right;">◀◀◀▶▶▶ /department of mechanical engineering 54/56</p>
<p style="text-align: right;">technische universiteit eindhoven</p> <p style="text-align: center;">TU/e</p> <p>Discrete-time approaches - continued</p> <p>van de Wouw, N., Nughshabrizi, P., Cloosterman, M., Hespanha, J.: Tracking control for sampled-data systems with uncertain sampling intervals and delays. <i>Intern. Journ. Robust and Nonlinear Control</i> 20(4), 387-411 (2010)</p> <p>Wittenmark, B., Nilsson, J., Törnren, M.: Timing problems in real-time control systems. In: <i>Proc. of the Amer. Control Conf.</i>, pp. 2000-2004. Seattle, USA (1995)</p> <p>Zhang, L., Shi, Y., Chen, T., Huang, B.: A new method for stabilization of networked control systems with random delays. <i>IEEE Trans. Autom. Control</i> 50(8), 1177-1181 (Aug. 2005)</p> <p style="text-align: right;">◀◀◀▶▶▶ /department of mechanical engineering 55/56</p>	<p style="text-align: right;">technische universiteit eindhoven</p> <p style="text-align: center;">TU/e</p> <p>Some stochastic approaches</p> <p>Antunes, D., Hespanha, J., Silvestre, C.: Control of impulsive renewal systems: Application to direct design in networked control. In: <i>IEEE Conference on Decision and Control</i>, pp. 6882-6887 (2009)</p> <p>Antunes, D., Hespanha, J., Silvestre, C.: Stability of impulsive systems driven by renewal processes. In: <i>Proc. Amer. Contr. Conf.</i>, pp. 4932-4937 (2009)</p> <p>M.C.F. Donkers, W.P.M.H. Heemels, D. Bernardini and A. Bemporad, Stability Analysis of Stochastic Networked Control Systems, <i>American Control Conference</i> 2010, Baltimore, USA</p> <p>Montestrucque, L., Antsaklis, P.: Stability of model-based networked control systems with time-varying transmission times. <i>IEEE Trans. Autom. Control</i> 49(9), 1562-1572 (2004)</p> <p style="text-align: right;">◀◀◀▶▶▶ /department of mechanical engineering 56/56</p>

Part 4

List of Participants

Dr.Ir. A. Abate
Delft Center for Systems and Control
Delft University of Technology
Mekelweg 2
2628 CD Delft
The Netherlands
a.abate@tudelft.nl

Dr. Bouchra Abouzaid
Department of Mathematics
University of Namur (FUNDP)
8, Rempart de la vierge
5000 Namur
Belgium
bab@math.fundp.ac.be

Prof. Pierre-Antoine Absil
Dept. INMA
Université Catholique de Louvain/UCL
Avenue Georges Lemaître, 4
1348 Louvain-la-Neuve
Belgium
absil@inma.ucl.ac.be

Ir. J. Achterberg
Dept. of Electrical Engineering
Eindhoven University of Technology
PO Box 513
5600 MB Eindhoven
The Netherlands
j.achterberg@tue.nl

Ir. Sisdarmanto Adinandra
Dept. of Mechanical Engineering
Eindhoven University of Technology
PO Box 513
5600 MB Eindhoven
The Netherlands
s.adinandra@tue.nl

MSc I. Aladagli
Dept. of Mechanical Engineering
Eindhoven University of Technology
PO Box 513
5600 MB Eindhoven
The Netherlands
i.aladagli@tue.nl

Pedro Almeida
Automatic Control Laboratory
University of Mons
Boulevard Dolez
7000 Mons
Belgium
pedro.almeida@umons.ac.be

Alejandro Alvarez-Aguirre
Department of Mechanical Engineering
Eindhoven University of Technology
PO Box 513
5600 MB Eindhoven
The Netherlands
a.a.alvarez@tue.nl

Carlos Alzate
Dept. Electrical Engineering, SCD/SISTA
Katholieke Universiteit Leuven
Kasteelpark Arenberg 10 box 2446
3001 Leuven
Belgium
carlos.alzate@esat.kuleuven.be

Ir. J.M. Ast, van
Delft Center for Systems and Control
Delft University of Technology
Mekelweg 2
2628 CD Delft
The Netherlands
j.m.vanast@tudelft.nl

MSc B. Babakhani
Dept. Electrical Engineering
University of Twente
P.O. Box 217
7500 AE Enschede
The Netherlands
b.babakhani@ewi.utwente.nl

Prof.Dr.Ir. T. Backx
Dept. Electrical Engineering
Eindhoven University of Technology
P.O. Box 513
5600 MB Eindhoven
The Netherlands
a.c.p.m.backx@tue.nl

Kurt Barbé
Dept. ELEC
Vrije Universiteit Brussel
Pleinlaan 2
B-1050 Brussel
Belgium
kurt.barbe@vub.ac.be

Kim Batselier
Dept. of Electrical Engineering
Katholieke Universiteit Leuven
Kasteelpark Arenberg 10 - bus 2446
3001 Heverlee
Belgium
kim.batselier@esat.kuleuven.be

N.W. Bauer
Dept. of Mechanical Engineering
Eindhoven University of Technology
PO Box 513
5600 MB Eindhoven
The Netherlands
n.w.bauer@tue.nl

Ir. B. Besselink
Department of Mechanical Engineering
Eindhoven University of Technology
PO Box 513
5600 MB Eindhoven
The Netherlands
b.besselink@tue.nl

J.J.B. Biemond
Dept. Mechanical Engineering
Eindhoven University of Technology
PO Box 513
5600 MB Eindhoven
The Netherlands
j.j.b.biemond@tue.nl

Ir. Bikcora
Dept. of Electrical Engineering
Eindhoven University of Technology
PO Box 513
5600 MB Eindhoven
The Netherlands
c.bikcora@tue.nl

Ir. R.S. Blom
Delft Center for Systems and Control
Delft University of Technology
Mekelweg 2
2628 CD Delft
The Netherlands
r.s.blom@tudelft.nl

Max Boegli
Dept. of Mechanical Engineering
Katholieke Universiteit Leuven
Celestijnenlaan 300B, Box 02420, AFD PMA
B-3001 Leuven-Heverlee
Belgium
max.boegli@mech.kuleuven.be

Matthijs Boerlage
GE Global Research
Freisingerlandstrasse 50
85748 Garching bei Munchen
Germany
boerlage@ge.com

Pierre Borckmans
Dept. INMA
Université Catholique de Louvain/UCL
Avenue Georges Lemaître, 4
1348 Louvain-la-Neuve
Belgium
pierre.borckmans@uclouvain.be

Prof. O.H. Bosgra
Dept. of Mechanical Engineering
Eindhoven University of Technology
PO Box 513
5600 MB Eindhoven
The Netherlands
o.h.bosgra@tue.nl

Boulaïd Boulkroune
Control Engineering Department
Université Libre de Bruxelles
Av. F.D. Roosevelt 50
1050 Bruxelles
Belgium
bboulkro@ulb.ac.be

Windel Bouwman
Control Engineering
University of Twente
P.O. Box 217
7500 AE Enschede
The Netherlands
w.m.bouwman@utwente.nl

Maarten Breckpot
Dept. Electrical Engineering, SCD/SISTA
Katholieke Universiteit Leuven
Kasteelpark Arenberg 10 box 2446
3001 Leuven
Belgium
maarten.breckpot@esat.kuleuven.be

Arnaud Browet
Dept. INMA
Université Catholique de Louvain/UCL
Avenue Georges Lemaître, 4
1348 Louvain-la-Neuve
Belgium
arnaud.browet@uclouvain.be

A. Buttafuoco
Dept. of Control Engineering and System Analysis
Université Libre de Bruxelles
50 Av. F.D. Roosevelt, CP 165/55
B-1050 Brussels
Belgium
angelo.buttafuoco@ulb.ac.be

Dr. Cao
Discrete Technology and Production Automation
University of Groningen
Nijenborgh 4
9747AG Groningen
The Netherlands
ming.cao@ieee.org

Th. Cason
Dept. INMA
Université Catholique de Louvain/UCL
Avenue Georges Lemaître, 4
1348 Louvain-la-Neuve
Belgium
thomas.cason@uclouvain.be

Chia-Tche Chang
Dept. INMA
Université Catholique de Louvain/UCL
Avenue Georges Lemaître, 4
1348 Louvain-la-Neuve
Belgium
chia-tche.chang@uclouvain.be

C. Cochior
Dept. of Electrical Engineering
Eindhoven University of Technology
PO Box 513
5600 MB Eindhoven
The Netherlands
c.cochior@tue.nl

Anne Collard
Dept. of Electrical Engineering and Computer Science
Université de Liège
Bât. B28 Systèmes et modélisation Grande Traverse 10
4000 Liège
Belgium
anne.collard@ulg.ac.be

Dr. P. J. Collins
Modelling, Analysis and Simulation
Centrum Wiskunde en Informatica
Postbus 94079
1090 GB Amsterdam
The Netherlands
Pieter.Collins@cwi.nl

Z. Cong
Delft Center for Systems and Control
Delft University of Technology
Mekelweg 2
2628 CD Delft
The Netherlands
z.cong@tudelft.nl

Sebastien Coppe
Dept. INMA
Université Catholique de Louvain/UCL
Avenue Georges Lemaître, 4
1348 Louvain-la-Neuve
Belgium
sebastien.coppe@uclouvain.be

Ir. C.H.A. Chris Criens
Dept. of Mechanical Engineering
Eindhoven University of Technology
PO box 513
5600 MB Eindhoven
The Netherlands
c.h.a.criens@tue.nl

Thibault Dasnoy
Dept. INMA
Université Catholique de Louvain/UCL
Avenue Georges Lemaître, 4
1348 Louvain-la-Neuve
Belgium
thibault.dasnoy@uclouvain.be

Dr. Robert David
Dept. INMA
Université Catholique de Louvain/UCL
Avenue Georges Lemaître, 4
1348 Louvain-la-Neuve
Belgium
robert.david@uclouvain.be

Pierre Daye
Dept. INMA
Université Catholique de Louvain/UCL
Avenue Georges Lemaître, 4
1348 Louvain-la-Neuve
Belgium
pierre.daye@uclouvain.be

J.J.T.H. de Best
Mechanical Engineering
University of Technology Eindhoven
PO Box 513
5600 MB Eindhoven
The Netherlands
j.j.t.h.d.best@tue.nl

Bram de Jager
Dept. of Mechanical Engineering
Eindhoven University of Technology
PO Box 513
5600 MB Eindhoven
The Netherlands
A.G.de.Jager@tue.nl

Prof. C. De Persis
Lab of Mechanical Automation and Mechatronics
University of Twente
PO Box 217
7500 AE Enschede
The Netherlands
c.depersis@ctw.utwente.nl

Prof.Dr.Ir. B. De Schutter
Delft Center for Systems and Control
Delft University of Technology
Mekelweg 2
2628 CD Delft
The Netherlands
bart@deschutter.info

Jérémy Dehaye
Département de Mathématiques, Unité d'Optimisation et
Contrôle - Théorie et Applications
FUNDP Namur
Rempart de la Vierge, 8
5000 Namur
Belgium
jeremy.dehaye@fundp.ac.be

MSc Ir. del Puerto-Flores
Dept. of Discrete Technology and Production Automation
Groningen University
Nijenborgh 4
9747 AG Groningen
The Netherlands
d.del.puerto.flores@rug.nl

Dr. G.A. Delgado Lopes
Delft Center for Systems and Control
Delft University of Technology
Mekelweg 2
2628 CD Delft
The Netherlands
g.a.delgadolopes@tudelft.nl

Benoit Delhayé
Dept. INMA
Université Catholique de Louvain/UCL
Avenue Georges Lemaître, 4
1348 Louvain-la-Neuve
Belgium
benoit.delhayé@uclouvain.be

Dr. J-Ch. Delvenne
Department of Mathematics
FUNDP
Rempart de la Vierge, 8
5000 Namur
Belgium
jean-charles.delvenne@math.fundp.ac.be

Thomas Delwiche
FMTC
FMTC
Celestijnenlaan 300D - bus 4027
3001 Leuven
Belgium
Thomas.Delwiche@fmtc.be

Ir. A. Denasi
Dept. of Mechanical Engineering
Eindhoven University of Technology
PO Box 513
5600 MB Eindhoven
The Netherlands
A.Denasi@tue.nl

Bruno Depraetere
Dept. of Mechanical Engineering, division PMA
Katholieke Universiteit Leuven
Celestijnenlaan 300B
3001 Heverlee
Belgium
bruno.depraetere@mech.kuleuven.be

Ir. L.D. Dewasme
Service d'Automatique
University of Mons
Boulevard Dolez 31
7000 Mons
Belgium
Laurent.Dewasme@umons.ac.be

Ir. D.A. Dirks
Faculty of Mathematics and Natural Sciences
University of Groningen
Nijenborgh 4
9747AG Groningen
The Netherlands
d.a.dirks@rug.nl

Ignat Domanov
Dept. Electrical Engineering, SCD/SISTA
Katholieke Universiteit Leuven
Kasteelpark Arenberg 10 box 2446
3001 Leuven
Belgium
ignat.domanov@esat.kuleuven.be

M.C.F. Donkers
Dept. of Mechanical Engineering
Eindhoven University of Technology
PO Box 513
5600 MB Eindhoven
The Netherlands
m.c.f.donkers@tue.nl

Philippe Dreesen
Dept. Electrical Engineering, SCD/SISTA
Katholieke Universiteit Leuven
Kasteelpark Arenberg 10 box 2446
3001 Leuven
Belgium
philippe.dreesen@esat.kuleuven.be

Guillaume Drion
Department of Electrical Engineering and Computer Science
Université de Liège
Bldg B32, Systems and modeling, Grande Traverse 10
B-4000 Liège
Belgium
gdrion@ulg.ac.be

Ir. Abhishek Dutta
Electrical Energy, Systems & Automation
Ghent University
Home Vermeylen 240, Stalhof 6
9000 Gent
Belgium
Abhishek@autoctrl.UGent.be

Caroline Ego
Dept. INMA
Université Catholique de Louvain/UCL
Avenue Georges Lemaître, 4
1348 Louvain-la-Neuve
Belgium
caroline.ego@uclouvain.be

Ir. J. Elfring
Dept. of Mechanical Engineering
Eindhoven University of Technology
PO Box 513
5600 MB Eindhoven
The Netherlands
j.elfring@tue.nl

J.C. Engwerda
Dept. of econometrics and O.R.
Tilburg University
P.O. Box 90153
5000 LE Tilburg
The Netherlands
engwerda@uvt.nl

Damien Ernst
Department of Electrical Engineering and Computer Science
Université de Liège
Institut Montefiore
B-4000 Liège
Belgique
dernst@ulg.ac.be

MSc Ezzeldin Mahdy
Electrical Engineering / Control System
Eindhoven University of Technology
PO Box 513
5600 MB Eindhoven
The Netherlands
m.ezz@tue.nl

S. Farahani
Delft Center for Systems and Control
Delft University of Technology
Mekelweg 2
2628 CD Delft
The Netherlands
s.safaeifarahani@tudelft.nl

Hans Joachim Ferreau
Dept. Electrical Engineering, SCD/SISTA
Katholieke Universiteit Leuven
Kasteelpark Arenberg 10 box 2446
3001 Leuven
Belgium
joachim.ferreau@esat.kuleuven.be

S. Fiaz
Johann Bernoulli Institute for Mathematics and Computer
Science
University of Groningen
P.O. Box 407
9700 AK Groningen
The Netherlands
S.Fiaz@math.rug.nl

Raphael Fonteneau
Department of Electrical Engineering and Computer Science
Université de Liège
Grande Traverse, 10
4000 LIÈGE
BELGIUM
raphael.fonteneau@ulg.ac.be

Florence Fonteneau-Belmudes
Department of Electrical Engineering and Computer Science
Université de Liège
Grande Traverse, 10 - Batiment B28
4000 Liège
Belgium
florence.belmudes@ulg.ac.be

M. Forgione
DCSC
Delft University of Technology
Mekelweg 2
2628 CD Delft
The Netherlands
m.forgione@tudelft.nl

M. Gálvez
Dept. of Control Engineering and System Analysis
Vrije Universiteit Brussel
50 Av. F.D. Roosevelt, CP 165/55
B-1050 Brussels
Belgium
mgalvezc@ulb.ac.be

Eloisa Garcia-Canseco
Fac. of Mechanical Engineering
Eindhoven University of Technology
PO Box 513
5600 MB Eindhoven
The Netherlands
e.garcia.canseco@tue.nl

M.P. Gerard
Delft Center for Systems and Control
Delft University of Technology
Mekelweg 2
2628 CD Delft
The Netherlands
m.p.gerard@tudelft.nl

Ir. R.H. Gielen
Dept. of Electrical Engineering
Eindhoven University of Technology
PO Box 513
5600MB Eindhoven
The Netherlands
r.h.gielen@tue.nl

Dr.Ir. G. Gins
Dept. of Chemical Engineering - BioTeC
Katholieke Universiteit Leuven
W. de Croylaan 46
3001 Heverlee (Leuven)
België
geert.gins@cit.kuleuven.be

Drs. S.V. Gottimukkala
Johann Bernoulli Institute for Mathematics and Computer
Science
University of Groningen
P.O. Box 407
9700 AK Groningen
The Netherlands
s.v.gottimukkala@rug.nl

N.B. Groot
Delft Center for Systems and Control
Delft University of Technology
Mekelweg 2
2628 CD Delft
The Netherlands
n.b.groot@tudelft.nl

A. Haber
Delft Center for Systems and Control
Delft University of Technology
Mekelweg 2
2628 CD Delft
The Netherlands
a.haber@tudelft.nl

Dr.Ir. W.B.J. Hakvoort
-
DEMCON Advanced Mechatronics
Zutphenstraat 25
7575 EJ Oldenzaal
The Netherlands
wouter.hakvoort@demcon.nl

Dr. W.P.M.H. Heemels
Mechanical Engineering
Eindhoven University of Technology
Dept. of Mechanical Engineering
PO Box 513 5600 MB
Eindhoven
TheNetherlands

Bart Hennen
Dept. of Mechanical Engineering
Eindhoven University of Technology
PO Box 513
5600 MB Eindhoven
The Netherlands
b.a.hennen@tue.nl

Ir. R.M. Hermans
Dept. of Electrical Engineering
Eindhoven University of Technology
P.O. Box 513
5600 MB Eindhoven
The Netherlands
r.m.hermans@tue.nl

Dr. P.S.C. Heuberger
Delft Center for Systems and Control
Delft University of Technology
Mekelweg 2
2628 CD Delft
The Netherlands
p.s.c.heuberger@tudelft.nl

Samuel Hiard
Montefiore/Systems and Modeling
Université de Liège
10, Grande Traverse
4000 Liège
Belgium
S.Hiard@ulg.ac.be

Z. Hidayat
Delft Center for Systems and Control
Delft University of Technology
Mekelweg 2
2628 CD Delft
The Netherlands
z.hidayat@tudelft.nl

Dr. H. Hjalmarsson
School of Electrical Engineering
Royal Institute of Technology
Osquidas v 10
10044 Stockholm
Sweden
hakan.hjalmarsson@ee.kth.se

Ir. P.G.M. Hoeijmakers
Dept. of Mechanical Engineering
Eindhoven University of Technology
PO Box 513
5600 MB Eindhoven
The Netherlands
p.g.m.hoeijmakers@tue.nl

Dr.Ir. S.W. Hoeven, van der
Delft Center for Systems and Control
Delft University of Technology
Mekelweg 2
2628 CD Delft
The Netherlands
s.w.vanderhoeven@tudelft.nl

Ir. R. Hoogendijk
Dept. of Mechanical Engineering
Eindhoven University of Technology
PO Box 513
5600 MB Eindhoven
The Netherlands
r.hoogendijk@tue.nl

Ir. I. Houtzager
Delft Center for Systems and Control
Delft University of Technology
Mekelweg 2
2628 CD Delft
The Netherlands
i.houtzager@tudelft.nl

R. Huisman
DTPA
Groningen University
Nijenborgh 4
9747 AG Groningen
The Netherlands
r.huisman@sron.nl

Bart Huyck
Dept. Electrical Engineering, SCD/SISTA
Katholieke Universiteit Leuven
Kasteelpark Arenberg 10 box 2446
3001 Leuven
Belgium
bart.huyck@esat.kuleuven.be

Dr. Mariya Ishteva
Dept. INMA
Université Catholique de Louvain/UCL
Avenue Georges Lemaître, 4
1348 Louvain-la-Neuve
Belgium
mariya.ishteva@uclouvain.be

Tzvetan Ivanov
Dept. INMA
Université Catholique de Louvain/UCL
Avenue Georges Lemaître, 4
1348 Louvain-la-Neuve
Belgium
tzvetan.ivanov@uclouvain.be

Ir. Rob Janssen
Dept. of Mechanical Engineering
Eindhoven University of Technology
PO Box 513
5600 MB Eindhoven
The Netherlands
r.j.m.janssen@tue.nl

Ir. Pieter Janssens
Dept. of Mechanical Engineering
Katholieke Universiteit Leuven
Celestijnenlaan 300B
3001 Heverlee
Belgium
pieter.janssens@mech.kuleuven.be

Dr. B. Jayawardhana
Discrete Technology and Production Automation
Groningen University
Nijenborgh 4
9747AG Groningen
The Netherlands
b.jayawardhana@rug.nl

M.D. Kaba
Dept. of Mathematics
Groningen University
Bernoulliborg 380, Nijenborgh 9
9747 AG Groningen
The Netherlands
m.d.kaba@rug.nl

A. Katalenic
Dept. of Electrical Engineering
Eindhoven University of Technology
P.O. Box 513
5600 M Eindhoven
The Netherlands
a.katalenic@tue.nl

Karel Keesman
Systems & Control Group
Wageningen University
P.O. Box 17
6700 AA Wageningen
The Netherlands
karel.keesman@wur.nl

F.J. Kerber
Institute of Mathematics and Computing Science
University of Groningen
P.O. Box 407
9700 AV Groningen
The Netherlands
f.j.kerber@rug.nl

A.A. Khalate
Delft Center for Systems and Control
Delft University of Technology
Mekelweg 2
2628 CD Delft
The Netherlands
a.a.khalate@tudelft.nl

M. Kinnaert
Control Engineering Dept.
Université Libre de Bruxelles
Avenue F.D. Roosevelt 50 – CP165/55
1050 Brussels
Belgium
Michel.Kinnaert@ulb.ac.be

Dr.Ir. S.H. Koekebakker
Control Systems Technology
Eindhoven University of Technology - Océ Technologies
PO Box 513
5600 MB Eindhoven
The Netherlands
s.h.koekebakker@tue.nl

Ir. J.J. Koopman Koopman
Delft Center for Systems and Control
Delft University of Technology
Mekelweg 2
2628 CD Delft
The Netherlands
j.j.koopman@tudelft.nl

Dr. H. Koroglu
Dept. of Electrical Engineering - Control Systems
Eindhoven University of Technology
PO Box 513
5600 MB Eindhoven
The Netherlands
h.koroglu@tue.nl

Dr. D. Kostic
Dept. of Mechanical Engineering
Eindhoven University of Technology
PO Box 513
5600 MB Eindhoven
The Netherlands
d.kostic@tue.nl

Gautier M. Krings
Dept. INMA
Université Catholique de Louvain/UCL
Avenue Georges Lemaître, 4
1348 Louvain-la-Neuve
Belgium
gautier.krings@uclouvain.be

Prof. A. Kugi
Electrical Engineering and Computer Science
Technical University of Vienna
Gußhausstraße 27-29/350
1040 Vienna
Austria
Kugi@acin.tuwien.ac.at

S. Kuiper
Delft Center for Systems and Control
Delft University of Technology
Mekelweg 2
2628 CD Delft
The Netherlands
stefan.kuiper@tudelft.nl

MSc G.K.H. Larsen
Institute for Technology, Engineering & Management
University of Groningen
Nijenborgh 4
9747 AG Groningen
The Netherlands
g.k.h.larsen@rug.nl

John Lataire
Dept. ELEC
Vrije Universiteit Brussel
Pleinlaan 2
B-1050 Brussel
Belgium
john.lataire@vub.ac.be

Quang Thuan Le
Department of Mathematics
University of Groningen
P.O. Box 800
9700 AV Groningen
The Netherlands
t.q.le@rug.nl

Guillaume Leclercq
Dept. INMA
Université Catholique de Louvain/UCL
Avenue Georges Lemaître, 4
1348 Louvain-la-Neuve
Belgium
guillaume.leclercq@uclouvain.be

Prof. Philippe Lefèvre
Dept. INMA
Université Catholique de Louvain/UCL
Avenue Georges Lemaître, 4
1348 Louvain-la-Neuve
Belgium
philippe.lefevre@uclouvain.be

Ir. M. Leskens
Delft Center for Systems and Control
Delft University of Technology
Mekelweg 2
2628 CD Delft
The Netherlands
m.leskens@tudelft.nl

Dr. S. Lichiardopol
Dept. of Mechanical Engineering
Eindhoven University of Technology
PO Box 513
5600 MB Eindhoven
The Netherlands
s.lichtiardopol@tue.nl

Dr.Ir. C.M.M. Lierop, van
Dept. of Electrical Engineering
Eindhoven University of Technology
PO Box 513
5600 MB Eindhoven
The Netherlands
c.m.m.v.lierop@tue.nl

Ms. H. Liu
Faculty of Mathematics and Natural Sciences
University of Groningen
Nijenborgh 9
9747 AG Groningen
The Netherlands
hui.liu@rug.nl

Dr.Ir. F. Logist
Chemical Engineering / BioTeC
Katholieke Universiteit Leuven
W. de Croylaan 46
3001 Leuven
Belgium
filip.logist@cit.kuleuven.be

Ebrahim Louarroudi
Dept. ELEC
Vrije Universiteit Brussel
Pleinlaan 2
B-1050 Brussel
Belgium
ebrahim.louarroudi@vub.ac.be

Heather Maclean
Dept. INMA
Université Catholique de Louvain/UCL
Avenue Georges Lemaître, 4
1348 Louvain-la-Neuve
Belgium
heather.maclean@uclouvain.be

Johan Mailier
Automatic Control Laboratory
University of Mons
31 Boulevard Dolez
B-7000 Mons
Belgium
johan.mailier@umons.ac.be

Anna Marconato
Dept. ELEC
Vrije Universiteit Brussel
Pleinlaan 2
B-1050 Brussel
Belgium
anna.marconato@vub.ac.be

Alexandre Mauroy
Department of Electrical Engineering and Computer Science
Université de Liège
Grande Traverse, 10
4000 Liège (Sart-Tilman)
Belgium
alexandre.mauroy@ulg.ac.be

Gjerrit Meinsma
Dept. of Applied Mathematics
University of Twente
PO Box 217
7500 AE Enschede
The Netherlands
g.meinsma@utwente.nl

Anup Menon
IWI, Mathematics and Natural Sciences
University of Groningen
PO Box 800
9700 AV Groningen
The Netherlands
a.menon@rug.nl

A. Mesbah
Delft Center for Systems and Control
Delft University of Technology
Mekelweg 2
2628 CD Delft
The Netherlands
ali.mesbah@tudelft.nl

Gilles Meyer
Montefiore Institute
Université de Liège
Grande Traverse, 10
4000 Liège
Belgium
G.Meyer@ulg.ac.be

Dr. S. Misra
Control Engineering (EWI)
University of Twente
Hogekamp 8256, P.O. Box 217
7500 AE Enschede
The Netherlands
s.misra@utwente.nl

Nima Monshizadeh Naini
Control systems and applied analysis
University of Groningen
Antillenstraat 1-19
9714 JT Groningen
The Netherlands
n.monshizadeh@rug.nl

Griet Monteyne
Dept. ELEC
Vrije Universiteit Brussel
Pleinlaan 2
B-1050 Brussel
Belgium
griet.monteyne@vub.ac.be

Mohammad Moradzadeh
department of Electrical energy, systems and automation
University of Gent
Isabellakaai 14
9000 gent
Belgium
mm.moradzadeh@yahoo.com

Mr. S. Muhammad
Delft Institute of Applied Mathematics
Delft University of Technology
HB04.110 EWI Building, Mekelweg 4
2628 CD Delft
The Netherlands
s.muhammad@tudelft.nl

Ir. Munoz Arias
Wiskunde en Natuurwetenschappen
Groningen University
Nijenborgh 4
9747 AG Groningen
The Netherlands
m.munoz.arias@rug.nl

Ir. M.E.C. Mutsaers
Dept. of Electrical Engineering
Eindhoven University of Technology
PO Box 513
5600 MB Eindhoven
The Netherlands
m.e.c.mutsaers@tue.nl

Ir. Naus
Dept. of Mechanical Engineering
Eindhoven University of Technology
PO Box 513
5600 MB Eindhoven
The Netherlands
g.j.l.naus@tue.nl

MSc D.V. Ngo
Mechanical Engineering Department,
Eindhoven University of Technology
PO Box 513, WH -1.121
5600MB Eindhoven
The Netherlands
d.v.ngo@tue.nl

H. Nijmeijer
Mechanical Engineering
Eindhoven University of Technology
PO Box 513
5600 MB Eindhoven
The Netherlands
h.nijmeijer@tue.nl

Dr.Ir. P.W.J.M. Nuij
Dept. of Mechanical Engineering
Eindhoven University of Technology
PO Box 513
5600 MB Eindhoven
The Netherlands
p.w.j.m.nuij@tue.nl

Victor Onclinx
Dept. INMA
Université Catholique de Louvain/UCL
Avenue Georges Lemaître, 4
1348 Louvain-la-Neuve
Belgium
victor.onclinx@uclouvain.be

Tom Oomen
Dept. of Mechanical Engeneer
Eindhoven University of Technology
PO Box 513
5600 MB Eindhoven
The Netherlands
t.a.e.oomen@tue.nl

François-Xavier Orban de Xivry
Dept. INMA
Université Catholique de Louvain/UCL
Avenue Georges Lemaître, 4
1348 Louvain-la-Neuve
Belgium
fx.orban@uclouvain.be

Ir. R.Y. Ouyang
Mathematics and Natural Science
university Groningen
Nijenborgh 4 office 5117.0122
9747AG Groningen
The Netherlands
r.ouyang@rug.nl

Dr. L. Ozkan
Dept. of Electrical Engineering
Eindhoven University of Technology
PO box 513
5600 MB Eindhoven
The Netherlands
l.ozkan@tue.nl

MSc B. Peerdeman
EWI
University of Twente
Matenweg 32-106
7522 LK Enschede
The Netherlands
b.peerdeman@utwente.nl

Rik Pintelon
Dept. ELEC
Vrije Universiteit Brussel
Pleinlaan 2
B-1050 Brussel
Belgium
rik.pintelon@vub.ac.be

Douglas Plaza Guingla
Electrical Energy Systems and Automation
University of Ghent
Technologiepark 914
B - 9052 Gent - Zwijnaarde
Belgium
Douglas.PlazaGuingla@UGent.be

Dr. J.W. Polderman
Dept. of Applied Mathematics
University of Twente
P.O. Box 217
7500 AE Enschede
The Netherlands
j.w.polderman@math.utwente.nl

S.V. Polenkova
Department of Applied Mathematics
University of Twente
P.O. Box 217
7500 AE Enschede
The Netherlands
s.v.polenkova@utwente.nl

Quentin Rentmeesters
Dept. INMA
Université Catholique de Louvain/UCL
Avenue Georges Lemaître, 4
1348 Louvain-la-Neuve
Belgium
quentin.rentmeesters@uclouvain.be

Ir. C. Retamal
Service d'Automatique
University of Mons
Boulevard Dolez 31
7000 Mons
Belgium
cristina.retamal@umons.ac.be

Ir. A. Rezapour
Delft Center for Systems and Control
Delft University of Technology
Mekelweg 2
2628 CD Delft
The Netherlands
a.rezapour@student.tudelft.nl

David Rijlaarsdam
Mechanical Engineering / Control Systems Technology
Eindhoven University of Technology
PO 513, WH -1.133
5600 MB Eindhoven
The Netherlands
d.j.rijlaarsdam@tue.nl

Yves Rolain
Dept. ELEC
Vrije Universiteit Brussel
Pleinlaan 2
B-1050 Brussel
Belgium
yves.rolain@vub.ac.be

Ir. M.J.C. Ronde
Dept. of Mechanical Engineering
Eindhoven University of Technology
PO Box 513, WHoog -1.127
5600 MB Eindhoven
The Netherlands
m.j.c.ronde@tue.nl

Pierre Sacré
Department of Electrical Engineering and Computer Science
Université de Liège
Bât. B28 Systems and modeling, Grande Traverse 10
4000 Liège
Belgique
pierre.sacre@ulg.ac.be

Prof. L. O. Santos
Dep. of Chemical Engineering
University of Coimbra
Pólo II, R. Sílvio Lima
3030-790 Coimbra
Portugal
lino@eq.uc.pt

Ines Saraiva
Automatic Control Laboratory, Polytechnic Faculty
University of Mons
Boulevard Dolez, 31
7000 Mons
Belgium
ines.saraiva@umons.ac.be

Prof.Dr.Ir. J.M.A. Scherpen
fac. Mathematics and Natural Sciences
University of Groningen
Nijenborgh 4
9747 AG Groningen
The Netherlands
j.m.a.scherpen@rug.nl

Johan Schoukens
Dept. ELEC
Vrije Universiteit Brussel
Pleinlaan 2
B-1050 Brussel
Belgium
johan.schoukens@vub.ac.be

Dr. R. Sepulchre
Systems and Modeling / ECE
Université de Liège
Institut Montefiore, B28
4000 Liège Sart Tilman
Belgium
r.sepulchre@ulg.ac.be

Mr. Marko Seslija
Faculty of Mathematics and Natural Sciences, DTPA
University of Groningen
Nijenborgh 4
9747 AG Groningen
The Netherlands
m.seslija@rug.nl

Hanumant Singh Shekhawat
Dept. Of Applied Mathematics
University of Twente
P.O. Box 217
7500 AE Enschede
The Netherlands
h.s.shekhawat@ewi.utwente.nl

Marco Signoretto
Dept. Electrical Engineering, SCD/SISTA
Katholieke Universiteit Leuven
Kasteelpark Arenberg 10 box 2446
3001 Leuven
Belgium
marco.signoretto@esat.kuleuven.be

Emile Simon
Dept. INMA
Université Catholique de Louvain/UCL
Avenue Georges Lemaître, 4
1348 Louvain-la-Neuve
Belgium
emile.simon@uclouvain.be

A. Simonetto
Delft Center for Systems and Control
Delft University of Technology
Mekelweg 2
2628 CD Delft
The Netherlands
a.simonetto@tudelft.nl

Jonas Sjöberg
Dept. ELEC
Vrije Universiteit Brussel
Pleinlaan 2
B-1050 Brussel
Belgium
jonas.sjoberg@chalmers.se

V. Spinu
 Dept. of Electrical Engineering
 Eindhoven University of Technology
 PO Box 513
 5600 MB Eindhoven
 The Netherlands
v.spinu@tue.nl

Dr. Alexandru Stancu
 Automatic Control Laboratory
 Universite de Mons
 Boulevard Dolez, 31
 7000 Mons
 Belgium
Alexandru.Stancu@umons.ac.be

Ir. N.E. Stein
 Systems and control group
 Wageningen UR/ Wetsus
 postbus 1113
 8900CC Leeuwarden
 The Netherlands
nienke.stein@wetsus.nl

Prof.Dr.Ir. M. Steinbuch
 Dept. of Mechanical Engineering
 Eindhoven University of Technology
 PO Box 513, wh 0.141
 5600 MB Eindhoven
 The Netherlands
m.steinbuch@tue.nl

Ir. E. Steur
 Dept. Mechanical Engineering
 Eindhoven University of Technology
 P.O. Box 513
 5600 MB Eindhoven
 The Netherlands
e.steur@tue.nl

Dr.Ir. J.D. Stigter
 Biometris
 Wageningen UR
 PO Box 100
 6700 AC Wageningen
 The Netherlands
hans.stigter@wur.nl

Julian Stoev
 Ecological Machines
 Flanders' MECHATRONICS Technology Centre
 Campus Arenberg, Celestijnenlaan 300D
 B-3001 Heverlee
 Belgium
julian.stoev@gmail.com

Ir. J. Stolte
 Dept. of Electrical Engineering
 Eindhoven University of Technology
 PO Box 513
 5600 MB Eindhoven
 The Netherlands
j.stolte@tue.nl

Prof.Dr. A.A. Stoorvogel
 Department of Electrical Engineering, Mathematics and
 Computing Science, P.O. Box 217
 University of Twente
 P.O. Box 217
 7500AE Enschede
 The Netherlands
A.A.Stoorvogel@utwente.nl

Jean-François Stumper
 Dept. of Electrical Engineering and Information Technology
 Technische Universität München
 Arcisstraße 21
 80333 München
 Germany
jean-francois.stumper@tum.de

Ir. Herman Sutarto
 EESA-Research Group SYSTeMS
 University of Ghent
 Technologiepark-Zwijnaarde 914
 B-9052 Zwijnaarde Ghent
 Belgium
herman.sutarto@ugent.be

Jan Swevers
 Dept. of Mechanical Engineering
 Katholieke Universiteit Leuven
 Celestijnenlaan 300B
 B-3001 Heverlee
 Belgium
jan.swevers@mech.kuleuven.be

Dr.Ir. A.N. Tarau
 Dept. of Mechanical Engineering
 Eindhoven University of Technology
 PO Box 513
 5600 MB Eindhoven
 The Netherlands
A.N.Tarau@tue.nl

Falck Tillmann
 Dept. Electrical Engineering, SCD/SISTA
 Katholieke Universiteit Leuven
 Kasteelpark Arenberg 10 box 2446
 3001 Leuven
 Belgium
tillmann.falck@esat.kuleuven.be

Quoc Tran Dinh
Dept. Electrical Engineering, SCD/SISTA
Katholieke Universiteit Leuven
Kasteelpark Arenberg 10 box 2446
3001 Leuven
Belgium
quoc.trandinh@esat.kuleuven.be

Laura Trotta
Montefiore Institute
Université de Liège
Grande Traverse, 10
4000 Liège
Belgium
l.trotta@ulg.ac.be

Ir. F van Belzen
Dept. of Electrical Engineering
Eindhoven University of Technology
PO Box 513, PT 4.09
5600 MB Eindhoven
The Netherlands
f.v.belzen@tue.nl

Ir. K. van Berkel
Dept. of Mechanical Engineering
Eindhoven University of Technology
PO Box 513
5600 MB Eindhoven
The Netherlands
k.v.berkel@tue.nl

Dr. N. van de Wouw
Mechanical Engineering
Eindhoven University of Technology
Dept. of Mechanical Engineering
PO Box 513 5600 MB
Eindhoven
The Netherlands
[TheNetherlands](mailto:N.J.M.v.Dijk@tue.nl)

Lieboud Van den Broeck
Dept. of Mechanical Engineering
Katholieke Universiteit Leuven
Celestijnenlaan 300b
3000 Leuven
Belgium
lieboud.vandenbroeck@mech.kuleuven.be

Prof.Dr.Ir. P.M.J. Van den Hof
Delft Center for Systems and Control
Delft University of Technology
Mekelweg 2
2628 CD Delft
The Netherlands
p.m.j.vandenhof@tudelft.nl

Ir. P. Van den Kerkhof
Dept. of Chemical Engineering - BioTeC
Katholieke Universiteit Leuven
W. de Croylaan 46
3001 Heverlee
Belgium
Pieter.VandenKerkhof@cit.kuleuven.be

Ir. P. van der Hulst
R&D
Piak electronic design b.v.
Markt 49
4101 BW Culemborg
The Netherlands
paul@piak.nl

Prof. Dr. A.J. van der Schaft
Johann Bernoulli Institute for Mathematics and Computer
Science
University of Groningen
PO Box 407
9700 AK Groningen
The Netherlands
a.j.van.der.schaft@rug.nl

Dr.Ir. E. Van Derlinden
Dept. of Chemical Engineering
Katholieke Universiteit Leuven
W. de Croylaan 46
3001 Leuven
Belgium
eva.vanderlinden@cit.kuleuven.be

Ir. N.J.M. van Dijk
Department of Mechanical Engineering
Eindhoven University of Technology
PO Box 513
5600 MB Eindhoven
The Netherlands
N.J.M.v.Dijk@tue.nl

Prof. Paul Van Dooren
Dept. INMA
Université Catholique de Louvain/UCL
Avenue Georges Lemaître, 4
1348 Louvain-la-Neuve
Belgium
paul.vandooren@uclouvain.be

Ir. P.M.M. Van Erdeghem
Dept. of Chemical Engineering
Katholieke Universiteit Leuven
W. de Croylaan 46
3001 Heverlee
Belgium
peter.vanerdeghem@cit.kuleuven.be

Ir. R.W. van Gils
Dept. of Mechanical Engineering
Eindhoven University of Technology
PO Box 513
5600 MB Eindhoven
The Netherlands
r.w.v.gils@tue.nl

Ir. R. M. A. van Herpen
Dept. of Mechanical Engineering
Eindhoven University of Technology
PO Box 513, WH -1.127
5600 MB Eindhoven
The Netherlands
r.m.a.v.herpen@tue.nl

Prof.Dr.Ir. Jan F.M. Van Impe
Dept. of Chemical Engineering
Katholieke Universiteit Leuven
W. de Croyllan 46 Bus 2423
3001 Heverlee
Belgium
jan.vanimpe@cit.kuleuven.be

Wendy Van Moer
Dept. ELEC
Vrije Universiteit Brussel
Pleinlaan 2
B-1050 Brussel
Belgium
wendy.vanmoer@vub.ac.be

S. van Mourik
Plant Sciences Group
Wageningen University and Research Center
P.O. Box 100
6700 AC Wageningen
The Netherlands
simon.vanmourik@wur.nl

Anne Van Mulders
Dept. ELEC
Vrije Universiteit Brussel
Pleinlaan 2
B-1050 Brussel
Belgium
anne.van.mulders@vub.ac.be

Ir. G. van Oort
EWI - Control Engineering
University of Twente
PO Box 217
7500 AE Enschede
The Netherlands
g.vanoort@ewi.utwente.nl

Prof. Dr.Ir. G. van Straten
Agrotechnology and Food Sciences
Wageningen University
Bornse Weilanden 9
6708 WG Wageningen
The Netherlands
gerrit.vanstraten@wur.nl

Dr. G.A.K. Van Voorn
Biometris
Wageningen University
P.O. Box 100
6700 AC Wageningen
The Netherlands
george.vanvoorn@wur.nl

Ir. P.W.M. van Zutven
Dept. of Mechanical Engineering
Eindhoven University of Technology
PO Box 513
5600 MB Eindhoven
The Netherlands
p.w.m.v.zutven@tue.nl

Laurent Vanbeylen
Dept. ELEC
Vrije Universiteit Brussel
Pleinlaan 2
B-1050 Brussel
Belgium
laurent.vanbeylen@vub.ac.be

Prof. Alain Vande Wouwer
Control Department
University of Mons
31 Boulevard Dolez
7000 Mons
Belgium
alain.vandewouwer@umons.ac.be

Jeroen Vandersteen
Dept. of Mechanical Engineering
Katholieke Universiteit Leuven
Celestijnenlaan 200 D
B-3001 Heverlee
Belgium
jeroen@ster.kuleuven.be

Jef Vanlaer
Dept. of Chemical Engineering - BioTeC
Katholieke Universiteit Leuven
W. de Croylaan 46
3001 Heverlee
Belgium
jef.vanlaer@cit.kuleuven.be

Ir. G.J. Veen, van der
Delft Center for Systems and Control
Delft University of Technology
Mekelweg 2
2628 CD Delft
The Netherlands
g.j.vanderveen@tudelft.nl

M. Verhaegen
DCSC
Delft University of Technology
Mekelweg 2
2628 CD Delft
The Netherlands
m.verhaegen@moesp.org

J. Verspecht
Dept. of Control Engineering and System Analysis
Université Libre de Bruxelles
50 Av. F.D. Roosevelt, CP 165/55
B-1050 Brussels
Belgium
jonathan.verspecht@ulb.ac.be

Mr. Vinjamoor
Mathematics and computing science.
University of Groningen
PO BOX 407
9700 AK Groningen.
The Netherlands.
h.g.vinjamoor@rug.nl

A. Virag
Dept. of Electrical Engineering
Eindhoven University of Technology
PO Box 513
5600 MB Eindhoven
The Netherlands
a.virag@tue.nl

Ir. J.A.W. Vissers
Dept. of Electrical Engineering
Eindhoven University of Technology
PO Box 513
5600 MB Eindhoven
The Netherlands
j.a.w.vissers@tue.nl

M.L.J.V. Volckaert
Dept. of Mechanical Engineering
Katholieke Universiteit Leuven
Celestijnenlaan 300B
B-3001 Heverlee
België
Marnix.Volckaert@mech.kuleuven.be

T. Voss
Dept. of Electrical Engineering
Eindhoven University of Technology
PO Box 513
5600 MB Eindhoven
The Netherlands
t.voss@tue.nl

MSc S.K. Wattamwar
Electrical Engineering
Eindhoven University of Technology
PO Box 513
5600 MB Eindhoven
The Netherlands
s.wattamwar@tue.nl

Dr. S. Weiland
Dept. Electrical Engineering
Eindhoven University of Technology
P.O. Box 513
5600 MB Eindhoven
The Netherlands
s.weiland@tue.nl

Dharmika Widanage
Dept. ELEC
Vrije Universiteit Brussel
Pleinlaan 2
B-1050 Brussel
Belgium
wwidanag@vub.ac.be

Prof. Joseph WINKIN
Department of Mathematics
FUNDP
Rempart de la Vierge, 8
5000 Namur
Belgium
Joseph.Winkin@fundp.ac.be

Mr. W Xia
Faculty of Mathematics and Natural Sciences
University of Groningen
Nijenborgh 4
9747 AG Groningen
The Netherlands
w.xia@rug.nl

Gang Xu
PMA
Katholieke Universiteit Leuven
Celestijnenlaan 300B
3001 Leuven
Belgium
wolfgang.xu@gmail.com

Tao Yang
Dept. of Applied Mathematics
University of Twente
P O Box 217
7500 AE Enschede
The Netherlands
tyang1@eecs.wsu.edu

Ir. Zamorano
Service d'Automatique
University of Mons
Boulevard Dolez 31
7000 Mons
Belgium
francisca.zamorano@umons.ac.be

Keivan Zavari
PMA Division, Dept. of Mechanical Engineering
Katholieke Universiteit Leuven
Celestijnenlaan 300B, Box 02420, AFD PMA
B-3001 Leuven-Heverlee
Belgium
keivan.zavari@student.kuleuven.be

Dr.Ir. Zhu
Electrical Engineering
Eindhoven University of Technology
PO Box 513
5600 MB Eindhoven
The Netherlands
y.zhu@tue.nl

Part 5

Organizational Comments

Welcome

The Organizing Committee has the pleasure of welcoming you to the 29th *Benelux Meeting on Systems and Control*, at the “Kapellerput Conference Centre” in Heeze, The Netherlands.

Aim

The aim of the Benelux Meeting is to promote research activities and to enhance cooperation between researchers in Systems and Control. This is the twenty-ninth in a series of annual conferences that are held alternately in Belgium and The Netherlands.

Overview of the Scientific Program

1. Plenary lectures by invited speaker *Håkan Hjalmarsson* (Royal Institute of Technology, Stockholm, Sweden) on
 - **System Identification of Complex and Structured Systems (Part I)**
 - **System Identification of Complex and Structured Systems (Part II)**
2. Plenary lectures by invited speaker *Andreas Kugi* (Technical University of Vienna, Austria) on
 - **Control of PDEs I: Trajectory Planning and Feedforward Control**
 - **Control of PDEs II: Feedback and Tracking Control**
3. Mini course by *Maurice Heemels and Nathan van de Wouw* (Eindhoven University of Technology, The Netherlands) on
 - **Networked Control Systems**
4. Contributed short lectures. See the list of sessions for the titles and authors of these lectures.

Directions for speakers

For a contributed lecture the available time is 25 minutes. Please leave a few minutes of this period for discussion and room changes and adhere to the indicated schedule. In each room overhead projectors and beamers will be available. Be careful with this equipment, because the beamers are supplied by some of the participating groups. *When using a beamer/projector, you have to provide a notebook yourself and you have to start your lecture with the notebook up and running and the external video port switched on.*

Registration

The Benelux Meeting registration desk, located in the foyer, will be open on Tuesday, March 30, from 10:00 to 14:00. Late registrations can be made at the Benelux Meeting registration desk, when space is still available. The on-site fee schedule is:

Arrangement	Price
single room	€495.–
twin-bedded room	€415.–
meals only (no dinner)	€285.–
one day (no dinner)	€145.–

The registration fee includes:

- Admission to all sessions.
- A copy of the Book of Abstracts.
- Coffee and tea during the breaks, and ice water and mints in the session rooms.
- In the case of an accommodation arrangement: lunch and dinner on Tuesday, breakfast, lunch, and dinner on Wednesday, and breakfast and lunch on Thursday.
- In the case of a “meals only” arrangement: lunch on Tuesday, Wednesday, and Thursday.
- In the case of a “one day” arrangement: lunch on Tuesday, or Wednesday, or Thursday.
- Free use of a wireless Internet connection (WiFi) at the conference location

The registration fee does *not* include:

- Cost of phone calls
- Special ordered drinks during lunch, dinner, in the evening, etc.

Organization

The Organizing Committee of the 29th Benelux Meeting consists of

D. Aeyels (Gent University),
 X.J.A. Bombois (Delft University of Technology),
 O.H. Bosgra (Delft University of Technology),
 M. Cao (University of Groningen),
 M. Gevers (Université Catholique de Louvain),
 M. Heemels (Eindhoven University of Technology),
 P. M. J. Van den Hof (Delft University of Technology),

J.F.M. van Impe (Katholieke Universiteit Leuven),
 T. Keviczky (Delft University of Technology),
 M. Lazar (Eindhoven University of Technology),
 G. Meinsma (University of Twente),
 B. De Moor (Katholieke Universiteit Leuven),
 H. Nijmeijer (Eindhoven University of Technology),
 A.J. van der Schaft (University of Groningen),
 J. Schoukens (Free University Brussel),
 M. Steinbuch (Eindhoven University of Technology),
 J.D. Stigter (Wageningen University),
 S. Stramigioli (University of Twente),
 A.A. Stoorvogel (University of Twente),
 G. van Straten (Wageningen University),
 S. Weiland (Eindhoven University of Technology).

The meeting is sponsored or supported by the following organizations:

- Dutch Institute for Systems and Control (DISC),
- Nederlandse Organisatie voor Wetenschappelijk Onderzoek (NWO).

The meeting has been organized by Hans Stigter (Wageningen University) and Gjerrit Meinsma (University of Twente).

Conference location

The lecture rooms of “Kapellerput Conference Centre” are situated on the ground floor in the eastern part. Consult the map at the end of this book to locate rooms and to avoid getting lost. During the breaks, coffee and tea will be served in the foyer, while ice water and mints are available in the session rooms. Announcements and personal messages will be posted near the main conference room. Accommodation is provided in the conference center for most participants. Breakfast will be served between 7:30 and 8:30. Room keys can be picked up at lunch time on the first day and need to be returned before 10:00 on the day of departure. Luggage storage is provided in room “de Aa” (in the old chapel to the left of the entrance). Parking is free of charge. The address of “Kapellerput Conference Centre” is

Somerenseweg 100
 5591 TN Heeze
 The Netherlands
 tel: +31 (0) 40 224 19 22
 fax: +31 (0) 40 226 54 47

Facilities

The facilities at the center include a restaurant, bar, and recreation and sports facilities. We refer to the reception desk of

the center for detailed information about the use of these facilities.

Best junior presentation award

Continuing a tradition that started in 1996, the Benelux meeting will close with the announcement of the winner of the Best Junior Presentation Award. This award is given for the best presentation at the meeting given by a junior researcher (*i.e.*, someone working towards a PhD degree). The award is specifically given for quality of presentation rather than quality of research, which is judged in a different way. At the meeting, the chairs of sessions will ask three volunteers in the audience to fill out an evaluation form. After the session, the evaluation forms will be collected by the Prize Commissioners who will then compute a ranking. The winner will be announced on Thursday April 1 in room **Samenspel**, immediately after the final lectures of the meeting and he or she will be presented with the award, which consists of a trophy that may be kept for one year and a certificate. The evaluation forms of each presentation will be returned to the junior researcher who gave the presentation. The Prize Commissioners are Peter Heuberger (Delft University of Technology), Jan van Impe (Katholieke Universiteit Leuven), and Filip Logist (Katholieke Universiteit Leuven).

The organizing committee counts on the cooperation of the participants to make this contest a success.

Website

An *electronic version* of the Book of Abstracts can be downloaded from the Benelux Meeting [web site](#).

Meetings

The following meetings are scheduled:

- Management Team DISC on Tuesday, March 30, room Visie, 21:00–22:00.
- Graduate School Committee Belgium on Tuesday, March 30, room Inspanning, 19:30–21:00.
- UNIT DISC on Wednesday, March 31, room Inspanning, 12:30–13:30.
- Board DISC on Wednesday, March 31, room Visie, 21:00–22:00.

Tuesday March 30

11:25 – 11:30	P0 Samenspel <i>Opening</i>						
11:30 – 12:30	P1 Samenspel “ <i>System Identification of Complex and Structured Systems (part I)</i> ” Håkan Hjalmarsson						
12:30 – 13:45	Lunch						
Room	Samenspel	Samenkomst	Samenwerking	Visie	Uitdaging	Interactie	
TuM	TuM01 <i>System Theory A</i>	TuM02 <i>Optimal Control A</i>	TuM03 <i>System Identification A</i>	TuM04 <i>Optimization A</i>	TuM05 <i>Mechanical Engineering A</i>	TuM06 <i>Robotics A</i>	
13:45 – 14:10	Seslija	Depraetere	Bezapour	Boreckmans	Hoelijmakers	Lopes	
14:10 – 14:35	Vinjamoor	Voleckaert	van Herpen	Cong	Kuiper	Adimandra	
14:35 – 15:00	van der Schaft	Janssens	Monteyne	Mahdy	van der Veen	Elfring	
15:00 – 15:25	Krings	Folandi	Ruiz	Ishteva	Houtzager	van Zutphen	
15:25 – 15:50	Seslija	Criens	Huyck	Van Erdeghem	Naus	Kostic	
15:50 – 16:15	Break with snack						
TuP	TuP01 <i>System Theory B</i>	TuP02 <i>Optimal Control B</i>	TuP03 <i>Systems Biology + Medical App. A</i>	TuP04 <i>Biochemical Engineering A</i>	TuP05 <i>Electro-Mechanical Engineering A</i>	TuP06 <i>Non-Linear Control A</i>	
16:15 – 16:40	Zapreev	Engwerda	Barbé	David	Gálvez	Vanbeylen	
16:40 – 17:05	Collins	Fonteneau	Buttafuoco	Retamal	Bakbakhani	Zivanovic	
17:05 – 17:30	Abate	Ferreau	Sacré	Saraiva	Steur	Katalenic	
17:30 – 17:45	Coffee Break						
17:45 – 18:10	Ivanov	Breckpot	Coppe	Delmotte	Achterberg	Alvarez-Aguirre	
18:10 – 18:35	Fiaz	Ngo	Leclercq	Dewasme	Huisman	Steur	
18:35 – 19:00	Haber	van Dijk	Daye	van der Linden	Ouyang	Gielen	
19:30 – 21:00	Dinner						
19:30 – 21:00	Graduate School Committee Belgium (room Inspanning)						
21:00 – 22:00	Management Team DISC (room Visie)						

Wednesday March 31

8:30 – 9:30	P2 Samenspel “Control of PDEs (part I)” Andreas Kugi Break					
9:30 – 10:00	P3 Samenspel “Control of PDEs (Part II)” Andreas Kugi Break					
10:00 – 11:00	P4 Samenspel “System Identification of Complex and Structured Systems (part II)” Håkan Hjalmarsson					
11:00 – 11:20	P4 Samenspel “System Identification of Complex and Structured Systems (part II)” Håkan Hjalmarsson					
11:20 – 12:20	P4 Samenspel “System Identification of Complex and Structured Systems (part II)” Håkan Hjalmarsson					
12:20 – 12:30	“DISC PhD Award and Certificates”					
12:30 – 13:30	UNIT DISC Meeting (room Inspanning)					
12:30 – 13:45	Lunch					
Room	Samenspel	Samenkomst	Samenwerking	Visie	Uitdaging	Interactie
WeM	WeM01 <i>Systems Theory C</i>	WeM02 <i>Optimal Control C</i>	WeM03 <i>System Identification B</i>	WeM04 <i>Optimization B</i>	WeM05 <i>Networks and Distributed Control</i>	WeM06 <i>Robotics B</i>
13:45 – 14:10	Chang	Farahani	Marconato	Alzate	Liu	-
14:10 – 14:35	Zavari	Logist	Widanage	Browet	Bauer	van Oort
14:35 – 15:00	Muhammad	Simon	Falek	Meyer	Groot	Janssen
15:00 – 15:25	Dreesen	Sutarto	Van Mulders	Collard	Larsen	Denasi
15:25 – 15:50	Shekhawat	van Keulen	Barbé	Dinh Quoc	Cason	Lichiardopol
15:50 – 16:15	Break with snack					
WeP	WeP01 <i>Distributed Parameter Systems</i>	WeP02 <i>Optimal Control D</i>	WeP03 <i>Systems Biology + Medical App. B</i>	WeP04 <i>Biochemical Engineering B</i>	WeP05 <i>Electro-Mechanical Engineering</i>	WeP06 <i>Non-Linear Control B</i>
16:15 – 16:40	van Gils	Hermans	Mauroy	Zamorano	Fontaneau-Belmudes	Biemond
16:40 – 17:05	Visiers	Van den Broeck	Fey	Maclean	Moradzadeh	Delvenne
17:05 – 17:30	Xia	Stumper	Trotta	Stein	de Best	Ceragioli
17:30 – 17:45	Coffee Break					
17:45 – 18:10	Witvoet	Dutta	Verspecht	Gins	Hennen	Dirksz
18:10 – 18:35	Leskens	Zhu	van Mourik	Van den Kerkhof	Ronde	del Puerto-Flores
18:35 – 19:00	Abouzaid	Khalate	Drion	Vanlaer	Gérard	Collins
19:30 – 21:00	Dinner					
21:00 – 22:00	Board DISC (room Visie)					

Thursday April 1

8:30 – 9:30	P5 Samenspel “ <i>Networked Control Systems (Part I)</i> ” Maurice Heemels and Nathan van de Wouw						
9:30 – 10:00	Break						
10:00 – 11:00	P6 Samenspel “ <i>Networked Control Systems (Part II)</i> ” Maurice Heemels and Nathan van de Wouw						
11:00 – 11:30	Break						
11:30 – 12:30	P7 Samenspel “ <i>Networked Control Systems (Part III)</i> ” Maurice Heemels and Nathan van de Wouw						
12:30 – 13:45	Lunch						
Room	Samenspel	Samenkomst	Samenwerking	Visie	Uitdaging	Interactie	
ThP	ThP01 <i>Systems Theory A</i>	ThP02 <i>Optimal Control E</i>	ThP03 <i>System Identification C</i>	ThP04 <i>Optimization and Model Reduction</i>	ThP05 <i>Modeling</i>	ThP06 <i>Observers</i>	
13:45 – 14:10	Yang	Xu	Rijlaarsdam	Wattamwar	Stolte	Hidayat	
14:10 – 14:35	Polenkova	Hoogendijk van Berkel	Louarroudi Lataire	van Belzen Mutsaers	Donkers van der Hulst	Simonetto Plaza	
14:35 – 15:00	Thuan	Mesbah	Blom	Besselink	Alladagli	Rentmeesters	
15:00 – 15:25	Kerber	van Voorn	Domanov	Signoretto	Garcia-Canseco	Vandersteen	
15:25 – 15:50							
16:00 – 16:15	Best Junior Presentation Award						
16:15	Closure of 29th Benelux Meeting						

